RUHR-UNIVERSITÄT BOCHUM

Yasir Mawla Hammood Al-Badran

Volumetric Yielding Behavior of Unsaturated Fine-Grained Soils

Bochum 2011 Heft 46

Schriftenreihe des Lehrstuhls für
Grundbau, Boden- und Felsmechanik

Herausgeber: Tom Schanz

ISSN 2190-3255

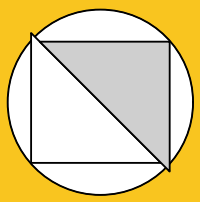

Ruhr-Universität Bochum
Schriftenreihe Grundbau, Boden- und Felsmechanik
Heft 46

Herausgeber:
Prof. Dr. -Ing. habil. Tom Schanz
Ruhr-Universität Bochum
Fakultät für Bau- und Umweltingenieurwissenschaften
Lehrstuhl für Grundbau, Boden- und Felsmechanik
44801 Bochum
Telefon: 0234/ 3226135
Telefax: 0234/ 3214236
Internet: www.gbf.ruhr-uni-bochum.de

ISSN 2190-3255

Volumetric Yielding Behavior of Unsaturated Fine-Grained Soils

Dissertation
as a requirement for the degree of
Doktor – Ingenieur

at the Faculty of Civil and Environmental Engineering
Ruhr-Universität Bochum

submitted by
Yasir Mawla Hammood Al-Badran
from Baghdad / Iraq

Bochum
May 2011

Reviewers:
Prof. Dr.-Ing. habil. Tom Schanz
Prof. Dr. Sai Vanapalli
Prof. Dr. Pierre Delage
Prof. Dr. Maria Datcheva

This work is dedicated to
my parents, my wife Susan, my daughter
Hawraa, and my son Yousif

RUHR – UNIVERSITÄT BOCHUM
Fakultät für Bau- und Umweltingenieurwissenschaften
Lehrstuhl für Grundbau, Boden- und Felsmechanik
Univ.-Prof. Dr.-Ing. habil. Tom Schanz

Vorwort des Herausgebers

Die vorliegende Promotionsarbeit von Herrn Yasir Al-Badran beschäftigt sich mit dem volumetrischen Verhalten von teilgesättigten feinkörnigen Böden. Im Speziellen geht es um Beanspruchungszustände, bei denen Erstbelastung, d.h. im bodenmechanischen Sinne, Fließen auftritt. Teilgesättigte Böden haben eine weitreichende Bedeutung in der Ingenieurpraxis. Diese reicht von den sog. problematischen Böden, welche z.B. zum Quellen, zum Schrumpfen und zum Kollaps neigen, in ariden- und semiariden Gebieten,
der Problematik von künstlich verdichteten Böden im Erd- und Straßenbau bis hin zur Frage der langfristigen Verwahrung von hochgiftigen Abfällen in Endlagern.
Herr Al-Badran benutzt in seiner Arbeit das Konzept der Zustandsflächen, bei dem eine Zielgröße wie die Porenzahl als Funktion verschiedener Zustandsgrößen, wie etwa der Saugspannung, der Sättigung oder der Nettospannung dargestellt werden. Das von Herrn Al-Badran vorgeschlagene Modell hat als zentrale Aussage, dass es eine derartige Zustandsfläche für einen Boden, bei unterschiedlichem initialen Sättigungsgrad und unterschiedlicher initialer Dichte, einen eindeutigen Zusammenhang zwischen der Porenzahl, der Nettospannung und dem Sättigungsgrad gibt.
Ein zweiter wesentlicher Teil der Arbeit von Herrn Al-Badran ist es, ein weiteres theoretisches Modell zur Beschreibung der vollständigen Verdichtungskurve von Böden über den gesamten Bereich der möglichen Wassergehalte aufzustellen. Dieses zweite Modell basiert auf den zunächst behandelten Zustandsflächen. Als praktische Anwendung wird ein Konzept vorgeschlagen, was mit wenigen Eingangsdaten eine Ableitung des optimalen Wassergehaltes und der maximalen Trockendichte ermöglicht. Beide Modelle wurden umfangreich an Ergebnissen aus der Literatur kalibriert, verifiziert und validiert. Es zeigt sich, dass beide Modelle jeweils die Daten aus der Literatur sehr gut wiedergeben können. Neben den theoretischen und analytischen Arbeitspaketen beinhaltet die Promotion von Herrn Al-Badran umfangreiche eigene experimentelle Untersuchungen zur Verifizierung seiner Konzepte. Als Materialien werden ein Calciumbentonit und ein Sand in zwei verschiedenen Lagerungsdichten herangezogen. Bentonit-Sand-Mischungen haben im Bereich des deutschen Konzeptes zur Endlagerung radioaktiver Abfälle eine zentrale Bedeutung.
Es ist zu betonen, dass die notwendigen experimentellen Prozeduren in ihrer Durchführung sehr komplex sind. Es existieren nur wenige Anleitungen zur Durchführung der entsprechenden Versuche. Hierbei ist besonders die Genauigkeit der zu messenden bzw. aufzubringenden Saugspannung zu nennen. Schwankungen der Saugspannung hängen neben der gewählten Methode vor

allen Dingen von der Möglichkeit ab, die Temperatur während der oftmals monatelang andauernden Experimente möglichst genau zu kontrollieren.
Besonders betonen möchte ich abschließend einen Typ von Experiment, den Herrn Al-Badran in seiner Arbeit neu entwickelt und zur Anwendung gebracht hat. Derartige Versuche sind mir aus der Fachliteratur nicht bekannt. Es handelt sich um ein Experiment, bei dem der Versuchskörper während der gesamten Belastungsdauer im Zustand der konstanten Sättigung gehalten wird. Da sich unter z.B. Änderungen der Nettospannung die Porenzahl ändert und somit auch die Sättigung ändern würde, muss permanent in Funktion der Volumenänderung die Kapillarspannung derartig geregelt werden, dass sich ein Wassergehalt ergibt, der in Zusammenhang mit der jeweiligen Porenzahl zu einer konstanten Sättigung führt.
Die vorliegende Arbeit von Herrn Al-Badran ist ein wesentlicher Schritt zur Weiterentwicklung des Verständnisses der Volumenänderung teilgesättigter feinkörniger Böden. Sie verwendet aktuellste theoretische und experimentelle Konzepte, und bringt diese einen entscheidenden Schritt vorwärts.

Bochum, im Sommer 2011

Prof. Dr.-Ing. habil. Tom Schanz

Acknowledgements

Praise be to God, the most gracious and the most merciful, for His helps that enable me to finish this work. I would like to express my deep gratitude, sincere appreciation first and foremost to my supervisor, Prof. Tom Schanz, Head of the institute of Foundation Engineering, Soil- and Rock mechanics for his meticulous guidance and patience throughout my period of candidature. No doubt, this doctoral research would not have been possible without his support.

I would like to acknowledge the financial support for my PhD research provided by Deutsch Akademischer Austausch Dienst, DAAD (German Academic Exchange Service). Many thanks go to Prof. Sai Vanapalli, Prof. P. Delage, and Dr. M. Datcheva for their agreement to be reviewers of this dissertation.

I want to express my deep and sincere gratitude to Dr. Snehasis Tripathy for their useful discussions and help in my study.

My gratitude also is extended to my former colleagues from the Laboratory of Soil Mechanics at Bauhaus-Universität Weimar including the research and laboratory staffs. Special thanks to Ms. Gabriel Tscheschlok, Mr. Frank Hoppe (Alma), Mr. Milad Asslan, Dr. Yulian Arifin, and Dr. Jamal Alabdoula for their assistance in the experiments, discussion, and sharing the ideas. My deep thanks to my colleagues (research and laboratory staffs) at Ruhr-Universität Bochum. I would like to thank my roommate Mr. Khan for shearing ideas and comments. I would like pass my gratefulness to all people who indirectly assisted me during my period of stay in Weimar and Bochum.

I also warmly thank my unending gratitude to my family, specially my parents for their help, support, and encouragement throughout my live.

At last but most, I would like to express my deepest gratitude to my wife Susan for her continuous support and caring, and to my daughter Hawraa and my son Yousif for their amusing and cheerful behavior at home.

Yasir Al-Badran
Bochum-Germany, May 2011

Zusammenfassung

In der geotechnischen Praxis ist der Zustand des Bodens häufig ungesättigt, z.B. oberflächennahe Schichten in den ariden oder semi-ariden Regionen und der verdichtete Boden in Erddämmen und schließlich die Abdichtung für nukleare Endlager. Der ungesättigte Zustand des Bodens kann viele geotechnische Probleme infolge von Sättigungs- und Trocknungszyklen mit sich bringen, wie die Volumenänderung und daraus resultierender Kollaps oder Schwellen, die Änderung der Scherfestigkeit (Entfestigung oder Verfestigung) oder eine Änderung der Wasserdurchlässigkeit. Die klassischen Prinzipien der Bodenmechanik für gesättigte Böden sind oft nicht geeignet für die Erklärung dieser Phänomene.

Viele Modelle haben die Volumenänderung von ungesättigten Böden behandelt, aber bis jetzt ist nur eine begrenzte Anzahl an Untersuchungen zur Volumenänderung im Fließzustand für den gesamten Bereich der Netto- und Saugspannungen, die ein Boden erfahren kann, präsentiert worden.

Das Ziel dieser Arbeit ist die Entwicklung eines neuen Modells für ungesättigte, feinkörnige Böden unter Verwendung einer konstitutiven Zustandsfläche im Porenzahl-Nettonormalspannungs-Saugspannungs-Raum. Das Modell schlägt vor, dass es für den gleichen Boden mit unterschiedlichem initialen Sättigungsgrad (d.h. gesättigt und ungesättigt) und unterschiedlicher initialer Dichte (d.h. verdichtet und locker) eine eindeutige Fläche im Porenzahl-Nettovertikalspannungs-Sättigungsgrad-Raum gibt, die die Zustandsfläche im Fließzustand repräsentiert. Das neue Modell basiert auf dem S_r-Linien-Konzept (Al-Badran, 2001), dass hier gemäß der mikrostrukturellen Betrachtung von (Nagaraj et al., 2006a und b) weiter modifiziert wird.

Außerdem wird ein theoretisches Modell der Verdichtungskurve von Böden mit unterschiedlichem Verdichtungsaufwand für den gesamten Bereich des Wassergehalts vorgestellt. Die Vorhersagemethode der Verdichtungskurve basiert auf der Annahme, dass die Verdichtungskurve die Zustandsfläche des Fließzustands reproduziert. Darüber hinaus können die Linien gleicher Saugspannung in den Verdichtungskurven bestimmt werden, wenn der Sättigungspfad der Saugspannung-Wassergehalts-Beziehung bekannt ist. Es wird ein schrittweises Vorgehen für die schnelle und zielgerichtete Schätzung des optimalen Wassergehalts w_{opt} und die maximale Trockenwichte vorgeschlagen.

Es wurde ein umfangreiches experimentelles Programm durchgeführt, um das volumetrische Fließverhalten (Volumenänderung im Fließzustand) zu untersuchen, und die

Zusammenfassung

Ergebnisse werden in dieser Arbeit diskutiert. Zwei Materialien wurden in dieser Arbeit getestet, nämlich reines Calcigel-Bentonit (100B) und eine Mischung aus 30% Calcigel-Bentonit und 70% Haider Sand (30B). Die Ergebnisse der experimentellen Untersuchungen wurden verwendet, um das neue konstitutive Modell für die Zustandsfläche des Fließzustands zu verifizieren. Die Ergebnisse zeigen, dass die Modellvorhersagen sehr gut mit Daten aus Experimenten, sowohl in dieser Arbeit durchgeführten als auch aus der Literatur gewonnenen, übereinstimmen.

Abstract

In geotechnical practice the condition of soil in many cases is unsaturated e.g., shallow layers in the arid and semi-arid regions and the compacted soil used in earth embankments, and finally the sealing and buffer materials for the nuclear repository. The unsaturated state of soil can raise many geotechnical problems upon wetting-drying cycles such as volume change resulting in collapse or swell, change in the shear strength (softening or hardening), and change in the hydraulic conductivity. The classical principles of soil mechanics for saturated soil are often not suitable for explaining these phenomena.

Many models have dealt with the volume change of unsaturated soil before, but till now limited studies have been presented on the volume change at the yield state for the entire range of net stress and suction that may be experienced by the soil.

This study aims at developing a new model for unsaturated fine-grained soils employing a constitutive state surface in void ratio-net normal stress-suction space. The model suggests that, for the same soil, and for different initial degree of saturation (i.e. saturated and unsaturated) and different initial densities (i.e., compacted and loose) there is a unique surface in void ratio-net vertical stress-degree of saturation space representing the state surface at yield state. The new model is based on the S_r-lines concept (Al-Badran, 2001) that is further modified here according to the microstructural consideration of (Nagaraj et al., 2006a and b).

A theoretical model of the compaction curve of soils at various compaction efforts for the entire range of water content is presented as well. The prediction method of compaction curve is based on the assumption that the compaction curves reproduce the state surface at yield state. Moreover, the lines of equal suctions on the compaction curves can be determined, if the wetting path of the soil water characteristic curve is known. A stepwise procedure is proposed for fast and straightway estimation of the optimum water content *OWC* and the maximum dry unit weight γ_{dmax}.

An extensive experimental work was carried out to study the volumetric yielding behavior (volume change at yield state) and the results are discussed in this thesis. Two materials namely pure Calcigel bentonite (100B) and a mixture of 30% Calcigel bentonite and 70 % Haider sand (30B) were tested in this study. The results of experimental tests were used to verify the new constitutive model for the state surface at yield state. The results show that the model predictions match very well with the data from the experiment both performed within this study and gathered data from literature.

Contents

List of Figures

List of Tables

List of Symbols

γ : A parameter that induces further stiffness in the 'intra-aggregate governing suction' zone.
ϕ : Coefficient.
β : Parameter controlling the rate of increase of soil stiffness with suction.
ν : Poisson's ratio.
χ : Effective stress parameter.
λ : Slope of the yield line under constant suction condition.
κ : Stiffness parameter for changes in net mean stress for saturated reversible (elastic) states of the soil.
σ : Total stress.
ϕ' : Effective angel of friction
λ^* : Slope of the yield line under constant suction condition.
σ' : Effective stress.
σ'_{vms} : Preconsolidation stress of saturated state.
σ'_{vmn} : Preconsolidation stress of unsaturated state (natural water content).
σ_a^{net} : Net axial stress.
γ_d : Dry density (or dry unit weight).
γ_{dmax} : Maximum dry density.
Δe : The change in void ratio upon wetting.
$(u_a\text{-}u_w)_b$: Air entry value.
λ_{vp} : Slope of NCL under constant suction condition.
100B : Pure bentonite (Calcigel).
1D-NCL : One-dimensional normal consolidation line.
30B : 30 % Bentonite (Calcigel) + 70 % Sand.
a : Ratio of the maximum yield stress at unsaturated state to yield stress at saturated state, p'_{sat}.
A_d : Constant (fitting parameter which controls the values of dry density at *DOP*).
a_e : Material parameter.
ATT : Axis-translation technique.
A_w : Constant (fitting parameter which controls the values of dry density at *WOP*).
B_d : Constant (fitting parameter which controls the degree of water sensitivity or slope of compaction paths at *DOP*).
B_w : Constant (fitting parameter which controls the degree of water sensitivity or slope of compaction paths at *WOP*).
C : A parameter relating to soil moisture.

c' : Effective cohesion.
C_c : Compression index.
CE : Compaction effort.
CEC : Cation Exchange Capacity.
com : Denoted to the compacted initial state.
CP : Collapse potential (%).
CP : Concave point.
C_r : Rebound index.
C_s : Swelling index.
C_{sat} : A parameter corresponds to saturation.
CSSS : constant void ratio cross-section of state surface.
d : Denoted to the drying test.
dl : Change in height of sample from natural content to saturated sample.
D : Dilatancy coefficient.
$D\gamma_{dmax}$: Maximum dry density at the lower *OWC*.
D10 : Grain size diameter corresponding to 10 % passing (mm).
D30 : Grain size diameter corresponding to 30 % passing (mm).
D60 : Grain size diameter corresponding to 60 % passing (mm).
DOP : Dry of optimum.
DOWC : Dry optimum water content.
DPCP : Dry peak compaction point.
e : Void ratio.
EC : Electrical conductivity (mS/cm).
e_{dry} : Void ratio of the fully dry soil.
e_L : Void ratio at liquid limit.
e_{max} : Maximum void ratio in the send interval.
e_{NCL} : Void ratio of the saturated NCLunder a specific net stress.
e_o : Initial void ratio.
e_s : Void ratio under saturated condition.
G_s : Specific gravity.
I_p : Plasticity index.
iso-NCL : Isotropic normal consolidation line.
K : Constant.
k_1 : Constant = $\frac{v_w}{n \Pi l}$.
l : Length of cylindrical pore.
LC : Loading-collapse curve.
LL : Liquid limit.
Lo : Denoted to the loose initial state.
l_o : Original height of sample.
LOO : line of optimum.
m : Molal salt solution (mol/Kg).
$M + C$: Silt + clay fraction.
M : Slope of critical state line(the ratio *q/p'* on critical state).
M : Parameter that controls the position of e_{max} in the second interval under each net stress.

MIP : Mercury intrusion porosimetry.
MP : Modified Procter.
M_w : Molecular weight of water (18.016 kg/kmol).
n : Number of capillary pores enclosed due to number of clusters enclosed by a capillary pore.
n : Shaping parameter.
NC : Normal consolidated state.
NCL : Normal consolidation line.
OC : Over consolidated state.
OMC : Optimum moisture content.
OMC_{SP} : Optimum moisture content for Standard Procter.
OWC : Optimum water content.
p : Excess of mean stress over air pressure (net mean stress).
P : Net stress.
$p_{(s)}$: Unsaturated preconsolidation stress under constant suction.
p' : Mean effective stress
p'_{sat} : Yield stress at saturated state.
p_0 : Saturated preconsolidation stress.
p^c : Reference stress state for which $v = N(s)$.
Pcom : Denoted to the constant net stress applied in static compaction.
PCP : Peak compaction point.
PL : Plastic limit.
P**X** : Denoted to the constant net vertical stress test of **X** MPa.
q : Deviator stress.
r : Parameter defining the maximum soil stiffness or post-yield compressibility parameter (for an infinite suction).
R : Universal gas constant (i.e., 8.31432 J/mol K).
R : Parameter that controls the influence of the degree of saturation to increase the void ratio under constant net stress.
R-A : Net forces of the difference between Repulsive and Attractive forces between clay particles.
RH : Relative humidity.
RP : Reduced Proctor (248 kJ.m/m^3).
S : Sand fraction.
s : Matric suction.
s : Suction.
*s** : Effective suction stress.
s_{aev} : Air entry value of soil.
s_c : Critical suction.
SD : Suction-decrease curve.
s_e : Air entry suction.
Se : Effective degree of saturation.
SEM : Scanning electron microscope.
SI : Suction-increase curve.
Sl : Denoted to the slurry initial state.
s_{min} : A reference suction value.

s_o : Hardening parameter of the suction increase yielding curve represents the maximum suction value for elastic deformation.
SP : Standard Proctor.
S_r : Degree of saturation.
$S_{r(e_{max})}$: Degree of saturation at maximum void ratio in the send interval.
S_{rc} : Critical degree of saturation.
S_r-lines : NCL's under constant degree of saturation condition.
Sr**X** : Denoted to the constant degree of saturation test of **X** %.
SSA : Total specific surface area.
s_{sep} : Separation suction.
s_t : Total suction.
SWCC : Soil water characteristic curve.
SWRC : Soil water retention curve.
S**X** : Denoted to the constant suction test of **X** MPa.
T : Absolute temperature in Kelvin.
U : Denoted to the identical specimen was tested in different devices under that same conditions for comparison.
u_a : Pore-air pressure.
USCS : Unified Soil Classification System.
u_w : Pore-water pressure.
ver : Denoted to the verification test by testing identical specimens with different paths but the same initial and final points.
VET : Vapour equilibrium technique.
w : Denoted to the wetting test.
w : Water content.
$W\gamma_{dmax}$: Maximum dry density at the high *OWC*.
$w_{(e_{max})}$: Water content of the maximum void ratio in the send interval.
WOP : Wet of optimum.
WOWC : Wet optimum water content.
WRC : Water retention curve.
XRD : X-ray diffraction.
ε^p_v : Plastic volumetric strain.
$\lambda(0)$: Stiffness parameter for changes in net mean stress for virgin states of the soil (Slope of saturated NCL).
$\lambda(s)$: Stiffness parameter for changes in net mean stress for saturated virgin states of the soil (Slope of NCL under constant suction condition).
ξ : Bonding variable.
π : Osmotic suction.
ρ_w : Unit weight of water in kg/m^3 as a function of temperature.
σ^*_{ij} : Average skeleton stress variable.
σ_v : Vertical net stress.
v : Specific volume.
ZAV : Zero air void line.

Chapter 1
Introduction

1.1 Background and motivations

The soil forming in shallow layers in the arid and semi-arid regions and the compacted soil used in earth dams, highways, embankments, airport runways, and the sealing and buffer materials engineering barriers e.g., used for the nuclear repository are in unsaturated conditions. Whenever the water interacts with a soil that is in a state of unsaturated condition volume change may occur. Such soil-water interaction may cause collapse or swell depending on soil condition. Moreover the wetting may cause reduction of the shear strength (softening) and increase of the hydraulic conductivity. In case of increasing the suction (drying) for initially saturated soils, slurry or compacted, the resulted curve is named the soil water characteristic curve (SWCC), while in case of initial unsaturated state soils, the curve will identify as soil-water retention curve (SWRC). The classical principles and concepts of soil mechanics for saturated soil are often not suitable for describing such problems. Therefore, special theories and models were proposed in the literature by several investigators (e.g., Ho, 1988; Fredlund and Rahardjo, 1993; Alonso et al, 1990; Gens and Alonso, 1992; Kohgo et al., 1993; Wheeler and Sivakumar, 1995; Bolzon et al., 1996; Cui and Delage, 1996; Pereira and Fredlund, 2000; Loret and Khalili, 2002; Datcheva and Schanz, 2003; Khalili et al., 2004; Fredlund and Pham, 2007; and Sheng et al., 2008a) to describe and analyse the behavior of unsaturated soils.

In nuclear (or radioactive) and high-level toxic waste disposal repositories, temperature of the waste elevates due to radioactivity processes which causes drying of the soil and alters the degree of saturation of the soil. The safe disposal of high-level radioactive nuclear waste generated from nuclear power plants is of great concern in many countries due to nuclear waste long-term (at least 10,000 years) detrimental impact on humans if released into the environment. In many countries, the chosen emplacement depth for the waste repositories has been found to vary between 500 to 1000 m (e. g., Swedish Nuclear Fuel and Waste Management, 1992 and Japan Nuclear Cycle Development Institute, 2000). A geologic

disposal facility generally consists of metallic canisters containing the radioactive nuclear wastes, buffer materials between the waste canister and bedrock, and backfill materials that would fill the spaces in the excavated access tunnels and pits. The basic functions of the barrier materials used in the waste repositories require a very low hydraulic conductivity in order to provide long-term stability to the barrier system under the high overburden pressure, and the materials should possess a high radionuclide adsorption capacity and a high heat transfer capacity (Brookins, 1984).

Therefore, it is important to investigate the materials that have been proposed (such as bentonite-sand mixtures) as these materials are to be used as sealing and buffer elements for the repository beside the studies performed on the host rock site characterization. The unsaturated condition of the repository induces hydro-mechanical processes of its buffer materials engineering barriers. The volume change behavior of unsaturated bentonite-sand mixtures is one of the main hydro-mechanical processes.

To precisely understand this behavior the volumetric yielding for unsaturated soils should also be investigated. Limited studies are reported in the literature the volume change beyond the preconsolidation stress (yield state) for a large range of net stress and suction that may be experienced by the soil. Here the definition of the state surface is the surface that consists of points of the preconsolidation pressures from any initial degree of saturation and different initial density. The loading path that provide sufficient information for determining the state surface, are either (*i*) increasing the net stress under constant suction (or constant water content) or (*ii*) reducing the suction (wetting) under constant net stress. In addition there is another condition of state surface; (*iii*) in case of increasing the suction (drying); (*a*) in the range of saturation zone (before the air-entry value), and (*b*) in the specific range of high suction. The volume change behavior in this study represents the consolidation, compression and collapse, while the fine-grained soils refer to the clayey and silty soils.

1.2 Objectives and Scopes

This study aims at developing a new model for constitutive state surface in void ratio-net normal stress-suction space for unsaturated soils. The new model is based on the Sr-lines concept (Al-Badran, 2001), which are the NCL's under constant degree of saturation condition, that is further modified using the microstructural consideration introduced by (Nagaraj et al, 2006a and b). A new model is also proposed to describe the compaction curve behavior. The work aims to provide additional understanding to the volume change behavior of unsaturated soils such as: compaction, compression, collapse. It is assumed that the compaction curves correspond to the state surface at yield state of unsaturated condition

(loading under constant water content for loose initial condition). Therefore, when the state surface at yield state is provided the compaction curves, compression curves, and collapse curves may determine and vice versa.

Two materials: pure bentonite (100B) and a mixture of 30% bentonite and 70 % sand (30B) were used in this study. The bentonite is Calcigel and the sand is Haider sand. Perform an extensive experimental work to study the volumetric yielding behavior (volume change at yield state) of pure bentonite and bentonite-sand mixture. The results of experimental tests were used to verify the new constitutive model of state surface. The experimental program consists of constant degree of saturation tests, constant net stress tests, constant suction test, changing both net stress and suction tests, compaction tests, high stress one-dimensional consolidation tests, and SWCC tests.

1.3 Organization of the Dissertation

The thesis consists of eight chapters. The first chapter describes the background and motivations, objectives of the thesis as well as the organization of the thesis.

The second chapter summarizes literature review on unsaturated soils. The concepts for unsaturated soils namely effective stress and the independent two stress variables, the features of volume change of unsaturated soil and the models to estimate the volume change of unsaturated soil are presented. The collapse phenomenon and the method to calculate the collapse are discussed as well. Moreover, survey on the experimental tests to measure the volume change of the unsaturated soil (i. e., constant net stress test, constant suction test, constant water content test, constant volume test, and the SWCC) are given. Finally the theoretical concept and the models from the literature to predict the compaction curve are reviewed.

The third chapter presents the basic physical properties of the materials used. Two materials: pure Calcigel bentonite (100B) and a mixture of 30% Calcigel bentonite and 70 % sand (30B) were used in this study. Additionally, the testing program to assess the volumetric yielding for unsaturated pure bentonite and bentonite sand mixture is presented.

In the fourth chapter, the equipment used in this work is introduced, namely modified controlled-suction oedometer cells, UPC-Barcelona cell, UPC-isochoric cell, high stress oedometer cell (HSC). The calibration of the used equipment is presented as well.

The fifth chapter presents the results of the assessment of volumetric yielding for unsaturated bentonite sand mixture. Here the results of SWCC tests are also summarized. The results of constant degree of saturation test, constant net stress test, constant suction test,

changing both the net stress and suction test are presented. Then the compaction results are presented. Finally the results of one-dimensional high stress consolidation are shown.

In the sixth chapter, a new model for volumetric yielding behavior to determine the state surface at yield state for unsaturated fine-grained soils is presented. The new model is based on the S_r-lines concept (Al-Badran, 2001) that is further modified here using the concept of microstructural consideration introduced by (Nagaraj et al, 2006a and b). The new model was verified by means of the results of the experimental program. Moreover, validity of this model was tested using different soils data from the literature.

Chapter seven presents a new method to model the compaction curve employing the proposed new model in chapter 6. It is assumed that the compaction curves reproduce the state surface at yield state of unsaturated condition. The model is analyzed, discussed, and verified using the experimental results of compaction tests for the pure bentonite and bentonite-sand mixture. Additionally, the model was applied to four different soils that were chosen from literature. Furthermore, a simple chart based on liquid limit values for quick estimation of the maximum dry density (γ_{dmax}) and the optimum water content (OWC) without performing laboratories Proctor tests is also presented.

Finally, Chapter eight summarizes the main results and the related conclusions of this study and provides an outlook for further studies in this field.

Chapter 2

Review of Literature

2.1 Introduction

This chapter provides an overview of the concept of soil suction and summaries the different approaches of stress state in fine-grained for unsaturated soils in the literature. The volume change and collapse behavior for unsaturated soils and models used are summarized. The soil condition on the compaction curve is unsaturated; therefore emphasis will be given to the compaction concept.

2.2 Unsaturated soil

The soil near the ground surface, especially in arid or semi-arid regions, is mostly unsaturated. Compacting, excavating, and remoulding soil processes used in several engineering constructions, such as earth dams, highways, embankments, and airport runways, result in unsaturated soils. These soils are difficult to consider within the framework of classical (saturated) soil mechanics.

An unsaturated soil has more than two phases, and the pore-water pressure is negative relative to the pore-air pressure. An unsaturated soil is commonly defined as having three phases: namely; solids; water; and air (Fredlund and Rahardjo, 1993).

2.2.1 Concept of suction

The concept of suction was developed by several researches (e.g., Buckingham, 1907; Edlefsen and Anderson, 1943; Bolt and Miller, 1958; and Aitchison, 1965). Soil suction, generally, consists of two components: matric component and osmotic component (Fredlund and Rahardjo 1993). The sum of these two components (i.e., matric suction, s, and osmotic suction, π) is called total suction, s_t.

$$s_t = s + \pi \tag{2.1}$$

The matric component is related to the difference between pore-air pressure (u_a) and pore-water pressure (u_w) in the soil (the air-water interface or surface tension) giving rises to the capillary phenomenon. Considering the general concept of suction and the soil-water potential in expansive soil (e.g., bentonite), the matric component of soil suction comes from

the hydration forces and capillary component effects (Pusch and Yong, 2003; Arifin 2008; and Arifin and Schanz, 2009). Therefore, in expansive soils, the matric suction is the sum of the hydration forces and the capillary forces. The osmotic suction component is related to the dissolve solutes in bulk water which is defined as the "free water".

2.2.2 State of stress

Currently, there are two approaches to describe the unsaturated soil behavior (volume change and the shear strength behaviors): the effective stress approach (Bishop, 1959) and the two independent state variables approach (Fredlund and Morgenstern, 1977).

2.2.2.1 Effective stress approach

Effective stress concept was proposed firstly by Terzaghi (1936). Effective stress (σ') represents the average stress carried by the soil skeleton and it is calculated from the difference between two parameters, total stress (σ) and pore water pressure (u).

Croney et al., 1958; Bishop, 1959; and Aitchison, 1960 all proposed modified forms of effective stress equation (Equation 2.2) to account for the two-phase nature of the pore fluid in the unsaturated soil.

$$\sigma' = (\sigma - u_a) + \chi(u_a - u_w) \tag{2.2}$$

where σ' = effective stress; σ = total stress; u_a = pore air pressure; u_w = pore water pressure; χ = effective stress parameter, which has a value of 1 for saturated soils and 0 for dry soils.

2.2.2.2 Two independent stress variables approach

Difficulties in finding a single effective stress equation, illustrated in the works of (Aitchison and Donald, 1956; Bishop and Donald, 1961; Jennings and Burland, 1962; Bishop and Blight, 1963; and Burland, 1965), progressively led to the acceptance of the two independent stress state variables fields as a necessary framework to describe the observed features of unsaturated soil behavior under paths involving the variation of total stress and pore-water pressure deficiency (or suction).

Fredlund and Morgenstern, (1977) proposed the state of stress in unsaturated soils to be describe in terms of two independent (two independent stress variables), namely (σ - u_a), at the macroscopic scale and (u_a - u_w) at the pore scale, to avoid the introduction of a material parameter in the effective stress equation. A separate set of material properties was then introduced for each of the stresses. This was in contrast with the usual approach in continuum mechanics, in which the state variables are averaged over the elemental volume (i.e.,

described at the macroscopic scale) and the macroscopic observations are described in terms of entities which are measured and/or defined at a macroscopic level. In general, mixing of scales can lead to complex constitutive equations with intractable stress-strain relationships (Lu and Likos, 2006).

2.3 Volume change behavior of unsaturated fine-grained soils

The classical one-dimensional theory of consolidation estimates the change in volume with respect to pore-water pressure and time due to the change in effective stress. The theory of consolidation does not play important role for unsaturated soils as it does for saturated soils (Fredlund and Rahardjo, 1993). The volume change problems involve negative pore-water pressures or suction that has received the most attention are that of swelling (Fredlund and Rahardjo, 1993) and collapsing soils.

Many models dealt with the volume change-stress-suction relationships for unsaturated soil (e.g., Ho, 1988; Fredlund and Rahardjo, 1993; Alonso et al, 1990; Gens and Alonso, 1992; Kohgo et al., 1993; Wheeler and Sivakumar, 1995; Bolzon et al., 1996; Cui and Delage, 1996; Pereira and Fredlund, 2000; Loret and Khalili, 2002; Datcheva and Schanz, 2003; Khalili et al., 2004; Fredlund and Pham, 2007; and Sheng et al., 2008a).

Other studies dealt with particular topics of volume change of unsaturated soils, such as the collapsibility of soil (Jennings and Knight, 1957; Knight, 1963; Lawton et al., 1991; Al-Badran, 2001; and Kanazawa et al., 2009). The collapse behavior and the methods to determine it and the relevant literature of the collapse potential will be discussed later in this chapter.

In the following sections the description of the volume change behavior for unsaturated soils will be divided, regarding to the state of stress, into two approaches: the effective stress approach (Bishop, 1959) and the two independent stress state variables approach (Fredlund and Morgenstern, 1977).

2.3.1 Volume change behavior: effective stress approach

Many attempts have been made earlier to describe the unsaturated soil behavior using the effective stress approach. In these attempts the relationship between the effective stress parameter, χ, and the degree of saturation, S_r, has been determined (Aitchison and Donald, 1956; Aitchison, 1960; Bishop, 1959; Bishop and Donald, 1961; Jennings and Burland, 1962; Croney and Coleman, 1961; Bishop and Blight, 1963; and Burland, 1965). Attempts have also been made later to quantify χ using simple capillary models.

Gens (1996) proposed categorization of the effective stress parameter χ: class 1 models are defined by $\chi = 0$ (at fully dried state), in class 2 models χ is a function of matric suction (at saturated state) and in class 3 models χ is a function of degree of saturation, S_r, and suction and, s, (at unsaturated condition). The formulations of class 2 and class 3 may be defined to satisfy the definition of the effective stress in unsaturated soils. Class 3 formulations (χ is a function of S_r and s) are popular in the literature of unsaturated soil modelling such as Aitchison, (1960) and Karube and Kawai, (2001). Bishop (1959) proposed $\chi = S_r$ using a phenomenological approach. The same formulation was subsequently derived from different theoretical considerations by Houlsby, (1997) and Hutter et al., (1999) and it was used in many constitutive models for unsaturated soils (Jennings and Burland, 1962; Jommi and Di Prisco, 1994; Bolzon et al., 1996; Jommi, 2000; Gallipoli et al., 2003b; Wheeler et al., 2003; and Tamagnini, 2004). Although the assumption of $\chi = S_r$ is often used; its validity has not been proved experimentally (e.g., Jennings and Burland, 1962). Jennings and Burland (1962) discussed the validity of the effective stress principle in unsaturated soils arguing that it can not explain the collapse phenomenon upon wetting path. They conducted a series of consolidation tests on several unsaturated soils, and showed that upon flooding (i.e., reducing suction) all samples collapsed rather than expand as expected when using the effective stress principle. Jennings and Burland (1962) used the same equation of Bishop, (1959) to determine the parameter χ which is equal to the ratio of net normal stress to the effective stress on the normal consolidation line (NCL), at the same void ratio of unsaturated condition, as shown in Figure (2.1).

Aitchison (1960) showed that, by making use of an idealized model of an unsaturated soil, the parameter χ is given by the expression:

$$\chi = \frac{\sigma'}{s} = S_r + \frac{1}{s}\sum_0^s 0.3 s \Delta S_r \qquad (2.3)$$

Another limitation of the effective stress principle is that there is no unique relationship between χ and the degree of saturation, S_r. The argument of this limitation was pointed out by (Croney and Coleman, 1961) that χ is a parameter strongly related to the soil structure and therefore one should not be surprised if no direct correlation is found between χ and a volumetric parameter such as the degree of saturation.

Burland (1965) reported that, from a microscopic viewpoint, it is incorrect to combine $(\sigma\text{-}u_a)$ and $(u_a\text{-}u_w)$ in a single equation. Similar arguments were also put forward by (Aitchison, 1965; Matyas and Radhakrishna, 1968; Brackley, 1971; Fredlund and Morgenstern, 1977; and Gens et al., 1995).

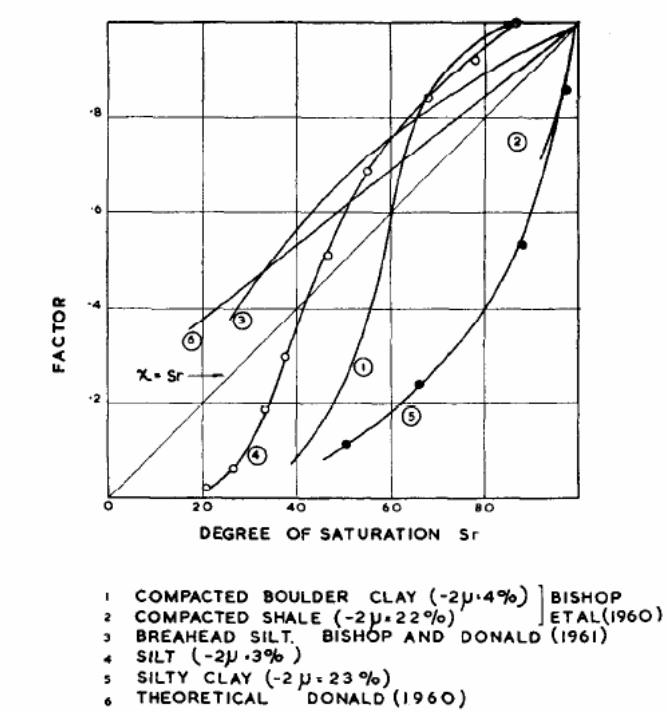

Figure 2.1 Curves of effective stress parameter or "Factor" χ against degree of saturation S_r for various soils (Jennings and Burland, 1962).

Several researchers described nonrecoverable deformations such as collapse within an effective stress framework by defining the state surface as a function of suction (Kohgo et al., 1993a; Modaressi and Abou- Bekr, 1994; Bolzon et al., 1996; Khalili and Khabbaz, 1998; Loret and Khalili, 2000; Khalili and Loret, 2001; and Khalili et al., 2004). Moreover, Khalili et al., (2004) noted that even in saturated soils, nonrecoverable deformations such as dilation and/or collapse (i.e., in metastable structures) can not be explained in terms of effective stress alone.

Kohgo et al. (1993a) tried to interpret the mechanical behavior of unsaturated soils from micro and macro structure aspects and proposed a simple elastoplastic model for unsaturated soils. They described the possible saturation conditions that named: insular air saturation, fuzzy saturation and pendular saturation, to examine the mechanical behavior of unsaturated soils, as shown in Figure (2.2). Suction effects are clarified for each state and are used to interpret the overall mechanical behavior of unsaturated soils. They classified the suction effects into two categories. First is that an increase in suction induces an increase in effective stresses and the second is that an increase in suction induces an increase in both yield stress and the stiffness of the soil skeleton. The first effect of suction can be estimated by formulating the relationship between suction and shear strength at the wet side of the critical state. According to the experimental results, they found that it is reasonable that the

relationship between shear strength and suction is postulated as a hyperbolic function, so the χ will be:

$$\chi = \begin{cases} 1 & (s \le s_e) \\ \dfrac{a_e (s_c - s_e)}{(s^* + a_e)^2} & (s > s_e) \end{cases} \qquad (2.4)$$

where s = suction; s^* = the effective suction stress (which represents the excess suction over the air-entry value); s_e = the air-entry suction; s_c = the critical suction; a_e = material parameter.

The second effect of suction can be estimated from the state surface concept. The modified Cam clay model with these suction effects is proposed. Figure (2.3) presents the state surface plotted by Kohgo et al., (1993a). Moreover, Figure (2.3) shows that the slope of the state line at yield state of constant suction (λ^*) decreases by increasing the suction. This model has been examined by (Kohgo et al., 1993b).

Bolzon et al. (1996) proposed a generalized model to simulate the experimentally observed behavior of unsaturated soils. It has been obtained by introducing elasto-plastic relationships for unsaturated soils by using Bishop's effective stress and suction (effective stress equation) as independent stress parameters and by modifying the hardening parameter and the yield condition to take into account the role of suction. The effective stress parameter (or the weighting parameter as used in the article) χ was assumed to be equal to the degree of saturation S_r, ($\chi = S_r$).

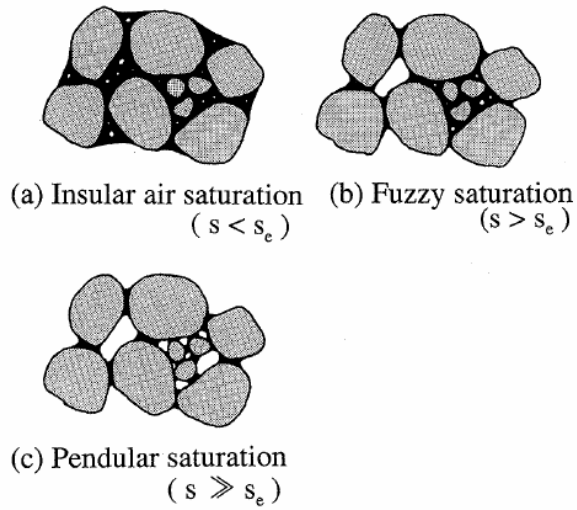

Figure 2.2 Possible saturation conditions in real soils (Kohgo et. al., 1993a).

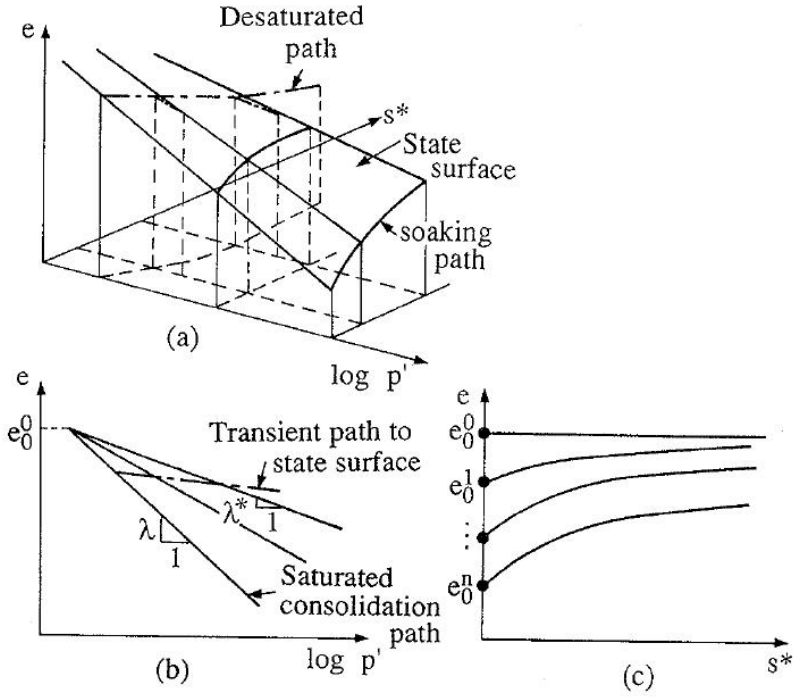

Figure 2.3 The generalized state surfaces (Kohgo et al., 1993a).

Khalili and Khabbaz (1998) presented a relationship between the effective stress parameter χ and the suction ratio $(u_a\text{-}u_w)$ / $(u_a\text{-}u_w)_b$, Figure (2.4). The term $(u_a\text{-}u_w)_b$ represents the air-entry value of soil, s_{aev}. They showed that the effective stress parameter χ can be calculated as in equation (2.5) and the best-fit value of the exponent $\gamma = -0.55$ is appropriate to represent the behavior of different soil types. The parameter γ can therefore be considered as a material-independent constant. The air-entry value, s_{aev} depends on the soil type and on the void ratio, though in the original formulation it was considered, for simplicity, as void ratio independent constant.

$$\chi = \begin{cases} 1 & for \quad s < s_{aev} \\ \left(\dfrac{s}{s_{aev}}\right)^{\gamma} & for \quad s \geq s_{aev} \end{cases} \tag{2.5}$$

The parameter χ was determined from shear strength data based on the assumption that the parameters c' and ϕ' are independent of matric suction $(u_a\text{-}u_w)$. But the experimental evidence indicates that ϕ' increases slightly with increasing the suction (Escario and Saez, 1986; Drumright, 1989). Later, Khalili et al. (2004) used the calculated χ values to predict the elastic deformation of unsaturated state, but in case of the normal consolidated state for unsaturated condition, the application of χ values is not presented. Equation (2.5) does not

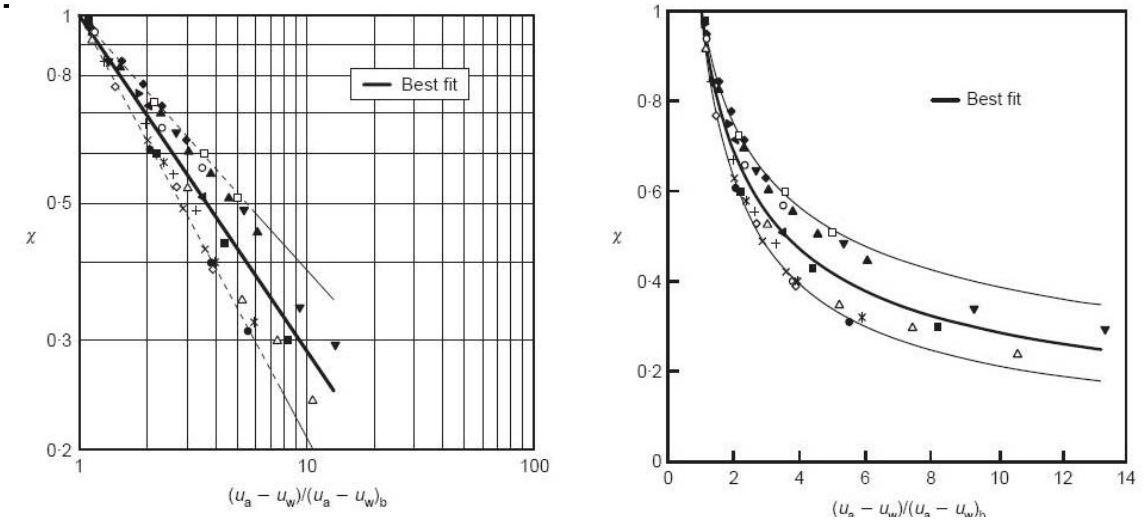

(a) (b)

Figure 2.4 Relationship between the effective stress parameter χ and the suction ratio $(u_a\text{-}u_w)$ / $(u_a\text{-}u_w)_b$: (a) log-log scale, (b) liner scale (Khalili and Khabbaz, 1998).

consider the hydraulic hysteresis. In other words the equation is applicable only for states following the drying path of soil water characteristic curve SWCC. Mašín (2010) had the same argument. This means that Equation (2.5) does not represent the normal consolidated state of unsaturated soils, which following in most cases the wetting path of the SWCC (as will be represented later in Chapter 6). A method to incorporate the effects of hydraulic hysteresis has been proposed by Khalili et al., (2008).

The effective stress formulation from Equation (2.5) has been already applied in many constitutive models for unsaturated soils by Khalili et al., (e.g. Loret and Khalili, 2000; Loret and Khalili, 2002; Russel and Khalili, 2006; Khalili et al., 2008; Masin and Khalili, 2008a; Masin and Khalili, 2008b; and Masin, 2009).

Loret and Khalili (2000) applied, within a three-phase framework using effective stress concept, an extension of elastic–plastic model of saturated soils to unsaturated state. In this model, the total volume changes of the solid skeleton and the fluid phases require a general three phase framework.

Khalili and Loret (2001) proposed an elasto-plastic model for non-isothermal analysis of flow and deformation in unsaturated porous media. The model takes into account the thermo-hydro-mechanical coupling processes.

Loret and Khalili (2002) presented an extension of elastic–plastic model of saturated soils to unsaturated states. The main concern point of the model is on the behavior of the solid skeleton. They used the modified Cam–Clay model as a plastic driver. The application of the

model is demonstrated using a comprehensive set of data reported by Wheeler and Sivakumar, (1995).

Other forms of elasto-plastic models that are presented in terms of two independent modified stress variables have been proposed by Karube and Kawai (2001); Gallipoli et al. (2003a); and Wheeler et al. (2003). The model stated by Karube and Kawai, (2001) has more complex variables than the other two models, associated with multiple surfaces and stress (Jotisankasa, 2005).

The models of Gallipoli et al., (2003a) and Wheeler et al., (2003) separate two mechanical effects in the unsaturated soil: i) the first effect results on the soil skeleton and the bulk water of the soil, and ii) the second effect is due to the stabilising action exerted at the inter-particle contacts of the soil, provided by the water menisci. These two mechanical effects influence directly the distribution of soil water. In the models the basic stress variable is representing (the first effect) the average skeleton stress (Jommi, 2000), which is equivalent to the Bishop, (1959) effective stress parameter space ,χ , in Equation (2.2): χ is equal to the degree of saturation, S_r. The average skeleton stress variable σ^*_{ij} is called the average skeleton stress by Gallipoli et al. (2003a) and Bishop's stress by Wheeler et al. (2003). The second effect is a function of the suction, the degree of saturation and the porosity. The models proposed by Gallipoli et al. (2003a) and Wheeler et al. (2003) use different approaches in considering this effect. Both models evaluate this effect based on the same analysis proposed by Fisher (1926), (Jotisankasa, 2005).

Gallipoli et al. (2003a) proposed that the second variable, ξ, is defined as the product of two factors, the degree of saturation of air ($1 - S_r$), and a function of suction, $f(s)$. Based on a physical argument, this model assumes that, during the elasto-plastic loading of a soil element, the ratio e/e_s is a unique function of the bonding variable, ξ. e is the void ratio under unsaturated conditions and e_s is the void ratio under saturated conditions at the same average skeleton stress state. Figure (2.5) shows the derivation of the yield locus in the isotropic plane: (a) change of void ratio; (b) stress path.

Based on the work by Houlsby (1997), Wheeler et al. (2003) introduced the second stress variable. The second stress variable, termed modified suction, $n.s$ (suction multiplied by porosity). The use of the stress variables σ^*_{ij}, and $n.s$ results in strain increment variables that are integrable of elastic behavior, *LC, SI* and *SD* yield curves, associated flow rules on all three yield curves, and soil constants.

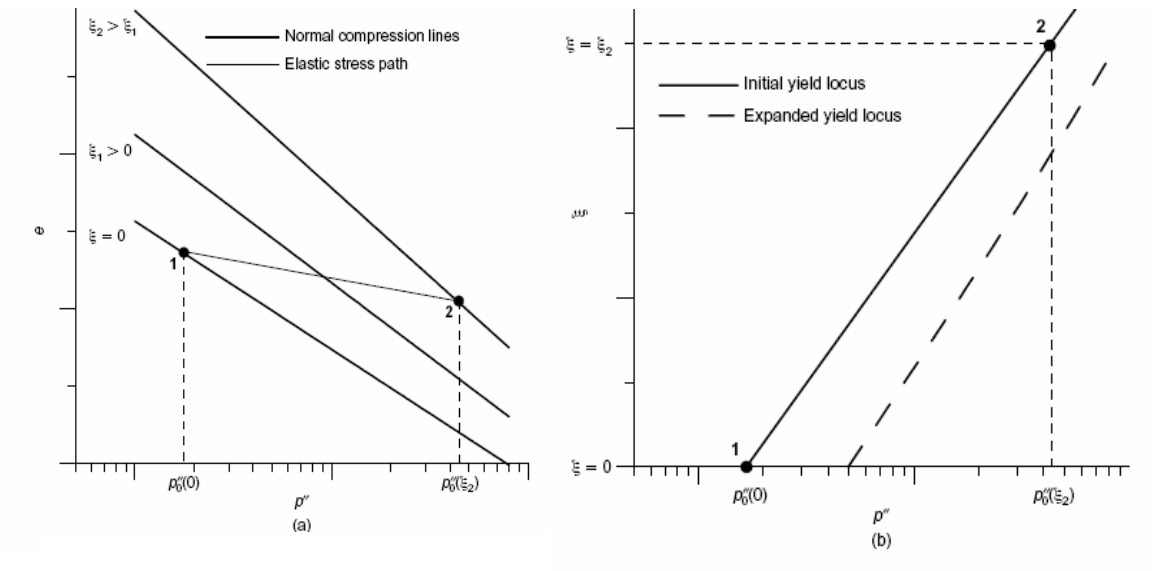

Figure 2.5 Derivation of the locus in the isotropic plane: (a) change of void ratio; (b) stress path (Gallipoli et al., 2003b).

Tamagnini (2004) proposed a constitutive model for unsaturated soils incorporating hydraulic hysteresis following the framework suggested by Jommi (2000), but introducing the formulation of the water retention curve *WRC*. The formulation of this model contains the original saturated Cam-clay as a limiting case (when S_r is equal to 1), and the transition between saturated and unsaturated conditions takes place without discontinuity ($\chi = S_r$).

Khalili et al. (2004) investigated the uniqueness of the critical state line in the deviatoric stress–effective mean stress plane for saturated as well as unsaturated soils, and derived the incremental form of the effective stress parameter, depending on χ established by Khalili et al, (1998), Figure (2.6). Khalili et al. (2004) observed that the state of stresses in a material is controlled by the state of elastic straining within that material. Thus, to explore the validity of the effective stress principle in a material, they assumed that the elastic response of the material is uniquely controlled by the effective stresses within that material (for both saturated and unsaturated states).

Moreover, Khalili et al. (2004) mentioned that in a drying test, as the sample undergoes volumetric contraction, at a certain value of suction, it separates from the confining ring and the incremental response of the sample changes from oedometric to axial loading condition. This value of suction, referred as the separation suction, can be calculated as:

$$s_{sep} = \frac{\nu.\sigma_q^{net}}{\chi(1-2\nu)} \qquad (2.6)$$

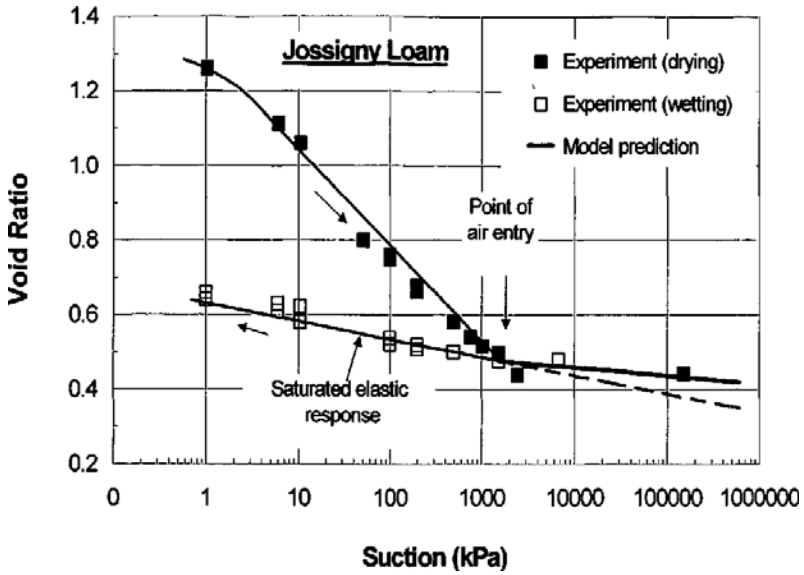

Figure 2.6 Predicted versus measured volume change, Jossigny loam (data from Fleureau et al., 1993, after Khalili et al., 2004).

where s_{sep} = separation suction; ν = Poisson's ratio; σ_a^{net} = the net axial stress.

Khalili et al. (2004) has been pointed the following behavior of unsaturated soils:

1. The process of desaturation occurs only at suction values higher than the air-entry value. At suction values lower than the air-entry value, the soil will be in a saturated state and the mechanics of saturated soils.

2. Suction has a dual effect on the behavior of unsaturated soils. It affects the effective stress as well as the preconsolidation pressure or the yield stress of the soil. Much of the debate in the literature as to the applicability of the effective stress principle to unsaturated soils has in fact been due to this dual effect. Collapse upon wetting, for instance, is a direct consequence of a shift in the preconsolidation pressure with suction.

3. In collapsible unsaturated soils, the rate of increase in the preconsolidation pressure is greater than the rate of increase in the effective stress with suction (Loret and Khalili, 2000). These soils exhibit irreversible volumetric contraction upon wetting at a critical combination of suction and the net stress. A characteristic feature in the behavior of collapsible soils is that, upon desaturation, the soil response enters the elastic region (e.g., see Fleureau et al., 1993). A direct consequence of this behavior is that the elastic coefficient of compressibility must be used in the volume change analysis of such soils subject to a drying test. This fundamental aspect has been neglected in the previous analyses of volume change in collapsible soils, leading to erroneous conclusions as to the applicability and/or uniqueness of the effective stress parameter in unsaturated soils.

4. In noncollapsible unsaturated soils, the rate of increase in the preconsolidation pressure with suction is smaller than the rate of increase in the effective stress. In these soils, collapse upon wetting could not be induced regardless of the value of the net stress and/or the suction. Furthermore, in this case, the response of a normally consolidated noncollapsible unsaturated soil, subject to a drying test, will involve both elastic and plastic volumetric changes. Here, a complete analysis of the soil response will require knowledge of the shift in the preconsolidation pressure with suction as well as the elastoplastic properties of the soil.

Kayadelen (2008) developed five artificial neural networks (ANNs) models with different input parameters. Feed-forward back propagation was applied in the analyses as a learning algorithm. Different input parameters were trained by data collected from the available literature for training the ANN models and then they were tested by the data collected from five different unsaturated tests as well as the data obtained from the unsaturated drained triaxial tests that performed in the study. The test results showed that the matric suction contributes to the shear strength of unsaturated soils. This contribution called suction strength exhibits nonlinear behavior with respect to the matric suction. Performances of the models were examined in terms of some statistical criteria. The best results and high correlation coefficient were produced by Model I with six input parameters: matric suction ($u_a - u_w$), angle of shearing resistance (ϕ'), air-entry value (s_{aev}), sand fraction (S), silt + clay fraction ($M + C$) and plasticity index (I_p) .

Khalili et al. (2008) presented a coupled elasto-plastic constitutive model using the effective stress parameters for describing the flow and deformation behavior of unsaturated soils. Attention is also given to the interrelations between the effective stress and wetting and drying paths, and the shift in the SWCC with the matrix deformation (to correct the effects of hydraulic hysteresis on the effective stress parameter χ proposed by Khalili and Khabbaz, 1998).

M**ašín** (2010) presented an approach to predicting variation of a degree of saturation in unsaturated soils with void ratio and suction. He used Equation (2.5) of Khalili and Khabbaz (1998) as a basis for developments the approach. The approach focuses on the main drying and wetting paths and does not incorporate the effects of hydraulic hysteresis. It leads to the dependency of soil water retention curve (SWRC) on void ratio, which does not require any material parameters apart from the parameters specifying SWRC for the reference void ratio.

2.3.2 Volume change behavior: two independent stress variables approach

The deformation state variables associated with the soil structure and the water phase are commonly used in a volume change of unsaturated soils analysis (Biot, 1941; Bishop and Donald, 1961; Croney and Coleman, 1961; Matyas and Radhakrishna, 1968). Void ratio changes or porosity changes can also be used as deformation state variables representing the soil structure deformation. On the other hand, changes in water content can be considered as the deformation state variable for the water phase (Fredlund and Rahardjo, 1993).

Fredlund and Morgenstern (1977) proposed the state of stress in unsaturated soils in terms of two independent (two independent stress variables), namely net stress (σ-u_a), at the macroscopic scale and matric suction (u_a-u_w), at the pore scale, which σ is the total stress, u_a and u_w are the air and water pore pressure respectively.

Moreover, Fredlund and Morgenstern (1977) argued that the mechanical behavior of soils is controlled by the same stress variables which control the equilibrium of representation value of the soil and the effective stress equation (2.2), contains material parameter (the effective stress parameter, χ). According to that the variables used for the description of a stress should be independent of the material properties. But Khalili et al., (2004) stated that the theoretical basis for the perceived limitations of the effective stress that reported by Fredlund and Morgenstern (1977) is not clear. Moreover, it is evident that the case of "the stress variables should be independent of the material properties" may only be applicable to single-phase homogeneous materials. In multiphase systems, such as saturated and unsaturated soils, the stress state within each phase will naturally be a function of the properties of that phase as well as the other phases within the system. This is required in order to ensure deformation compatibility between the phases.

Different models have been presented for the volume change-stress-suction relationship using the two independent stress variables approach for unsaturated soil (e. g., Lloret and Alonso, 1980; Ho, 1988; Fredlund and Rahardjo, 1993; Alonso et al, 1990; Gens and Alonso, 1992; Wheeler and Sivakumar, 1995; Pereira and Fredlund, 2000; Pham, 2005; Pham and Fredlund, 2005; Fredlund and Pham, 2006; Fredlund et al., 2007; Fredlund and Pham, 2007; and Sheng et al., 2008a). Several constitutive equations and stress variables are used in these models.

Lloret and Alonso (1980) established general equations expressing air and water continuity in an unsaturated soil from the basis of a comprehensive model of volume change behavior of unsaturated soil, in particular the existence of state surfaces for volume change as a mean to accommodate, within the same framework, swelling and collapse behavior.

Ho (1988) and later Ho et al. (1992) and Fredlund and Rahardjo (1993) presented constitutive surfaces for an unsaturated soil, using soil mechanics terminology by means of the two independent stress variables (Figure 2.7). Fredlund and Rahardjo (1993) mentioned that the uniqueness of the two constitutive surfaces for an unsaturated soil (i. e., soil structure and water phase) was restricted to monotonic deformation. Uniqueness is used to indicate that there is one and only one relationship between the deformation and stress state variables. It appears that a reversal in direction of deformation (i. e., an increase and then a decrease in volume) results in different constitutive surfaces. Both of constitutive surfaces require experimental data in order to examine their uniqueness. In additional they reported that the complete uniqueness of constitutive relationship under loading and unloading conditions is virtually impossible. It is important to mention that these surfaces represent a specific paths which consist of reversible and irreversible states.

Alonso et al. (1990) presented a constitutive model (Barcelona Basic Model BBM), which is one of the essential models for unsaturated soils, for describing the stress-strain behavior of unsaturated soils. Gens and Alonso (1992) presented an extension model for unsaturated expansive clays. The model is formulated within the framework of hardening plasticity using two independent sets of stress variables: the excess of total stress over air pressure and the suction. Alonso et al. (1990) showed that, the volumetric response of unsaturated soils depends not only on the initial and final stress and suction values but on the particular path followed from the initial to the final state.

They cited that for isotropic stress conditions the model is characterized, for each initial condition, by two yield curves (*LC*; loading-collapse and *SI*, after suction-increase), Figure (2.8), whose hardening laws are controlled by the total plastic volumetric deformation, Equation (2.7).

$$\left(\frac{p_0}{p^c}\right)=\left(\frac{p_{(s)}}{p^c}\right)^{[\lambda(0)-\kappa]/[\lambda(s)-\kappa]} \tag{2.7}$$

p = excess of mean stress over air pressure (net mean stress); p_0 = saturated preconsolidation stress; $p_{(s)}$ = unsaturated preconsolidation stress under constant suction; p^c = reference stress state for which $\upsilon = N(s)$; s = suction $(u_a - u_w)$; s_o = hardening parameter of the suction increase yield curve represents the maximum suction value for elastic deformation (Figure 2.8c); υ = specific volume; $\lambda(0)$ = stiffness parameter for changes in net mean stress for virgin states of the soil; $\lambda(s)$ = stiffness parameter for changes in net mean stress for saturated virgin states of the soil; κ = stiffness parameter for changes in net mean stress for saturated reversible (elastic) states of the soil.

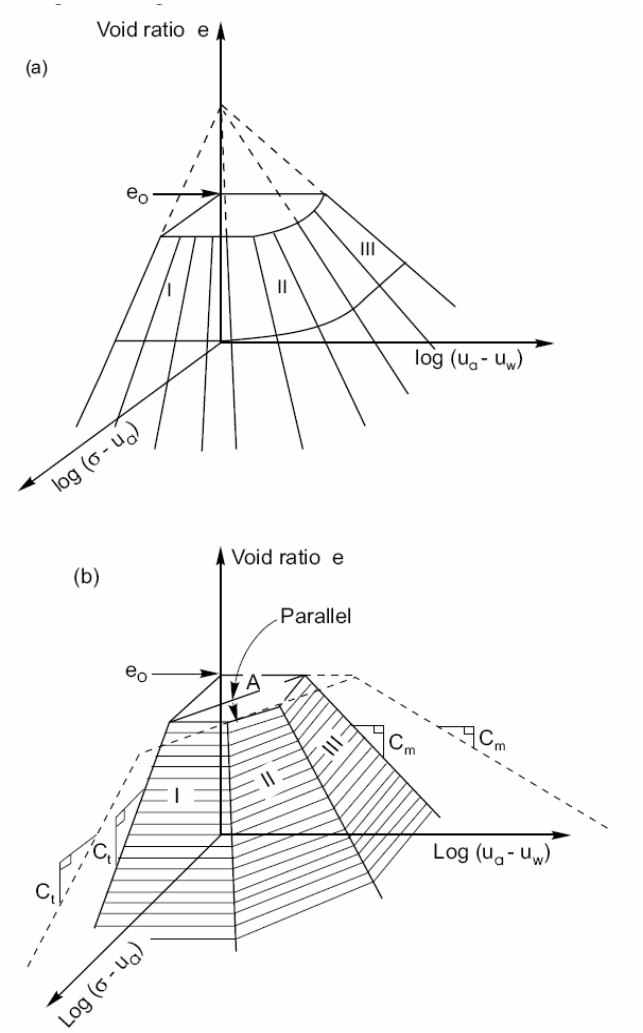

Figure 2.7 Logarithmic forms of void ratio constitutive surface for loading conditions (Ho, 1988): (a) void ratio constitutive surfaces for loading as plotted logarithmically; (b) approximated form of the void ratio constitutive surface in the logarithmic plot.

Equation (2.7) beside plays a central role in the BBM, estimates and explains not only the apparent increase in preconsolidation stress associated with increasing suction, but also the collapse phenomena observed in wetting paths. Note that when $P_{(s)} = p^c$, the LC yield curve becomes a straight line. In this case, changes in suction, *s*, do not result in plastic deformations, only the elastic component is maintained. Equation (2.7) defines the set of yield *p*. values for each associated suction (it can be considered therefore as a family of yield curves in a *p*-*s* space). In order to isolate a single yield curve it is necessary to specify the preconsolidation. These curves become yield surfaces when a third axis (accounting for shear stress) is introduced to model triaxial stress states. The behavior of saturated soils is a particular case of the model developed which is reached when suction becomes zero. In the

BBM, the value of maximum stiffness $\lambda(s)$ is assumed to vary exponentially with suction, from a value $\lambda(0)$ at zero suction, to a value r $\lambda(0)$ as suction tends to infinity by adopting the following alternative empirical equation:

$$\lambda(s) = \lambda(0)\left[(1-r)e^{(-\beta s)} + r\right] \tag{2.8}$$

$$r = \lambda(s-\infty)/\lambda(0) \tag{2.9}$$

where: r = parameter defining the maximum soil stiffness or post-yield compressibility parameter (for an infinite suction); β = parameter controlling the rate of increase of soil stiffness with suction.

Alonso et al. (1990) assumed that $\lambda(s)$ decreased with increasing suction (Figure 2.8b), so the value of r was less than 1. They presented experimental results from Josa (1988) (on compacted low plasticity kaolin) and Maswoswe (1985) (on a compacted sandy clay) showed normal compression lines where $\lambda_{(s)}$ decreased with increasing suction ($r > 1$). Furthermore, according to the BBM (Alonso et al., 1990), the potential collapse on wetting would increase indefinitely with increasing net stress. This formulation is thus not capable of modelling the maximum potential collapse (the normal compression line of constant suction will diverge from the saturated one, r > 1), and only valid for a range of applied net stress that is dependent upon the type of material and value of suction involved. Nevertheless, for many soils the complete picture, if examined over a sufficiently wide range of net mean pressure p; is probably that normal compression for different values of suction initially diverge with increasing and then subsequently converge at higher values of net mean stress. This type of behavior has been observed by numerous researchers (e. g., Maswoswe, 1985; Josa et al., 1992; Sivakumar, 1993; Wheeler and Sivakumar, 1995; Wheeler and Karube, 1996; Sharma, 1998; Matsuoka et al., 2002; Wheeler et al., 2002; Gallipoli et al., 2003b; Georgiadis, 2003; Jotisankasa, 2005; Casini et al., 2007; and Benatti et al., 2010). Figure (2.9) shows that the contour of normal compression lines (NCL's) at constant suctions have slopes more that the saturated NCL (r > 1) (Jotisankasa, 2005).

This means that the maximum potential for wetting-induced collapse compression occurs at an intermediate value of p. Moreover, the studies applied BBM on unsaturated soils show that the post-yield compressibility parameters (r and β) depend on the density (e. g., Romero, 1999). The results of Romero (1999) show that the parameter (r) increases with increasing density and parameter (β) decreases as density increases.

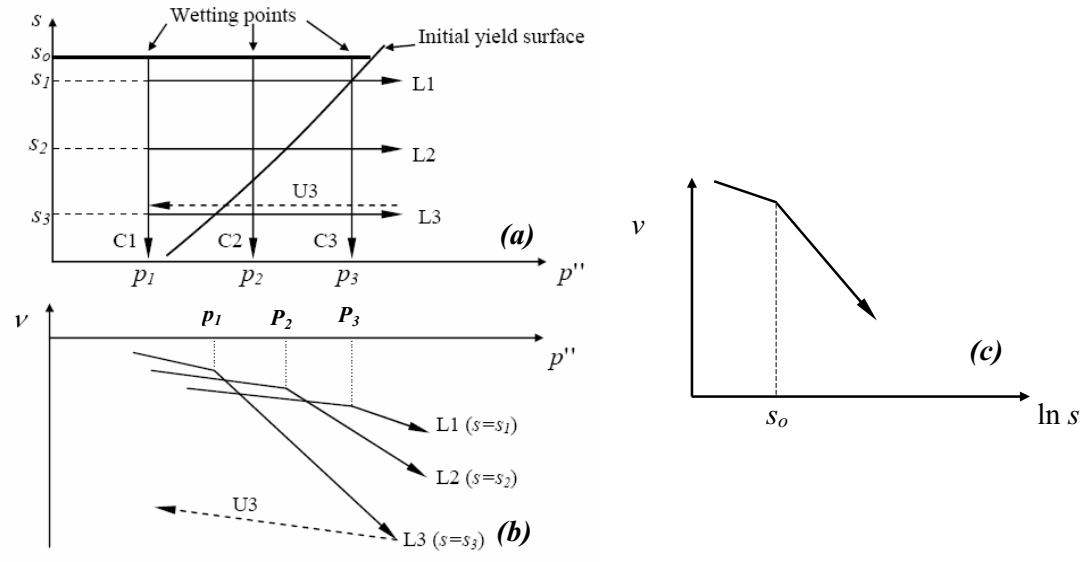

Figure 2.8 Barcelona basic model BBM concepts: (a) Stress paths of LC curve in the (p:s) space; (b) Volume change during compression.(c) Volume change during increase in suction.

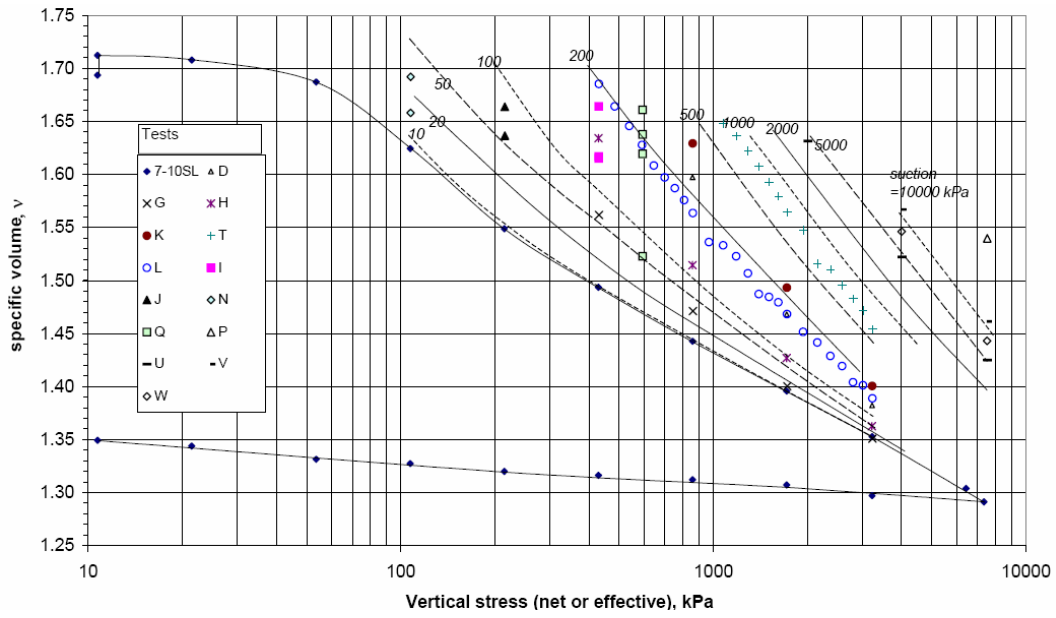

Figure 2.9. Contour of normal compression lines (NCL's) at constant suctions (Jotisankasa, 2005).

The Loading-Collapse (*LC*) yield surface (Figure 2.8a), according to the BBM, projected onto an *s:p* plot as the yield locus in Figure (2.8b), predicts irreversible compressive volumetric strains for any paths moving outside the locus with either an increase of p, decrease of *s* or both. Increase of *p* path represents loading at constant suction, while decrease

of s path represents wetting at constant net stress. For the range within the yield surface, elastic behavior is predicted for both changes in suction and net mean stress. Any decrease or increase in suction within the elastic zone induces reversible swelling or shrinkage respectively. The irreversible strain induced by increase of p path will be equal to that induced by decrease of s path, which is related to the hardening parameter $P_{(s)}$. In other words the irreversible strains induced by both paths will be equivalent to compression along the normal compression line *NCL* at zero suction (fully saturated) from $P_{(1)}$ to $P_{(2)}$. The shape and position of the *LC* yield curve locus (in an *s-p* plot) and its evolution with the hardening parameter, $P_{(s)}$, can be derived from a set of compression curves for different suctions in a $v- p$ plot, as illustrated in Figure (2.8). By tracing the points of preconsolidation pressures through the compression curves, the (*s-p*) points at the intersections between the elastic path and the compression curves form the coordinates; the *LC* yield curve can be drawn.

Alonso et al. (1990) proposed that an increase in suction, for a given soil and applied load, can provide irreversible volumetric strains and this can be taken into account by a Suction Increase (SI) yield surface. Figure (2.8c) shows the SI yield surface as formulated by Alonso et al. (1990) assumed to correspond to the past maximum suction experienced by the sample. It is important to note that the linear relationship between v and ln s is only realistic over a range of suctions, depending on the degree of saturation (Jotisankasa, 2005). As the degree of saturation decreases and approaches the residual state, due to increase the suction, the specific volume will almost unchanged. Here the linear relationship in v - ln s space is invalid.

The original BBM (Alonso et al., 1990) can not represent the behavior of expansive soils due to strongly path-dependent. It is recognized that within the 'elastic zone' that proposed in the BBM (Alonso et al., 1990), significant irreversible strains can occur due to the accumulated shrinkage over a number of wetting-drying cycles. In order to model this aspect of expansive soils, Gens and Alonso, (1992) established the double-structure concept, as an extension to the original BBM by Alonso et al. (1990). This concept is based on an idealization that the structure of the clay soils can be divided into two levels, namely macro- and micro- structural levels. According to the formulation of Gens and Alonso (1992), the clay 'packets' or clusters are assumed to be fully saturated and their volume change can be characterized by the two yield surfaces (SI and SD) as shown in Figure (2.10). The behavior at the macro-structural level is then assumed to be characterized by the Loading-Collapse (LC) yield curve as in the original BBM.

Numerous works used BBM to interpret the unsaturated soil behavior (i.e., Cui and Delage, 1996; Romero, 1999; Gallipoli et al., 2002, and Alonso et al., 2005).

Cui and Delage (1996) carried out experimental programme with the osmotically controlled triaxial apparatus using unsaturated compacted an Aeolian silt. They concluded that the main features of the BBM model have been confirmed (i.e., *LC, λ(s), P(s)*, and the expansions of the yield curves in the *q-p* space as increases suction).

Romero (1999) investigated the effects of temperature and hydration/drying paths on reversible and irreversible features of volume change behavior (swell, collapse and shrinkage, thermal dilatation and contraction), under oedometer and isotropic stress state conditions. The study used two artificial prepared packings of Boom clay powder with a dominant aggregated fabric. He carried out different controlled suction oedometric and isotropic tests: compression, collapse, swelling, shrinkage, and constant volume tests. One more parameter was added to the general empirical equation of BBM for the value of maximum stiffness *λ(s)* to include the effect of the further intra-aggregate stiffness as below:

$$\lambda(s) = \lambda(0)\left[(1-r).e^{(-\beta.s)} + r - \gamma \ln\left(\frac{s}{s_{\min}}\right)\right] \tag{2.10}$$

where γ = a parameter that induces further stiffness in the 'intra-aggregate governing suction' zone; s_{min} = a reference suction value.

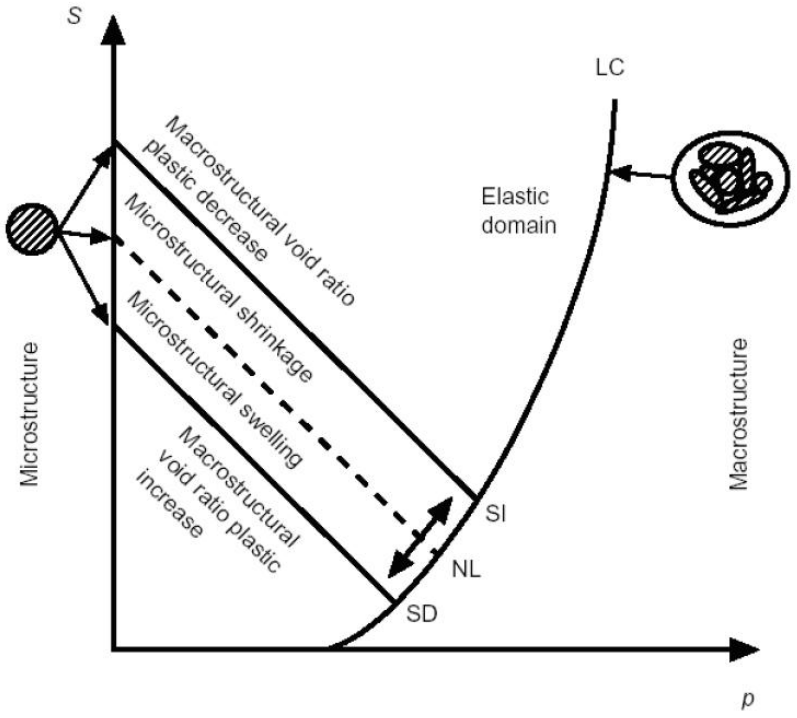

Figure 2.10 Graphical summary of the double-structure elasto-plastic, BBM, model for expansive soils (Lloret et al., 2003).

In additional, Romero (1999) reported that the value of the parameter (γ), as well as (r and β), depends on the density .The parameter (γ) increases with increasing density.

Gallipoli et al. (2002) presented the results of numerical modelling of pressure meter expansion in an unsaturated soil, using BBM of Alonso et al. (1990). They proposed a new relationship for degree of saturation or a conventional state surface expression for degree of saturation. Their results showed significant differences between the two sets of analyses, and thus provided an example of the practical significance of improved modelling of the variation of degree of saturation.

Many models presented later (i.e., Josa et al., 1992; Wheeler and Sivakumar, 1995; Delage and Graham, 1995; Alonso et al., 1999; Gallipoli, 2000; Cui et al., 2002; Wheeler et al., 2002; Blatz and Graham, 2003; and Sheng et al., 2008a and b) deal with the volume change-stress-suction relationships for unsaturated soil, based on the same basic assumptions and framework of BBM (Alonso et al., 1990 and Gens and Alonso, 1992). The models vary in detail, but are based on the consistent principle that the volume change behavior can be separated and additive the recoverable (elastic) and nonrecoverable (plastic) components due to both mechanical and suction effect defined by a state boundary surface.

Josa et al. (1992) presented a modified elasto-plastic model for unsaturated soils, which incorporates curved normal compression lines that initially diverge and then converge. For most practical applications, however, the range of net stress, p, of interest will be sufficiently limited that it will normally be acceptable to assume straight normal compression lines in the v-ln p plane that diverge or converge with increasing p. To include the latter possibility within the BBM, extend the applicability of the model, it is essential to consider the possibility of $\lambda(s)$ increasing with increasing suction ($r > 1$). When plotting data from experimental normal compression lines in the manner shown in Figure (2.11b), it will often be found that the various lines intersect at very different values of p. This is an indication that the behavior of the particular soil is not well predicted by the BBM and, irrespective of the values selected for the various model parameters, it will be very difficult to match correctly the locations of the normal compression lines for different values of suction (and hence the changing shape of the LC yield curve as it expands and the variation of collapse potential with stress level). A degree of judgement will be required to select an optimum set of parameter values, and then to decide whether the resulting match between experimental and predicted normal compression lines is sufficiently accurate for the purposes required.

Wheeler and Sivakumar (1995) suggested an elasto-plastic critical state model for unsaturated soil in terms of four state variables: mean net stress, p, deviator stress, q, suction,

s, and specific volume, *v*. The model was developed using data from a series of controlled suction triaxial tests on samples of compacted speswhite kaolin that perfumed by Sivakumar (1993). They assumed that the virgin compression takes place only when the applied the net stress, *p*, is greater than the point of maximum potential collapse. The gradient of the normal compression line, $\lambda(s)$, then increases with increasing suction Figure (2.11c). They stated that the pattern of swelling and collapse observed during wetting, the elastic-plastic compression behavior during isotropic loading and the increase of shear strength with suction were all related to the shape of the yield surface and the hardening law defined by the form of the state boundary.

Delage and Graham (1995) proposed constant-suction yield model. They suggested that plastic hardening caused by increases in mean stress, *p*, might cause microstructural rearrangements that would increase the yield suctions in tests where the suctions are increased, with the pressure being kept constant. They presented, as Alonso et al. (1990) and Wheeler and Sivakumar (1995), yield ellipses in constant-suction (*q*-*s*) plane.

Later Blatz and Graham (2003) examined a model which is one of a family of constant-suction yield models by Delage and Graham (1995) for triaxial stress fields of a compacted highly plastic sand–clay mixture. Three series of tests evaluated components of a possible elastic-plastic constitutive model for unsaturated stress–strain behavior. The tests studied the influence of suction on yield stress with external isotropic loading and the influence of suction on shear strength. The model presents three-dimensional surfaces relating five variables, mean stress, $p = (\sigma_1 + 2\sigma_3/3)$, deviator stress, $q = (\sigma_1 - \sigma_3)$, suction, s, specific volume, *v*, and water content, *w*. Figure (2.12) illustrates the conceptual model proposed (without detailed experimental evidence) by Delage and Graham (1995) based on earlier work by Alonso et al. (1990) and Wheeler and Sivakumar (1995). The model requires six parameters to define the *p*–*v*–*s* state boundary surface assuming isotropic behavior and no suction yielding.

Gallipoli (2000) presented an attempt to fit the experimental data of Wheeler and Sivakumar (1995) for compacted speswhite kaolin to the BBM. In this case, use of a value for $r > 1$ was clearly appropriate, but the best match that could be achieved between model predictions and experimental normal compression lines was still far from perfect.

Cui et al. (2002) proposed an elastic non-linear model based on experimental results. They carried out hydration, wetting–drying, and loading–unloading tests on dense compacted French FoCa7 clay. Some basic concepts were taken from the model of Gens and

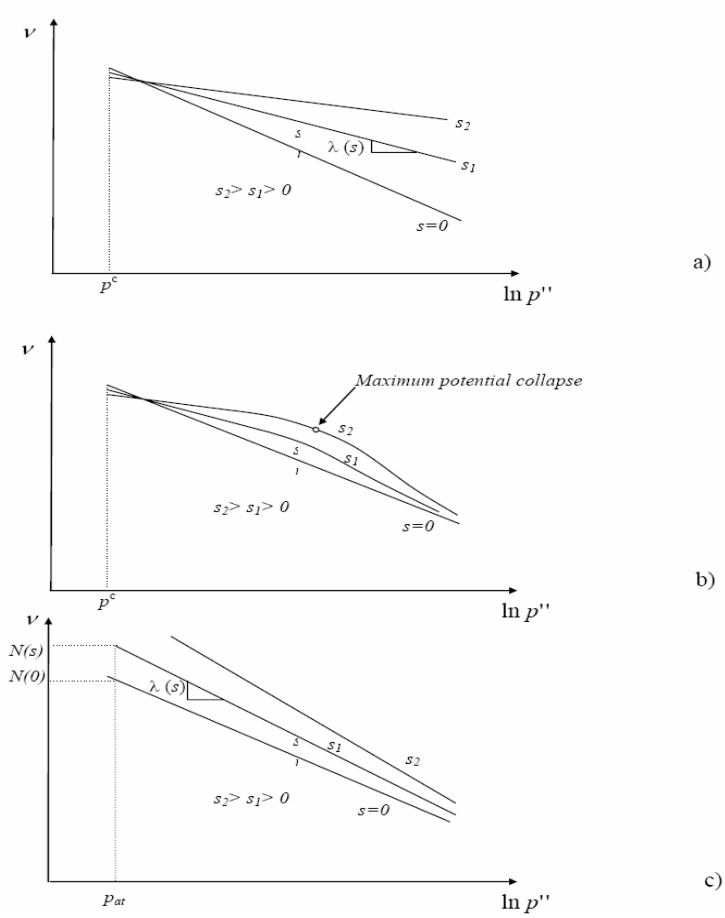

Figure 2.11. The normal compression lines (NCL's) assumed by: (a) Alonso et al. (1990); (b) Josa et al. (1992) and Georgiadis (2003); (c) Wheeler and Sivakumar (1995), (Jotisankasa, 2005).

Alonso (1992) with substantial changes due to the absence of the macropores in dense compacted clays. The model requires six parameters. An original feature of the model is the new concept of critical swelling curve, named CSC (Figure 2.13), which accounts for the effects of hydraulic–mechanical couplings on the volume change behavior of the clay.

Wheeler et al. (2002) reported that the main reason for any difficulty in fitting normal compression lines predicted by the BBM to corresponding experimental results is the constraint imposed by the assumption in the model that there is a stress p^c at which the yield curve becomes a straight vertical line in the *s-p* plane. In practice, they added, this is unlikely to be true. Consider the original model presented by Alonso et al. (1990), that $\lambda(s)$ decreases as suction increases *(r < 1),* as shown in Figure (2.8b and 2.11a). Although this means that the *LC* yield curve must get steeper in the *s-p* plane as it is traced back towards the origin (i.e. as $p_{(s)}$ decreases), for a real soil there is no reason that the curve must ever reduce to a vertical straight line. Wheeler et al. (2002) stated that the hypothesis in the BBM that there is a pressure p^c at which the yield curve is a straight vertical line is a major assumption of the model. This is not made entirely clear in the original paper by Alonso et al. (1990) and

appears not to have been fully appreciated by many subsequent users of the BBM. A consequence of this assumption is that, for a given soil, it may be impossible to match accurately the locations of the normal compression lines for different values of suction, and hence the shape of the *LC* yield curve as it expands and the variation of collapse compression with stress level.

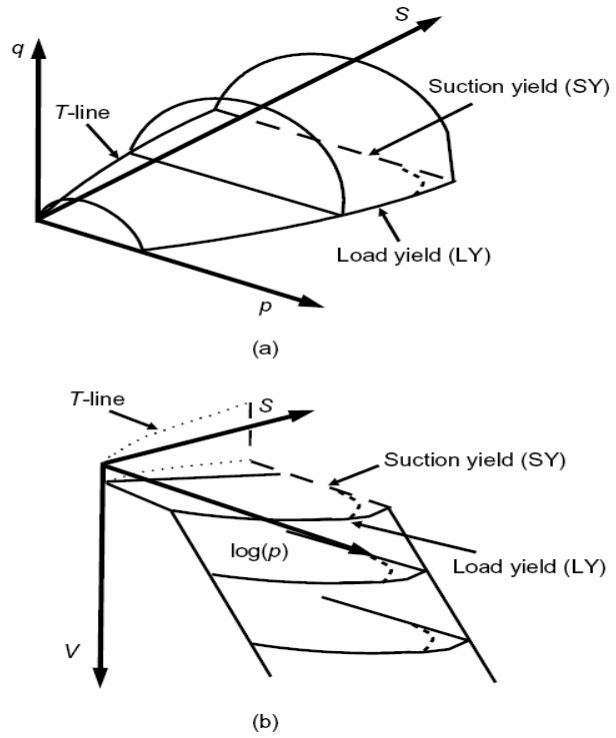

Figure 2.12 Conceptual elastic-plastic framework for unsaturated soils (Delage and Graham, 1995): (a) three-dimensional stress state space; (b) three-dimensional volume state space.

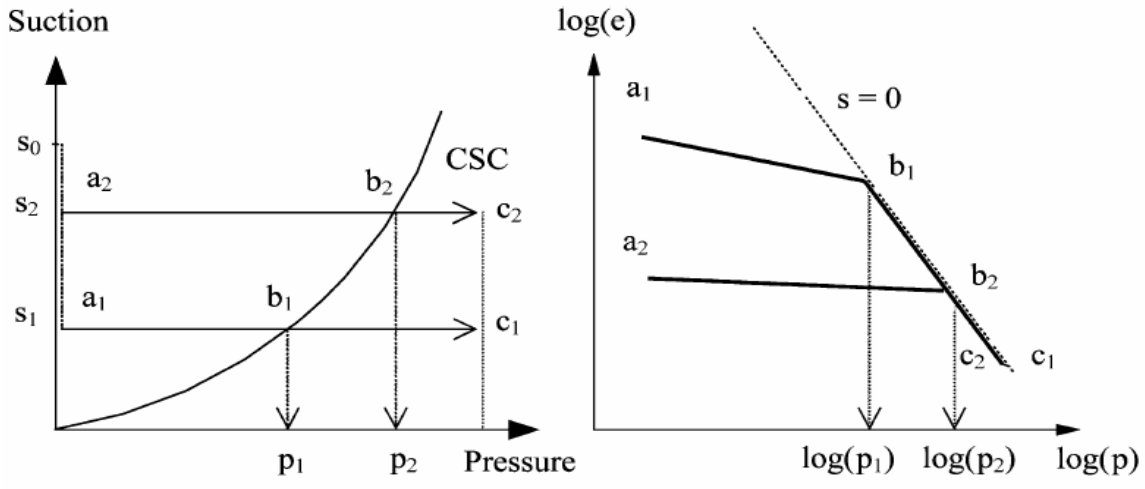

Figure 2.13 Operating model of Cui et al. (2002) during suction controlled compression tests.

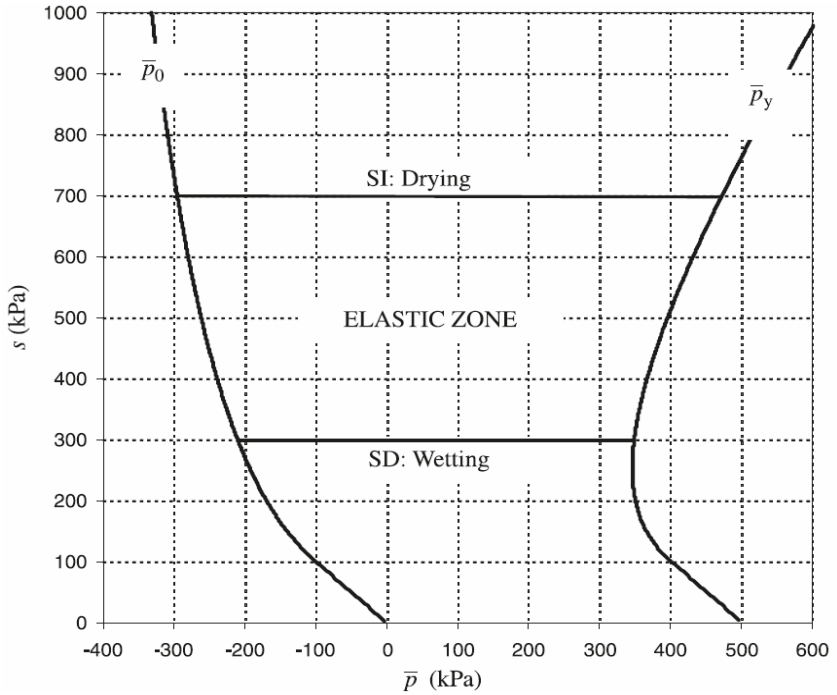

Figure 2.14 Initially yield surface includes the elastic zone and the drying and wetting surfaces using SFG model, (after Sheng et al. 2008a).

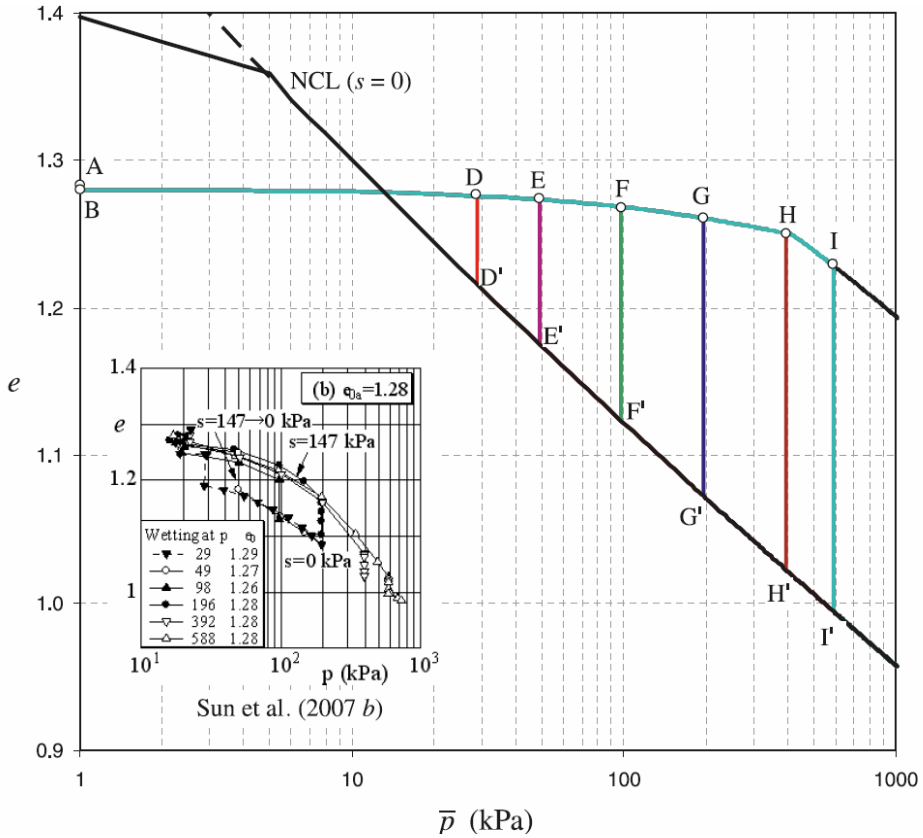

Figure 2.15 Predicted volume collapse during the final wetting paths using SFG model, experimental results of Sun et al. (2007) shown in the lower left corner, (Sheng et al., 2008a).

Georgiadis (2003) made some further refinements to the BBM. Nevertheless, both models assumed the existence of $p_{(s)}$, Figure (2.11b).

Jotisankasa (2005) investigated the validation of the assumption of the Gallipoli et al. (2003) model, which employs modified stress variables. He proposed a new formulation of the Loading Collapse surface to provide a better fit to the results of oedometer tests. The assumption involves the analysis of stabilizing force provided by the meniscus water lenses and the relationship between the numbers of these lenses with the degree of saturation. It appears to be valid for suctions less than 1500 kPa and for degrees of saturation greater than 30 %. For samples drier than these conditions, some modification is required to the model. This observation also applies to the application of the modified stress approach for shear behavior.

Sheng et al. (2008a) presented different approach to model the basic features of unsaturated volume change soil behavior under the framework of elastoplasticity using independent stress variables named SFG model. The SFG model used the modified Cam Clay (MCC) model (Roscoe and Burland, 1968) as the base model for saturated soils. The model assumes that λ_{vp} (the slope of NCL under constant suction) is constant, i. e., the unsaturated *NCL* is parallel to the saturated NCL. The model considers the effect of the hysteresis associated with the SWCC. The volumetric model is then used to derive the yield surface in suction-mean stress space. The yield stress, according to the SFG model, initially decreases with increasing suction below the saturation suction, in (p-s) space, but may increases or decreases, depending on the stress path, Figure (2.14). The experimental results, for compacted Pearl clay, of Sun et al. (2007) were used to simulate the initially unsaturated soil using the SFG model. Figure (2.15) shows the experimental and predicted results of void ratio changes during the wetting paths (collapse) at different net stresses for compacted Pearl clay (Sun et al., 2007) using the SFG model. Sheng et al. (2008a) attributed the discrepancy between the predicted and measured results to the Cam Clay elastoplasticity. Moreover, the simplicity nature of the constant the slope of saturated NCL (λ_{vp}) used in the proposal model can also be attributed for this discrepancy.

Sheng et al. (2008b) presented an overview of constitutive modelling and the numerical solution of the unsaturated soils problems (e. g., effective stress, shear strength, volume change, soil water characteristic curves and hysteresis problems). They stated some conclusions: *i)* The use of Bishop's effective stress for unsaturated soils can leads to a smooth transition between saturated and unsaturated states, but the effective stress formulations is carrying light weight, since the stress space is constantly changing with the material state due

to its definition can depend on material states and stress beside the experimental difficulties of such tests. *ii)* Most elasto-plastic models have embodied shear strength criteria, in which the friction angle ϕ^b is a function of suction and the air-entry value. *iii)* Hysteresis in the soil water characteristic curves can be presented in the framework of elasto-plasticity.

Beside the Barcelona basic model BBM several research groups are working to develop improved constitutive models of the volume change for unsaturated soil (i.e., Pereira and Fredlund, 2000; Al-Badran, 2001; Pham, 2005; Nagaraj et al, 2006a; Pham and Fredlund, 2005; Fredlund and Pham, 2006; Fredlund et al., 2007; Fredlund and Pham, 2007; Sun et al., 2007; and Kanazawa et al, 2009).The studies had been dealt with collapse behavior (i. e., Pereira and Fredlund, 2000; Al-Badran, 2001; Nagaraj et al, 2006a; Sun et al, 2007; Kanazawa et al, 2009) will be mentioned later in collapse section.

Fredlund and Pham proposed by several studies (i.e., Pham, 2005; Pham and Fredlund, 2005; Fredlund and Pham, 2006; Fredlund et al., 2007; and Fredlund and Pham, 2007) volume-mass constitutive model for unsaturated soils depending on independent stress variable. The proposed model is for isotropic loading condition only (i.e., ignoring the existence of the shear stress). The model is capable of predicting volume and water content, the hysteresis nature in the soil water characteristic curve, and the elastic and plastic deformations in the soil which include both swelling and collapsible behavior of an unsaturated soil, Figure (2.16).

The main assumptions were adopted for the proposed model are a particular pore in the soil has only two states: water-filled pore and the air-filled pore (which is assumed incompressible), and pores are deformed and water is absorbed and drained independently. According to the model, the yield stress of the soil structure surrounding a water-filled pore is considered to be maximum effective stress that ever acted on the pore. If a pore is dried under zero net mean stress, the yield stress of the pore is equal to the air-entry value of the pore. If a pore is dried under a constant net mean stress of, p, the yield stress of the pore can be calculated according to a proposed equation depending on the net mean stress and air-entry value and the applied suction. When a pore is filled with air, the pore is incompressible; therefore, yield stress of the soil structure surrounding the pore does not change with net mean stress and soil suction.

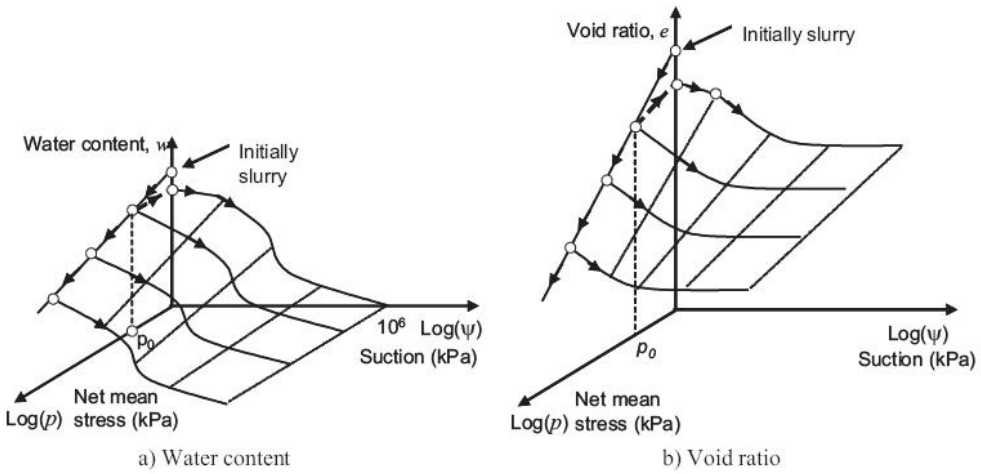

Figure 2.16 Schematic illustrations of the volume-mass constitutive surfaces of an initially slurred specimen that id dried under various constant net men stresses, (Fredlund and Pham, 2007).

2.4 Collapsibility of soils

2.4.1 General

A collapsible soil is defined as any unsaturated soil that goes through a radical rearrangement of particles and great loss of volume upon wetting with or without additional loading (Clemence and Finbarr, 1981). The collapse occurs when the dry or semi-dry (unsaturated) soil is soaked with water under a considerable load.

Cause of phenomenon.

In any case of collapse the addition of water to the soil is the triggering action (Dudley, 1970). According to (Dudley 1970; Barden, 1973; and Mitchell, 1993) appreciable collapse of soil requires the following three conditions:

1. An open (large void ratio), potentially unstable, unsaturated structure.
2. A high enough value of an applied or existing stress component to develop a metastable condition.
3. A strong soil bonding or cementing agent to stabilize intergranular contacts, with a reduction which, upon wetting will produce collapse.

Many cases studied have shown that these soils have a honeycomb structure of bulky-shaped grains with the grain held in place by some bonding material or force. The bonding material or force must be susceptible to removal or reduction by the arrival of additional water. When the support is removed, the grains are able to slide (shear) on one another moving into the vacant space (Dudley, 1970 and Clemence and Finbarr, 1981).

Therefore collapsible soils can be divided depending on the materials and the mode of formation of the soil mass into three types (Dudley, 1970; Barden, 1973; and Clemence and Finbarr, 1981):

A- Sand with some silt binder (strength due to capillary tension).

B- Clay particles in the bonds between the bulky or and silt grains (strength due to buttresses of clay).

C- Soil with cementing agent like (iron oxide, calcium sulfate and calcium carbonate).

2.4.2 The methods to calculate the collapse potential

In order to calculate the collapsibility of a soil, a method was proposed by Jennings and Knight, (1957) to compute the collapse potential named double oedometer test (*DOT*). In this method two identical samples are tested in an oedometer. One of them is tested in its natural water content and the other one in a pre-saturated condition. The difference between the two strain curves ($\Delta\varepsilon$) quantifies the amount of deformation that would occur at any stress level when soil is saturated. The collapse potential (*CP*) is then defined at a specific pressure as

$$CP \ \% = \frac{\Delta e}{1 + e_o} = \Delta \varepsilon = \frac{dl}{l_o} * 100 \ \% \qquad (2.10)$$

where Δe = the change in void ratio upon wetting; e_o = the initial void ratio; $d\,l$ = Change in height of sample from natural content to saturated sample; l_o = Original height of sample.

Knight (1963) proposed a laboratory test using a single odometer test (*SOT*). A single sample at natural water content is placed in the odometer and loaded progressively until the pressure reaches 200 kPa. At the end of this loading stage the sample is flooded with water and left for 24 hrs. During this time the volume change is recorded. The sample will then be loaded to a specific pressure.

Jennings and Knight (1975) suggested a description to the severity of collapse problems according to the collapse potential of soils as table (2.1).

Table (2.1): The severity of collapse potential (Jennings and Knight, 1975).

collapse potential, CP %	Severity of Problem
0-1	No problem.
1-5	Moderately Trouble.
5-10	Trouble.
10-20	Severe Trouble.
20	Very Severe Trouble.

The standard test method (ASTM D5333-96, 1998) determines the one-dimensional collapse potential of soils at vertical pressure equals the anticipated overburden pressure plus the weight of the structure.

2.4.3 Collapse behavior

Several studies dealt with the particular topics of volume change of soils, such as the collapsibility of soil (Jennings and Knight 1957; Kezdi, 1960; Jennings and Burland, 1962; Knight, 1963; Abeyesekera, 1977; Johnson and Lovell, 1979; Lawton et al., 1989; Lawton et al., 1992; Reznik, 1995; Pereira and Fredlund, 2000; Al-Badran, 2001; Rao and Revanasiddappa, 2002; Delage et al., 2005; Jotisankasa, 2005; Aziz et al., 2006; Nagaraj et al., 2006a; Sun et al,, 2007; and Kanazawa et al., 2009).

Kezdi (1960) referred to another method in which a single oedometer test is run with a sample initially at its natural water content. After a particular load increment (usually 300 kPa in Hungarian practice), water is added to the sample while the applied load is maintained constant. The resulting additional settlement is recorded and then further load increments are applied under soaked conditions. The potential volume change is expressed by relative collapse (i), which can be calculated similar to Equation (2.10).

Jennings and Burland (1962) studied the validity of the effective stress principle for a unsaturated soil. In every case when the unsaturated silt was soaked under constant applied load underwent additional settlement or "collapse". This occurred even when soaking took place at small values of applied load. They stated that the "collapse" is the reverse of the behavior predicted on the basis of the effective stress principle.

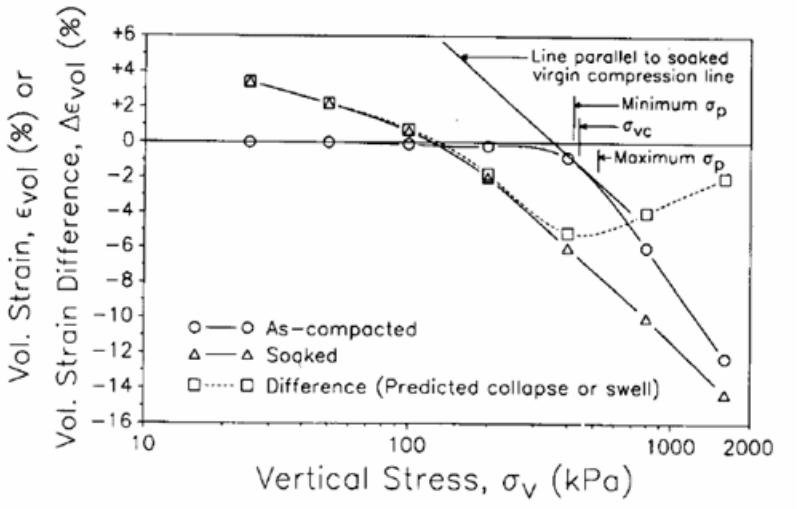

Figure 2.17 Typical double oedometer test results (Lawton et al., 1992).

Abeyesekera (1977) and Johnson and Lovell (1979) tested samples using standard triaxial equipment. Each sample was first consolidated under isotropic confining pressure, then saturated under high back pressure and the resulting total volume change determined (similar to the single oedometer test).

Lawton et al. (1989) showed that in case of wetting induced collapse in compacted soils, the collapse potential would be a maximum at some critical value of vertical stress, beyond which the collapse potential decrease with the increase in vertical stress. The same characteristics were found in the results of Lawton et al. (1992). This should be true for all soils although the critical vertical stress for certain conditions may be so large that it may not be found in usual laboratory stress ranges. The reduction in collapse potential at high stress levels is due to the densification and the increase in degree of saturation resulting from the applied stress. The maximum collapse potential occurs at a value of vertical stress approximately equal to the preconsolidation stress for the as-compacted soils. Figure (2.17) shows typical results of volume change due to wetting at different net applied stress by Lawton et al. (1992).

A double-triaxial test procedure similar to the double-oedometer test was developed by Lawton et al. (1991) to determine the wetting-induced collapse potential of soils subjected to anisotropic stress states. The difference between the equilibrium void ratios for the two specimens (as-compacted and wetted specimens) at each level of stress was used to calculate the volumetric strain difference. The volumetric strain difference at any level of stress is assumed to be approximately the same as the volumetric strain that would occur if the soil was loaded to that stress level in the as-compacted state, when soaked with water.

Reznik (1995) determined empirical relationships between oedometer deformation moduli for collapsible loessial soils deposited in the vicinity of the city of Odessa (Ukraine) and soil void ratios and degrees of saturation are introduced and analyzed.

Pereira and Fredlund (2000) experimentally investigated the collapse behavior of compacted silty sand (metastable-structured) residual soil using both a conventional oedometer cell (*Ko*-condition) and triaxial system (isotropic condition). They used best-fit modelling for predicting the volume change behavior of the compacted metastable-structured residual soil during Wetting-induced collapse. They classified the deformations during wetting process into three phases. The first phase of deformation occurs at high matric suction and is characterized by small volumetric deformation in collapsing soil and is term the ‘precollapse’ phase. The second phase of deformation occurs at intermediate value of matric suction and is characterized by significant volumetric deformation in collapsing soil and is term the ‘collapse’ phase. The third phase of deformation occurs at low matric suction and

requires no additional volumetric deformation in collapsing soil and is named the 'postcollapse' phase.

Al-Badran (2001) examined and reanalyzed previous published results and produced a different approach for better understanding volumetric deformation behavior l. A theoretical approach for collapse potential of unsaturated soil was also presented and applied to gypseous soils. The theoretical model, depending on S_r-lines, can estimate the collapse and the unsaturated compression curves for soils of any initial state (dry density and water content). The model was applied on the compacted clayey sand (Lawton et al., 1989 and Lawton et al., 1992) and additionally on gypseous soil. The study concluded, according to the S_r-lines concept, that the unsaturated soils exhibit a significant collapse potential when the wetting takes place under net stress more than the saturated preconsolidation stress. As net stress increases the collapse potential increases linearly with logarithmic net stress until reaches to the preconsolidation stress of unsaturated state, then the collapse potential starts decreasing. In other word, the maximum collapse potential happens under wetted net stress equals to the unsaturated preconsolidation stress. The conclusion is agreed with the observed behavior of soils by (Lawton et al., 1989; Lawton et al., 1992; and Wheeler and Sivakumar, 1995).

2.4.4 S_r-lines concept

As mentioned above, the S_r-lines concept was presented to describe and estimate the collapse and compression curves for unsaturated soils of any initial state. The main assumptions of S_r-lines concept of Al-Badran (2001), Figure (2.18) and (2.19), can be summarized as following:

1. For each degree of saturation a line parallel to the soaked compression curve can be drawn what represents the normal consolidated state. In other words, S_r-line is the NCL under constant degree of saturation condition. A family of such lines may be located by performing a double oedometer test (DOT) for single initial state (preferred high void ratio and low water content to pass a larger number of such lines). These lines will be called *S_r-lines*.
2. The compression *e-log* σ_v curve of an unsaturated soil changes its trend from an over consolidated soil, OC, to a normal consolidated soil, NC, when the degree of saturation of the soil becomes equal to that of the S_r -line passing over the point.
3. To predict all expected collapse potential, CP, values it is important to use a value for C_r. Here it is assumed that C_r is almost equal for all states. Hence only one rebound is enough to assess C_r. A support to this assumption may be found in (Jennings and Knight, 1957).

4. To unify all calculations a seating load of 1 kPa will be considered as the initial state corresponding to initial void ratio and water content.

Rao and Revanasiddappa (2002) investigated the collapse behavior of an unsaturated bonded (undisturbed) red soil, from India, referenced to tests on samples in an unbounded (remoulded) state. They used single collapse and double oedometer methods to find out the collapse strains and filter paper method to determine the matric suction of the bonded and unbounded specimens, and mercury intrusion porosimetry (MIP) was used to determine the pore size distribution. Analysis of the experimental results shows that bonding plays an important role in the collapse behavior of the unsaturated residual soil. The results showed that the unsaturated bonded and unbounded specimens exhibit either no or small volumetric strains at low consolidation pressure. As the consolidation pressure increases the unbounded specimen collapses significantly more than the bonded specimen. The tendency of the bonded specimen to collapse by a lesser amount than the unbounded specimen at the higher consolidation pressure implies that its soil structure is more resistant to wetting under load. They concluded that on wetting below the yield locus, the unsaturated bonded specimen did not swell, as its swelling pressure did not exceed the bond yield stress. On wetting beyond the yield locus, the unsaturated bonded specimen collapsed by an amount smaller than or equal to that of the unsaturated unbounded specimen, depending on the magnitude of the applied load. The preconsolidation pressure of the unsaturated unbounded specimen and the bond yield stress of the unsaturated bonded specimen were similar in magnitudes. Despite having similar void ratio and water content, the unbounded specimen was less porous than the bonded specimen, which imparted to it a high matric suction and large preconsolidation pressure.

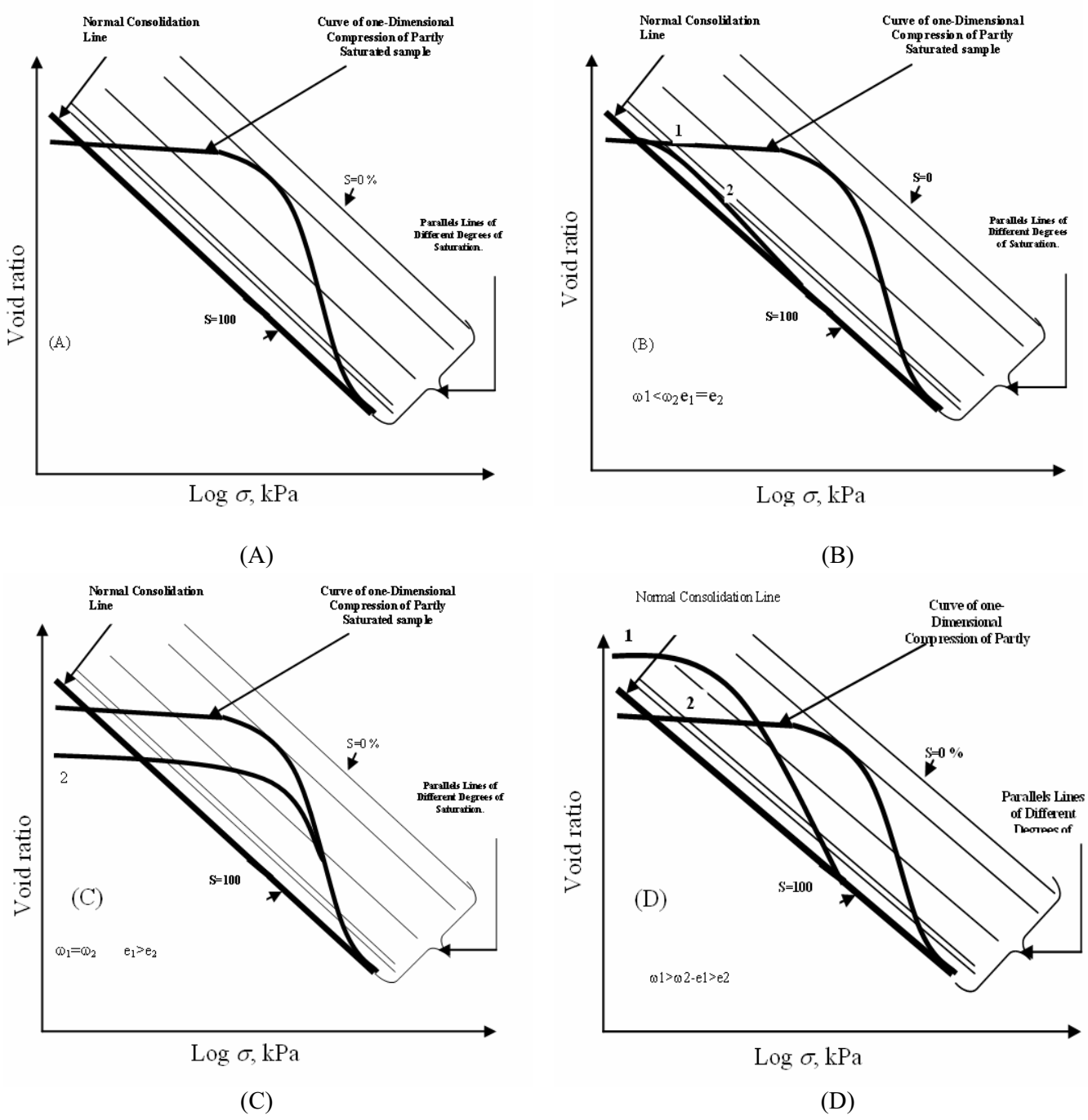

Fig.(2.18) Typical compression curves of unsaturated soil according to the S_r-lines concept (original study was *S*-lines): (A) Constant water content test (B) Constant initial void ratios and different water contents ;(C) Constant water content and variation initial void ratios ;(D) Combined effect of water content and void ratio (Al-Badran, 2001).

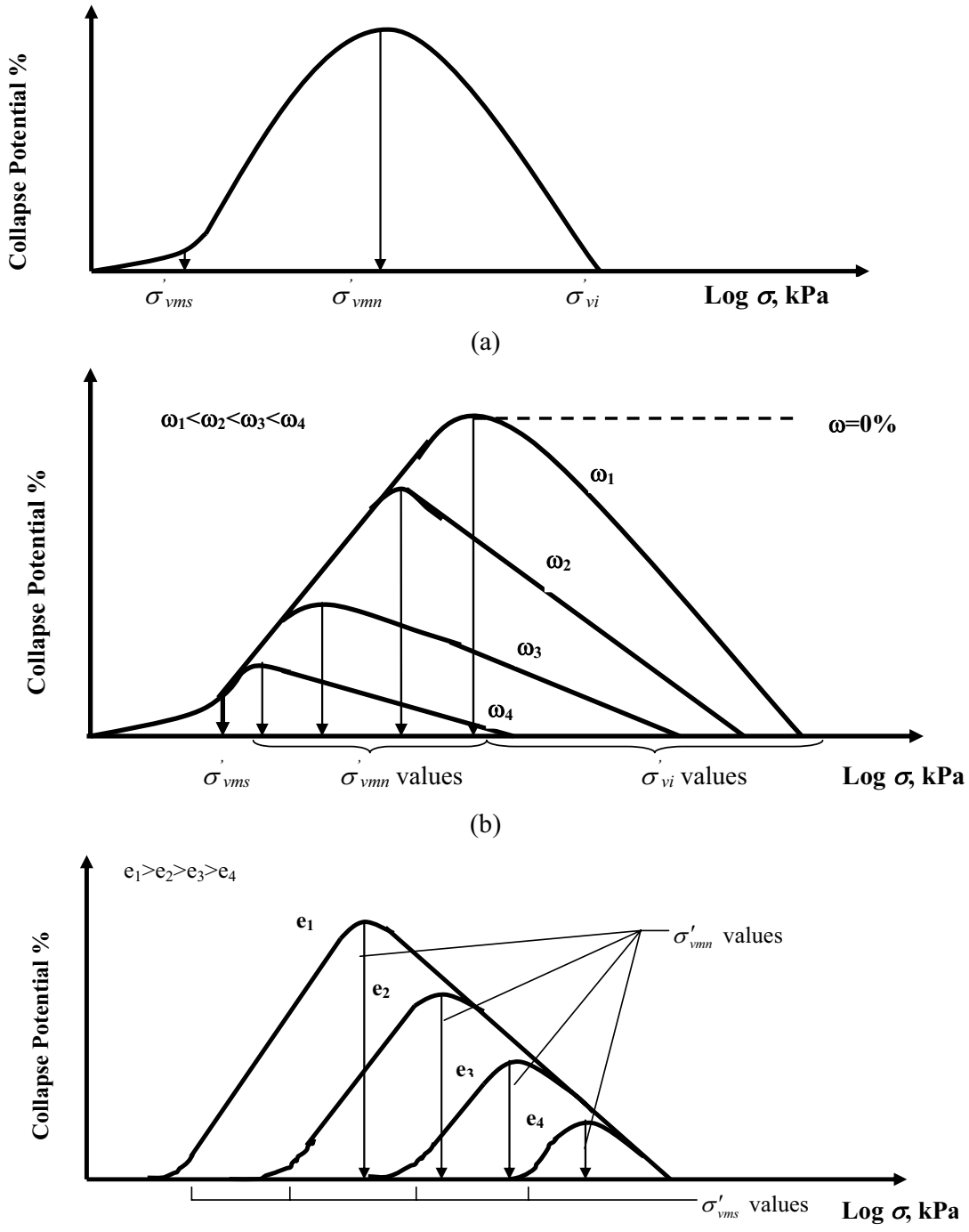

Figure 2.19-1 Typical curve of (collapse potential – log pressure) of unsaturated soil according to the S_r-lines concept: (a) Constant water content test (b) Constant initial void ratios and different water contents ; (c) Constant water content and variation initial void ratios ;(d) Combined effect of water content and void ratio. σ'_{vms} = preconsolidation stress of saturated state; σ'_{vmn} = preconsolidation stress of unsaturated (natural water content) state (Al-Badran, 2001).

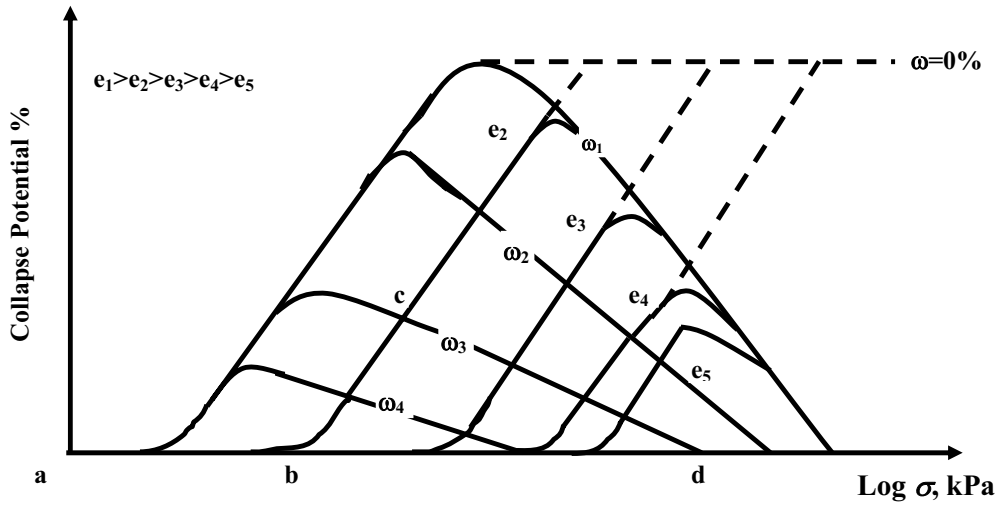

(d)

Figure 2.19-2 Typical curve of (collapse potential – log pressure) of unsaturated soil according to the S_r-lines concept: (a) Constant water content test (b) Constant initial void ratios and different water contents ; (c) Constant water content and variation initial void ratios ;(d) Combined effect of water content and void ratio. σ'_{vms} = preconsolidation stress of saturated state; σ'_{vmn} = preconsolidation stress of unsaturated (natural water content) state. (Al-Badran, 2001).

Khalili et al. (2004) stated that, by investigating some data from literature, with applying suction most of the results showed a normally consolidated isotropic compression until the point of air-entry. Beyond the point of air-entry, the samples enter the elastic region, marked by a strong reduction in the volume change with decreasing suction, a characteristic feature in the behavior of collapsible unsaturated soils. Upon wetting (i.e., suction unloading), the samples undergo elastic dilatancy, with little or no hysteresis, until the suction attains the air-entry value. At suction values below the air-entry, wetting results in stress paths increasingly entering the saturated elastic region, yielding a greater level of elastic dilatancy than in the unsaturated region.

Jotisankasa (2005) investigated the collapse behavior of compacted silty clay using a developed suction-controlled triaxial apparatus that incorporates the tensiometer at Imperial College. This apparatus was used to investigate the collapse, shear, and water-retention behaviors of a loosely compacted mixture of 70 % silt, 20 % kaolin, and 10 % London clay. In addition, other experiments carried out included the suction-controlled oedometer, unconfined drying/wetting tests and a fabric study using a petrological microscope in order to gain a more complete understanding of the behavior. The influence of fabrics induced by differing compaction properties was also examined in relation to the water retention and collapse behavior. Two main types of constitutive elasto-plastic models were used to describe the collapse behavior of unsaturated soils to fit the experimental results: first one is related to

those using the stress variables (two independent stress variables approach) of Wheeler and Sivakumar (1995) and second one is related to the models that using modified stresses (effective stress approach) of Gallipoli et al. (2003b). The main assumption regarding the uniqueness of the Loading-Collapse surface was validated as identified by results of loading and wetting tests. The model employing the modified stress approach could not reproduce accurately the test results at suctions greater than about 3000 kPa. The evidence for critical states for compressive shearing has also been examined using stress-dilatancy plots. The concept of soil-water-retention surface has been validated and extended to cover the influence of different components of strain.

Delage et al. (2005) studied collapse susceptibility in the light of microstructure observation, examined the dependence of collapse to water content changes, and investigated the validity of various existing collapse criteria. The collapse susceptibility of samples was conducted for samples extracted from a profile located neer Paris, by using the single and double oedometer methods. The scanning electron microscope (SEM) and mercury intrusion porosimetry (MIP) were carried out to investigate the microstructure and the pore size distribution of soil. They observed that the collapsibility appeared to be significantly sensitive to changes in water content with collapse volume decrease higher than 5 % at water contents smaller than 12%. They concluded that, by examining the SEM results, a porous microstructure with heterogeneous scattering of clay aggregations that filled the inter-grains pores and worked as a linking agent between the grains in some areas. In areas with no clay, they observed sharp edge angular silt grains (15 to 30 μm in diameter) with large inter-grains pores. These pores located in the areas with no clay probably significantly contribute to collapse volume decrease. MIP results pointed out the changes in inter-grains pores that occurred during collapse and showed that the smaller pores inside the clay aggregations were not affected. The structure after collapse structure is apparently more organised with a well graded pore size distribution curve.

Nagaraj et al. (2006a and b) showed that, according to the microstructural consideration, for each soil all unsaturated normal consolidated compression data (compressed from loose state) can be normalized in one line by multiplying void ratio with the square root of the degree of saturation. They reported that the change in microstructure of unsaturated soil, at constant water content, due to compression under applied net pressure (p-u_a) or applied suction (u_a–u_w) is due to change in the radius of air-water interface in the micropore enclosed by saturated clay clusters. This concomitantly alters the inter-cluster physico-chemical net repulsive forces. Consequently the clay attains a new equilibrium state. To represent these changes, the parameter $w/\sqrt{S_r}$ (or $e\sqrt{S_r}$) is a convenient parameter to account

for the effects of degree of saturation in the range of 40 to 90 percent. Normalization of data points due to compression by (p-u_a) and their inundation disposition, by the void ratio at liquid limit (e_L), would render this state parameter independent of soil properties. This generalized state parameter, [(e/e$_L$) $\sqrt{S_r}$] bears a direct relationship with stress state variables, (p-u_a) and (u_a-u_w). They added that the distinct advantage of the proposed state parameter approach by using the degree of saturation as a distinct parameter is that the measurement of matric suction at varies stages would tend to be optional.

2.4.5 Microstructure consideration of Nagaraj et al. (2006a and b)

The examinations of pore size distribution and permeability data of saturated clays infer that micro-fabric is made up of clay particle aggregates enclosing capillary micro pores as large as 5000 angstroms (Nagaraj et al., 1990; Mitchell, 1993; and Nagaraj and Miura, 2001). If the clays exhibit interacting particulate behavior then the effective stress relations for saturated clays with interparticle forces and soil state variables possible are (Nagaraj et al., 1994):

$$\sigma' = \sigma - u = R - A = f(e, e_L) \tag{2.11}$$

R-A is the reaction to conventional effective stress which is characterized by the equilibrium state which is a function of e and e_L. This resulting micro-fabric model consists of aggregated clay particles with inter –cluster interactions consequently enclosing capillary pore (filled with water or air), Figure (2.20). As the water admixed clay is further incrementally statically compacted, since there is no immediate access to water, the radius 'R' of the area of the pore, changes with the incremental total pressure (p) to which soil is subjected to;

$$R = f(p) \tag{2.12}$$

Degree of saturation, S_r is given by

$$S_r = \frac{Volume\,of\ water}{Volume\ of\ voids} = \frac{v_w}{v_v} = \frac{v_w}{n\pi R^2 l} \tag{2.13}$$

where l = length of cylindrical pore ; n = number of capillary pores enclosed due to number of clusters enclosed by a capillary pore.

For constant water content during the change in equilibrium state upon loading with the pore length (l) remaining constant, the degree of saturation is;

$$S_r = \frac{k_1}{R^2} \quad or \quad R = \frac{k_1'}{\sqrt{S_r}} \tag{2.14}$$

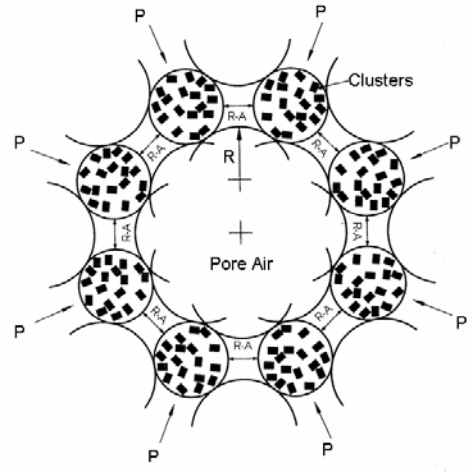

Figure 2.20 Equilibrium states in unsaturated soils "idealized microfabric model" (Nagaraj et al., 2006a).

where $k_1 = \frac{v_w}{n\Pi l} =$ constant; k_1' = a constant = $\sqrt{k_1}$.

On substituting (2.14) in equation (2.12),

$$\frac{k'_1}{\sqrt{S_r}} = f(p) \tag{2.15}$$

In an unsaturated soil compression under externally applied load occurs due to expulsion of air with water content being constant. Hence equation can be represented as

$$\frac{w}{\sqrt{S_r}} = f(p) \tag{2.16}$$

For the condition of constant water content, if there is a change in applied pressure, the radius of air-water interface changes, concomitantly altering the physico-chemical net repulsive forces. Consequently the soil attains a new equilibrium state. To represent these changes, the parameter $w / \sqrt{S_r}$ (or $e/\sqrt{S_r}$ obtained from $G\,w = S_r\,e$) is a convenient parameter to account for the effects pore water tension through the degree of saturation in the range of 40 to 90 percent.

Figure (2.21) shows the compression data of dry Black Cotton soil (*LL* = 84 %) mixed with water content of 35 % and compressed from its loose state and its corresponding collapse upon inundation along with its degree of saturation shown in parenthesis. It is interesting to note that the two compression paths reduce to one path upon considering $e/\sqrt{S_r}$ in place of *e*. Three such soils from their dry state (Red earth, *LL* = 50 %, Black Cotton soil *LL* = 84 % Brown soil *LL* = 62 %) admixed with different initial water contents and monotonically compressed up to 1000 kPa show unique paths on $e/\sqrt{S_r}$ versus *p* plots (Figure 2.22). Data points along the equilibrium paths, both at constant water content and inundation conditions,

(Figure 2.23) when normalized with respect to their respective e_L ($e_L = w\ G_s$) values, collapse on to a narrow band. This consideration of liquid limit values subdue the type of clay to result in a generalized constitutive relation between generalized state parameter $[(e/e_L)\sqrt{S_r}]$, independent of clay properties, and equilibrium pressure ($p - u_a$) of the form:

$$\left\{\frac{e}{e_L}\right\}\sqrt{S_r} = 1.00 - 0.21 \log\ (P - u_a) \tag{2.17}$$

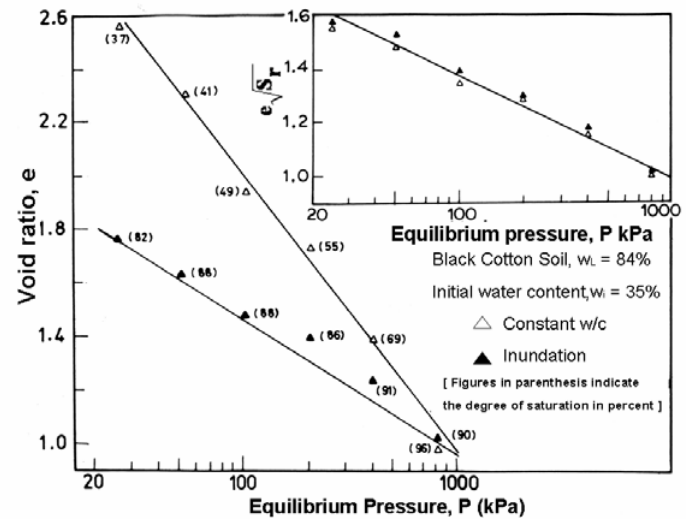

Fig. 2 21 Compression paths of unsaturated soil and its inundated states and its generalized path for Black Cotton soil (Nagaraj et al., 2006a).

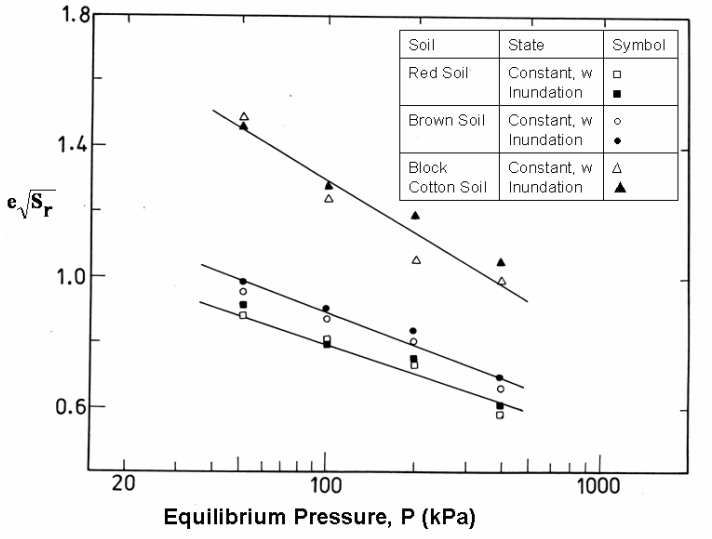

Fig. 2.22 Equilibrium constant water content paths and their inundated condition of three soils, date from Nagaraj, et al. (1988),(Nagaraj et al., 2006a).

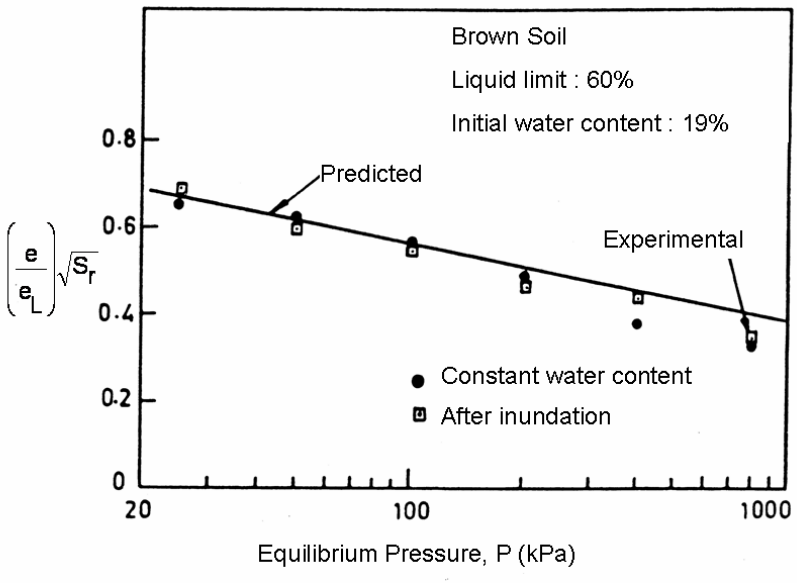

Fig. 2.23 Validation of Generalized State Parameter –pressure relation, date from Nagaraj, et al. (1988),(Nagaraj et al., 2006a).

Equation (2.17) has correlation coefficient of 0.940. The data points along the compression path of unsaturated Brown soil with altogether different initial water content at different applied equilibrium pressure levels and the corresponding inundated locations are very close to the predicted path using the generalized constitutive relation.

Aziz et al. (2006) examined the collapsibility and volume change behavior specifically of an unsaturated residual soil under various levels of applied matric suction and net mean stress. The volume change of the soil was found to be sensitive to both the applied matric suction and net mean stress. The results showed that there is an apparent unique relationship between the void ratio, matric suction and net mean stress. The unique relationship between void ratio and matric suction was observed when there is collapse (decrease in void ratio) due to the reduction in applied matric suction at constant net mean stress. This decrease in void ratio is believed to be due to loss of additional rigidity provided by the suction to the soil structure as the suction is suddenly reduced. At a similar net mean stress level, the void ratio of the soil subjected to matric suction of even as low as 25 kPa appear to have marked difference from soil not subjected to matric suction.

Sun et al. (2007) presented the results of a series of controlled-suction triaxial tests on the collapse behavior (includes volume changes and hydraulic characteristic) of an unsaturated compacted Pearl clay with different initial dry densities and suction. They stated that the wetting-caused collapse mainly depends on the mean net stress and the initial density.

SWCC in term of suction and degree of saturation shifts upwards with increasing density. Moreover, they showed that the collapse occurs mainly in a middle range of suction levels, and that the wetting-caused volume decrease is a companied by an increase in the degree of saturation. The same observation was found by Pereira and Fredlund (2002).

Kanazawa et al. (2009) suggested a constitutive model to predict the elasto-plastic behavior of unsaturated soils, which can express the volume changes and hydraulic characteristic behavior of unsaturated soil. The model uses the effective degree of saturation, *Se*, as a parameter related to stiffness. In addition, they found that all compression lines of normal consolidated state with various applied suction that follow the contours of the degree of saturation are parallel, (Figure 2.24). They used Cam-clay model to format the yield function of unsaturated soil (Equations 2.18 and 2.19) by using an empirical equation for value of the ratio of the yield stress at unsaturated state to yield stress at saturated state, ξ, Equation (2.20) :

$$f(\sigma', C, \varepsilon_v^p) = MDLn\ \frac{p'}{\xi P'_{sat}} + D\frac{q}{P'} - \varepsilon^p{}_v = 0 \tag{2.18}$$

$$\xi = \xi(C) \tag{2.19}$$

$$\text{where} \quad \xi = 1 \quad \text{when} \quad C = C_{sat}$$

$$\xi = a \quad \text{when} \quad C = C_{\max}$$

$$\xi = \exp\left((1 - S_e)^n \ln a\right) \tag{2.20}$$

where: The value of C = a parameter relating to soil moisture; $C_{sa\,t}$= a parameter corresponds to saturation; $\varepsilon^p{}_v$ = the plastic volumetric strain, p' = the mean effective stress, q = the shear stress, M = the ratio q/p' on critical state; D = the dilatancy coefficient; Se = the effective

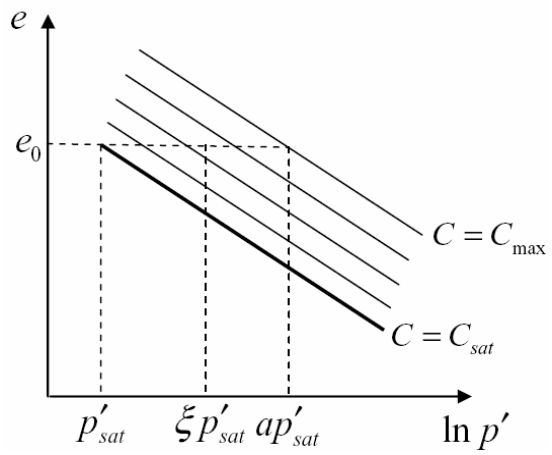

Figure 2.24 Conceptual compression lines of unsaturated soil (Kanazawa et al., 2009).

degree of saturation; n = shaping parameter; a = the ratio of the maximum yield stress at unsaturated state to yield stress at saturated state, p'_{sat}.

2.5 Unsaturated volume change behavior: experimental tests

Several types of volume change tests are presented for unsaturated soils, for one-dimensional and isotropic compression, such as; constant net stress test, constant suction test, constant water content test, and constant volume tests.

The difference in the initial condition and type of the test leads to the variation in the outcome of volume change. The details of performing the constant net stress and suction tests will explain later in Chapter 4.

2.5.1 Constant net stress test

The constant net stress (σ- u_a) test can be carried out by increasing the suction (drying) or decreasing the suction (wetting). The increase in suction can be applied starting from unsaturated and/or saturated conditions. The decrease in suction can be applied for compacted and/or loosely initial state of unsaturated soils. As suction decreases (wetting) swelling is expected for initially compacted state, while collapse is expected in case of initially loose state (Lawton et al., 1989; Lawton et al., 1992; and Al-Badran, 2001). The net stress during decreasing the suction is an additional considerable factor that controls the swelling and collapse phenomena beside the initial state. Al-Badran (2001) reported that the considerable collapse is expected if the wetting takes place at net stress more than the saturated preconsolidation stress, while the maximum collapse is expected when the wetting happens at net stress equals to the unsaturated preconsolidation stress. The same characteristics were found in the results of (Lawton et al., 1989 and Lawton et al., 1992).

In case of swelling, by decreasing the suction, the swelling strain and swell pressure depend on the stress path. Gens and Alonso, (1992) gave a good example for this case by using the results of Brackley (1975) tests, (Figure 2.25). Brackley (1975) performed three tests to determine swelling at 50 kPa: (1) free swell (wetting) from the beginning and then loading to the specific load, (2) loading to the specific load and then swell (wetting) at this load, and (3) saturation (wetting) at constant volume and then unloading to the specific load. The first test gives the maximum swelling (d-a in Figure 2.25), the third test shows the smallest swelling (d-c in Figure 2.25), and the second test gives an intermediate swelling value (d-b in Figure 2.25).

In cases of collapse and swelling the addition of water to the soil (decreasing of the suction) is the triggering action (Dudley, 1970). Moreover, in both cases the volume (or void

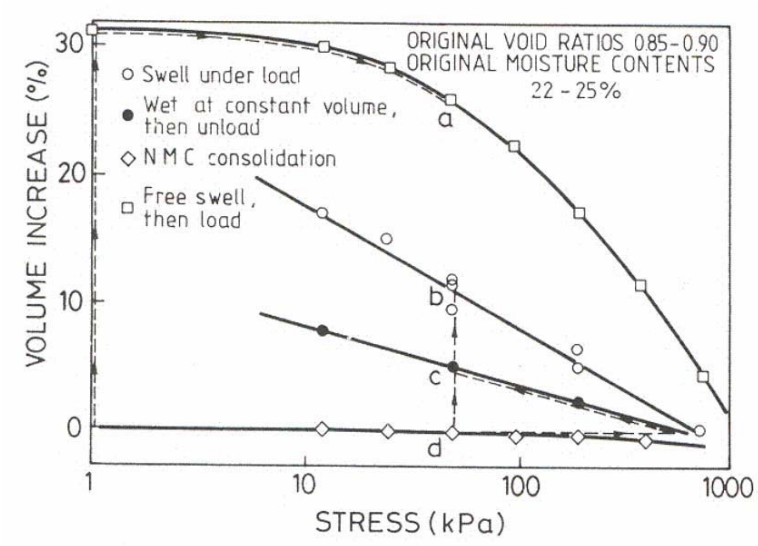

Figure 2.25 Procedures for swell prediction, NMC is the natural moisture content (Brackley, 1975).

ratio) of soil in the unsaturated state (before wetting) is changed to be sits mostly on the saturated normal consolidation line, NCL, after wetting. Therefore, the main factor that sets the type (collapse or swelling) and the amount of the deformation is the location of void ratio before the wetting with respect to the saturated NCL (in net vertical stress vs. void ration relationship).

In case of increasing the suction (drying) for initially saturated soils, slurry or compacted, the resulted curve is named the soil water characteristic curve (SWCC), while in case of initial unsaturated state soils, the curve will identify as soil-water retention curve (SWRC).

2.5.2 Soil water characteristic curve (SWCC)

The soil water characteristic curve (SWCC) is very important to estimate the hydromechanical behavior of unsaturated soils such as volume change, shear strength and hydraulic conductivity (Fredlund and Rahardjo, 1993 and Fredlund, 2000). The SWCC describes the relationship between suction and the corresponding state of wetness (i.e., gravimetric, volumetric water content, and degree of saturation-suction relationships) for specimen full dried first from saturated condition (drying path) and then wetting the specimen to full saturated condition (wetting path) under any loading condition (Figure 2.26). The increasing of the suction starting from saturated condition can be performed under zero net applied stress (unconfined) or under any specific net stress (isotropic or one-dimensional compression), Figure (2.16). The volume of saturated soil reduces significantly as the suction

increases until reaching to the air-entry value suction s_{aev} (i. e., saturation zone). The amount of this volume reduction decreases with increasing the value of the constant net stress. Then, with increasing the suction, the reduction in volume will be very small comparison with the first stage, (Figure 2.16b). The reduction of water content continues as the suction increases following a drying path (i.e., before and after S_{aev}), Figure (2.16a). The reverse (i.e., wetting path) is the process where the water content of soil increases with decreasing the suction. Usually, the drying path is ended to oven-dried condition. The suction corresponding to the oven-dried condition is about 1000000 kPa. Croney and Coleman (1961) found that the total suction at zero water content for a variety of soils was slightly below 1000000 kPa. Fredlund and Rahardjo (1993) also found from the gravimetric water content versus suction relationship for various sand and clay soils that at zero water content the suction approaches a value of approximately 980000 kPa. This value is also supported by thermodynamic considerations (Richards, 1965).

The reduction of volume with increasing the suction before air-entry value suction s_{aev} relates to increasing of the isotropic effective stress according to Equation (2.2) with $\chi = 1$, and this means that the increase in suction in this case has similar effect as the increase in isotropic effective stress, and the amount of volume change can be calculate as in case of the saturated condition, but according to the new effective stress as Equation (2.2). When the suction overtakes the air-entry value, s_{aev}, the effect of the suction on the reduction in volume will be very small, because even when the effective stress increases with increasing the suction (Equation 2.2 with $\chi < 1$ for unsaturation condition) but the soil will be more stiff, hardening), (Kohgo et al., 1993a and Khalili and Khabbaz, 1998). Vesga (2008) reported that in case of unconfined condition of Kaolinite clay there is small amount of increasing in volume after increasing the suction more than the residual suction. The increase in suction, for soils have initial suction more than the air-entry value, s_{aev}, almost dose not lead to a significant volume change, Figure (2.27).

The SWCC is influenced by type of soil, texture, and mineralogy. The soil behavior can be indicated by the consistency limits, i.e., Atterberg limits, (Sridharan and Nagaraj, 1999). Atterberg limits indicate variation of the soil properties with water content. The value of total suction at any water content can be correlated to the total suction at a reference state. Nelson and Miller (1992) used liquid and plastic limits as the reference states and reported that at the liquid limit of clays had suction in the range between 0.5 kPa and 1 kPa. At the plastic limit, suction in the clay was about 250 kPa. Fleureau et al. (2002) presented a correlation between the liquid limit and slope of void ratio versus suction and

liquid limit and slope of water content versus suction for wetting path. Marinho (2005) used liquid limit of clay (i.e., higher than 25 %) combined with suction capacity (i.e., reduction in water content over one logarithmic scale) and stress history to predict SWCC.

Specimens compacted at different water contents result in different fabric of the soil (Lambe, 1979; Gens et al., 1995; and Delage and Graham, 1996). Vanapalli et al. (1999)

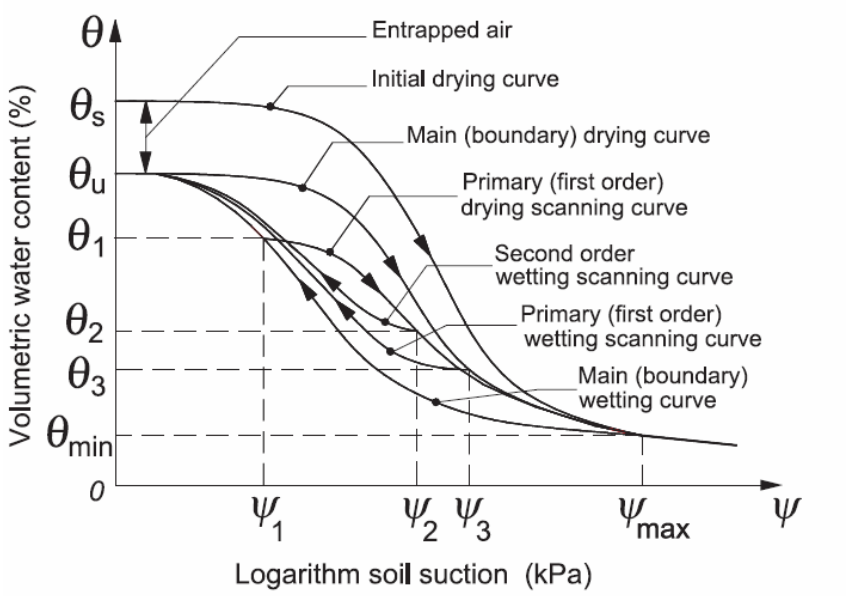

Figure 2.26 Main drying, wetting, and hysteresis paths of soil water characteristic curve, SWCC (Pham et al., 2005).

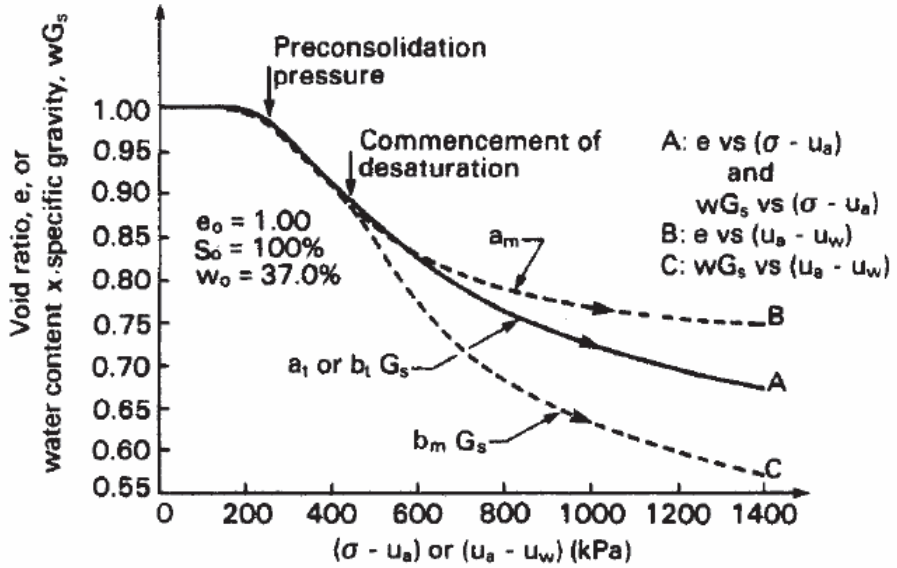

Figure 2.27 Relationship among volumetric deformation moduli for an initially saturated soil (Fredlund and Rahardjo, 1993).

stated that there is a significant difference in the SWCC of clay till compacted at different water content (i.e., at wet of optimum, optimum, and dry of optimum) using the same compaction energy. They cited that the SWCC appears to be approximately the same over suction ranging from 20000-1000000 kPa for specimens tested with different initial water content. Fleureau et al. (2002) found that drying path of specimen from slurry represent the highest capability to retain water or can be used as main drying curve of a soil. They also reported that the wetting path of specimen compacted at optimum water content was almost the same as wetting path of specimen from slurry.

Delage et al. (1998) investigated the water retention and swelling properties of the FoCa7 clay with controlled suction and zero applied stress. They found reversible responses of suction cycles, in terms of water content and volume change. During these changes, it was observed that the air volume remained constant. They reported that the reversibility is due to the predominant role of a saturated microstructural level, strongly influenced by the physicochemical bonds existing between water and the active clay minerals.

Al-Mukhtar et al. (1999) investigated the effect of axial compaction stress on the drying curve of compacted smectite. It was found that the drying curve, in term of water content for relative humidity (*RH*) range from 100 % to 98 % , for specimen having lower axial stress was placed over that of specimen having higher axial stress. For *RH* less than 98 % (or total suction higher than 2700 kPa), the drying curves of specimens were similar. Al-Mukhtar et al. (1999) stated that for *RH* ranging from 0 to 98 %, suction is controlled by micro-pores; their size and distribution are not influenced by the compaction process, while suction is controlled by macro-pores at $RH > 98$ %.

Romero (1999) carried out compaction curves and determined the contour lines of equal suction, Figure (2.28). He observed that suction increases as water content reduces, being the high suction value lines with values 3 MPa nearly vertical, which indicates that at water content values less than approximately 15 %, increasing by compaction the dry unite weight (or in an equivalent form increasing the degree of saturation) does not change significantly the initial total suction value. However, the results of (Delage and Graham, 1995; Gens et al., 1995; Li, 1995; Romero, 1999 as Figure 2.28; Tarantino and Tombolato, 2005; Agus, 2005 as Figure 2.29; and Ferrari, 2007) showed that for the dry side of compaction curve the density has no effect on the suction water content relationship for fine-grained soils. Romero (1999) attributed this behavior to the effects of loading mechanism on the macroporosity that does not contain free water, since at low moisture content levels (less than the optimum moisture content for each compaction effort), water is mainly absorbed or contained in intra-aggregate scale. In which, the degree of saturation changes are associated

with macroporosity changes under constant intra-aggregate water content. Romero (1999) added more, that as matric suction values approach the saturation line, the loading mechanism affects inter-aggregate water and the contour lines of equal suction try to incline in order to converge to the limit condition of matric suction equals to zero at full saturation condition (S_r = 100 %). Romero (1999) concluded that the drying-wetting path, after main wetting, shows a remarkable plastic shrinkage that also increases at higher temperatures. Maximum shrinkage and water content changes appear when matric suction is increased over the air-entry value of the packing, which is associated with the suction increase SI yield locus as defined by Alonso et al, (1990).

Agus (2005) studied the drying-wetting behavior of a heavily compacted 100, 70/30, 50/50, and 30/70 bentonite-sand mixtures. Different initial dry densities were prepared with water content of 9 %, and total suction of 22700 kPa. The specimens were saturated (wetted) to full saturation in two conditions (i.e., under seating load of 7 kPa and constant volume condition) before drying process. It was found that the drying-wetting curves of the as-prepared specimen used were reversible as long as the drying and wetting paths do not ever touch the boundaries. He indicated that the triggering action in the suction versus water content relationship of bentonite-sand mixture is the bentonite water content (Figure 2.29). He stated that the difference in the total suction for different mixtures (or bentonite contents) at the same mixture water content is believed to be due to the difference in the sum of osmotic suction and sportive forces, whereas surface tension or capillary action has an insignificant influence.

Arifin (2008) presented an experimental study on the temperature effects on the hydro-mechanical behavior of compacted bentonite and bentonite-sand mixtures. He concluded that at given water content, increase in temperature results in decreasing total suction. The reduction of the total suction is due to reduction in the capillary component of total suction for total suction less than 2000 kPa. For total suction higher than 2000 kPa, the reduction in total suction is due to reduction of capillary component and/or hydration force.

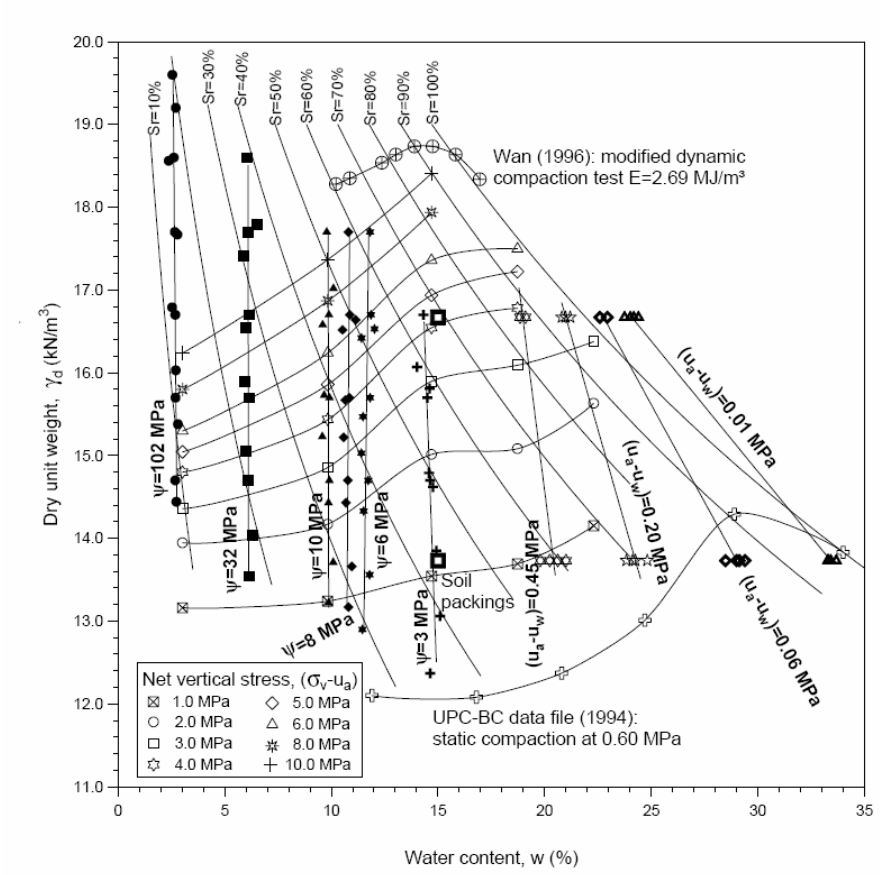

Figure 2.28 Static compaction curves with contours of equal suction (Romero, 1999).

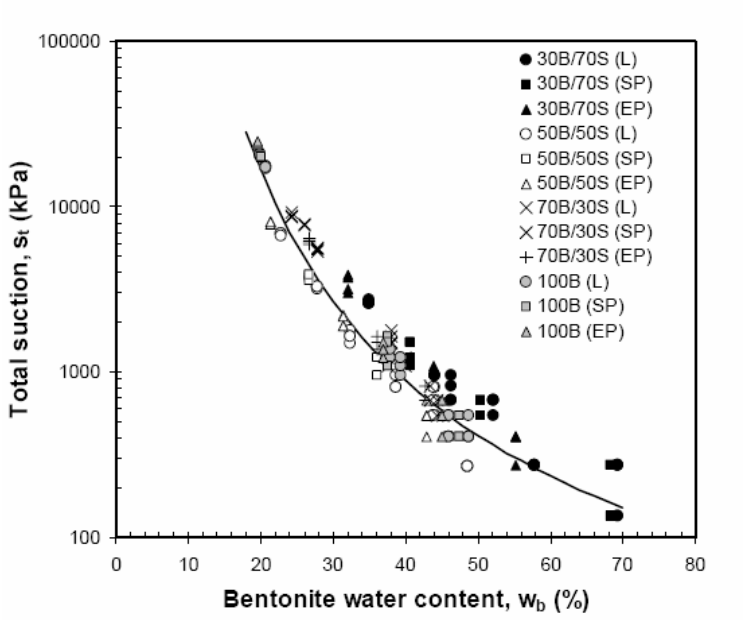

Figure 2.29 Total suction versus bentonite water content of the four mixtures at different states (Agus, 2005), Note: 'L' means loose state, 'SP' means compacted to standard proctor density, and 'EP' means compacted to enhanced proctor density.

2.5.2.1 Hysteresis models for soil water characteristic curve

The gravimetric water content at a given suction for a wetting path of SWCC is less than that for a drying path (i.e. the SWCC is hysteretic). There are an infinite number of scanning curves inside the hysteresis loop. The hysteresis of SWCC caused by the following points (Klausner, 1991):

- Irregularities in the cross-sections of the void passages or the "ink-bottle" effect (Haines, 1930).
- The contact angle being greater in an advancing meniscus than in a receding meniscus.
- Entrapped air, which has a different volume when the soil suction is increasing or decreasing.
- Thixotropic regain or aging due to the wetting and drying history of the soil.

Slope ratio is the ratio between the slope of boundary drying curve to the slope of boundary wetting curve. Pham et al. (2005) reported that there are particular ranges of values for the slope ratio and the distance between the two boundary curves for the collected soil datasets. Values for the slope ratio between the two boundary curves on the semi logarithmic soil suction scale vary from 2.5 for sand to1 for clay (the value of 1.5~1 can be considered for fine-grained soils). The values of the distance between the two boundary curves on the logarithmic soil suction scale for sand and clay are from 0.2 to 0.5 (log-cycles). The simplified version of Feng and Fredlund (1999) model assumes that the boundary wetting curve and the boundary drying curve are parallel when soil suction is plotted in a logarithmic scale (i. e. the slope ratio equals to 1).

2.5.3 Constant suction test

The constant suction test is achieved by means of increasing net stress (loading). Regarding to the initial density and soil type, for each suction there is preconsolidation stress (e. g., see the results of Maswoswe, 1985; Alonso et al., 1990; Gens and Alonso, 1992; Sivakumar, 1993; Wheeler and Sivakumar, 1995; Wheeler and Karube, 1996; Sharma, 1998; Matsuoka et al., 2002; Cui et al., 2002; Gallipoli et al, 2003b; Jotisankasa, 2005 as Figure 2.9; and Casini et al., 2007). The loading collapse curve (LC) in Alonso et al. (1990) and Gens and Alonso (1992), BBM, represents the positions of the preconsolidation stress of the different suctions for the same initial density (Figure 2.8). In the constant suction test the increase in the initial density leads to increase the preconsolidation stress. However, the results of constant applied suction and increase in net stress test for as compacted sample (unsaturated), appear that the compression curve in normal consolidated state (for void ratio-log net stress relationship) is

upper than the saturated normal consolidation line NCL and the unsaturated soil on the normal consolidated state suffers collapse with reduce suction (wetting). Moreover, the results of (Bishop and Blight, 1963; Alonso et al, 1990; Wheeler and Sivakumar, 1995; and Casini et al, 2007) for constant suction test show that the soil firstly suffer from slightly compression until the soil reaches to specific value of net stress, the preconsolidation stress, then the compressibility of soil increases as the net stress increases.

2. 5.4 Constant water content test

The constant suction test, for fine–grained soils, is very close to the constant water content test as long as the applied suction is higher than the air-entry value s_{aev}. The reason of such behavior is that, for fine–grained soils, the density has no effect on water content-suction relationship when the suction is higher than S_{aev}, as mentioned in section (2.3.1.1), (Delage and Graham, 1995; Gens et al., 1995; Li, 1995; Romero, 1999 as Figure 2.28; Tarantino and Tombolato, 2005; and Agus, 2005 as Figure 2.29).

The concept of S_r-lines (Al-Badran, 2001) shows that the compression curves in normal consolidated state for constant water content condition results in straight lines with slope more than the saturated NCL. The slope of such lines decreases with increasing water content which reflected in the results of the expected collapse (collapse will reduce), Figure. (2.18).

Honda et al. (2007) confirmed the observations of Al-Badran (2001). They cited that in constant water content test, the normal compression line is straight in semi-logarithm scale as long as the degree of saturation is not high (Figure. 2.30). The same consequences can be found in the results of Trantino and Tombolato (2008). In general, the normal consolidated lines for constant suction condition or constant water content condition are straight lines on logarithm scale of net mean stress as long as the suction higher than S_{aev} or as the degree of saturation is not high.

2. 5.5 Constant volume test

Constant volume test can be carried out mostly for unsaturated soils by reducing the suction (wetting) and increasing net stress to keep the volume constant through the test. When the compacted saturated soil is under stress, constant volume test can be applied by increasing the suction (drying) and decreasing the net stress. In this case constant volume state is valid for limited value of suction due to shrinkage of soil when the net stress value reduces to zero. Many studies investigated and tried to explain this type of test (e. g., Gens and Alonso, 1992;

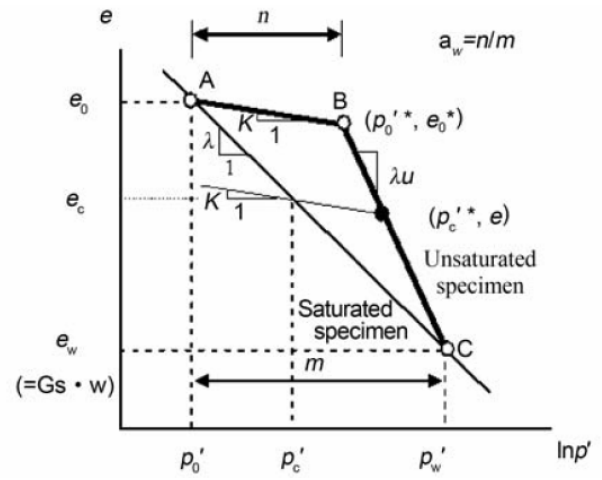

Figure 2.30 Compression curve for unsaturated specimen for constant water content test (Honda et al., 2007).

Romero, 1999; Agus 2005; and Arifin, 2008). Figure (2.31) shows the constant volume tests of Romero (1999) with vertical and horizontal swelling and shrinkage pressure paths.

The magnitude of pressure acting on an expansive soil at which the soil swells upon wetting represents the swelling pressure of the soil at the equilibrium void ratio. Swelling pressure is defined as the pressure needed to maintain constant volume conditions when water is added to an unsaturated expansive soil. Three different methods namely: swell-load, swell-under-load, and constant volume test were reported by Sridharan et al. (1986) and Gens and Alonso (1992). Swelling pressure measurements using oedometer are also described in ASTM D 4546 (ASTM, 1997). The magnitude of swelling pressure of compacted expansive soils is controlled by initial dry density of the specimen (Sridharan et al., 1986; Gens and Alonso, 1992; Komine and Ogata, 2003; Villar and Lloret, 2004; and Agus and Schanz, 2005). In case of bentonite-sand mixtures, the swelling pressure of bentonite-sand mixture is a function of bentonite dry density (Agus and Schanz, 2005 and Agus and Schanz, 2008).

Romero (1999) investigated the effects of temperature and hydration/drying paths by caring out suction controlled swell and shrinkage pressure tests under constant volume condition using prepared packings of Boom clay powder with a dominant aggregated fabric with two different densities (13.7 kN/m^3 and 16.7 kN/m^3). The results showed that the swelling stress reaches a maximum controlled by the microstructural yield surface and then decreases upon subsequent wetting following this yield locus at constant volume (Figure 2.31).

Agus (2005) studied the swelling pressure and constant volume wetting behavior of heavily compacted 50/50 bentonite-sand mixture specimen. He used two different methods

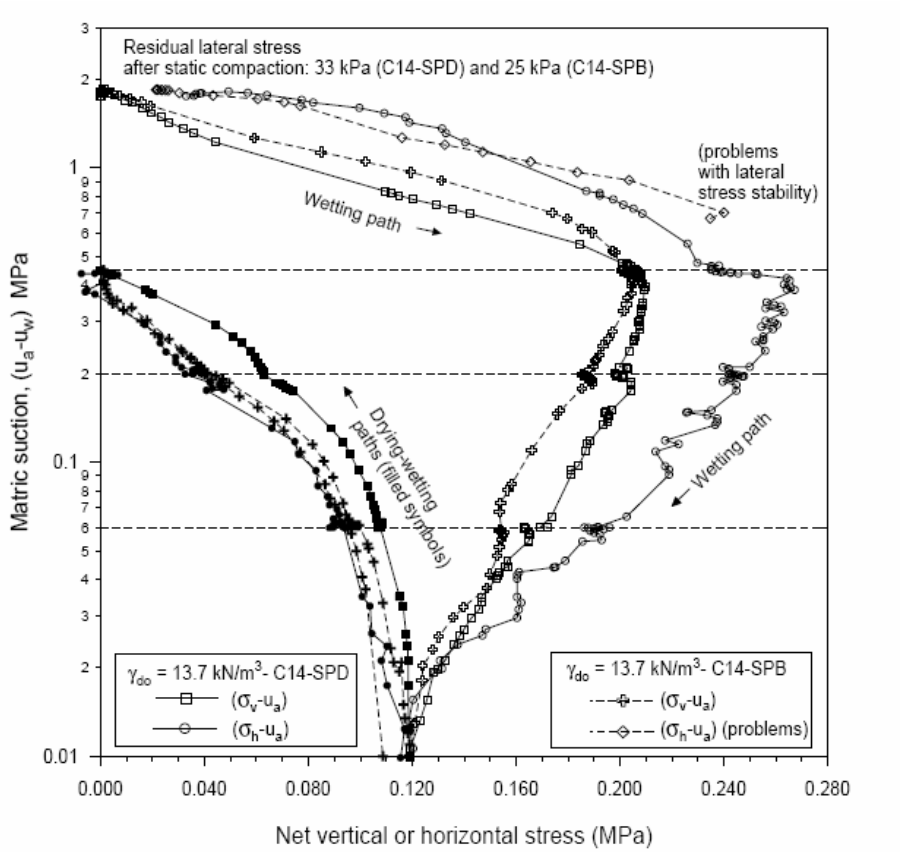

Figure 2.31 Vertical and horizontal swelling and shrinkage pressure paths in the high-porosity packing (Romero, 1999).

(i.e., vapor equilibrium technique, VET for suction higher than 2000 kPa and axis translation technique, ATT for suction less than 2000 kPa). He found that, at constant volume test, very

small development of swelling pressure occurs upon wetting from the as-prepared suction (i.e., 22700 kPa) to about 2000 kPa suction. A rapid development of swelling pressure occurred afterward. Very small increase happened in swelling pressure at suction higher than 2000 kPa is related to the method application suction to the specimen (i.e., vapor equilibrium technique, VET. For the specimen exposed to water vapor, the water molecules migrate into the open channels (i.e., macro-pores) and absorbed on exposed mineral surface. An internal redistribution of water occurs in order to balance the water potential gradient exist between macro-pores and micro-pores. Agus (2005) stated that the insignificant swelling pressure development during wetting up to 2000 kPa suction might be due to a delayed 'true' equilibrium in the specimen and the 'true' equilibrium might be attained after long test duration. He also investigated swelling pressure development for different initial conditions and bentonite content of the specimens. It was found that different initial conditions of

50B/50S specimens (i.e., as-prepared and oven-dried conditions) do not influence the swelling pressure development of the specimens.

Arifin (2008) investigated the thermo-hydro-mechanical behavior of compacted bentonite and bentonite-sand mixtures by carrying out constant volume tests. It was found that the increase in temperature results in reduction in swelling pressure and this reduction of swelling pressure is reversible.

In constant volume test of swelling pressure measurement, at saturation condition (i.e., at the end of the test) the matric and osmotic potentials are balanced by pressure potential or swelling pressure. Thus, at this condition, the soil suction of the specimen is equal to swelling pressure (Agus and Schanz, 2008). Agus and Schanz (2008) extended this idea to predict the swelling pressure of unsaturated by using the SWRC as a tool.

2.6 Compaction Test

2. 6.1 Introduction

Control specifications for the compaction of cohesive soils were developed by Procter (1933); thus, the standard laboratory compaction test is commonly called the proctor test. The compaction effort (*CE*) is a measure of the mechanical energy applied to the soil mass. In SI units, the *CE* is in kJ.m/m^3 (which is equal to kN/m^2 for static compaction), e.g., *CE* = 594.8 KJ/m^3 for Standard Proctor and 2694 KJ.m/m^3 for Modified Proctor). In FPS units, 1 Ib·ft/ft^3 = 0.04796 kJ.m/m^3. Table (2.2) presents the size of the hammer, height of the drop, number of the drops, number of the layers of soil, and volume of the mold.

Table (2.2) The size of the hammer, height of the drop, number of the drops, number of the layers of soil, and volume of the mold.

	Standard		Modified	
	SI Units	FPS Units	SI Units	FPS Units
Weight of hammer	24.5 (N)	5.5 (Ib)	44.5 (N)	10(Ib)
Height of fall	0.305 (m)	12 (in)	0.457 (m)	18 (in)
Number of layers	3	3	5	5
Blows per layer	25	25	25	25
Mold volume(105-mm-diameter)	0.0009422 (m^2)	1130 (ft^3)	0.0009422 (m^2)	1130 (ft^3)
Size of soil used	(-)No.4 sieve	(-)No.4 sieve	(-)No.4 sieve	(-)No.4 sieve
Compaction effort or energy	594.8 (kJ.m/m^3)	12400 (ft.Ib/ft^3)	2698 (kJ.m/m^3)	56255 (ft.Ib/ft^3)

Compaction is commonly practiced in engineering projects in which main components of the structure are made of soil (e.g., highway embankments, earth dams, landfill clay liners). Generally, compaction reduces permeability, compressibility (settlements), and shrinkage, and it increases the soil strength and bearing capacity because of the reduction in the void ratio. In the laboratory, the compaction effort may be determined by impact or dynamic (most common) kneading or static methods.

The compaction curve (Figure 2.32) usually represents the relationship between the moulding water content (w) of the soil and its dry unit weight or dry density (γ_d). Figure (2.32) shows the results of soil that tested by Benson et al. (1997), which is classified as CL in the USCS and is composed of 1% gravel, 85% fines, and 42 % clay with LL = 41%. The two important keys of compaction curve are: the maximum dry density (γ_{dmax}) and the corresponding optimum water content, *OWC* (or optimum moisture content, *OMC*). The portion of the curve that has water content lower than the *OWC* is labelled dry of optimum (*DOP*), and the region with water content greater than the *OWC* is wet of optimum (*WOP*).

For a given type of soil, as the compaction effort increases, the maximum dry density increases and the optimum water content decreases. The points of maximum dry density and optimum water content for the various compaction efforts tend to fall along a line named line of optimum (*LOO*).

Several experimental studies showed that in some cases compaction curve has double peaks (Figure 2.32), where the compaction curve has initially decreasing then increasing dry

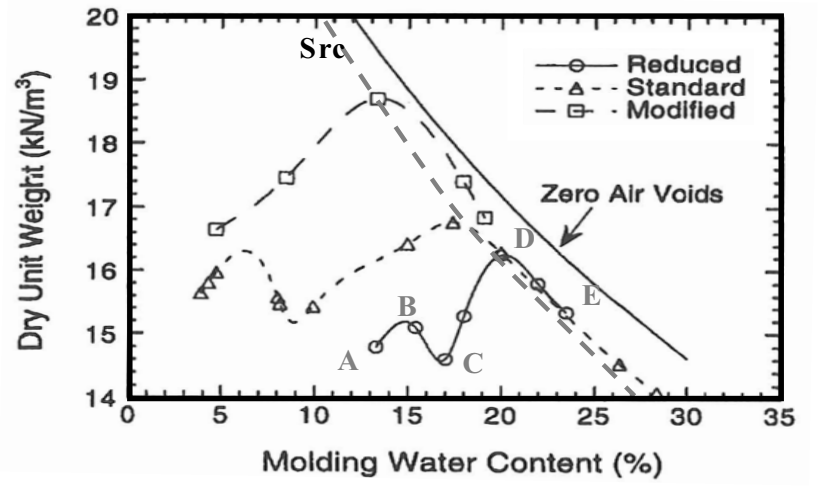

Figure 2.32 Compaction curves for Reduced, Standard, and Modified compaction effort (Benson et al., 1997).

density as the water content increases. Thus the compaction curve identifies two maximum dry densities and two optimum water contents (e.g., the results of Hindi, 1967; Lee and Suedkamp, 1972; Ellis, 1980; Razouki et al., 1980; Dixon et al., 1985; Benson et al., 1997; Sun et al., 2007; and Razouki et al., 2008). To differentiate between the maximum dry densities Razouki et al. (1980) referred to the maximum dry density at the lower *OWC* as the day maximum dry density $D\gamma_{dmax}$, and the maximum dry density at the high *OWC* as the wet maximum dry density $W\gamma_{dmax}$. Because of the bell-, S-, and M-shaped nature of the compaction curve, some soil may be compacted to equal density at two, three, or four different water contents.

For a given compaction effort and dry unit weight, the soil structure tends to be more flocculated for compaction on the dry side of optimum as compared to the dispersed soil compacted on the wet side of optimum. In dry of optimum, the particles or particle groups general alignment in horizontal planes, because the hammer (dynamic compaction) does not penetrate the soil as in case of the piston (static compaction), (Mitchell, 1993). However, when fine-grained soil is sufficiently wet of optimum, the compaction rammer penetrates the soil surface as a result of a bearing capacity failure under the rammer face; alignment of particles along the failure surface develops as a result of successive rammer blows.

2.6.2 Compaction modelling

Previous studies on soil compaction models can be divided into two main groups:

1) Models that use empirical correlations for both cohesive and cohesionless soils, which relate optimum water content *OWC* and maximum dry density or unit weight γ_{dmax} to soil properties such as the Atterberg index (liquid limit, *LL*, and plastic limit, *PL*), specific gravity of solids (G_s), and grain-size distribution (Davidson and Gardiner 1949; Turnbull 1948; Ring et al., 1962; Ramiah et al., 1970; Jeng and Strohm, 1976; Livneh and Ishai, 1978; Wang and Huang, 1984; Korfiatis and Manikopoulos, 1982; Al-Kafaji, 1993; Basheer and Najjar, 1995; Najjar and Basheer, 1996; Blotz et al., 1998; Sridharan and Nagaraj, 2005; Gurtug and Sridharan, 2002; and Jesmani et al., 2008).

2) Models for the entire range of the compaction curve describing the compaction characteristics (Joslin, 1959; Rethati, 1988; Hilf, 1991; Howell et al., 1997; Nagaraj and Bindumadhava, 1992; Nagaraj, 1994; Pandian et al., 1997; Basheer, 1998; Li and Sego, 2000;

Basheer, 2001; Nagaraj et al., 2006b; Honda et al., 2007; Kurucuk et al., 2008; and Horpibulsuk et al., 2008a and b).

An early work by Joslin (1959) yielded 26 typical standard Proctor curves (named Ohio's curves). Rethati (1988) presented an empirical approach to modelling the compaction curve based on fitting a simple quadratic equation to the dry density- water content relationship. Hilf (1991) and Howell et al. (1997) used second-, third-, and fourth-degree polynomial equations to model the compaction curve. Nagaraj and Bindumadhava (1992) and Nagaraj (1994) developed a semi-empirical phenomenological model to determine the w-γ_d relationship separately for the *DOP* and *WOP* based on the liquid limit and specific gravity for each compaction effort. Pandian et al. (1997) presented the linear relationships of w-*LL*, $[w/(S_r)^{0.5}]$-*LL*, $[w\ (S_r)^2]$-*LL*, for the standard Proctor test. Basheer (1998) developed based models for both the compaction characteristics and compaction curves. Li and Sego (2000) derived an equation with both soil and compaction effort parameters to predict complete compaction curves of fine-grained soils for all $w > 0$.

Basheer (2001) suggested empirical models using both statistical regression and ANNs to predict the compaction curves of cohesive soils based on soil properties and compaction effort.

Nagaraj et al. (2006b) introduced an ideal pore model (linear relationships) depends on the microstructural consideration to estimate the compaction curves of fine-grained soils quickly for different compaction efforts for the *DOP* and *WOP*. Based on their ideal model, parameters $w/\ S_r^{\ 0.5}$ and $w/\ S_r^{\ 2}$ were proposed for the *DOP* and *WOP*, respectively. Honda et al. (2007) presented a method to determine the dry density- water content relationship based on the assumptions that the unsaturated normal compression lines in the constant water content condition (although the degree of saturation is increasing) are straight in the void ratio-lnσ plot, as long as the degree of saturation is not close to 100%. Several studies yielded a set of compaction curves that are nearly parallel for all soils (Joslin, 1959; Nagaraj and Bindumadhava, 1992; Nagaraj, 1994; and Nagaraj et al., 2006b). Basheer (2001) and Horpibulsuk et al. (2008a, b) have demonstrated that the compaction curves of natural soils are rarely parallel to each other (some of them have flatter curves and others have sharp peaks).

Kurucuk et al. (2008) presented an approach to predict the soil compaction curve during undrained loading. They investigated the effect of soil suction, stiffness, and pore air pressure on the shape of the compaction curve.

Horpibulsuk et al. (2008a) showed that the two parameters $w/S_r^{0.5}$ and $w/S_r^{\ 2}$ (from Nagaraj et al., 2006b) are not the state parameters for all clays. They proposed a more general relationship between the water content, w, and the degree of saturation, S_r, for a particular compaction effort as a power function of the form:

$$w = A_d S_r^{\ Bd} \qquad for \quad DOP \tag{2.21a}$$

$$w = A_w S_r^{\ Bw} \qquad for \quad WOP \tag{2.21b}$$

where w is the water content (decimal); S_r is the degree of saturation (decimal); and A_d, B_d, A_w, and B_w are constants.

B_d and B_w are 0.5 and 2.0 for the model proposed by Nagaraj et al., (2006 b). For a particular clay and compaction effort, the parameters A_d and A_w control the values of dry density. The parameters B_d and B_w control the degree of water sensitivity (slope of compaction paths) in the *DOP* and *WOP* regions, respectively. They also observed that, even though the *OMC* values are different for different soils, their rate of decrease with compaction effort is almost the same for all fine-grained soils, which is evident because the ratios OMC/OMC_{SP} (or $A_d/A_{d\text{-}SP}$ or $A_w/A_w\text{-}_{SP}$) are almost the same for any compaction effort as fitting equation (2.22).

$$\frac{OMC}{OMC_{SP}} = 2.09 - 0.39 \log(CE) \tag{2.22}$$

where OMC_{SP} is the *OMC* for a standard proctor.

Horpibulsuk et al. (2008b) extended the work of Horpibulsuk et al. (2008a) for coarse and fine grained soils. They found that Equation (2.22) is almost the same (2.09 and 0.39 became 2.02 and 0.37 respectively) for all different coarse and fine soils used in the study. Based on this finding, they modified Ohio's curves under different compaction efforts (0.5*SP*, *SP*, 0.5*MP*, and *MP*).

2.7 Summary

Several of the issues relevant to the volume change of unsaturated soils are summarized in this chapter. Suction concept, state of stress, volume change and collapse of unsaturated soil are briefly presented. In addition, a review of the volume change models of unsaturated soils is presented. The volumetric models of unsaturated soils are classified into two groups; one used the effective stress (Bishop) approach and the other used the two independent stress variables (net stress and suction) approach. Laboratory techniques used to measure the volume change of unsaturated soil are also elaborated. The concept of compaction and a review of compaction modelling are presented.

Chapter 3

Material Used and Experimental Program

3.1 Introduction

The focus of the experimental program is to study the volumetric behavior of unsaturated fine-grained soils. Two materials are used: high plasticity soil material i. e., pure bentonite (calcigel), 100B, and low plasticity soil material i. e., 30 % bentonite and 70 % sand, 30B, with two different initial conditions i. e., slurry and loose. The study aims to investigate and determine the state surface of unsaturated fine-grained soils in void ratio-net stress-suction space. Therefore, experimental program consists of several controlled-suction volume change tests for100B and 30B soils, is presented.

3.2 Material used

The materials used in this study are Calcigel and quartz sand. The Calcigel was mined from Bavaria, Southern part of Germany. The sand used in this study for mixture is named Haider sand. The most of the main properties of the bentonite (Calcigel) used were obtained from the experiments in this study. The other properties of bentonite and the properties of sand were collected from previous studies.

3.2.1 Basic properties

The basic properties investigated in this study included the determination of specific gravity, grain-size distribution, and Atterberg limits. The tests were performed based on ASTM standards (ASTM, 1987) and DIN standards (DIN, 1987).

For specific gravity determination, method proposed in DIN 18124 KP (DIN, 1987) was adopted in this study. The method proposed in ASTM D 854 (ASTM, 1987) for high plastic clay was performed for comparison. In order to release entrapped air in the specimen, the picnometer with the saturated specimen was placed on sand bath and stirred carefully. The specific gravity of 2.744 and 2.756 were obtained from the tests based on DIN and ASTM standards, respectively. The average specific gravity of 2.75 was used in this study.

The grain size distribution of Calcigel was investigated using sedimentation method (i.e., DIN 18123-7) (DIN, 1987). The sample was dispersed using a dispersing solution (i.e., sodium pyrophosphate) during experiment. The results of grain size distribution for calcigel

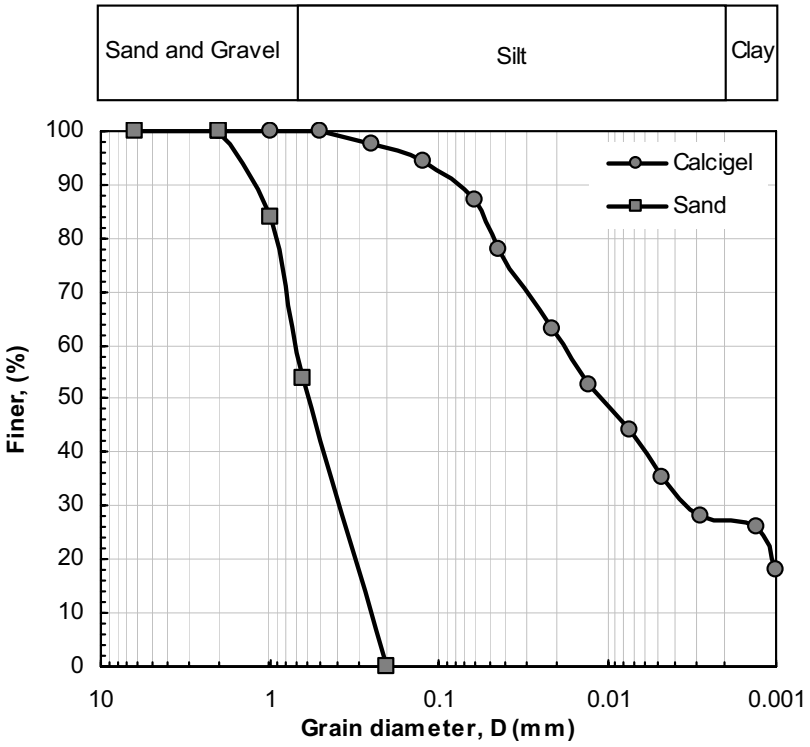

Figure (3.1) Grain-size distribution curves of the bentonite (calcigel) and sand used, data of sand from Agus (2005).

and quartz sand are presented in Figure (3.1). Figure (3.1) shows that the amount of clay particle size fraction is 27 %.

The Atterberg limits were performed according to DIN 18 122 (DIN, 1987). The tests included the liquid limit using Casagrande, the plastic limit, and the shrinkage limit determination. The samples were mixed with distilled water to reach different values of water content and remixed everyday for minimum one week before investigation. The liquid limit, the plastic limit, and the shrinkage limit obtained were 89.1%, 35.9%, and 14%, respectively.

Table (3.1) presents the basic properties materials used (100B and 30B soils) in this study. The properties of sand used in this study reported by Agus (2005) and Arifin (2008) are summarized in Table (3.2).

3.2.2 Physico-chemical characterization

In this study, the physical, chemical, and mineralogical properties of the bentonite are of concern since it has been known that the bentonite behavior such as compressibility, swelling behavior, permeability, etc are controlled by its physical, chemical, and mineralogical

properties. The physical, chemical, and mineralogical characterization of bentonite used in this study included determination of specific surface area (SSA), cation exchange capacity (CEC), mineralogical and chemical compositions, and osmotic suction.

Specific surface area

The total specific surface area (SSA) was determined using Ethylene Glycol Monoethyl Ether (EGME) method (Cerato and Lutenegger, 2002). The amount of EGME, age of desiccant, amount of soil tested, and size of desiccator used were considered carefully. The total specific area of material used in this study was 400 m^2/g.

Cation Exchange Capacity (CEC)

The CEC data was collected from Schanz et al. (2010) due to using the same bentonite (Calcigel II in article). The amount of basic exchangeable cations (i.e., Na^+, K^+, Ca^{2+}, and Mg^{2+}) was determined using inductively couples plasma atomic emission (ICP) according to the European Standard EN ISO 11885, (1985). The amount of cations (i.e., Na^+, Ca^{2+}, Mg^{2+}, and K^+) are 2, 50, 13, and 1 meq/100g, respectively. Therefore, the total of basic exchangeable cations is 66 meq/100g.

Müller-Vonmoos and Kahr (1982) reported the CEC for Calcigel is 62 meq/100g with the amount of Na^+, Ca_2^+, Mg_2^+, and K^+ exchangeable cations of 1.8, 37.6, 22.4, and 0.2 meq/100g, respectively.

Mineralogy and Chemical Compositions

The mineralogy of Calcigel was investigated using X-ray diffraction (XRD) method. The result is shown in Figure (3.2). The result shows that the predominant clay mineral of Calcigel used in this study are montmorillonite, muscovite which is known as common mica, quartz, chlorite, Anorthite which is one of the plagioclase feldspars, and Dolomite which is the sedimentary carbonate rock and composed of calcium-magnesium carbonate in crystals.

Osmotic suction determination

The squeezing process to extract the specimen's pore-water was performed using a squeezer that has similar shapes and dimensions to the squeezer used by Krahn and Fredlund (1972). The same squeezer was used by Arifin, (2008). Figure 3.3a shows the squeezer used in this study. As shown in the figure, the squeezer is divided into three main parts (i.e., ram, cylinder, and base). The squeezer was equipped by accessories such as Teflon disk, rubber disk, filter holder, and rubber washer. The Teflon disk was used to separate the ram and rubber disk and to avoid damage in the rubber disk. The rubber disk and rubber washer were used to avoid leakage in the cylinder and between filter holder and base, respectively. The filter holder was used for placing the wire mesh and filter paper.

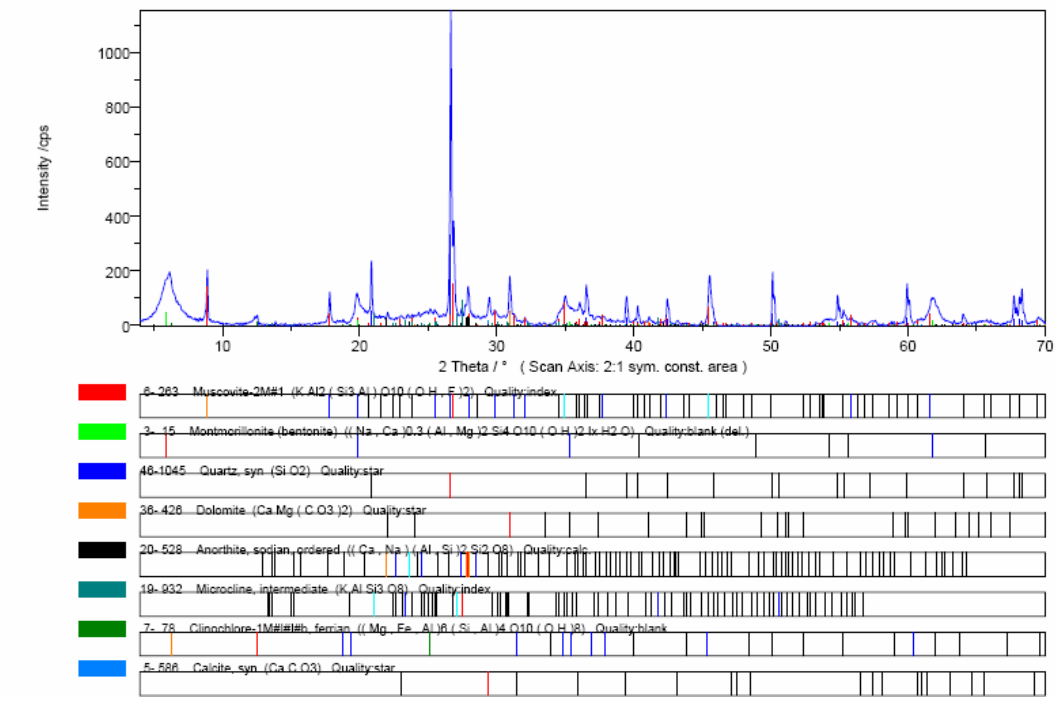

Figure 3.2 The predominant clay mineral of Calcigel used in this study.

Figure 3.3 Device used in the squeezing technique (a) squeezer (b) squeezer in the triaxial load frame (Arifin, 2008).

Using the suggested empirical relationship (Equation 3.1) by Arifin (2008), the osmotic pressure of the pore-water obtained from the squeezing technique was measured using a conductivity meter. The calibration of the conductivity meter was performed using molal NaCl solutions.

Arifin (2008) found that the calibration curve obtained is in a good agreement with the calibration curve presented by USDA (1950) which was established for salt mixtures in saline soils. Rao and Shivananda (2005) found a single calibration line for sodium chloride and calcium chloride. The osmotic suction can be computed from the measured electrical conductivity using the following equation (Arifin, 2008).

$$\pi = 38.54EC^{1.0489} \quad (3.1)$$

where π is osmotic suction (kPa) and EC is electrical conductivity (mS/cm).

The osmotic suction measurement using the squeezing technique was performed on several statically compacted specimens. After compaction, the specimen with diameter of 5 cm was trimmed to reach the same diameter as the squeezer. Pressure was applied one dimensionally using triaxial-load frame (Figure 3.3b) until the first drop of pore-water expelled. The pressure of 500, 1000, 2000, 4000, 8000, 15000, 20000, 25000, 30000, 35000, 40000, 45000, 50000, 55000, 60000, 65000, 70000, 75000, 80000 kPa were applied with duration for each pressures of 5 minutes. The use of low pressure is not favourable since it requires longer time to obtain the first drop of soil pore-water (Arifin, 2008). This will change the salt concentration due to evaporation or cation exchange in between elementary layers and in the free pore-water in order to balance the external pressure applied (Sacchi et al., 2001). The soil pore-water was collected using a syringe and was subsequently transferred to the conductivity meter to measure its electrical conductivity. About 2 ml of soil pore-water is required for the measurement of osmotic suction. The pore-water was carefully placed on the sensor surface of the conductivity meter. In about less than 5 seconds after the pore-water placement, the value of the electrical conductivity in μS/cm or mS/cm was shown on the digital display of the equipment. In order to investigate the squeezing pressure effect, the pressure was subsequently increased until the next drop of water was obtained. The osmotic pressure of the extracted soil pore-water was determined from the electric conductivity reading and calculated using Equation 3.1. The obtained of Physico-chemical properties are summarized in Table 3.1.

Table 3.1 Summary of soil properties for materials used, 100B and 30B soils.

Properties of soils	100B	30B
Specific gravity	2.75	2.695
Liquid limit (%)	89.1	30
Plastic limit (%)	35.9	-
Plasticity index (%)	53,2	-
Shrinkage limit (%)	14	-
Clay content (%)	27	8.1
Fine content (%)	95	28.5
Total specific surface area (m^2/g)*	400	120
Basic exchangeable cation Na^+, Ca^{2+}, Mg^{2+}, K^+ (meq/100g)**	2, 50, 13, 1	-
Total Cation exchange capacity (meq/100g)	66	-
Monmorillonite content (%)***	45	-
Hygroscopic water content (%)	7.2	1.5
Total suction at hygroscopic water content (kPa)	207500	297000
Osmotic pressure, π (kPa)	50	-

*determined using the Ethylene glycol monethyl ether (EGME) method (Cerato and Lutenegger, 2002).
** Schanz et al. (2010)
*** determined using X-ray diffraction method.

Table 3.2 Summary of sand characteristics used (from Agus, 2005 and Arifin, 2008).

Properties	Haider sand
Specific gravity	2.65
D10	0.25
D60	0.40
D30	0.70
Specific surface area (m^2/g)	0.25

3.3 Experimental program

The study seeks to investigate and determine the state surface of unsaturated fine-grained soils in void ratio-net stress-suction space. Therefore, several volume change tests for 100B and 30B soils were performed for slurry and loose initial states. The experimental program consists from (i) volumetric yielding tests for unsaturated fine-grained soils, (ii) compaction tests, and (iii) SWCC tests. The values of two stress variables (net vertical stress and suction) in the experimental program are limited to the ability of the used equipments. Moreover, in experimental program several cells were used to perform the big experimental program, therefore some identical specimens were tested in different devices for comparison (U symbol). The following nomenclatures will be used as abbreviation in this work for the mixture percent, type of test, initial condition (e.g. 30B-S39-Sl = 30B mixture with 39000 kPa constant suction test for slurry initial condition): 30B = 30% bentonite (calcigel) and 70%

sand; 100B = 100% bentonite (calcigel); Sr**X** = constant degree of saturation test of **X** %; S**X** = constant suction test of **X** MPa; P**X** = constant net vertical stress test of **X** MPa; ve r= verification test by testing identical specimens with different paths but the same initial and final points; Lo = loose initial state; Sl = slurry initial state; com: compacted initial state; U = comparison test for specimen with other cell under that same conditions; w = wetting test; d: drying test; SP= Standard Proctor; MP= Modified Proctor; RP= Reduced Proctor (248 kJ.m/m^3); Pcom= constant net stress applied in static compaction.

3.3.1 Volumetric yielding tests for unsaturated soil

One-dimensional compression tests were carried out for pure bentonite (calcigel), 100B, and 30 % bentonite- 70 % sand mixture, 30B, to investigate the characteristics and determine the volumetric yielding for both of saturated and unsaturated states. Loose state was chosen as initial state when wetting process was applied to investigate the volumetric yielding of unsaturated soils. While initially slurry state was used when drying process was applied to determine the volume change when soil state changes from saturated to unsaturated. Different types of controlled suction oedometer (one-dimensional) tests were performed to determine the volume change of unsaturated 30B and 100B soils to verify the proposed model in chapter 6 and determine the volume change of unsaturated state.

3.3.1.1 Constant degree of saturation test

To investigate the validity of *Sr*-lines concept (1st hypothesis in section 6.3) the constant degree of saturation test was proposed. Such tests were has been not carried out in the past to the best of the knowledge of the author. Two constant degrees of saturation tests for 30B soil were conducted to determine the NCL of 0.58 and 0.68. The initial condition of both tested specimens was unsaturated loose with details shown in Table (3.3). Figure (3.4) shows the stress path of each test in (net stress-suction) space. Procedure of the test will explain in chapter 4 (4.6.1.1).

Table 3.3 Initial conditions of specimens for the constant degree of saturation test.

The constant degree of saturation	0.58	0.68
Test name	30B-Sr58-com	30B-Sr68-com
soil/ Initial state	30B/ com	30B/ com
Initial void ratio	0.945	0.80
Initial dry density, (gm/cm^3)	1.39	1.5
Initial water content	0.16	0.24
Initial degree of saturation	0.46	0.81

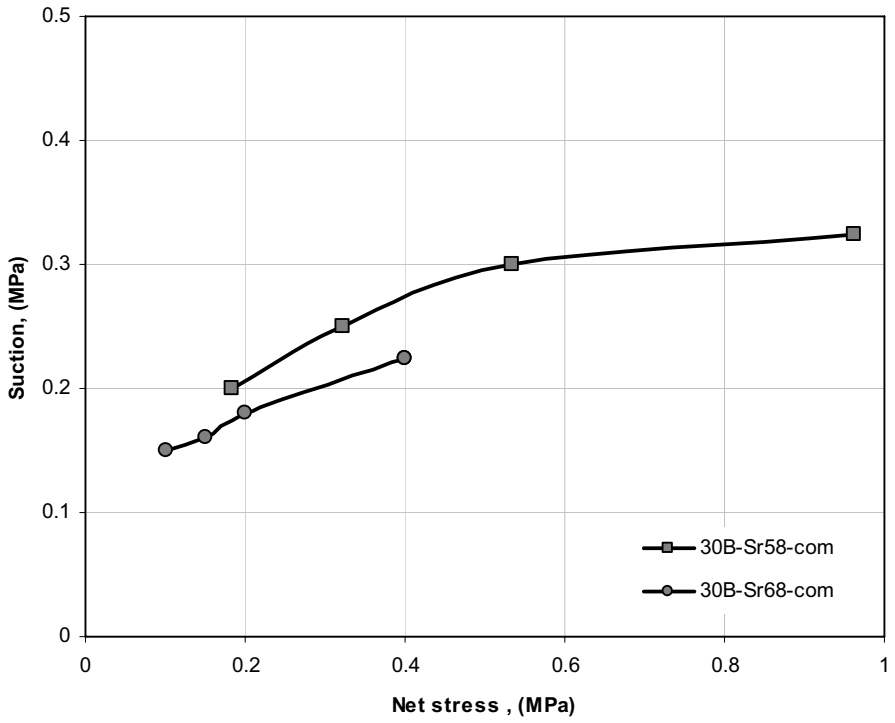

Figure 3.4 Stress path of NCL's for constant degree of saturation tests for 30B soil.

3.3.1.2 Constant net stress test

The constant net stress test divides into two main categories: drying test (increase suction) and wetting test (decrease suction). The net stress is kept constant through the test. The SWCC tests under unconfined condition for both soils will point out later in section (3.2.3.2).

Constant net stress test with increasing the suction (drying).

The drying tests were performed for initially slurry state specimens to investigate the volume change of soil when the soil state is transferred from saturated to unsaturated. Seven 30B specimens and four 100B specimens were tested under drying condition. In addition two 30B specimens were prepared in order to carry out for comparison between different cells.

Constant net stress test with decreasing the suction (wetting)

Three 30B specimens were collected for wetting (collapse) test with initially loose unsaturated state specimens to determine the volumetric yielding of unsaturated state. The initial states for constant net stress tests and the stress paths for each test in (net stress-suction) space are shown in Table (3.4) and Figure (3.5), respectively.

Table 3.4 Initial conditions of specimens for the constant net stress test.

Nr	Test name	soil/ Initial state	constant net stress , (MPa)	Initial void ratio	Initial dry density (gm/cm^3)	Initial water content,	Initial degree of saturation,	Initial total suction, (MPa)
1	30B-P0.001-d&w-Sl	30B/Sl	0.005	1.00	1.37	0.35	1.00	0
2	30B-P0.001- d&w -com1	30B/Sl	0.005	0.661	1.62	0.245	1.00	0
3	30B-P0.001- d&w -com2	30B/Sl	0.005	0.430	1.89	0.160	1.00	0
4	30B-P0.1-d-Sl	30B/Sl	0.1	1.09	1.29	0.370	0.92	0
5	30B-P0.22-d-Sl	30B/Sl	0.22	0.96	1.37	0.350	0.98	0
6	30B-P0.6-d-Sl	30B/Sl	0.6	0.96	1.37	0.355	0.994	0
7	30B-P1.0-d-Sl	30B/Sl	1.0	0.93	1.4	0.34	0.99	0
8	30B-P0.25-w-Lo	30B/Lo	0.25	1.47	1.09	0.065	0.12	12
9	30B-P0.6-w-Lo	30B/Lo	0.6	1.57	1.05	0.069	0.12	10
10	30B-P1.0-w-Lo	30B/Lo	1.0	1.51	1.07	0.075	0.135	9.0
11	100B-P0.001- d&w -Sl	100B/Sl	0.005	2.79	0.73	1.03	1.00	0
12	100B-P0.001- d&w -com1	100B/Sl	0.005	1.071	1.33	0.39	1.00	0
13	100B-P0.3-d-Sl	100B/Sl	0.3	2.83	0.72	1.00	0.975	0
14	100B-P0.6-d-Sl	100B/Sl	0.6	2.83	0.72	1.02	0.98	0
15	30B-P0.22-d-Sl-U	30B/Sl	0.22	0.88	1.43	0.321	0.99	0
16	30B-P0.6-d-Sl-U	30B/Sl	0.6	0.87	1.44	0.321	0.996	0

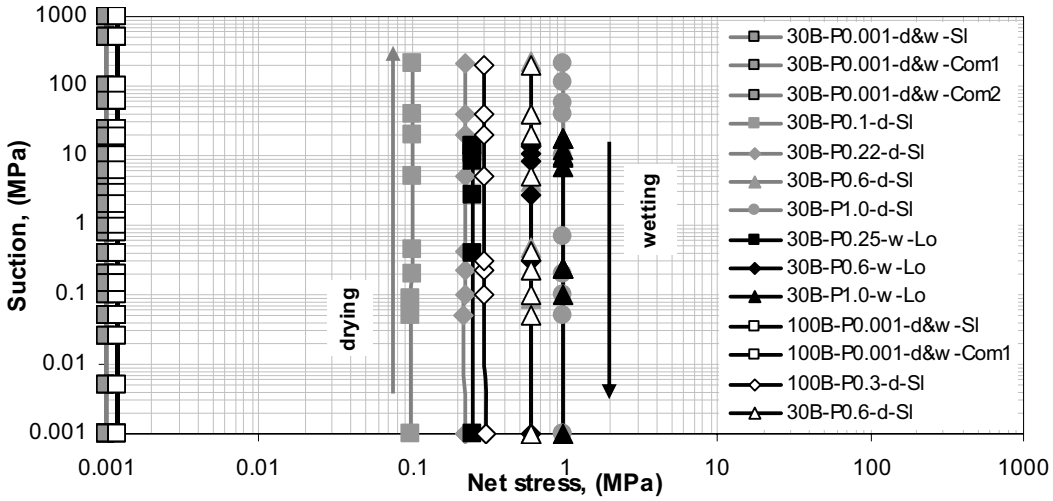

Figure 3.5 Stress paths of constant net stress tests for 30B soil, d = drying and w = wetting.

3.3.1.3 Constant suction test

In this type of test, the net stress is increased through the test while the suction is kept constant. Thirteen 30B specimens and two 100B specimens were tested under constant suction condition. Extra two tests on 30B specimens will be used for comparison of the test results between different cells. The initial states for constant net stress test and the stress paths for each test in (net stress-suction) space are shown in Table (3.5) and Figure (3.6), respectively. The tests 30B-S0.1-SL, 30B-S0.45-Sl, 30B-S0.05-Lo, and 30B-S0.1-Lo1 were loaded under constant suction condition then followed by wetting process (reduction in suction under constant net stress) at 0.91 MPa, 1.6 MPa, 0.92 MPa, and 0.925 MPa, respectively. The maximum constant applied suction in the cerise was 39000 kPa (30B-S39-Sl test) because of the possibility to increase the preconsolidation pressure (yield stress) more than 24000 kPa (the maximum limit of the used equipments).

3.3.1.4 Changing both net stress and suction test

This test was achieved to investigate the uniqueness of the state surface at yield state for unsaturated soil. This test was used to investigate the validity of the main hypothesis in this study (there is only one state surface in 'void ratio-net stress-suction' space, see chapter six). Three identical specimens were used in this test. The two stress variables (net stress and matric suction) for the three specimens are varied along three different paths. However, the initial and the final two stress variables for the three specimens were identical. Additionally, the stress paths intersect in different points. One of the criteria of the test was that the specimen should keep in normal consolidated state during the test. The coordinates (net stress in MPa, suction in MPa) of each point are: A (0.0, 80), B (0.6, 20), C (3.0, 40), D (3, 0.5), E (3, 0.0), F (25, 0.0b), G (3, 166), and H (0, 0.5). The initial states for change both net stress and suction test and the stress paths for each test in (net stress-suction) space are shown in Table (3.6) and Figure (3.7), respectively.

3.3.2 Compaction tests

As part of unsaturated volume change investigations, static and compaction tests were carried out for both 30B and 100B soils with different compaction efforts.

3.3.2.1 Static compaction

The static compaction tests were performed for both soils with reduced proctor compaction stress (RP) equals to 248 kPa.

3.3.2.2 Dynamic compaction

The Dynamic compaction tests were performed for both soils with standard proctor (SP), using ASTM D698 standard, and modified proctor (MP), using ASTM D1557 standard,

compaction efforts ([SP] =593 and [MP] =2694 kJ.m/m^3). One point from each soil was carried out with reduced proctor compaction energy (RP) equals to 248 kJ.m/m^3 or 248 kPa. The water contents of reduced dynamic compaction test (RP) of each soil are 31.2 % and 11.2% for 100B and 30B, respectively.

Table (3.7) shows the compaction tests conditions for both bentonite-sand soils used in study.

Table 3.5 Initial conditions of specimens for the constant suction test.

Nr	Test name	soil/ Initial state	constant suction, (MPa)	Initial void ratio	Initial dry density, (gm/cm^3)	Initial water content, (w)	Initial degree of saturation (S_r)	Initial total suction (MPa)
1	30B-S0-Sl	30B/Sl	0	0.89	1.42	0.33	1.00	0
2	30B-S0.05-Sl	30B/Sl	0.05	1.08	1.29	0.355	0.94	0
3	30B-S0.1-Sl	30B/Sl	0.10	1.02	1.33	0.375	0.994	0
4	30B-S0.255-Sl	30B/Sl	0.225	0.98	1.36	0.34	0.94	0
5	30B-S0.3-Sl	30B/Sl	0.3	0.98	1.36	0.344	0.943	0
6	30B-S0.4-Sl	30B/Sl	0.4	0.914	1.41	0.35	1.00	0
7	30B-S0.45-Sl	30B/Sl	0.45	1.03	1.31	0.365	0.952	0
8	30B-S39-Sl	30B/Sl	39	1.00	1.32	0.375	1.00	0
9	30B-S0.05-Lo	30B/Lo	0.05	1.65	1.04	0.085	0.14	5
10	30B-S0.1-Lo1	30B/Lo	0.1	1.83	0.95	0.100	0.147	3.5
11	30B-S4.3-Lo	30B/Lo	4.3	1.44	1.11	0.075	0.14	4.3
12	30B-S10-Lo	30B/Lo	10	1.50	1.08	0.07	0.126	10
13	30B-S39-Lo	30B/Lo	39	1.05	1.34	0.053	0.135	39
14	100B-S0-Sl	100B/Sl	0	2.71	0.74	0.994	1.00	0
15	100B-S4.3-Lo	100B/Lo	4.3	2.4	0.81	0.243	0.28	4.3
16	30B-S0-Sl-U	30B/Sl	0	1.02	1.34	0.377	0.999	0
17	30B-S0.05-Lo-U	30B/Lo	0.05	1.61	1.03	0.073	0.122	9.1

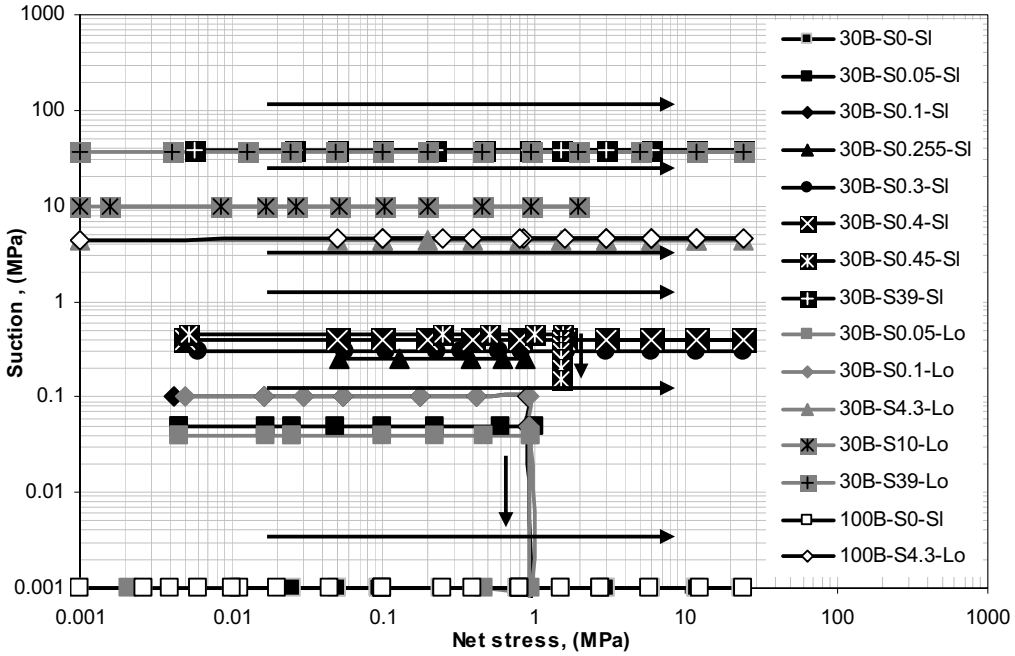

Figure 3.6 Stress paths of constant suction tests for 30B soil.

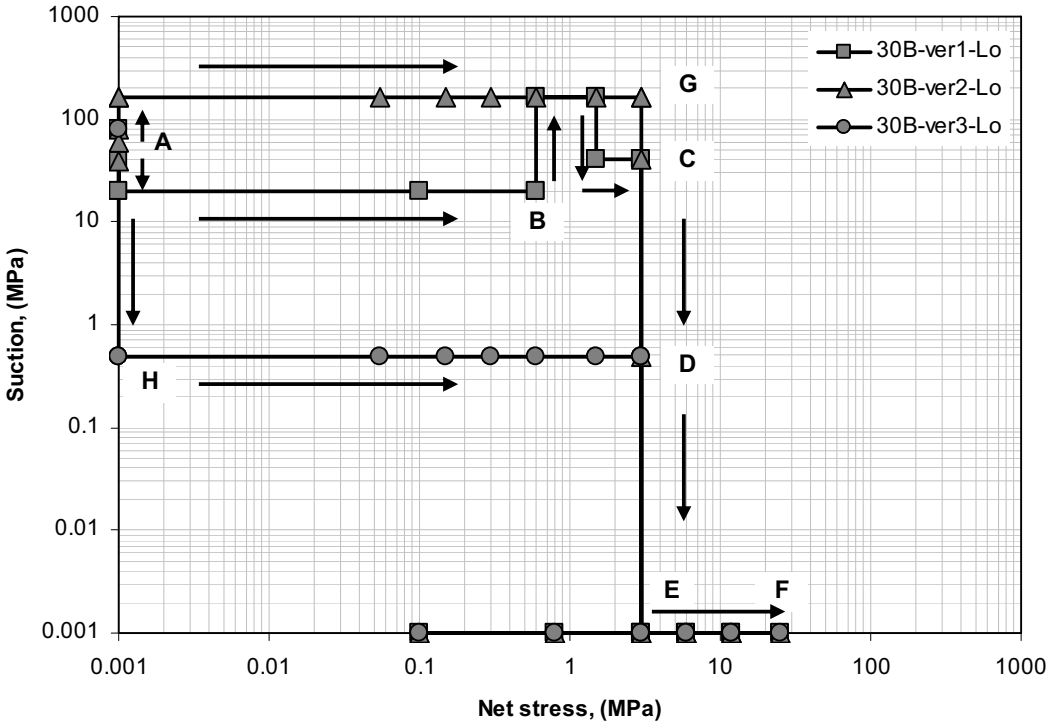

Figure 3.7 Stress paths of change both net stress and suction test for each test of 30B soil.

Table 3.6 Initial conditions of specimens for change both net stress and suction test.

Nr	Test name	soil/ Initial state	Path as shown in Figure (3.7)	Initial void ratio	Initial dry density (gm/cm^3)	Initial water content,	Initial degree of saturation,	Initial total suction, (MPa)
1	30B-ver1-Lo	30B/Lo	A-B-C-E-F	0.723	1.56	0.04	0.15	80
2	30B-ver2-Lo	30B/Lo	A-G-C-D-E-F	0.723	1.56	0.04	0.15	80
3	30B-ver3-Lo	30B/Lo	A-H-D-E-F	0.723	1.56	0.04	0.15	80

3.3.3 Soil water characteristic curve (SWCC) tests program

The relationship between the SWCC and consolidation test results was investigated. The experimental program to study this relationship consists of isotropic consolidation test (effect of suction on the soil skeleton is similar to the effect of isotropic consolidation) and determination of the SWCC.

3.3.3.1 Soil water characteristic curve test

The effect of suction on the 30B and 100B soils with different densities is investigated by performing a set of SWCCs tests under unconfined condition. The initial states and the applied suction for SWCCs tests for both soils are shown in Table (3.8).

Table 3.7 Compaction tests conditions for the soil used.

Nr.	Test name	Soil	Type of compaction	Compaction effort
1	30B-SP	30B	dynamic	Standard Proctor (593 KJ/m^3)
2	30B-MP	30B	dynamic	Modified Proctor (2694 KJ/m^3)
3	30B-RP	30B	dynamic	Reduced Proctor (248 KJ/m^3)
4	30B-Pcom0.248	30B	static	Net stress = 248 kPa
5	100B-SP	100B	dynamic	Standard Proctor (593 KJ/m^3)
6	100B-MP	100B	dynamic	Modified Proctor (2694 KJ/m^3)
7	100B-RP	100B	dynamic	Reduced Proctor (248 KJ/m^3)
8	100B-Pcom0.248	100B	static	Net stress = 248 kPa

Table 3.8 Initial conditions of specimens for SWCC test.

Nr	Test name	soil/ Initial state	Initial void ratio	Initial dry density, (gm/cm^3)	Initial water content,	Initial degree of saturation	Initial total suction (MPa)
1	30B-swcc1.31-Sl	30B/Sl	1.06	1.31	0.371	0.94	0
2	30B-swcc1.62-com	30B/com	0.66	1.62	0.224	0.91	0
3	30B-swcc1.89-com	30B/com	0.43	1.89	0.161	1.00	0
4	100B-swcc0.72-Sl	100B/Sl	2.84	0.72	1.01	0.98	0
5	100B-swcc1.33-com	30B/com	1.07	1.33	0.35	0.90	0

3.4 Summary

Two materials were selected for study in this research program: pure bentonite (calcigel), 100B with LL = 89.1 %, and 30 % bentonite and 70 % sand, 30B with LL = 30 %. The basic physico-chemical characterizations of the selected materials are presented. The physico-chemical characterizations include specific surface area, cation exchange capacity (CEC), mineralogy and chemical compositions, osmotic suction, as shown in Tables (3.1 and 3.2). In addition, the experimental program consists of several one-dimensional controlled-suction volume change tests (constant degree of saturation test, constant net stress test, constant suction test, changing both net stress and suction test, and compaction tests) is presented. Two different initial conditions are used: Slurry and loose.

Chapter 4

Experimental Techniques and Procedures

4.1 Introduction

Determination the volume change behavior of unsaturated fine-grained soils from experiments is difficult, time consuming, and requires special equipments which can be performed by high quality personnel. For fine-grained soils, these equipments should be capable to apply large range of suction (from zero to several hundreds thousands kPa) and large range of net stress (from zero to several tens kPa). In this chapter the specimen's preparation, devices, and experimental techniques and procedures used in determination of volume change of saturated and unsaturated states are summarized.

4.2 Samples preparation

To cover all the possible states of unsaturated volume change, the initial conditions of the specimens used are divided into two states: ((i) Slurry (Sl) when drying path was applied and (ii) Loose (Lo) when wetting path was applied. The initial slurry state was used to study the unsaturated volume change of drying path, whereas the initially loose state was used to study the unsaturated volume change of wetting path. The slurry specimens were prepared by mixing the soil with water content equal to 1.2 times its liquid limit (i.e., 36 % for 30B and 107 % for 100B). The soil was mixed daily for at least one week to produce homogonous mixture. The loose specimens were prepared to produce maximum void ratio of unsaturated state. Water content of range (0.65-0.10) to achieve suction ranges (12 MPa-3.5 MPa) brings into being maximum initial void ratio for 30B soil and water content 0.24 to achieve suction 10 MPa produces maximum initial void ratio for 100B soil.

4.3 Devices used for applying net vertical stress

In this study many compression devices were used due to different abilities of each one and the long duration of controlled-suction test (approximately 3-4 months for 30B soil and the doubled time for 100B soil). The state of the applied net stress in study is mainly one-dimensional using; the modified controlled-suction oedometer cell, UPC-Barcelona cell, UPC-Isochoric cell, and high stress oedometer cell. Only one test for each soil was carried out by applying isotropic stress using triaxial device to locate the position of isotropic normal consolidation line (iso-NCL).

The procedure followed for each test depends on the type of the test. Based on the pressure-deformation characteristic of all devices, the measured volume (i.e., dry density and void ratio) at each loading and unloading steps during the compression tests were corrected.

4.3.1 Modified controlled-suction oedometer cells (Red and Black cells)

The modified controlled-suction oedometer cells, (Figure 4.1a and 4.2) used by Lins (2009), enable to use axis-translation technique (ATT), and the vapour equilibrium technique (VET) to control the suction for determination of the one dimensional volume change under 1D strain condition (i) one and multi-step drying or wetting paths under constant net stress and (ii) increase net stress (loading) under constant suction. Thus suction is controlled in the cells. In the axis-translation technique, using ceramic disk, the change of water level of the attached burette that has a high accuracy is measured (change of water content). In the vapour equilibrium technique, using vapor circulation system with porous stone, the light weight cell can be weighted directly to measure the change of water content due to suction change. The valves were closed and the volume (height) of the specimen was kept constant through the weighting process by preventing the piston movement. The net stress is applied using the mechanical oedometer frame and the volume measurements are performed by the attached dial gauge (Figure 4.1b). The specimen ring has 70 mm in diameter and 20 mm high.

(a) **(b)**

Figure 4.1 modified controlled-suction oedometer cells: (a) Red and black cells. (b) appling net (vertical) stress.

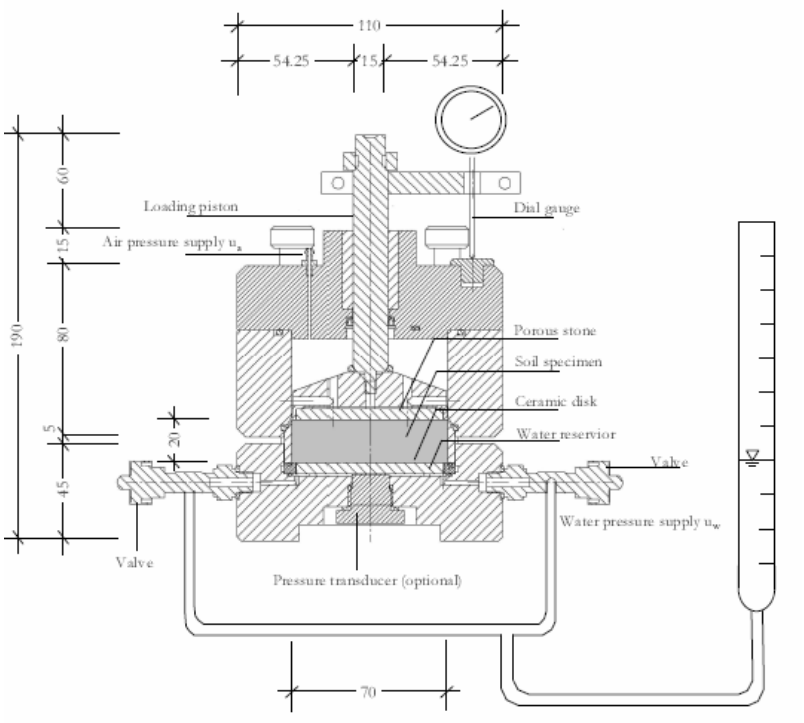

Figure 4.2 Cross sectional area of the modified controlled-suction oedometer device for the Black cell, all dimensions in mm, (Lins, 2009).

4.3.2 UPC-Barcelona cell

The cell was made by the workshop at Universitat Politècnica de Catalunya (UPC), Barcelona, Spain (Figure 4.3). The cell is controlled-suction oedometer and the suction can be controlled using either axis-translation technique or vapour equilibrium technique. The vertical or net stress is applied by air pressure using flexible membrane. Similar to the modified controlled-suction oedometer cells, the UPC-Barcelona cell was used for determination of the one dimensional volume change under 1D strain condition (i) one and multi-step drying or wetting paths under constant net stress and (ii) increase net stress (loading) under constant suction. The vapour equilibrium technique did not use in this cell. Therefore, the axis-translation technique is used only to control the suction. The UPC-Barcelona cell is connected with high accuracy burette, one air-pressure system for application of matric suction as well as one air-pressure system for application of vertical net stress. The diameter of the specimen is 50 mm and the high is 20 mm.

The pressure-deformability of UPC-Barcelona cell during loading and unloading was verified using dummy stainless steel specimen (Agus, 2005). The stainless steel specimen was placed in the oedometer cells with two dry filter papers (i.e., each on the top and bottom of the dummy specimen). When a real soil specimen is saturated, the filter papers used will be wet and therefore dummy tests were also performed with wet filter papers. The dummy stainless steel specimen with the filter papers was subjected to increasing and decreasing vertical pressure in the oedometer test system. Figure (4.4) shows the deformation characteristic of the UPC-Barcelona cell. The deformation characteristic of the systems was used to give correction to the one-dimensional unsaturated volume change tests.

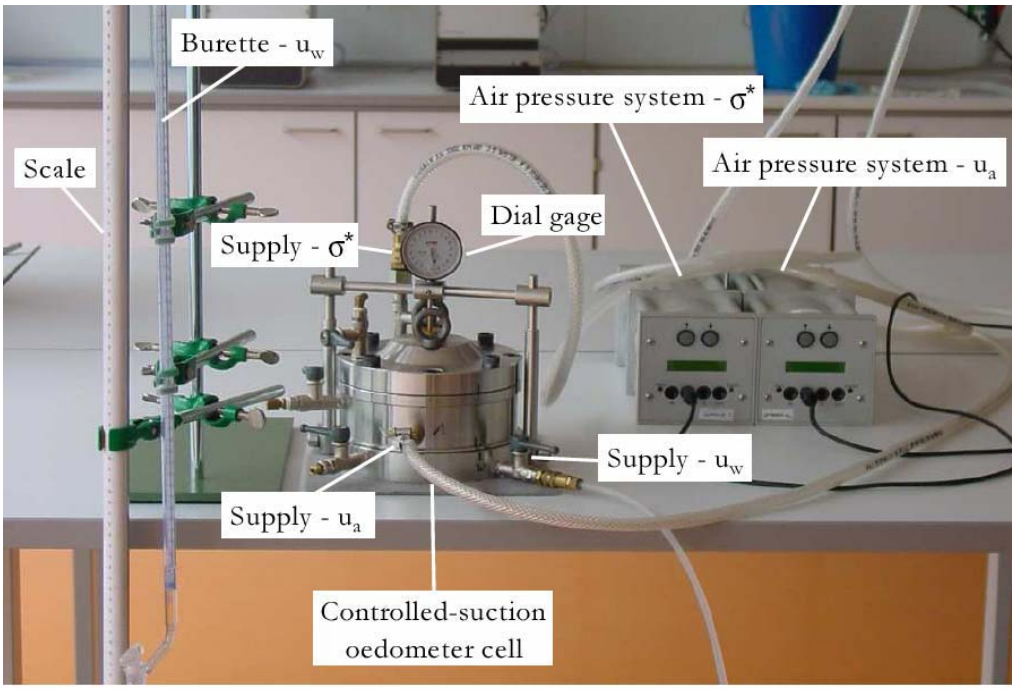

Figure 4.3 UPC-Barcelona cell setup.

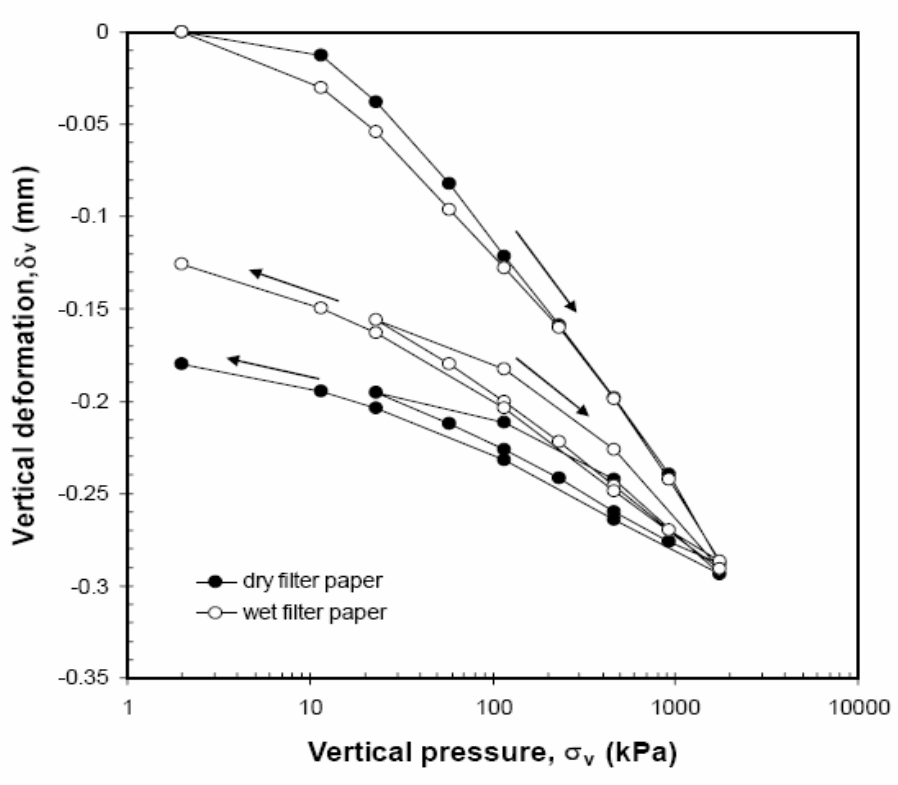

Figure 4.4 Pressure-deformation calibrations of the UPC-Barcelona cell (Agus, 2005).

4.3.3 UPC-Isochoric cell

The isochoric cell developed as well at the Universitat Politècnica de Catalunya (UPC), Barcelona, Spain (Figure 4.5a). The cell is designed to perform constant volume test. The cell has been used originally to measure swelling pressure of compacted soil during wetting at room temperature by Villar et al. (2001) and Agus (2005) and at high temperature by Arifin (2008). Both axis-translation technique and the vapour equilibrium technique can be used to control the suction in this cell. The cell mainly consists of a pedestal, a threaded top part with a top cap and a load cell. The pedestal is exchangeable that makes it possible to perform tests using the water circulation, axis-translation, and vapor equilibrium techniques. The pedestal used for the axis-translation technique was designed to have a grooved water compartment where a high-air-entry ceramic disk is seated flushed and glued. The grooves are 3 mm wide and 1.5 mm deep and form a spiral. The ceramic disk used has an air-entry value of 1500 kPa. The top cap has a corrosion resistant metal porous disk. In case of using the vapour equilibrium technique to apply suction, the cell was equipped with an Erlenmeyer flask and an air pump to circulate water vapor through the specimen bottom and top boundaries.

The cell was modified by adding a base plat to fix the cell on the mechanical oedometer frame (Figure 4.4b) to apply vertical net stress for determine the volume change. Therefore, the UPC-Isochoric cell was used in this study to apply controlled-suction one-dimensional deformation.

In the axis-translation technique, using ceramic disk, the change of water level of the attached burette that has a high accuracy is measured (change of water content). In the vapour equilibrium technique, using porous stone, the light weight cell can be weighted directly to measure the change of water content due to suction change (Figure 4.5c). Similar to the modified controlled-suction oedometer cells, the piston movement was prevented and the valves were closed to keep the volume of the specimen constant through the weighting process.

Four isochoric cells were used in this study. The pressure-deformability of four cells used was calibrated by pressurising the cells (with the load cells installed) with air (Agus, 2005). The cells were subjected to increasing and decreasing air pressures while the deformations were recorded using linear vertical displacement transducers (LVDT). Figure (4.6) shows vertical deformation of the cells as a function of applied air pressure.

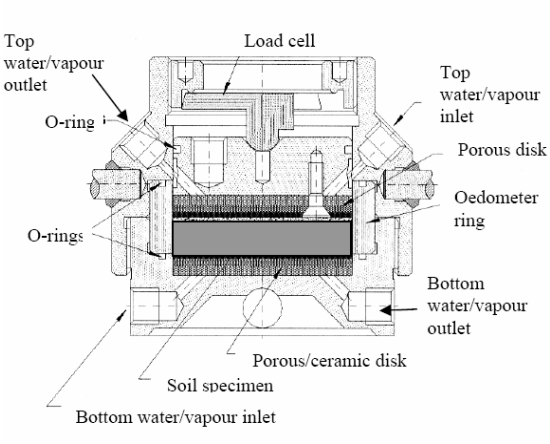

(a)

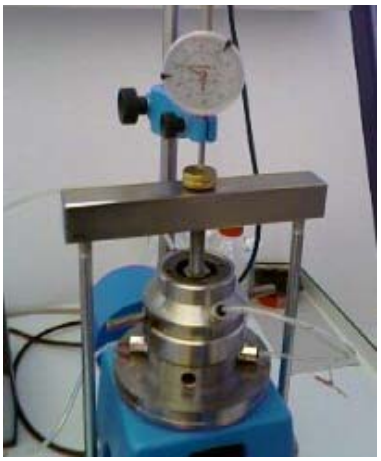

(b)

(c)

Figure 4.5 Isochoric-UPC cell: (a) Isochoric cell as used for constant volume test with schematic of the cell, (b) Isochoric cell with oedometer frame, (c) Measuring the water content during the test.

The movable piston of UPC-isochoric cell has O-ring. Therefore, there is a small amount of friction generated due to vertical movement of piston that leads to produce some error of the measured net stress. Two consolidation tests were performed using two identical slurry 30B soil specimens, as shown in Figure (4.7). One specimen was tested using UPC-isochoric cell and the other was tested using UPC-Barcelona cell. The figure clearly shows that the results of the UPC-isochoric cell provide reliable values for net stress more than 50 kPa. Therefore, the UPC-isochoric cell used to exam the volume change behavior with respect to net stresses values grater than 50 kPa.

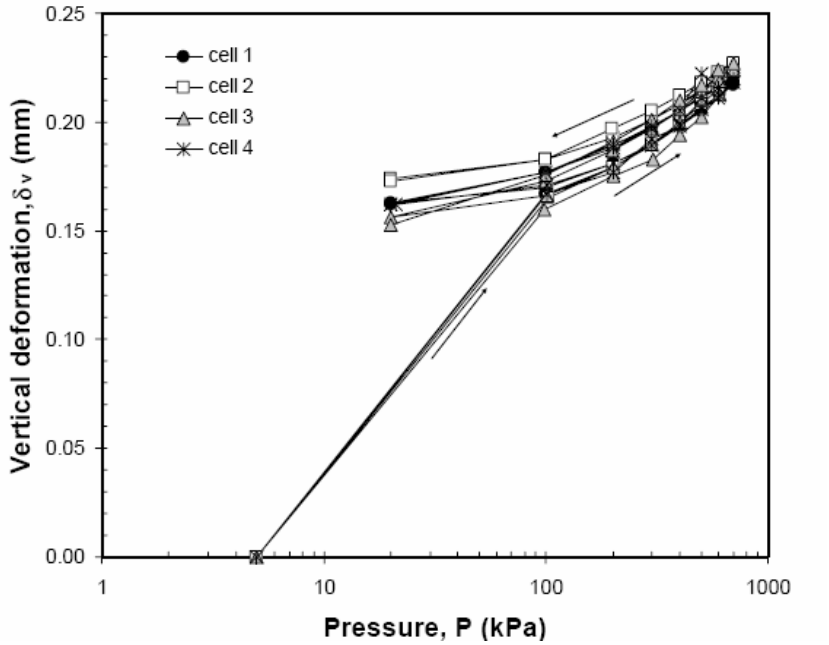

Figure 4.6 Pressure-deformation calibrations of the four UPC-isochoric cells as a function of applied air pressure (Agus, 2005).

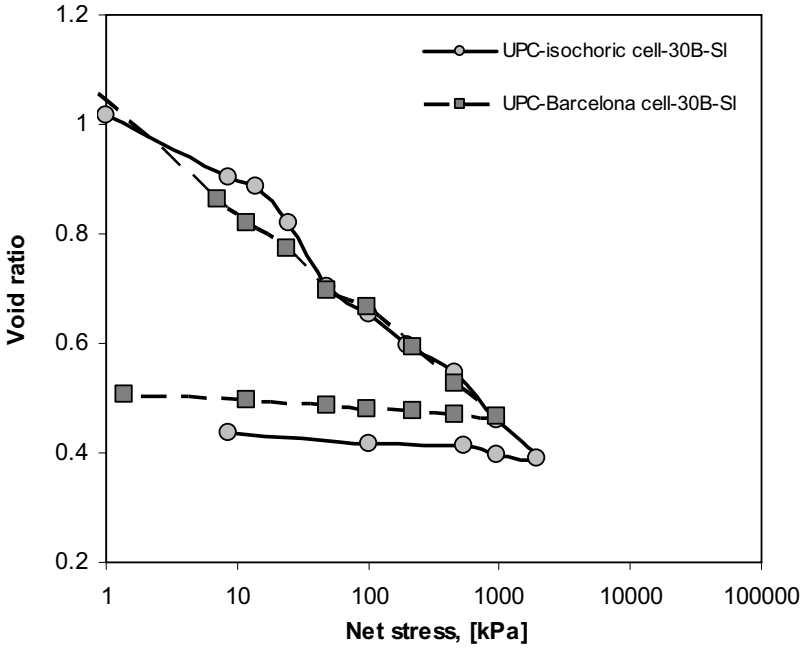

Figure 4.7 Comparison between two consolidation tests using UPC-isochoric cell and UPC-Barcelona cell for identical slurry 30B soil specimens.

4.3.4 High stress oedometer cell (HSC)

A newly developed high pressure oedometer device fabricated by Wille Company, Germany (Figure 4.8), as used by Baille et al. (2010), was used in this study. The cell enables to (i) loading the specimens (compression test) up to 25 MPa and (ii) measurement of swelling pressures of initially unsaturated compacted bentonite specimens constant volume test. The high stress oedometer cell was used for one-dimensional determination measurements (volume change) when the range of the applied net stress (>1 MPa) of (i) one and multi-step drying or wetting paths under constant net stress and (ii) increase net stress (loading) under constant suction.

In Figure (4.8), a bottom stainless steel base (no. 3) houses a porous stainless steel plate (no. 7) and the bottom water chamber (no. 19). The central part of the device (no. 2) holds a thick walled specimen ring of thickness 20 mm and 50 mm in diameter (no. 4) that accommodates a compacted clay specimen (no. 5), and a pressure pad with a porous stainless steel plate (no. 6). The top part carries the loading piston (no. 10) attached with a force transducer (no. 8). The force transducer used in this study had a maximum loading capacity of 50 kN with a precision of 0.001 kN. A strain gauge (no. 9) with a precision of 0.001 mm and a total run of 25 mm was connected directly to the loading piston to record the vertical deformation. The bottom and the central parts are connected with the help of heavy screws (no. 17), whereas the top part is directly screwed onto the central part. The force transducer together with the loading piston becomes fixed between the pressure pad (no. 6) and the upper restraint (no. 12).

The pressure-deformation characteristic of the device was calibrated using a steel dummy (Baille et al., 2010), Figure (4.9). The measured deformations during loading–unloading cycles included the deformation of the loading piston, the transducer, the oedometer cell, and the loading frame, and thus represent the total deformation of the system. Based on the pressure-deformation characteristic of the device, the volume change of the specimen during the test during the compression test was corrected.

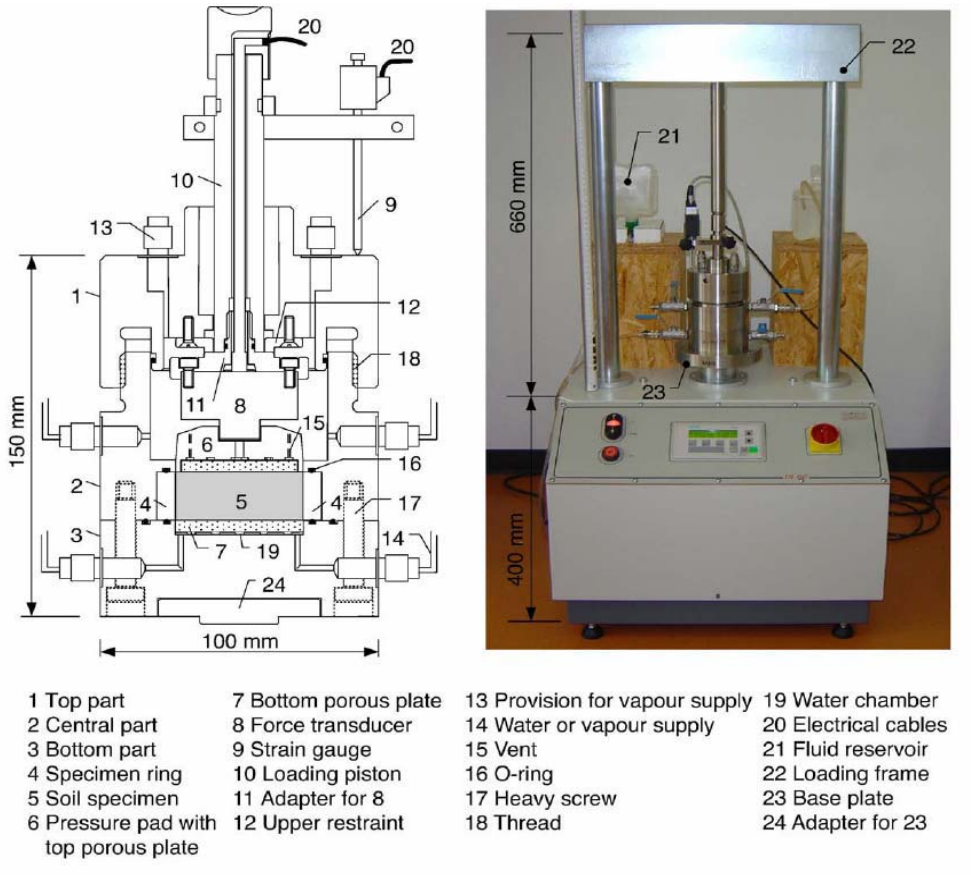

Figure 4.8 New HSC with sketch of the cell (left), and the test set up (right), (Baille et al., 2010).

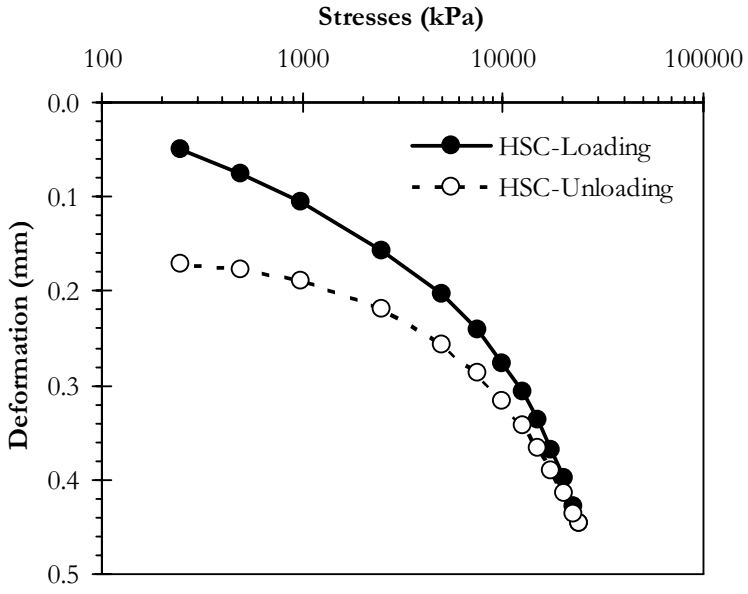

Figure 4.9 Pressure-deformation calibrations of HSC, (Baille et al., 2010).

4.4 Devices used for applying isotropic stress

The isotropic consolidation test was performed using triaxial cell (Fig. 4.10). The specimen has dimensions 50 mm diameter and 40 mm height. Figure (4.10) presents the triaxial cell capable of subjecting soil specimens to cell pressures up to 1700 kPa. The cell pressure is supplied using a digital volume pressure controller (VPC) device capable to pressurize water up to 4000 kPa (40 bar). While the back pressure is applied using air-water interface cell consist of twin-burette volume change indicators enable to apply the back pressure and measure the overall volume change of the specimen.

4.5 Techniques used for controlling suction

Two main types of techniques for controlling soil suction have been used in experimental program: the axis translation technique (ATT), and the relative humidity control or vapor equilibrium technique (VET).

4.5.1 Axis translation technique (ATT)

The technique was adopted to determine loaded (one dimensional) and unconfined drying and

Figure 4.10 Triaxial cell setup used in isotropic consolidation test.

wetting paths in the low suction range (i.e., less than 1500 kPa). In the technique, matric suction is applied. Matric suction is mostly associated with the soil matrix and is defined as the difference between pore-air and pore-water pressure of the soil (u_a-u_w). Therefore, measuring negative pore-water pressure can be avoided by increasing the pore-air pressure while maintaining the pore-water pressure to a positive reference pressure (i.e., axis-translation technique) (Hilf, 1956). The measurement of matric suction using this technique is only limited by the air-entry value of the ceramic disk (air-water interface) used since cavitations be avoided due to elevated pore-water pressure. Ceramic disks with a maximum air-entry value of 1500 kPa are available commercially. Olson and Langfelder (1965) developed a pressure plate apparatus for applying matric suction using the axis-translation technique. Since water pressure in the water compartment is maintained as close as possible at a zero value, the technique is called null-type axis-translation technique (Fredlund, 1989).

In the one-dimensional compression cells, porous stone is replaced by ceramic disk in order to use axis-translation technique for the application of controlled-suction test (i. e., modified controlled-suction oedometer cell, UPC-Barcelona cell, UPC-isochoric cell, and HSC cell). In this case, where there water content of the specimen is determined by measuring the water level in the accurate burette, the evaporation correction has to be assessed. For unconfined drying and wetting paths the pressure plate apparatus from Soil Moisture Company (Figure 4.14) was used.

4.5.2 Vapor equilibrium technique (VET)

The vapour equilibrium technique (VET) was used to determine loaded (one dimensional) and unconfined drying and wetting paths in the high total suction range (i.e., greater than 2000 kPa).

Flask with circulation system (loaded test, as Figure 4.11 for UPC-isochoric cell) and desiccator (unconfined test, Figure 4.14) were used to apply the vapor of molal salt solution to the specimens. Several aqueous and molal salt solutions were used to induce total suction to the specimen by changing the relative humidity of the vapour space in the desiccator. The total suction of salt solution can be calculated using osmotic coefficient data using Equation (4.1) suggested by Lang (1967).

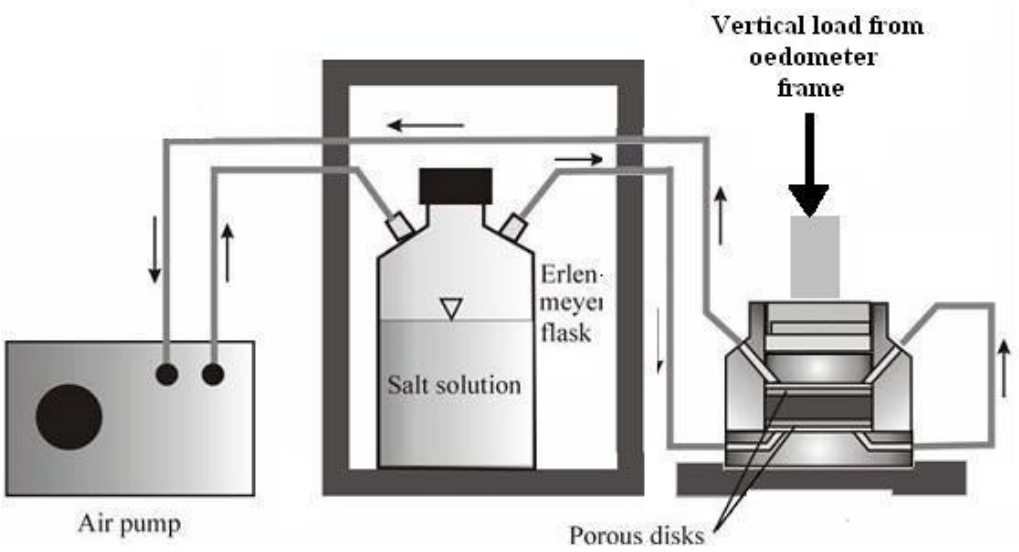

Fig. 4.11 Applying suction on the UPC-isochoric cell using vapor equilibrium technique with circulation system.

$$s_t = 2mRT\phi \qquad 4.1$$

where s_t is total suction in kPa, m molal salt solution (mol/Kg), R is the universal gas constant (i.e., 8.31432 J/mol K), T is absolute temperature in Kelvin, and ϕ is coefficient.

4.6 Measuring of suction

Ridley and Wray (1996) categorized the suction measuring devices into two types: those that measure the suction directly and others that measure it indirectly. With direct measurement, the relevant quantity is measured, namely the pore water energy or tensile stress. The indirect devices are ones that measure another parameter (e.g. relative humidity, resistively, conductivity or moisture content), which are related to the suction through calibration relationships. For both cases, they emphasize the importance of knowing whether total or matric suction is being measured. In general, if no contact is made between the measuring device and the soil water, the relative humidity of the ambient air within the soil is measured and so it is the total suction. If a good contact is assumed between the soil water and the measuring device, and the concentration of dissolved salts can be assumed to be the same everywhere, the matric suction is being measured. However at low degrees of saturation, the soil water might move away into the finer pores and become discontinuous, in which case it is normally difficult to guarantee that full contact is made and that the matric suction is being

measured. In the current study, only the chilled mirror technique (using relative humidity technique) was used.

4.6.1 Chilled mirror technique

The chilled-mirror technique is used for measuring the relative humidity of the air space over the soil specimen. Therefore, the technique used for total suction measurements. The chilled-mirror, in this study, was used for measuring the total suction of specimens and verifying the salt solution used in vapor equilibrium technique. The chilled-mirror used in this study was a water activity meter type 3TE produced by AQUA LAB device, Figure (4.12). The equipment has a special specimen closed chamber of about 12 cc in volume, where the soil specimen is placed. The components and principal working of the equipment were described in Leong et al., (2003); Albrecht et al., (2003); and Agus and Schanz, (2005b). The sensors in Chilled Mirror apparatus measure the relative humidity of the air space over the soil specimen at a given temperature. Agus and Schanz (2007) stated that the technique can be used for suction measurement as low as 1500 kPa if the maximum measurement error is limited to 30 %.

The total suction in the chilled-mirror technique can be calculated using Kelvin equation (Thomson, 1871) that is the thermodynamic relationship between total suction and relative humidity of the vapor space in the soil (Sposito, 1981).

$$s_t = -\frac{RT}{M_w(1/\rho_w)}\ln\left[\frac{RH}{100}\right] \qquad 4.2$$

where s_t is total suction in kPa, R is the universal gas constant (8.31432 J/mol K), T is absolute temperature in Kelvin, M_w is the molecular weight of water (18.016 kg/kmol), ρ_w is the unit weight of water in kg/m^3 as a function of temperature, and RH is the relative humidity.

The measurement of total suction using this technique was commenced by switch on the device for sufficient time (about 1-2 hours) to reach to equilibrated temperature. Then placing the soil specimen in the special chamber not more than half its capacity. Immediately, the chamber with the specimen inside was placed in the device. The soil in the specimen chamber in the device was allowed to reach isothermal equilibrium which was defined as the difference between temperature of the vapor space and the specimen. The device showed the difference in temperature between the headspace and the mirror. The chamber was closed and after reaching equilibrium in about 3 minutes, the relative humidity and the temperature of the vapor space were shown in the display. The measurement was performed many times for each

Figure 4.12 The chilled-mirror hygrometer (AQUA LAB) used in this study.

specimen until obtained two identical readings. The same procedure was applied for verifying salt solutions used in vapor equilibrium technique.

4.7 Experimental procedures

4.7.1 Volumetric yielding tests program for unsaturated soils

In this study the volumetric yielding tests are carried out to determine the volume change at normal consolidated (yield) state for unsaturated condition. All volumetric yielding tests are one-dimensional controlled-suction tests using the cells mentioned in section (4.3.1). The volumetric yielding tests include constant degree of saturation test, constant net stress test, constant suction test, and changing both net stress and suction test. Suction test takes considerable time, thus, in all type of tests the duration of each step of suction change takes 1-4 weeks for 30B and 1-3 months for 100B until the water content reaches to equilibrium condition.

4.7.1.1 Constant degree of saturation test

To investigate the validity of S_r-lines (Al-Badran, 2001), the constant degree of saturation test was proposed. The test was performed by controlled-suction one-dimensional compression device, in which both the net stress and the suction can be controlled. In this test the suction was applied by axis translation technique (ATT). During the test the deformation was measured and the degree of saturation was kept constant by controlling net stress and suction.

However, there are many difficulties in this test, such as when suction increases the reduction in water content needs time to equilibrate (1-4 weeks), while the volume change response faster (1-4 days) when the net stress increases. Firstly the suction is increased. The net stress was kept constant until the change of water content reaches to equilibrium (1-4 weeks), and then the net stress is increased slowly. At the end of each net stress level the degree of saturation was calculated (by computing the current volume of the specimen and the water content) until the degree of the saturation reaches to the target value. In this stage, one point of the constant degree of saturation test is obtained. Repeat the same steps starting by increasing suction to gain the other points.

4.7.1.2 Constant net stress test (multi-step controlled-suction test)

The net stress was kept constant through the test. This type of tests was divided into two categories: drying test (increase suction) and wetting test (decrease suction). In both cases the suction is applied by axis translation technique (suction < 1500 kPa) and vapor equilibrium technique (suction > 2000 kPa).

Constant net stress test with increasing the suction (drying)

The drying tests were performed for initially slurry specimens to investigate the volume change of soil when the soil state is transferred from saturated to unsaturated ones. The initially slurry specimen was loaded till reaching the target net stress under zero applied suction (saturated state). Then the suction was increased under the constant net stress. Through the test, variation in volume and water content of the specimen were measured.

Constant net stress test with decreasing the suction (wetting)

The wetting tests were performed for initially unsaturated loose specimens to determine the volumetric yielding at unsaturated state. The initially unsaturated loose state specimen was loaded till reaching the marked net stress under constant suction equal to corresponding suction of the initial water content. Then the suction was decreased under the constant net stress. Through the test, the change of the volume and the water content were measured.

4.7.1.3 Constant suction test

The applied suction was kept constant through this test. The suction was applied by axis translation technique (suction < 1500 kPa) and vapor equilibrium technique (suction > 2000 kPa). Both slurry and loose initial states were used in this type of test to investigate the volumetric yielding at constant suction under different initial soil structure. In case of slurry initial state the suction is increased up to the target suction under seating net stress (< 5 kPa). The constant suction of the initially loose state equals to the corresponding suction for the

initial water content. Then the net stress is increased in both states. Again through the test, the variation in the sample volume and water content were measured.

4.7.1.4 Changing both net stress and suction test

Three identical specimens were used in this series to investigate the uniqueness of the state surface. The two stress variables (net stress and matric suction) for the three specimens are varied along three different paths. However, the initial and the final two stress variables for the three specimens are identical. Additionally, the stress paths intersect in different points, see Figure (3.7). The initial state of the specimens is loose under unsaturated condition with following properties e_o = 0.723, w_o= 0.4, s_o = 80000 kPa, as in Table 3.5). The stress path of each test was given in Table (3.6) and Figure (3.7).

4.7.2 Soil water characteristic curve (SWCC) tests program

As mentioned in section (4.4), there are two types of techniques for unconfined controlling soil suction, which have been used in this study; the axis translation technique (ATT) (suction < 1500 kPa), and the vapor equilibrium technique (VET), (suction > 2000 kPa). The pressure plat with different air pressure values, was used to apply ATT, while desiccator, with different molal salt solutions, was used to apply VET. The duration of each step of suction change takes 1-3 months (in case of high suction increment it takes 6 months) until the water content reaches to equilibrium condition. The long duration is due to the mixing the specimens of 30B soil and of pure bentonite 100B have to be placed in the same pressure plate device in ATT and the same desiccator in VET during the tests. The total duration of SWCC's tests (30B-P0.001-d&w-Sl, 30B-P0.001-d&w-com1, 30B-P0.001-d&w-com2, 100B-P0.001-d&w-Sl, and 100B-P0.001-d&w-com1) is about three years by using four identical specimens for each specific test and then divided into two groups (each group two identical specimens) to reduce the time of the test.

Pressure plate (using ATT)

For unconfined drying and wetting paths the pressure plate apparatus from Soilmoisture (Figure 4.13) was used. The main part of the pressure plate apparatus is the high-air-entry ceramic plate. Three ceramic plates with different air-entry values; namely, 100 kPa, 500 kPa and 1500 kPa were used in the investigation depending on the applied matric suction. The use of ceramic plate with a high air-entry value is not desirable when lower matric suction value is

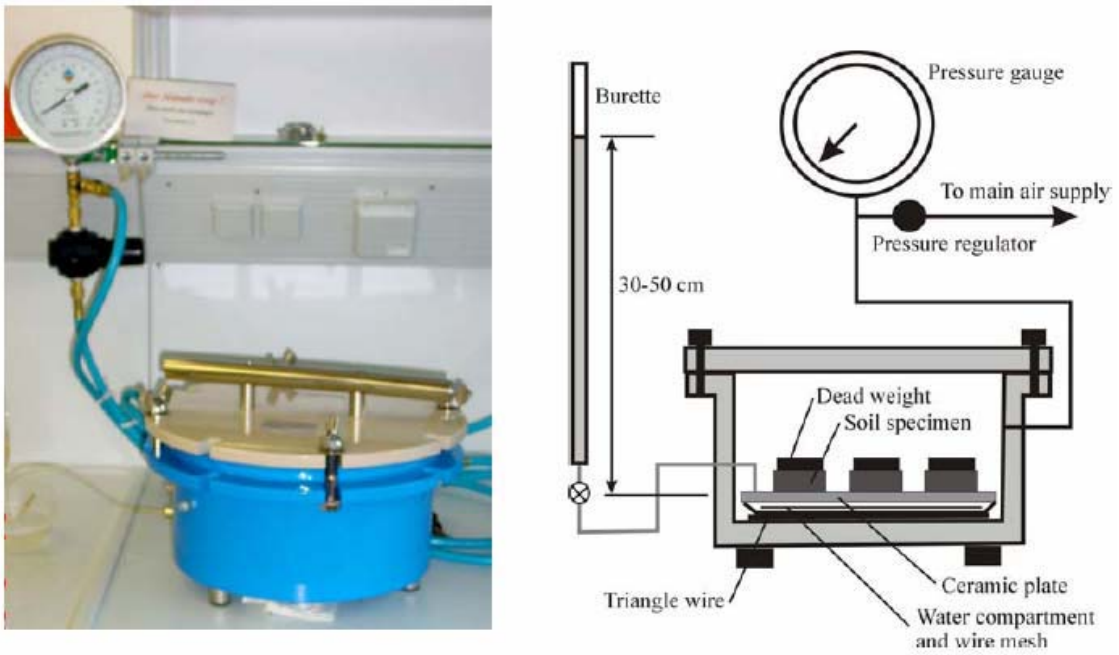

Figure 4.13 Pressure plate apparatus setup used in study.

to be applied (Agus, 2005). This is due to the fact that the coefficient of permeability of the ceramic plate with a higher air-entry value is lower than that of the ceramic plate with a lower air-entry value. Therefore, the test can run for long time duration. Slurry specimen and different densities of compacted bentonite-sand specimens were placed on the ceramic plate. A dead weight of about 50 g was placed on the specimen to maintain a good contact between the specimen and the ceramic plate.

An air pressure was slowly and carefully applied to reach the target matric suction by also considering the water column in the burette. The flushing of the water compartment was performed regularly to remove the diffused air bubbles collected beneath the ceramic disk. It is important to note that the existence of diffused air bubbles in the water compartment results in discontinuity between the water phase in the specimen and the source of water. The water phase continuity has to be established through out the experiment as to warrant liquid transfer of water into and out of the specimen. The water outlet in the pressure plate apparatus was connected to a burette for flushing purpose. The test started with saturating the ceramic plate with distilled deaired water. The water compartment located between the ceramic plate and the rubber membrane was filled with distilled deaired water. Low value of air pressure of (about 1half value of its air-entry value) was applied to pressurise water on the ceramic plate for several hours. The pressurisation was stopped when no air bubbles were observed to come out of the compartment and flowed towards the burette. Diffused air bubbles collected beneath the ceramic plate was flushed using sufficient amount of water in the burette. The

above flushing process repeated at least two times until no air bubbles were observed. The water left on the ceramic plate was wiped off and an air pressure as high as the air-entry value of the ceramic plate was applied. The water level in the burette was monitored. Initially, there was a small increase in burette water level. The water level in the burette stopped increasing indicating that there was no air flowed across the ceramic plate.

The change in mass and dimensions (i.e., the diameter and height) of the specimen were monitored. A precision weighing balance with an accuracy of 0.0001 g was used to weigh the specimen. The dimensions of the specimen were monitored using a digital vernier calipher that could measure to the nearest 0.01 mm. At low matric suction (i.e., below 80 kPa), the measurement of dimensions of the soil specimen was only performed after the specimen had reached equilibrium based on the water content versus time plot. At matric suction below 80 kPa, the specimen was soft enough such that the dimension measurement using the digital calliper could introduce disturbance along the circumference of the specimen. After each suction equilibration, the ceramic disk was resaturated. Both water content and void ratio of the specimen were used to judge the equilibrium conditions before applying the next matric suction increment or decrement.

Desiccator (using VET)

The experiment was conducted in a temperature-controlled room that could maintain a constant temperature of $22^oC \pm 0.5^oC$. In this study a large desiccators for testing up to eight specimens simultaneously (Figure 4.14) were used. Several aqueous and molal salt solutions were used to induce total suction to the specimen by changing the relative humidity of the vapour space in the desiccator. Procedures similar to those used in the pressure plate apparatus (ATT) to determine the changes in water content and void ratio was adopted. At the end of the test, the relative humidity of the solution was measured using chilled mirror technique to compute the actual total suction applied to the specimens.

4.8 Compaction procedure

Two different types of compaction were used in this study; static compaction and dynamic compaction. The steps of preparing the soil before performing the test are the same for both types of compaction and as follow. The preparation starts by mixing the soil with different amount of water and then stores the mixture for at least one week by remixing the soil daily to ensure of distribute the water homogenously.

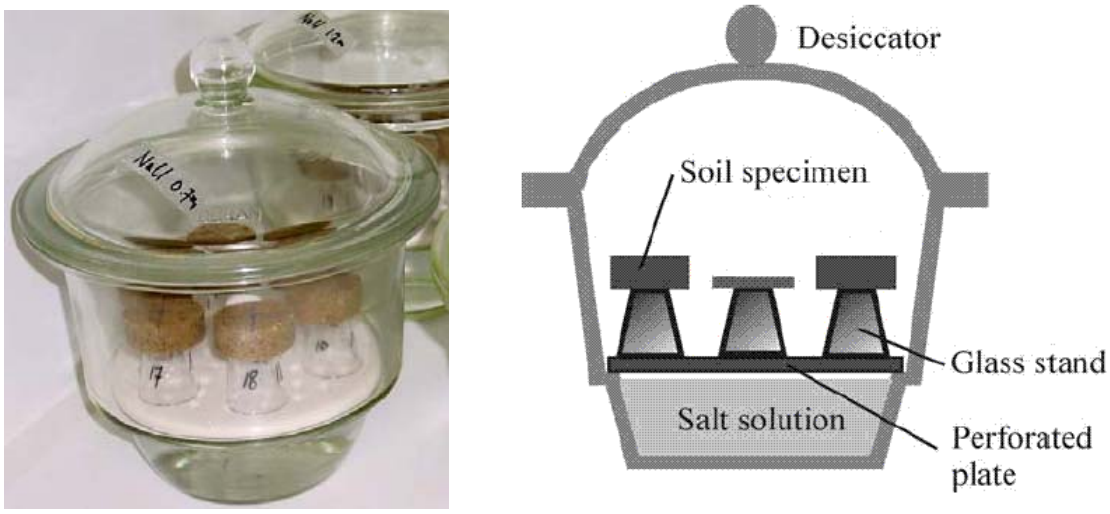

Figure 4.14 Large desiccator test setup used in study.

4.8.1 Static compaction

The static compaction was applied by means of one-dimensional (oedometer) compression cell and compression machine which enables to apply constant force. A specific amount of mixed soil was placed in the cell and then the constant force (stress) was applied until no further settlement is recorded. After that the displacement of the piston was recorded to know the volume of the mixed soil under the constant net applied stress. Then the wet weight of the soil and the water content were measured to calculate the dry density for this water content. These steps were repeated for different values of water contents to draw the static compaction curve of this applied stress.

4.8.2 Dynamic compaction

The dynamic compaction was performed by means of allowing the hammer to drop several times on a mixed soil in a mold according to ASTM D698 standard (SP), ASTM D1557 standard (MP). Then the wet weight of the soil and the water content were determined to calculate the dry density for this water content. These steps were repeated for different values of water contents to draw the dynamic compaction curve of this applied compaction effort. The size of mold, the weight and the height of fall of the hammer, number of blows, and the applied energy for Standard Proctor (SP) and Modified Proctor (MP) were shown in Table (2.3).

4.9 Summary

This chapter presents the specimens preparation, devices, and experimental techniques and procedures used in determination of volume change of saturated and unsaturated states. To cover all the possible states of unsaturated volume change, the initial conditions of the specimens used are divided into two states: (i) Slurry (Sl) when drying path was applied and (ii) Loose (Lo) when wetting path was applied. Two types of techniques for controlling soil suction have been used in this study; the axis translation technique ATT (suction <1500 kPa), and the vapor equilibrium technique VET (suction > 2000 kPa). The state of the applied net stress in study is mainly one-dimensional using; the modified controlled-suction oedometer cell, UPC-Barcelona cell, UPC-Isochoric cell, and high stress oedometer cell. Only one test for each soil was carried out by applying isotropic stress using triaxial device to locate the position of isotropic normal consolidation line (iso-NCL). The procedure followed for each test depends on the type of the test. Prior to the tests, all the devices were checked to confirm the applicability. The required devices calibrations are presented as well.

Chapter 5

Experimental Results

5.1 General

This chapter provides an extensive overview for the experimental results of the one dimensional volumetric yielding tests (constant degree of saturation test, constant net stress test, constant suction test, changing both net stress and suction test) and the compaction tests (static and dynamic compactions) for unsaturated pure bentonite (calcigel), 100B, and 30 % bentonite- 70 % sand mixture, 30B. In addition, the results of the soil water characteristic curve (SWCC) program and the consolidation tests are presented.

5.2 Volumetric yielding tests

In the following sections the results of 1D-volumetric yielding tests will be presented for 100B and 30B soils. Slurry and unsaturated loose conditions were chosen as initial states in the experimental program to cover the major ranges of soil structures. Initially slurry state was used and followed by drying process to determine the volume change when soil state changes from saturated to unsaturated. Unsaturated loose state was chosen as initial state followed by wetting process to investigate the volumetric yielding behavior of unsaturated soils. The volume-mass constitutive surface is stress path dependent (Fredlund and Rahardjo, 1993). Therefore, four different types of one-dimensional (oedometer) controlled-suction tests were performed for unsaturated 30B and 100B soils (constant degree of saturation test, constant net stress test, constant suction test, and changing both net stress and suction test) to determine and verify the volumetric yielding behavior of unsaturated state. The results of constant degree of saturation test are shown with three relationships i. e., void ratio-log net stress, degree of saturation- log net stress, and gravimetric water content- log net stress. Furthermore, for the other types of tests as explained earlier, the volume change behavior due to change in net stress and suction are presented with four relationships namely, a) void ratio-log net stress, b) void ratio-log suction, c) gravimetric water content-log suction, and d) degree of saturation-log suction. Due to the many presented relationships, each test is denoted by points (A, B, C, and D) to make the test easy to follow. The 1D-NCL for each soil was determined using high

oedometer stress cell (HSC), and the isotropic NCL for each soil was determined using a triaxial cell. These two NCL lines were denoted in most figures in this series of tests (Figures 5.5-5.47) to show the position of compression curves.

5.2.1 Constant degree of saturation test

The results of constant degree of saturation tests under one-dimensional controlled-suction compression condition are be presented. Such tests, to the best of the knowledge of the author have been not carried out earlier by other investigators. Two tests for compacted 30B soil were conducted to determine the normal consolidated lines (NCL's) of constant degrees of saturation equal to 0.58 and 0.68: 30B-Sr58-com and 30B-Sr68-com tests. The initial point is denoted as point A, whereas points B and C represent the point of the beginning and the end the constant degree of saturation condition, respectively.

Figure (5.1) shows the volume change at 0.58 constant degrees of saturation test for 30B soil, while Figure (5.2) shows the volume change at 0.68 constant degrees of saturation test for 30B soil. In Figures (5.1) and (5.2), the initial part (before the preconsolidation pressure) for both compression and degree of saturation curves give unsmooth relationship. This behavior is due to changing the two stress variables (net stress and suction) to achieve volumetric yielding under constant degree of saturation state. Figure (5.3) presents the gravimetric water content for both constant degrees of saturation tests (0.58 and 0.68). Figure (5.1) and (5.2) show that the condition of the volumetric yielding under constant degree of saturation is valid for net stress more than 183 kPa for 30B-Sr58-com test and more than 100 kPa for 30B-Sr68-com test (from B to C). Figure (5.4) presents the data of volumetric yielding under constant degrees of saturation state of 0.58 and 0.68 for 30B soil.

The results in Figure (5.4) show that the NCL for both tests are almost straight in semi-log scale, and have slopes near to the slope of the saturated normal consolidation line (NCL). Indeed, the slope of the compression line is slightly more than the slope of the saturated NCL. Moreover, Figure (5.4) depicts almost the same behavior as it was assumed in Al-Badran (2001) and Kanazawa et al. (2009). The models of Al-Badran (2001), see Figure (2.18) and Kanazawa et al. (2009), see Figure (2.24), assumed that the NCL at any constant degree of the saturation (S_r-lines in Al-Badran, 2001) is parallel to the saturated NCL. Net stress-suction relationships under volumetric yielding for both constant degree of saturation tests are presented in chapter 3, Figure (3.4).

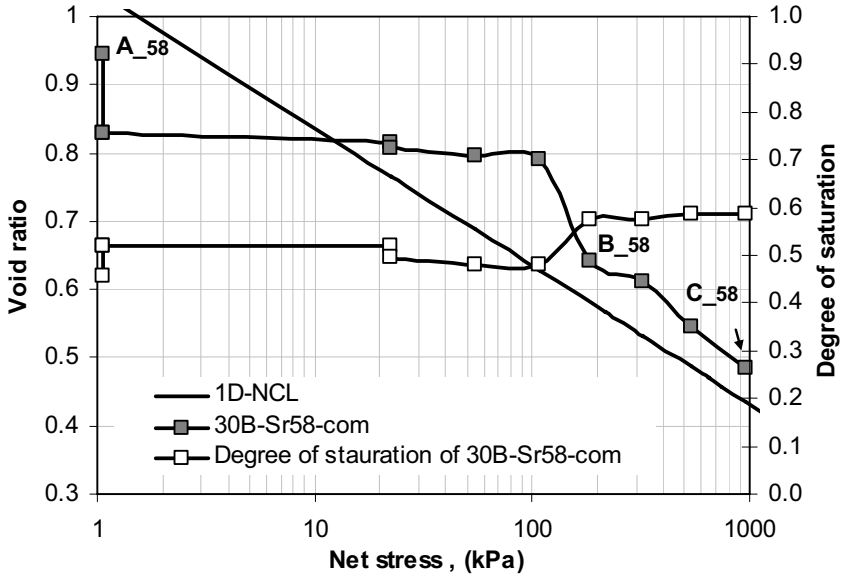

Figure 5.1 Volume change and the degree of saturation in drying path for 0.58 constant degrees of saturation test for 30B soil.

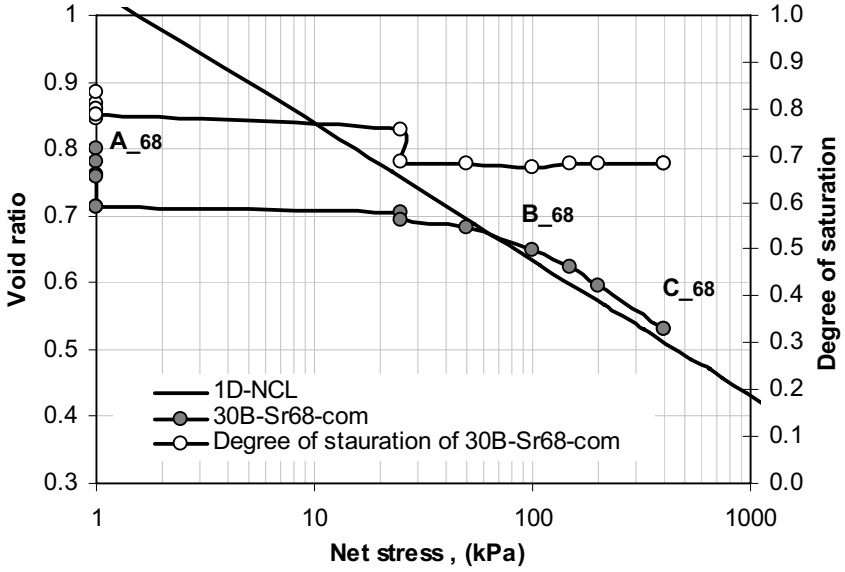

Figure 5.2 Volume change and the degree of saturation in drying path for 0.68 constant degrees of saturation test for 30B soil.

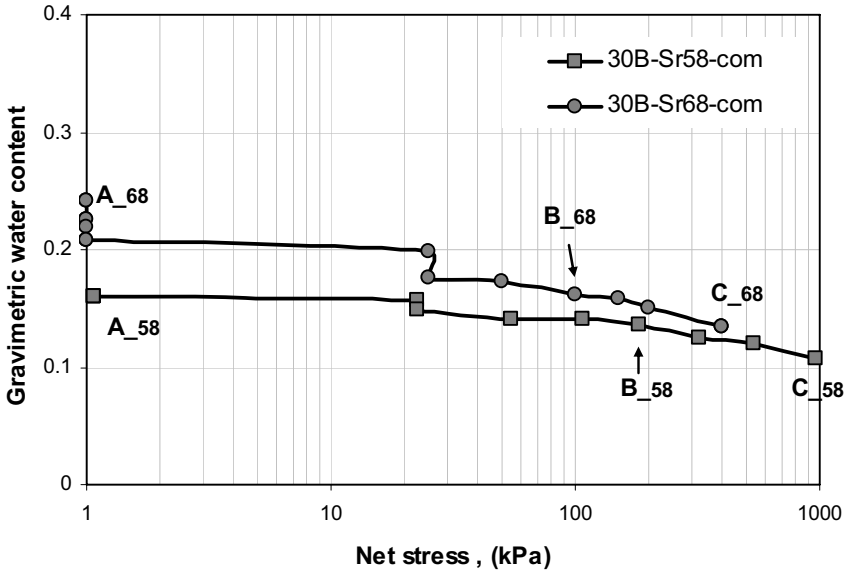

Figure 5.3 Gravimetric water content for constant degrees of saturation tests (0.58 and 0.68) for 30B soil.

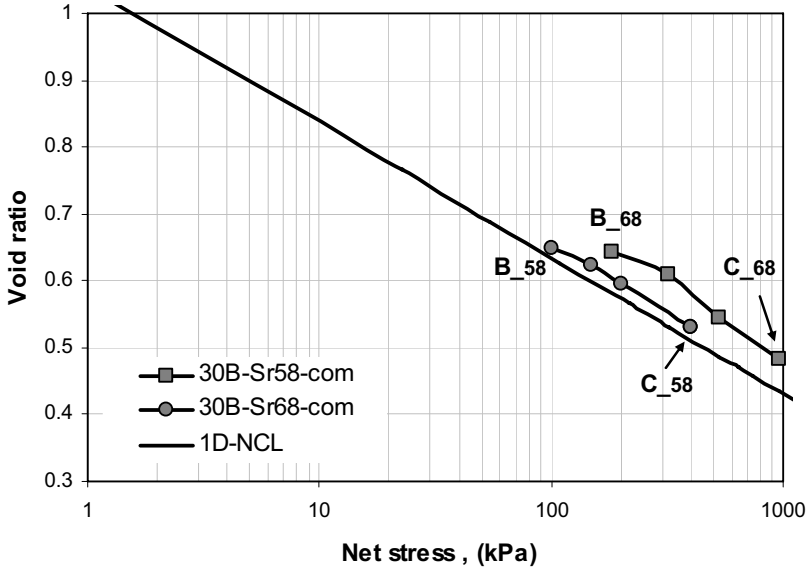

Figure 5.4 NCL's under constant degrees of saturation state (0.58 and 0.68) for 30B soil.

5.2.2 Constant net stress test

The results of the volume change test under constant net stress condition are presented in this section. Two types of tests are reported: drying test (increase suction) for initially slurry specimen and wetting test (decrease suction) for initially loose specimen. The net stress is kept constant through the test. The initial conditions of all constant net stress tests and the

stress paths for each test in (net stress-suction) space are shown in Table (3.4) and Figure (3.5), respectively.

Constant net stress test with increasing the suction (drying).

Seven specimens from 30B soil (30B-P0.001-d&w-Sl, 30B-P0.001-d&w-com1, 30B-P0.001-d&w-com2, 30B-P0.1-d-Sl, 30B-P0.22-d-Sl, 30B-P0.6-d-Sl, and 30B-P1.0-d-Sl) and four specimens from 100B (100B-P0.001-d&w-Sl, 100B-P0.001-d&w-com1, 100B-P0.3-d-Sl, and 100B-P0.6-d-Sl) were tested under drying condition. In addition two tests for two identical specimens (30B-P0.22-d-Sl-U and 30B-P0.6-d-Sl-U) were carried out for comparison between different cells. The initial point is denoted as point A, whereas point B represents the beginning of applying suction (drying) under constant net stress condition. Point C represents the air-entry suction, s_{aev}, and point D represents the end of drying path under constant net stress condition. In case of SWCC test, point E represents the end of wetting path under constant net stress condition. In the Figures of SWCC tests under unconfined condition (i.e., Figure 5.5 for 30B soil and Figure 5.12 for 100B soil) there is no loading stage, therefore A and B correspond to the same point.

Figures (5.5-5.10) show the results of void ratio, gravimetric water content, and degree of saturation versus net stress and suction under constant net stress condition with drying path followed by wetting path from SWCC tests (30B-P0.001-d&w-Sl, 30B-P0.001-d&w-com1, 30B-P0.001-d&w-com2) and drying path only for other tests for 30B soil. Figures (5.12-5.15) show the results of void ratio, gravimetric water content, and degree of saturation versus net stress and suction relationships under constant net stress condition with drying and wetting paths for SWCC tests (100B-P0.001-d&w-Sl, 100B-P0.001-d&w-com1) and drying path only for other tests for pure bentonite 100B.

The 30B-P0.001-d&w-Sl, 30B-P0.001-d&w-com1, 30B-P0.001-d&w-com2, 100B-P0.001-d&w-Sl, and 100B-P0.001-d&w-com1 tests are actually SWCC tests for unconfined condition with different initial densities.

The results in Figure (5.5d) show that the air-entry value s_{aev} of initially slurry 30B soil specimen (30B-P0.001-d&w-Sl) is about 80 kPa (point C) and the same value for initial moderate density specimen (30B-P0.001-d&w-com1), (point C_1). While the air-entry value of higher initial density specimen (30B-P0.001-d&w-com2) is about 600 kPa (point C_2). Figure (5.5b) shows that the air-entry value for 30B soil is very close to the isotropic preconsolidation pressure for each density. Furthermore, Figure (5.5b) shows that the volume decreases following initially overconsolidated path then the isotropic normal consolidation line (iso-NCL) for all specimens as suction increases until reaching air-entry value. Then the slope of the compression curve decreased until reaching a specific suction value when there is

no further reduction in volume with increasing suction. This suction value equals to 600 kPa for 30B-P0.001-d&w-Sl and 30B-P0.001-d&w-com1 tests and 3500 kPa for 30B-P0.001-d&w-com2. On other hand, the gravimetric water content, Figure (5.5c), continued decreasing as suction increased. The main remark in these tests is that all gravimetric water content curves for different initial densities almost joined after reaching a suction equal to the corresponding isotropic preconsolidation pressure for each initial density. The 30B-P0.001-d&w-Sl, 30B-P0.001-d&w-com1, and 30B-P0.001-d&w-com2 tests (SWCC tests) show that there is no residual suction for 30B soil. In other words, the SWCC (gravimetric water content and the degree of saturation verses suction relationship) for 30B soil has only one slope beyond the air-entry value. Moreover, the results of SWCC tests for different densities show significant hysteresis behavior. As a result, during drying path certain suction corresponds to higher gravimetric water content and degree of saturation then during wetting path.

Figures (5.6a, 5.7a, 5.8a, 5.9a, and 5.10a) show that the initial slurry 30B soil specimens follow the one-dimensional normal consolidation line (1D-NCL) as the net stress increases (from A to B).

The results in Figures (5.6d, 5.7d, 5.8d, 5.9d, and 5.10d) show that the air-entry values (points C's) are about 100 kPa for 30B-P0.1-d-Sl, 150 kPa for 30B-P0.22-d-Sl, 600 kPa for 30B-P0.6-d-Sl, and 1500 kPa for 30B-P1.0-d-Sl. It is noticeable here the effect of the constant net stress in the air-entry value.

Volume change results in Figures (5.6b, 5.7b, 5.8a, 5.9b, and 5.10b) show that the volume decreased with increasing suction until reaching air-entry value, then the reduction in volume reduced. For low constant net stress condition (up to 220 kPa) the amount of reduction in volume during drying path (increase in suction) decreased as the constant net stress increased. While the state changed oppositely for high constant net stress condition (higher than 220 kPa). Initially, all the slurry specimens followed the 1D-NCL as the net stress increased. The initially compacted specimens follow the over consolidation (OC) path until reach to the NCL. Actually, if the effective stress is considered for the saturated zone (before the air-entry value) as in Equation (2.2) with $\chi = 1$, and as suction increases all compression curves of initially slurry condition with constant net stress tests follow the iso-NCL after applying suction under constant net stress Figure (5.11a). After the air-entry value the slope of the compression curve decreased until the suction reaches value above that there is no further reduction in volume with increasing suction. This suction value is about 500 kPa for 30B-P0.1-d-Sl, 500 30B-P0.22-d-Sl, 5000 kPa for 30B-P0.6-d-Sl, and 1000 30B-P1.0-d-Sl.

The gravimetric water content, Figure (5.6c, 5.7c, 5.8c, 5.9c, and 5.10c), continued decreasing as suction increased. Similar observation is noticed again; all gravimetric water content curves for different constant net stress joined in one path after reaching the suction equal to the corresponded isotropic preconsolidation pressure regarding to density under constant net stress before applying the suction. As in void ratio-effective stress relationship, Figure (5.11b) shows that at saturation zone all gravimetric water content curves of initially slurry condition with different constant net stress follow the 1D-NCL, then after applying suction under constant net stress, they follow the iso-NCL.

The results in Figure (5.12d) show that the air-entry value, s_{aev}, (point C) of initially slurry 100B soil specimen (100B-P0.001-d&w-Sl) is about 15000 kPa and same value for other initial density 100B soil specimen (30B-P0.001-d&w-com1). In Figure (5.12b), it was observed that, as the suction increases (point B) the initially slurry specimen (100B-P0.001-d&w-Sl) followed the NCL path until reaching the air-entry value (point C), while the initial part of the curve for the initial compacted specimen (100B-P0.001-d&w-com1) swelled and followed the over consolidation path till reaching the NCL then it followed the NCL path until reaching the air-entry value(point C_1). Afterward the slope of the compression curve decreased until reaching the suction value when there is no further reduction in volume with increasing suction. This suction value equals to 3500 kPa for 100B-P0.001-d&w-Sl and 100B-P0.001-d&w-com1 tests. These results indicate that the air-entry value of initially slurry 100B specimen for unconfined condition is almost the same for all different initial densities (low to high). On other hand, the gravimetric water content, Figure (5.12c), continued decreasing as suction increased. It was observed that for 100B soil, as well as for 30B soil, all gravimetric water content curves for different initial densities joined after reaching a suction equal to the corresponding isotropic preconsolidation pressure of the compacted specimen see the isotropic NCL in the corresponded figures. Furthermore, the 100B-P0.001-d&w-Sl and 100B-P0.001-d&w-com1 tests (SWCC tests) show that there is no residual suction or the SWCC (gravimetric water content and the degree of saturation verses suction relationship) had only one slope beyond the air-entry value (from C to D). In addition, the results of SWCC tests for different densities show significant hysteresis behavior. As a result, during drying path certain suction corresponds to higher gravimetric water content and degree of saturation than during wetting path.

Figures (5.13a and 5.14a) show that the initially slurry 100B soil specimen followed the one-dimensional normal consolidation line (1D-NCL) as the net stress increased.

The results in Figures (5.13d and 5.14d) show that the air-entry values (points C's) are about 15000 kPa for both tests. Thus, the air-entry value of initially slurry 100B specimen for different constant net stress conditions is almost the same for all cases.

Volume change results in Figures (5.13b and 5.14b) show that the volume decreased with increasing suction until reaching air-entry value (points C's). The amount of reduction in volume during drying path (increase in suction) for 100B soil decreased as the constant net stress increased for the range of tested constant net stress values (up to 600 kPa). Afterward the slope of the compression curve decreased until reaching the suction value when there is no further reduction in volume with increasing suction. This suction value is about 3500 kPa for both 100B-P0.6-d-Sl and 100B-P0.6-d-Sl tests. Again, if the effective stress is considered for the saturated zone, as in Equation (2.2) with $\chi = 1$, and as suction increases all compression curves of initially slurry condition with constant net stress tests follow the 1D-NCL path then, after applying suction under constant net stress, they will follow iso-NCL, Figure (5.16a). The compression curves before applying the suction (before point B) seem to follow a path between the 1D-NCL and iso-NCL. This behavior is due to the fact that both paths are close to each other, as well the acceptable experimental error. The initially compacted specimens will follow the over consolidation (OC) path until reaching the NCL.

The gravimetric water content, Figure (5.13c and 5.14c), continued decreasing as suction increased. Again all gravimetric water content curves for different constant net stress joined in one path after reaching a suction equal to the corresponding isotropic preconsolidation pressure regarding to density under constant net stress before applying the suction. As in void ratio-effective stress relationship, Figure (5.16b) shows that at saturated zone all gravimetric water content curves of initially slurry condition with different constant net stress follow the 1D-NCL, then after applying suction under constant net stress, they follow the iso-NCL.

Agus (2005) cited that the as-prepared bentonite-sand mixtures show insignificant hysteresis in the void ratio versus suction relationships. The significant hysteretic behavior is seen in the water content and degree of saturation versus suction relationships. Furthermore, he added that during cyclic wetting and drying under constant load conditions, the specimen with a higher stress level exhibited a higher shrinkage on drying. This observation is similar to the observed behavior of high constant net stress condition for 30B soil.

Pham (2005) mentioned that at soil suction less than the air-entry value (for drying path) and the water entry value (for wetting path) all the pores are filled with water and the soil behavior exactly like that at saturation. Therefore, the volume change relationships are stress path independent. When all the pores are filled with water, all stress paths give the same

predictions for both void ratio and water content. Moreover, Pham (2005) pointed out that the air-entry and the water entry value were significant influenced by net vertical stress and the yield stress of the soil, while the gravimetric residual water content seemed to be essentially independent of net vertical stress and the yield stress.

Ferrari (2007) tested a kaolinitic–illitic clay with liquid limit LL = 58 % and plasticity index PI = 30 %. Ferrari (2007) showed that the air-entry value increases with increasing the density. This behavior agreed with the experimental results of 30B soil for different initial density and different constant applied net stress.

In addition two tests for two identical slurry specimens from 30B soil (30B-P0.22-d-Sl-U and 30B-P0.6-d-Sl-U) were carried out for comparison between the performances of the two available UPC-Isochoric cells and the standard oedometer cell (Black cell) for compression test with drying path for initially slurry condition. Figures (5.17 and 5.18) show that the two UPC-Isochoric cells give good agreement with the results of Black cell under the same conditions, thus the UPC-Isochoric cells were used in the one-dimensional controlled-suction compression tests.

Considering all the above results for the specific range of densities used in study, the following key observations can be derived:

- The suction stress has isotropic effect.
- For unconfined condition (SWCC tests), the results show significant hysteresis behavior associated with absence of residual suction (only one slope beyond the air-entry value) for both 30B and 100B soils.
- For unconfined condition (SWCC tests), the value of air-entry suction of initially slurry low expansive soil specimens, such as 30B soil, is the same for all specimens of low and moderate densities. As density increases, when its isotropic preconsolidation pressure is higher than the air-entry value of slurry condition, the air-entry value will be equal to the corresponding isotropic preconsolidation pressure.
- While the air-entry value of initially slurry high expansive soil specimen, such as 100B soil, for unconfined condition is almost the same for all different initial densities (low to high). This behavior is related to two facts: (1) the air-entry value of initially slurry high expansive soil specimens is already high (more than 10000 kPa), and this needs high density to reach to isotropic preconsolidation pressure higher than the air-entry value of slurry condition; (2) the initial high density will decrease due to swelling, and this leads to a reduction of the isotropic preconsolidation pressure.

- For constant net stress condition, the air-entry value of initially slurry low expansive soil specimens, such as 30B soil, is the same for all specimens under constant low net stress. When the applied net stress value passes the air-entry value of initially slurry specimen the air-entry value will be closed to the applied constant net stress. Indeed the air-entry value found be close to the isotropic preconsolidation pressure of the density under constant applied net stress before applying the suction.
- The air-entry value of initially slurry high expansive soil specimen, such as 100B soil, for different constant net stress conditions is almost the same for all cases due to the same first reason mentioned in the case of unconfined condition for high expansive soil that is (the high value of air-entry value).

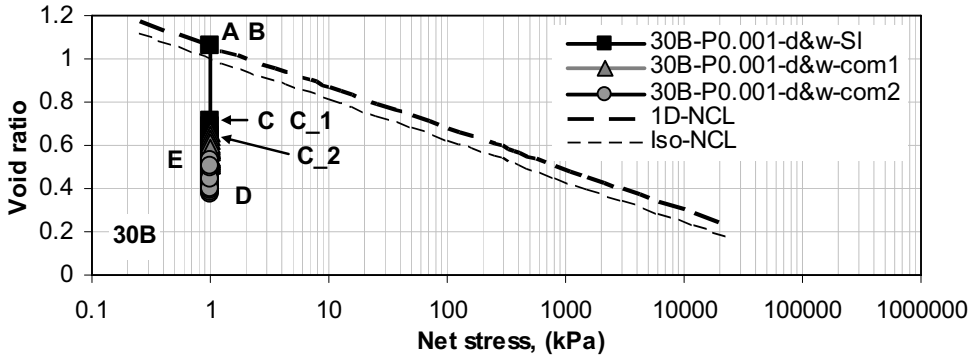

a

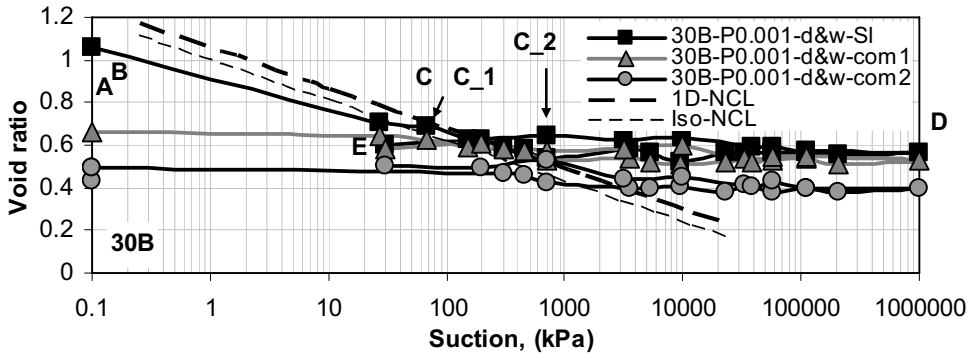

b

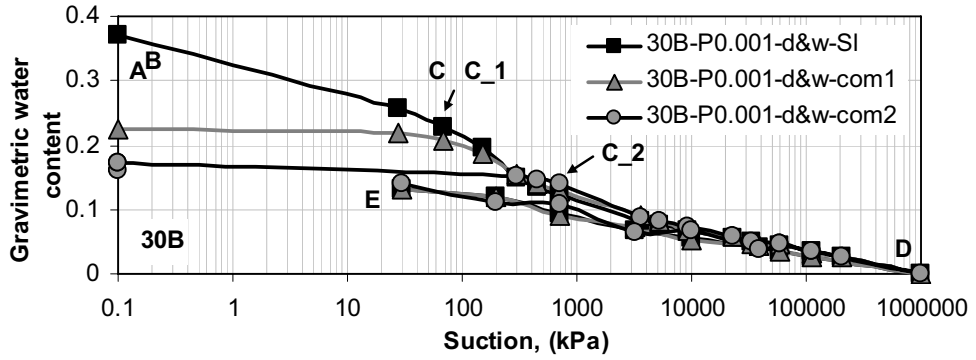

c

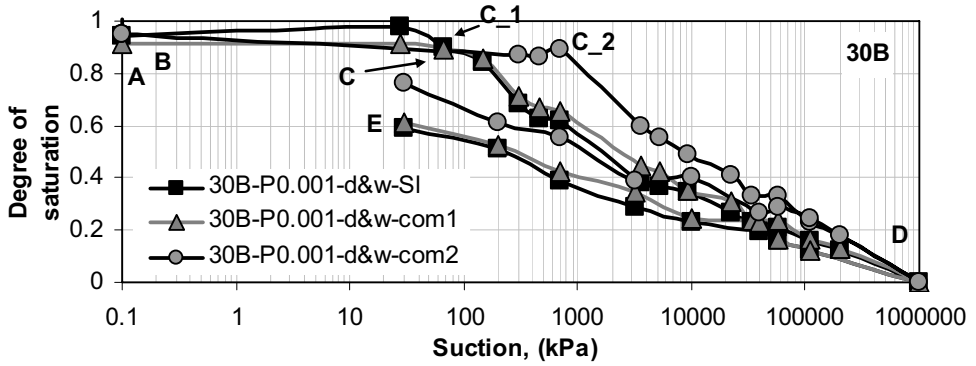

d

Figure 5.5 Void ratio, gravimetric water content, and degree of saturation results of unconfined stress condition with drying and wetting paths (SWCC tests) for 30B soil.

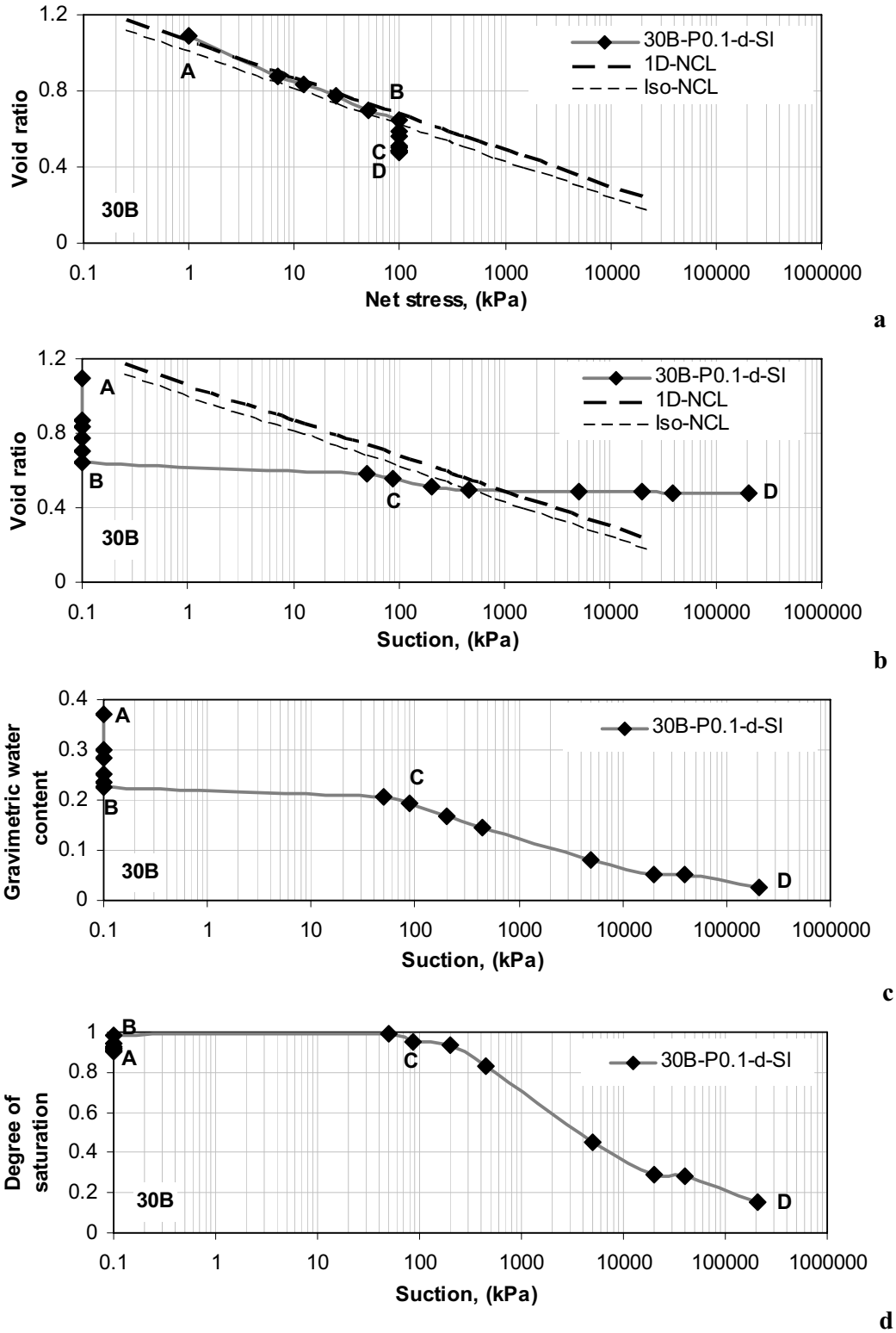

Figure 5.6 Void ratio, gravimetric water content, and degree of saturation results of constant net stress = 100 kPa condition with increasing the suction (drying path) for 30B soil.

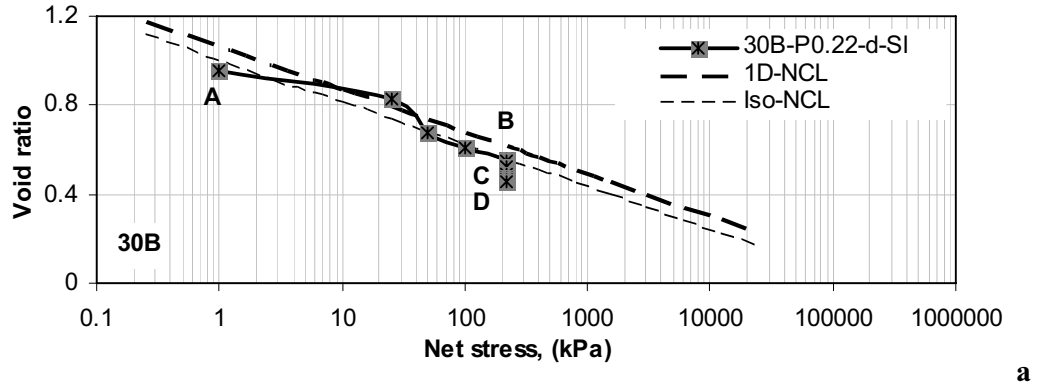

a

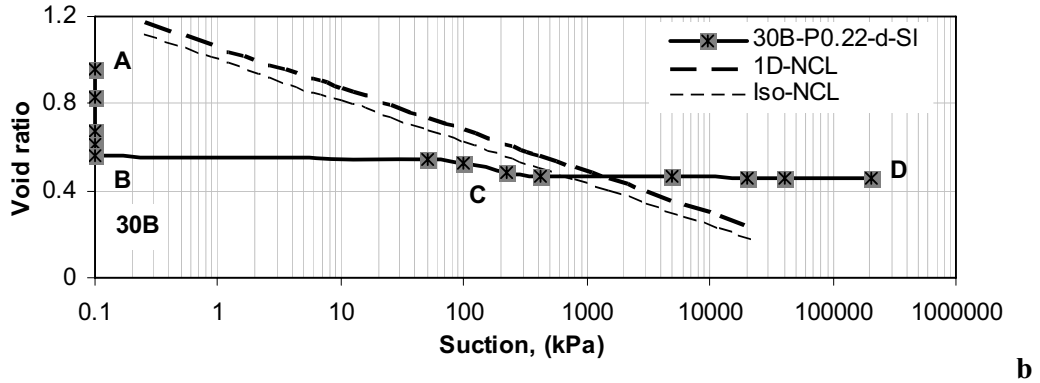

b

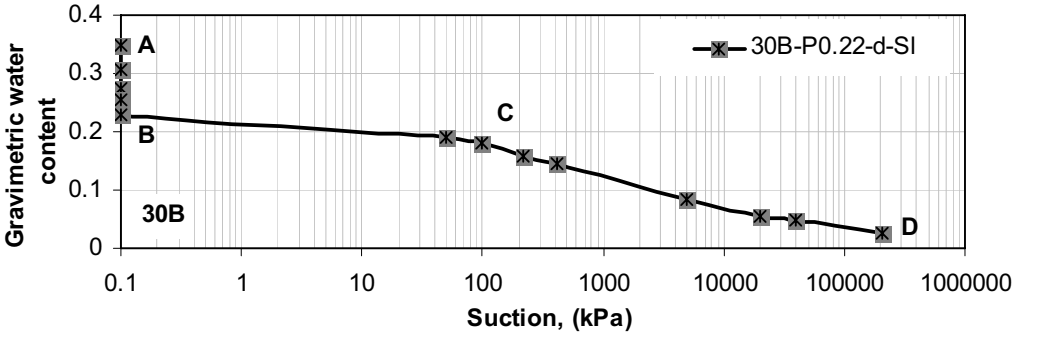

c

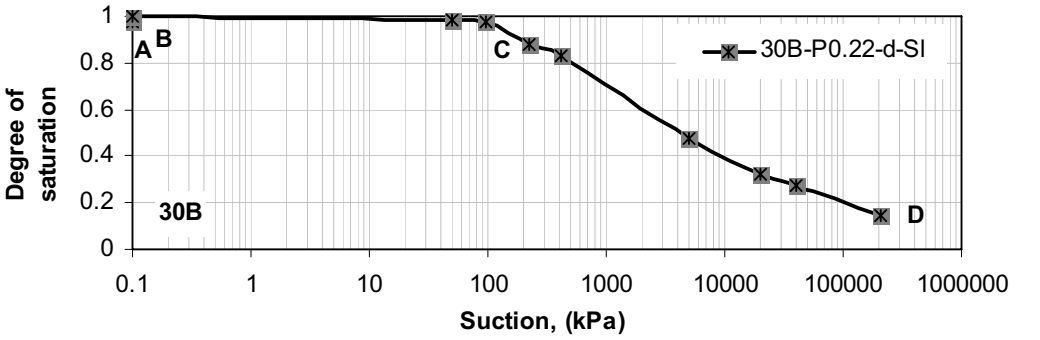

d

Figure 5.7 Void ratio, gravimetric water content, and degree of saturation results of constant net stress = 220 kPa condition with increasing the suction (drying path) for 30B soil.

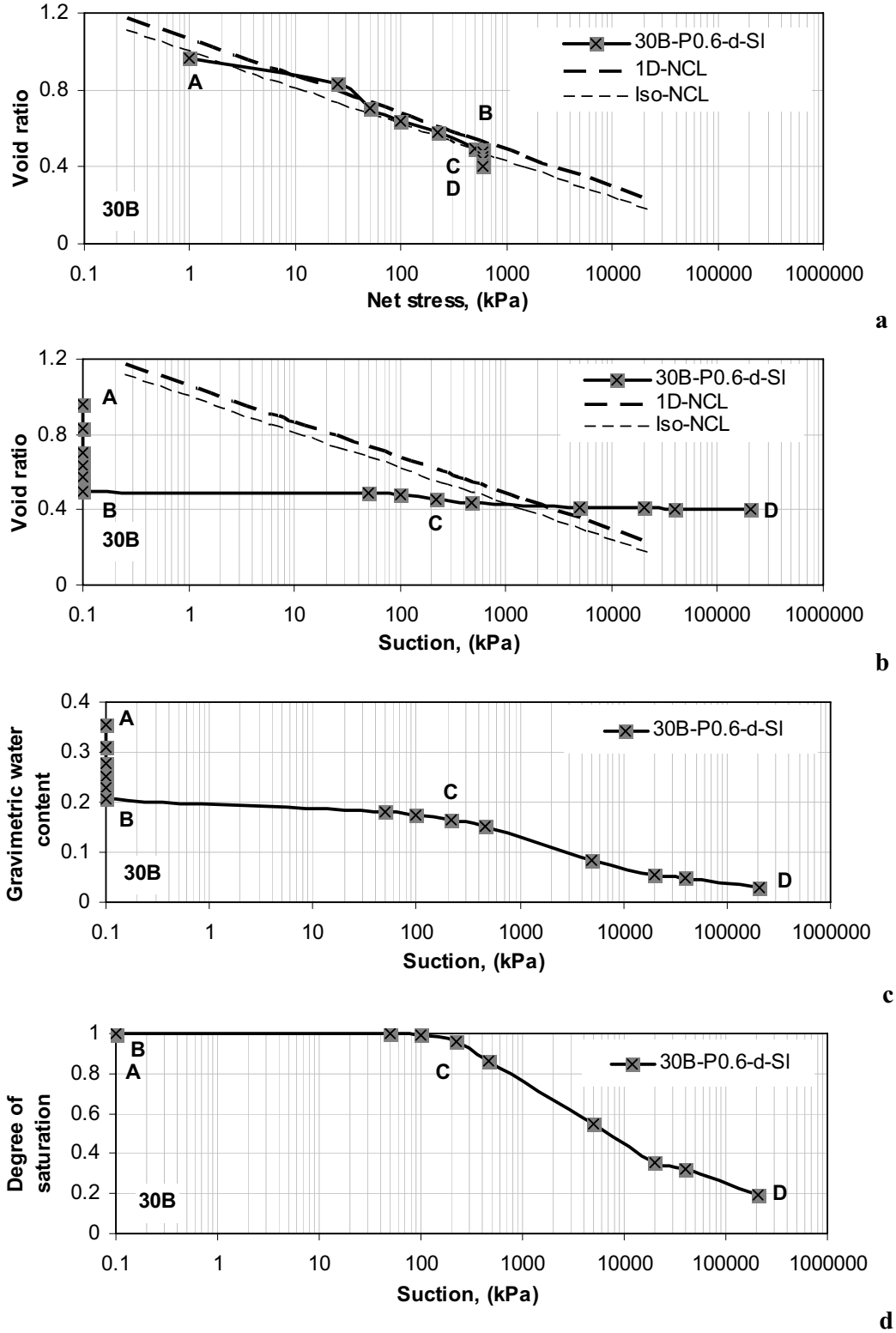

Figure 5.8 Void ratio, gravimetric water content, and degree of saturation results of constant net stress = 600 kPa condition with increasing the suction (drying path) for 30B soil.

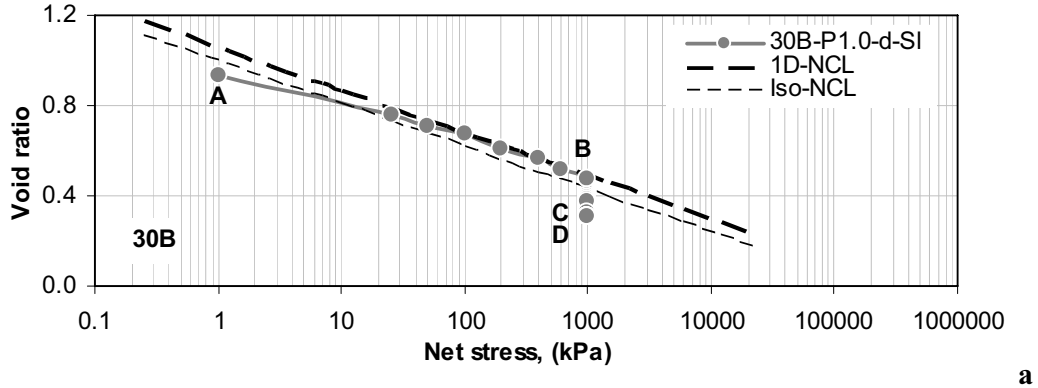

a

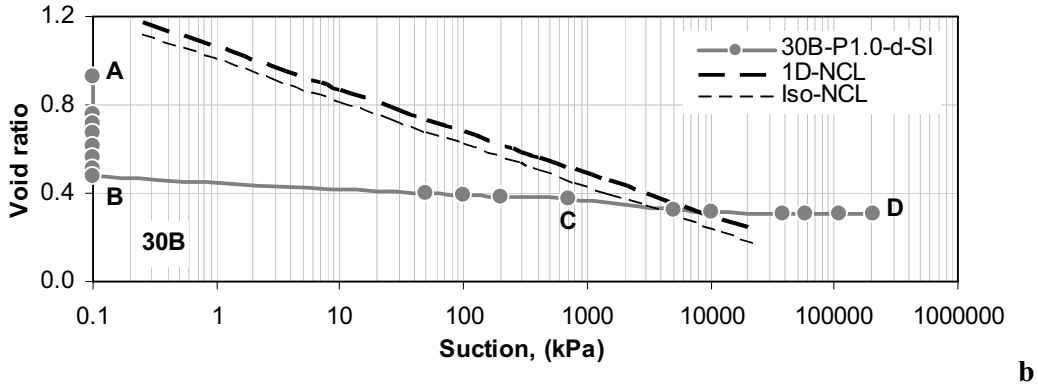

b

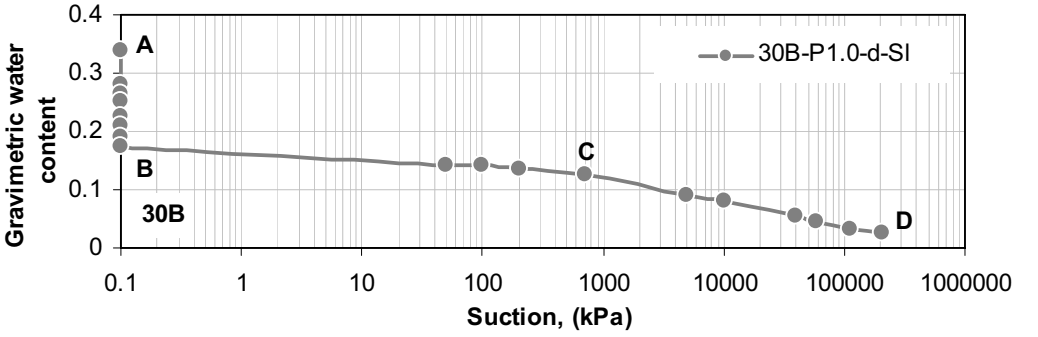

c

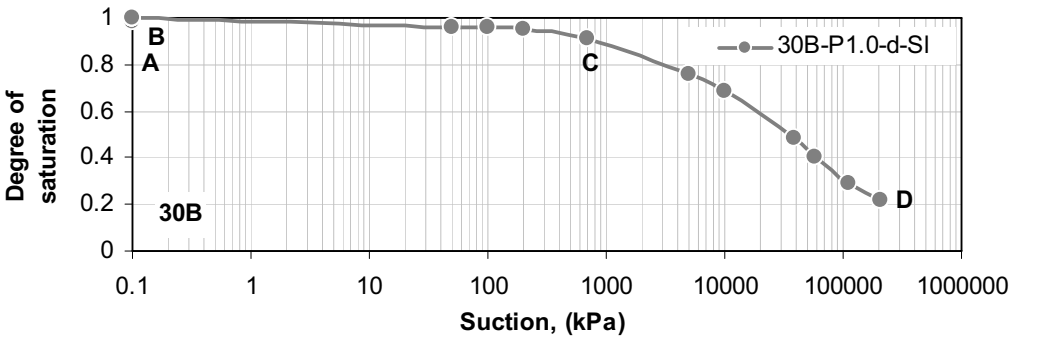

d

Figure 5.9 Void ratio, gravimetric water content, and degree of saturation results of constant net stress = 1000 kPa condition with increasing the suction (drying path) for 30B soil.

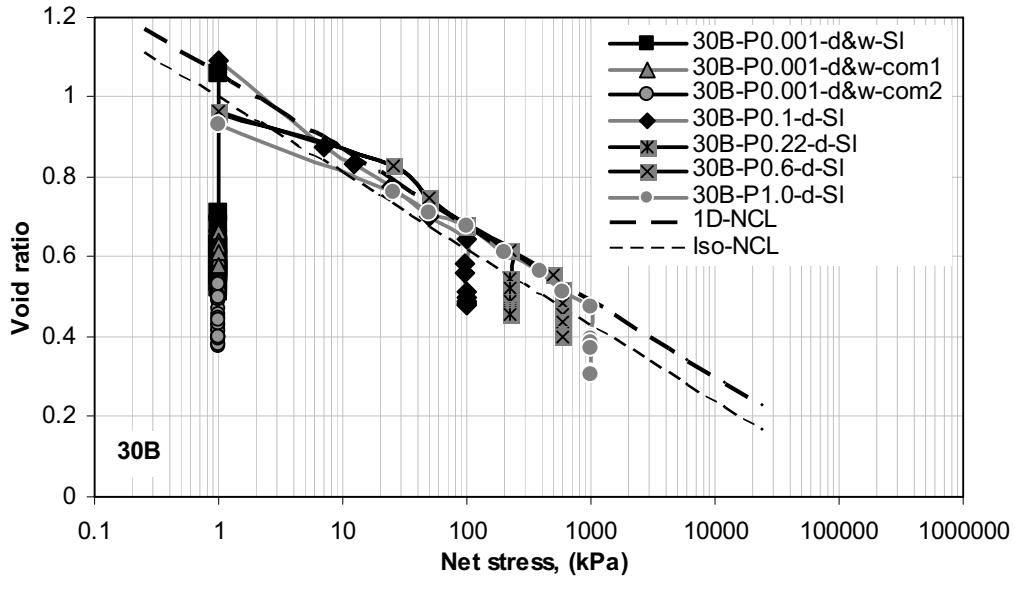

a

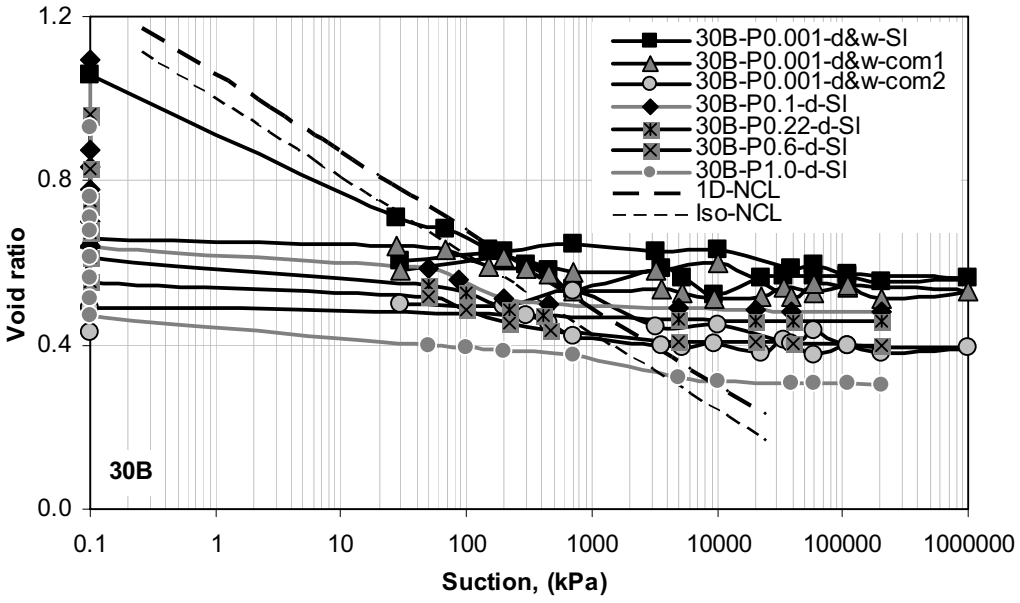

b

Figure 5.10-1 Void ratio, gravimetric water content, and degree of saturation results of all constant net stress tests condition with drying path (SWCC tests, P0.001, for drying and wetting paths) for 30B soil.

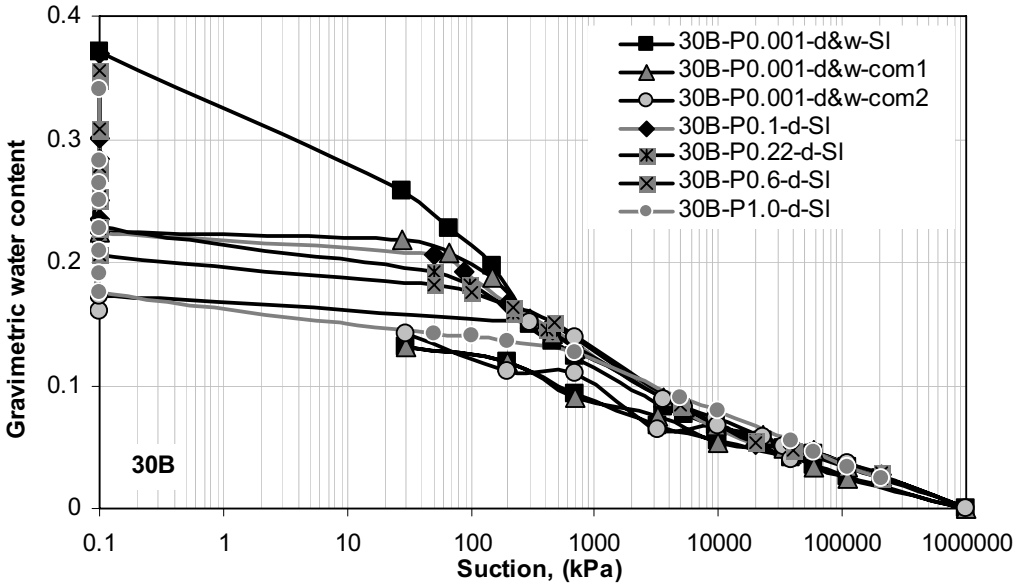

c

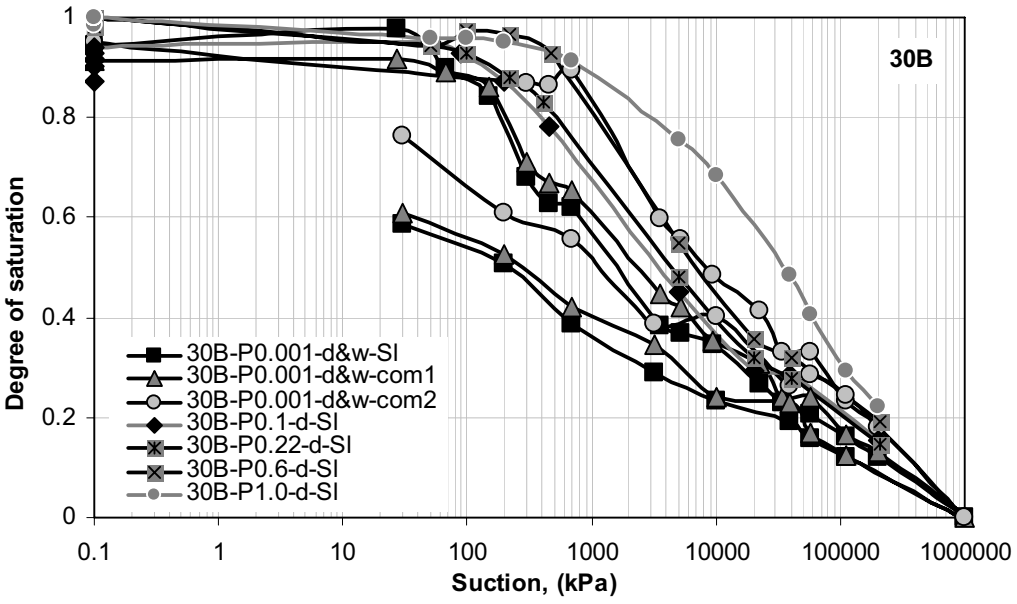

d

Figure 5.10-2 Void ratio, gravimetric water content, and degree of saturation results of all constant net stress tests condition with drying path (SWCC tests, P0.001, for drying and wetting paths) for 30B soil.

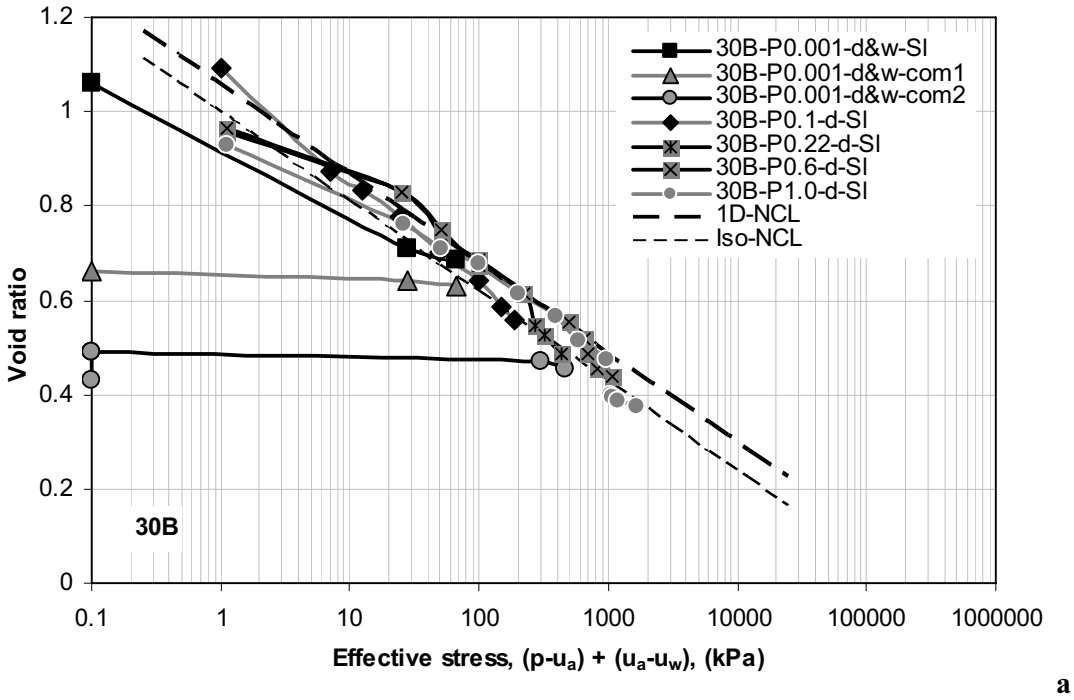

a

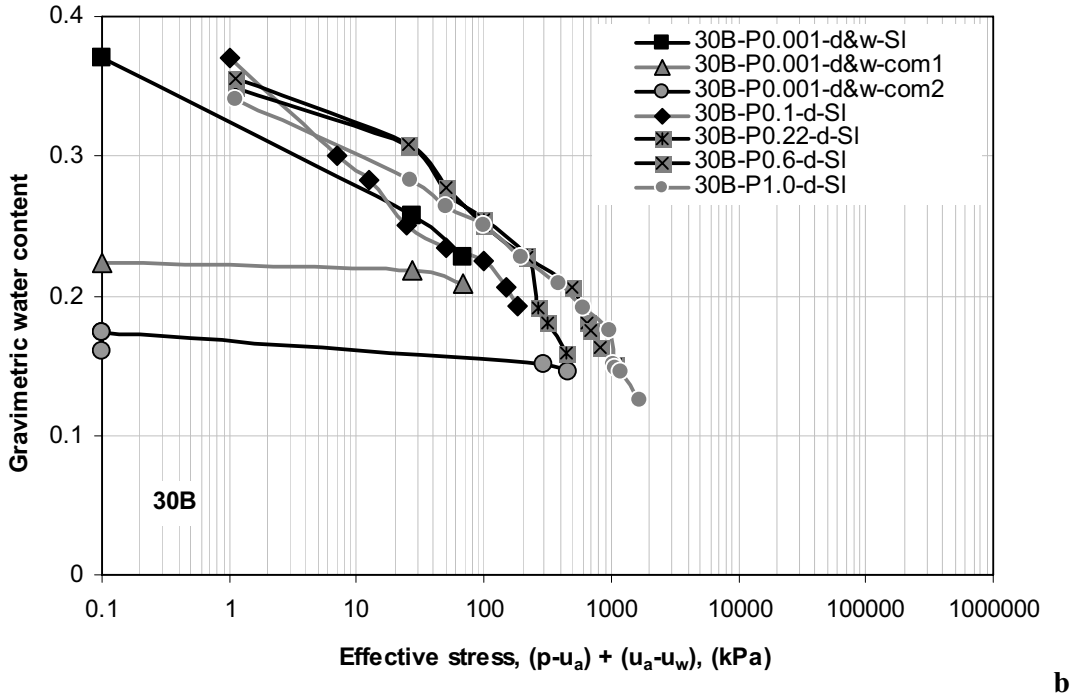

b

Figure 5.11 Void ratio and gravimetric water content verses effective stress relationships for saturation zone of all constant net stress tests condition with drying path for 30B soil.

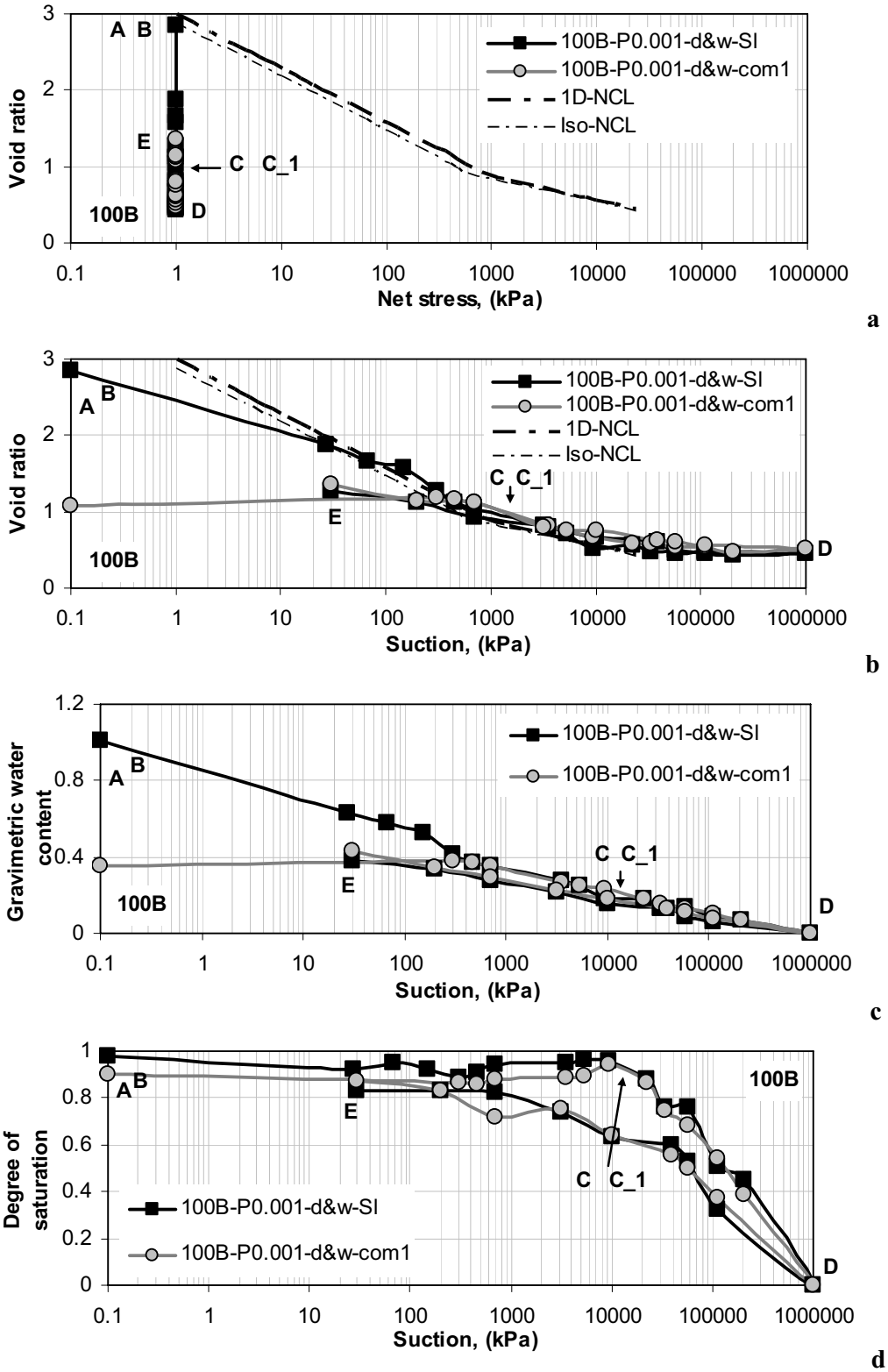

Figure 5.12 Void ratio, gravimetric water content, and degree of saturation results of unconfined stress condition with drying and wetting paths (SWCC tests) for 100B soil.

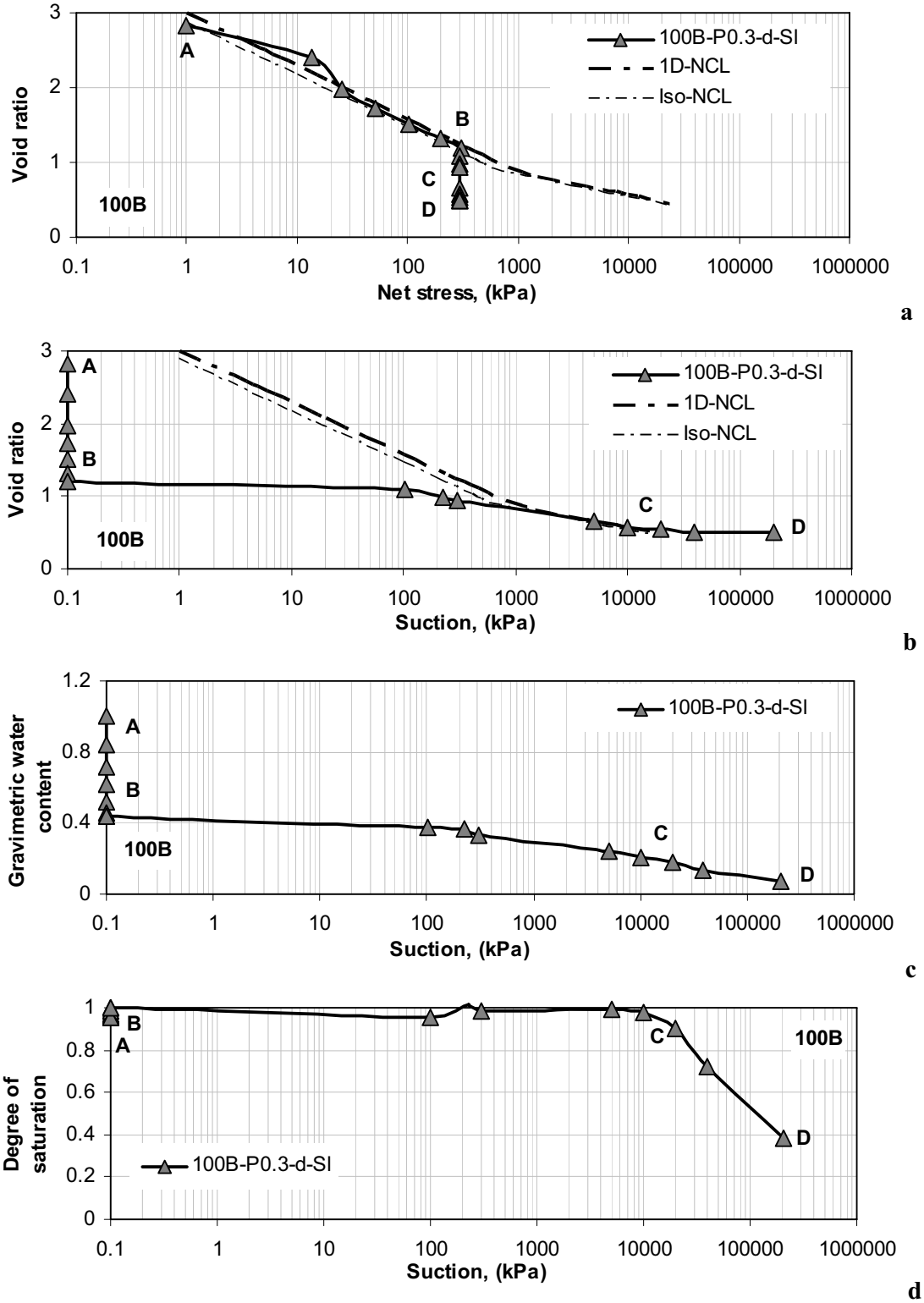

Figure 5.13 Void ratio, gravimetric water content, and degree of saturation results of constant net stress = 300 kPa condition with increasing the suction (drying path) for 100B soil.

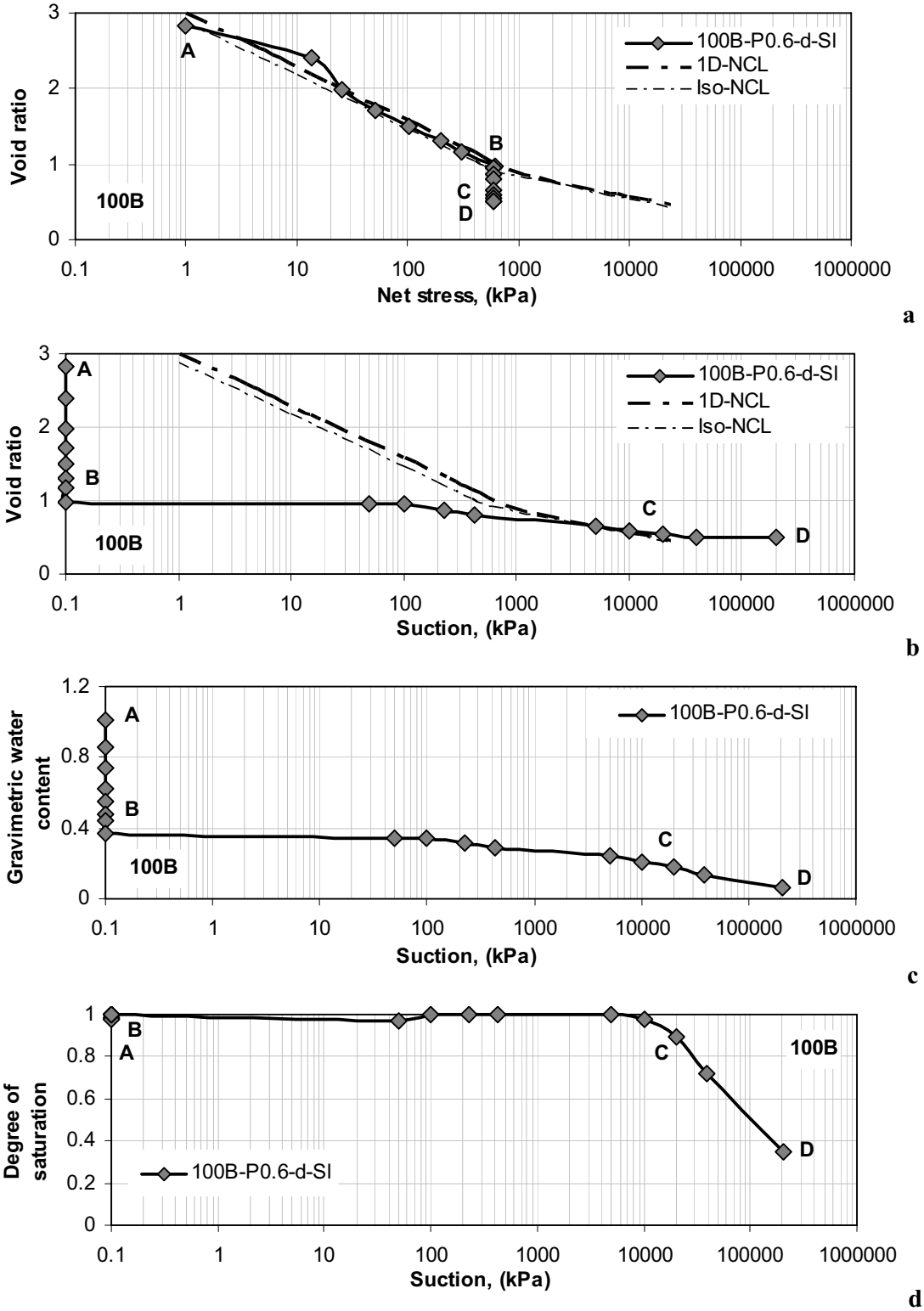

Figure 5.14 Void ratio, gravimetric water content, and degree of saturation results of constant net stress = 600 kPa condition with increasing the suction (drying path) for 100B soil.

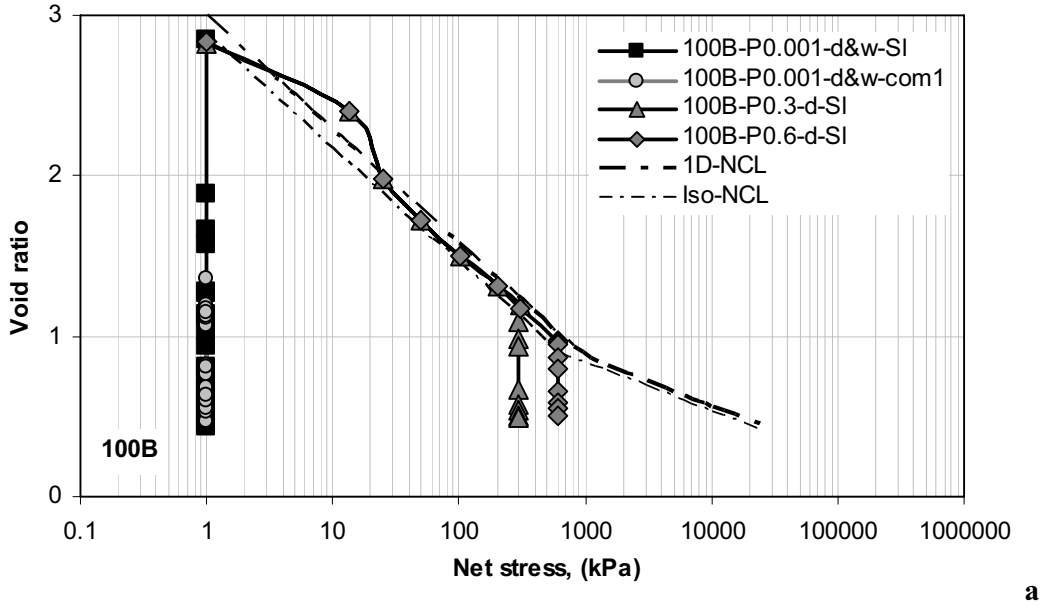

a

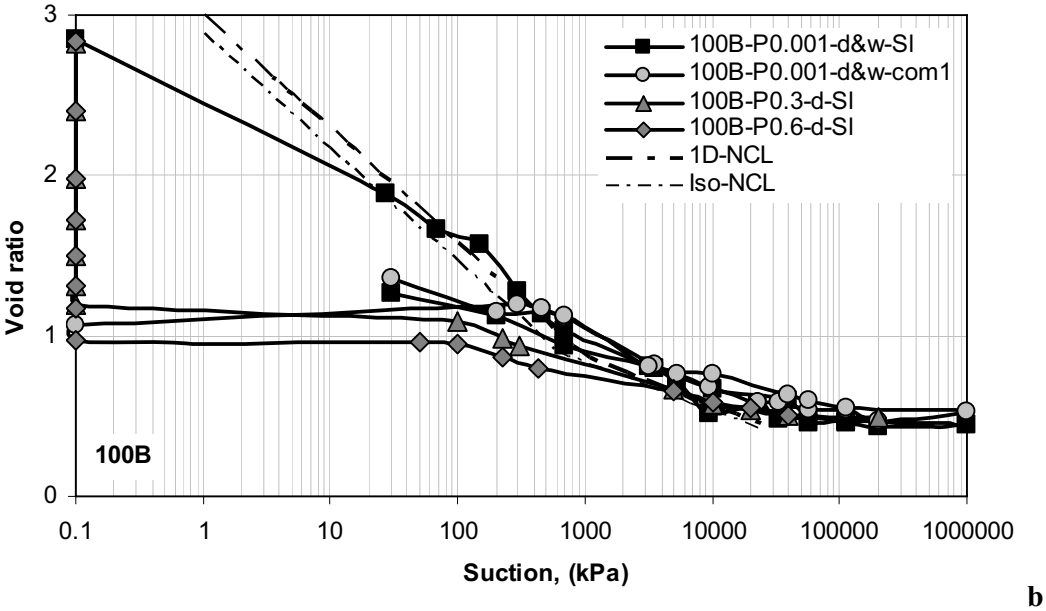

b

Figure 5.15-1 Void ratio, gravimetric water content, and degree of saturation results of all constant net stress tests condition with drying path (SWCC tests, P0.001, for drying and wetting paths) for 100B soil.

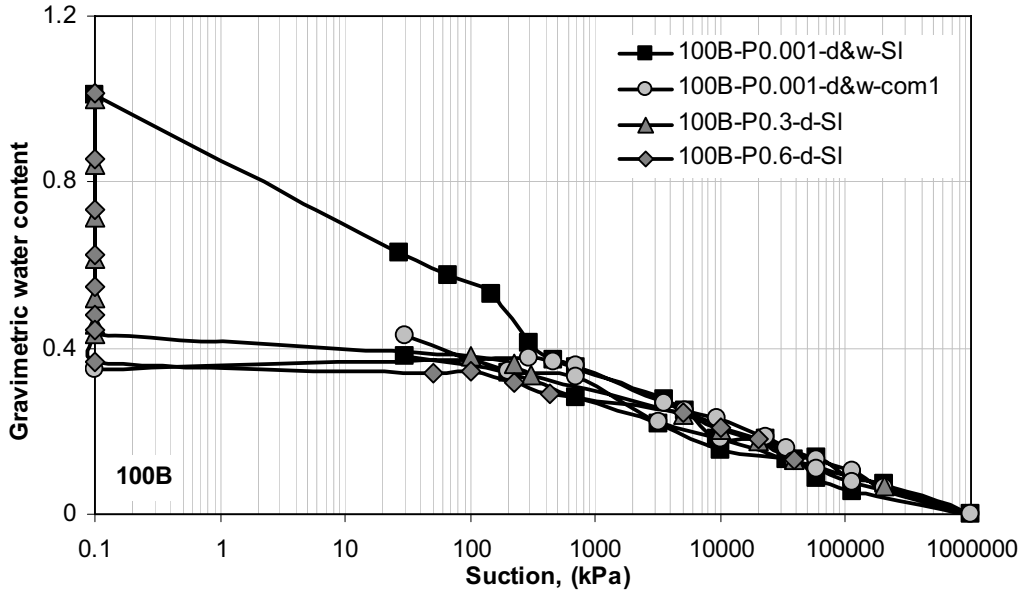

c

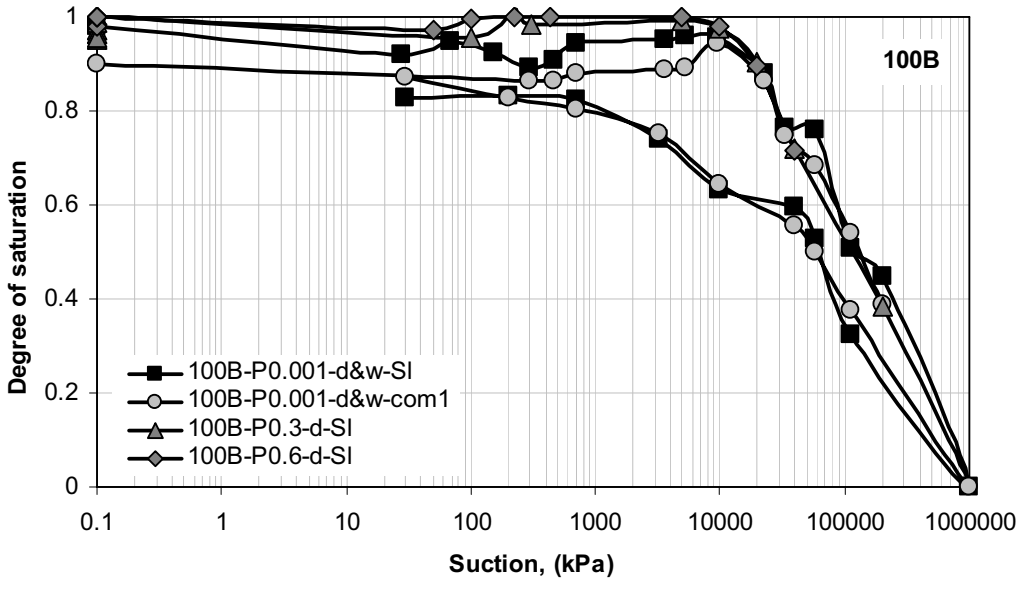

d

Figure 5.15-2 Void ratio, gravimetric water content, and degree of saturation results of all constant net stress tests condition with drying path (SWCC tests, P0.001, for drying and wetting paths) for 100B soil.

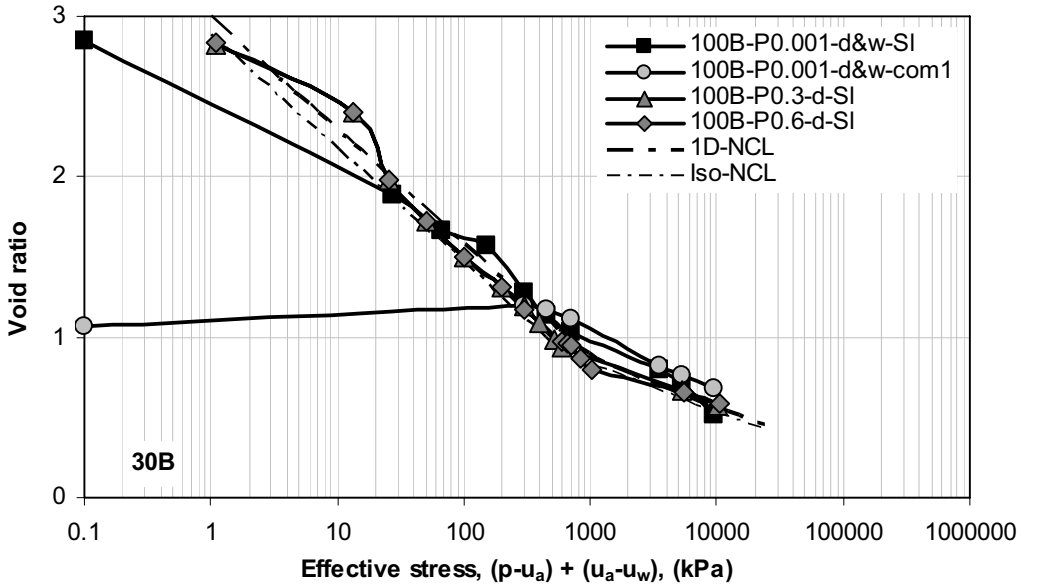

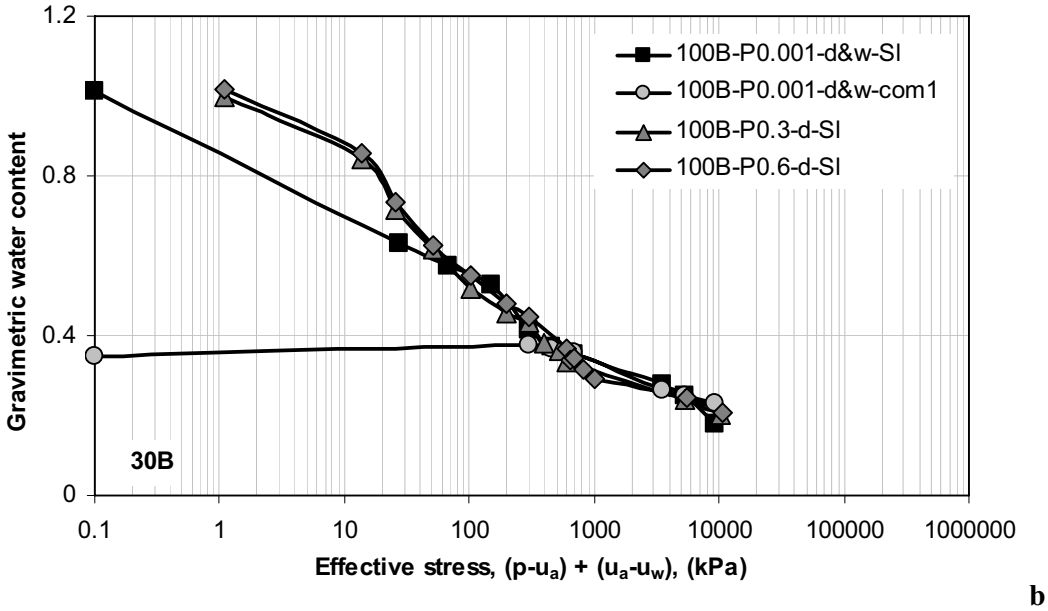

Figure 5.16 Void ratio and gravimetric water content verses effective stress relationships for saturation zone of all constant net stress tests condition with drying path for 100B soil.

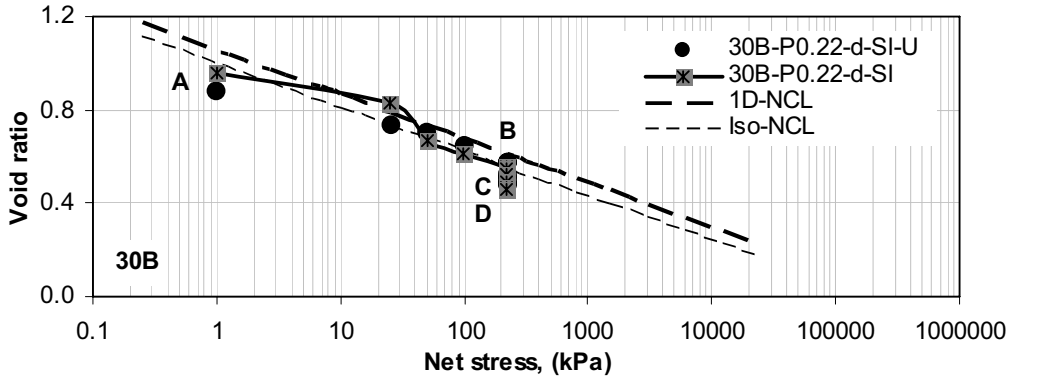

a

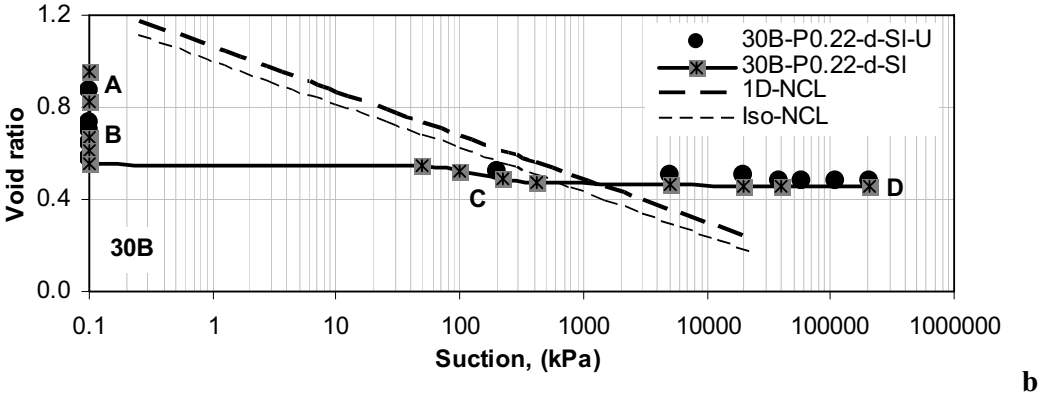

b

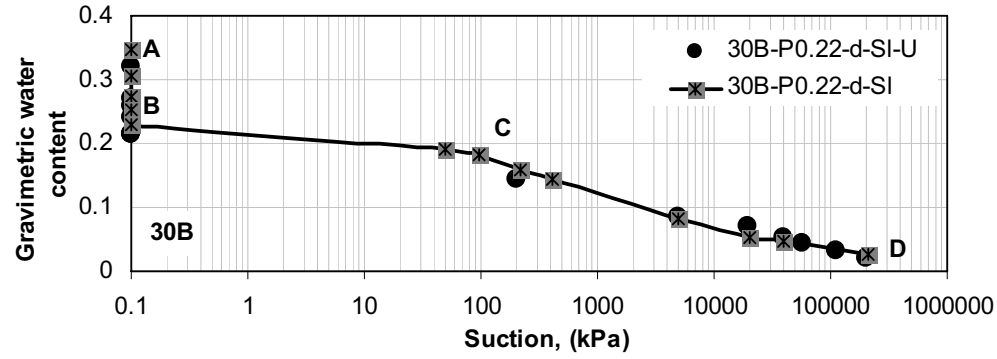

c

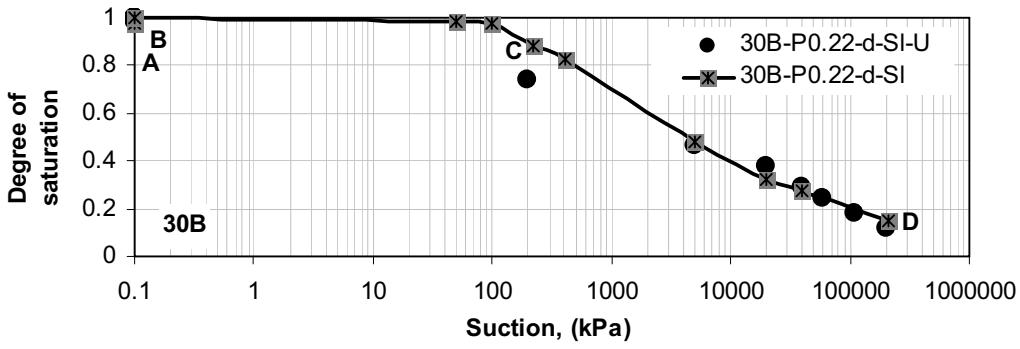

d

Figure 5.17 Results of the verifying test for comparison between the Black cell (original test) and UPC- Isochoric cell Nr. 1 (U test) for void ratio, gravimetric water content, and degree of saturation results of constant net stress = 220 kPa condition with increasing the suction (drying path) for 30B soil.

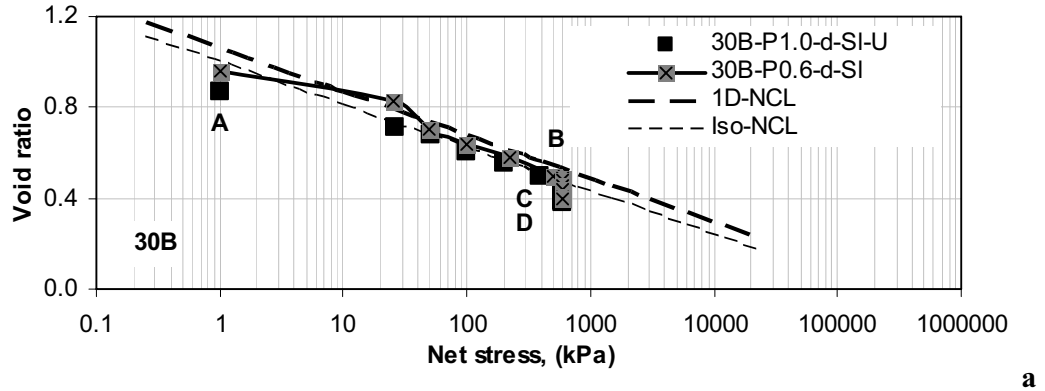

a

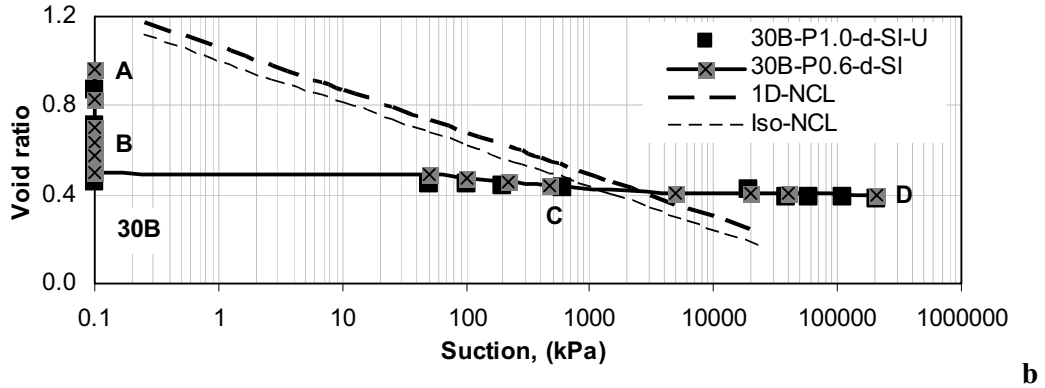

b

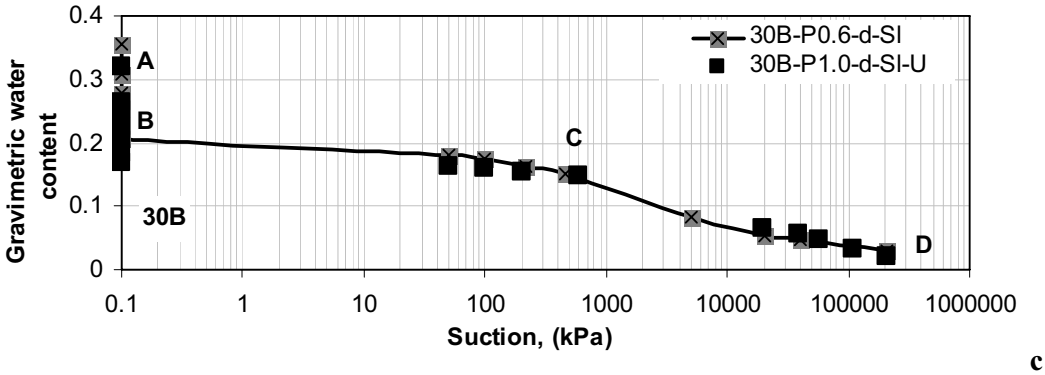

c

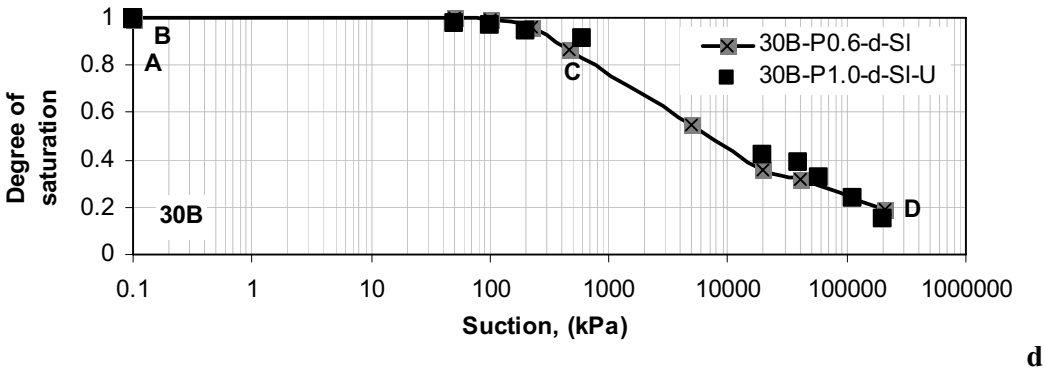

d

Figure 5.18 Results of the verifying test for comparison between the Black cell (original test) and UPC- Isochoric cell Nr.2 (U test) for void ratio, gravimetric water content, and degree of saturation results of constant net stress = 600 kPa condition with increasing the suction (drying path) for 30B soil.

Constant net stress test with decreasing the suction-wetting (collapse test).

Three tests on 30B specimens (30B-P0.25-w-Lo, 30B-P0.6-w-Lo, and 30B-P1.0-w-Lo) were conducted for wetting (collapse) test for initially unsaturated loose state specimens to determine the volumetric yielding at unsaturated state. The initial point is denoted as point A, whereas point B represents the beginning of constant net stress condition under wetting path. Point C represents the end of constant net stress condition under wetting path. Figures (5.19-5.22) show the results of void ratio, gravimetric water content, and degree of saturation versus net stress and suction under constant net stress condition with wetting paths for initially loose prepared 30B soil.

Each test in this series followed different path in order to pass different states (over consolidation and normal consolidation states) before attains the specific constant net stress state. Figure (5.19) shows that the volume of initially loose specimen 30B-P0.25-w-Lo decreased due to increase of applied suction from 12000 kPa to 13523 kPa. Then the net stress was increased that leads to compress the specimen until reaching 250 kPa (point B) and during loading the specimen reached the preconsolidation pressure at about 50 kPa. After that the suction was decreased which caused reduction in volume (collapse). The gravimetric water content and the degree of the saturation increased with decreasing the suction. The volume reduced initially rapidly with decreasing the suction (for suction 13523 kPa to 8100 kPa), then the rate of decreasing the volume reduced until reaching 2723 kPa applied suction. After that the rate of decreasing the volume increased again (till suction reaching 400 kPa). Finally, the rate of decreasing the volume reduced until reaching zero applied suction (point C).

Figure (5.20) demonstrates that the 30B-P0.6-w-Lo specimen compressed initially under suction equals to 11000 kPa (point A). The suction was increased to 13523 kPa for net stress range from 100 kPa to 600 kPa (point C). At 600 kPa the net stress was kept constant, while the suction was decreased (start the collapse stage). However, as the suction decreased the gravimetric water content and the degree of the saturation increased. In wetting (collapse) process, as the suction decreased, the volume initially decreased moderately till reaching suction 2732 kPa. Subsequently the reduction in volume increased rapidly for the suction range form 2732 kPa to 300 kPa. Then for the final range of suction (till zero suction, point C) the rate of decrease in volume reduced.

The third test in this series is 30B-P1.0-w-Lo, Figure (5.21). The suction initially was decreased from 10000 kPa (point A) to 6000 kPa and then, at net stress 100 kPa, the suction was again increased to about 18000 kPa. The suction was kept constant until net stress 1000 kPa (point B), in which the wetting (collapse) process started. Again, the gravimetric water

content and the degree of the saturation increased as the suction decreased. The volume change behavior of 30B-P1.0-w-Lo specimen under wetting condition was similar to the 30B-P0.6-w-Lo specimen. The volume reduced moderately till suction 900 kPa, and then the volume decreased rapidly till suction 245 kPa. Afterward, for suction range from 245 kPa to 0 kPa (point C), the amount of decreasing the volume reduced.

Figure (5.22a) shows that all the tests in this series almost joined the NCL after wetting process according to applied constant net stress. Actually they located a little bit lower than the 1D-NCL. Figure (5.22b) shows that, at wetting (collapse) process, all the specimens have almost the similar behavior consist of three stages except 30B-P0.25-w-Lo specimen. Specimen 30B-P0.25-w-Lo has four stages; as the suction starts decreasing for wetting process, from 13523 kPa to 8100 kPa, the specimen exhibited rapid decrease in volume before the three other stages. However, the three stages of collapse (reduction in suction under constant net stress) are : (i) the volume reduced moderately for the initial part of wetting (till suction 2732 kPa for both 30B-P0.25-w-Lo and 30B-P0.6-w-Lo and 9500 kPa for 30B-P1.0-w-Lo), (ii) then the volume decreased rapidly till intermediate suction value (till suction 400, 300, and 245 kPa for 30B-P0.25-w-Lo, 30B-P0.6-w-Lo and 30B-P1.0-w-Lo, respectively). (iii) Afterward, for the rest range of suction, the amount of decreasing the volume reduced.

Pereira and Fredlund (2000) observed the same behavior regarding to volume change-suction relationship during the wetting process. They classified the deformations during wetting process into three phases. The first phase of deformation occurs at high matric suction and is characterized by small volumetric deformation in collapsing soil and is termed the ‘precollapse’ phase. The second phase of deformation occurs at intermediate value of matric suction and is characterized by significant volumetric deformation in collapsing soil and is termed the ‘collapse’ phase. The third phase of deformation occurs at low matric suction with no additional volumetric deformation in collapsing soil and is named ‘postcollapse’ phase. The results of Jotisankasa (2005) and Sun et al. (2007) showed also the same three phases during the wetting process regarding to volume change-suction relationship.

Figure (5.22c) shows that the gravimetric water content -suction relationship is the same for all the specimens in the high suction values (>2732 kPa). After that each specimen follows particular path, where the specimen with lowest constant net stress value (30B-P0.25-w-Lo) is in the upper boundary while the specimen with highest constant net stress value (30B-P1.0-w-Lo) is in the lower boundary value. The relationship between degree of saturation and suction can be obtained from the void ratio and gravimetric water content versus suction relationships. However, each specimen has particular path, with opposite

behavior of the gravimetric water content -suction relationship, the specimen with lowest constant net stress value (30B-P0.25-w-Lo) is in the lower boundary while the highest constant net stress value (30B-P1.0-w-Lo) is in the upper boundary value. In other words, curves of degree of saturation-suction relationship for constant net stress tests condition with wetting path are shifted upward as the constant net stress increased. This shifting is due to increase of the density of the specimen with increasing constant net stress during the wetting process.

Jotisankasa (2005) investigated the collapse during the wetting under two different constant net vertical stresses (1184 kPa and 1691 kPa). The yield points are in a good agreement with the identified LC curve from the constant water content loading tests. Sun et al. (2007) tested the collapse for compacted Pearl clay in a controlled- suction triaxial cell with different initial void ratio (e_o = 1.28 and e_o = 1.36). It was detected that the collapse deformation due to a suction reduction depends mainly upon the density and stress state under which the collapse occurs. The results show similar behavior as in the presented test here regarding to the upward shift of the curves of degree of saturation-suction relationship during the wetting process with increasing the density. Furthermore, it was observed that the occurrence of the volume change due to a suction reduction is seem to be controlled by the changes in the degree of the saturation rather than by changes in the suction.

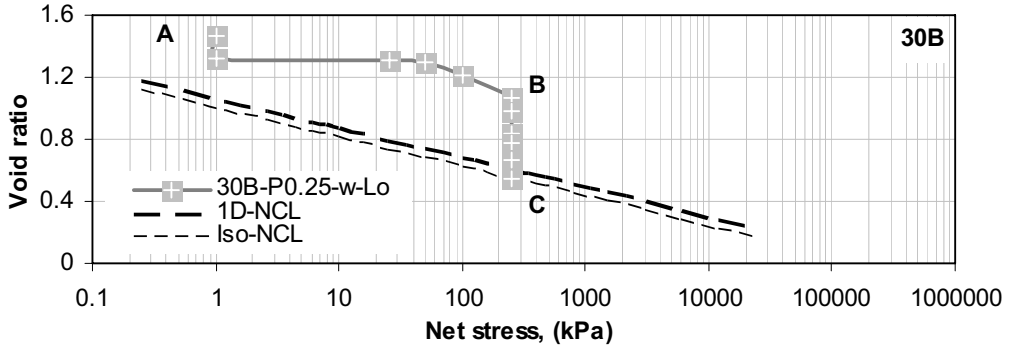

a

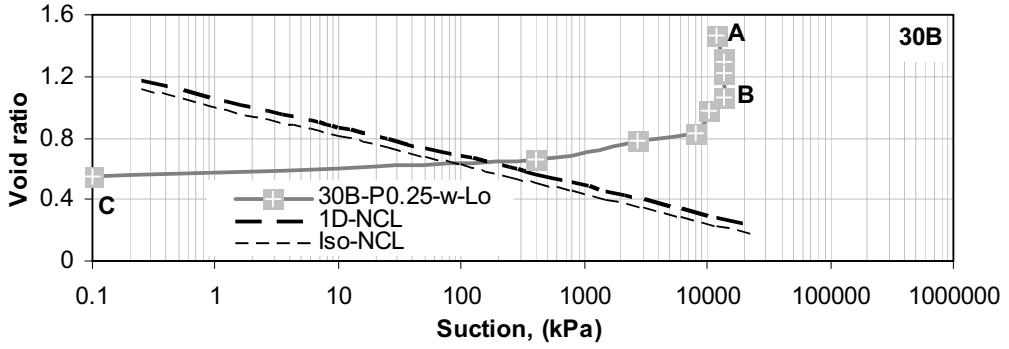

b

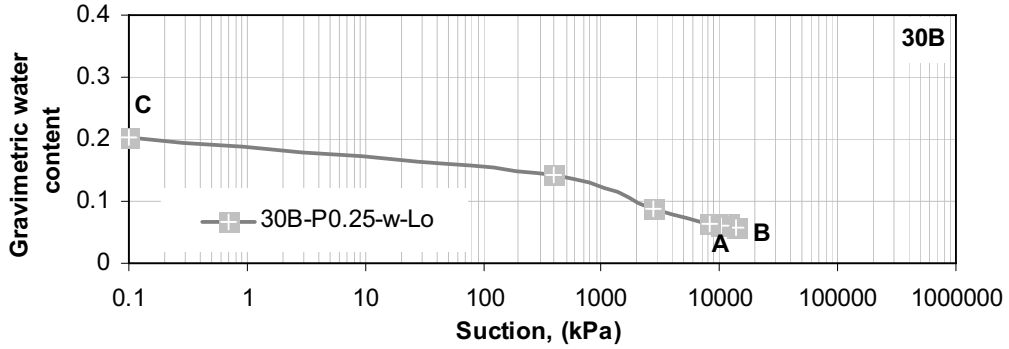

c

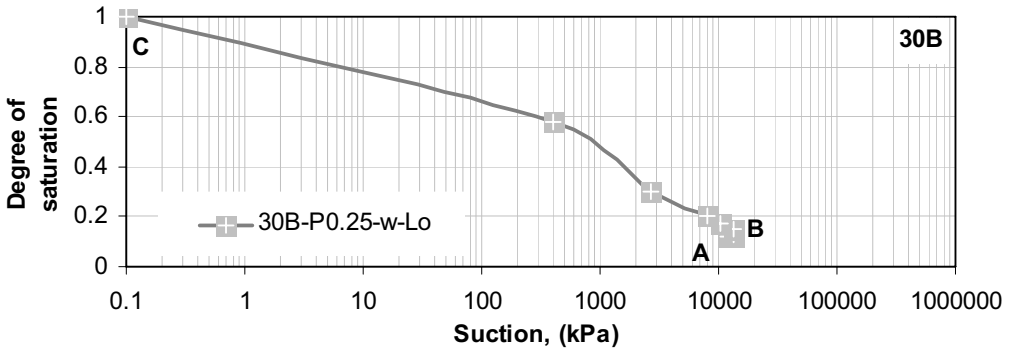

d

Figure 5.19 Void ratio, gravimetric water content, and degree of saturation results of constant net stress = 250 kPa condition with decreasing the suction (wetting path)-collapse test- for 30B soil.

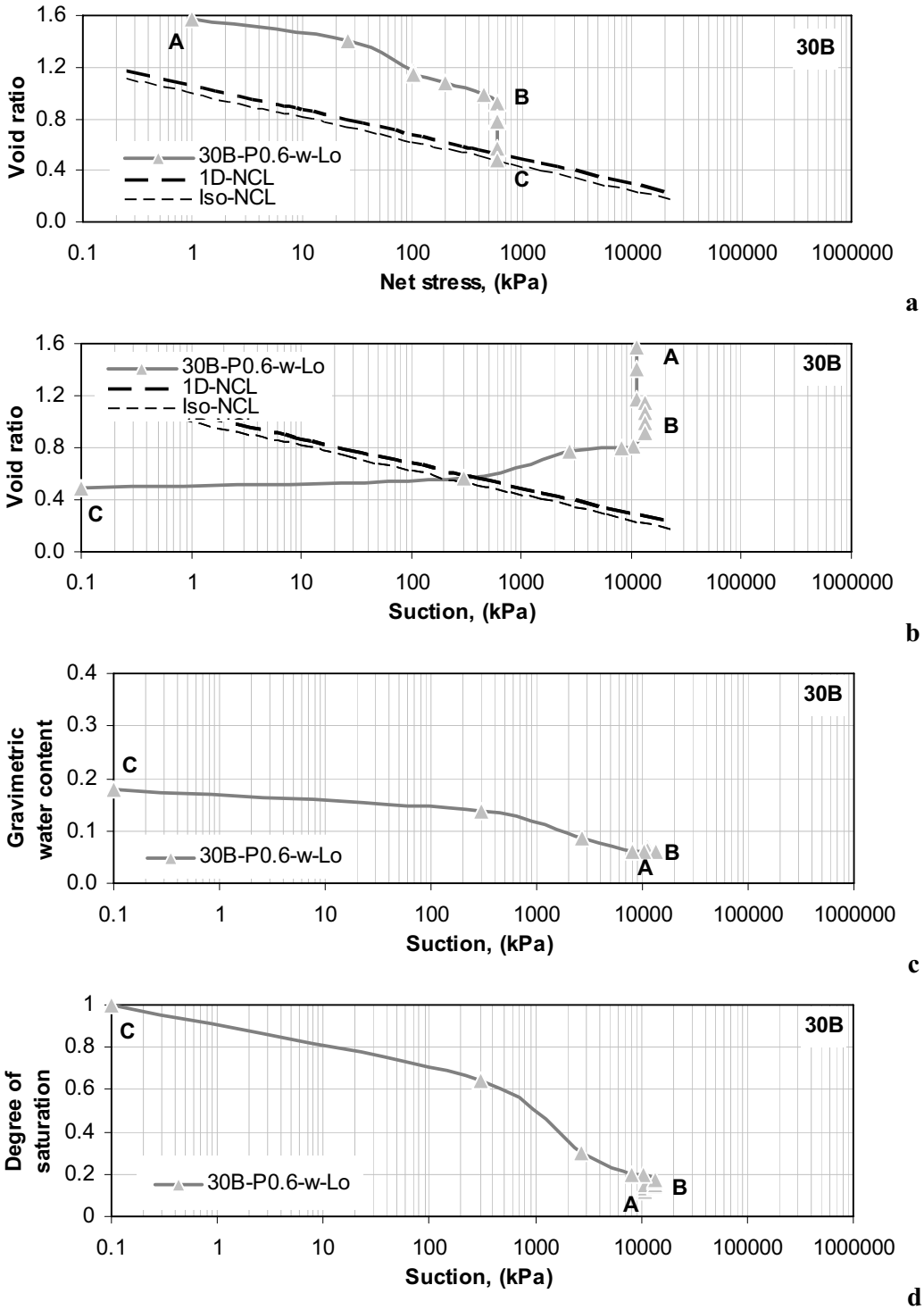

Figure 5.20 Void ratio, gravimetric water content, and degree of saturation results of constant net stress = 600 kPa condition with decreasing the suction (wetting path) -collapse test- for 30B soil.

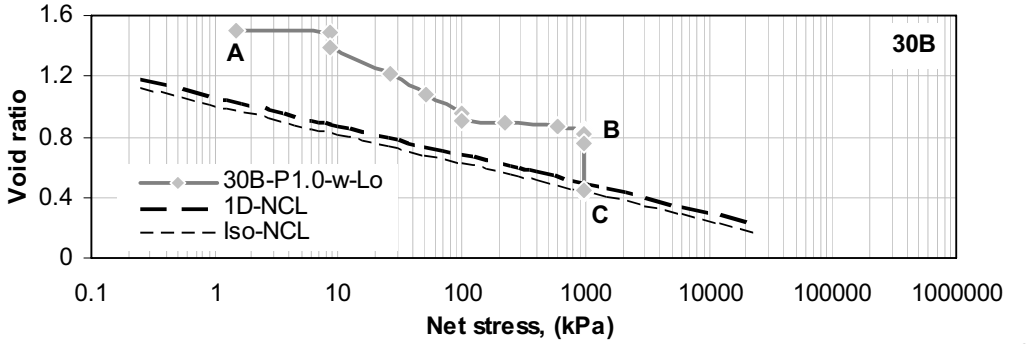

a

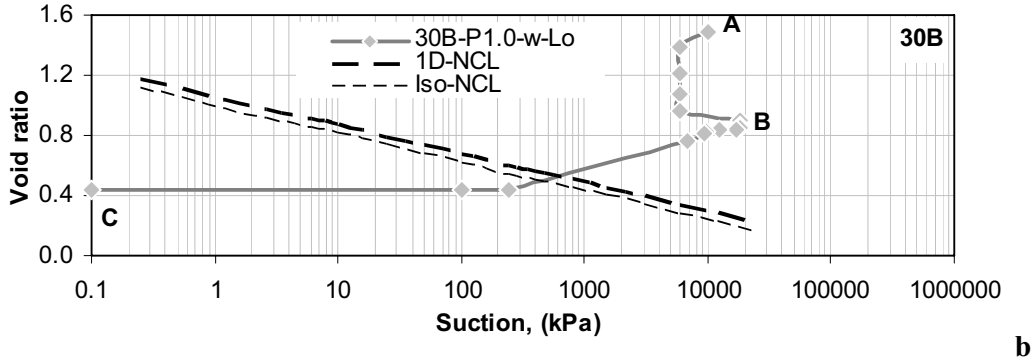

b

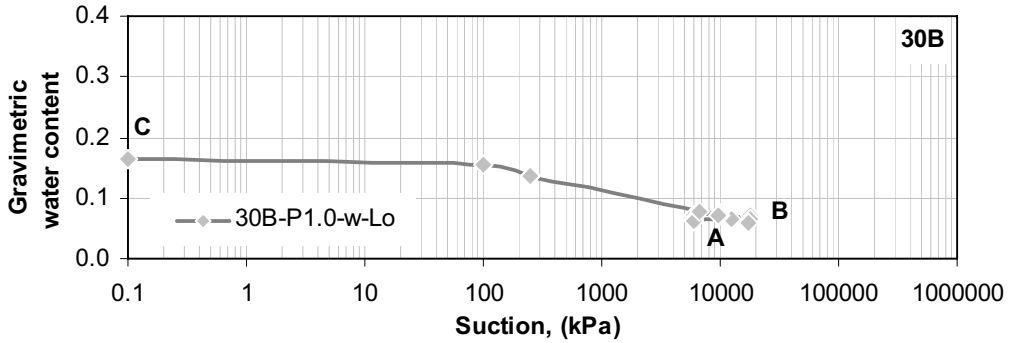

c

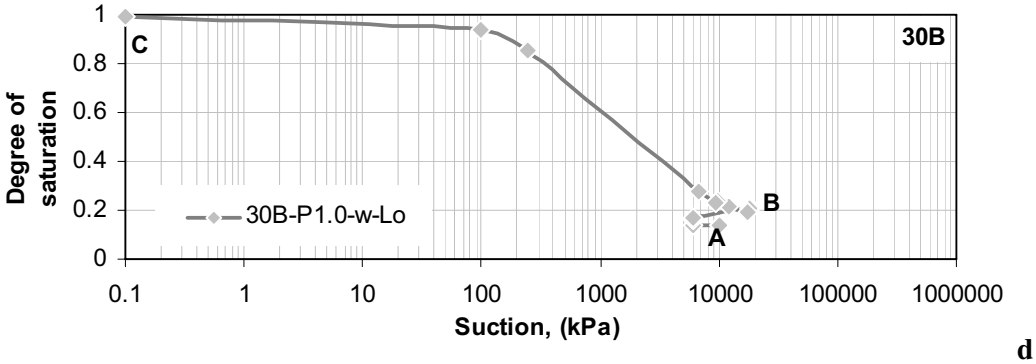

d

Figure 5.21 Void ratio, gravimetric water content, and degree of saturation results of constant net stress = 1000 kPa condition with decreasing the suction (wetting path) -collapse test- for 30B soil.

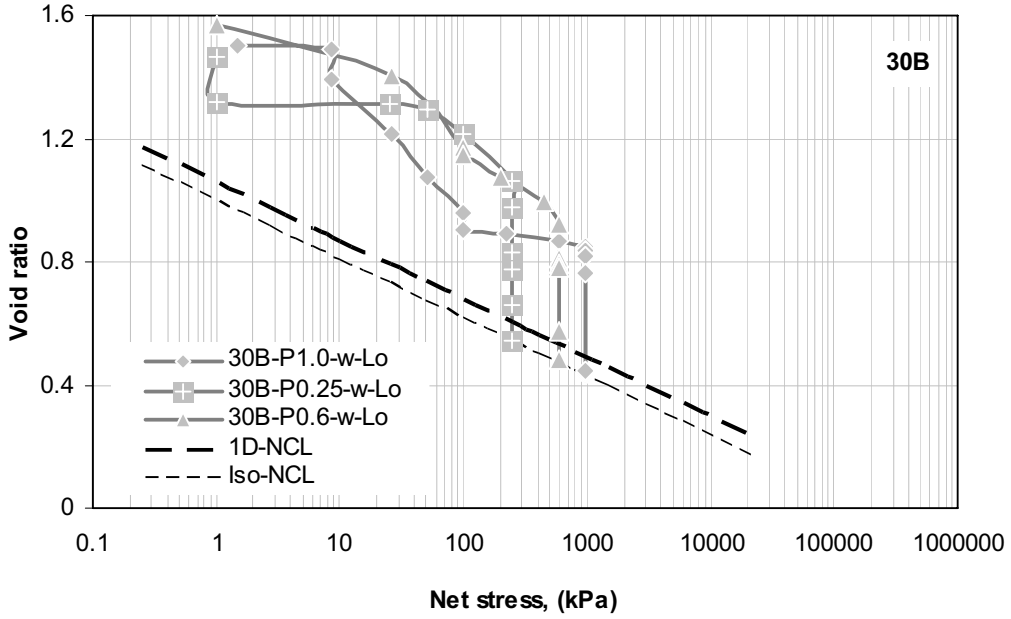

a

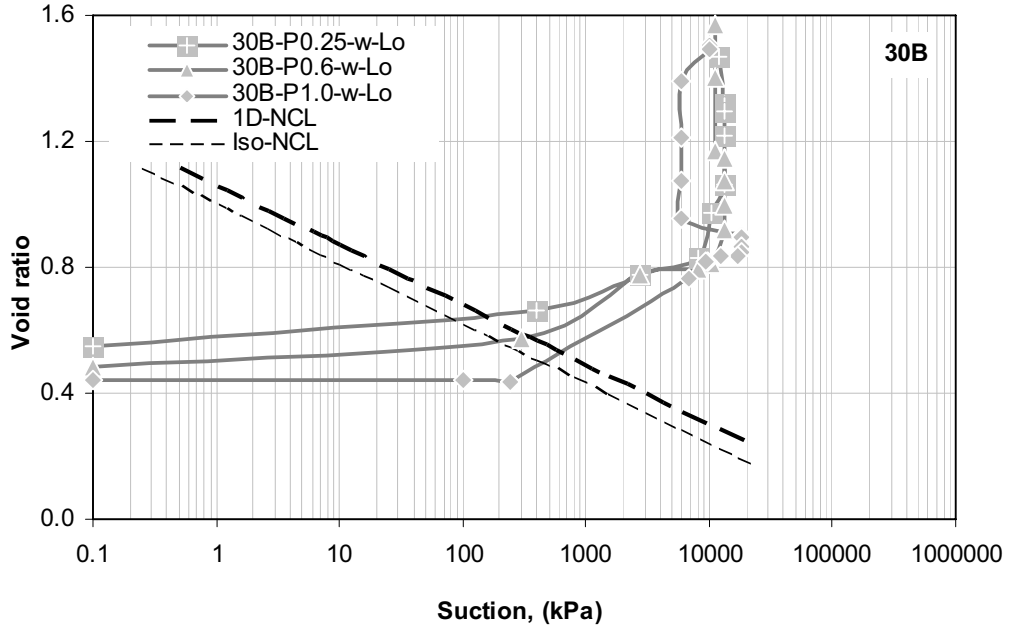

b

Figure 5.22-1 Void ratio, gravimetric water content, and degree of saturation results of all constant net stress tests condition with wetting path-collapse test-for 30B soil.

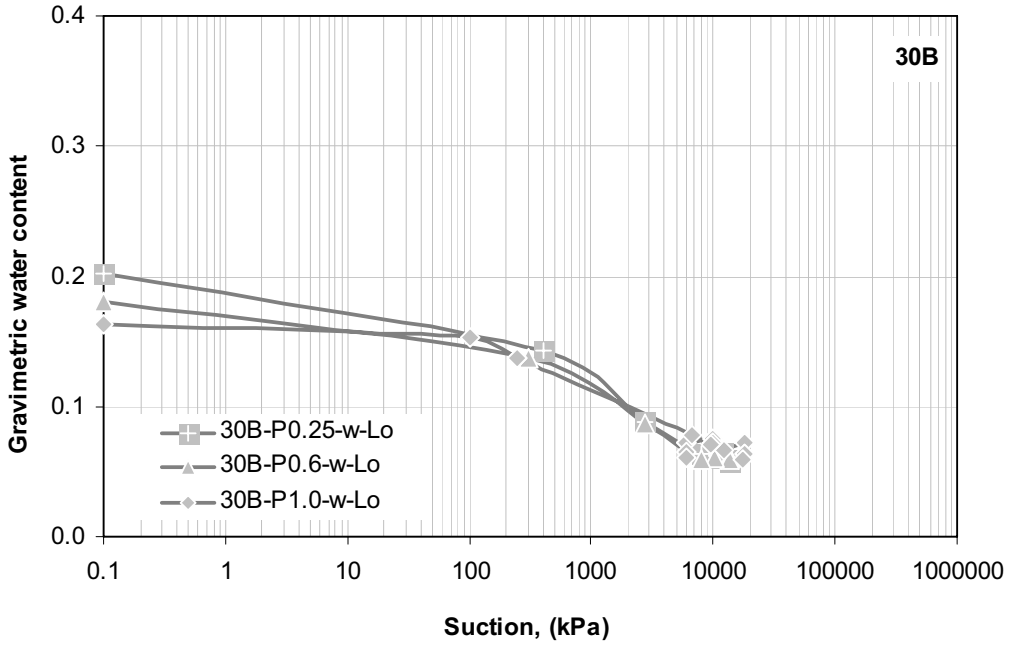

c

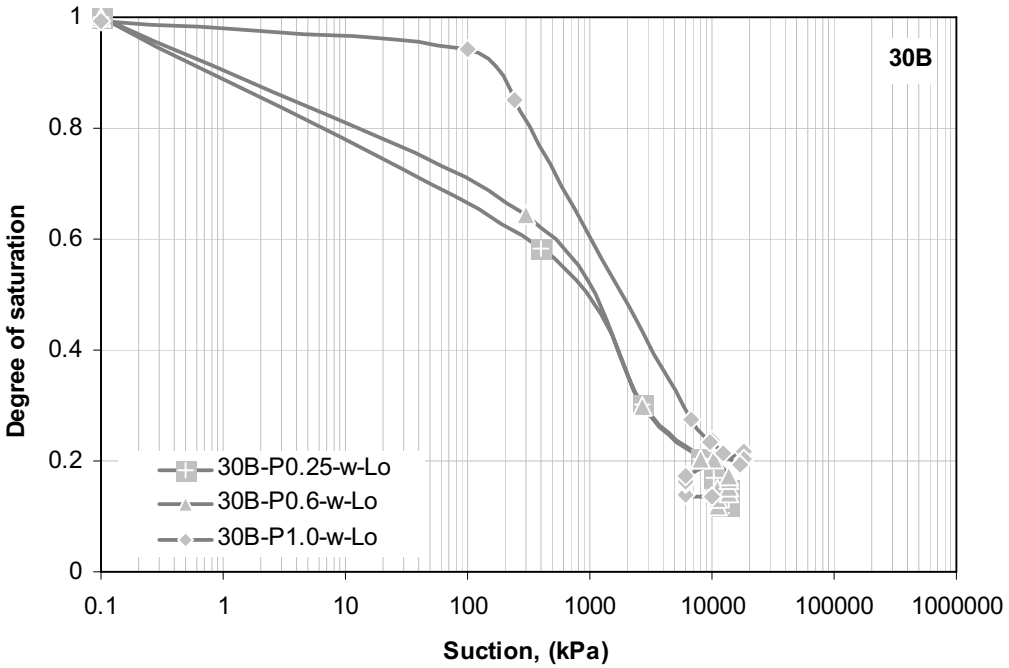

d

Figure 5.22-2 Void ratio, gravimetric water content, and degree of saturation results of all constant net stress tests condition with wetting path-collapse test-for 30B soil.

5.2.3 Constant suction test

The results of the volume change test under constant suction condition are presented in this section. Thirteen 30B specimens (8 specimens for initially slurry state and 5 specimens for initially loose state) and two 100B specimens (1 specimen for initially slurry state and 1 specimen for initially loose state) were tested under constant suction condition. Extra two 30B specimens were tested for comparison between the different cells. Two different initial states were chosen to examine the effect of initial state (slurry and loose) on the volumetric yielding at unsaturated state. The initial states for constant suction test and the stress paths for each test in (net stress-suction) space are shown in Table (3.5) and Figure (3.6), respectively. The initial point is denoted as point A, whereas point B represents the beginning of applying suction. Point C represents the beginning of loading under constant suction condition, and point D represents the end of constant suction condition. In the Figures (5.23, 5.39, and 5.35-5.37), the applied constant suction was equal to the initial suction, therefore A, B, and C correspond to the same point. Figures (5.23 and 5.39) were tested under zero suction condition (consolidation test).

Figures (5.23-5.32) show the results of first group (initially slurry state) of constant suction test for 30B soil. Within these tests, all the specimens start at slurry condition (point A) then the suction increases under seated load (4-7 kPa), (point B), till reaching a specific suction value (point C). Beyond that the net stress increases under constant suction condition.

The preconsolidation pressure are 7, 200, 300, 400, 600, 800, 1000, and 8000 kPa under 0, 50, 100, 255, 300, 400, 450, and 39000 kPa constant suction conditions respectively as shown in Figures (5.23a-5.31a). The increase in the preconsolidation pressure is due to (i) increase in the density before loading (as result of increasing the applied suction) and (ii) hardening of soil material as a result of increase in suction. Most of curves in this group (except 30B-S39-Sl test) joined the 1D-NCL as net stress increases. This behavior is attributed to increase in the degree of saturation during the loading that made the specimens reaching the saturation zone. The preconsolidation pressures, for tests with constant suction range from 0 to 450 kPa, locate on the saturated 1D-NCL and the values of these pressures increase as a result of increasing the density due to applying the suction. Note the values of the void ratio before start loading, Figures (5.23b-5.31b). The compression curve of 30B-S39-Sl test (Figure 5.30a) had undergone a high reduction in volume during the initial part of loading (between point C and 100 kPa net stress). This behavior can be attributed to separation of the sample from the confining ring due to high applied suction (39000 kPa) and the incremental response of the sample changes from oedometric to uniaxial. Therefore, initially the sample had high reduction in volume until it retain back, by filling the space

between the sample and the ring with soil material due to lateral deformation, to the oedometric loading condition. As the loading increased the compression curve passed the 1D-NCL till reaching 8000 kPa net stress. Beyond this point the state of the specimen changes from over consolidated to normal consolidated (yield) state with slope higher than the slope of saturated NCL. Once the suction was applied (after point B), the compressibility of the specimens in this group followed the isotropic NCL up to 255 kPa suction. Subsequently, the slope of compression curve decreased. The results of increasing suction for initially slurry state (Figure 5.5b) show that the slope of compression lines became near to zero (no compression with increasing the suction) for suction higher than 600 kPa. The same behavior was observed in case of 30B-S39-Sl test.

The gravimetric water content, of constant suction tests for initially slurry sate, decreased as suction increased along with drying path of SWCC, Figures (5. 24c-5.31c). The gravimetric water content decreased slightly as the net stress increased for over consolidation (before the preconsolidation pressure). The reduction in the gravimetric water content during the loading at the over consolidated state is believed to be due to change of the state from drying path (due to increasing the suction before loading) to wetting path (due to increase in the degree of saturation as a results of compression the specimen during loading). The results of controlled-suction collapse tests carried out by Sun et al. (2007) showed similar behavior during the over consolidated state. Beyond the preconsolidation pressure it seems to be that the gravimetric water content-suction relationship depends on the degree of saturation. If the degree of saturation is equal or higher than the degree of saturation at air-entry value (about 0.85 for 30B soil), as the case of 0, 25, 100, and 255 kPa constant suction conditions, the gravimetric water content decreased as net stress increased to keep the specimen in saturated zone. Whereas in case that the degree of saturation was moderately lower than the degree of saturation at air-entry value, as the case of 300, 400, and 450 kPa constant suction conditions, the gravimetric water content increased slightly as net stress increased till the degree of saturation reaches value around 0.85 (the degree of saturation at air-entry value), then the relationship followed similar behavior of first case. The third case is when the degree of saturation was significantly lower than the degree of saturation at air-entry value, as the case of 30B-S39-Sl test under constant suction of 39000 kPa. In this case the results show that the gravimetric water content remained unchanged regardless of increasing the density due to loading. Generally, the degree of saturation decreases with increasing the suction, then increases as the net stress increases, Figures (5.24d-5.31d).

For the initially slurry specimens under values for constant suction up to 255 kPa, the specimens remain in saturated state (except one point before loading in the 30B-S0.255-Sl

test). The soil before the air-entry value, s_{aev}, is in the saturated zone and its behavior as the saturated soil. Therefore, the effective stress (Equation 2.2 with $\chi = 1$) can be applied for void ratio and gravimetric water content, Figure (5.32). In other tests, the effective stress can be applied for range of suction before air-entry value (80 kPa) only.

Figures (5.33-5.38) show the results of second group of tests under constant suction condition for 30B soil: namely the initially loose state. The preconsolidation pressures are 5, 4, 100, 150, and 800 kPa under 50, 100, 4300, 10000, and 39000 kPa constant suction conditions respectively, Figures (5.33a-5.38a). The values of the void ratios in this group before loading (points C's) was 1.0, 1.1, 1.44, 1.05, and 1.05 under 50, 100, 4300, 10000, and 39000 kPa constant suction conditions respectively. These values can give some explanations about the relationship between the initial void ratio (initial density) and the unsaturated preconsolidation pressure. Again the increase in the preconsolidation pressure is due to the higher density before loading and hardening of soil material as suction increases. However, the yield states of 30B-S0.05-Lo and 30B-S0.1-Lo tests were achieved immediately when the suction was reduced from 5000 and 3500 kPa to 50 and 100 kPa, respectively. The results of 30B-S4.3-Lo, 30B-S10-Lo, and 30B-S39-Lo tests show that the unsaturated preconsolidation pressure increased from 100 kPa to 800 kPa as the constant suction increased from 4300 kPa to 39000 kPa. Moreover, Figure (5.38a) shows that the normal consolidated (yield) paths for both 30B-S10-Lo and 30B-S39-Lo tests are the same and the difference in the preconsolidation pressure is due to difference in the initial density. In other words, the results show that, for range of void ratio from 1.44 to 1.5, the unsaturated preconsolidation pressure remains almost constant when the suction was changed from 4300 kPa to 10000 kPa. The slopes of the unsaturated over consolidated path in all tests were closed to the slope of saturated over consolidated path (C_r), while the slopes of the unsaturated normal consolidated (yield) state are higher than the slope of saturated NCL. The specimen of 30B-S0.05-Lo test, Figure (5.33), had initially 5000 kPa suction (point A), and then the suction was reduced to 50 kPa under seating load (point B) which caused an increase of the gravimetric water content from 0.85 to 0.205 (point C), Figure (5.33b), and reduction in void ratio from 1.56 to 1.04, Figure (5.33c). While the initial suction for 30B-S0.1-Lo test, Figure (5.34), was 3500 kPa (point A), then it was reduced to 100 kPa under seating load (point B) which caused reduction in the gravimetric water content from 0.1005 to 0.190 (point C), Figure (5.34b), and reduction in void ration from 1.6 to 1.06, Figure (5.34c). The applied constant suction values of the other tests of this group (30B-S10-Lo, 30B-S4.3-Lo, and 30B-S39-Lo) were equaled to the initial suction. The gravimetric water content values remain almost unchanged during the yield state for high suction value (s > 4300 kPa), whereas the gravimetric water content

decreased slightly in case of 50 kPa and 100 kPa constant suction conditions, Figure (5.38c). The results show that all the tests, during yield state had gravimetric water content-suction relationship follows the wetting path of SWCC.

Figures (5.39-5.41) show the results of two different cases (slurry and loose) under constant suction condition for 100B soil. Figure (5.39) shows the results of initially slurry specimen under zero constant suction condition, 100B-S0-Sl. The test is a conventional one-dimensional high stress consolidation test (the specimen remains saturated during the test), in which the specimen was loaded till 24000 kPa net stress. Figure (5.39a) shows that, up to range of applied net stress, the 1D-NCL of the 100B soil has two different slopes. The first slope (C_{c1}) was 0.7 for net stress up to 900 kPa. Beyond this point the slope (C_{c2}) reduced to 0.37.

Figure (5.40) shows the results of initially loose specimen under 4300 kPa constant suction condition, 100B-S4.30-Lo. The initial void ratio was 2.4 and the preconsolidation pressure was about 375 kPa. The specimen had high reduction in volume after the preconsolidation pressure, then followed a path with slope higher than the slope of saturated NCL till joined the saturated NCL at 60000 kPa net stress, Figure (5.40a). The gravimetric water content values slightly changed (decreased) during the yield state, Figure (5.40c). The degree of saturation increased due to compression till reaching the full saturation state at 12000 kPa net stress (S_r = 90 % at 6000 kPa net stress when the curve joined the saturated NCL), Figure (5.40d). Figure (5.41) shows the results for both cases (slurry and loose) together.

The observed behavior, the slope of the unsaturated NCL is higher than the slope of saturated NCL, is similar to the results of (Maswoswe, 1985; Josa et al., 1992; Sivakumar, 1993; Wheeler and Sivakumar, 1995; Wheeler and Karube, 1996; Sharma, 1998; Sivakumar and Wheeler, 2000; Matsuoka et al., 2002; Wheeler et al., 2002; Gallipoli et al., 2003b; Georgiadis, 2003; Jotisankasa, 2005; Casini et al., 2007; and Benatti et al., 2010), see Figure (2.9) for the results of Jotisankasa (2005). This behavior confirms the assumption of some unsaturated soil models (e. g. Josa et al., 1992; Wheeler and Sivakumar, 1995; Georgiadis, 2003; and Gallipoli et al., 2003a), while it disagrees with other unsaturated soil models, where they are assumed that the slope of the unsaturated NCL is lower than the slope of saturated NCL (e. g. Alonso et al., 1990, Kohgo et al., 1993a)

Agus (2005) pointed out that the apparent pre-consolidation pressure of the 50 % bentonite-sand mixture specimens generally increases with increasing suction indicating that the material hardened as suction increases. This behavior is generally similar to the behavior of tested bentonite-sand mixtures (30B and 100B) in this study. Pham (2005) presented results

showing that during the compression process at constant soil suction for an unsaturated soil, the degree of the saturation always increases with an increment of net vertical stress. Jotisankasa (2005) cited that the contours of constant suction NCLs for suctions between 10 and 100 kPa appear to be slightly curved and converge towards the fully saturated (zero suction) NCL at high vertical stresses, Figure (2.9). But the NCLs for higher suction showed straight line behavior. It is expected that the NCLs for higher suction would also converge toward the fully saturated NCL if the samples are loaded to high enough net stresses. Moreover, his results show that all the contours of constant suction NCLs have a slope larger than the saturated NCL. The behavior of soil in the work of Jotisankasa (2005) is very close to the observed behavior of tested bentonite-sand mixtures in this study.

Moreover, two different tests (initially slurry and loose) for 30B soil, 30B-S0-Sl-U and 30B-S0.05-Lo-U were carried out. One was tested for comparison between the performance of other two UPC-Isochoric cells and HSC. The other one was tested for comparison between the performance of other two UPC-Isochoric cells and the modified oedometer cell (Red cell). Figures (5.42 and 5.43) show that the results obtained by the two UPC-Isochoric cells are in a good agreement with the results of HSC and Red cell. Thus, these two UPC-Isochoric cells were used in one-dimensional controlled-suction compression tests.

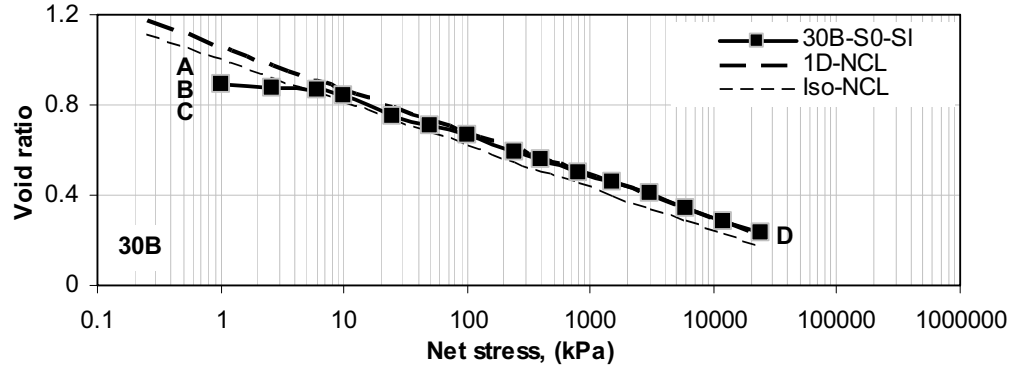

a

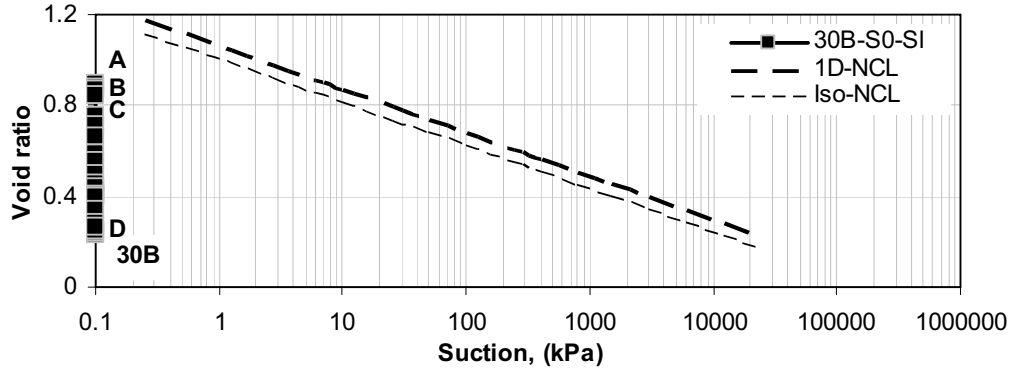

b

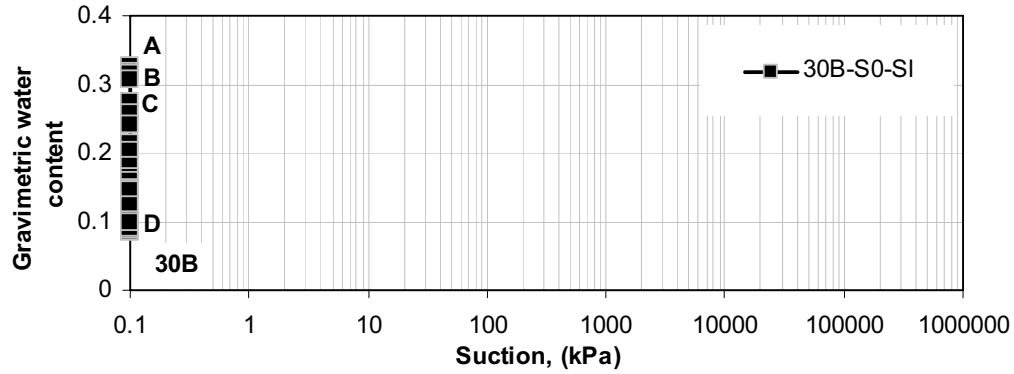

c

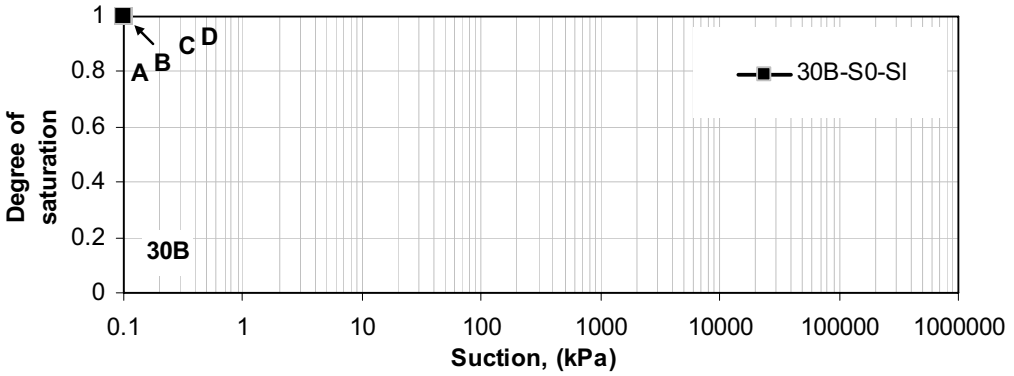

d

Figure 5.23 Void ratio, gravimetric water content, and degree of saturation results of constant suction = 0 kPa condition, saturated, (for log-scale of suction it is given as 0.1 kPa) for initially slurry 30B soil.

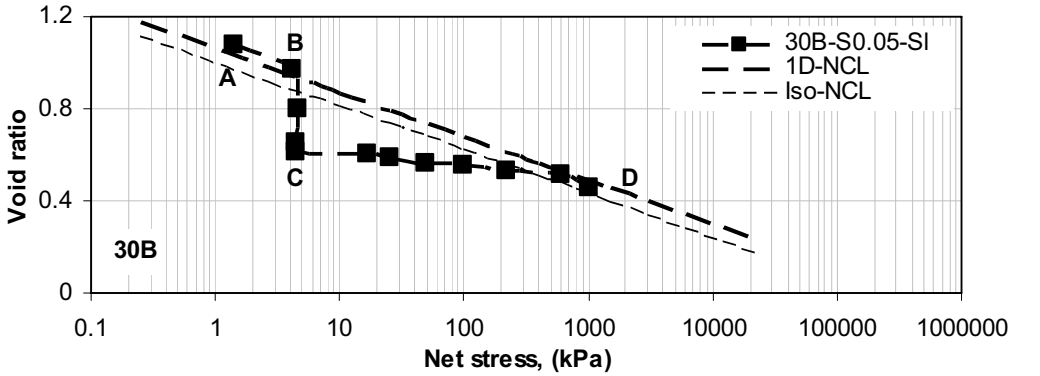

a

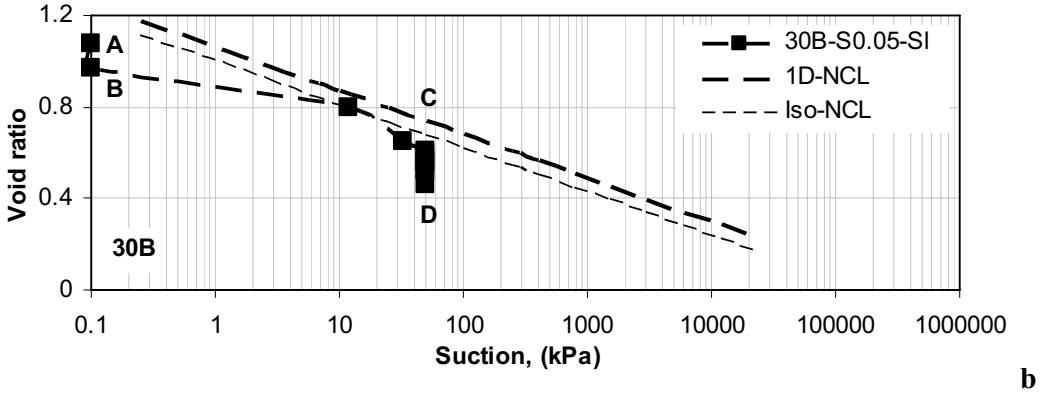

b

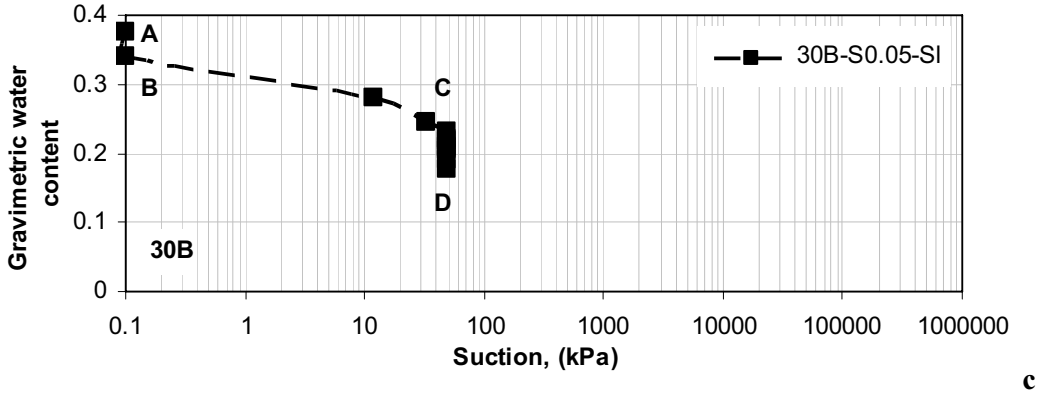

c

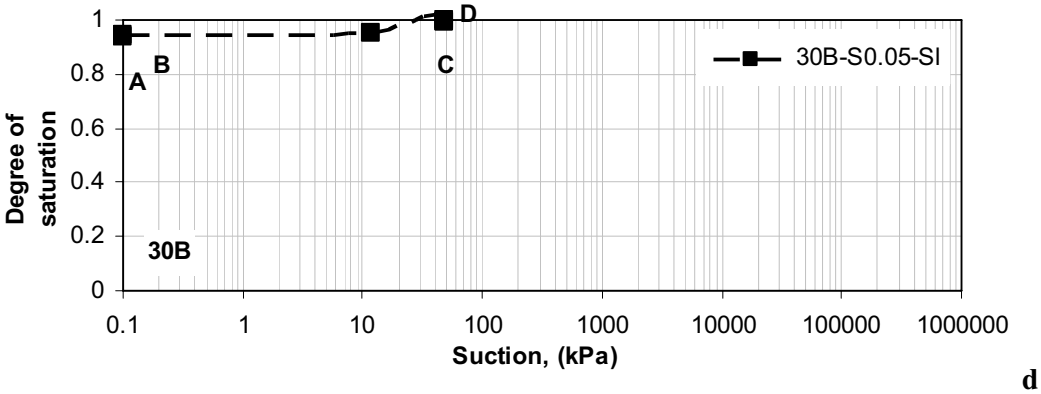

d

Figure 5.24 Void ratio, gravimetric water content, and degree of saturation results of constant suction = 50 kPa condition for initially slurry 30B soil.

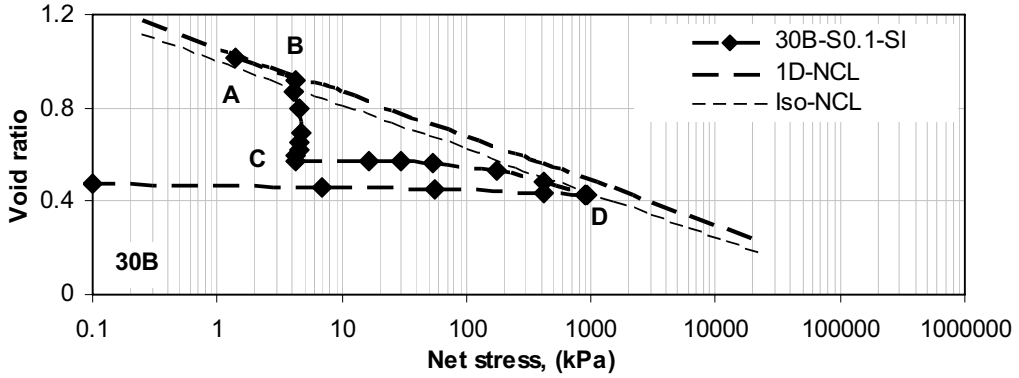

a

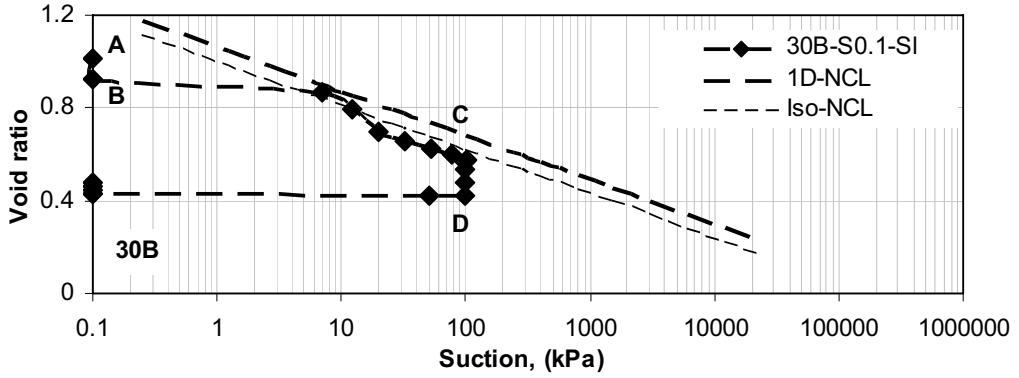

b

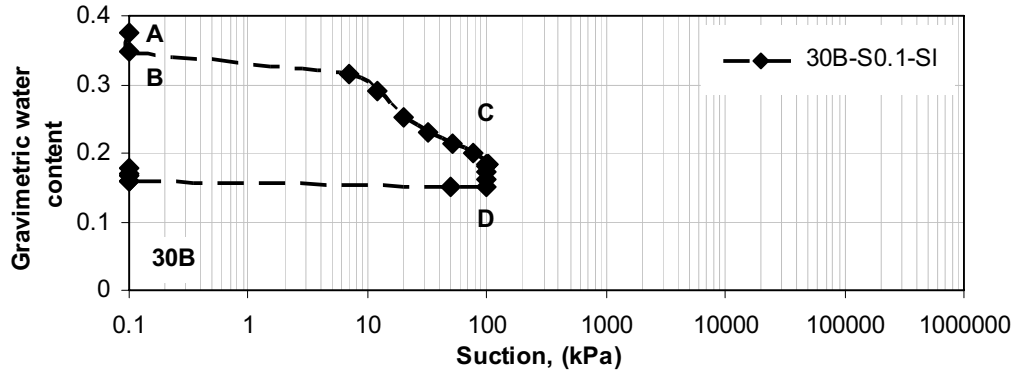

c

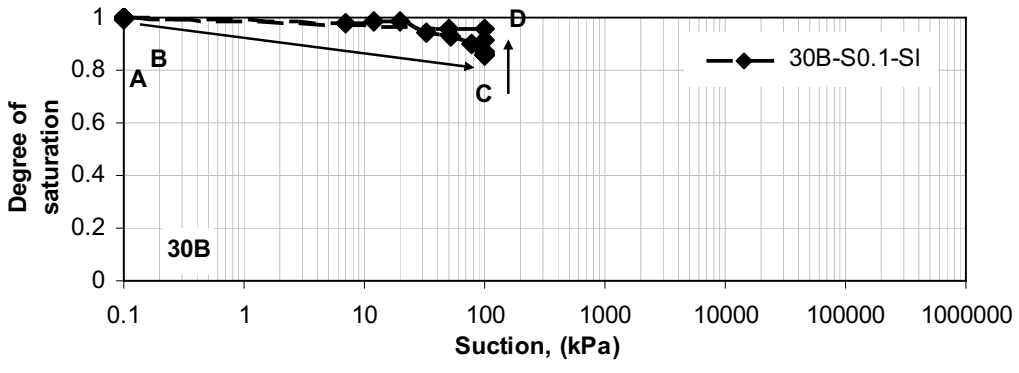

d

Figure 5.25 Void ratio, gravimetric water content, and degree of saturation results of constant suction = 100 kPa condition for initially slurry 30B soil.

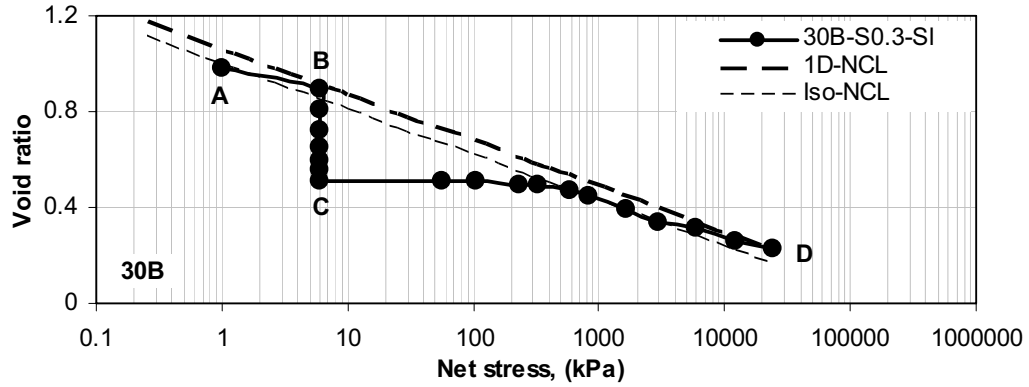

a

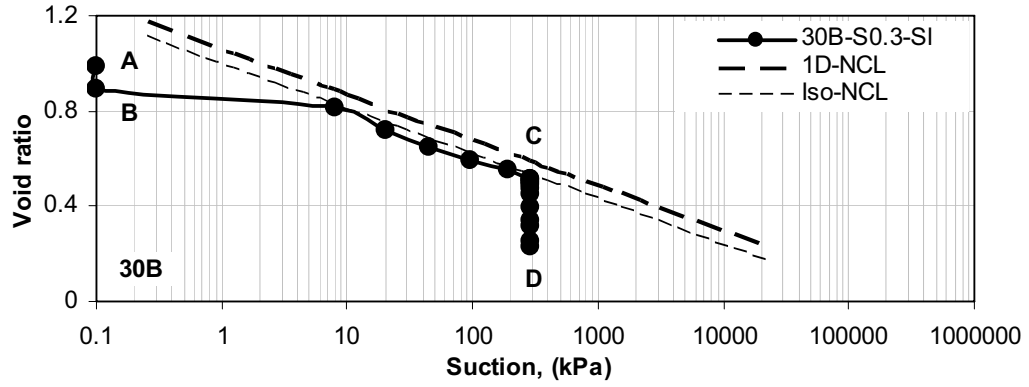

b

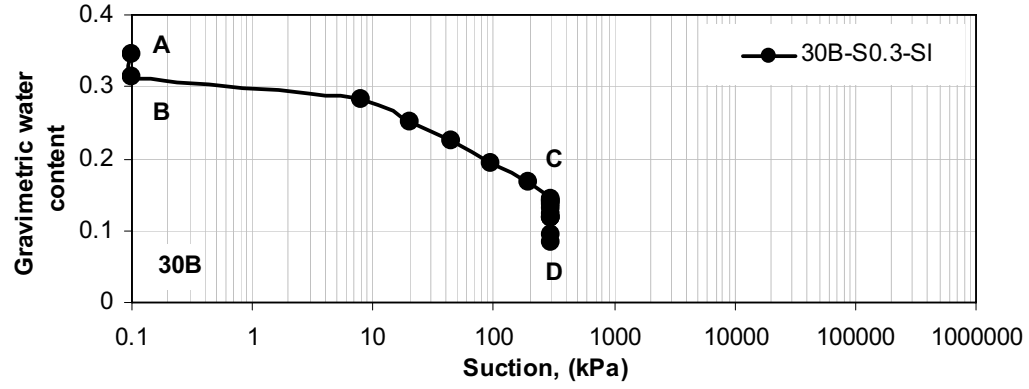

c

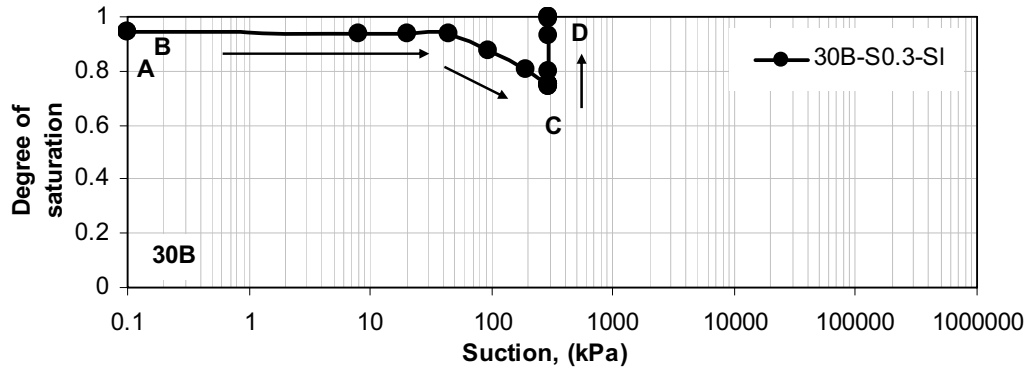

d

Figure 5.26 Void ratio, gravimetric water content, and degree of saturation results of constant suction = 255 kPa condition for initially slurry 30B soil.

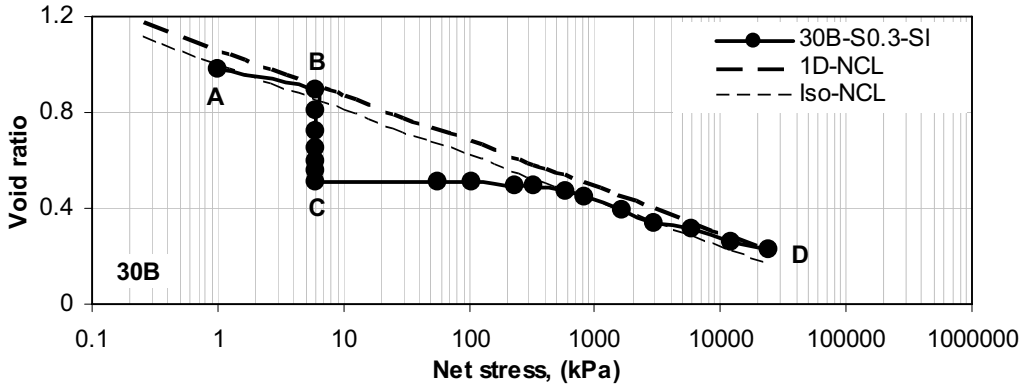

a

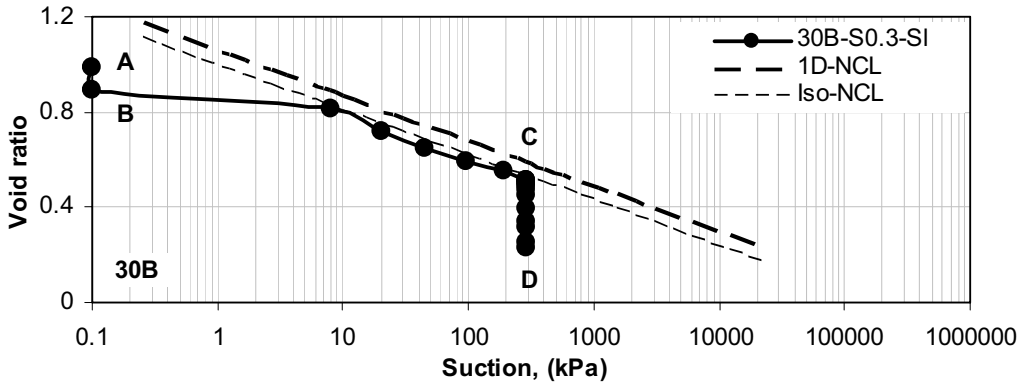

b

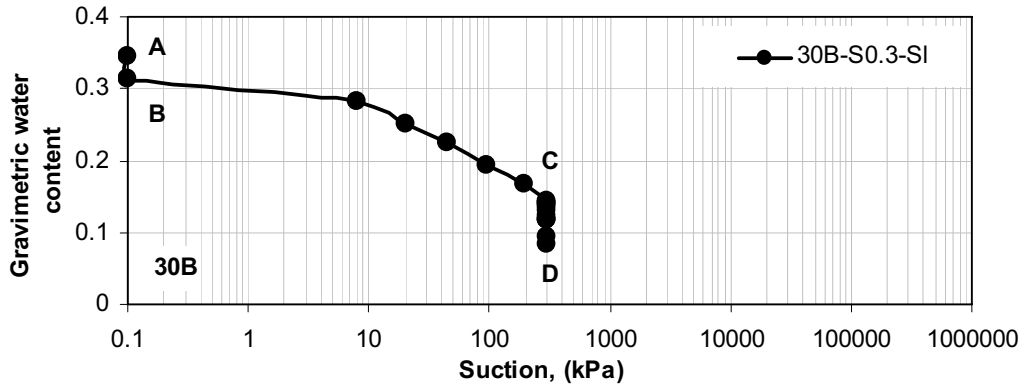

c

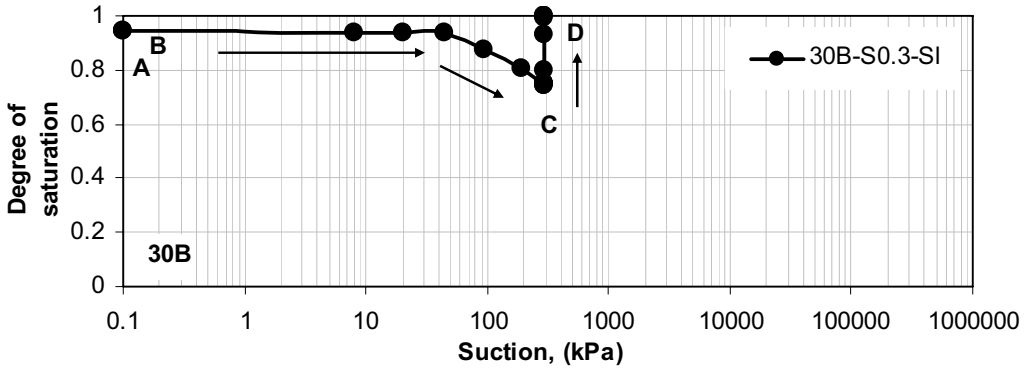

d

Figure 5.27 Void ratio, gravimetric water content, and degree of saturation results of constant suction = 300 kPa condition for initially slurry 30B soil.

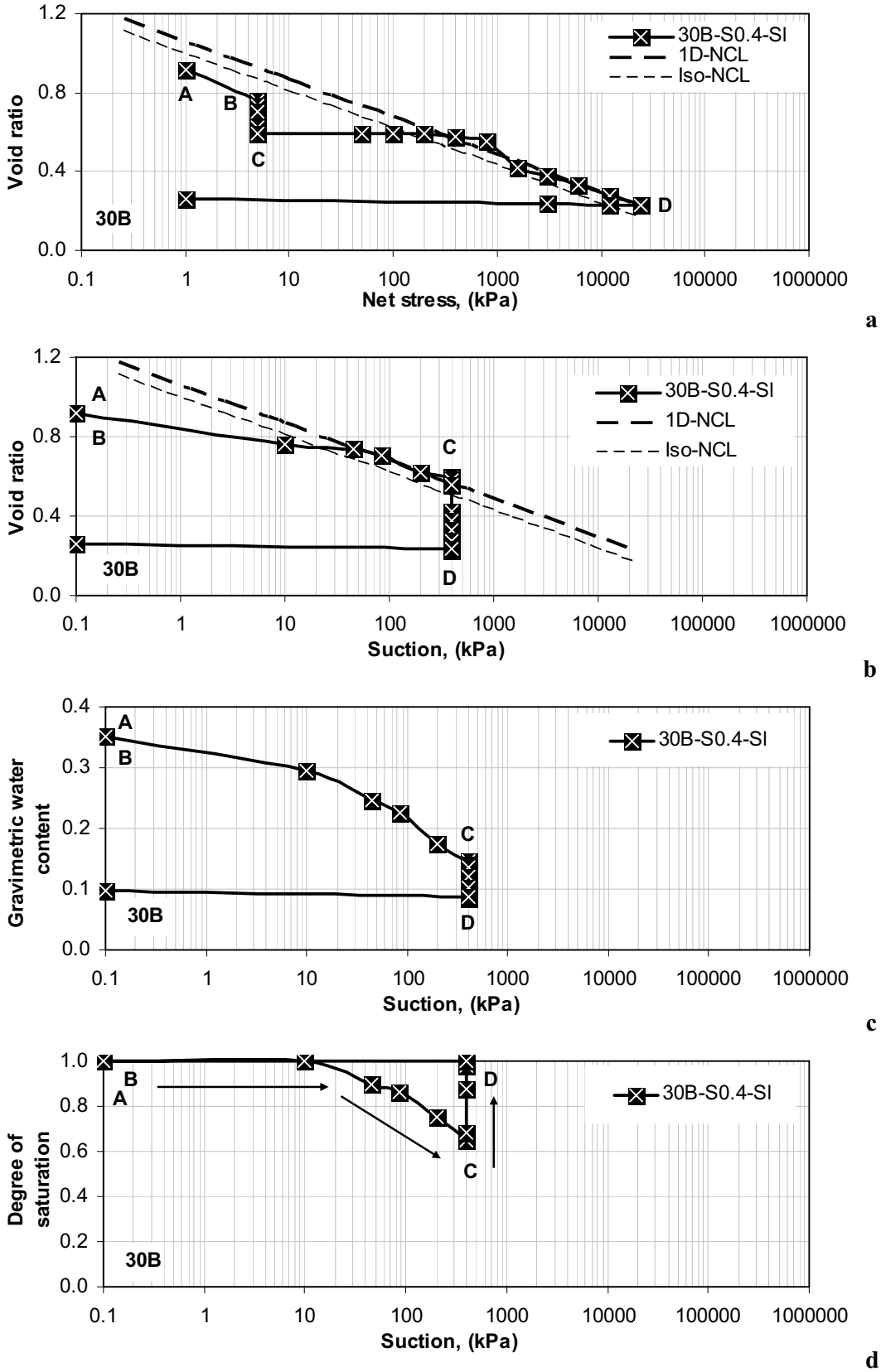

Figure 5.28 Void ratio, gravimetric water content, and degree of saturation results of constant suction = 400 kPa condition for initially slurry 30B soil.

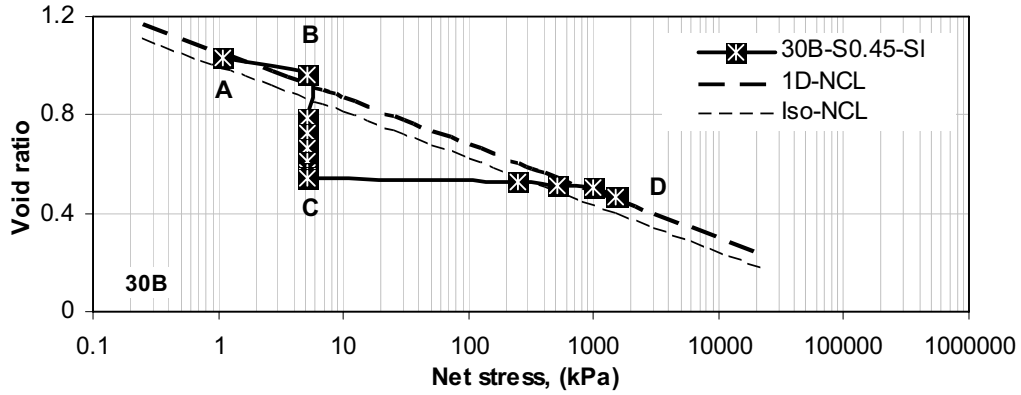

a

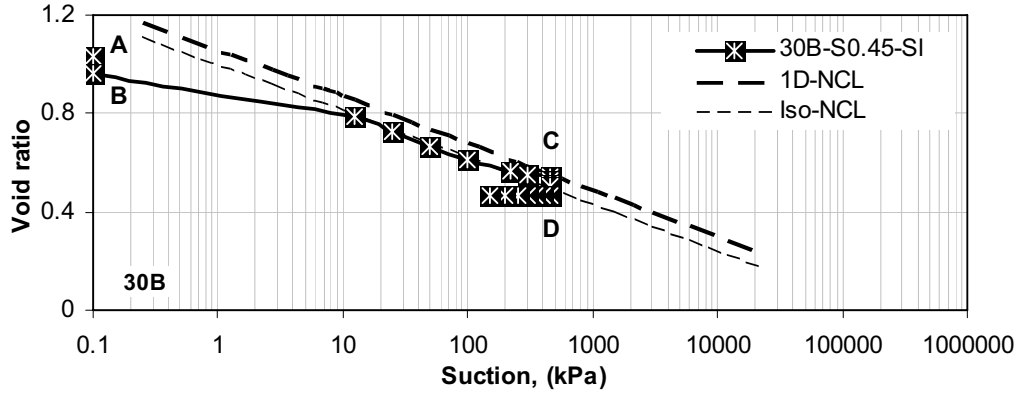

b

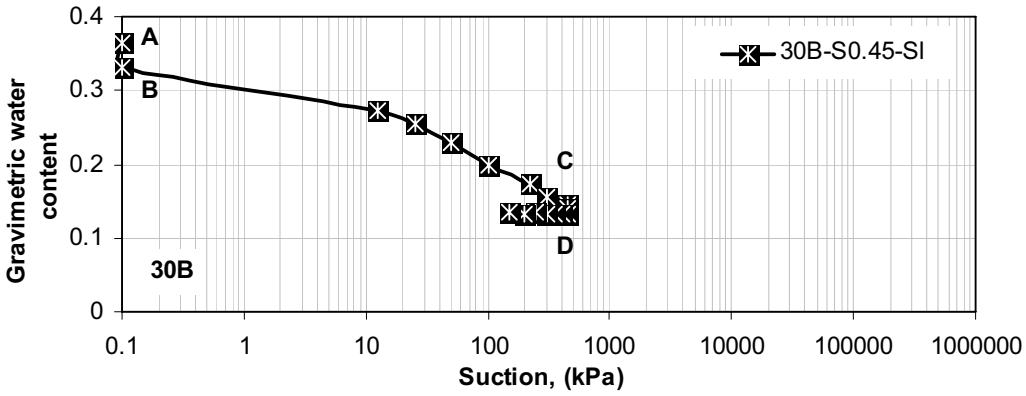

c

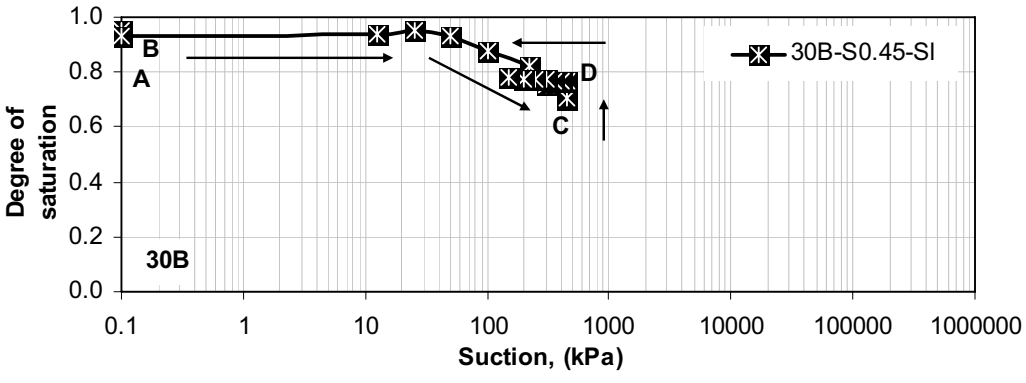

d

Figure 5.29 Void ratio, gravimetric water content, and degree of saturation results of constant suction = 450 kPa condition for initially slurry 30B soil.

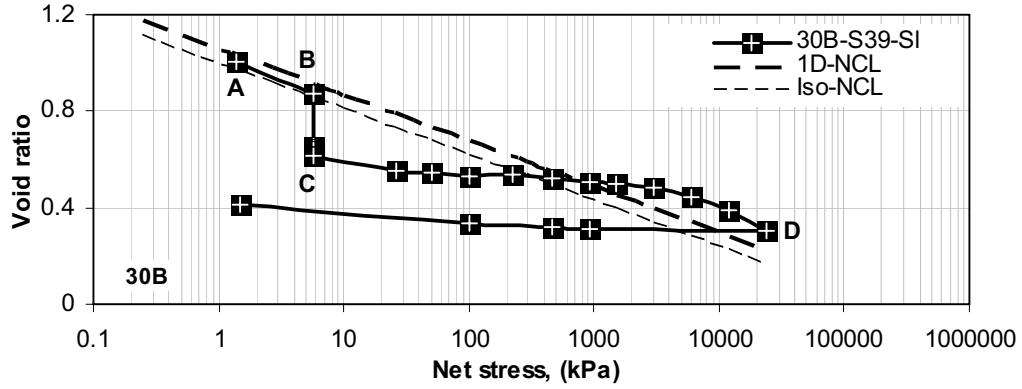

a

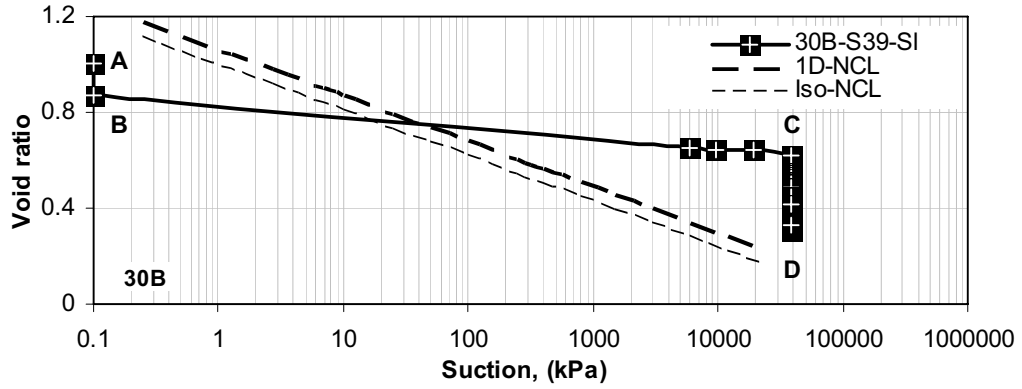

b

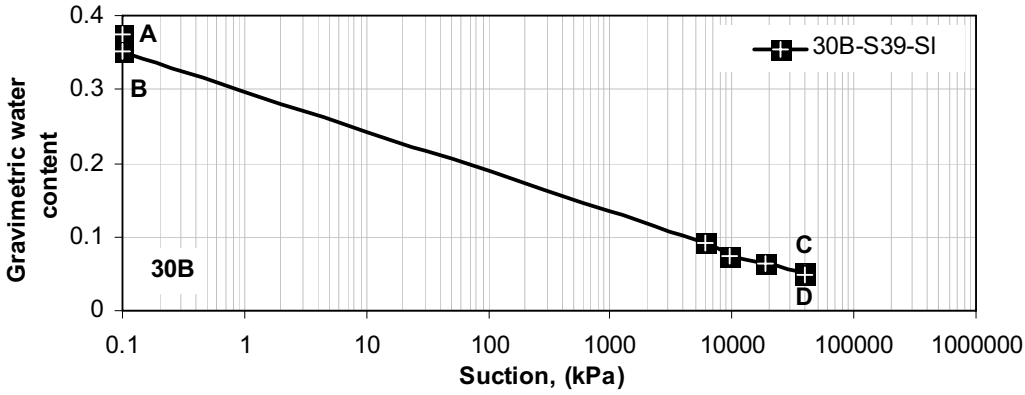

c

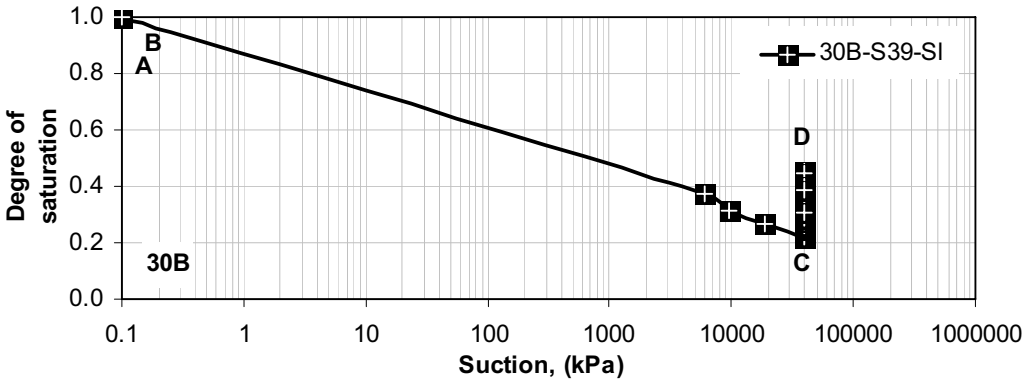

d

Figure 5.30 Void ratio, gravimetric water content, and degree of saturation results of constant suction = 3900 kPa condition for initially slurry 30B soil.

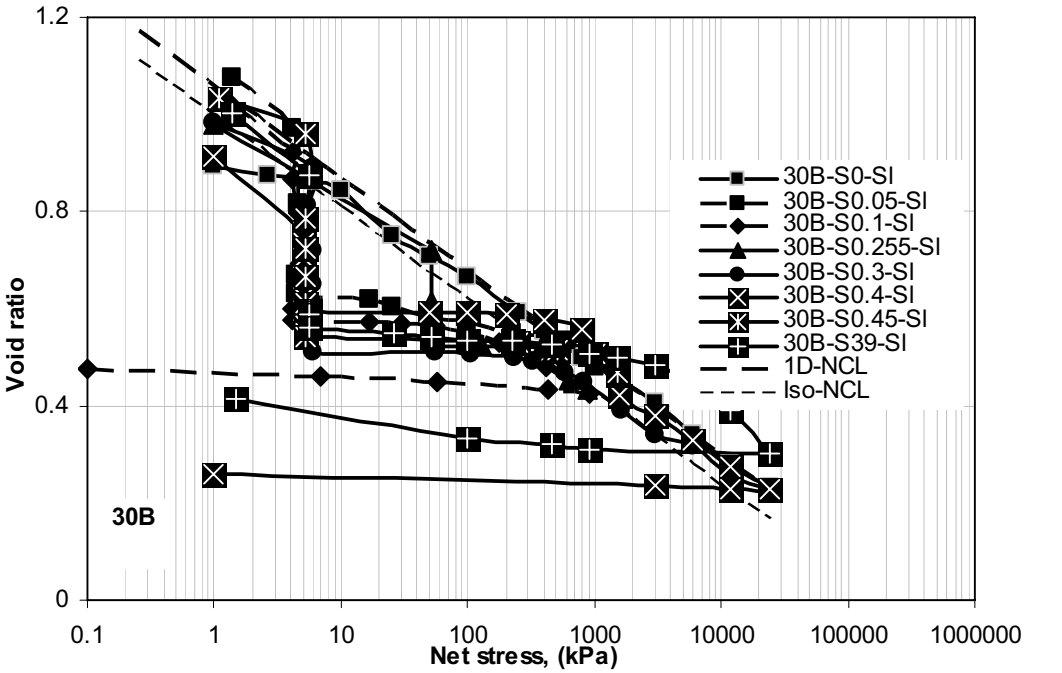

a

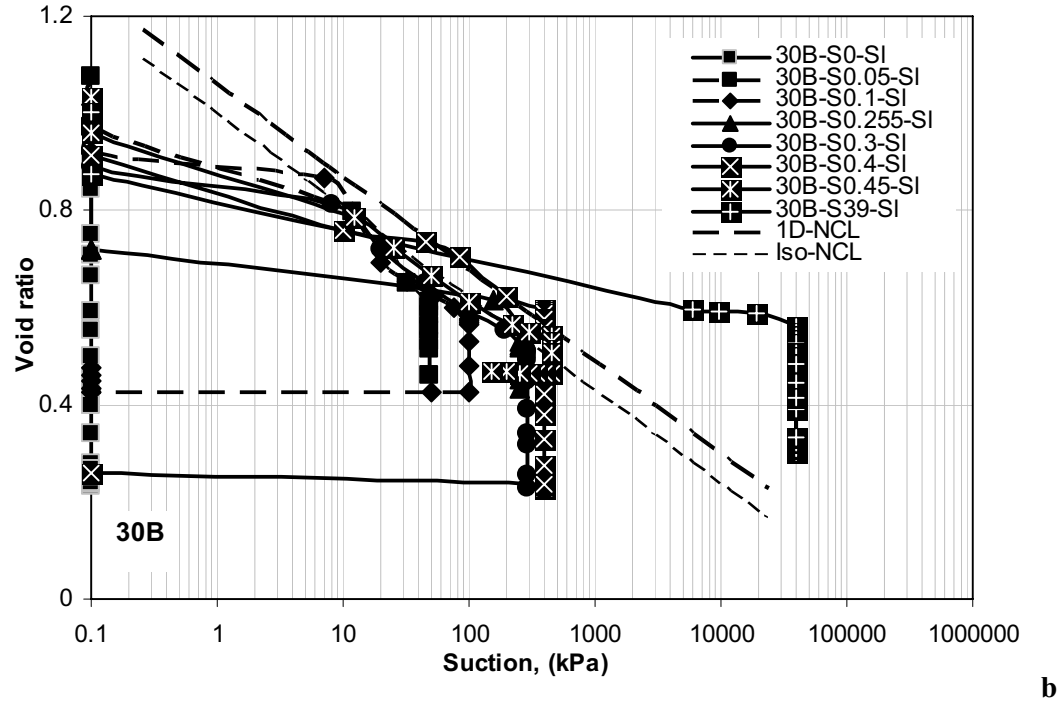

b

Figure 5.31-1 Void ratio, gravimetric water content, and degree of saturation results of all constant suction condition for initially slurry 30B soil.

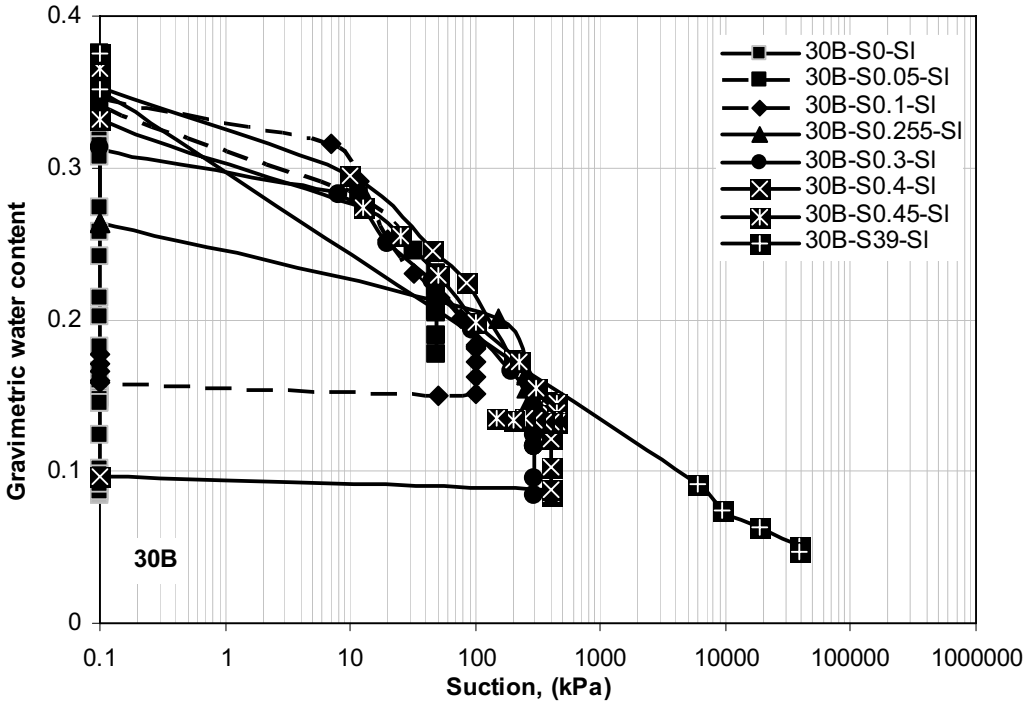

c

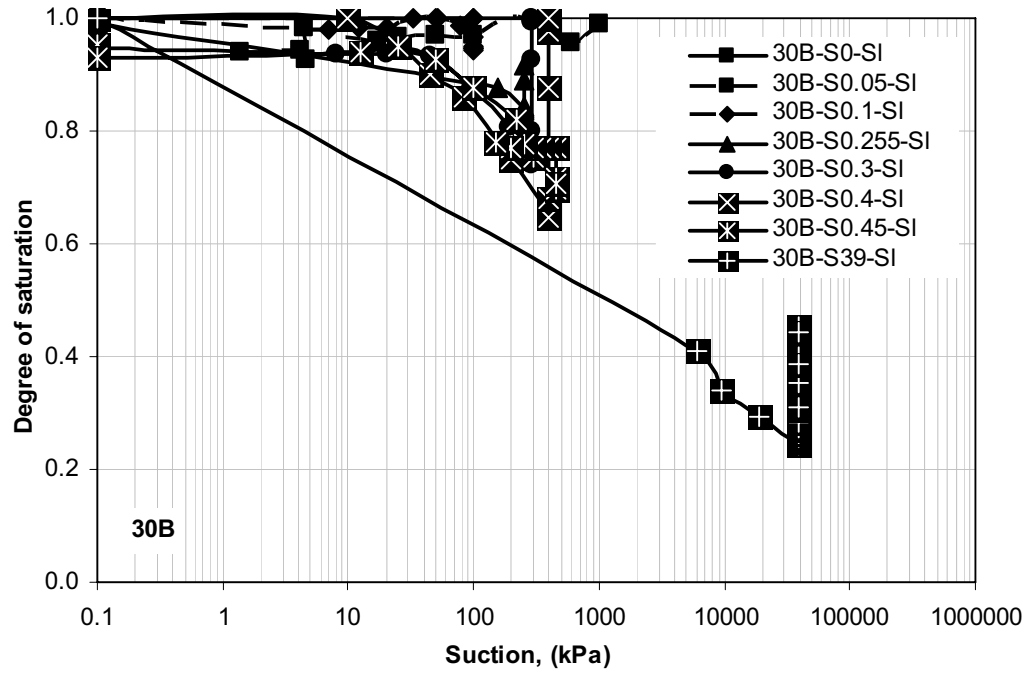

d

Figure 5.31-2 Void ratio, gravimetric water content, and degree of saturation results of all constant suction condition for initially slurry 30B soil.

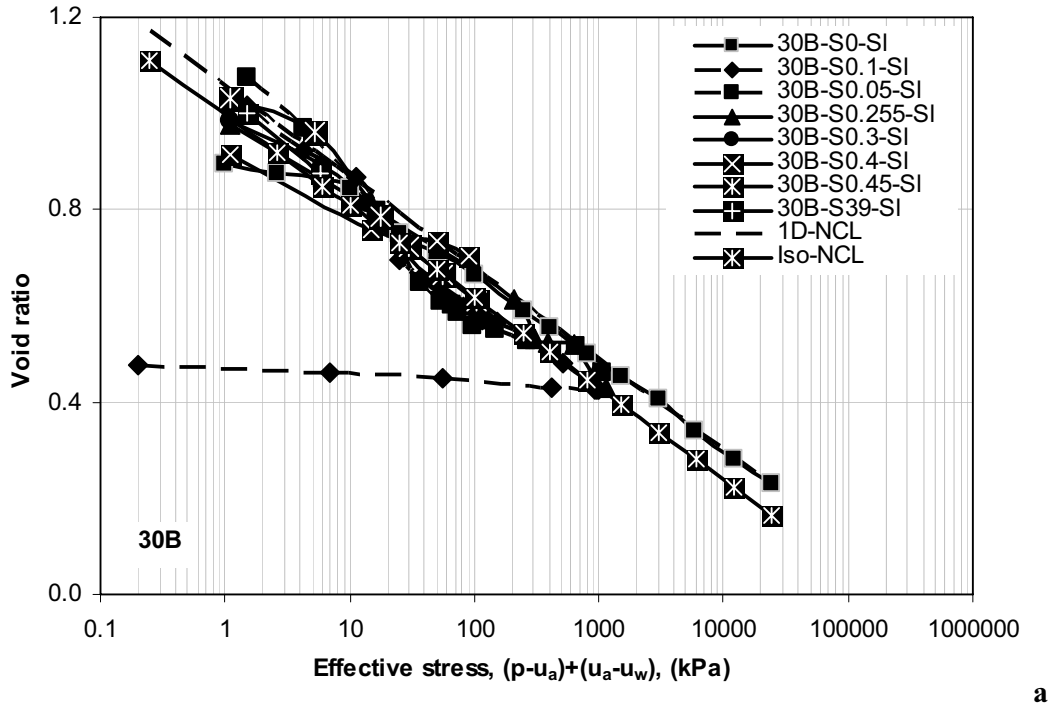

a

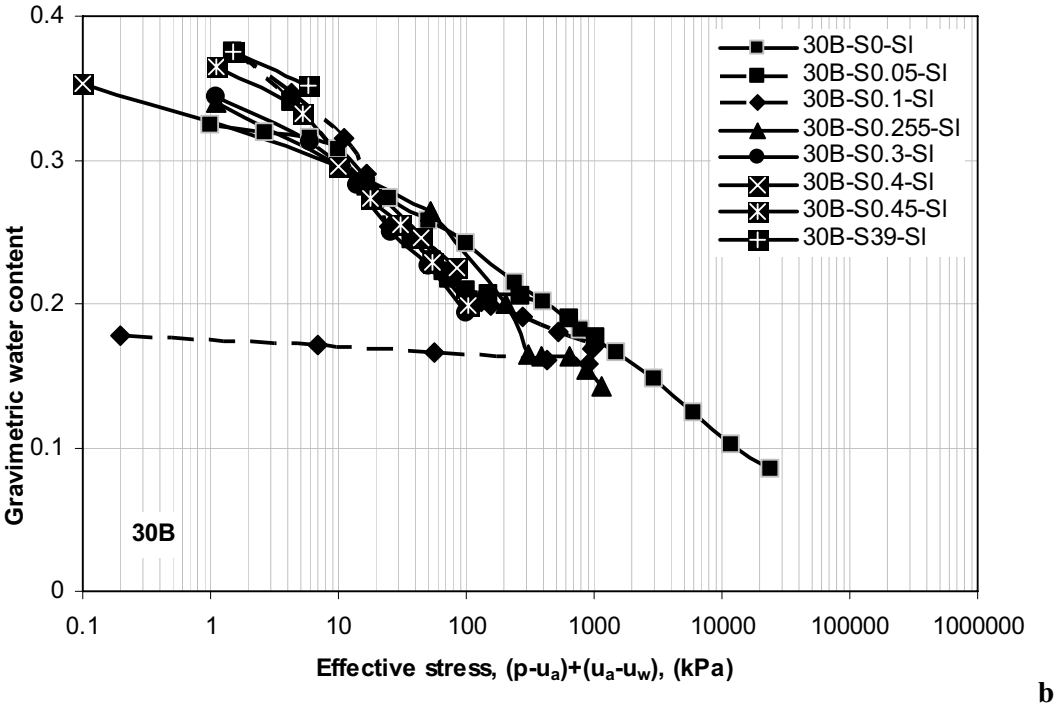

b

Figure 5.32 Void ratio and gravimetric water content verses effective stress relationships for saturation zone of all constant suction condition for initially slurry 30B soil.

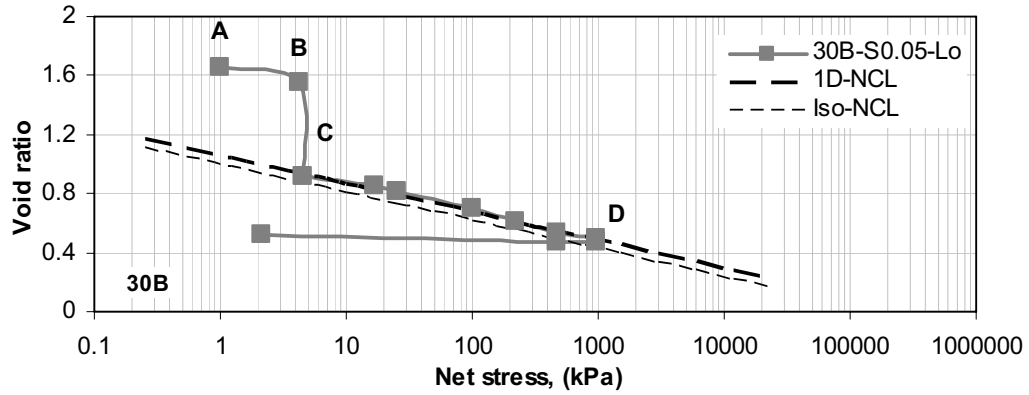

a

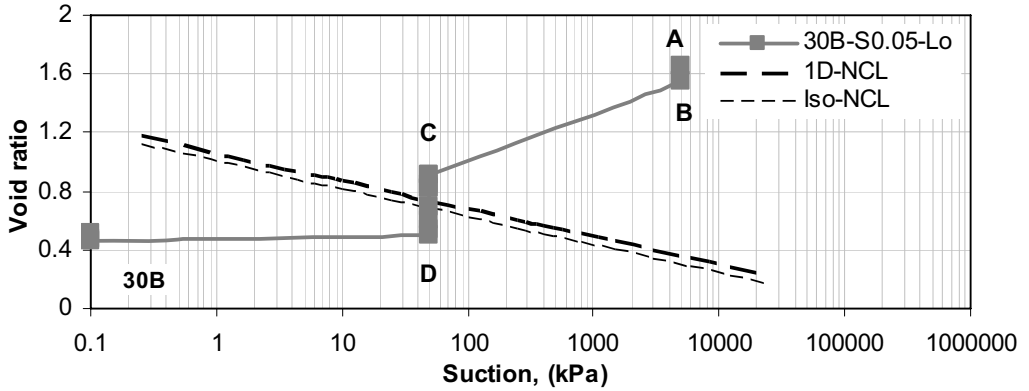

b

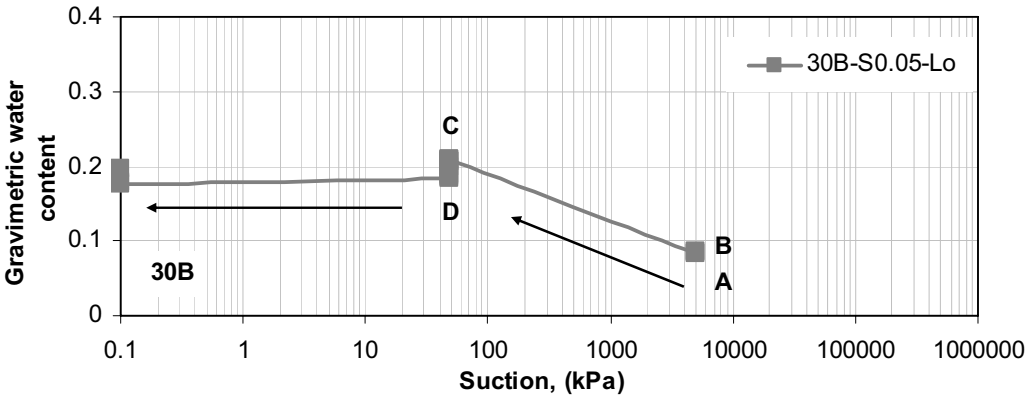

c

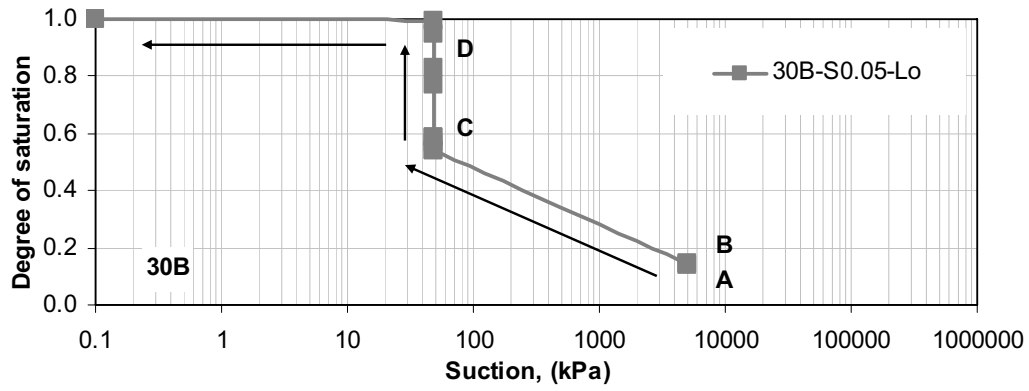

d

Figure 5.33 Void ratio, gravimetric water content, and degree of saturation results of constant suction = 50 kPa condition for initially loose 30B soil.

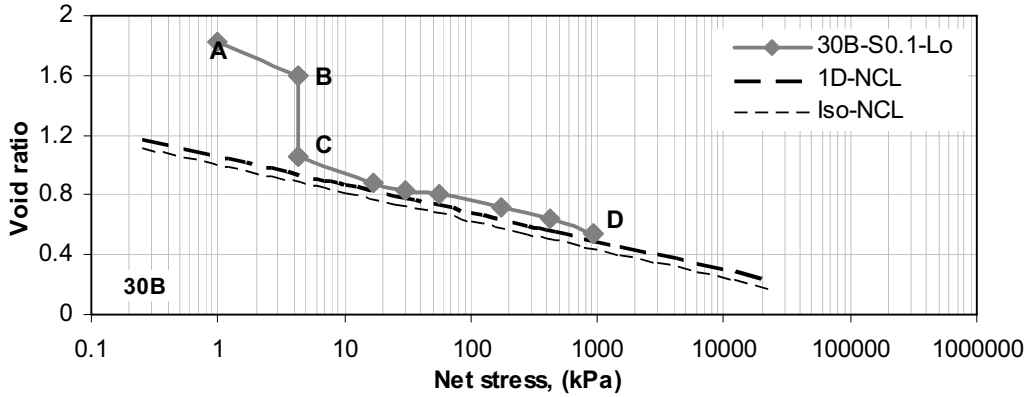

a

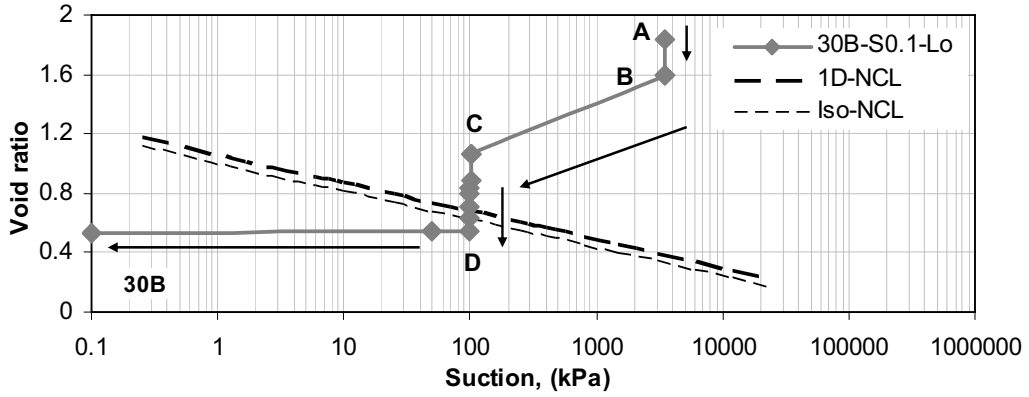

b

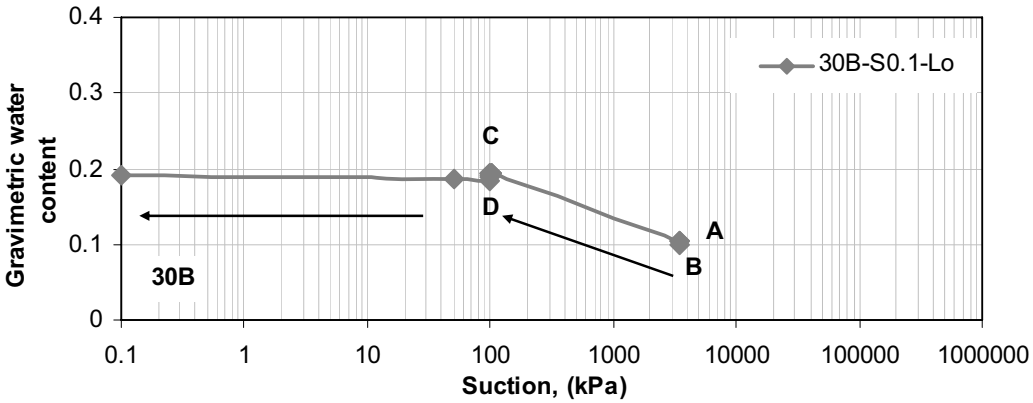

c

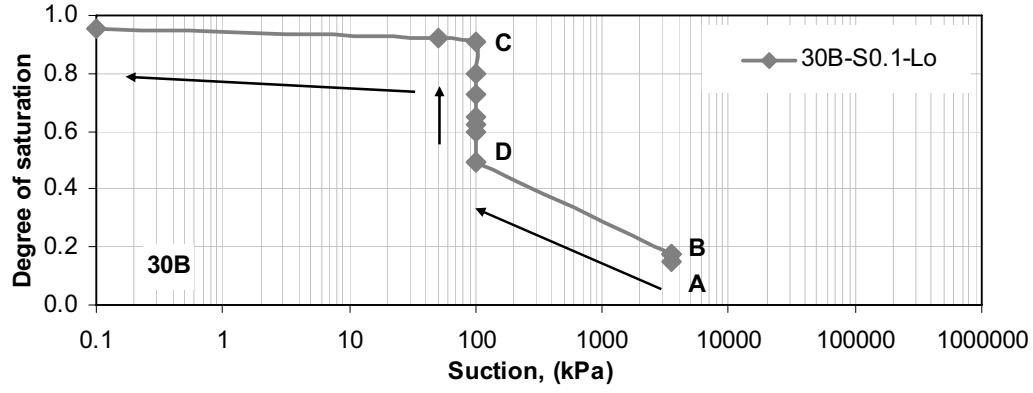

d

Figure 5.34 Void ratio, gravimetric water content, and degree of saturation results of constant suction = 100 kPa condition for initially loose 30B soil.

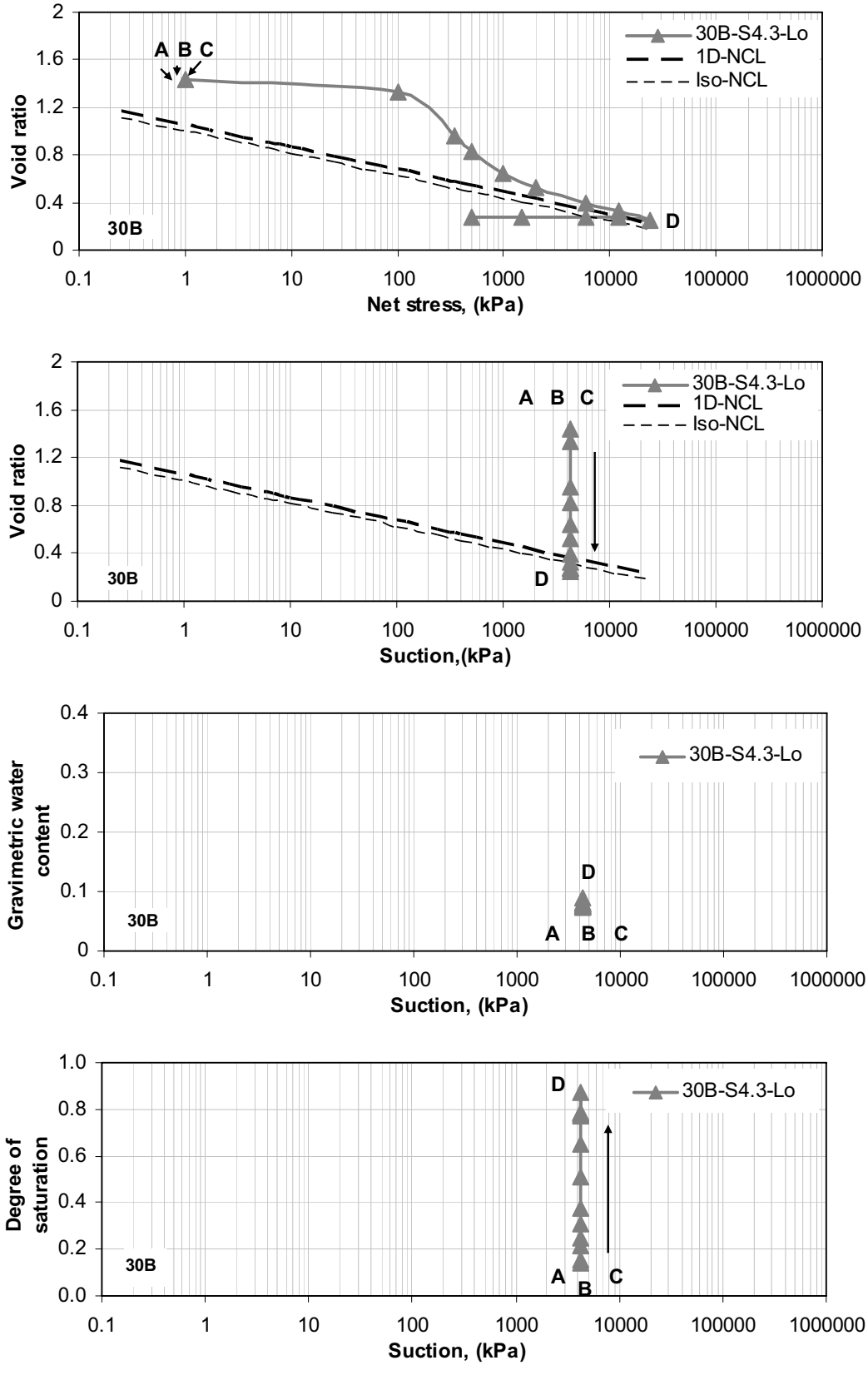

Figure 5.35 Void ratio, gravimetric water content, and degree of saturation results of constant suction = 4300 kPa condition for initially loose 30B soil.

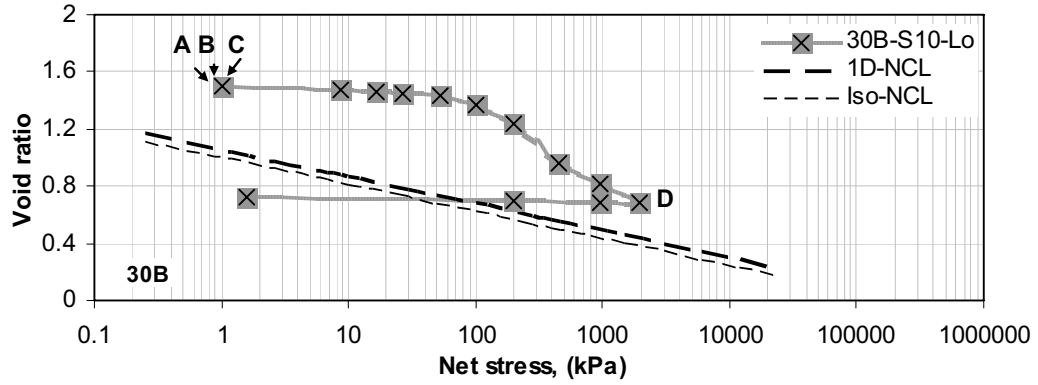

a

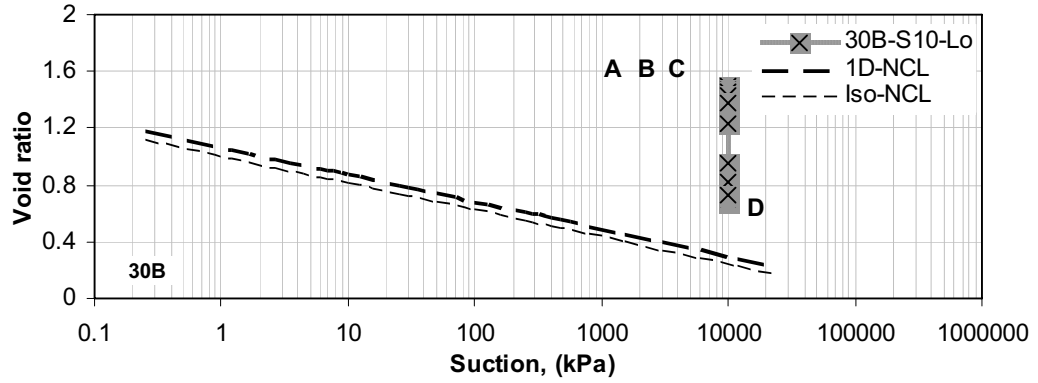

b

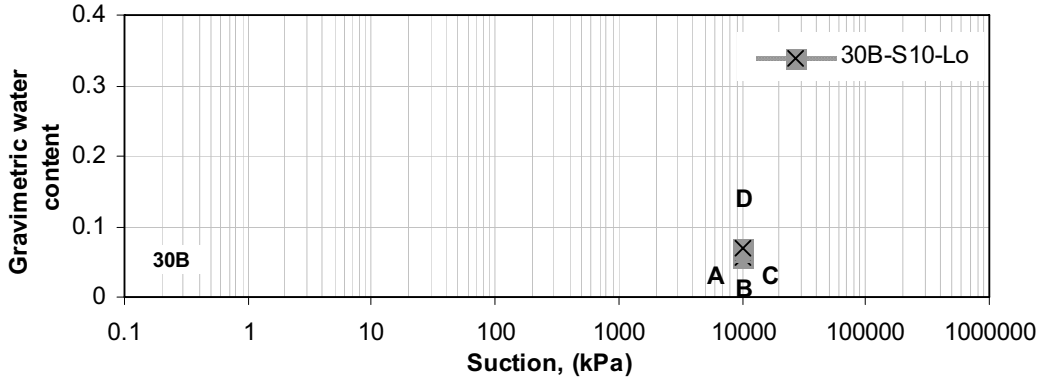

c

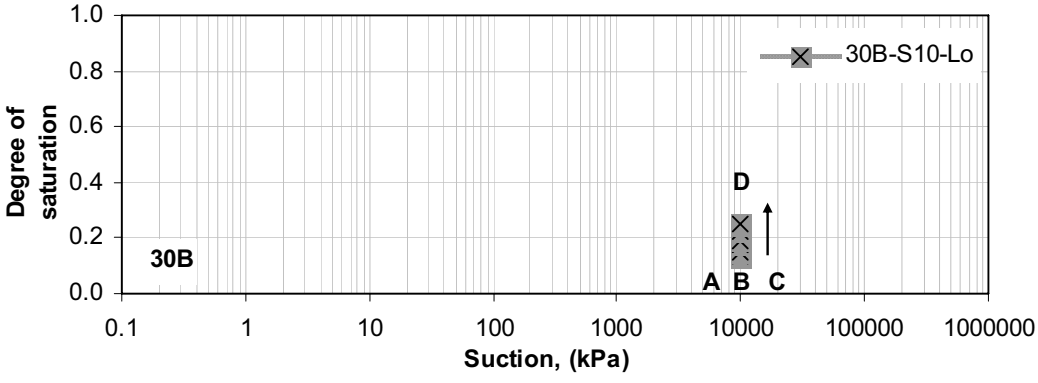

d

Figure 5.36 Void ratio, gravimetric water content, and degree of saturation results of constant suction = 10000 kPa condition for initially loose 30B soil.

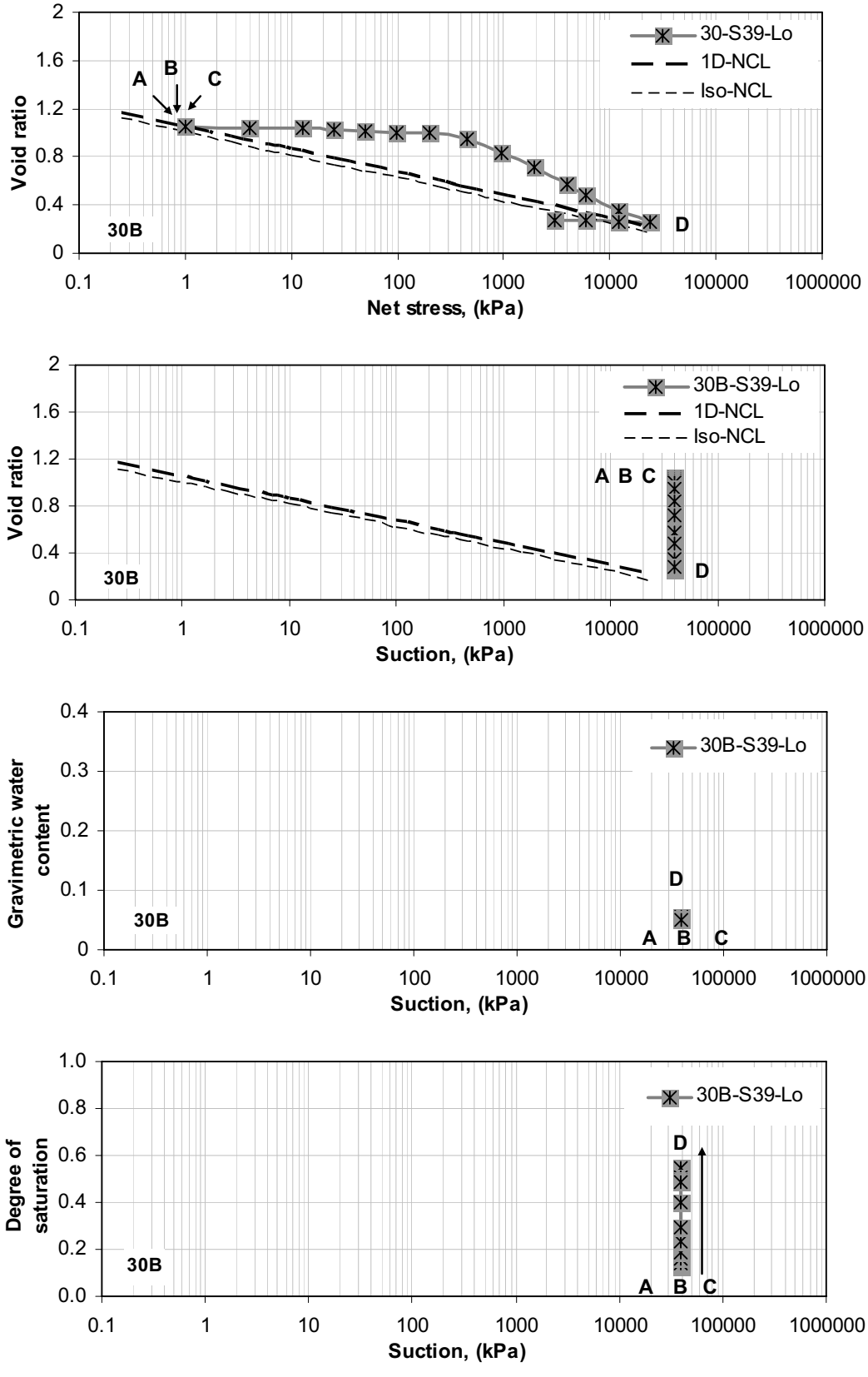

Figure 5.37 Void ratio, gravimetric water content, and degree of saturation results of constant suction = 39000 kPa condition for initially loose 30B soil.

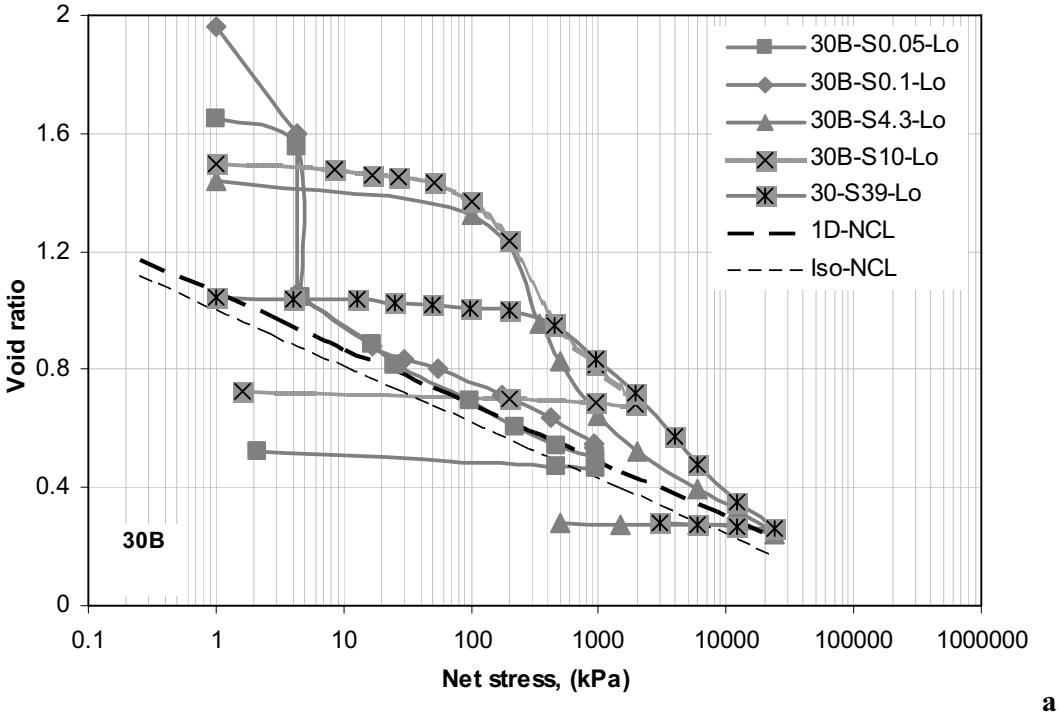

a

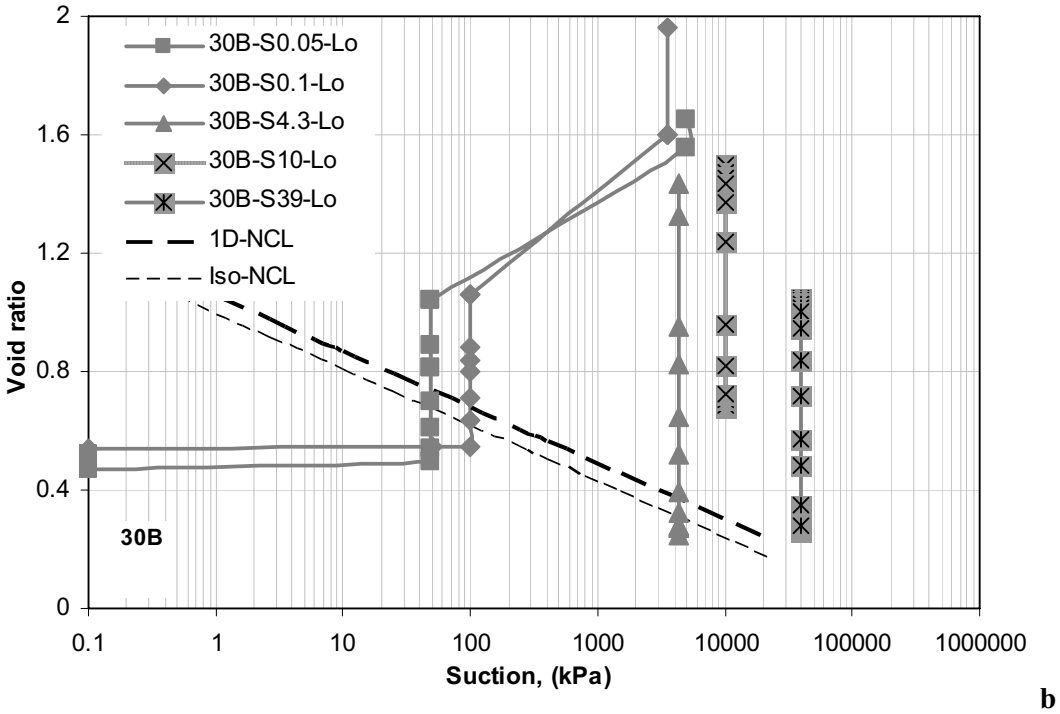

b

Figure 5.38-1 Void ratio, gravimetric water content, and degree of saturation results of all constant suction condition for initially loose 30B soil.

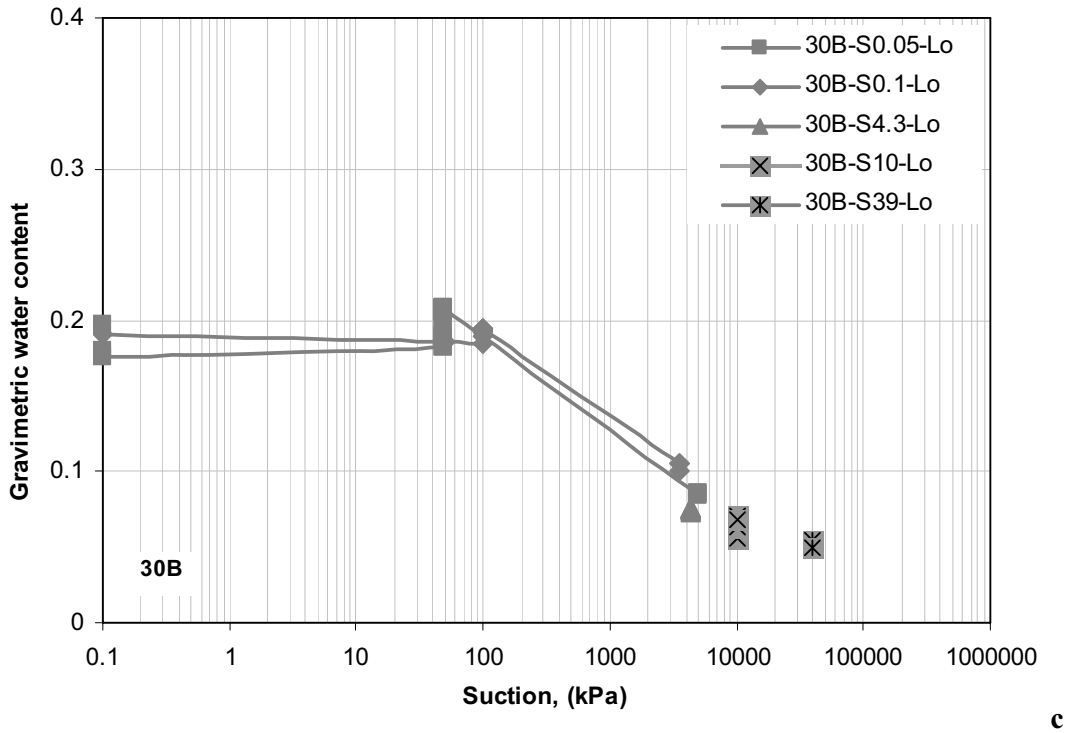

c

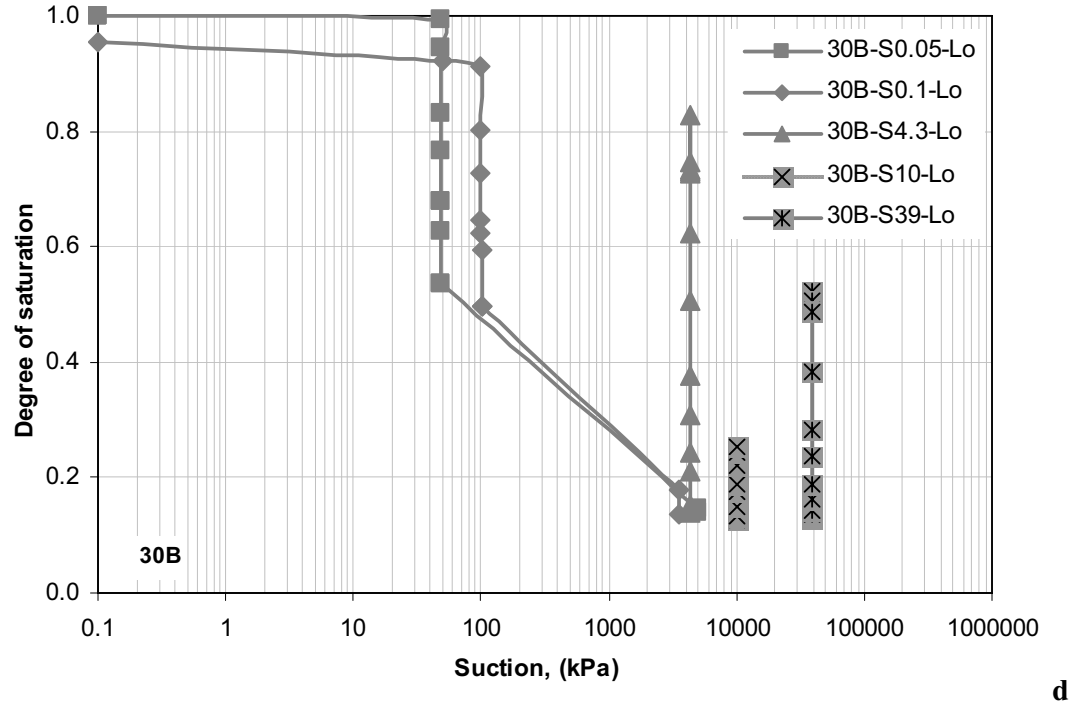

d

Figure 5.38-2 Void ratio, gravimetric water content, and degree of saturation results of all constant suction condition for initially loose 30B soil.

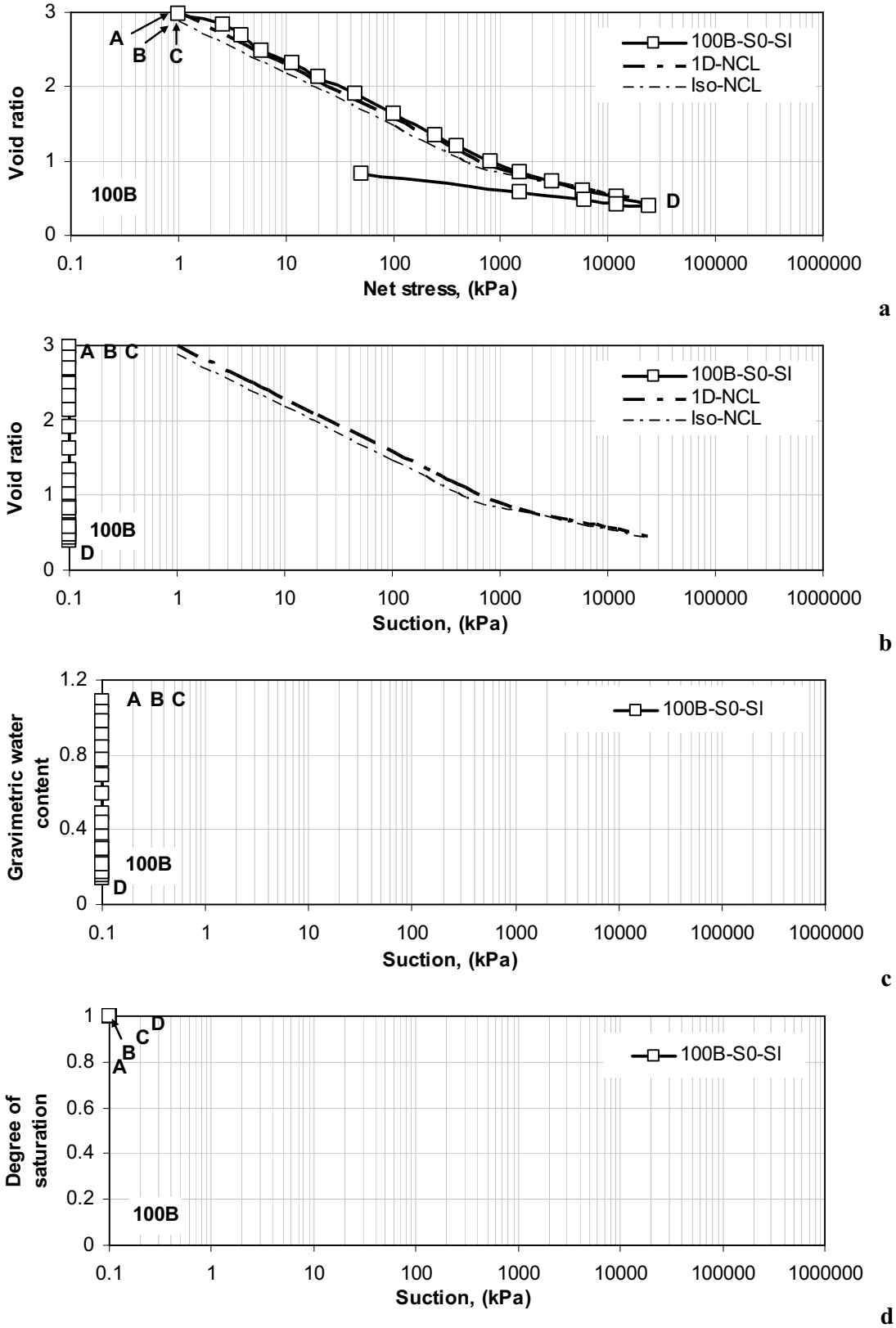

Figure 5.39 Void ratio, gravimetric water content, and degree of saturation results of constant suction = 0 kPa condition, saturated, (for log-scale of suction it is given as 0.1 kPa) for initially slurry 100B soil.

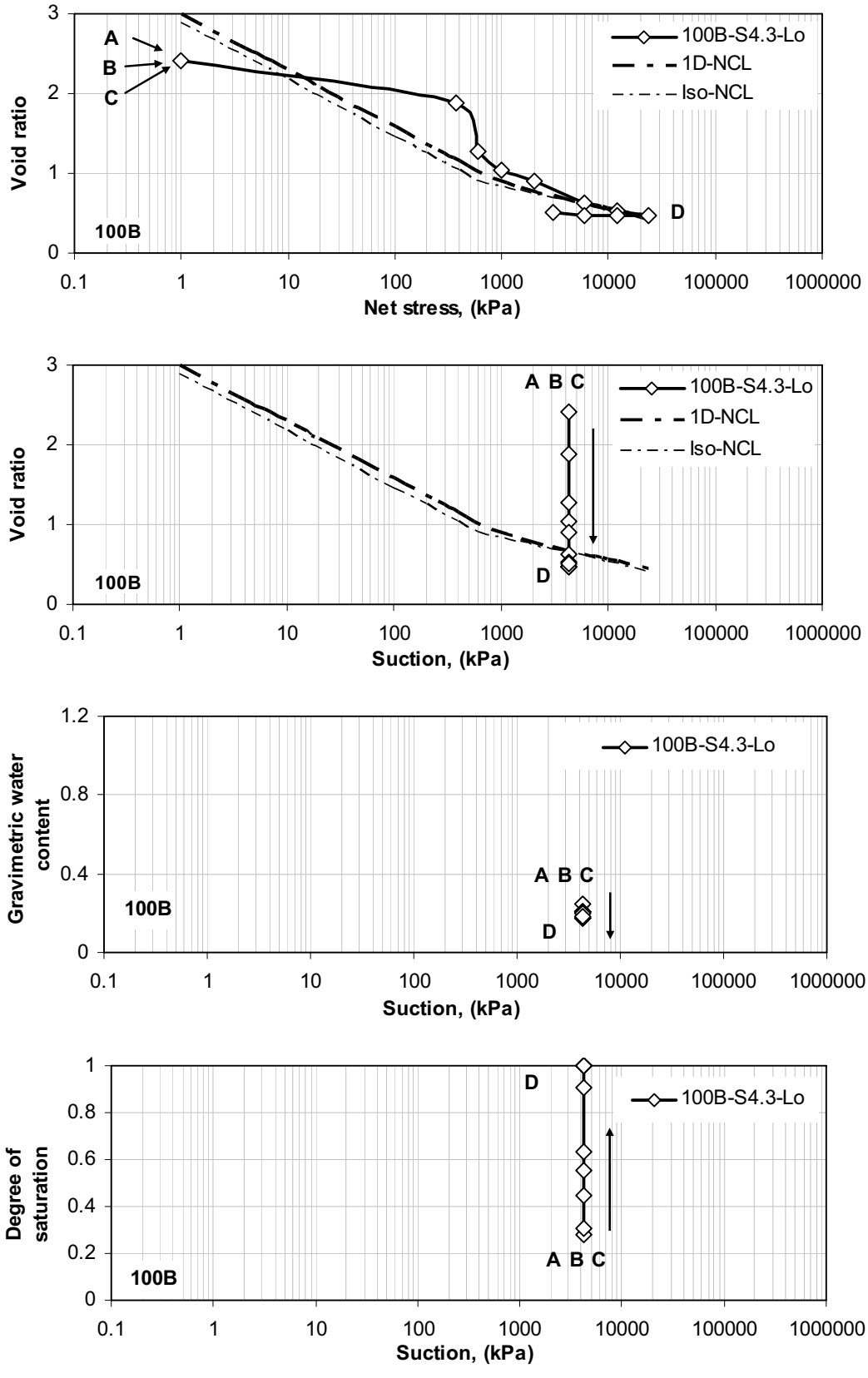

Figure 5.40 Void ratio, gravimetric water content, and degree of saturation results of constant suction = 4300 kPa condition (saturated) for initially loose 100B soil.

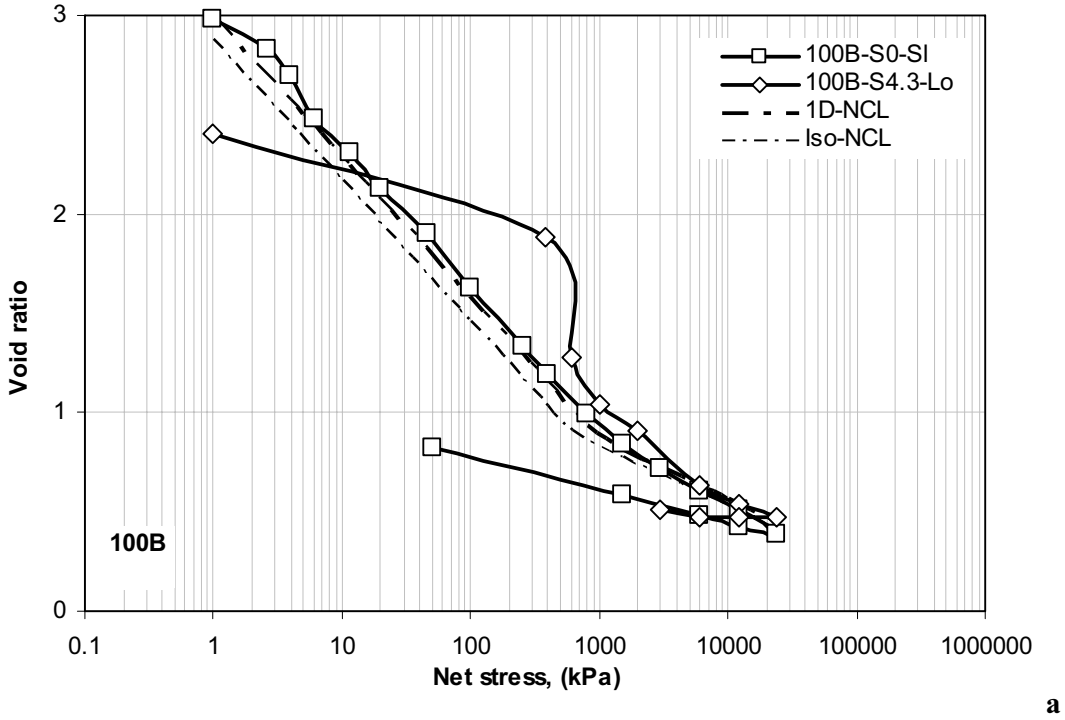

a

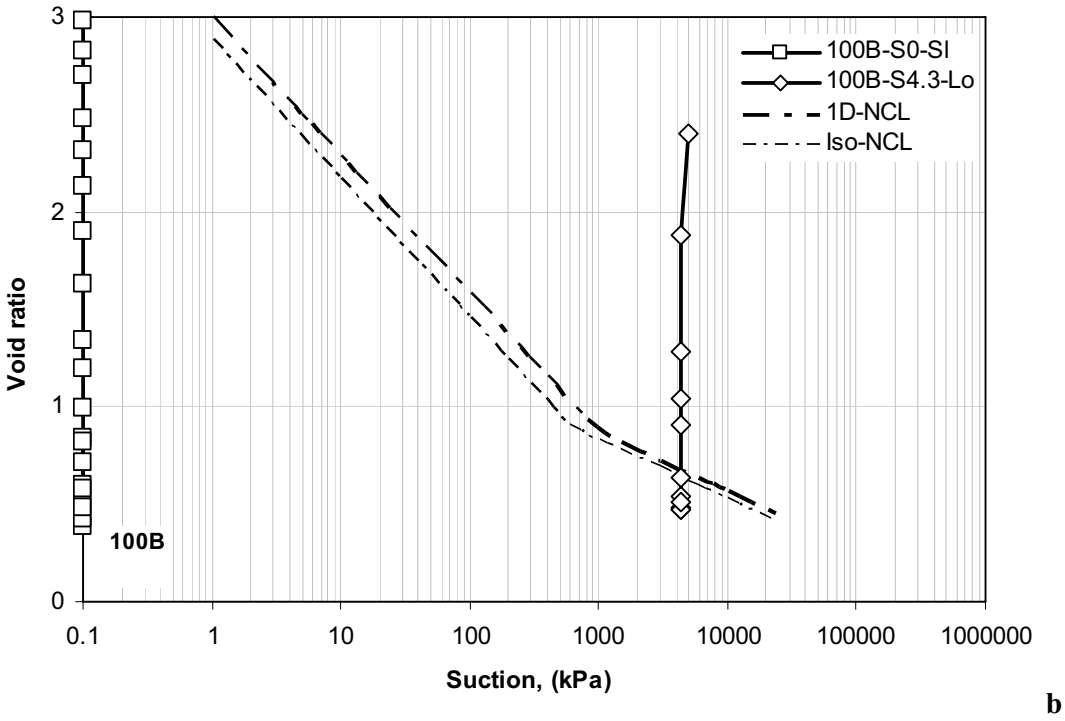

b

Figure 5.41-1 Void ratio, gravimetric water content, and degree of saturation results for both constant suction condition for initially slurry and loose 100B soil.

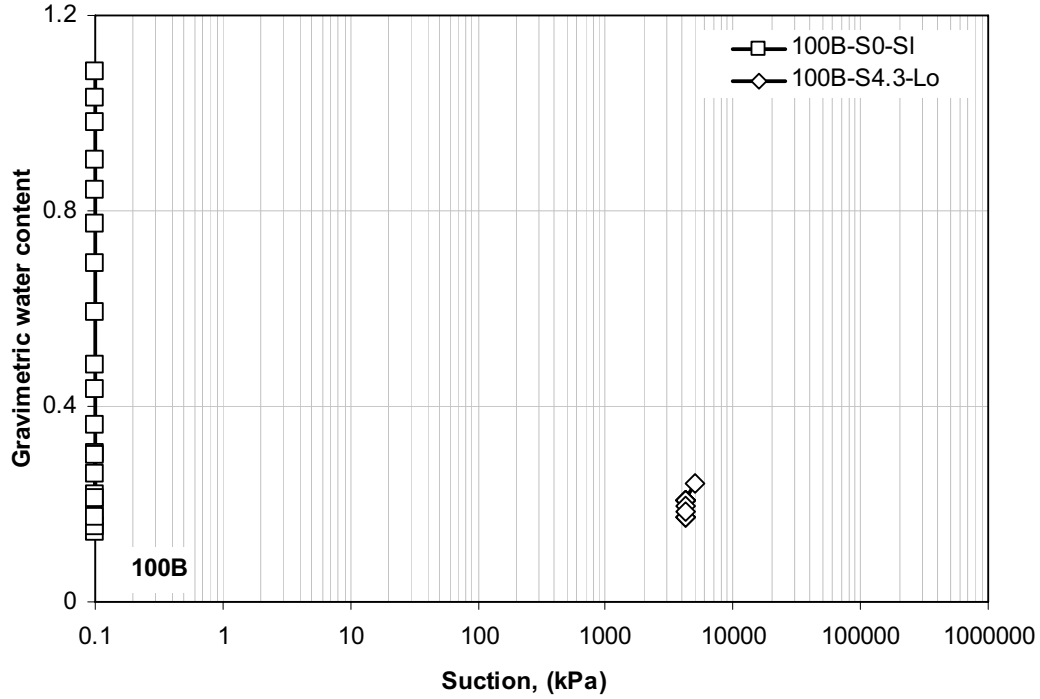

c

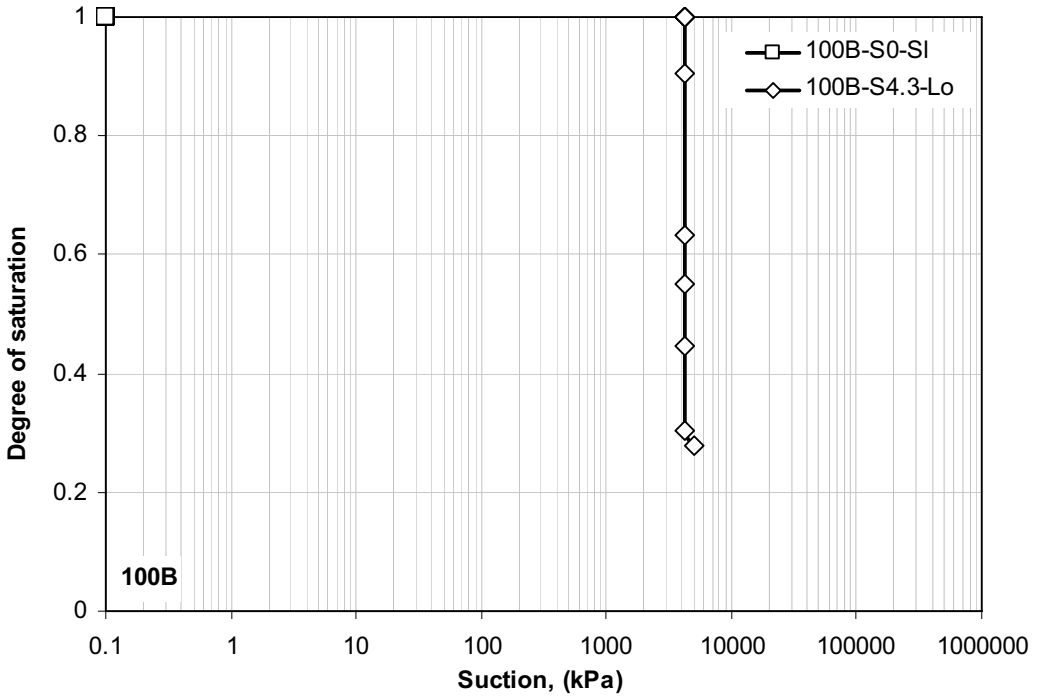

d

Figure 5.41-2 Void ratio, gravimetric water content, and degree of saturation results for both constant suction condition for initially slurry and loose 100B soil.

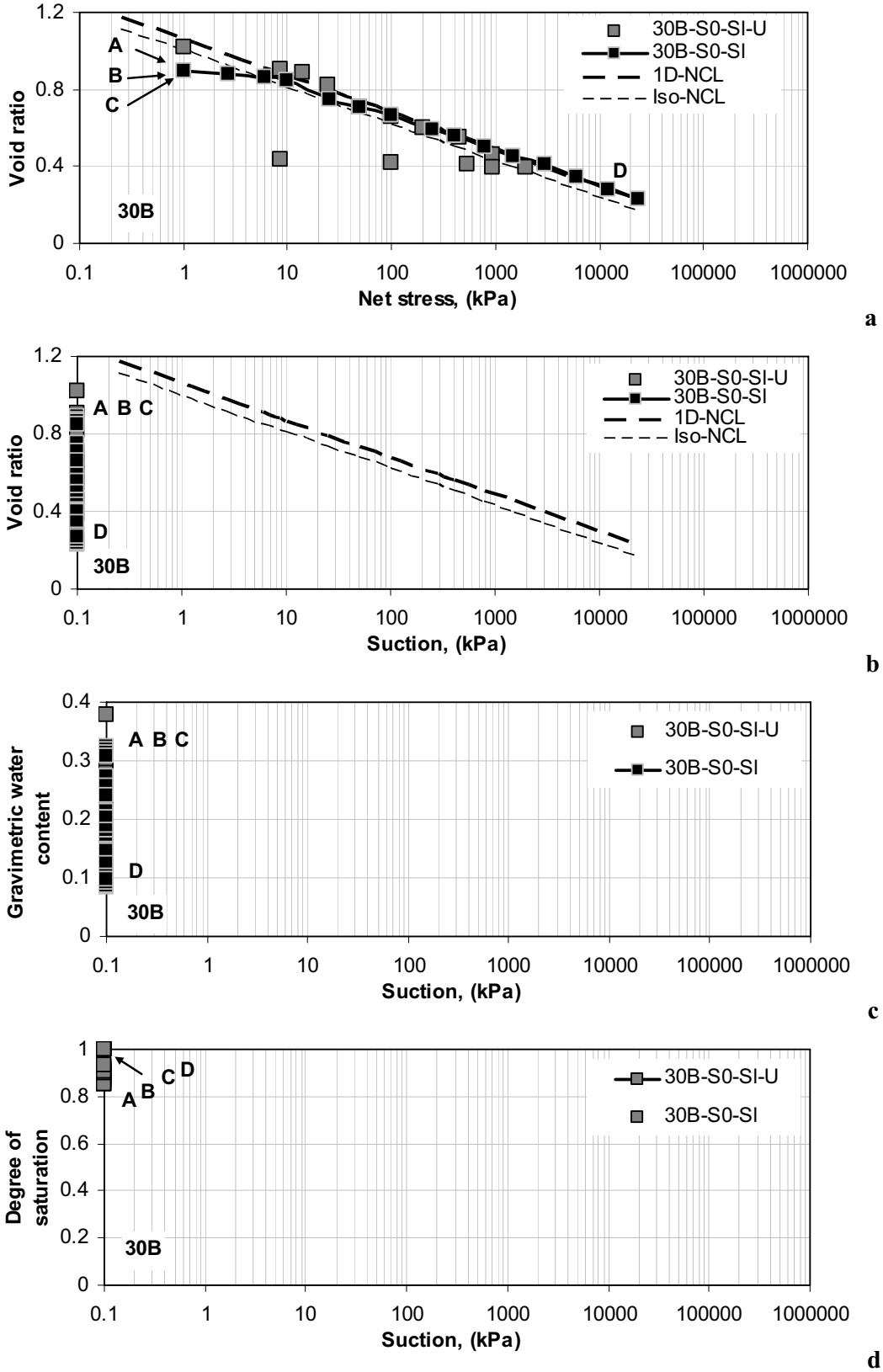

Figure 5.42 Results of the verifying test for comparison between the High oedometer stress cell, HSC, (original test) and UPC- Isochoric cell Nr. 3 (U test) for void ratio, gravimetric water content, and degree of saturation results of constant suction = 0 kPa condition, saturated, (for log-scale of suction it is given as 0.1 kPa) for initially slurry 30B soil.

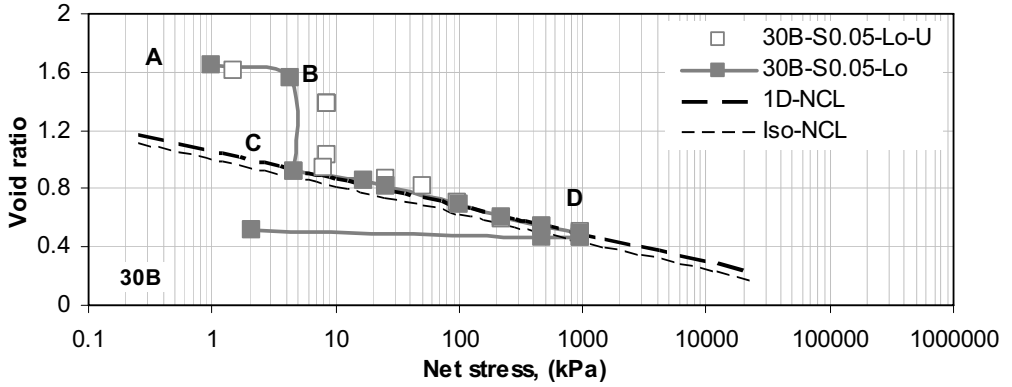

a

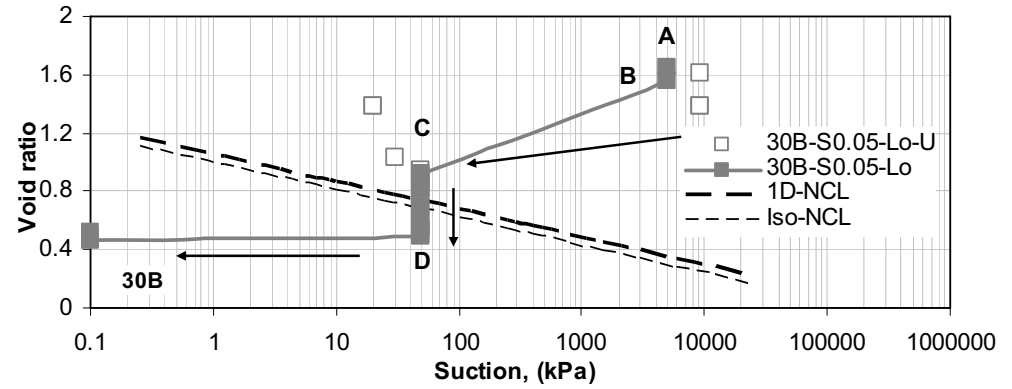

b

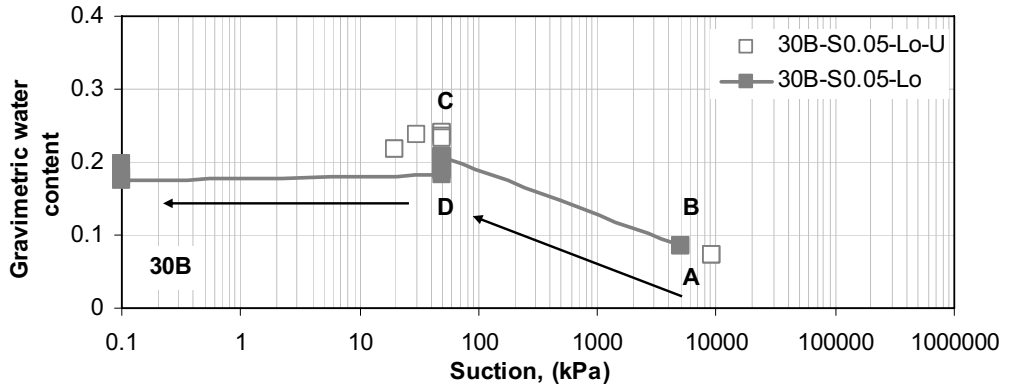

c

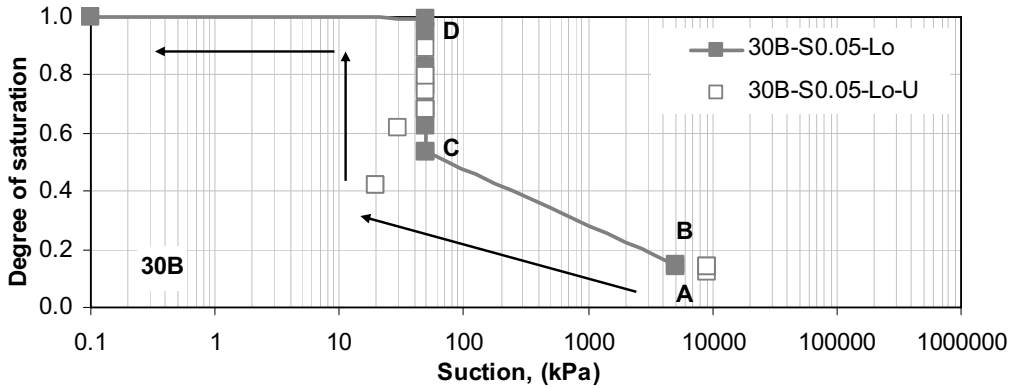

d

Figure 5.43 Results of the verifying test for comparison between the Black cell (original test) and Red cell (U test) for void ratio, gravimetric water content, and degree of saturation results of constant suction = 50 kPa condition for initially loose 30B soil.

5.2.4 Changing both net stress and suction test

This section presents the results of three identical specimens (30B-ver1-Lo, 30B-ver2-Lo, and 30B-ver3-Lo). The aim of this series is to investigate the uniqueness of the state surface at yield state for unsaturated soils. The two stress variables (net stress and matric suction) for the three specimens are varied along three different paths. The stress paths intersect in different points (initial, in-between, and final points). One of the criteria of this program was that the specimen, in most cases, should keep in yield state during the test. The initial states and the stress paths for the three tests are shown in Table (3.6) and Figure (3.7), respectively.

Figure (5.44) shows the results of 30B-ver1-Lo test which followed A-B-C-E-F path. The initial suction was 80000 kPa (point A), and then the suction was reduced till 20000 kPa. Beyond that the net stress was increased to 500 kPa (point B) followed by increase in suction to 166000 kPa which caused decrease in volume (Figure 5.44a). The net stress was increased after that till 1500 kPa. At this point, as shown in Figure (5.44b), the suction was decreased again from 166000 kPa to 40000 kPa which initiated reduction in volume followed by increasing the net stress till 3000 kPa (point C). Here, at 3000 kPa net stress, the suction was reduced to 0 kPa (point E), which leads to collapse of the specimen and the void ratio reduces to saturated 1D-NCL. Then the test followed the saturated 1D-NCL path as the net stress increased till 24000 kPa (point F). The gravimetric water content relationship for the tested points almost followed the main wetting path of SWCC (except the points of 0 kPa suction), Figure (5.44c). The degrees of saturation values before the saturation (point E) were between 0.15 and 0.275 during the test, Figure (5.44d).

Figure (5.45) shows the results of 30B-ver2-Lo test which followed A-G-C-D-E-F path. The initial suction was 80000 kPa (point A), then the suction was decreased to 40000 kPa and again was increased till 166000 kPa. The net stress was increased after that to 3000 kPa (point G). The soil behavior through this stage has a feature of over consolidated state and the soil response just starts to change to normal consolidated behavior (due to change of the slope of the compression curve, see Figure 5.45a). Then the suction was decreased to 40000 kPa (point C), 490 kPa (point D), and finally to 0 kPa (point E). The reduction in suction from 166000 kPa to 40000 kPa caused insignificant compression (Figure 5.45b) in spit of increase in the degree of saturation from 0.14 to 0.27 (Figure 5.45d) as a result of increasing the gravimetric water content from 0.27 to 0.53 (Figure 5.45c). While the reduction of suction, from 40000 kPa to 490 kPa, caused noteworthy reduction in volume and increase in degree of saturation from 0.27 to 0.96 and the gravimetric water content from 0.53 to 0.135. Again there is no significant change in volume in the case of decreasing the suction from 400 kPa to 0 kPa with final void ration closed to the void ratio of saturated 1D-NCL. The gravimetric water content

at 0 kPa suction was 0.139 which made the degree of saturation about 0.977. These three phases during collapse are similar to the observed response in the collapse tests (Figures 5.19 -5.21 for 30B-P0.25-w-Lo, 30B-P0.6-w-Lo, and 30B-P1.0-w-Lo tests) and the results of Pereira and Fredlund (2000). Then the specimen followed the saturated 1D-NCL path as the net stress increased till 24000 kPa (point F). The gravimetric water content for the tested points almost followed the main wetting path of SWCC (except the points of 0 kPa suction). The degrees of saturation till suction 40000 kPa (point C) was between 0.104 and 0.27 during the test, but it increased to about 0.905 at 400 kPa suction.

Figure (5.46) shows the results of 30B-ver3-Lo test which followed A-H-D-E-F path. The initial suction was 80000 kPa (point A), then the suction was decreased to 490 kPa (point H). After that the net stress was increased to 3000 kPa (point D). During the loading, the specimen passed the preconsolidation pressure at 600 kPa (with about 0.58 degree of saturation), Figures (5.46a and 5.46d). Then the specimen was compressed and ended in the normal consolidated or yield state with slope higher than the saturated NCL to reach void ratio a little bit below the saturated 1D-NCL at 1500 kPa net stress with 0.86 degree of saturation. As the net stress was increased above 1500 kPa, the slope of the compression curve reduced to a value lower than the value of slope of the saturated NCL. When the net stress was increased to 3000 kPa the void ratio located close to 1D-NCL with 0.88 degree of saturation (point D). Here, at 3000 kPa net stress, the suction was reduced till 0 kPa (point E) with trivial compression (Figure 5.46b). Then the specimen followed the saturated 1D-NCL path as the net stress increased till 24000 kPa (point F). The gravimetric water content relationship for the tested points was also similar to the previous two tests which followed the main wetting path of SWCC (Figure 5.46c). Even the suction was remained constant, for the path between H and D, but the gravimetric water content reduced slightly. This reduction in gravimetric water content was taking place in 1500 and 3000 kPa net stress when the degree of saturation were 0.86 and 0.88 (higher than 0.85 which is the degree of saturation at air-entry value). Again this behavior is similar to the observed results in 30B-S0.05-Sl, 30B-S0.1-Sl, and 30B-S0.255-Sl tests, Figures (5.24c-5.26c). The specimen was fully saturated when the suction was reduced to 0 kPa. The values of the degrees of saturation for points A and H were 0.15 and 0.515 respectively.

Figure (5.47) shows the results of all the three tests together. Generally, all the three tests had nearly the same void ratio-net stress, void ratio-suction, gravimetric water content-suction, and degree of saturation-suction relationships in intersects points. The compression path between net stress 500 kPa and 1500 kPa under 166000 kPa suction for 30B-ver1-Lo and 30B-ver2-Lo tests had the same values of void ratio (Figure 5.47a). The collapse behavior, in

yield state, between point C and E for 30B-ver1-Lo and 30B-ver2-Lo tests was the same. Furthermore, the collapse path between point D and E for 30B-ver2-Lo and 30B-ver3-Lo tests also showed indistinguishable difference. The three tests showed the same volumetric yielding behavior in the saturated state (Figure 5.47a). In which all the verification tests joined in the saturated 1D-NCL (from point E to point F). Finally, the verification tests obviously showed that the loaded volumetric yielding behavior is unique for unsaturated soil that is the same regardless of stress path of initial unsaturated loose soil.

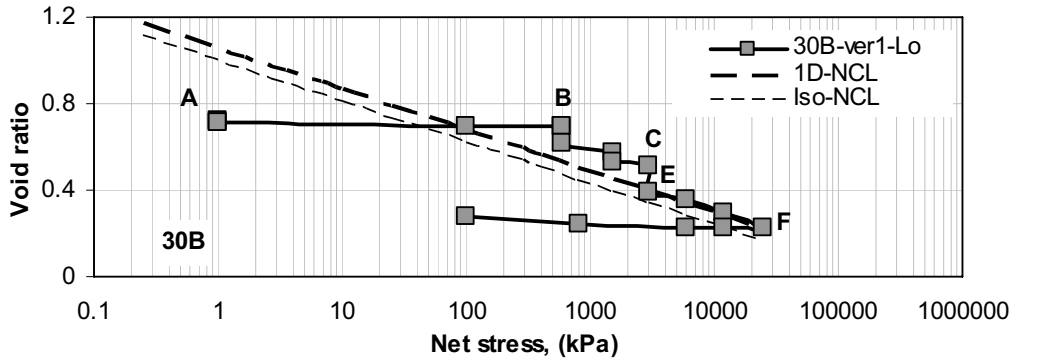

a

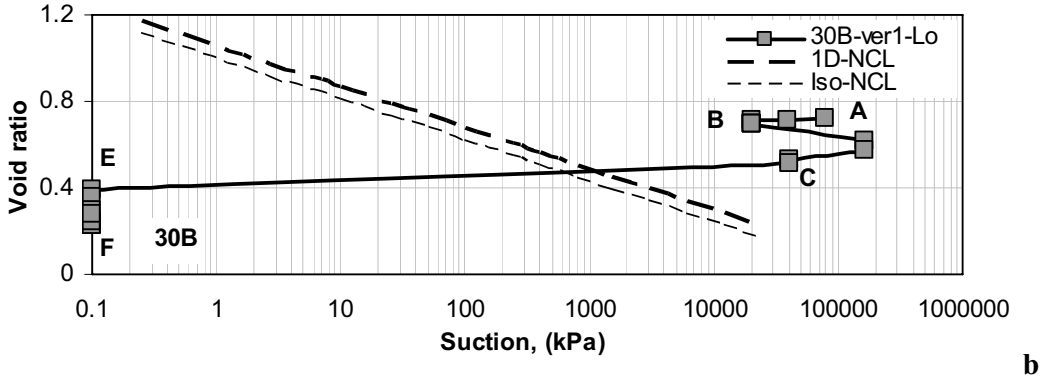

b

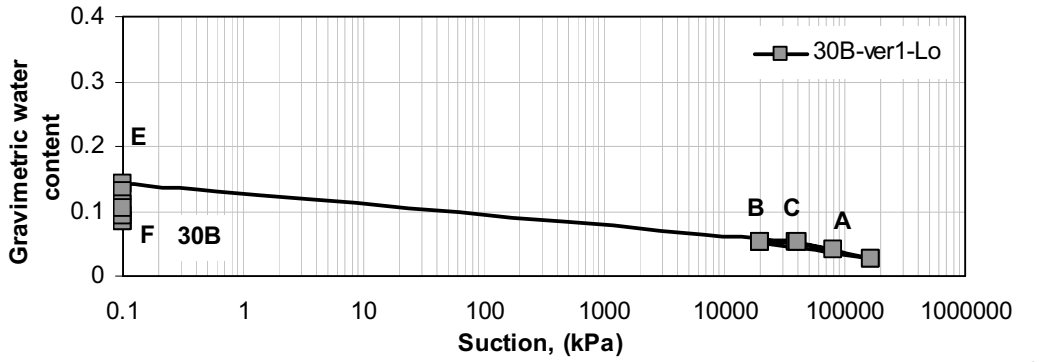

c

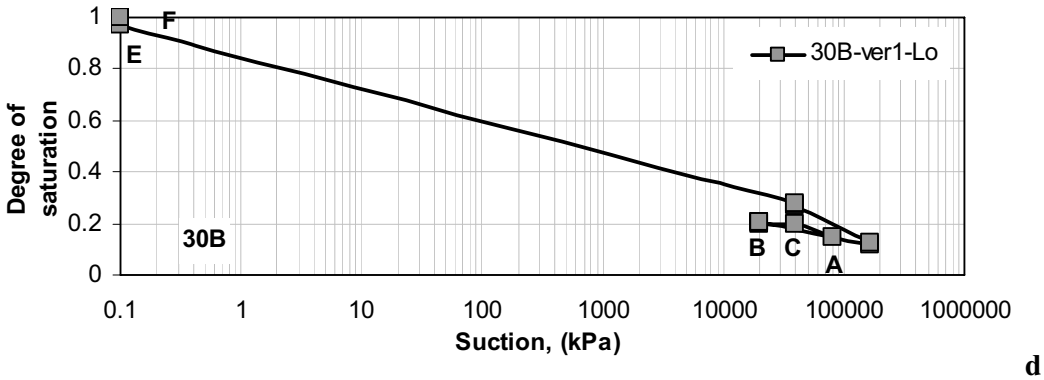

d

Figure 5.44 Void ratio, gravimetric water content, and degree of saturation results of Changing both net stress and suction test (verification test-1) A-B-C-E-F path for initially loose 30B soil.

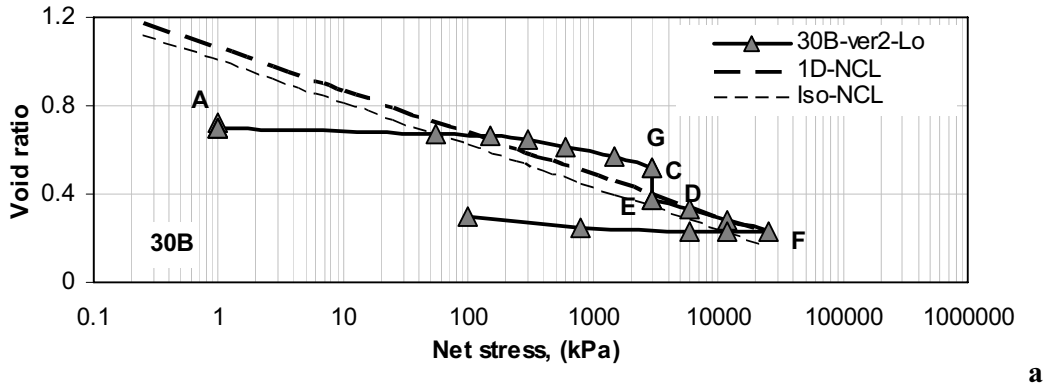

a

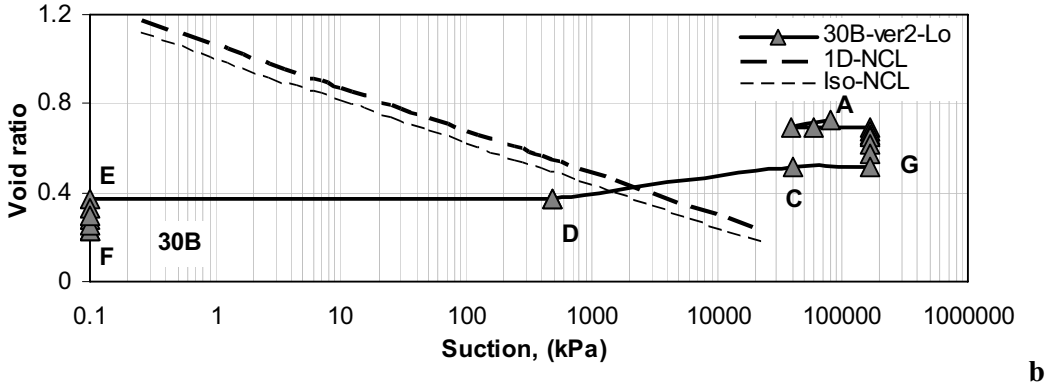

b

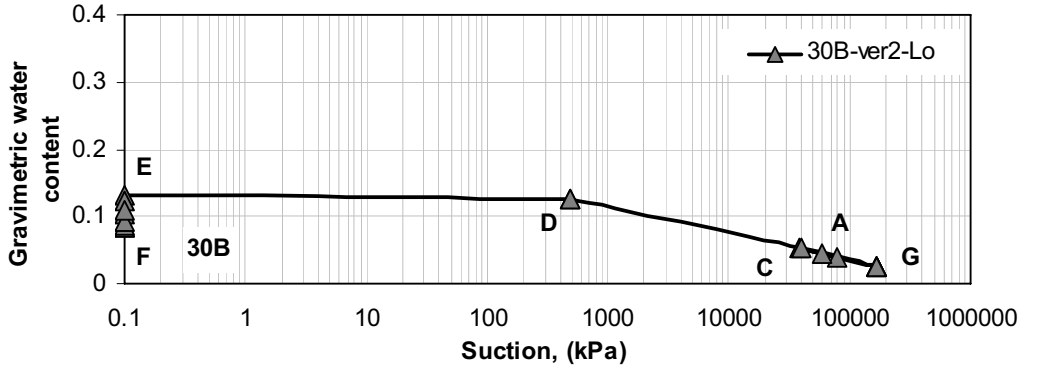

c

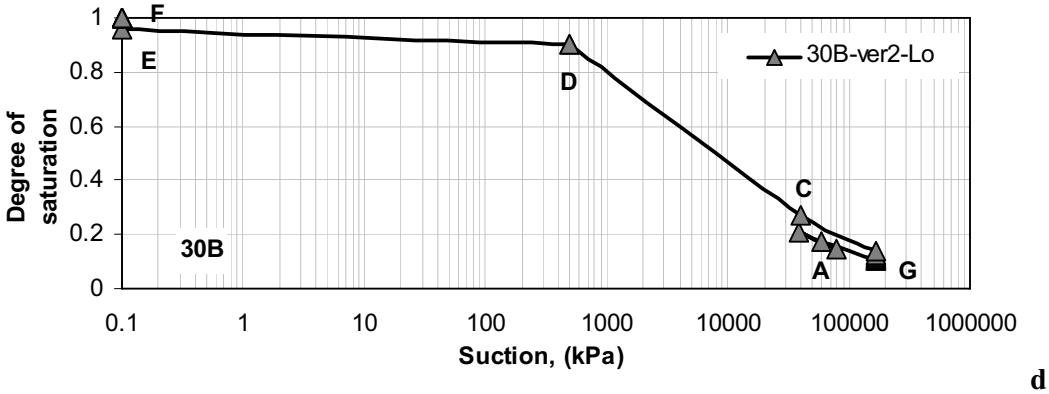

d

Figure 5.45 Void ratio, gravimetric water content, and degree of saturation results of Changing both net stress and suction test (verification test-2) A-G-C-D-E-F path for initially loose 30B soil.

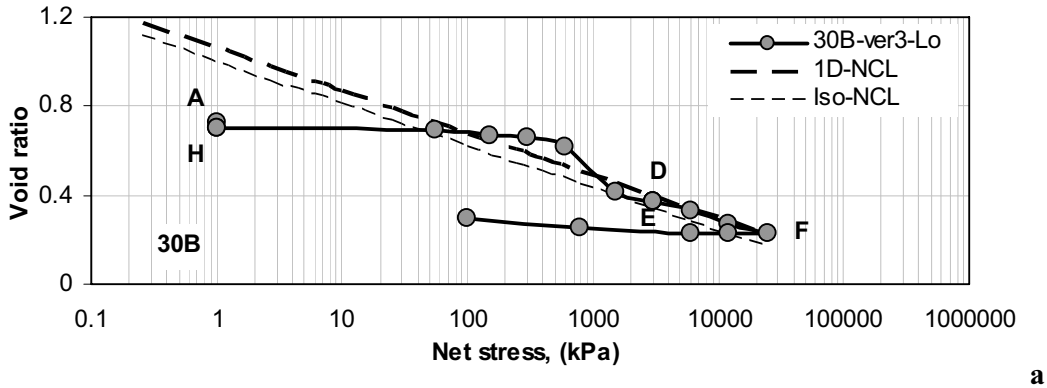

a

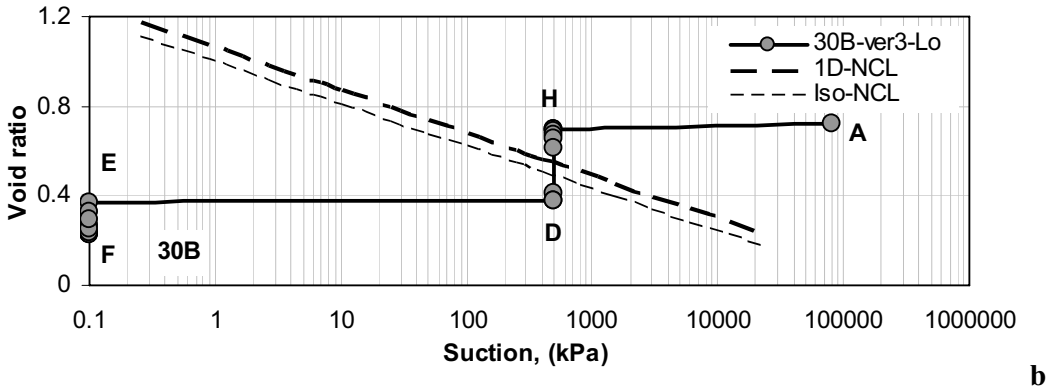

b

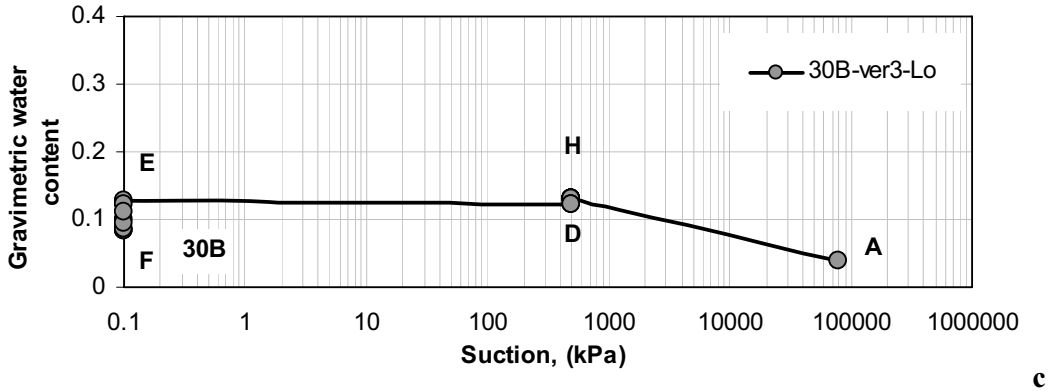

c

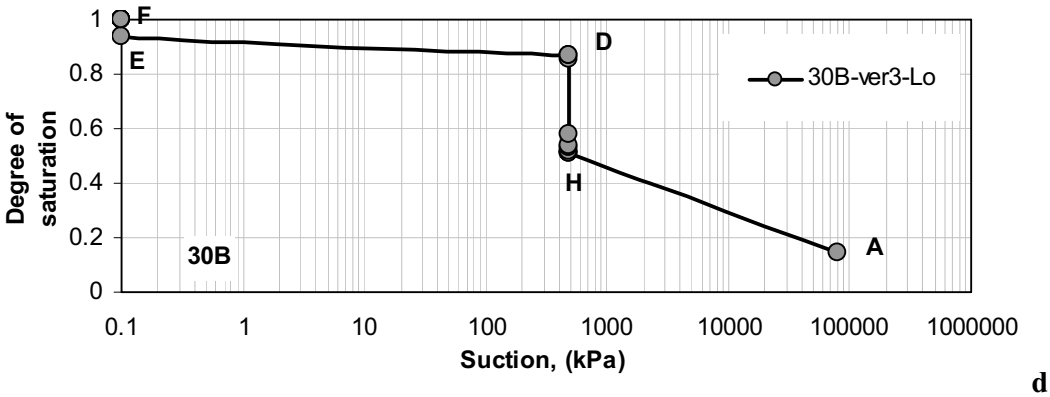

d

Figure 5.46 Void ratio, gravimetric water content, and degree of saturation results of changing both net stress and suction test (verification test-3) A-H-D-E-F path for initially loose 30B soil.

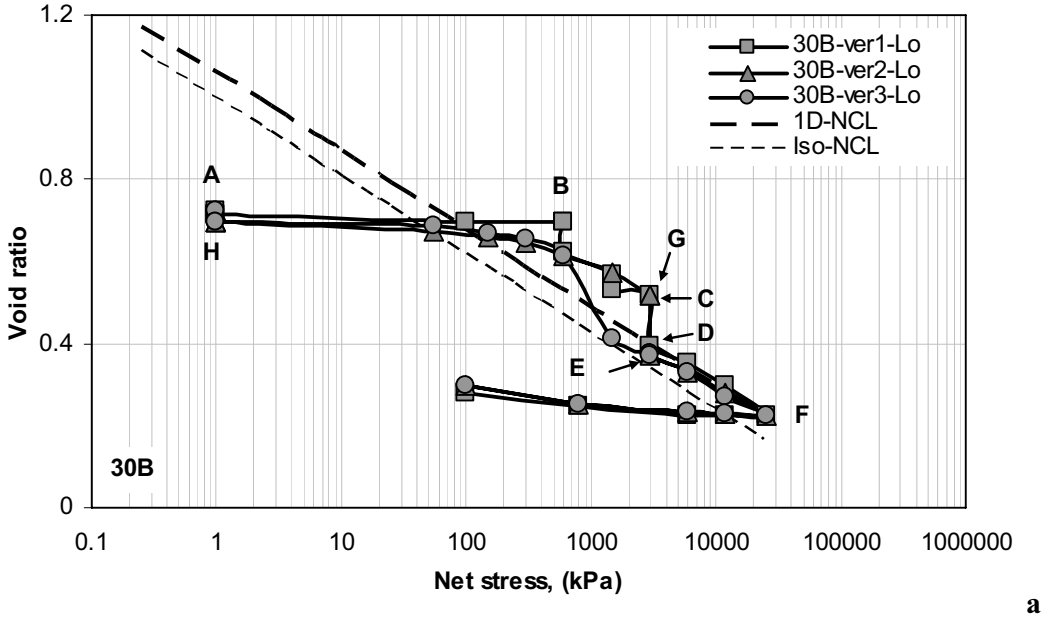

a

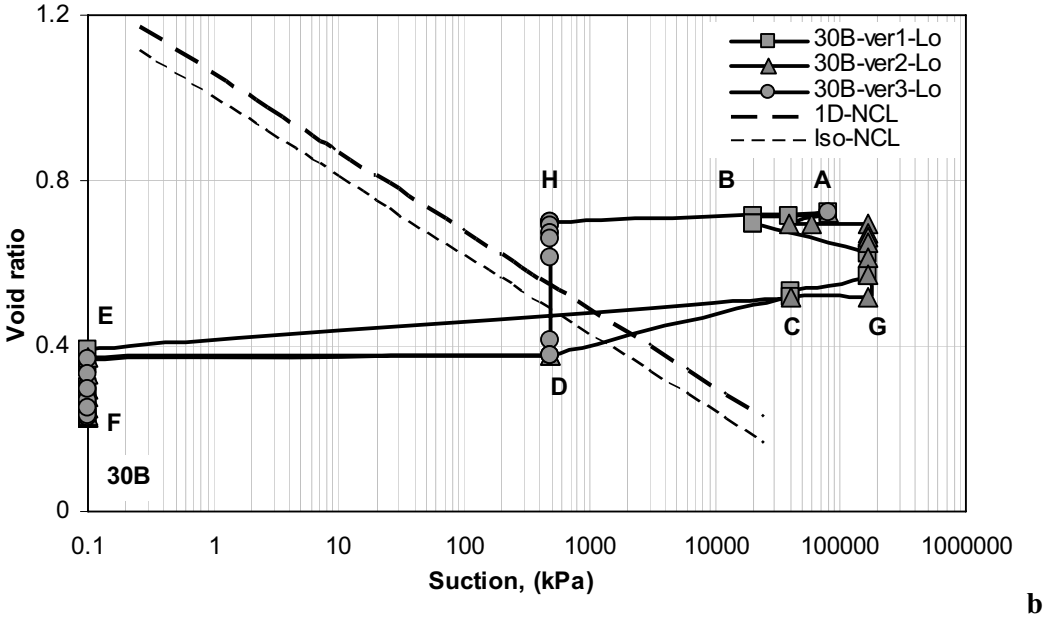

b

Figure 5.47-1 Void ratio, gravimetric water content, and degree of saturation results of all changing both net stress and suction test (verification test) with different paths for initially loose 30B soil.

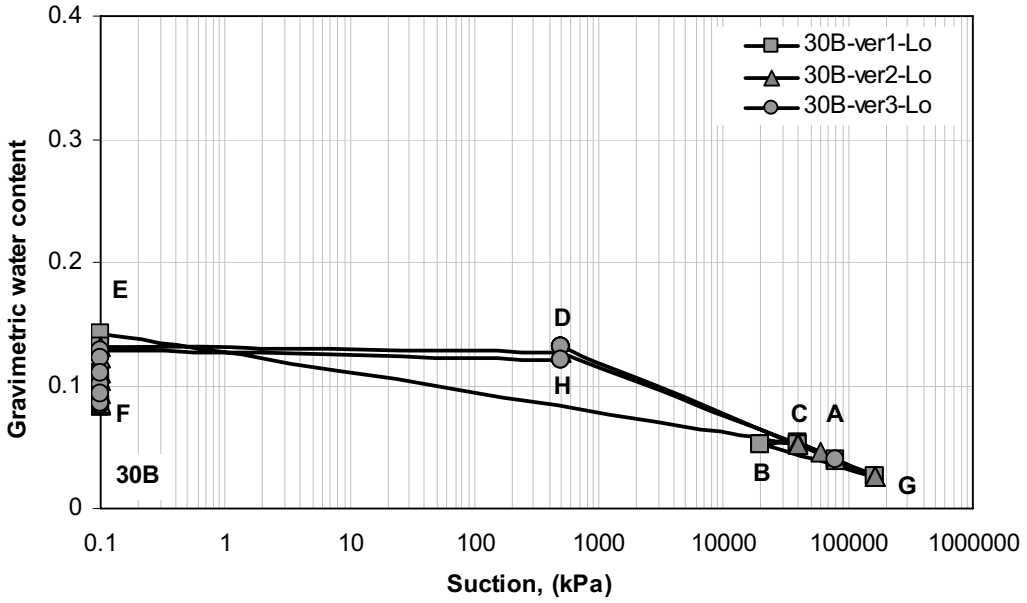

c

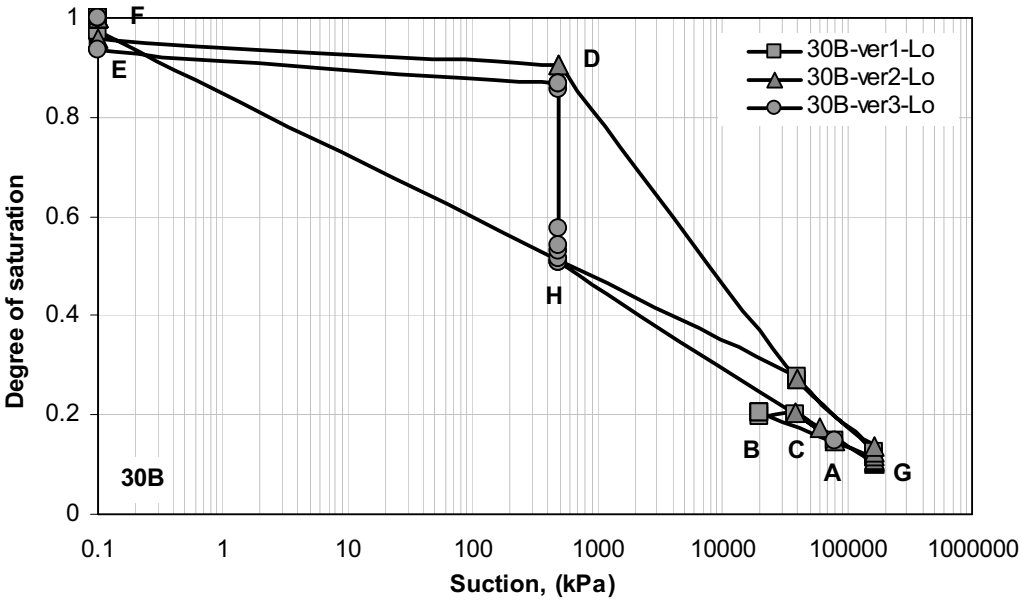

d

Figure 5.47-2 Void ratio, gravimetric water content, and degree of saturation results of all changing both net stress and suction test (verification test) with different paths for initially loose 30B soil.

5.3 Compaction Tests

The results of the static and dynamic compaction tests for both 30B and 100B soils with different compaction efforts (CE's) will be presented in this section. The static compaction tests were performed for both soils with reduced proctor compaction stress (RP) equal to 248 kPa. The Dynamic compaction tests were performed for both soils with Standard Proctor (SP) and Modified Proctor (MP) compaction efforts ([SP] =593 and [MP] =2694 kJ.m/m^3). One point from each soil was obtained by dynamic compaction with Reduced Proctor (RP) compaction energy equals to 248 kJ.m/m^3 or 248 kPa. Table (3.7) shows the compaction tests conditions for both soil materials used in this series. The total suction of the compaction tests was measured at the end of the test with a Chilled Mirror device. The results of equal total suction are shown together with the compaction results for each soil.

Figures (5.48) and (5.49) show the experimental results of compaction tests, dry density (γ_d)-water content (w) and the points of equal suction for soils used in the investigation.

The maximum dry density (γ_{dmax}) was 2.03 gm/cm^3 for *MP*, 1.85 gm/cm^3 for *SP*, and 1.75 gm/cm^3 for *RP* (static) for 30B soil, whereas it was 1.58 gm/cm^3 for *MP*, 1.36 gm/cm^3 for *SP*, and 1.21 gm/cm^3 for *RP* (static) for 100B soil. The optimum water content (*OWC*) was 0.104 for *MP*, 0.145 for *SP*, and 0.168 for *RP* (static) for 30B soil, while it was 0.241 for *MP*, 0.338 for *SP*, and 0.415 for 100B soil. The maximum dry density and the optimum water content and the degree of saturation at the optimum for 30B and 100B soils are listed in Table (5.1). For both 30B and 100B soils, the maximum dry density values increased as the compaction effort increased, whereas the optimum water content decreased with increasing compaction effort. Table (5.1) shows that the degree of saturation for each soil was changing in a narrow range as the compaction effort changed (± 0.7 % for 30B and ± 1.0 % for 100B). The degree of saturation for each soil was about 0.85 for 30B and 0.90 for 100B. However, the 100B soil had OWC (at S_r = 0.90) closer to the zero air void line (ZAV) than the optimum of 30B soil (S_r = 0.85). Similar behavior was observed for previous compaction tests with different bentonite-sand mixture that tested by (Agus, 2005 and Arifin, 2008).

Double peaks are observed in compaction curves especially in 30B soil. The first one locates in high water content (the original OMC), and the second finds at low water content (even the water content is different with compaction effort but it was close to the hygroscopic water content). Several experimental studies showed that in some cases the compaction curve has double peaks (e.g., the results of Hindi, 1967; Lee and Suedkamp, 1972; Ellis, 1980; Razouki et al., 1980; Dixon, 1985; Benson et al., 1997;Sun et al., 2007; and Razouki et al., 2008).

The results for equal total suction show that the water content-dry density relationship for constant suction represents almost a vertical line in w-γ_d plane. The suction values were 700 kPa and 6700 kPa when the water contents were between 0.125-0.13 and 0.07 respectively for 30B soil. In case of 100B soil, the suction was 1000 kPa for water content between 0.275-0.285 and the suction increased to 35000 kPa when the water content decreased to 0.11.

All the contour lines of equal suction were established in the dry of optimum (DOP) state only. This was due to that the points of the wet of optimum (WOP) suffered from high reduction in water content during measuring the suction which let to be close to the range of DOP.

The results of (Delage and Graham, 1995; Gens et al., 1995; Li, 1995; Romero, 1999 as Figure 2.28; Tarantino and Tombolato, 2005; Agus, 2005 as Figure 2.29; and Ferrari, 2007) showed that for the dry side of optimum the density has no effect on the suction water content relationship for fine-grained soils. Romero (1999) attributed this behavior to the effects of loading mechanism on the macroporosity that does not contain free water, since at low water content levels (which is equal or lower than the optimum water content for each compaction effort), water is mainly absorbed or contained in the less bonded diffuse layers at intra-aggregate scale. In intra-aggregate scale, the degrees of saturation changes are associated with macroporosity changes under constant intra-aggregate water content. While in case that the matric suction values approach the saturation line, the loading mechanism affects inter-aggregate water and the contours of equal suction try to incline in order to converge to the limit condition of matric suction equal to zero at fully saturated condition (S_r = 1.0).

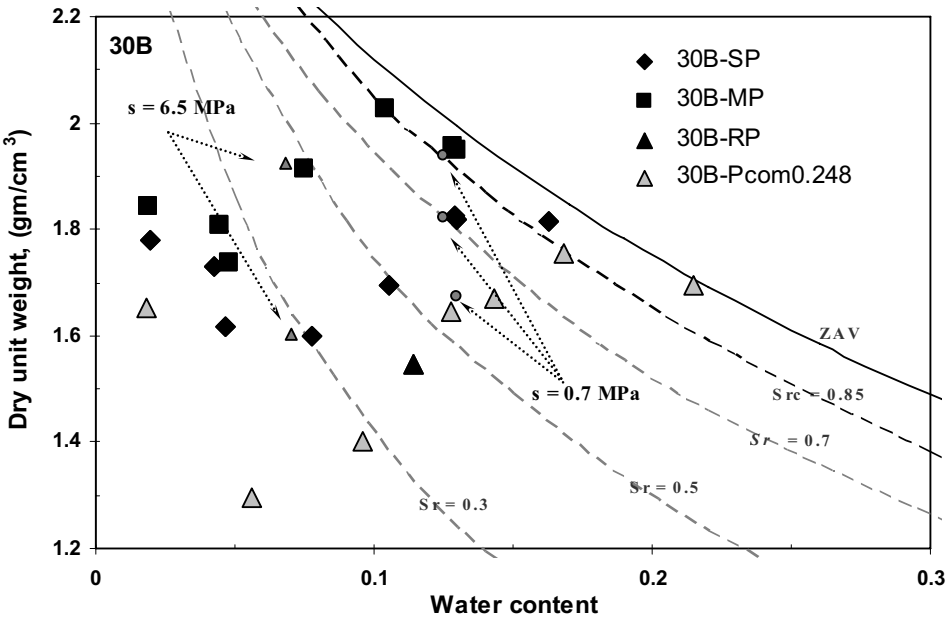

Figure 5.48 Dynamic and static experimental compaction tests for different CE, and points of equal suction for 30B soil.

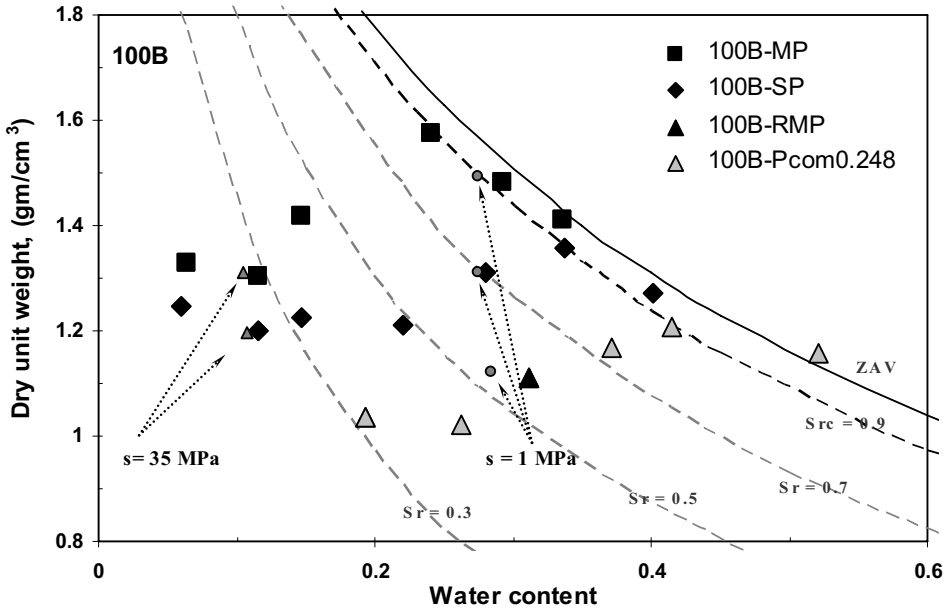

Figure 5.49 Dynamic and static experimental compaction tests for different CE, and points of equal suction for 100B soil.

Table 5.1 The maximum dry density and the optimum water content and the degree of saturation at the optimum for different compaction efforts for 30B and 100B soils.

Soils	**30B**			**100B**		
Compaction Effort (CE)	***MP***	***SP***	***RP***	***MP***	***SP***	***RP***
γ_{dmax}, gm/cm^3	2.03	1.85	1.75	1.58	1.36	1.21
OWC	0.104	0.145	0.168	0.241	0.338	0.415
S_r	0.851	0.855	0.844	0.891	0.905	0.895

5.4 Results of soil water characteristic curve program

This section contains the results of SWCC tests. The results of SWCC are already presented in the previous sections. The initial states and the applied suction for soil water characteristic curves SWCCs tests for both soils are shown in Table (3.8). The results and the discussions were given in section 5.2.1.2 (unconfined constant net stress tests with increasing and decreasing the suction). Namely: 30B-P0.005-d&w-Sl, 30B-P0.005-d&w-com1, and 30B-P0.005-d&w-com2 as in Figure (5.5) for 30B soil, whereas 100B-P0.005-d&w-Sl, and 100B-P0.005-d&w-com1 as in Figure (5.12) for 100B soils. In the SWCC tests, three different initial densities for 30B soils were used, while two different initial densities for 100B soils were used.

5.5 Consolidation tests

The 1D-NCL for each soil was determined using high oedometer stress cell (HSC). The isotropic NCL for each soil was determined using a triaxial cell.

5.5.1 One-dimensional consolidation test

Slurry was the initial condition for the one-dimensional test. Firstly 1D-consolidation test started with very small seated load (1 kPa) then the load increased gradually until reaching 24000 kPa. This test was performed for 30B and 100B soils.

The results and the discussions are shown in section 5.2.1.3 (constant suction test). The results of high oedometer stress cell are cited in Figure (5.23), 30B-S0-Sl test, for 30B soil and Figure (5.39), 100B-S0-Sl test, for 100B soil.

5.5.2 Isotropic consolidation test

The isotropic consolidation test was conducted for both 30B and 100B soils with maximum cell pressure 800 kPa.

Figures (5.50 and 5.51) show the results of both 1D-consolidation and isotropic-consolidation tests for 30B and 100B soils. The isotropic-NCL for both soils was parallel to the 1D- NCL. The isotropic-NCL of 30B soil, 30B-S0-com-iso, had 0.945 offset in void ratio value from the 1D-NCL. Whereas, the isotropic-NCL of 100B soil, 100B-S0-com-iso, had 0.96 offset in void ratio value from the 1D-NCL.

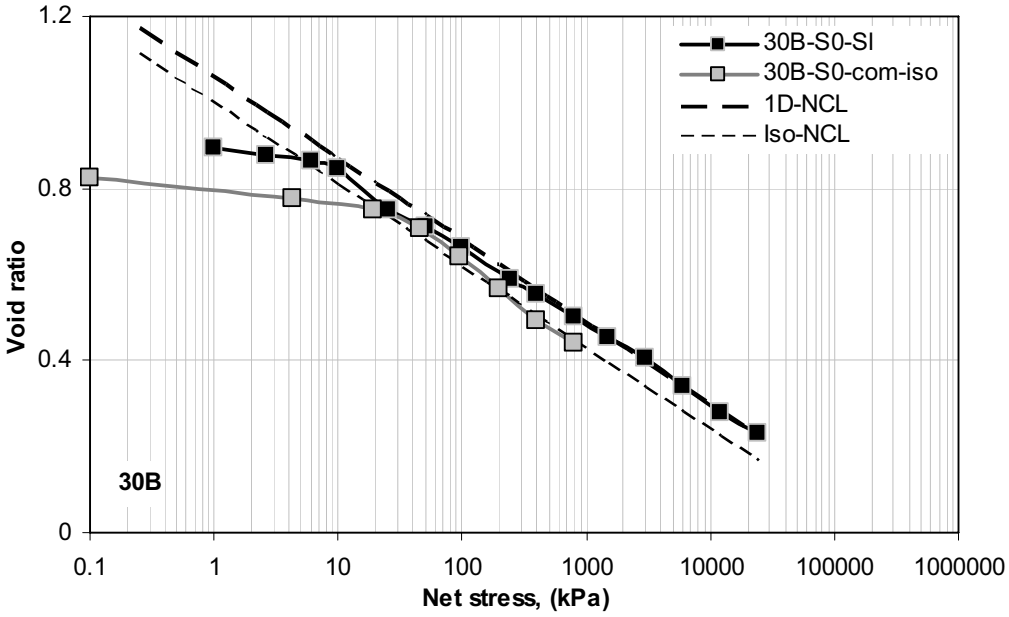

Figure 5.50 One-dimensional and isotropic consolidation tests for 30B soil.

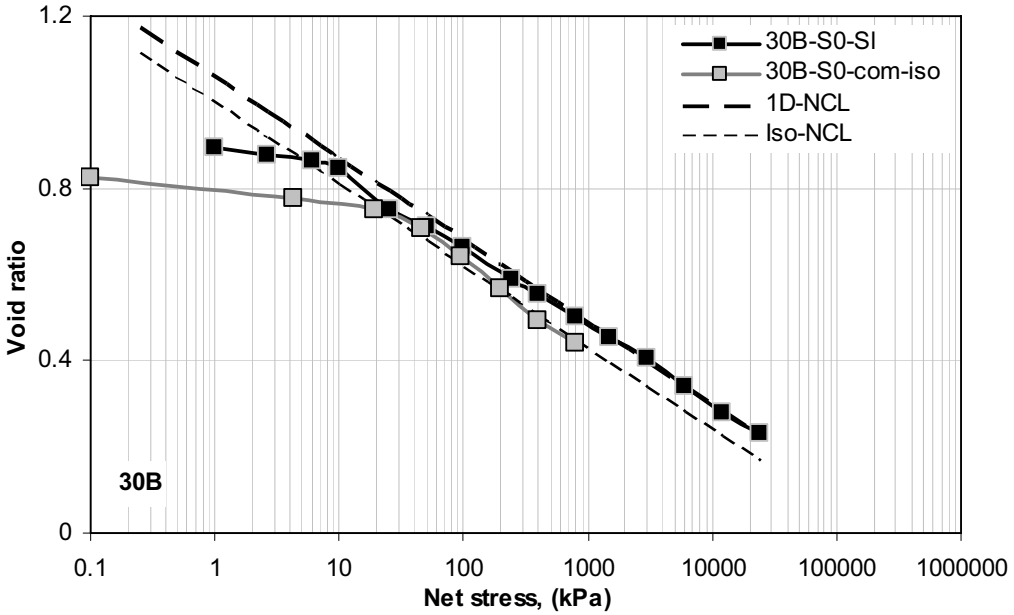

Figure 5.51 One-dimensional and isotropic consolidation tests for 100B soils.

5.6 Summary

The results of experimental tests of the volumetric yielding tests for 30B and 100B soils are presented and discussed. The volumetric yielding tests consist of five different types of 1D-compression tests: constant degree of saturation test, constant net stress test, constant suction test, changing both net stress and suction test, and the compaction tests. The results of the soil water characteristic curve (SWCC) program are presented as well. Four different controlled-suction 1D-compession cells are used to detect the volumetric yielding behaviour. Slurry and unsaturated loose conditions are chosen as initial states in the experimental program to cover the major ranges of soil structures.

The results of constant degree of saturation tests (Figures 5.1-5.4) show that the NCL's are almost straight in semi-log scale, and have slopes slightly more than the slope of the saturated NCL. This behavior depicts almost the same behavior as it was assumed in Al-Badran (2001) and Kanazawa et al. (2009).

The results of drying condition of constant net stress tests (Figures 5.6-5.18) show that for all initial densities the volume decreased with increasing suction until reaching air-entry value, then the reduction in volume reduced. The gravimetric water content continued decreasing as suction increased, and all gravimetric water content curves for different constant net stress joined as suction increases. The results of constant net stress tests with wetting for

initial loose condition (collapse test), Figures (5.19-5.22), show three different phases during reducing the suction (wetting) process.

The results of constant suction tests (Figures 5.23-5.43) show the position and the slope of NCL's depend on both net stress and suction. The NCL's either, for low suction value, has void ratio lower than the saturated NCL (associated with lower slope than the saturated NCL), or has void ratio higher than the saturated NCL (associated with higher slope than the saturated NCL) for higher suction value.

The verification tests (changing both net stress and suction test, Figures 5.44-5.47) obviously showed that the loaded volumetric yielding behavior is unique for unsaturated soil that is the same regardless of stress path of initial unsaturated loose soil.

Double peaks are observed in compaction curves (Figures 5.48-5.49). The contour lines of equal suction were established in the dry of optimum (DOP) state only. All these contour lines show vertical lines.

Finally, the results of SWCC tests under unconfined condition (Figures 5.5 and 5.12) show, (1) significant hysteresis behavior associated with absence of residual suction; (2) for low expansive soil (e.g., 30B soil) the value of air-entry suction of initial slurry condition remains constant initially then increases as the density increases; (3) while for high expansive soil (e.g., 100B soil) the density has no effect on the value of air-entry suction of initial slurry condition for the tested range of density.

Chapter 6
Modelling the Volumetric Yielding Behavior for Unsaturated Fine-Grained Soils

6.1 Introduction

The classical principles of soil mechanics for saturated soil are often not suitable for explaining the volume change behavior of unsaturated soils due to the influence of wetting-drying cycles. The volumetric yielding behavior for unsaturated soils is very important for analytical and practical purposes (collapse and swelling soil, design of footing, dams, embankments, and highways). Many models were undertaken to study the volume change of unsaturated soil before (Chapter 2), but till now limited studies have been revealed the volume change behavior beyond the preconsolidation pressure or at the yield state for the entire range of net stress and suction that may be experienced by the soil. The focus of present study is to develop a new model for constitutive state surface at the yield state in void ratio-net stress-suction space for unsaturated soils. The volume change in this model represents the consolidation, compression and collapse. In this study the fine-grained soils are clayey and silty soils.

6.2 New model for state surface at yield state for unsaturated fine-grained soils

The model supposed that, for the same soil, all points in void ratio-net vertical stress-degree of saturation space at normal consolidated (yield) state for different initial degree of saturation (i.e. saturated and unsaturated) and different initial densities (i.e. slurry, compacted and loose) relate to a unique surface. This unique surface represents the state surface. Each point on the state surface represents the preconsolidation pressure for a specific initial state. The loading paths, to obtain the state surface, are either (*i*) increasing the net stress (loading) under constant suction (or water content) or (*ii*) reducing the suction (wetting) under constant net stress. In addition there is another condition of state surface; (*iii*) in case of increasing the suction (drying); (*a*) in the range of saturation zone (before the air-entry value), and (*b*) in the specific range of high suction (in the second interval as shown later in Figure 6.18).

When the degree of saturation is replaced by gravimetric water content the state surface is still unique. The state surface for void ratio-net vertical stress-suction space is also unique in case of (*i*) and (*ii*) loading paths (i. e., the wetting conditions). In case of drying condition, (*iii*) loading path, the state surface will reflect the hysteresis behavior of SWCC.

The proposed model of unsaturated soil is based on the S_r-lines concept (Al-Badran, 2001), see section 2.4.4, which is modified according to the microstructural consideration of Nagaraj et al. (2006a and b), see section 2.4.5. The main parameters of the new model are: void ratio of the saturated NCL (e_{NCL}) under a specific net stress, critical degree of saturation (S_{rc}), parameter that controls the influence of the degree of saturation to increase the void ratio under constant net stress (R), parameter that controls the position of maximum value of void ratio under each net stress (M), and drying and wetting paths of SWCC (for suction space). The parameters R and M will be explained later in this chapter (section 6.4).

6.3 Hypotheses

As mentioned above, based on S_r-lines concept and the modification of this concept that is done in this study, there is a strong relationship between void ratio-net stress-degree of saturation at yield state. The model presents the relationship between void ratio, net stress and degree of saturation according to 1st hypothesis for S_r-lines. Then, to connect void ratio, net stress and degree of saturation with suction, 2nd and 3rd hypotheses are used.

The position of the state surface is defined by the NCL's of constant degree of saturation, S_r-lines (Al-Badran, 2001), Figure (2.18), according to the following hypothesis:

1st hypothesis: *The volume change behavior on the state surface is governed by degree of saturation, and for each degree of saturation there is a straight line representing the normal consolidation line for this degree of saturation (S_r-lines).*

The two experimental tests of constant degree of saturation condition, 30B-Sr58-com and 30B-Sr68-com tests as shown in Figure (5.4), were carried out to verify the 1st hypothesis. The results of these two tests show that the NCL's are almost straight, and have slopes slightly more than the slope of the saturated NCL. Moreover, the results in Figure (5.4) show almost good agreement with the *Sr*-lines assumption of Al-Badran (2001) and the work of Kanazawa et al. (2009). The models of Al-Badran (2001), Figure (2.18) and Kanazawa et al. (2009), Figure (2.24), assumed that the NCL of any constant degree of saturation (S_r-lines in Al-Badran, 2001) is a straight line and parallel to the saturated NCL. Moreover, the contour lines of constant degrees of saturation for yield state, after back calculations from unsaturated compression curves under constant water content condition, show a linear trend (Lawton et al., 1989; Al-Badran, 2001; Honda et al., and 2007; Sun et al., 2007).

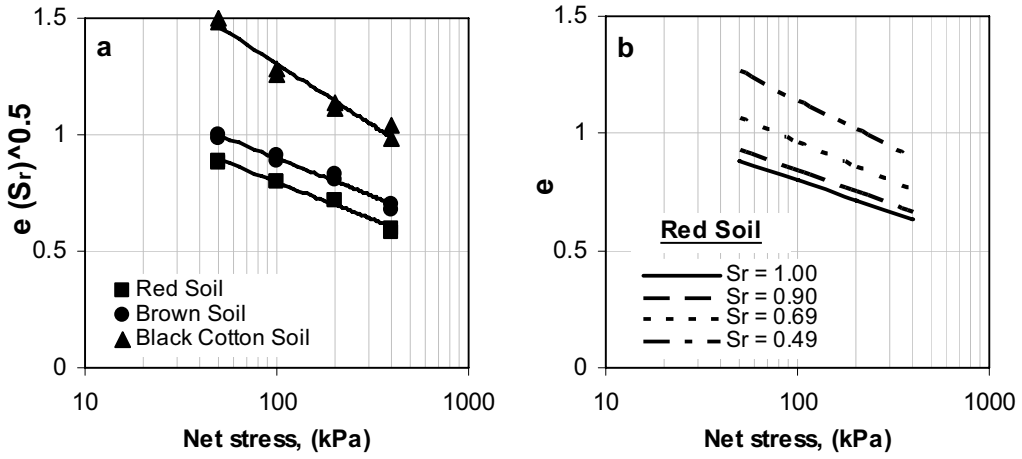

Figure 6.1 a- Nagaraj et al. (2006a) concept 'each soil has one NCL by normalization' (after Nagaraj et al., 2006a), b- S_r-lines concept 'straight NCL for each degree of saturation' for Red Soil.

The work of Nagaraj et al. (2006a and b) supports the relationship between the saturated NCL and S_r-lines from microstructural consideration, Figure (6.1). It was assumed that the change in microstructure of unsaturated soil at constant water content, due to change in net pressure (p- u_a) or suction ($u_a - u_w$), is due to change in the radius of air-water interface in the micropore enclosed by assuming to be saturated clay clusters. The parameter $w/\sqrt{S_r}$ (or $e\sqrt{S_r}$) is a convenient parameter to account for the effects of degree of saturation in the range of 0.4 to 0.9. Actually, Figure (6.1a) is the same as Figure (2.22) from Nagaraj et al. (2006a) and Figure (6.1b) represents the void ratio data for constant degree of saturation from the normalized compression line of the Red soil. The data for constant degree of saturation condition show that there is a straight line in void ratio-log net stress space for each degree of saturation. The slope of these lines increases as the degree of the saturation increases starting from the slope of the saturated NCL. Therefore, the new state surface model of unsaturated soil relates the saturated NCL and unsaturated NCL (S_r-lines) using empirical equations, as other unsaturated models do, but here the microstructural evidence is considered.

Some objections may be raised against 1st hypothesis. Firstly, the model was applied for the net normal stress not for the effective stress. Secondly, the variables used for determining the yield stress (or preconsolidation pressure) must be independent of material properties (i. e. water content or degree of saturation). For the first objection, it is too difficult to determine exactly the value of effective stress for entire range of suctions (i.e. for unsaturated state). Also, it can be possible to find a relationship between void ratio and the net vertical stress, like other relationships (empirically or statistically) for maximum dry density and equivalent energy in compaction test (Pandian et al., 1997 and Nagaraj et al., 2007). In

addition, till now there is no unique and standard method to determine effective stress for unsaturated soil for entire range of suctions. Nevertheless there are some recent attempts for special tests for unsaturated soils (Khalili and Khabbaz, 1998 and Khalili et al., 2004). Regarding the second objection Khalili et al. (2004) and Lu and Likos (2006) supported the 1st hypothesis. In multiphase systems, such as saturated and unsaturated soils, the stress state within each phase will naturally be a function of the properties of that phase as well as the other phases within the system (Khalili et al., 2004). Moreover, Honda et al., (2007) presented a model to determine yield stress for unsaturated soil depending on the water content.

A change in the number of meniscus water bridges in unsaturated soil (as degree of saturation changes), produces a change in their stabilising effect and hence leads to the possibility of yielding and plastic compression during an increase in degree of saturation (wetting), (Wheeler et al., 2003). However, in addition to the effect of net vertical stress, there is a strong relationship between the volume change and suction, considered by the change of the degree of saturation, according to following hypothesis:

2nd hypothesis: *If the fine-grained soils are kept in drying or wetting state for unsaturated state (when the degree of saturation is lower than the degree of saturation at air-entry value) the suction is a function of the gravimetric water content only.*

The air-entry value, s_{aev}, is the value of suction when the degree of saturation starts decreasing sharply upon increase in suction. The value of air-entry suction can be determined by the intersection point between the straight sloping line at the transition zone and the straight line at the saturation zone in S_r-log s space, Figure (6.2). In the transition and residual zones when the degree of saturation is lower than the degree of saturation at air-entry value, there is no density effect on the gravimetric water content-suction relationship for fine-grained soils. The degree of saturation at the air-entry value will be named as critical degree of saturation (S_{rc}), and it is close to the degree of saturation at the optimum water content *OWC*. Figure (6.2) presents the drying path of the SWCC for 30B and 100B soils. Figure (6.2) shows that the values of the degree of the saturation at the air-entry value (i. e. critical degree of saturation) are the same as the values of the degree of the saturation at *OWC* of compaction curve, see Table (5.1). The results of contour lines of equal suction in the compaction curves of the experimental programme, Figures (5.50 and 5.51) and the results of (Delage and Graham, 1995; Gens et al., 1995; Li, 1995; Romero, 1999 as Figure 2.28; Tarantino and Tombolato, 2005; Agus, 2005 as Figure 2.29; and Ferrari, 2007) support the 2nd hypothesis. The results showed that at the dry side of compaction curve, when the soil is in unsaturated state, the lines of constant suction are almost vertical and therefore the density has no effect on the suction-water content relationship for fine-grained soils. Romero (1999) attributed this feature to the

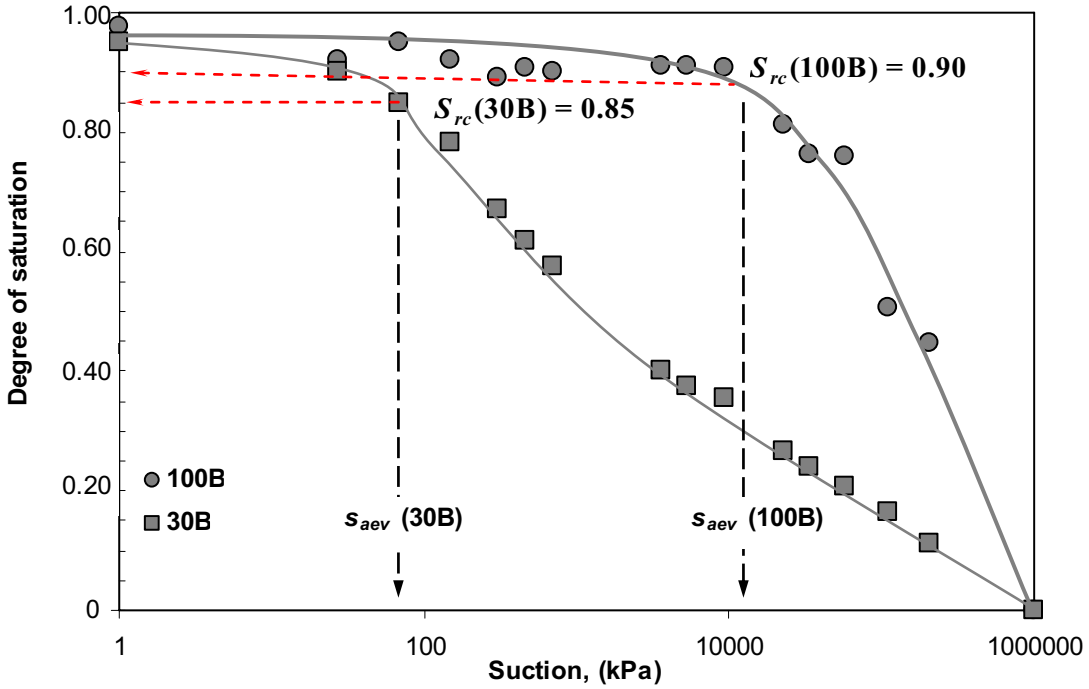

Figure 6.2 The drying paths for 100B and 30B soils showing the degree of saturation at s_{aev}.

effects of loading mechanism on the macroporosity that does not contain free water, since at low water content levels water is mainly absorbed or present in diffuse layers at intra-aggregate scale. The degrees of saturation changes, in these diffuse layers at intra-aggregate scale, are associated with macroporosity changes under constant intra-aggregate water content. While in case that the matric suction approaches the saturation zone, the loading mechanism affects inter-aggregate water and the contours of equal suction try to incline in order to converge to the limit condition of matric suction equal to zero at full saturation condition (S_r = 1.0). However, the contour lines of equal suction in the compaction curves of Romero (1999) work, Figure (2.28), that pass the optimum water content (*OWC*) may need some corrections. Some of the contour lines were established using two different positions only (one on the wet side and the other on the dry side). Using two points will produce only a straight line, which is not necessary to represent the actual behavior. The structure and the behavior of the wet side are different from the dry side, thus it is important to use many points from different locations to draw the contour lines of equal suction when the line passes the transition from the dry side to the wet side.

The proposed model here assumes that the structure of the fine-grained soils has a double porosity system: macro pores and micro pores (Alonso et al., 1990). The macropores compress when low and intermediate net stress is applied. The micropores remain unchanged at this level of net stress. Subsequently, at high net stress, the average diameter of macropores

will highly reduce due to high compression. Here the average macropores size decrease to a level minimizes most of the large pores from soil structure system (change in soil fabric from open pore state to close pore state, see Figure 6.3). Figure (6.3) shows the pore size distribution of different densities for different types of soils; silty clay with *LL* = 41 %, high-plasticity clay with *LL* = 98 % (Ferber et al., 2008), and a mixture of 50 % bentonite-50 % sand, 50B/50S, with *LL* = 74 % (Arifin, 2008). The silty clay and high-plasticity clay prepared into two different conditions: a well-compacted and loosely compacted conditions. The 50B/50S mixture has also two conditions: compaction for dry of optimum, DOP, in Standard Proctor and Modified Proctor or highly compacted, HC. The figure shows that the percentage of the large pores size (macro level) reduces as the density increases, whereas the percentage of the small pores size (micro level) remain almost unchanged or increases with increasing the density. The changes in the pores level are believed to be associated with change of the shape of compression lines (change the slope of the saturated NCL). This changing of the macropores level can be also taken place by steps, especially in high expansive soils, which means different slopes for the saturated NCL.

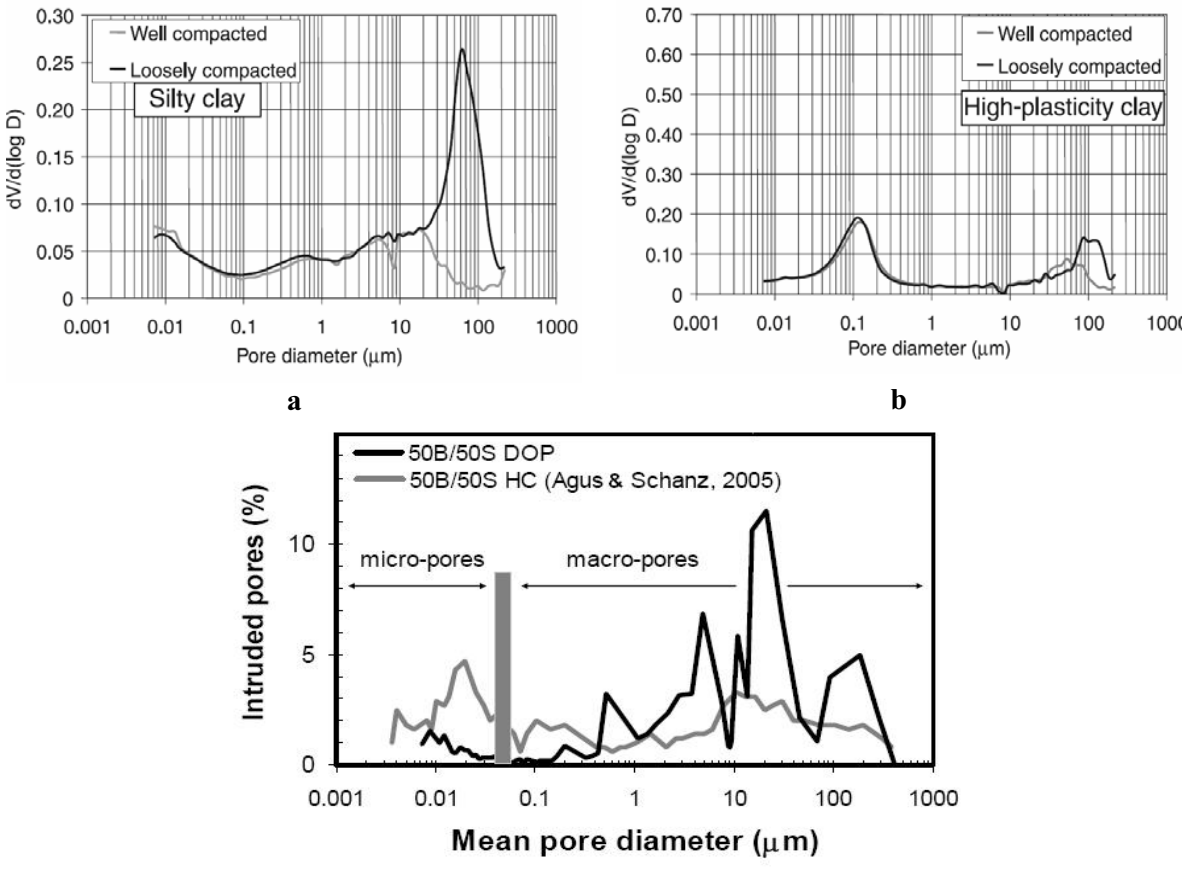

Figure 6.3 Pore-size distributions for: (a) & (b) Silty clay and high-plasticity clay (Ferber et al., 2008), and (c) A mixture of 50 % bentonite-50 % sand (Arifin, 2008).

The model proposed here assumes that when the applied suction is higher than the air-entry value the pore water will locate in the fine pores only (Backer and Frydman, 2009). These fine pores are not affected by the density changes (Figure 6.3a, b), even their percentage may increase with increasing the density (Figure 6.3c). Therefore, at high suction level (higher than the air-entry value), there is no density effect on gravimetric water content-suction relationship. While when applied suction is lower than the air-entry value the pore water is believed to locate at both fine pores as will as the large pores. Therefore, at low suction level (lower than the air-entry value), both density and the gravimetric water content have an effect on suction value or the suction is a function of volumetric water content. At the saturation zone (suction lower than the air-entry value) the model assumes, according to on the experimental results of this study, a linear relationship between the degree of saturation and suction, see the data of Figure (6.2). In other words, below the air-entry value, the suction is a function of volumetric water content, while at suction range higher than the air-entry value, the suction is a function of gravimetric water content only.

It is important to clarify that up to here the state surface (except the saturation zone and the specific part of drying state, Figure, 6.18) can be established by wetting process only. By increasing the net stress, the soil at unsaturated NCL under constant suction or constant water content conditions results in increase in the degree of saturation due to compression which means wetting process. To consider the effect of hysteresis behavior of SWCC 3rd hypothesis, depending on the experimental results in chapter 5, is adopted.

3rd hypothesis: *The state surface for unsaturated state, under mechanical loading path (increase in net stress) or wetting condition (increase in water content), represents the wetting path. Therefore the gravimetric water content-suction relationship in this surface follows the main wetting path of SWCC.*

In other words, in case of loading paths (*i*) increase in net stress (loading) and (*ii*) decrease in suction (wetting) the suction value at state surface follows the main wetting path of SWCC. Whereas, in case of third loading path, (*iii*) increase in suction (drying), the suction value at state surface follows the main drying path of SWCC.

6.4 Locations of S_r-lines on the state surface for constant net vertical stress condition

The locations of S_r-lines can be determined by performing double oedometer test (DOT) for the same initial state (preferred high void ratio and low water content to intersect a large number of S_r-lines). Analyzing unsaturated volume change data in normal consolidated state (compression curves and static compaction data for different net stress and different water

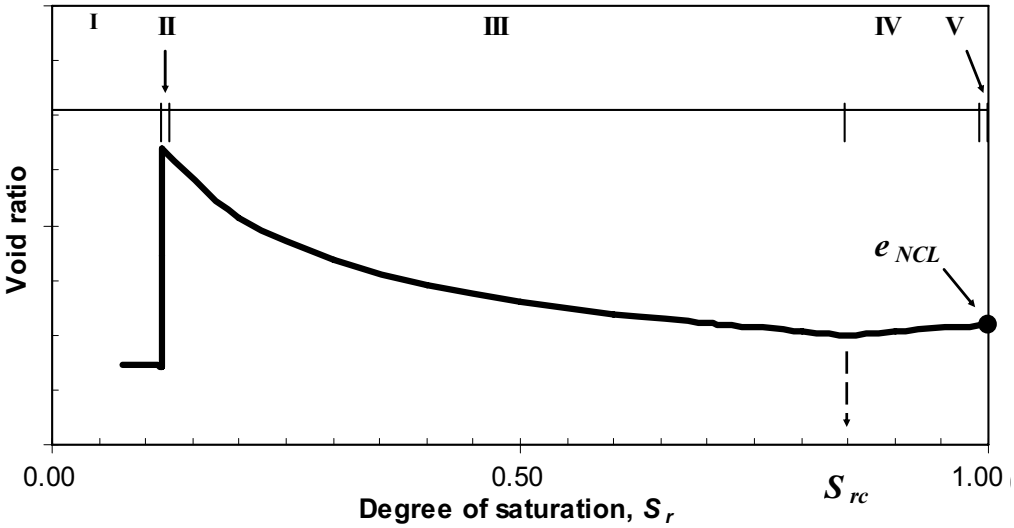

Figure 6.4 The proposed void ratio-degree of saturation relationship at normal consolidated state under constant net vertical stress condition with five characteristic intervals of degree of saturation (S_{rc} = 0.85).

content of 30B and 100B soils) drive the following interesting phenomenon. For constant net vertical applied stress, the entire range of the degree of saturation (from fully dry to fully saturated condition) shows five different trends. Thus, the entire range of the degree of saturation, for each net stress, is divided into five intervals from fully dry to fully saturated state, Figure (6.4). The behavior of the soil in the five ranges depends on the saturated NCL, the degree of saturation (S_r) and the critical degree of saturation (S_{rc}). Figure (6.4) shows the curve of void ratio-degree of saturation relationship (at normal consolidated state) under constant net stress for the entire range of the degree of saturation (five intervals).

Therefore, the volumetric behavior of initial loose soil condition under constant net vertical stress will track the following five intervals. The first interval starts from zero degree of saturation in which the void ratio is constant due to absence of any bonding forces between soil particles. Then, with increasing the degree of saturation, the second interval comes about when water attracts the soil particles through the capillary forces. The second interval is for constant degree of saturation (Figure 6.4). The soil stiffness in the second interval increases (hardening), which causes increase in the void ratio as the water content increases under constant net vertical stress till reaching the maximum void ratio in the second interval e_{max}. Afterwards the third interval sets off in which the void ratio decreases as the degree of saturation increases. The third interval is the main part of volumetric yielding behavior and it is the same part that Nagaraj et al., (2006a and b) established the relationship for normalizing the unsaturated void ratio under yield state. The third part continues till reaching the critical degree of saturation (S_{rc}) with the lowest void ratio (or highest density) can be reached under

a specific net vertical stress. Then the fourth interval is reached and the void ratio increases again as the degree of saturation increases till reaching the full saturation condition (the fifth interval) and the void ratio here equal to the void ratio at saturated NCL under the specific net stress (e_{NCL}).

The hardening in the second interval is believed to be related to the increase in the capillary force. When the water content increases (degree of saturation remains constant) the void ratio increases (Equation 6.2) as result of increase in the capillary force which attracts the soil particles together. Here the curve of the second interval is not related to one test (when the void ratio increases with increasing the water content) but each point represents the preconsolidation pressure for a specific initial condition. The experimental results of compression curves, static and dynamic compaction for 30B and 100B soils show that the degree of saturation at maximum void ratio $S_{r(e_{max})}$ increases when the net applied vertical stress or compaction effort (*CE*) increases. It is important to note, that the second interval appears if the void ratio at dry condition is less than maximum void ratio in the second interval (e_{max}) which is the case in low range of net vertical stress.

The equations that govern the five intervals are: The first interval is from zero degree of saturation to the degree of saturation at the maximum void ratio in the second interval $S_{r(e_{max})}$.

$$e_{uns-I} = e_{dry} \tag{6.1}$$

where e_{dry} is the void ratio of the fully dry soil.

The second interval represents the degree of saturation at the maximum void ratio in the second interval $S_{r(e_{max})}$. In this interval, the degree of saturation shows almost constant value, see the points between S_r = 0.1 to S_r = 0.15 in Figure (6.5), resulting in the following equation:

$$G_s w = S_{r\,(e\max)} e_{uns} \rightarrow e_{uns-II} = \frac{G_s w}{S_{r\,(e\max)}} \tag{6.2}$$

where G_s is the specific gravity.

The water content of the maximum void ratio in the second interval, $w_{(e_{max})}$, can be calculated according to Equation (6.3). Equation (6.3) is a fitting equation established from the experimental data for 30B and 100B soils as shown in Figure (6.6). The model predictions in this figure are achieved using the equations of five intervals for different compaction effort. The behavior of soil in the second interval produces maximum void ratio that can the soil reach under a specific net stress.

$$w_{(e_{\max})} = G_s + \left(\left(\frac{e_{NCL}}{G_s} \right).100 - G_s \right) M \tag{6.3}$$

where e_{NCL} is the void ratio of the saturated NCL; M is the fitting parameter that controls the position of e_{max} in the second interval.

The third interval is from the degree of saturation at the maximum void ratio $S_{r(e_{max})}$ to the critical degree of saturation S_{rc}. The following general equation (Equation 6.4) can be used for low to high plasticity fine-grained soils, which is equivalent to the approach used by Nagaraj et al., (2006b) and Horpibulsuk et al., (2008a and b), see Figure (6.7). Nagaraj et al. (2006b) introduced an ideal pore model (linear relationships) depends on the microstructural consideration to estimate the compaction curves of fine-grained soils quickly for different compaction efforts for the *DOP* and *WOP*. Based on their ideal model, parameters $w/ S_r^{0.5}$ and w/ S_r^{2} were proposed for the *DOP* and *WOP*, respectively.

$$e_{uns-III} = \frac{e_{NCL} S_{rc}}{(S_r)^R} \tag{6.4}$$

where R is the fitting parameter that controls the influence of the degree of saturation on the increase of the void ratio under constant net stress in the third interval.

The fourth interval is from the critical degree of saturation up to fully saturated state (S_r = 1.0). All the degrees of saturation in the fourth interval are greater than the critical

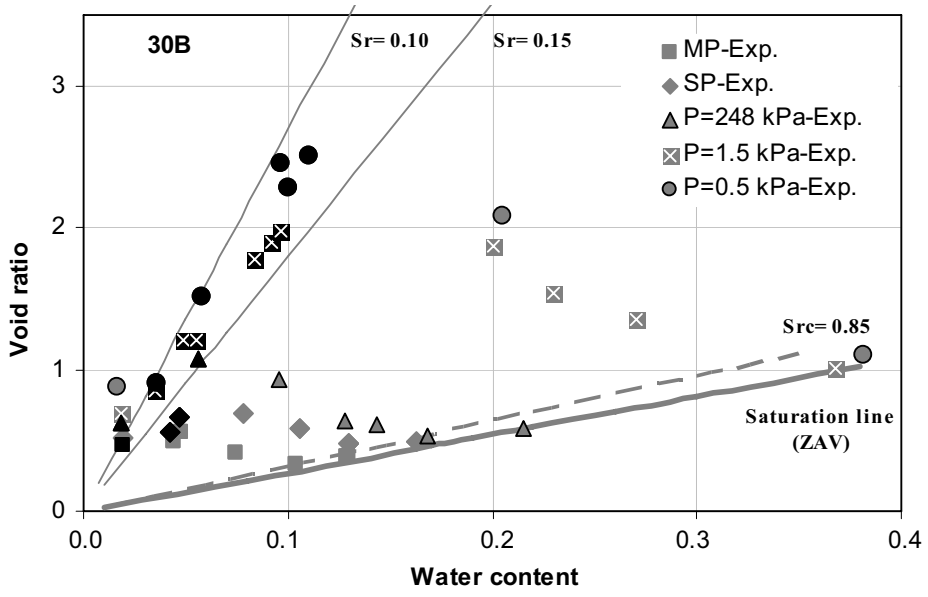

Figure 6.5 Volumetric yielding behavior within the second interval of degree of saturation (between 0.10 to 0.15 degree of saturation with black color) during compression (static and dynamic) for different net stress and compaction effort for 30B soil. MP and SP are the Modified and Standard Proctor tests.

degree of saturation; therefore, the current degree of saturation is used in Eq. (6.4) instead of the critical degree of saturation:

$$e_{uns-IV} = \frac{e_{NCL} S_r}{(S_r)^R} \longrightarrow e_{uns-IV} = e_{NCL} (S_r)^{1-R} \tag{6.5}$$

The fifth interval is defined by degree of saturation equal to 1.0; the void ratio equal to the void ratio at saturated NCL (i.e., e_{NCL}).

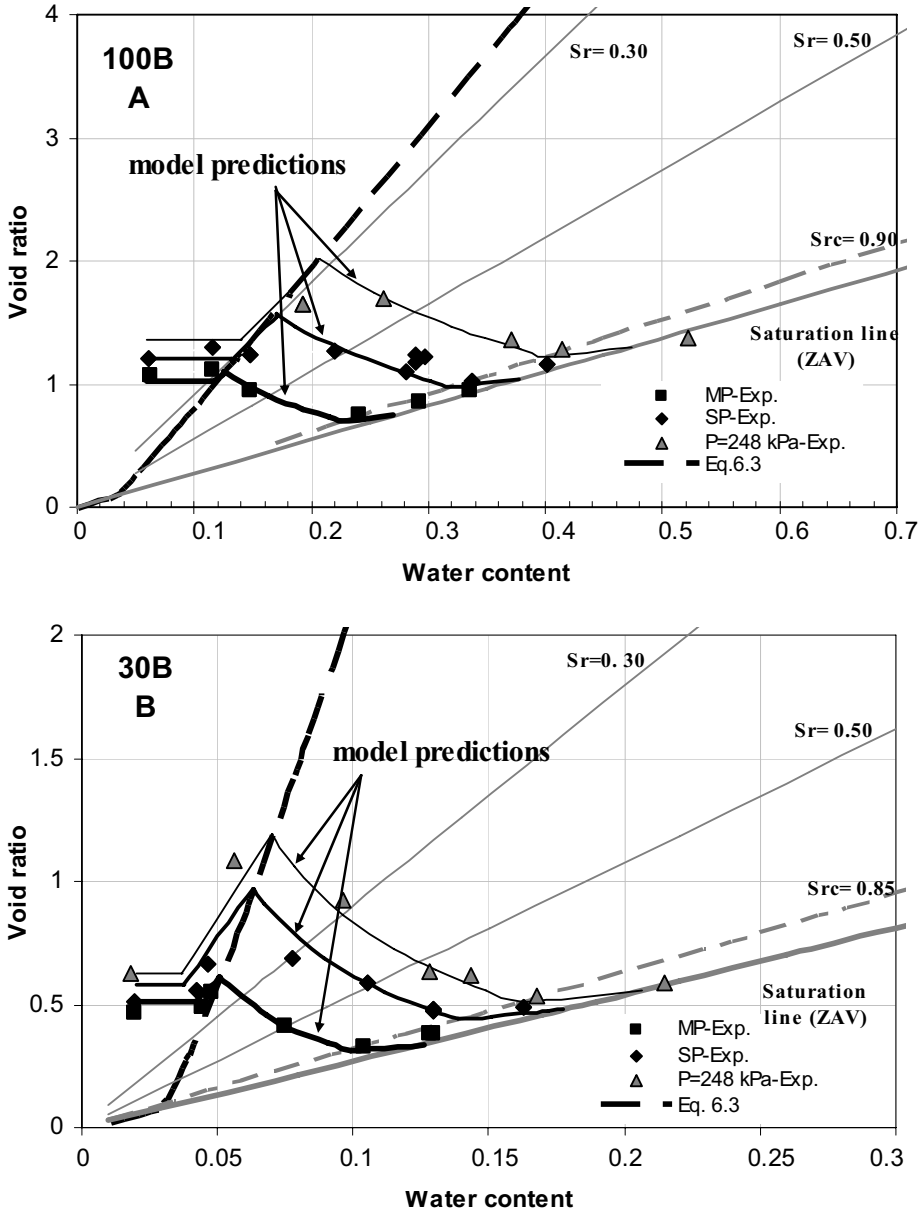

Figure 6.6 The predicted line (Eq. 6.3) of the maximum void ratio in the second interval, e_{max}, for: (A) 100B soil (S_{rc} = 0.90, R = 0.43, M = 0.4) and (B) 30B soil (S_{rc} = 0.85, R = 0.5, M = 0.24).

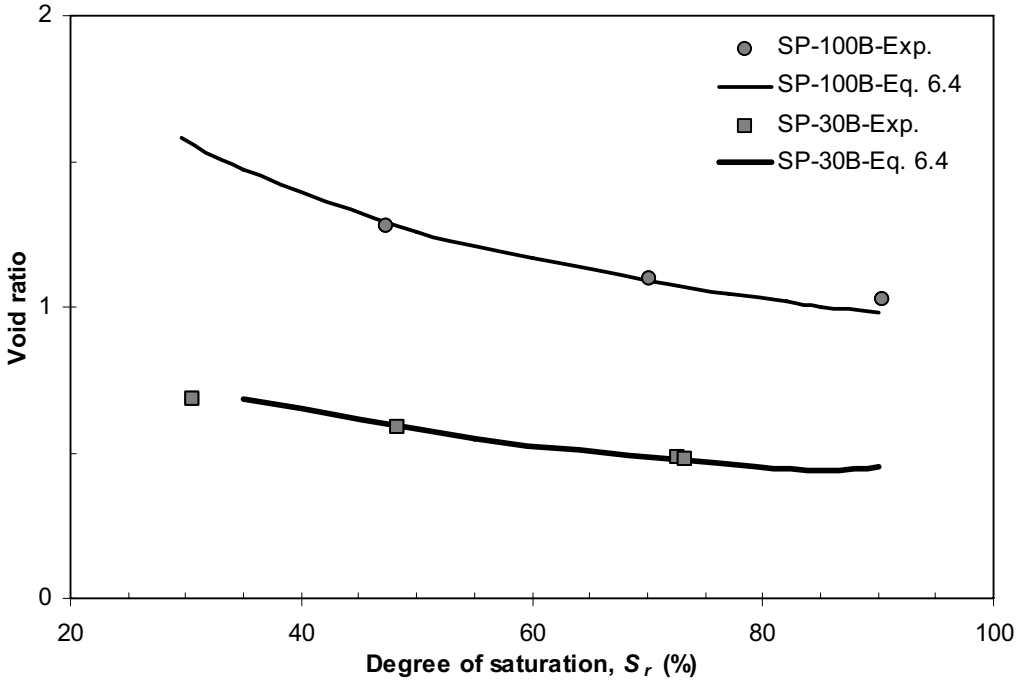

Figure 6.7 Comparison between exp. results of standard compaction tests and Eq. (6.4) for 100B (S_{rc} = 0.90, R = 0.43) and 30B (S_{rc} = 0.85, R = 0.5) soils.

6.5 Two- and three-dimensional relationships (2D and 3D) of volumetric yielding for unsaturated fine-grained soils.

In the proposal model there are four characteristic properties to be known: (1) saturated NCL from consolidation test; (2) the critical degree of saturation S_{rc} from SWCC or from the optimum water content *OWC*; (3) the gravimetric SWCC; and (4) the R and M parameters from unsaturated compression test preferable using samples with initially loose state.

The saturated NCL for initially slurry specimen represents the yield line for the saturated state or at S_r = 1.0. In addition, the saturated NCL is adopted in this model to determine the parameter e_{NCL}. To estimate the complete compression curve (over and normal consolidated states) the model assumes that the rebound index (C_r) at unsaturated state is the same as the rebound index at saturated state. If the soil was at the drying path, the hydration process in soil will change from drying to wetting during loading under constant suction condition. All the model predictions in Figures (6.8-6.13) are for 30B soil. The values of the main parameters for 30B soil are: critical degree of saturation (S_{rc}) = 0.85, R = 0.5, and M = 0.24.

Hysteresis of SWCC is the main cause of nonuniqueness of volume change and water content constitutive surfaces in net normal stress-suction space (Fredlund and Rahardjo, 1993). But on other hand the state surface for (i) and (ii) loading paths, as explained earlier in section 6.1 and 6.2, represents a wetting path (3rd hypothesis). Practically, the problem of hysteresis may come into picture when the soil state initially, before loading, is located on the drying or scanning path of SWCC. As mentioned before if the net stress increases under constant suction condition or constant water content the state of specimen will change from drying to wetting path due to increase in the degree of the saturation. In some cases the state of the specimen may not reach the main wetting path when the state of the specimen changes from over consolidated to the normal consolidated or yield state. However, as the loading increases at normal consolidated state, under constant suction or constant water content, the state of the specimen will force to be at the wetting path as a result of high increase in the degree of saturation, see Figure (5.30) for 39 MPa constant suction test.

Figures (6.8-6.11) represent the state surface in 2D space for the relationships between net stress, void ratio, water content, and the degree of the saturation, (e-logσ / e-S_r / e-w) respectively. Figure (6.8) shows that the unsaturated NCL's for low range of the degree of saturation are not continuing in the same straight line as the net stress increases, but they collapse to the full dry NCL path. This behavior relates to the path of the maximum void ratio in second interval (e_{max}). The maximum void ratio decreases as the net stress increases, Figure (6.6), and in the same time associates with increase in both values of the degree of the saturation, Figure (6.10), and water content, Figure (6.11). Therefore, the path of the unsaturated NCL for low range of constant degree of saturation will intersect the path of the maximum void ratio as the net stress increases. Then the unsaturated NCL will follow the path of first interval i. e., the path of fully dry NCL. The value of the net stress, in which the intersection between the path of the unsaturated NCL under constant degree of saturation condition and the maximum void ratio in the second interval takes place, increases with increasing the value of degree of saturation until reaching a specific net stress, in which the second interval ends. Moreover, the model predictions show that the slope of the unsaturated NCL's for each degree of saturation (S_r-lines) firstly decreases as the degree of saturation decreases until reaching the critical degree of saturation (S_{rc}), then the slope increases until finally the slope reduce rapidly to the slope of the fully dry NCL, Figure (6.9).

Figures (6.12 and 6.13) represent the state surface in 3D-space for the relationships between net stress, void ratio, water content, and the degree of the saturation, (e-logσ-Sr and e-logσ-wc) respectively. For each stress level, the void ratio-gravimetric water content relationship can be predicted from void ratio-degree of saturation relationship. Then, from

void ratio-gravimetric water content and wetting path of gravimetric water content-suction relationship (i. e. SWCC), the 3D proposed state surface (void ratio-net stress-suction) can be established, Figure (6.14). In other words, the state surface of void ratio-net stress-suction relationship results from Figure (6.11) and SWCC.

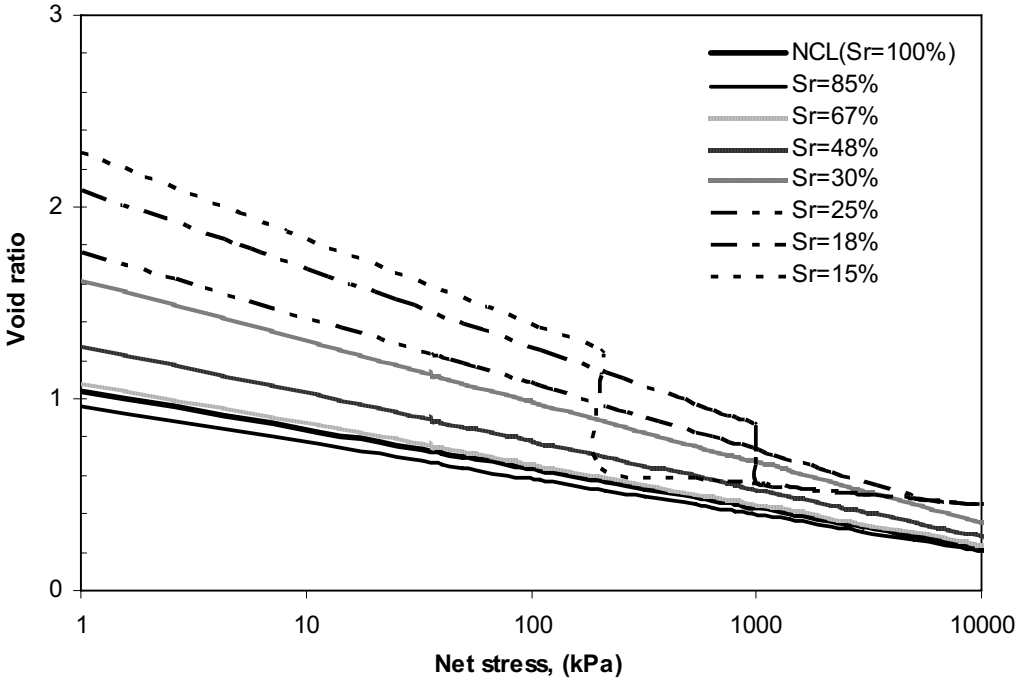

Figure 6.8 The model prediction of NCL for each degree of saturation in e-logσ space, for 30B soil.

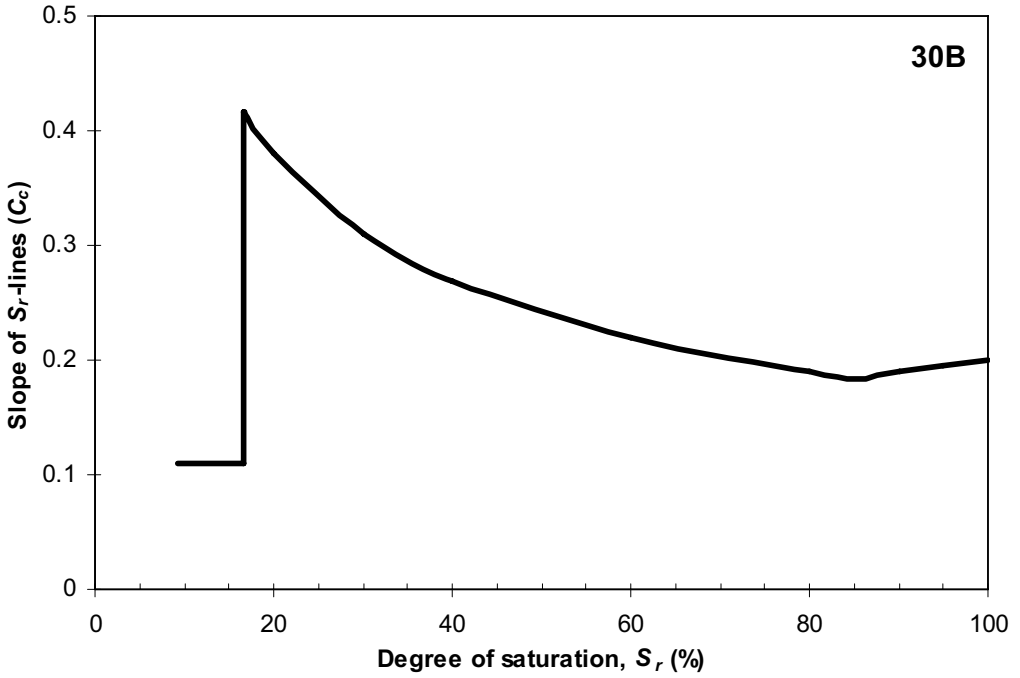

Figure 6.9 The model prediction of the relationship between the slope of predicted

unsaturated NCL's (S_r-lines) and the degree of saturation for 30B soil.

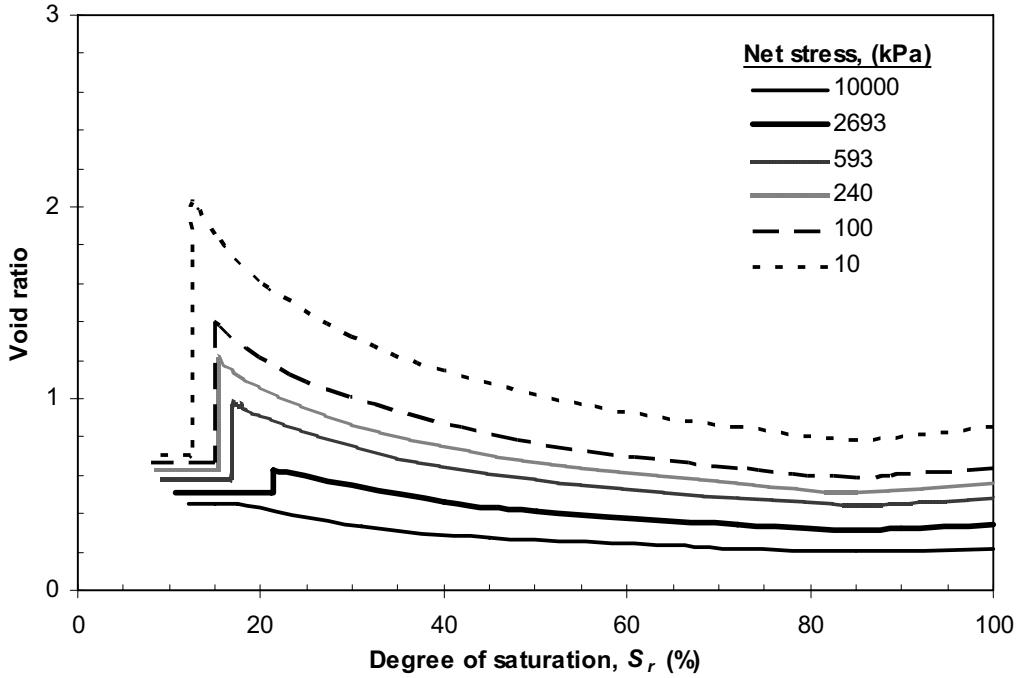

Figure 6.10 The model prediction of void ratio-degree of saturation relationship at normal consolidated state under constant net stress condition, for 30B soil.

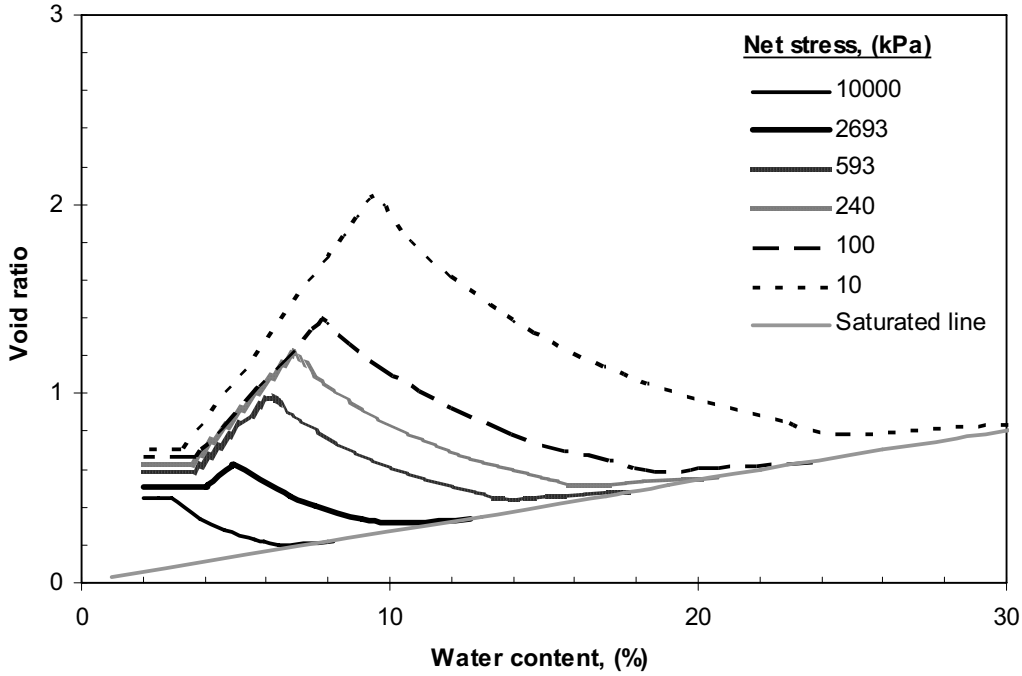

Figure 6.11 The model prediction of void ratio-gravimetric water content relationship at normal consolidated state under constant net stress condition, for 30B soil.

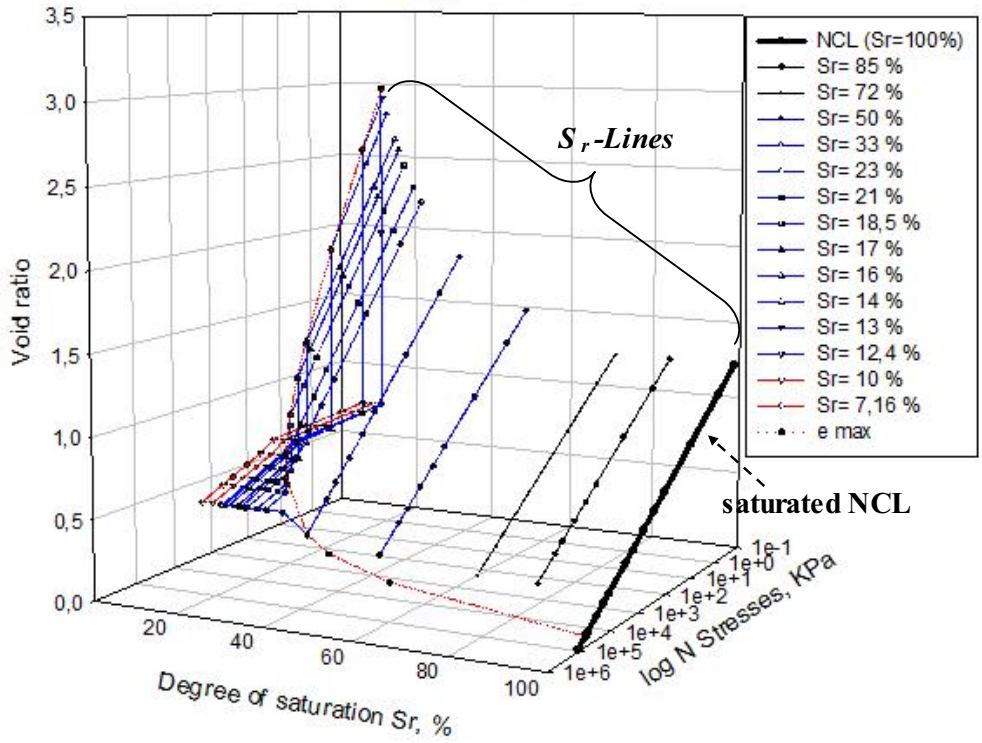

Figure 6.12 The model prediction of 3D state surface in void ratio-log net stress-degree of saturation space for 30B soil.

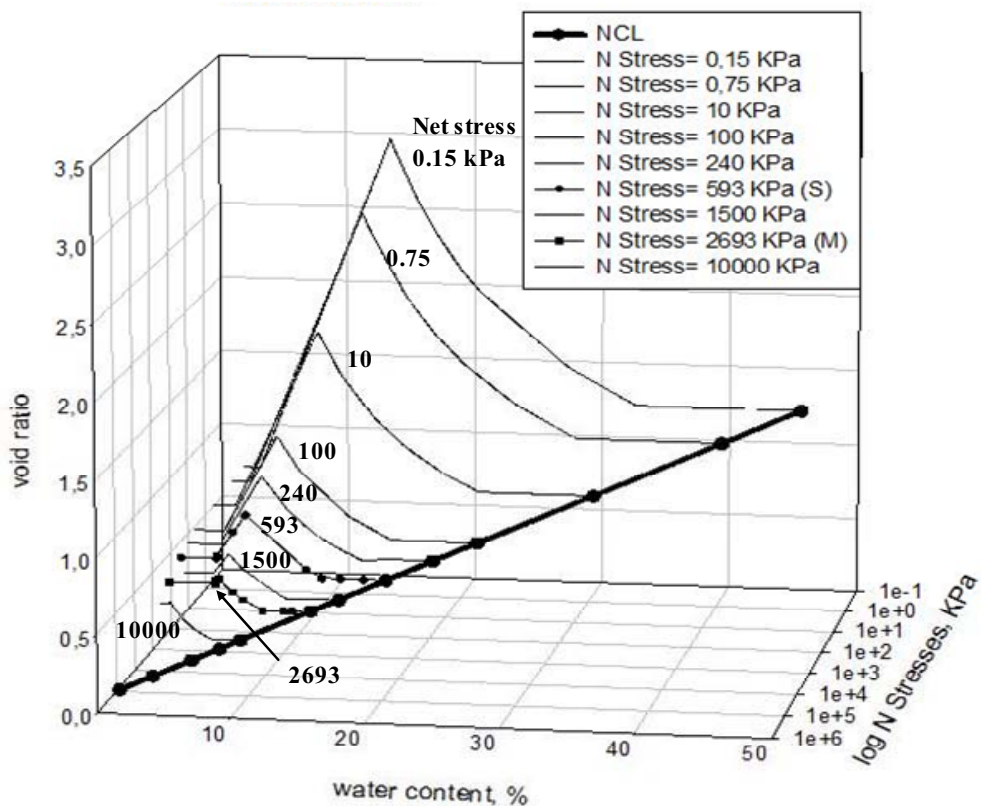

Figure 6.13 The model prediction of 3D state surface in void ratio-log net stress- gravimetric water content space for 30B soil.

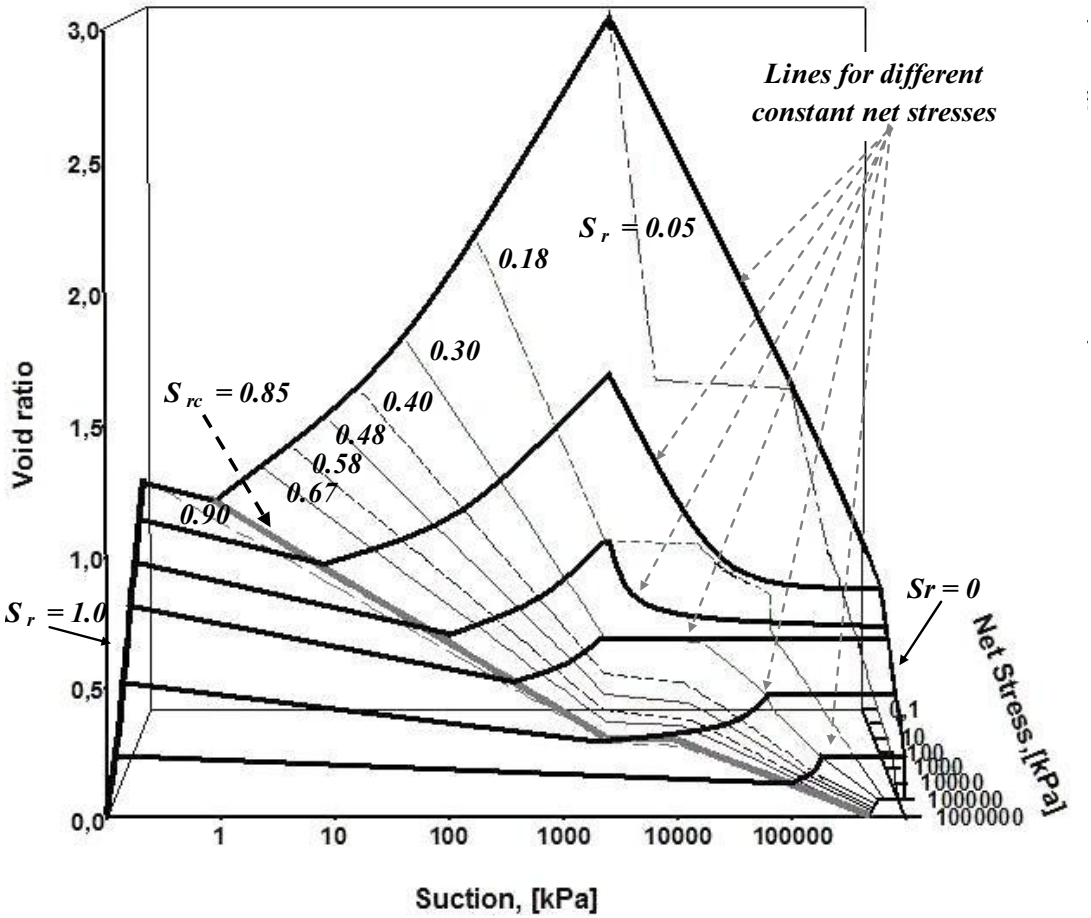

Figure 6.14 The model prediction of 3D state surface in void ratio-log net stress- log suction space for 30B soil.

Figures (6.15-6.17) show the typical shape of curve at normal consolidated state in case of constant suction, constant net stress, and constant volume conditions respectively. Figure (6.15) shows the predicted NCL's under constant suction condition in net stress-void ratio plane for 30B soil. The figure shows that the slope NCL under low constant suction condition decreases as the suction increases, s = 20 kPa, until reaching the air-entry value (fourth interval). The slope of the NCL increases, s = 1000 kPa, with increasing the constant suction condition (third interval). Consequently, with increasing the suction (second interval) the slope starts to decrease again (s = 10000 kPa) until reaching the slope of the fully dry condition (first interval) as in case of s ≥ 100000 kPa. The behavior of the initial void ratio has the same tendency as the slope of the NCL. Initial void ratio decreases with increasing the value of constant applied suction, then the increases after the air-entry value till reaching to the maximum initial void ratio and finally decreases to value of void ratio of the fully dry condition which is lower than the initial void ratio of saturated state (saturated NCL). The

above two characteristics determine the following behavior for the NCL's of constant suction condition. The NCL for low values of the applied constant suction (below the air-entry value or in the fourth interval, s = 20 kPa in Figure 6.15) starts with void ratio below the saturated NCL. The NCL for low values of the applied constant suction will be closer to the saturated NCL as the net stress increases until joins the saturated NCL (NCL for low values of the applied constant suction has slope smaller than the saturated NCL) as in case of s = 20 kPa. As the value of the applied constant suction increases and become larger than the air-entry value (third interval, s = 1000 kPa in Figure 6.15) both the initial void ratio and the slope of the NCL will start to increase until the maximum void ratio in the second interval is reached. The NCL in this case also will be closer to the saturated NCL as the net stress increases until joins the saturated NCL, s = 1000 kPa. With increasing the applied constant suction value (second interval l, s = 10000 kPa in Figure 6.15) both the initial void ratio and the slope of the NCL will decrease. But with increasing the net stress the NCL will pass from second interval to the third interval, which yields the increase of the slope and again the NCL will be closer to the saturated NCL as the net stress increases until joins the saturated NCL, s = 10000 kPa. In case of NCL for high applied constant suction (the first interval, s ≥ 100000 kPa in Figure 6.15) the NCL initially follows the behavior of fully dry NCL, which is starting with low values for the void ratio and the slope (lower than the values of the saturated NCL). As the net

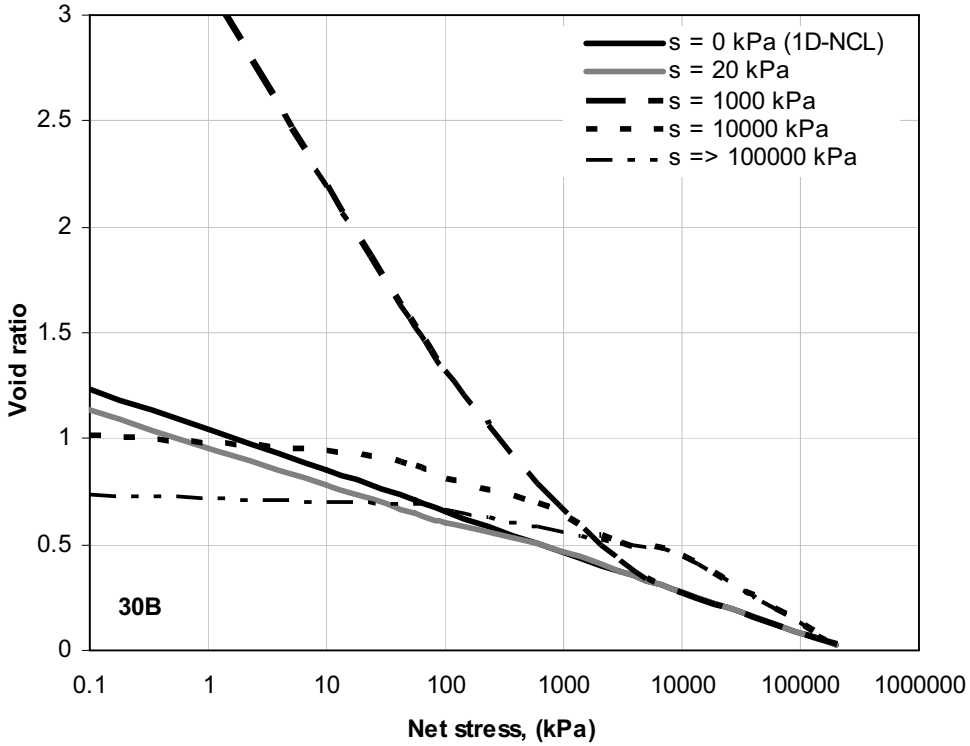

Figure 6.15 The model prediction of NCL's under constant suction condition in void ratio-log net stress space for 30B soil.

stress increases the NCL will transfer from the first interval to the third interval, as in case of net stress higher than 10000 kPa for s ≥ 100000 kPa in Figure 6.15, (because the second interval will end in the high net stress range). The last action leads to increase the slope and here again the NCL will be closer to the saturated NCL as the net stress increases until joins the saturated NCL. Figure (6.15) obviously shows that the trend of all the NCL's of constant suction condition (except the fully dry condition) towards the saturated NCL as the net stress increases until join the saturated NCL.

Figure (6.16) is similar to Figures (6.10 and 6.11), but it shows the relationship with suction not with degree of saturation or water content. Figure (6.16) shows that as the suction increases initially the curve for normal consolidated state decreases till air-entry value, S_{aev}, (fourth interval) is reaches, then the curve increases with increasing the suction (third intervals). After that the curve decreases (second interval) and then keep constant (first interval) as in case of low and intermediate constant net stress (p = 100 kPa and p = 593 kPa), or directly after the maximum void ratio is reached the curve keep constant (first interval) as in case of high constant net stress (p = 10000 kPa).

Figure (6.17) shows that in the curve for normal consolidated state under constant

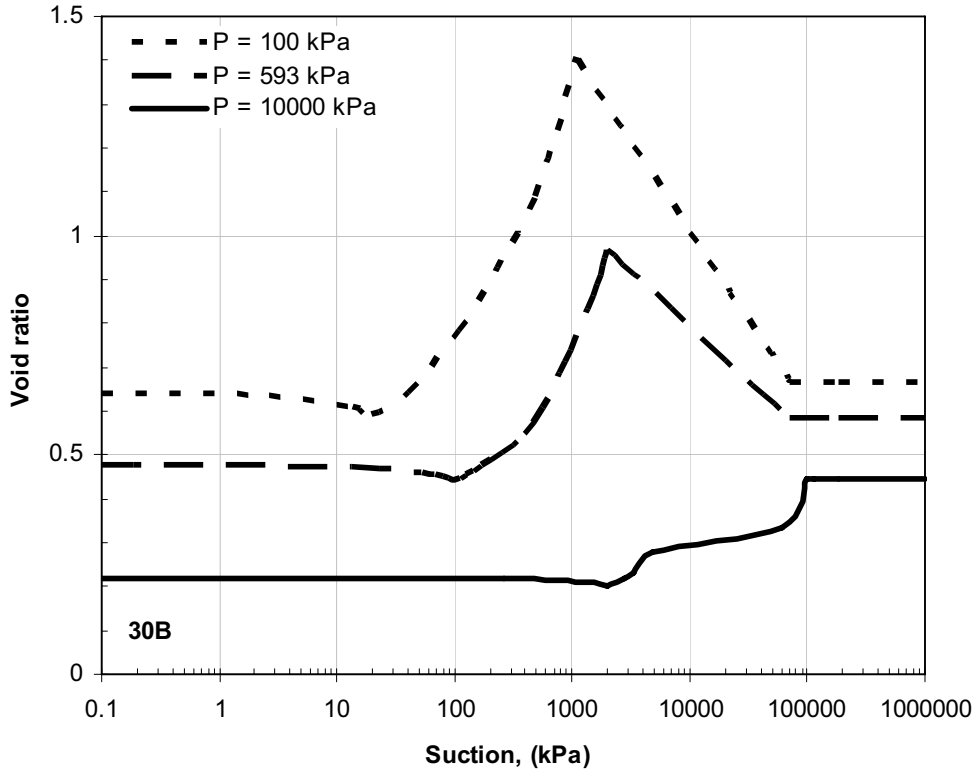

Figure 6.16 The model prediction of void ratio-log suction relationship at normal consolidated state under constant net stress condition, for 30B soil.

volume condition or constant void ratio cross-section of state surface (CSSS), the yield net stress (or the preconsolidation pressure) initially decreases as the suction increases (fourth interval), then increases after air-entry value (third interval). The yield net stress continues increasing as suction increases until reaching the maximum value at the beginning of the second interval, in which the yield net stress decreases again with increasing the suction. Finally the yield net stress reaches the net stress of the fully dry condition (first interval). After this value the yield net stress unchanged with increasing the suction. The typical CSSS curve consists of four intervals and can be represented by the curve of the intermediate constant density (e = 0.695 in Figure 6.17). In case of the low constant density (e = 1.00), the CSSS curve consist only of parts of the third and second intervals. While in case of high constant density (e = 0.486) the part of the second interval will not be present. Therefore the yield net stress has three intervals only (fourth, third and first intervals). It is worthy to mention that the CSSS curve is different from the loading collapse (LC) curve of Barcelona basic model, BBM (Alonso et al., 1990), even both of them represent the points of preconsolidation pressure for different suction values. First difference is that the LC curve represents originally the isotropic condition (but some times the 1D-compression tests were used to determine the BBM's parameters as in case of Alonso et al., 2005) while the CSSS curves represent the 1D-compression state. The second difference is the LC curve does not represent the constant volume condition which is the case in the CSSS curve. Figure (2.8) shows that as the suction increases the void ratios at preconsolidation stresses, which represent the LC curve, will increase. Generally, the LC curve has yield net stress higher than the CSSS curve in case of equal initial saturated density due to the lower density of LC with increasing the suction. However, the shape of the LC curve that established by Sheng et al. (2008a) is more similar to the predicted CSSS curve, even it has not the last two intervals (the second and first intervals).

As mentioned in section (6.1), to create the state surface, the loading path can be established either (*i*) by increasing the net stress (loading) under constant suction (Figure 6.15) or (*ii*) by reducing the suction (wetting) under constant net stress (Figure 6.16) or (*iii*) in case of increasing the suction (drying) with two positions; initially for saturated soil in the range of saturation zone (before the air-entry value) and other part in the specific range of high suction (in the second interval), as shown in Figure (6.18). The curve of drying state divides into two parts due to that the drying curve does not represent the yield state after passing the air-entry value. If the initially unsaturated loose soil (high void ratio) is dried with suction in the range of interval (with or without increasing the net stress) the other part of curve of drying state will appear. Figure (6.18) shows the comparison between the two

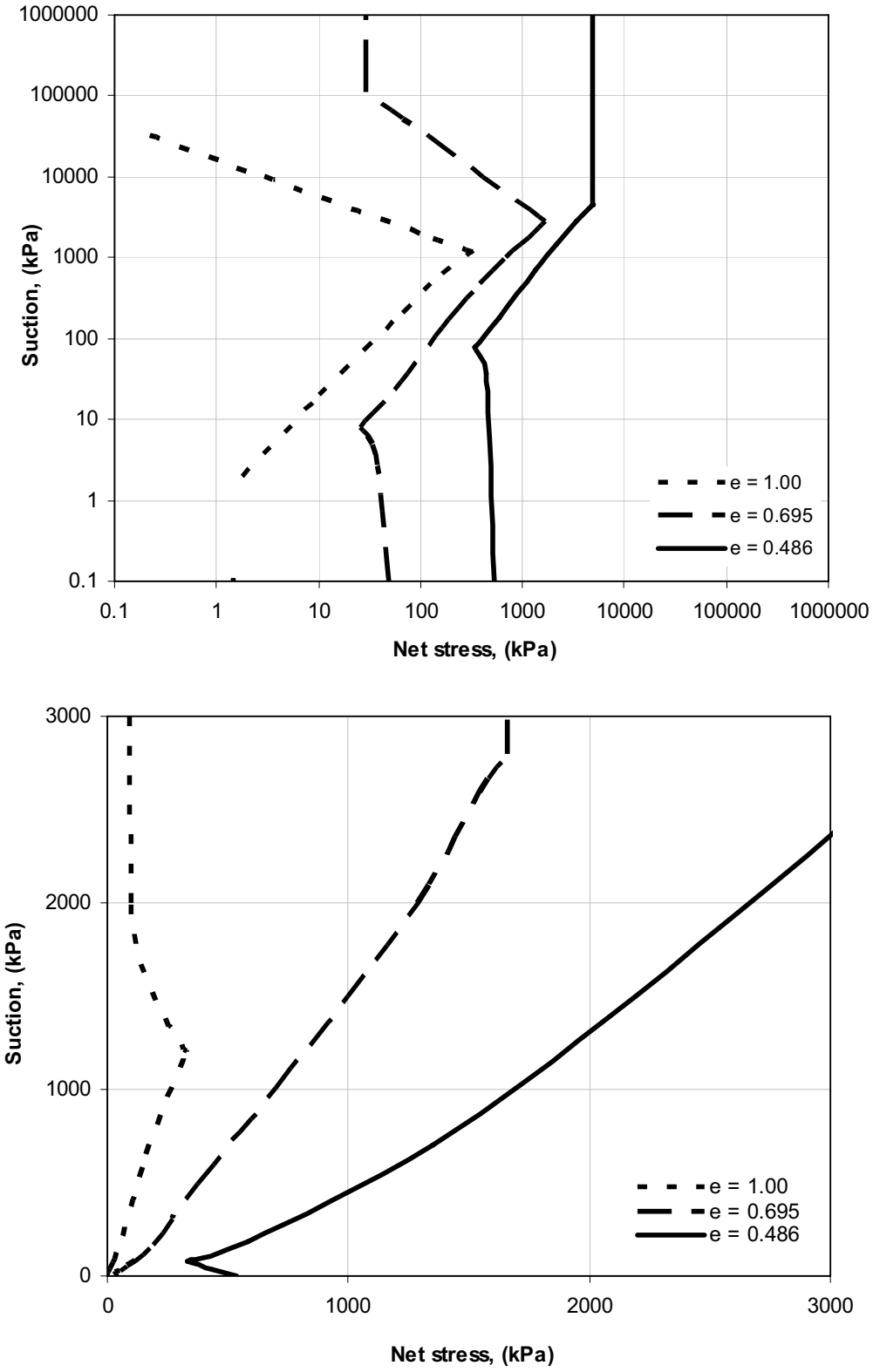

Figure 6.17 The model prediction of curves of constant void ratio cross-section of state surface (CSSS curves) in net stress-suction space for 30B soil. (a) in log-log scale and (b) in the normal scale.

possible cases of predicted yield state; wetting the unsaturated soil (in case of *i* and *ii* loading paths) under constant net stress (Wetting under P) and increase the suction or drying the soil (in case of *iii* loading path) under constant net stress (Drying under P). Bishop's Equation (2.2) is used to predict the initial part of drying curve under constant net stress (before the air-entry value). While other part of drying condition, the curve is established using the equation of the second interval (Equation 6.3) and the main drying path (initially it starts with scanning path then follows the drying path). Both wetting and drying curves before the air-entry value are almost following the same path but the drying curve will extend for more suction value. This behavior attributes to the difference in the value of air-entry value between drying and wetting paths. Moreover the initial part of drying curve (before the air-entry value) is slightly higher than the wetting curve specifically in the high suction value. This variation decreases as the value of constant net stress increases.

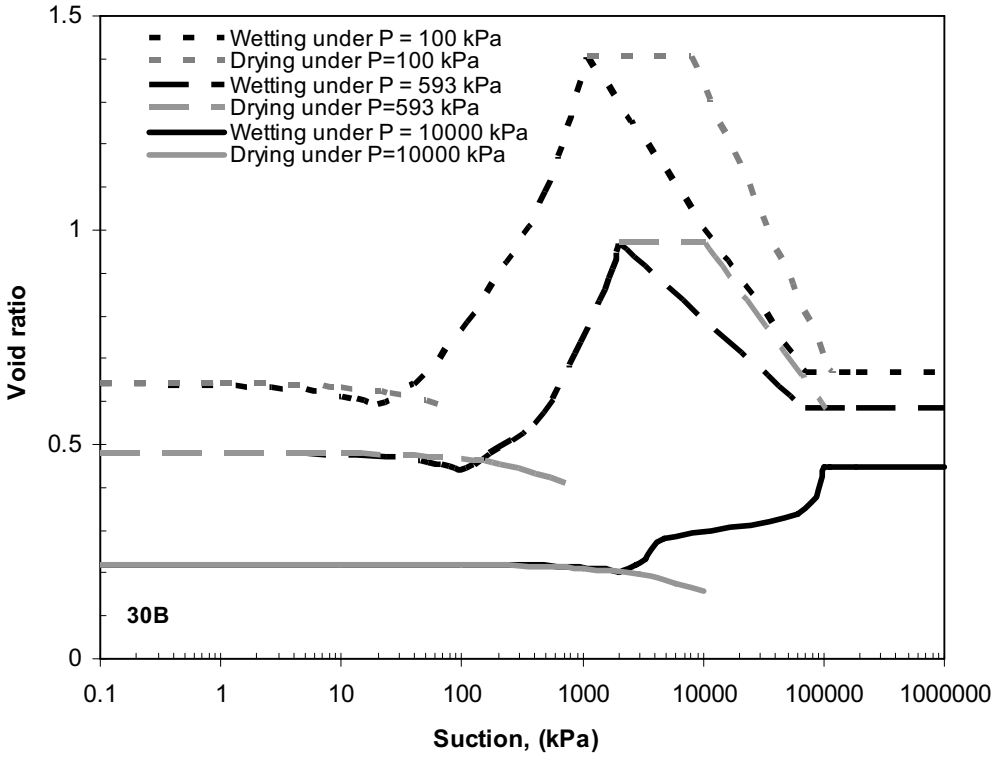

Figure 6.18 Comparison between the model predictions of void ratio-log suction relationships at normal consolidated state for 30B soil due to two different cases: wetting conditions for *i* and *ii* loading paths (Wetting under P) and drying condition for *iii* loading path (Drying under P).

6.6 Verification of model

The verification of the new model and its hypotheses are examined by investigating the relationship between the predicted and the experimental results of different controlled-suction one-dimensional compression tests.

6.6.1 Constant degree of saturation test

This type of tests considers a direct verification of 1st hypothesis. Figure (6.15), shows the result of constant degree of saturation tests (S_r = 0.58 and 0.68) for initially loose 30B soil. Figure (6.19) represents the experimental volumetric yielding or NCL's, Figure (5.4), and the predicted NCL's (using Equation 6.4) under constant degree of saturation condition. The figure shows that the points at normal consolidated state are located on straight lines and have a good fitting with the predicted lines. The predicted lines depend on the saturated NCL (from oedometer test) and S_{rc} = 0.85 (from SWCC) by using Eq. (6.4).

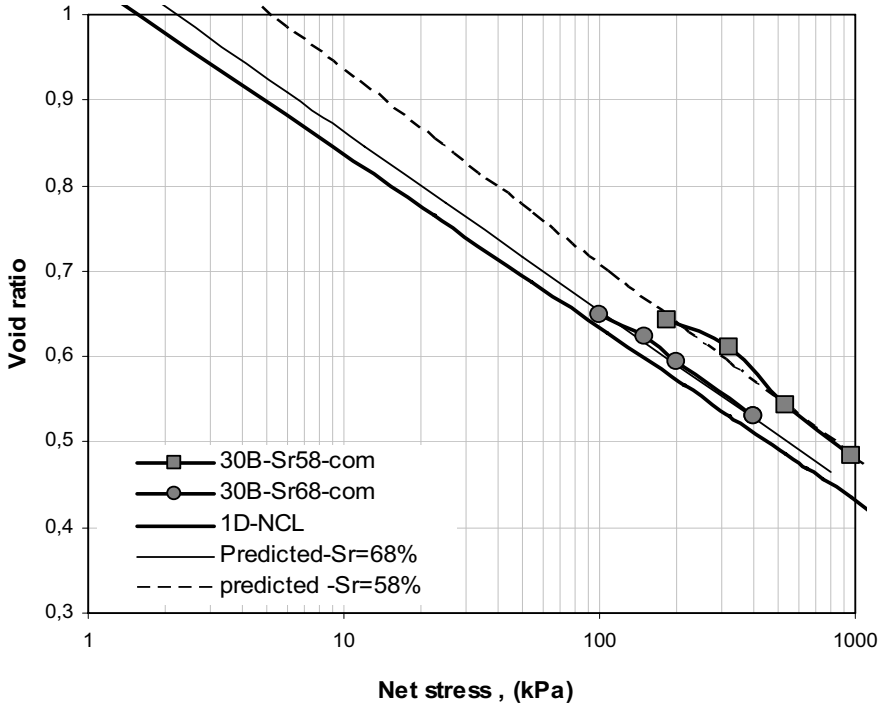

Figure 6.19 Experimental and model prediction of NCL's under constant degrees of saturation state of 0.58 and 0.68 for 30B soil.

6.6.2 Constant net stress tests

6.6.2.1 Constant net stress test with increasing the suction (drying) for initially slurry condition

In this type of tests the initially slurry specimens were loaded under saturated condition then were dried (by increasing the suction) under a specific net stress. The normal consolidated or yield state in these tests starts from the beginning of the test until reaching the air-entry value (the loading stage under saturation condition and the first part of the drying path), then the soil behavior changes from normal consolidated state to over consolidated state as the suction increases. The volume change of the yield state can calculate by using the effective stress concept (Equation 2.2.) with χ = 1, as shown in Figures (5.11 and 5.16) for 30B and 100B soils. In other words, the yield state in this type of tests represents the saturated NCL i. e., the fifth interval.

6.6.2.2 Constant net stress test with decreasing the suction-wetting for initially loose condition (collapse test)

The three tests of the initially loose 30B specimens (30B-P0.25-w-Lo, 30B-P0.6-w-Lo, and 30B-P1.0-w-Lo) were tested under wetting (collapse) condition as shown in Figures (5.19-5.22). Figures (6.20-6.23) show the comparison between the experimental and model predictions of void ratio, gravimetric water content, and degree of saturation versus net stress and suction relationship of all constant net stress tests condition with wetting path-collapse test-for 30B soil. Generally, the model predictions show a good agreement with the experimental data. Figure (6.23d) shows that the degree of saturation-suction relationship (SWCC) shifts upright as the net stress during wetting increases. Moreover, the model predictions show that the three different stages during the wetting (collapse) process can be attributed to the degree of the saturation-gravimetric water content- suction relationship as shown in Figure (6.24). The first stage occurs when the state of the specimen before wetting is over consolidated state. The second stage relates to state surface. While the behavior during the third stage is a composition between the effect of the net stress and suction when the soil reaching the saturation zone, in which the water content increases slightly when the suction reduces rapidly, Figure (6.24d). The behavior of the first stage is due to either when the state of the soil before wetting and during this stage is over consolidated (as the case of 1000 kPa constant net stress). Or when the state of the soil before wetting is normal consolidated (yield) but located in the first or second interval of state surface (as the case of 250 kPa and 600 kPa constant net stress). When the suction decreases the water content and the degree of saturation increase (wetting), the specimen will not swell, to follow the state surface, but follows the over consolidated state until reaching the state surface in the third interval. There is also

another possibility for this case when the wetting occurs under high net stress in which the second interval disappears. The first interval of state surface (the horizontal surface) will cover wide range of suction. Moreover, the soil state of the third stage represents unloading path (not yield). The effective stress (Equation 2.2) with $\chi = 1$ can apply for the third stage (saturation zone). The effective stress will reduce as a result of decreasing the suction under constant net stress condition. This behavior explains why the final void ratios, after the wetting process, locate a little bit lower than the NCL. However, it is difficult practically to measure with this decrease and then increase in the void ratio during the collapse test due to fast wetting by adding water directly to specimen (in case of one step wetting) or when the suction steps not cover the third stages of collapse (in case of multi-steps wetting). The 30B-P0.25-w-Lo test exhibited a rapid decrease in volume before the three stages of collapse. Regarding to the model predictions, the specimen showed low volume change with relative to the volumetric yielding before wetting. Afterward, as the suction reduced the volume decreased rabidly to the corrected position before following the three stages of collapse. The low volume change may be possible to happen in the low range of net stress as in case of 250 kPa due to rearrangement of particles of loose state specimen. Generally, any wetting collapse test may pass all or parts of the three stages of collapse as shown in Figure (6.24). The soil will pass all the three stages of collapse when the condition of the specimen is: ether (i) in the first stage (normal or over consolidated state), or (ii) over consolidated state regardless of stages). While the soil will pass one or more of the three stages of collapse when the conditions of specimen before wetting are: (i) normally consolidated state, and (ii) within the second or third stage.

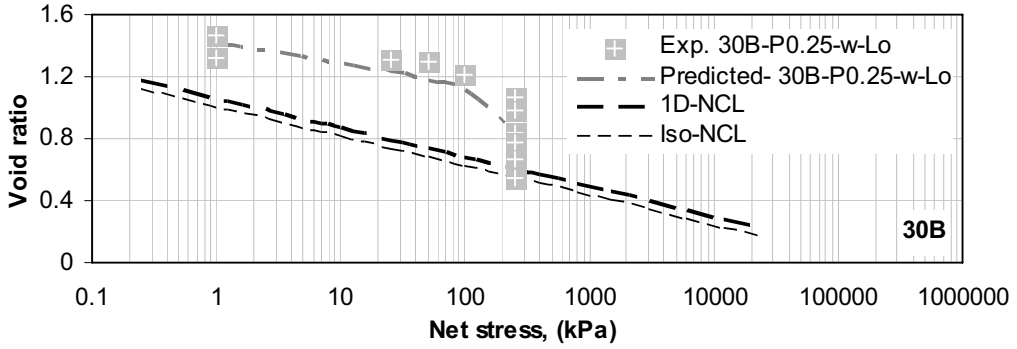

a

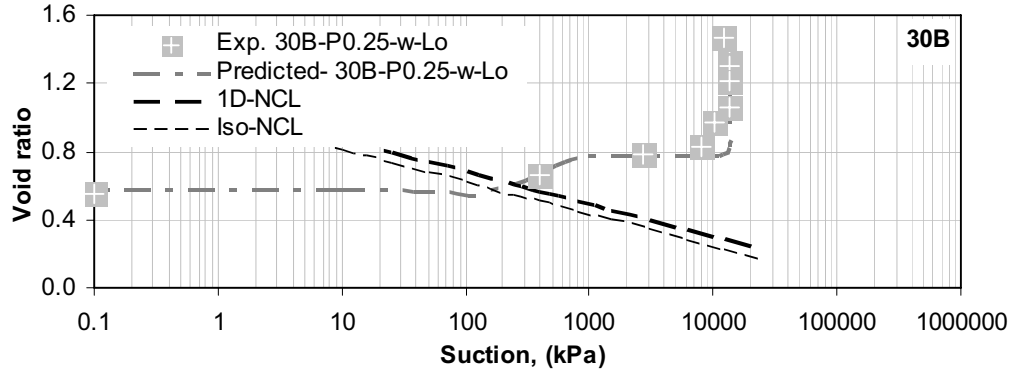

b

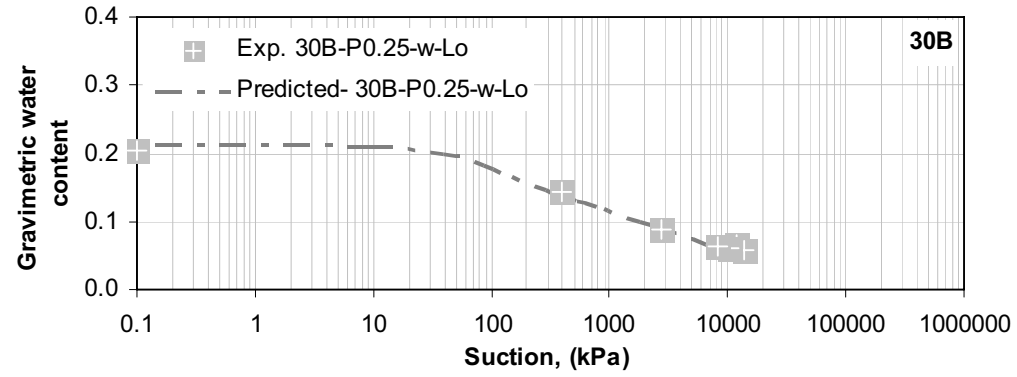

c

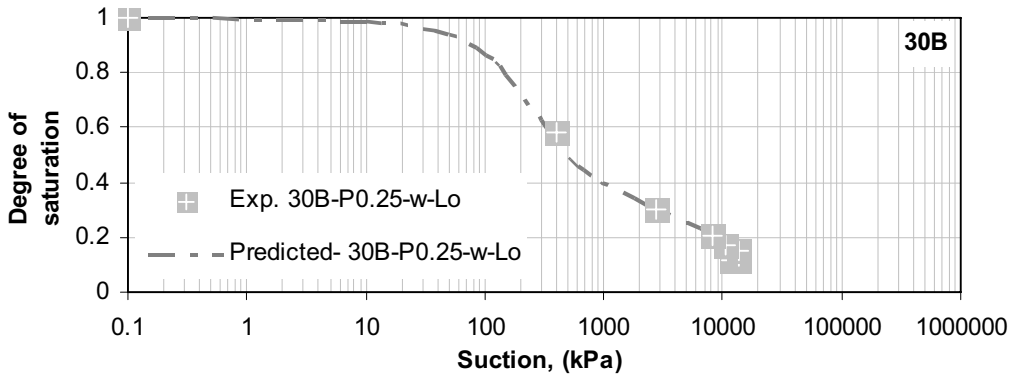

d

Figure 6.20 Experimental and model predictions of constant net stress = 250 kPa condition with decreasing the suction (wetting path)-collapse test- for 30B soil.

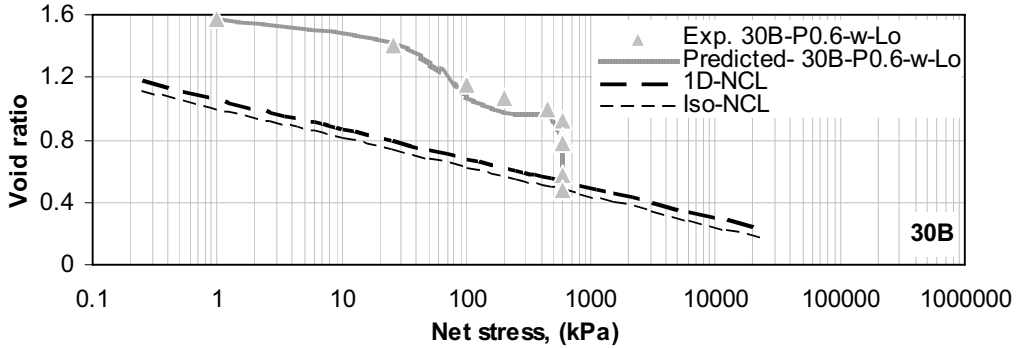

a

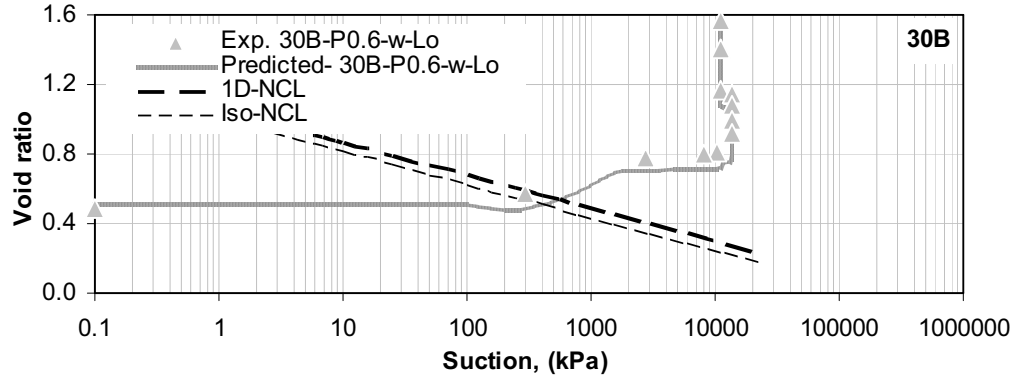

b

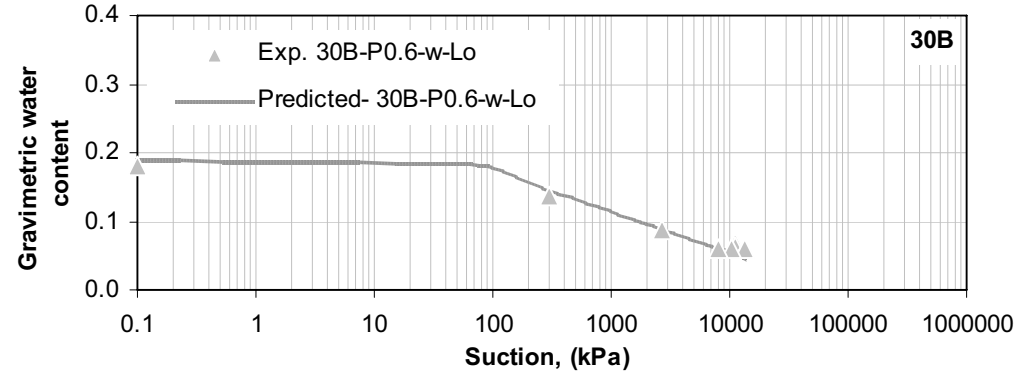

c

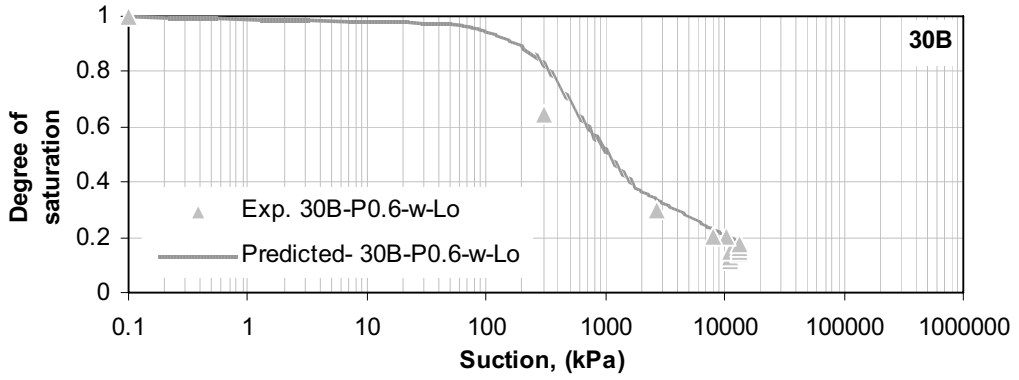

d

Figure 6.21 Experimental and model predictions of constant net stress = 600 kPa condition with decreasing the suction (wetting path)-collapse test- for 30B soil.

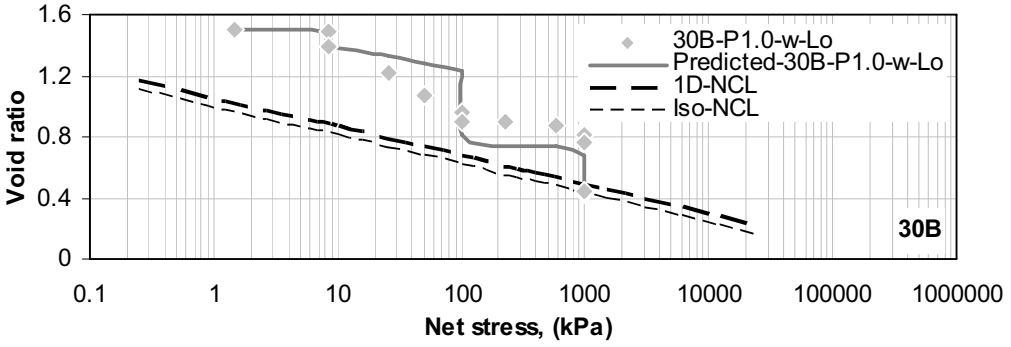

a

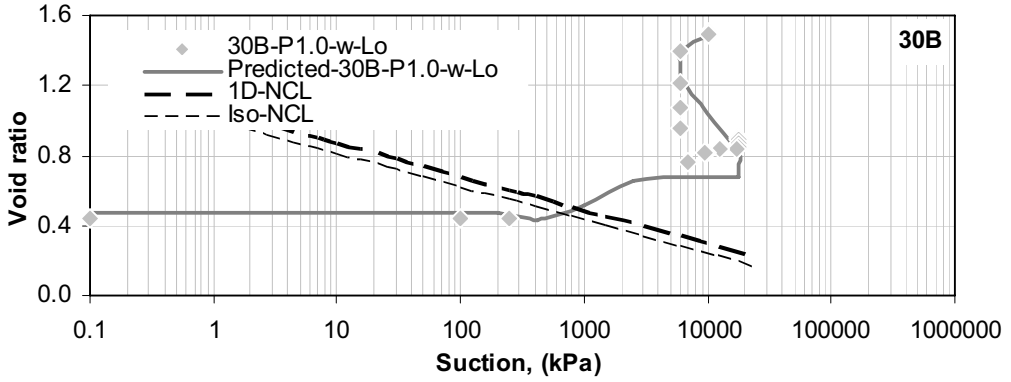

b

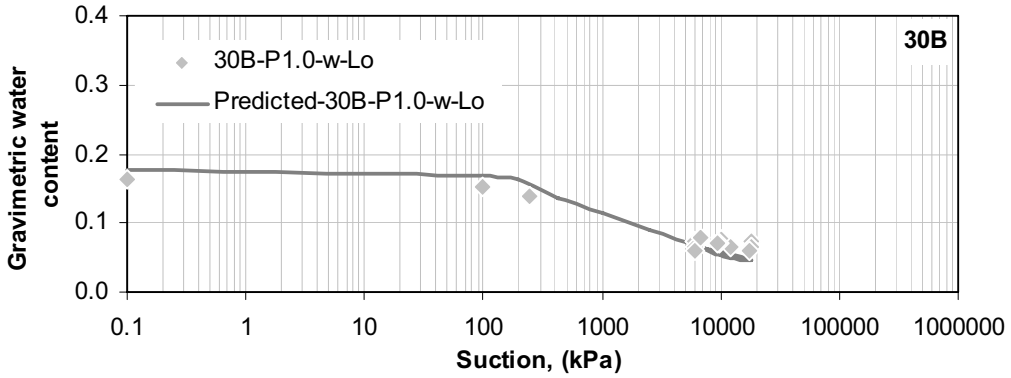

c

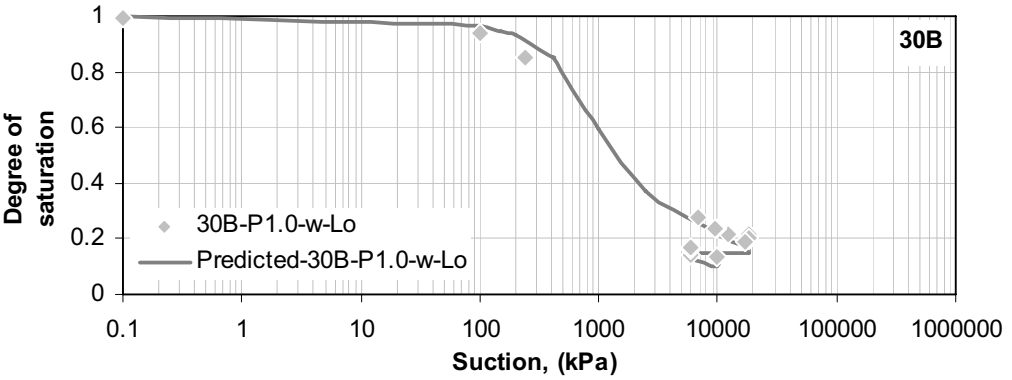

d

Figure 6.22 Experimental and model predictions of constant net stress = 1000 kPa condition with decreasing the suction (wetting path)-collapse test- for 30B soil.

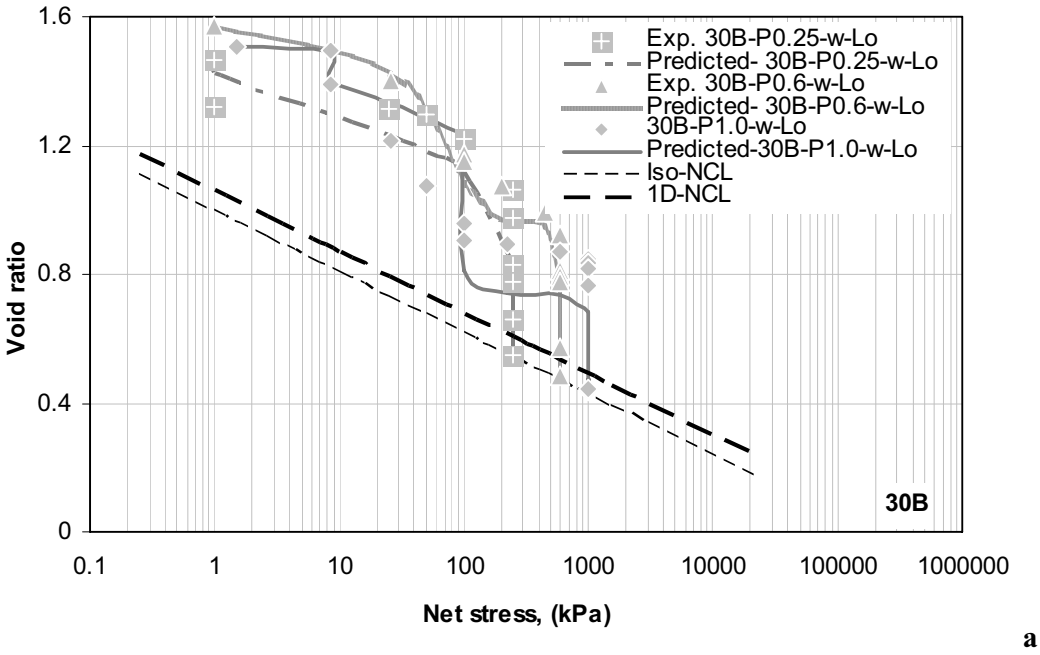

a

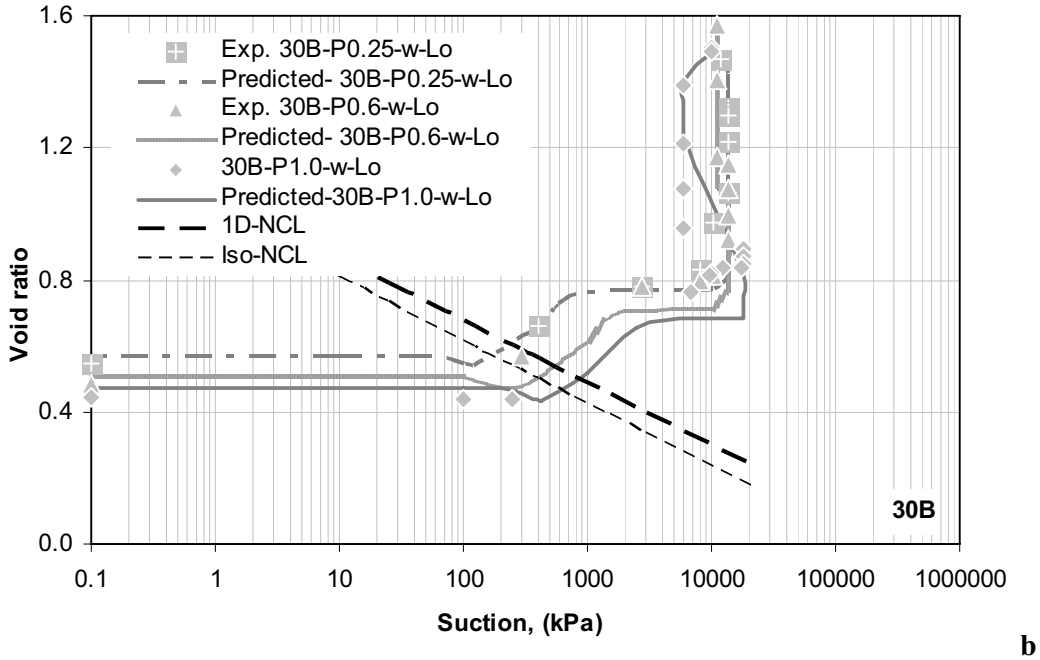

b

Figure 6.23-1 Experimental and model predictions of all constant net stress tests condition with wetting path-collapse test-for 30B soil.

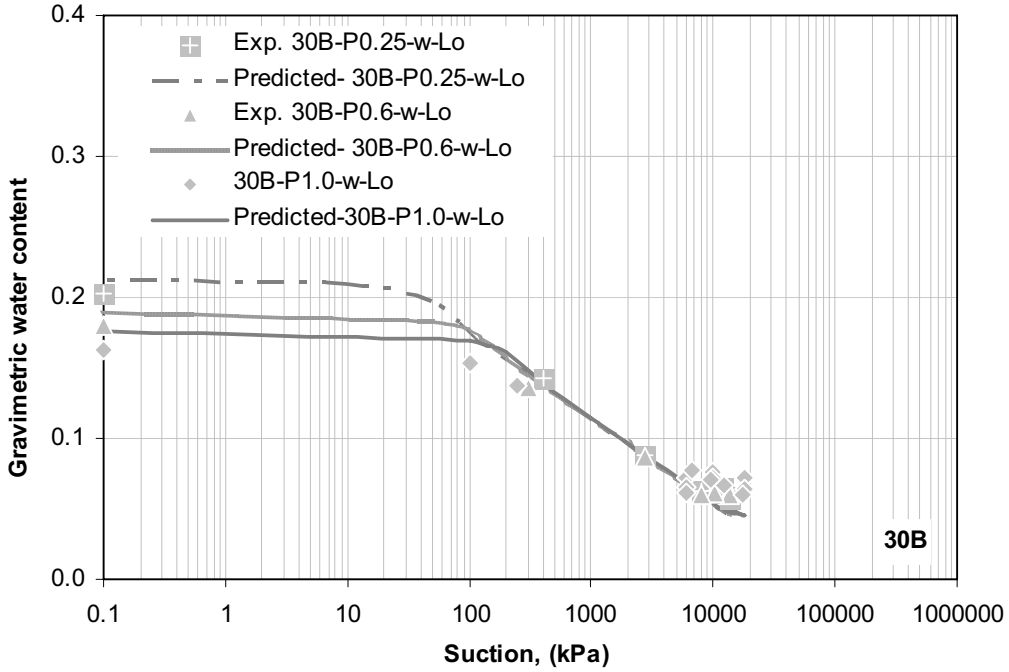

c

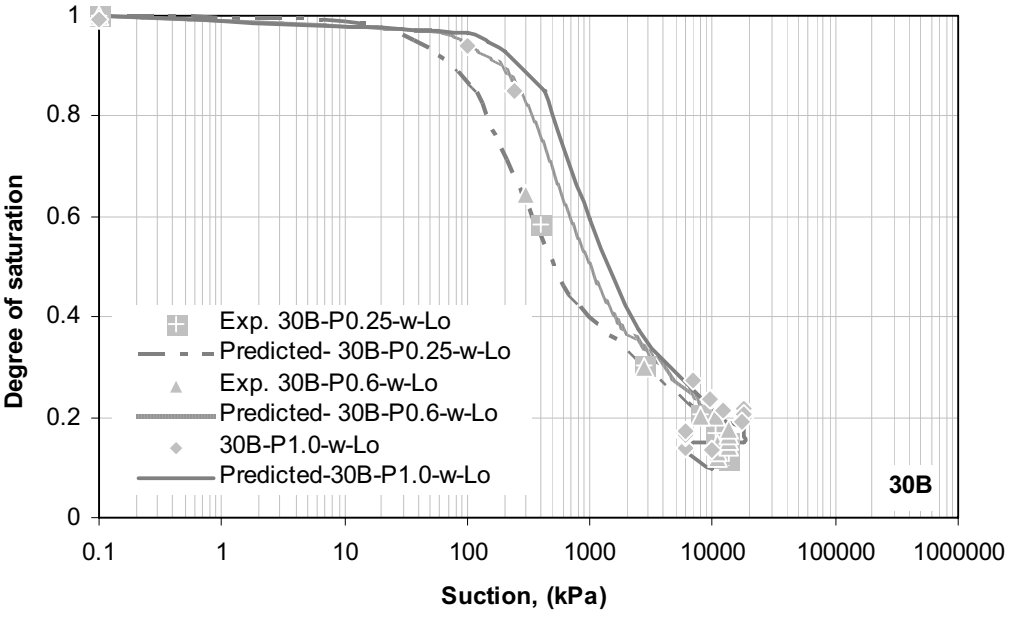

d

Figure 6.23-2 Experimental and model predictions of all constant net stress tests condition with wetting path-collapse test-for 30B soil.

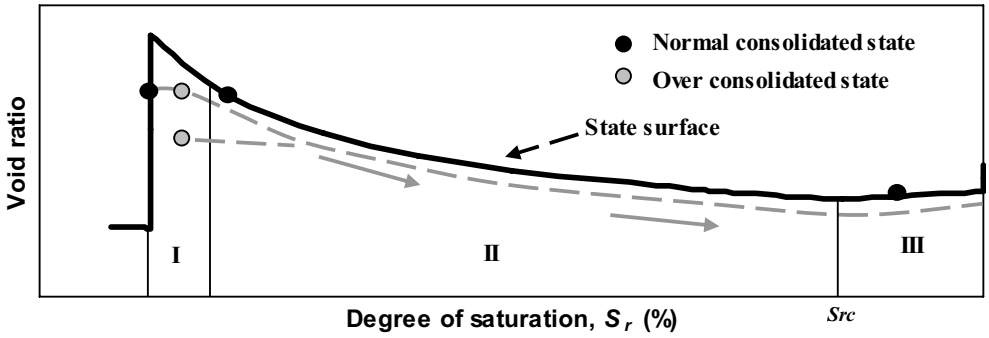

a

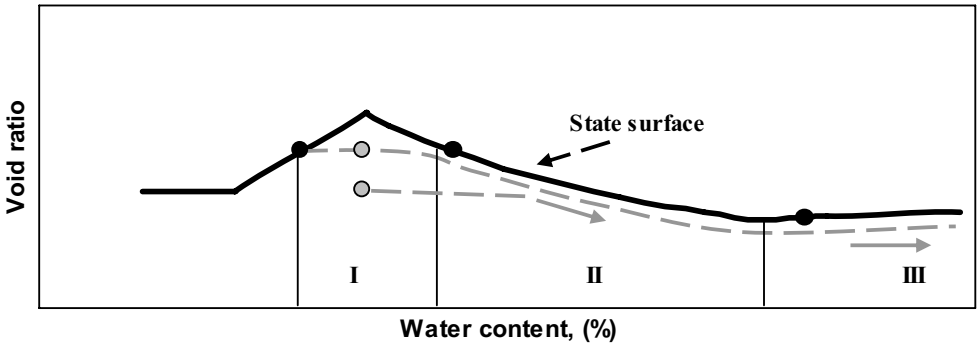

b

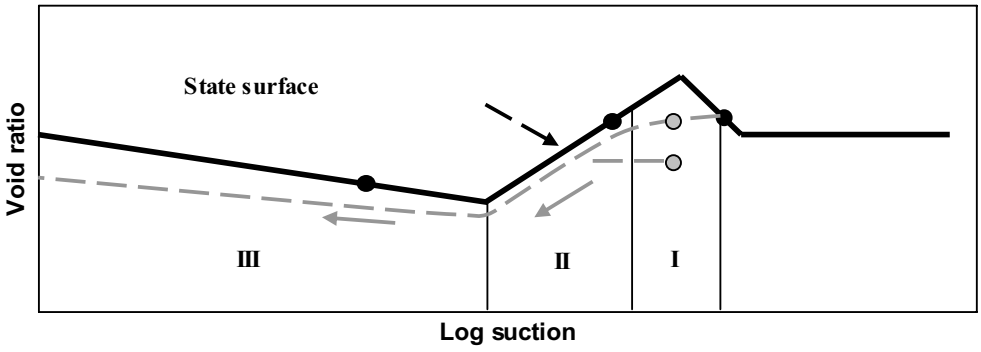

c

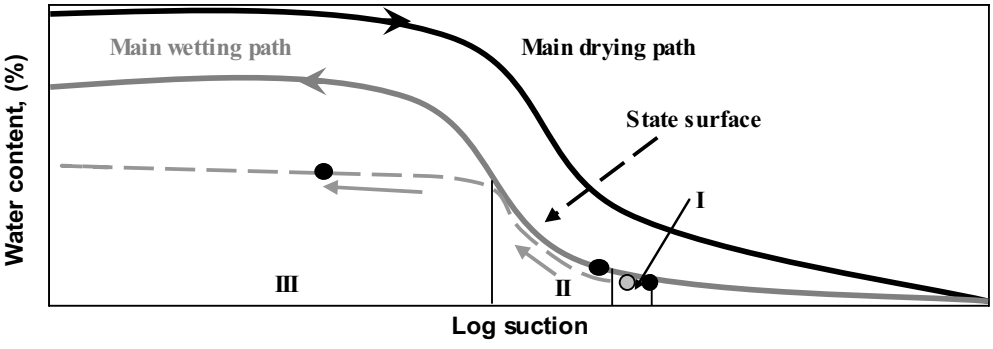

d

Figure 6.24 Proposed three stages of collapse behavior during wetting and the possible conditions of specimens before wetting according to the new proposed model.

6.6.3 Constant suction test

The initially slurry specimens follow the isotropic NCL with increasing the suction before the air-entry value. When the net stress increases under constant suction condition the degree of saturation will increase due to the compression. If the degree of the saturation is higher than the critical degree of saturation the complete path of the volume change will follow the yield state according to the effective stress concept (Equation 2.2) with $\chi = 1$. When the suction passes the air-entry value the experimental results show that when the degree of the saturation reached to value equal to $(S_{rc})^{1/R}$ the volume almost will remain constant. Before this value of degree of saturation the volume change in the drying path is assumed follows the model used the effective stress concept (Equation 2.2) with $\chi = S_r$, while the volume remains constant for lower degree of saturation value. The value of $(S_{rc})^{1/R}$ is 0.72 for 30B soil and 0.78 for 100B soil. According to the above concepts, the initially slurry specimens under constant suction condition can be predicted, as in Figures (6.25-6.32) for 30B soil and Figure (6.38) for 100B soil. The experimental and model predictions of the initially loose specimens under constant suction condition are presented in Figure (6.33-6.37) for 30B soil and Figure (6.39) for 100B soil. Generally, the prediction results show a good agreement with the experimental data.

Figures (6.33 and 6.34) show that the predicted voids ratios after wetting are higher than the experimental voids ratios. These differences are probably due to the one-step wetting that causes extra energy as result of high falling of piston upon wetting. The other reason for these differences can be related to that the initially loose state is not completely homogeneous which makes large voids in the soil structure that leads to high settlement during wetting.

The model predictions of some initially loose state specimens: 30B-S10-Lo, 30B-S39-Lo, and 100B-S4.3-Lo as shown in Figures (6.36, 6.37, and 6.39) show that the soil state during compression under the constant suction condition was initially over consolidated then reaches to normal consolidated or yield state but in the second interval (constant degree of saturation state as Equation 6.2). Afterwards the tests followed the yield state regarding to third, fourth, and fifth intervals (Equations 6.4 and 6.5).

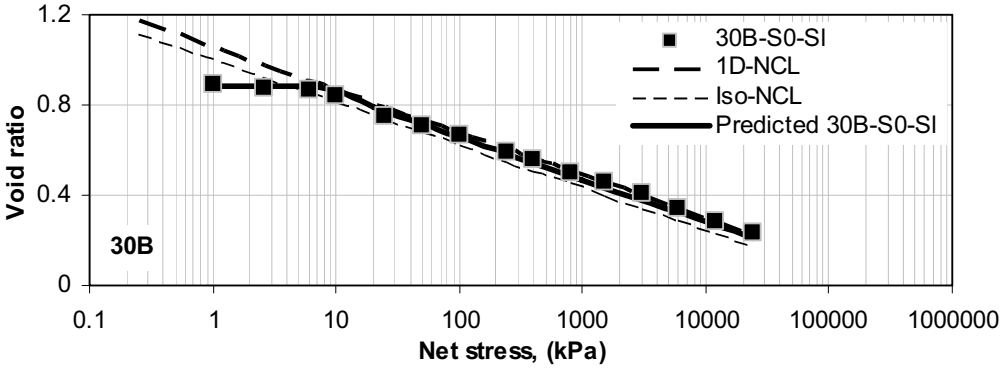

a

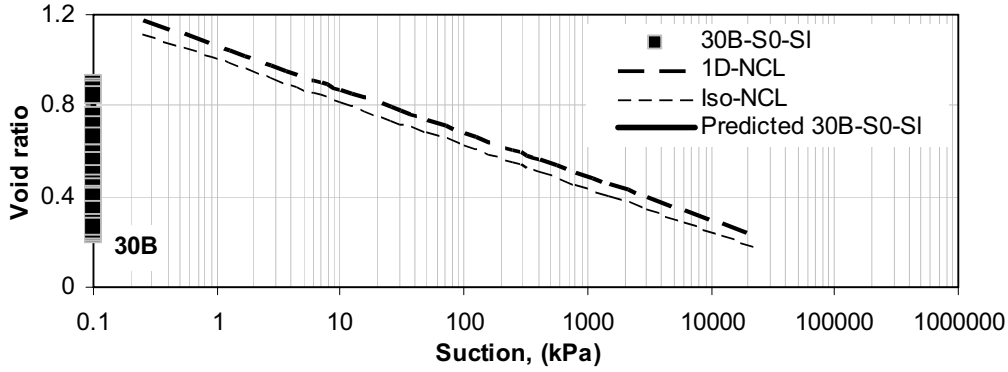

b

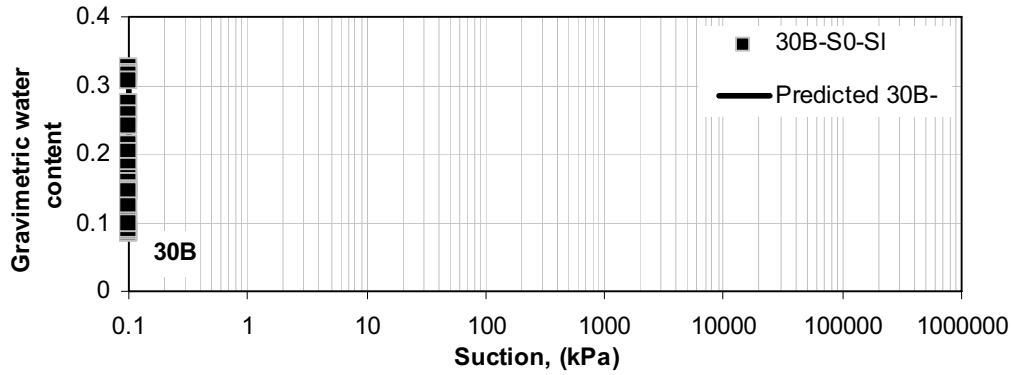

c

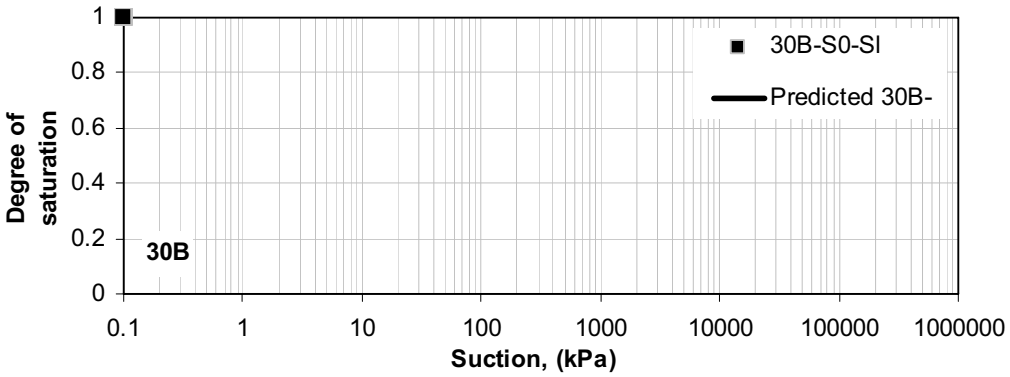

d

Figure 6.25 Experimental and model predictions of constant suction = 0 kPa condition of initially slurry specimen for 30B soil.

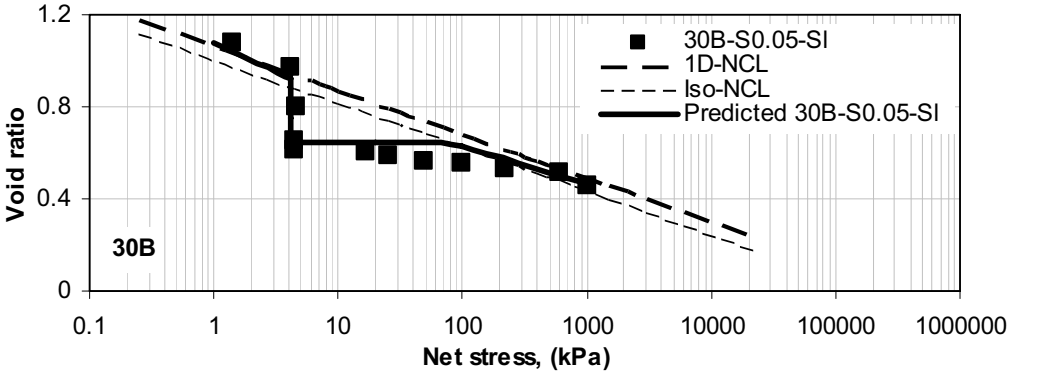

a

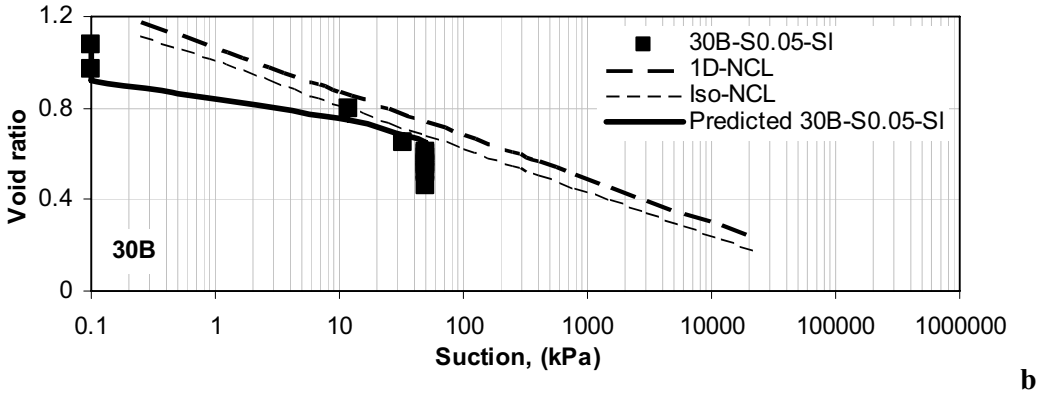

b

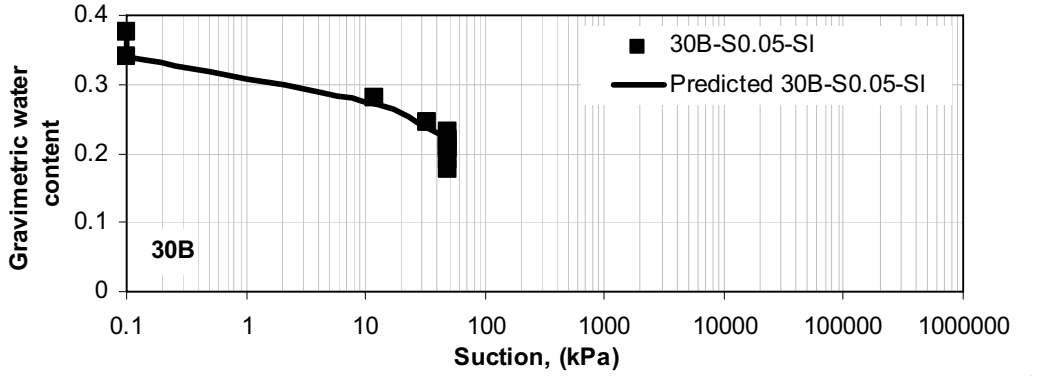

c

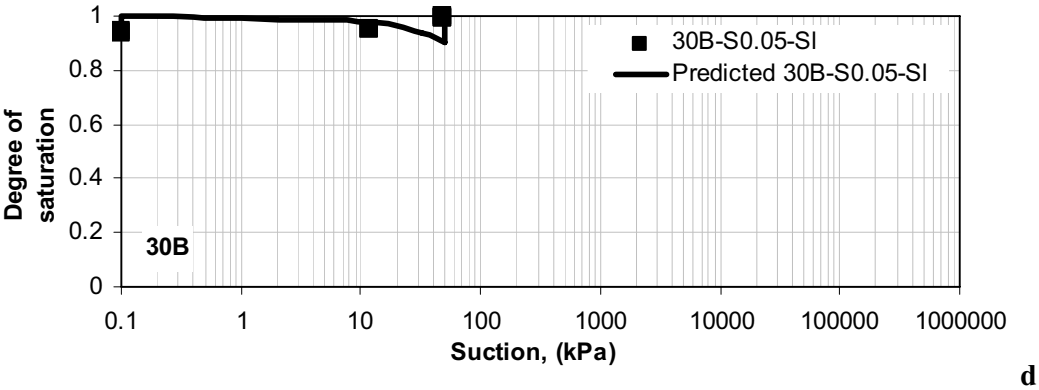

d

Figure 6.26 Experimental and model predictions of constant suction = 50 kPa condition of initially slurry specimen for 30B soil.

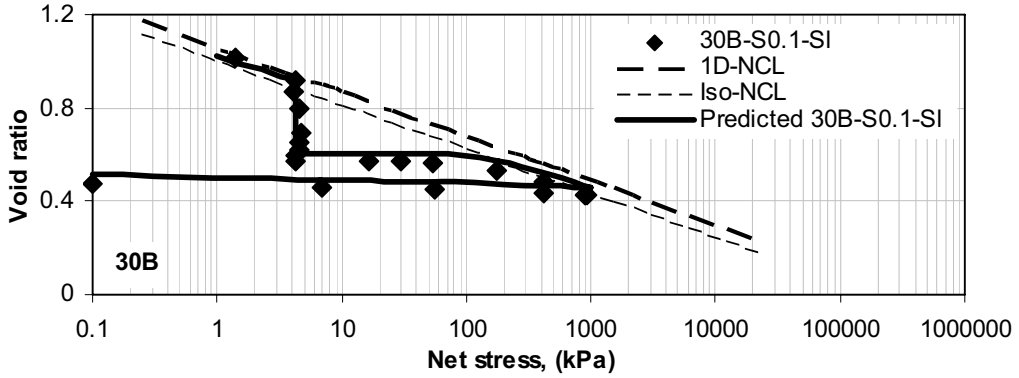

a

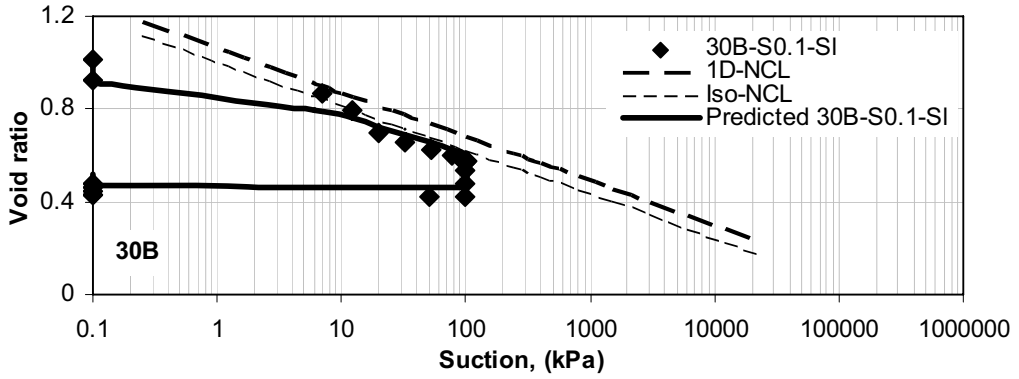

b

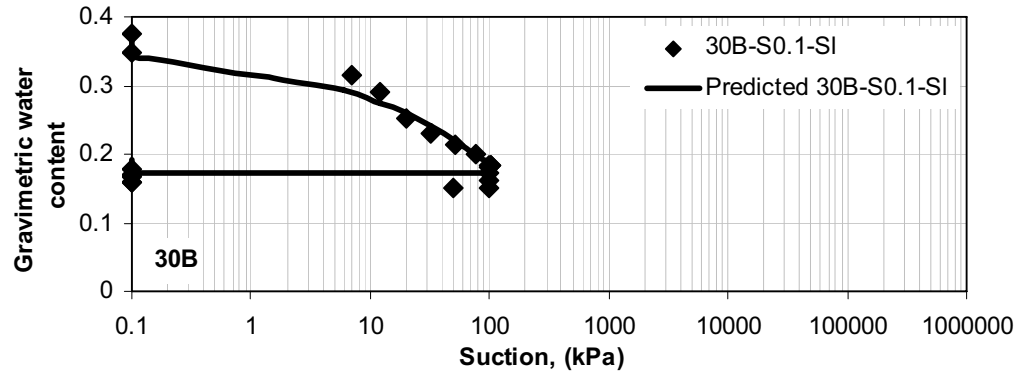

c

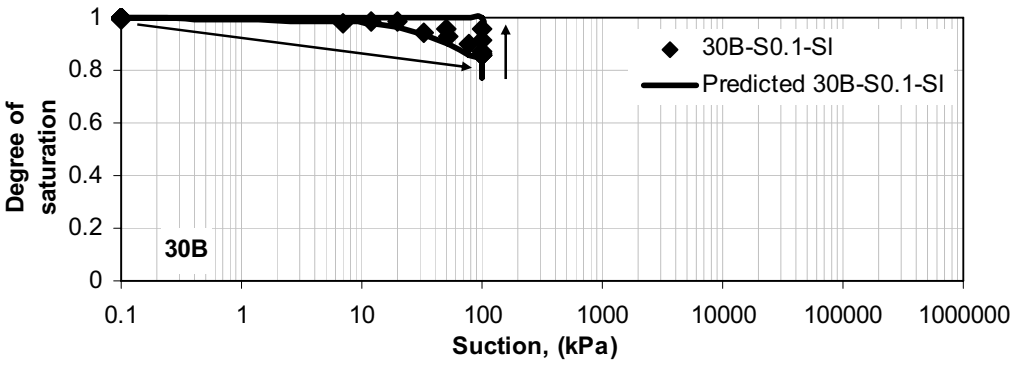

d

Figure 6.27 Experimental and model predictions of constant suction = 100 kPa condition of initially slurry specimen for 30B soil.

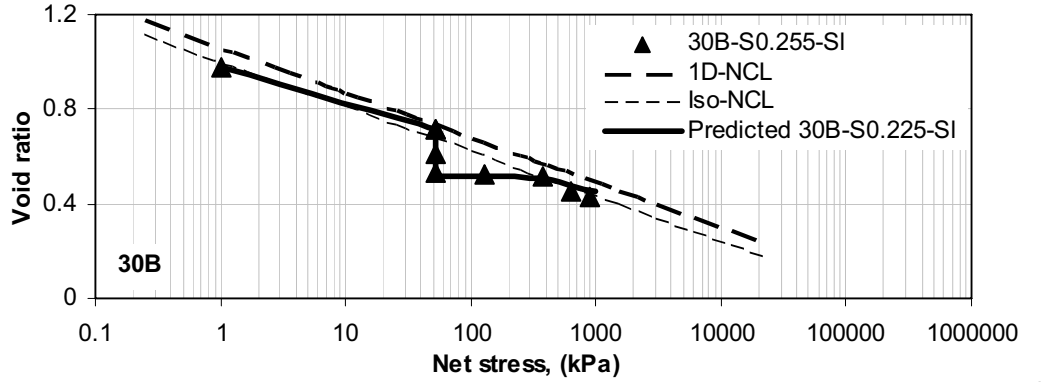

a

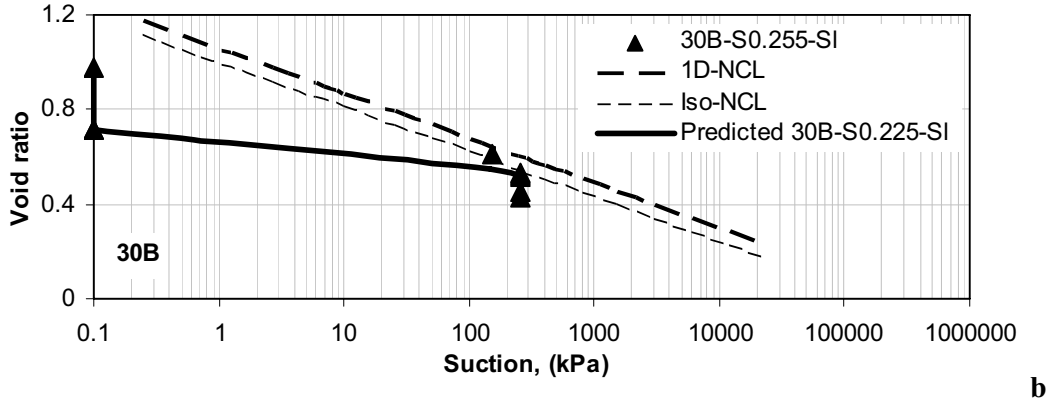

b

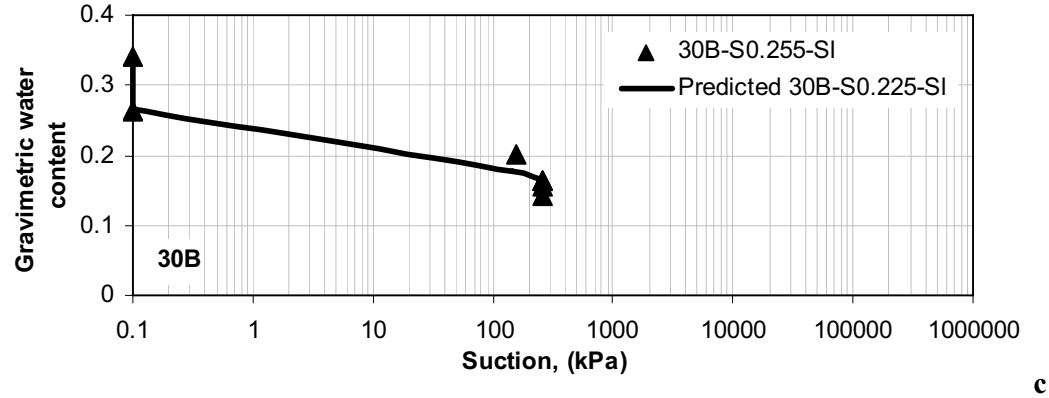

c

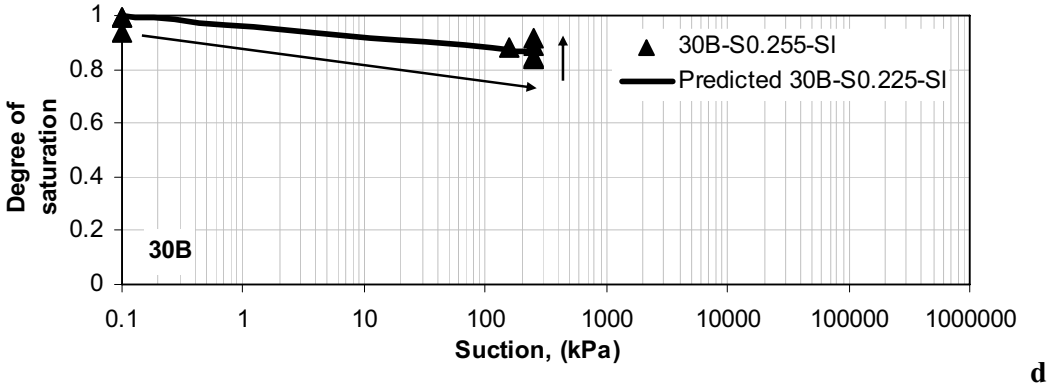

d

Figure 6.28 Experimental and model predictions of constant suction = 255 kPa condition of initially slurry specimen for 30B soil.

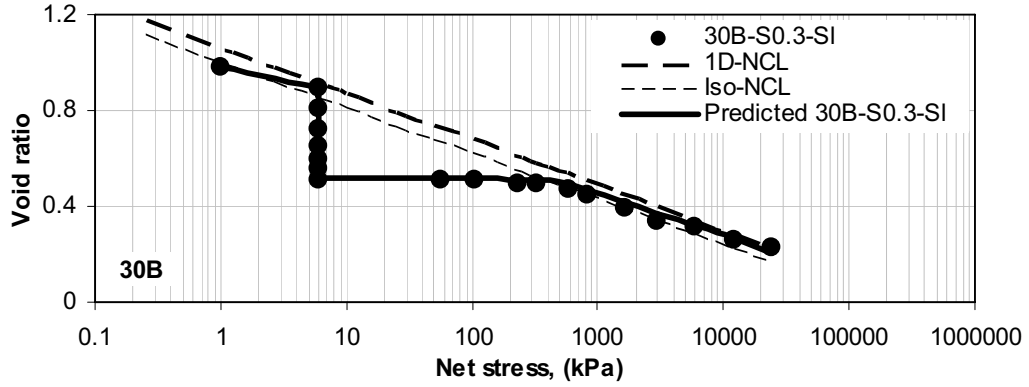

a

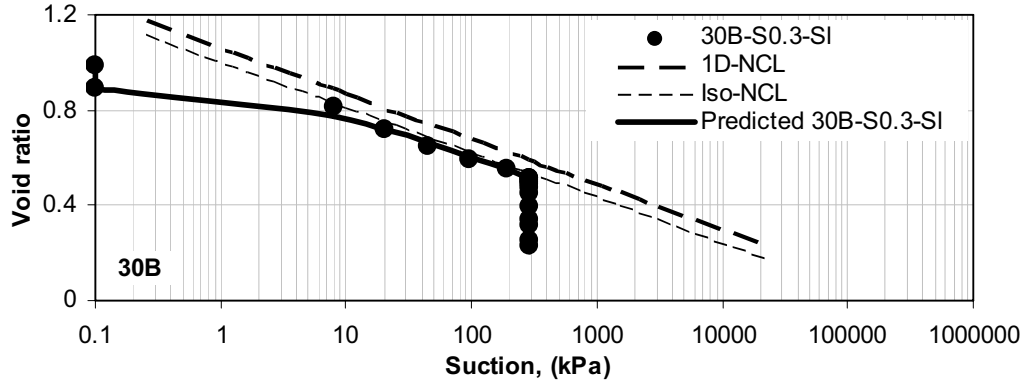

b

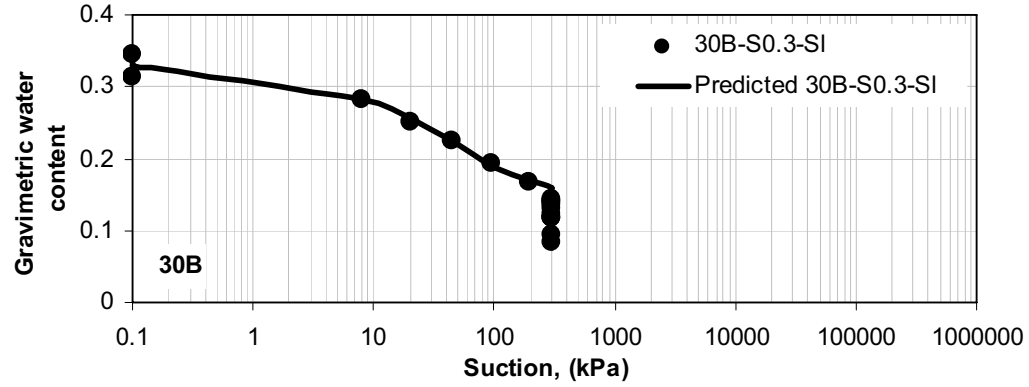

c

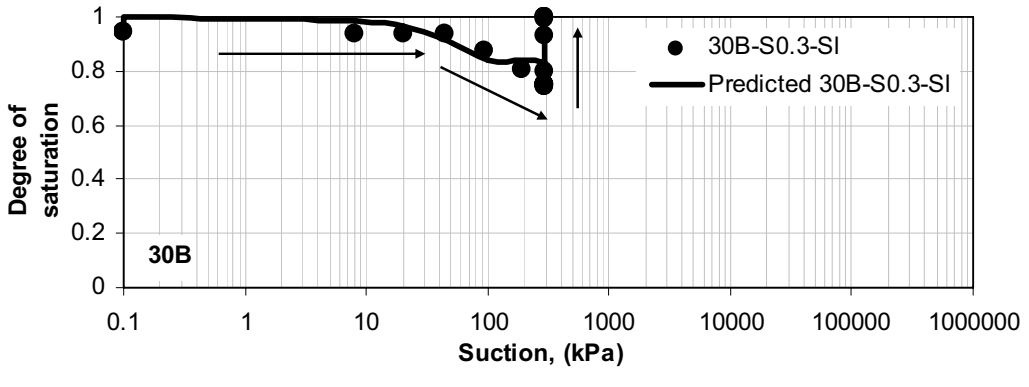

d

Figure 6.29 Experimental and model predictions of constant suction = 300 kPa condition of initially slurry specimen for 30B soil.

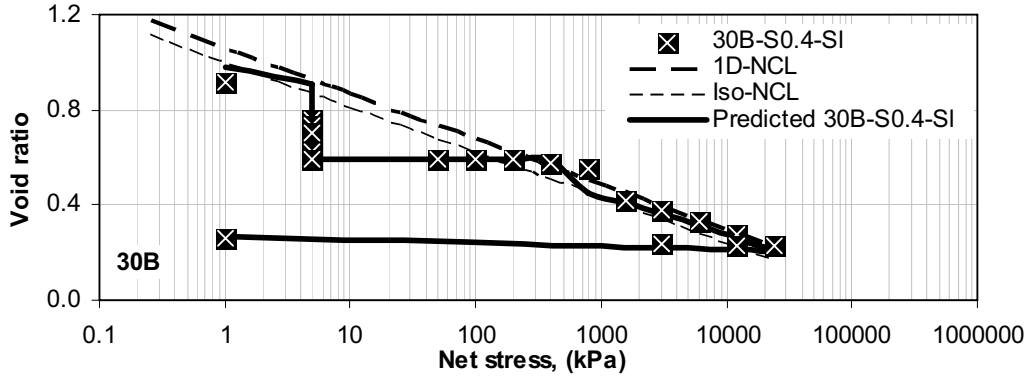

a

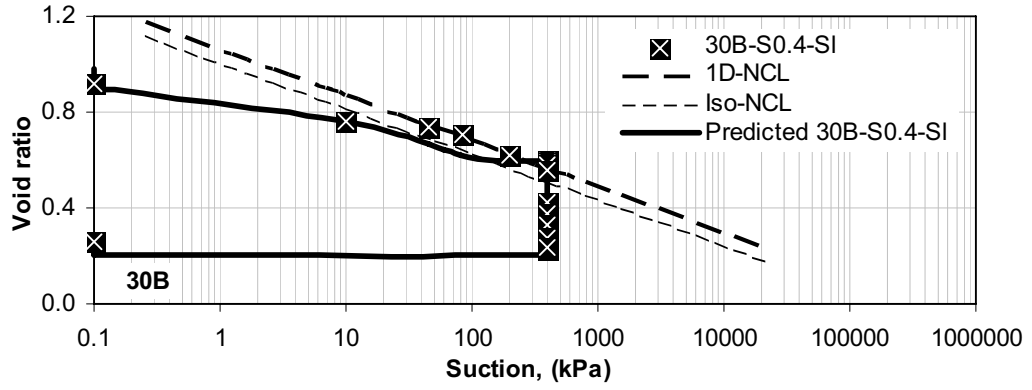

b

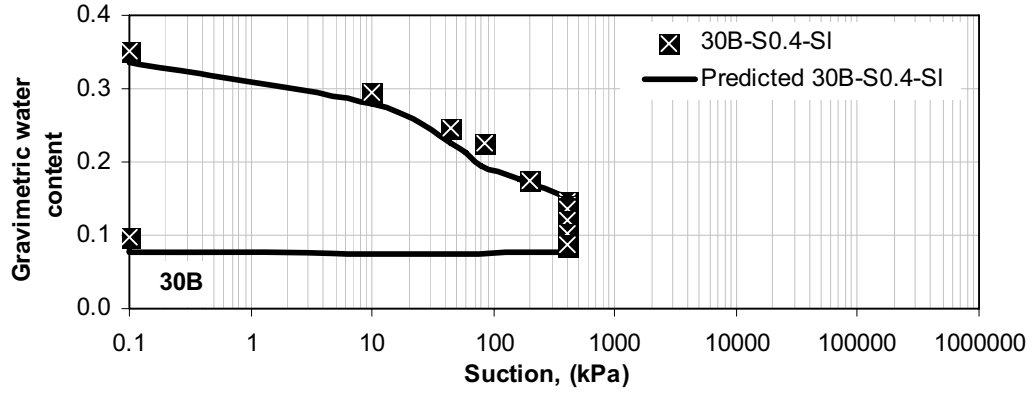

c

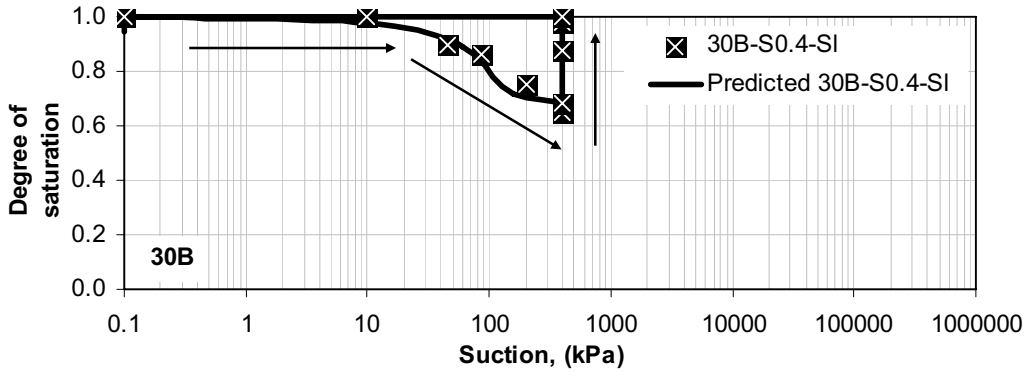

d

Figure 6.30 Experimental and model predictions of constant suction = 400 kPa condition of initially slurry specimen for 30B soil.

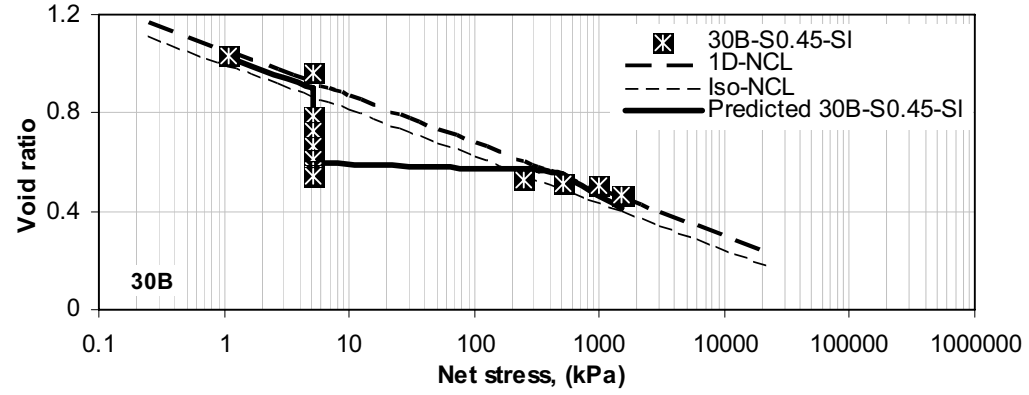

a

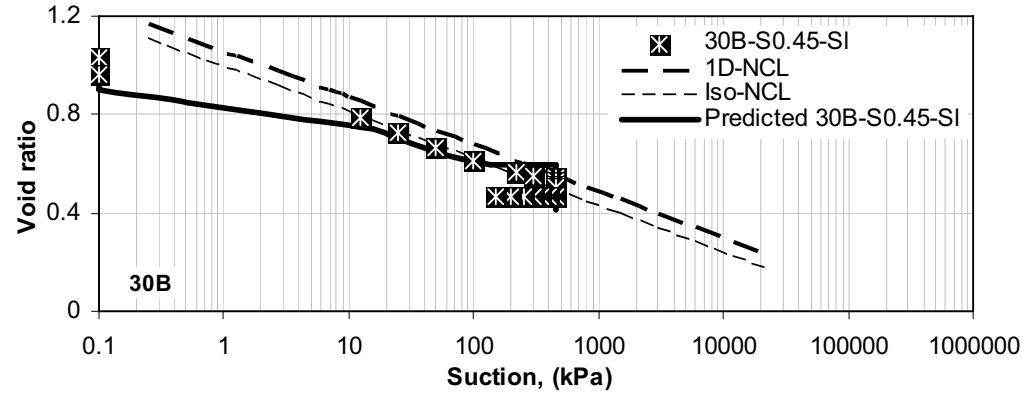

b

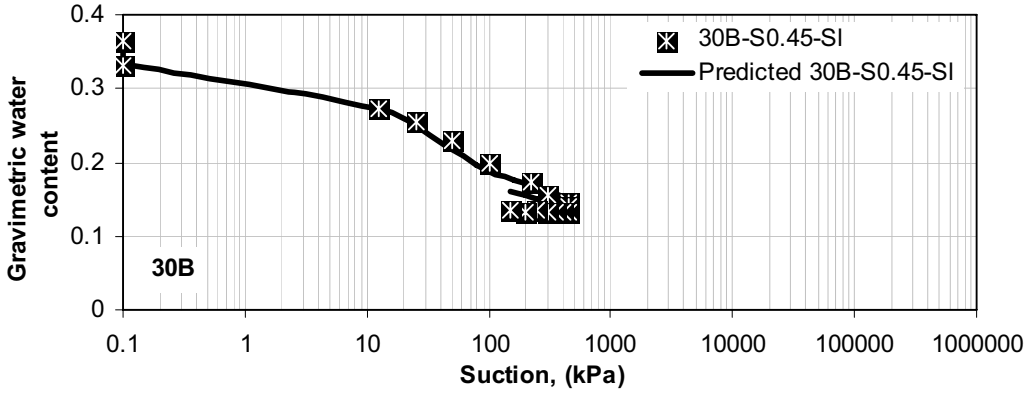

c

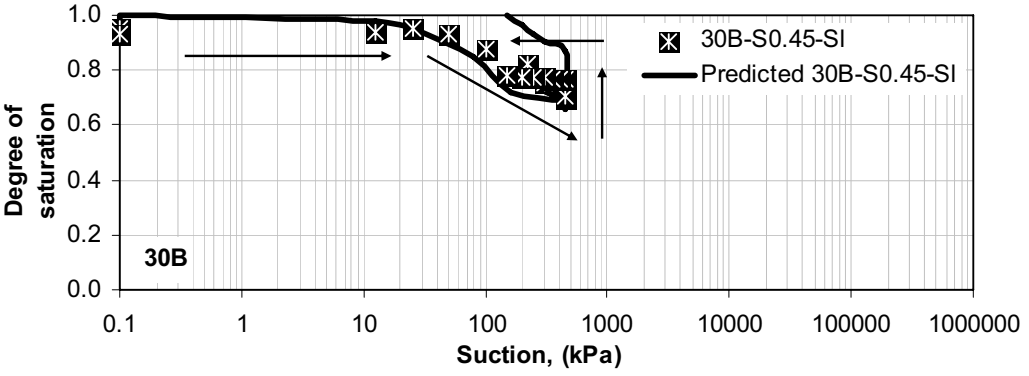

d

Figure 6.31 Experimental and model predictions of constant suction = 450 kPa condition of initially slurry specimen for 30B soil.

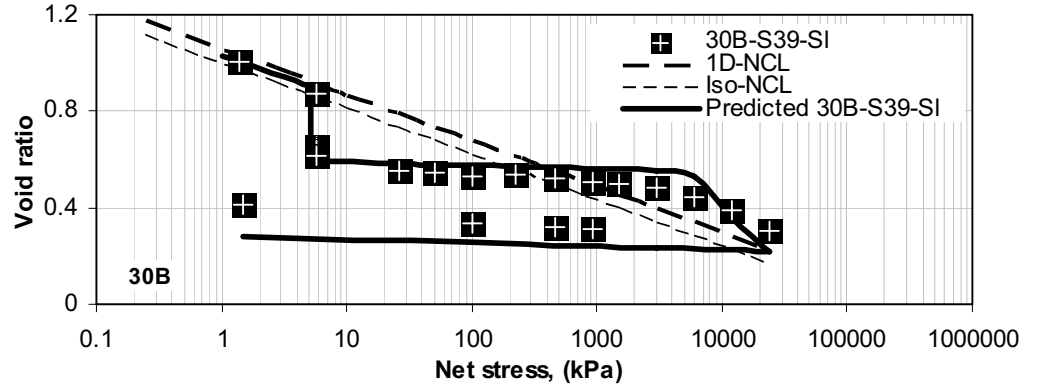

a

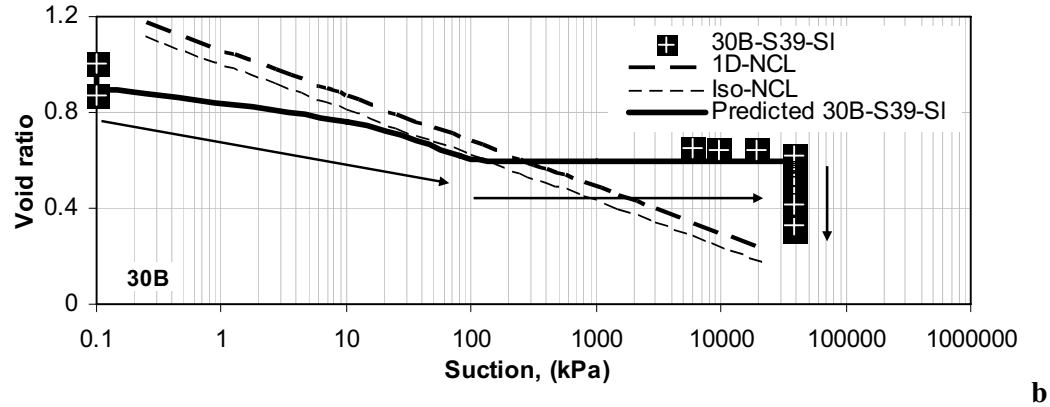

b

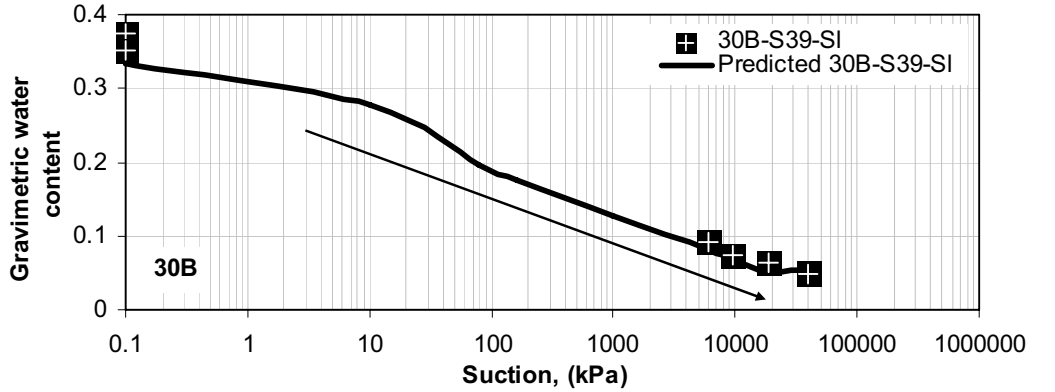

c

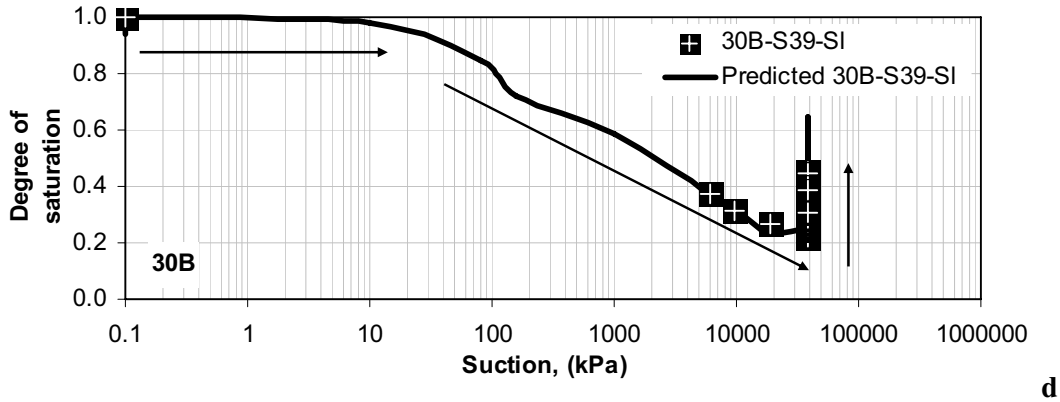

d

Figure 6.32 Experimental and model predictions of constant suction = 39000 kPa condition of initially slurry specimen for 30B soil.

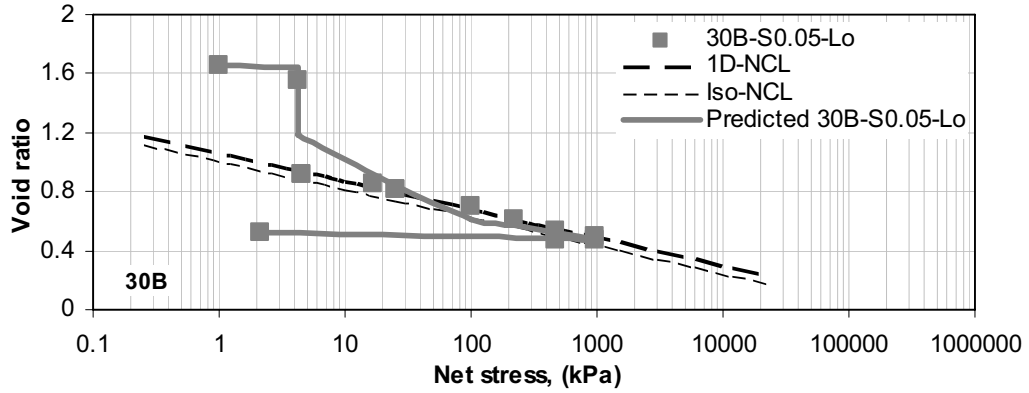

a

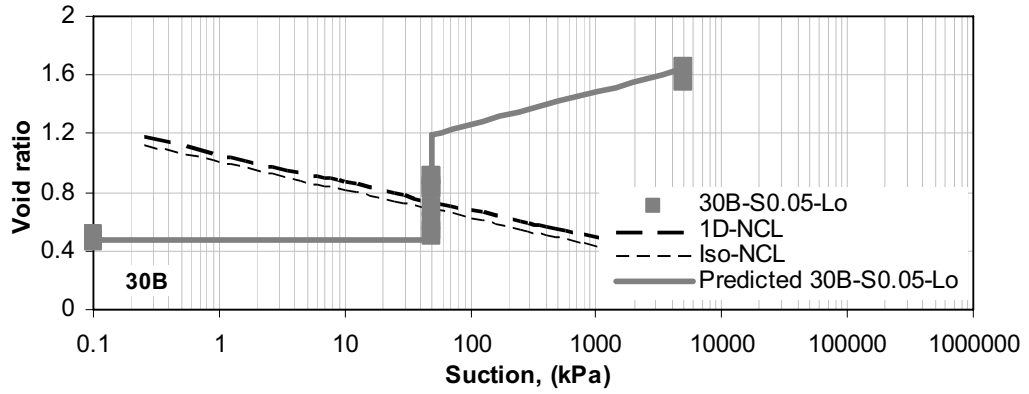

b

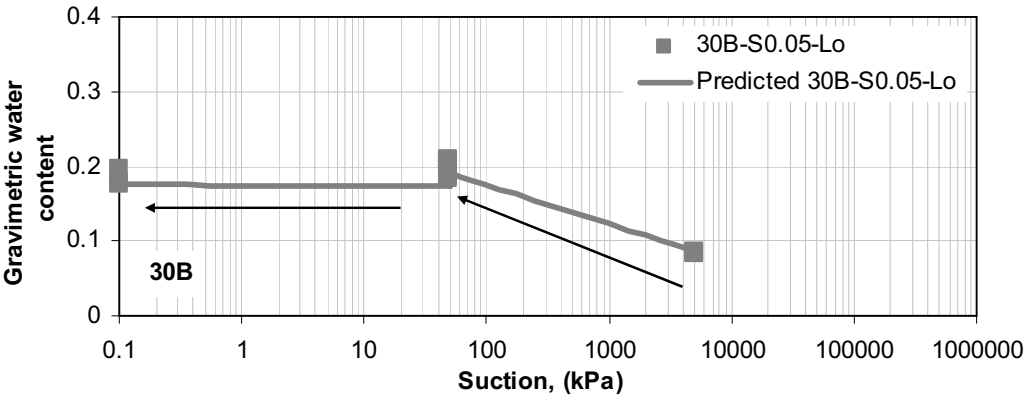

c

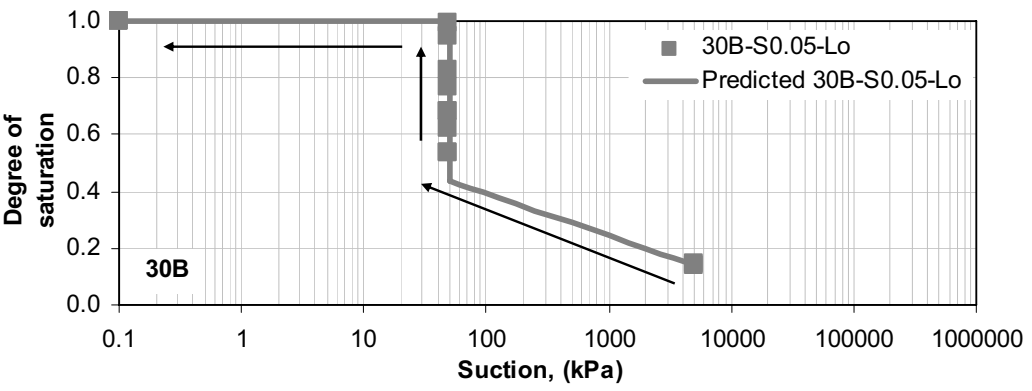

d

Figure 6.33 Experimental and model predictions of constant suction = 50 kPa condition of initially loose specimen for 30B soil.

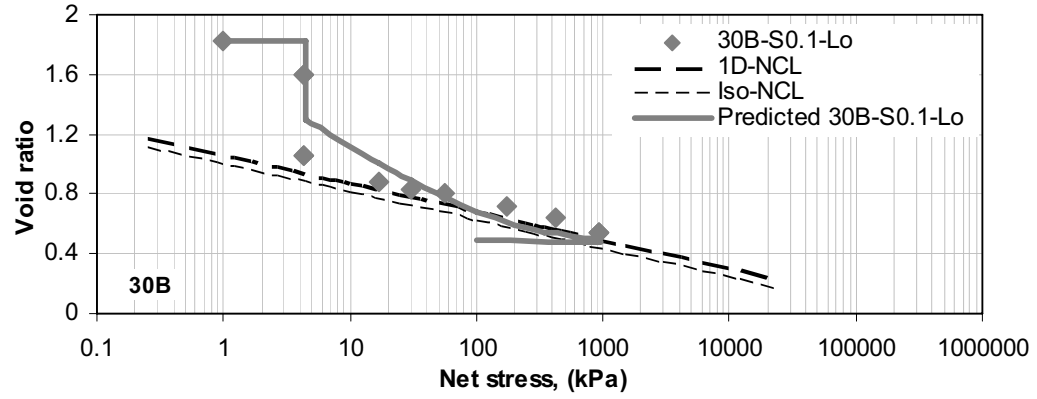

a

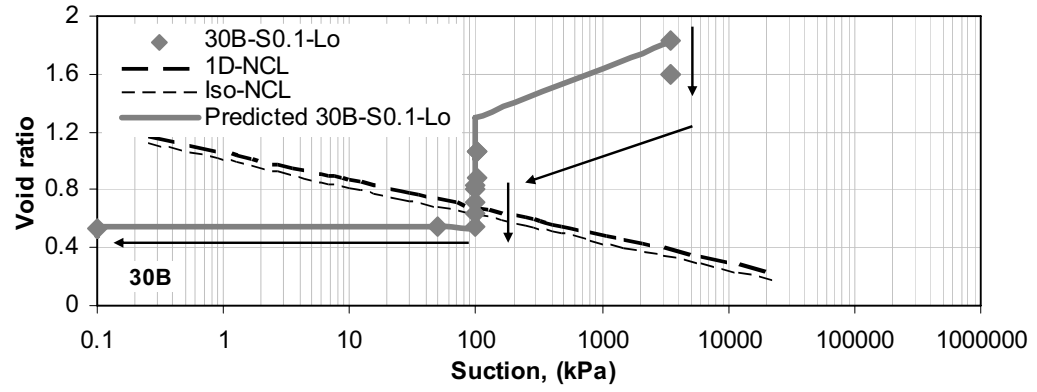

b

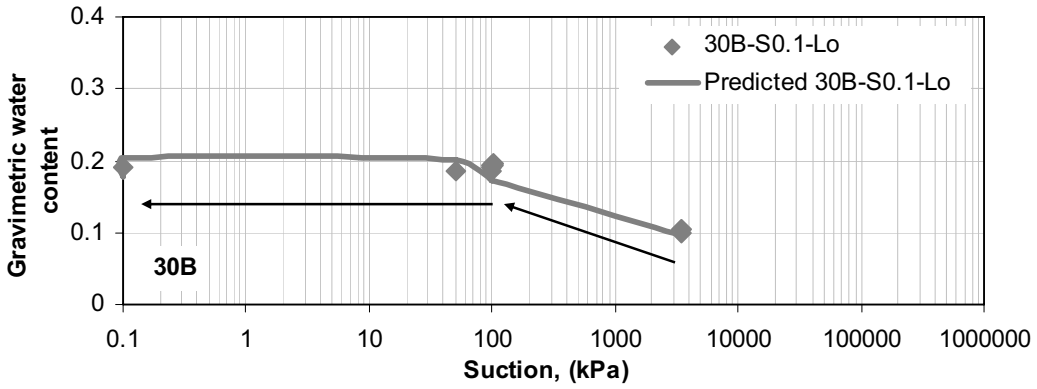

c

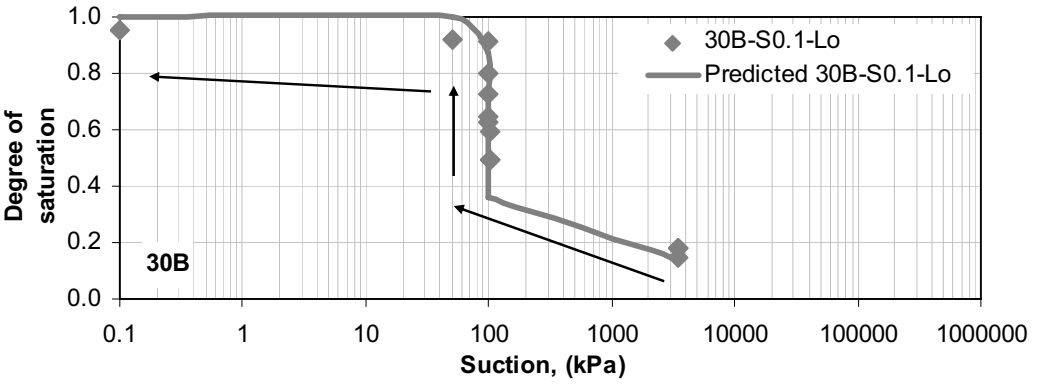

d

Figure 6.34 Experimental and model predictions of constant suction = 100 kPa condition of initially loose specimen for 30B soil.

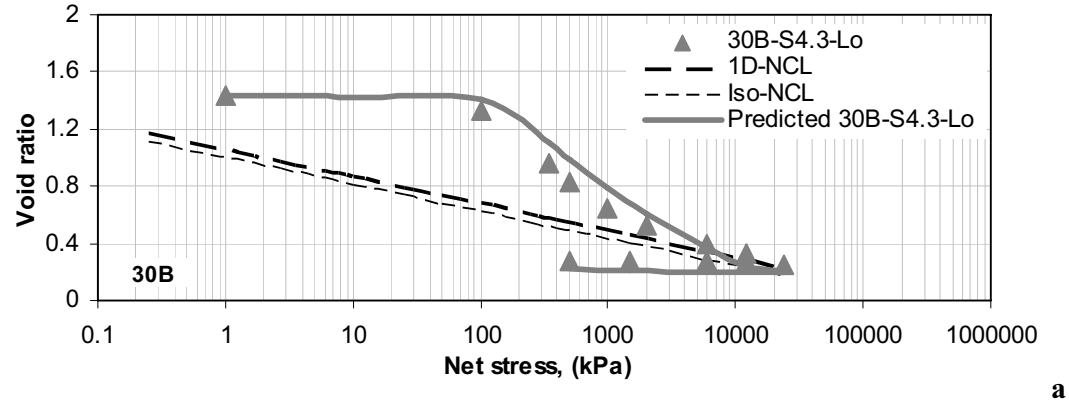

a

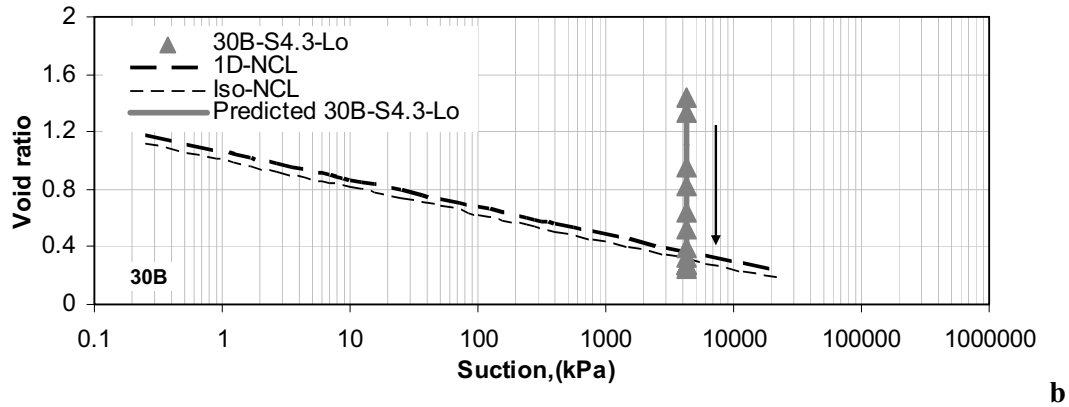

b

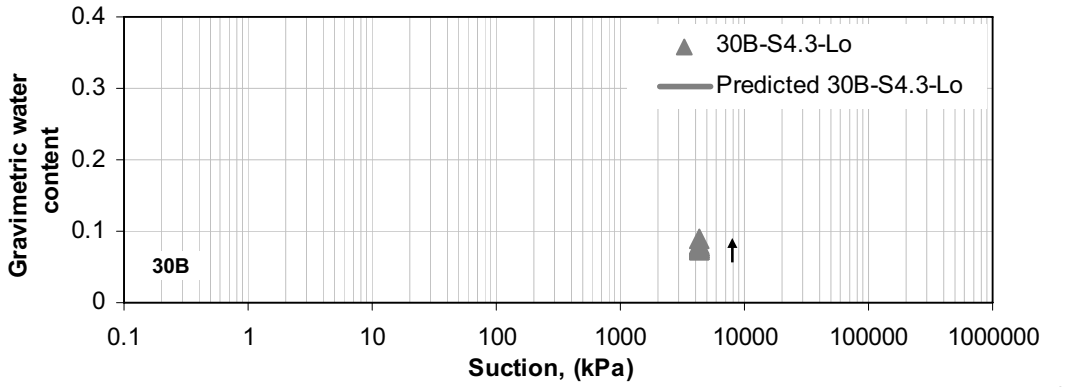

c

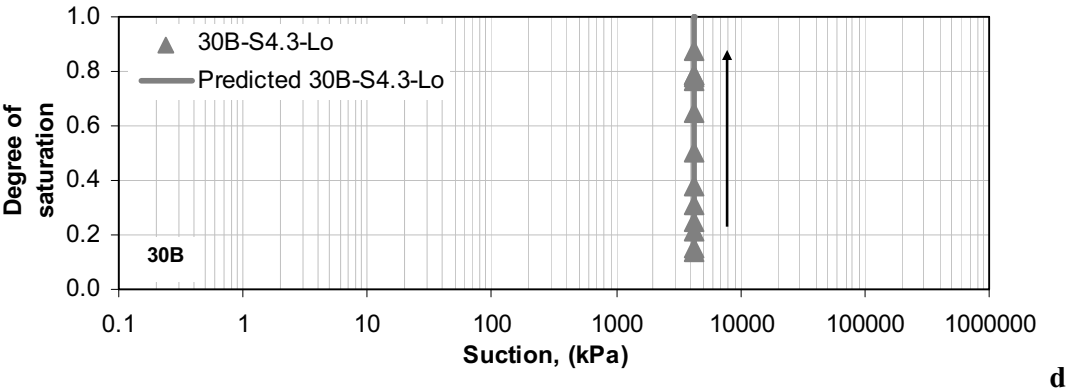

d

Figure 6.35 Experimental and model predictions of constant suction = 430 kPa condition of initially loose specimen for 30B soil.

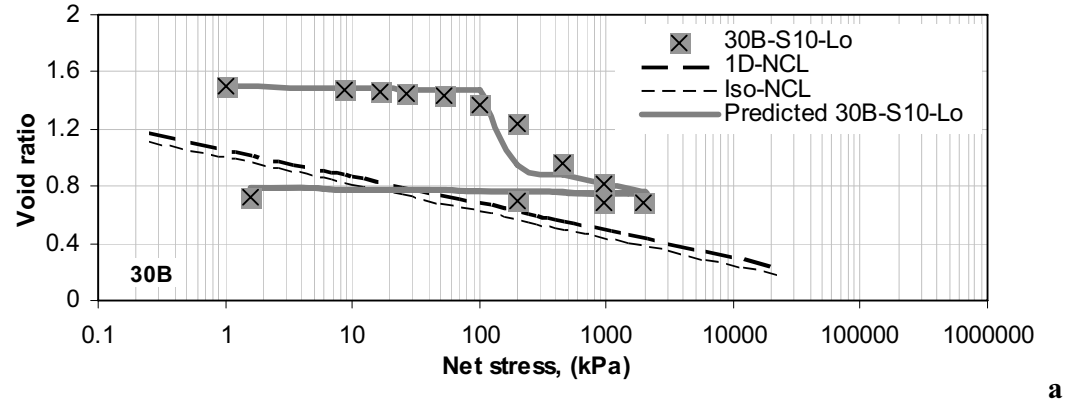

a

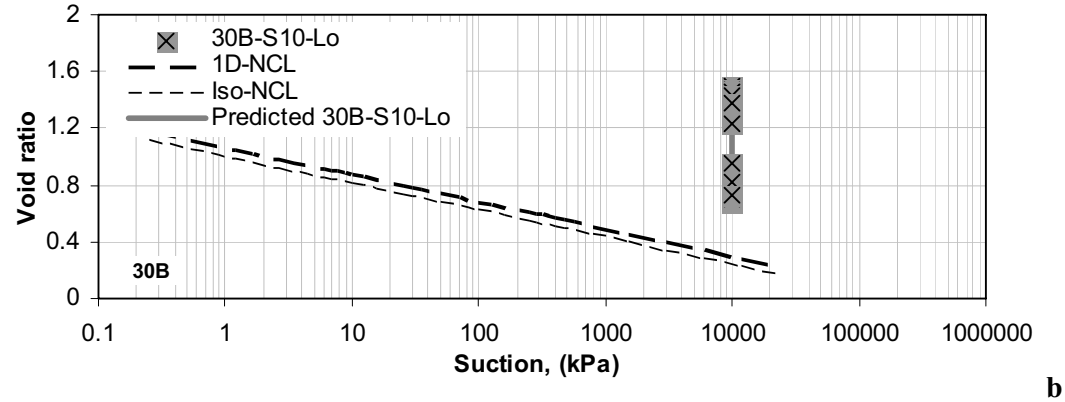

b

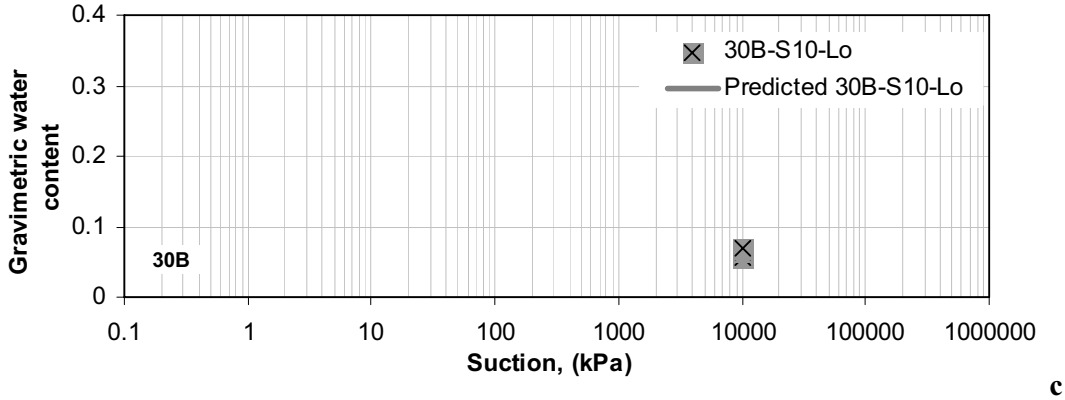

c

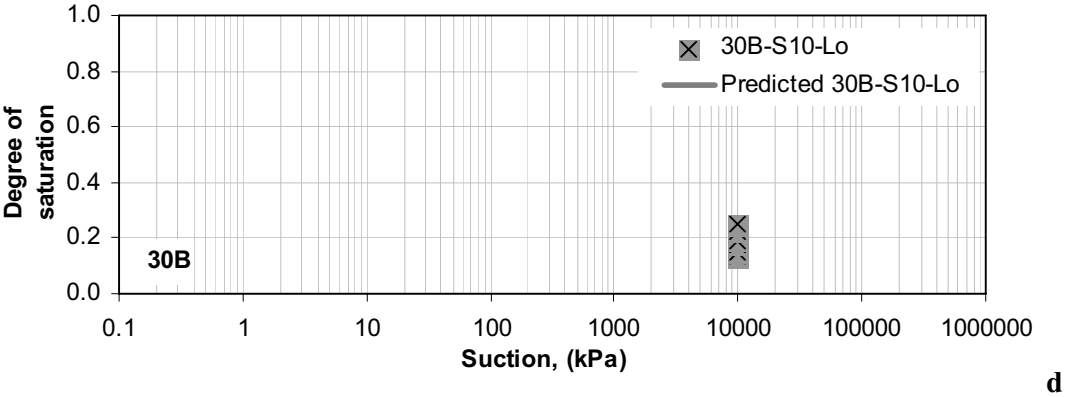

d

Figure 6.36 Experimental and model predictions of constant suction = 10000 kPa condition of initially loose specimen for 30B soil.

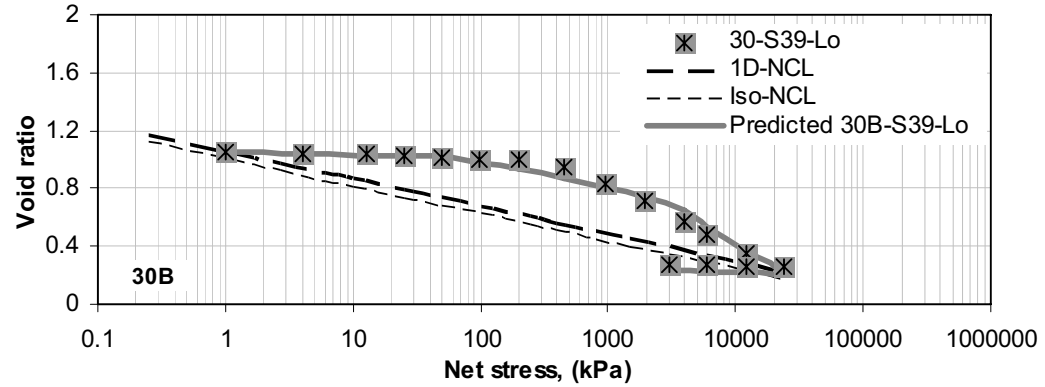

a

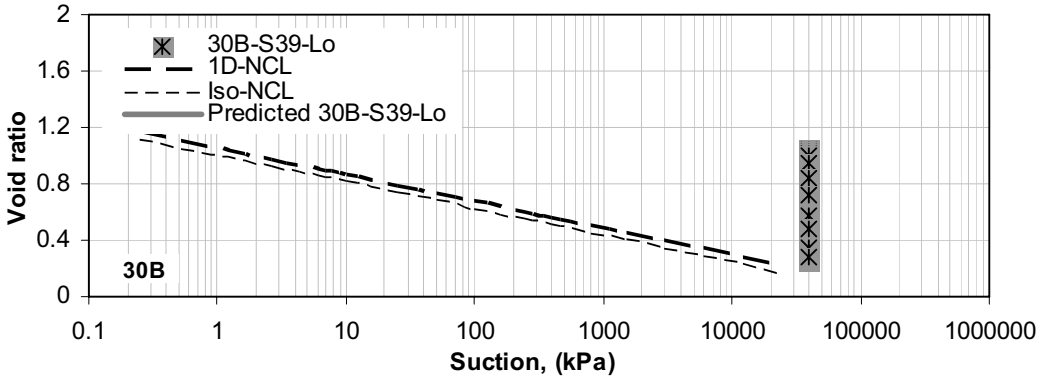

b

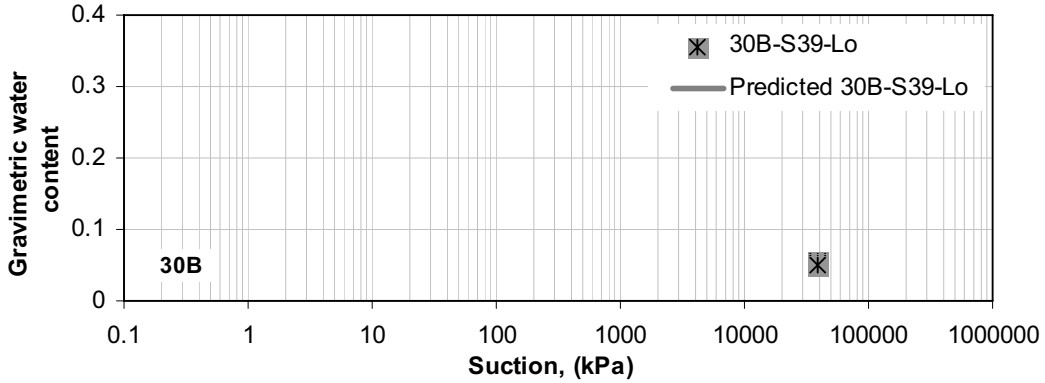

c

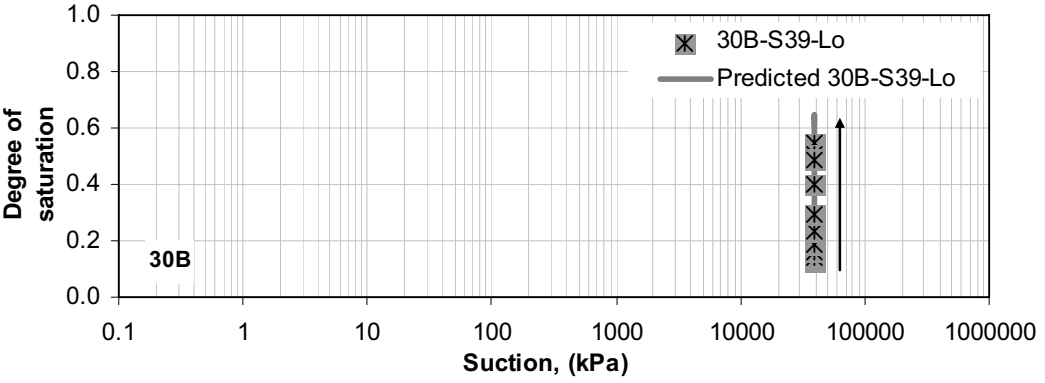

d

Figure 6.37 Experimental and model predictions of constant suction = 39000 kPa condition of initially loose specimen for 30B soil.

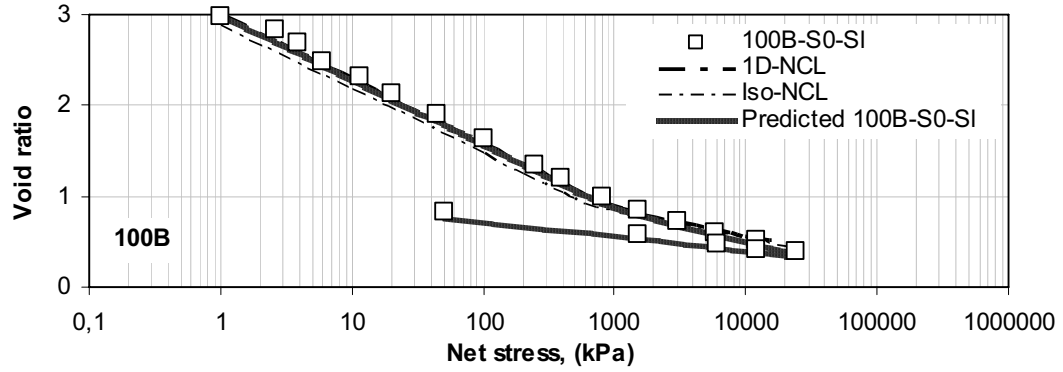

a

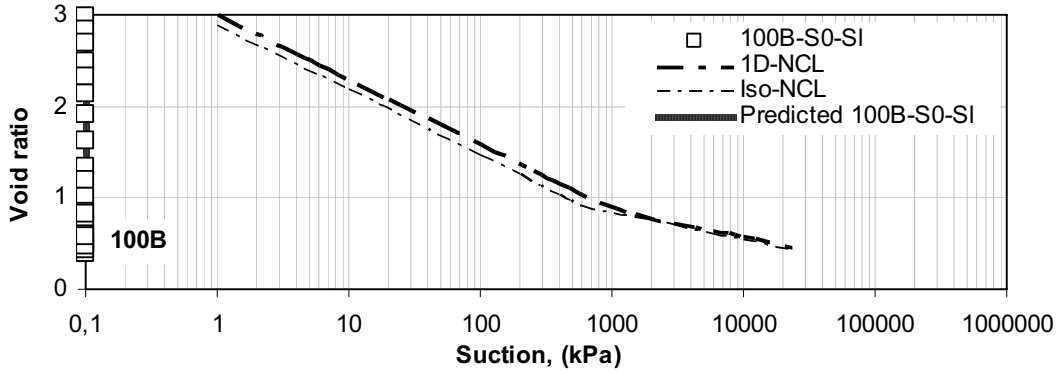

b

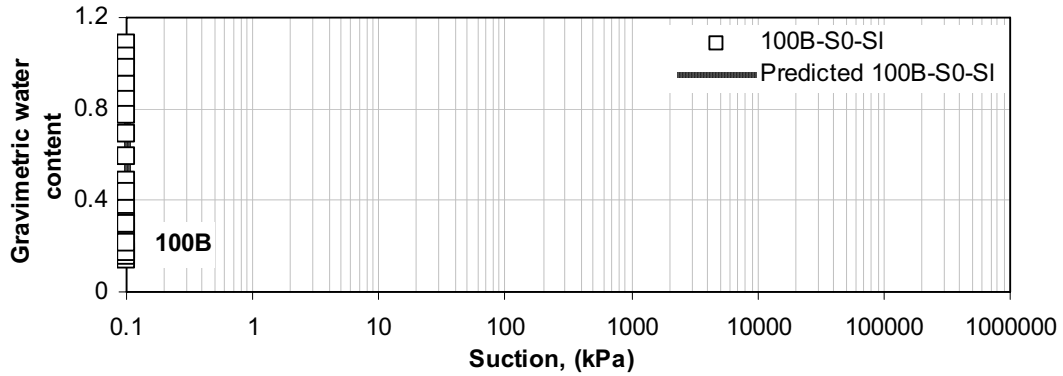

c

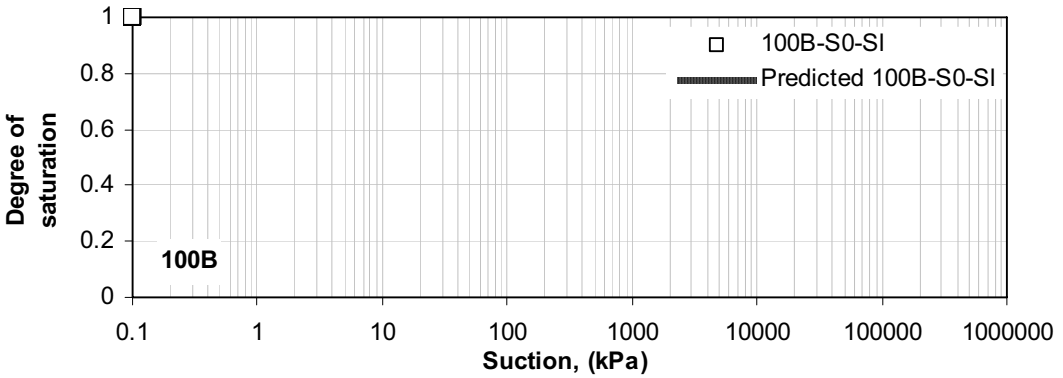

d

Figure 6.38 Experimental and model predictions of constant suction = 0 kPa condition of initially slurry specimen for 100B soil.

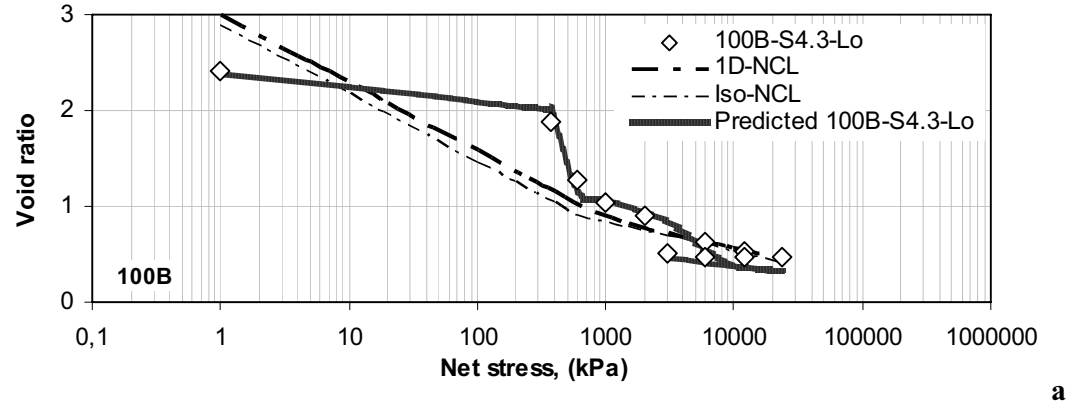

a

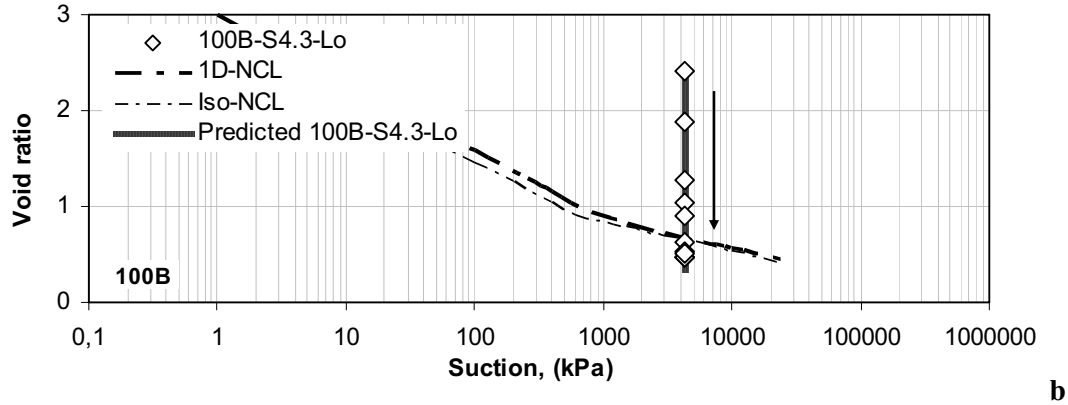

b

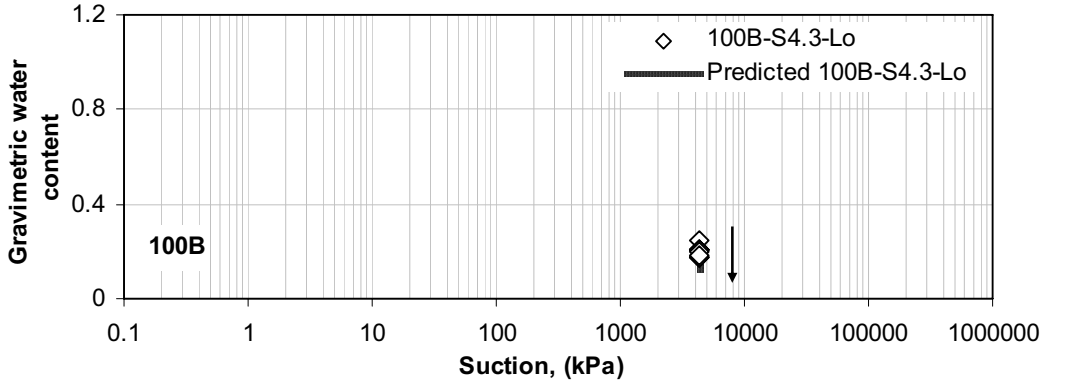

c

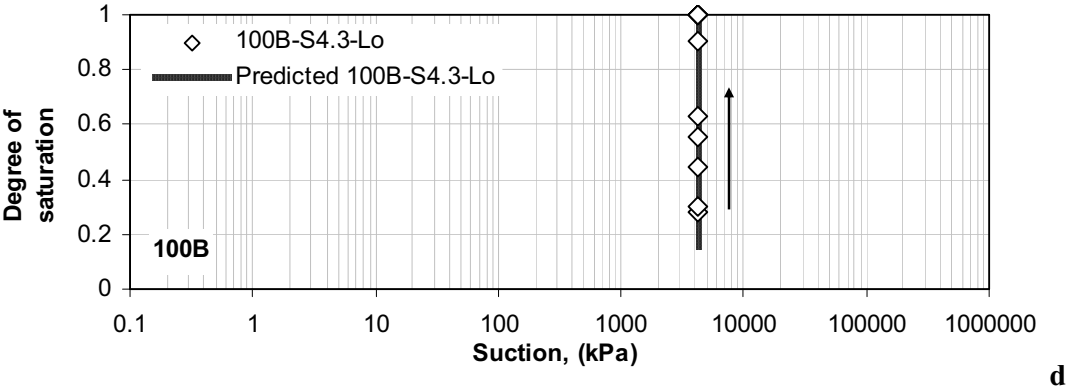

d

Figure 6.39 Experimental and model predictions of constant suction = 4300 kPa condition of initially loose specimen for 100B soil.

6.6.4 Verification tests for uniqueness of the 3D state surface: Changing both net stress and suction test

This test was performed to investigate the uniqueness of the state surface. This test is used to investigate the validity of the main hypothesis in this study (there is only one state surface in void ratio-net stress-suction space). One of the criteria of the test is that the specimen should keep in yield state during the test. The important outcome of the test is that the intersection points of the three specimen (having same net stress and suction values) should have the same volume change (void ratio or density). Figures (6.40-6.42) show the experimental and the model predictions of the three tests (30B-ver1-com, 30B-ver2-com, and 30B-ver3-com) in this program. Figure (6.43) shows the experimental and the model predictions of the three tests together. The model predictions show a good agreement with the experimental data.

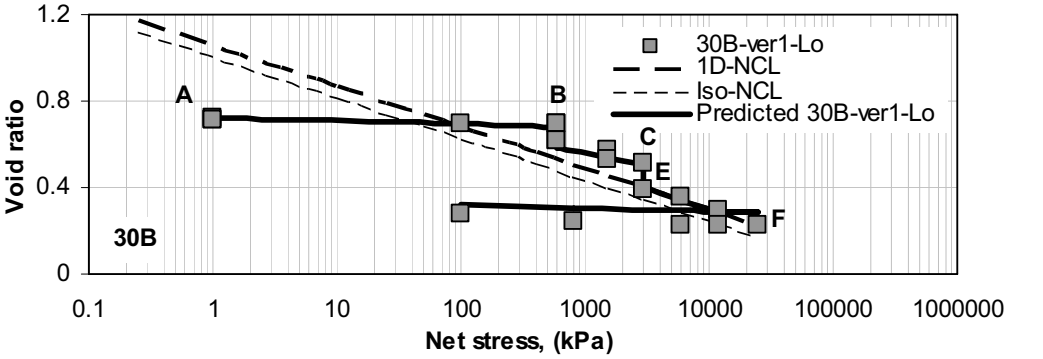

a

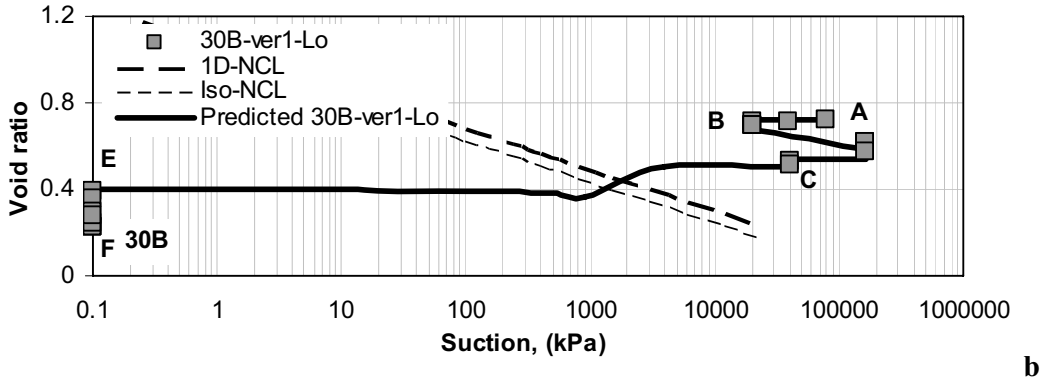

b

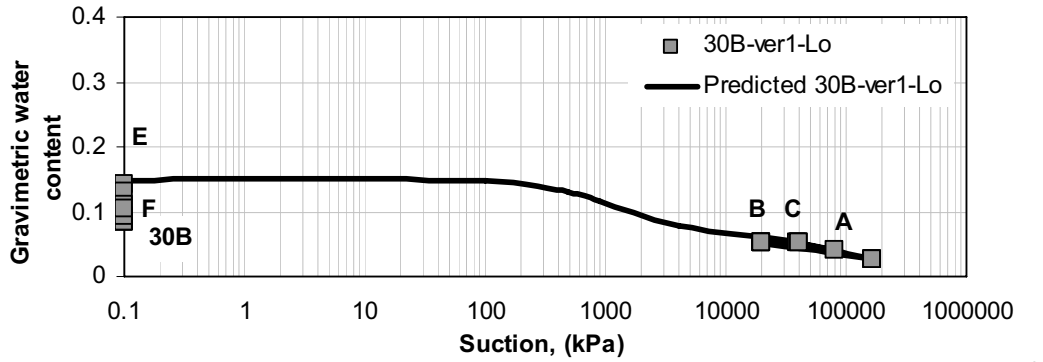

c

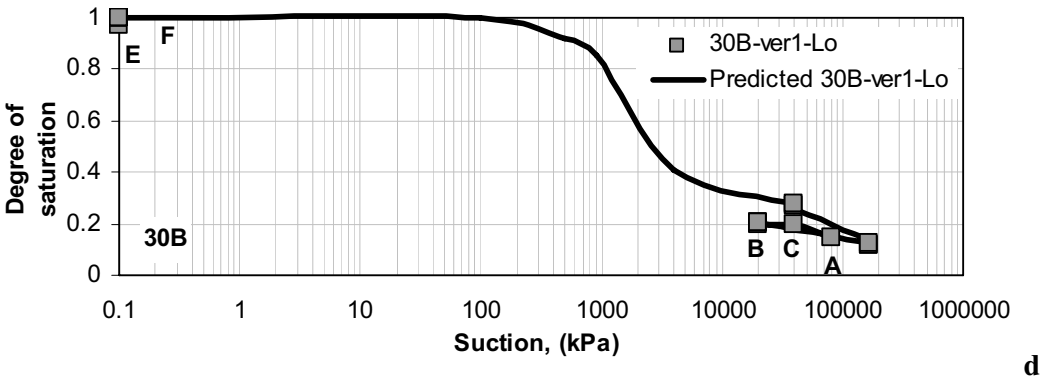

d

Figure 6.40 Experimental and model predictions 30B-ver1-com test for 30B soil.

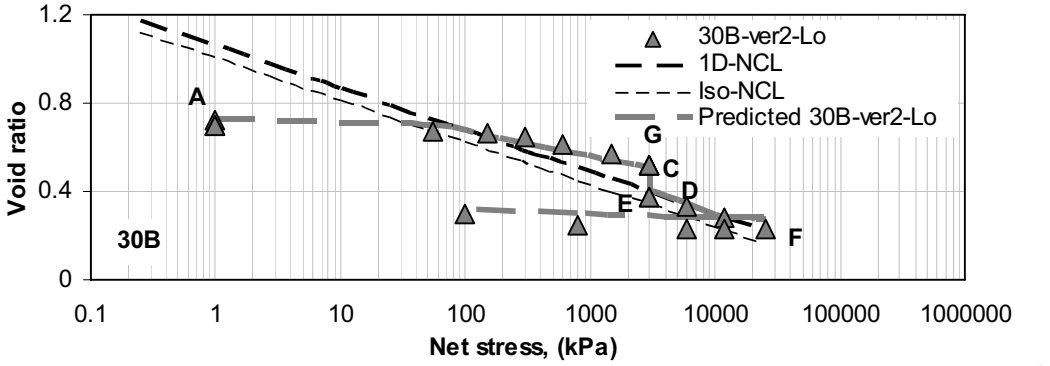

a

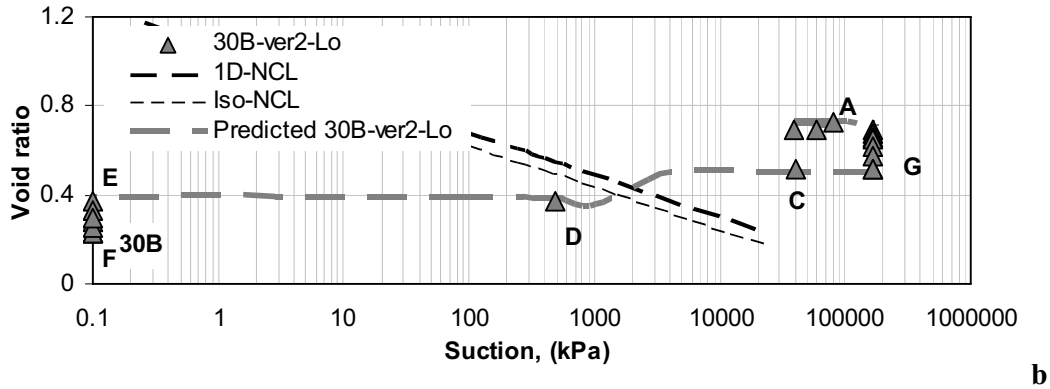

b

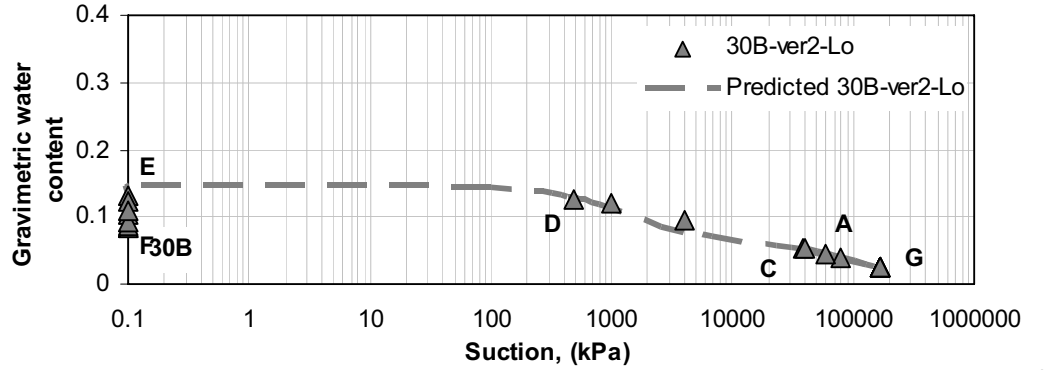

c

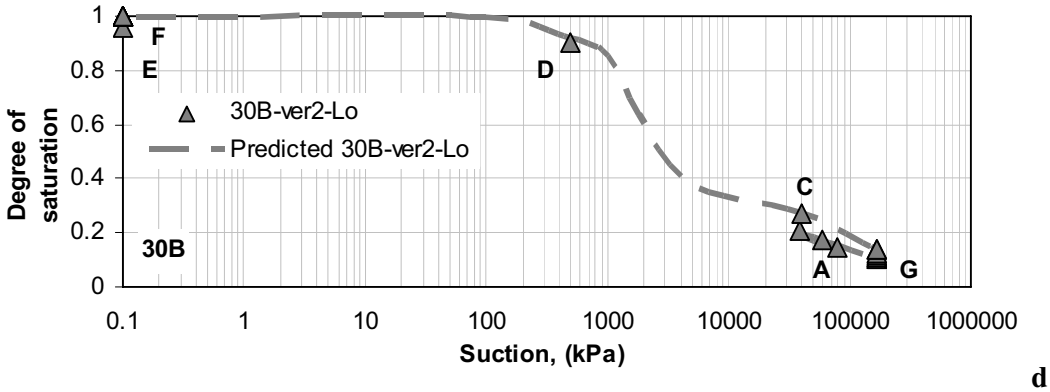

d

Figure 6.41 Experimental and model predictions of 30B-ver2-com test for 30B soil.

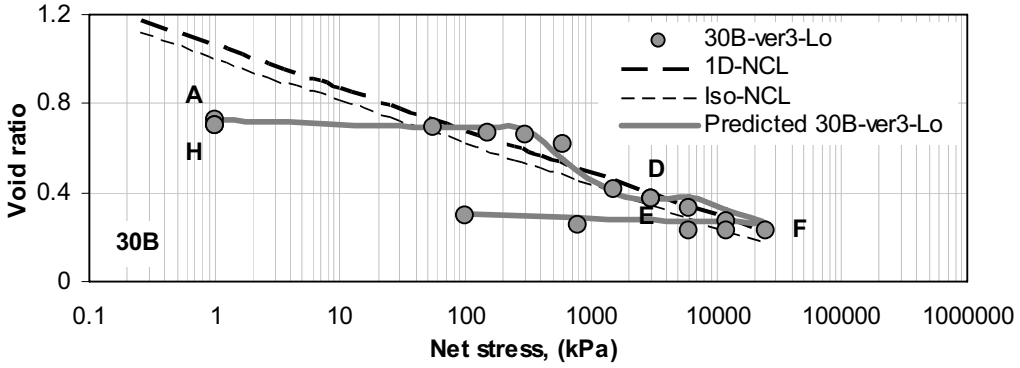

a

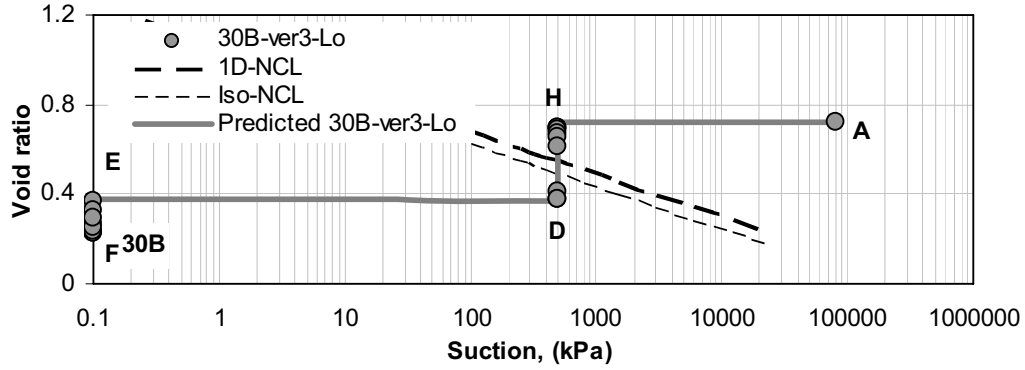

b

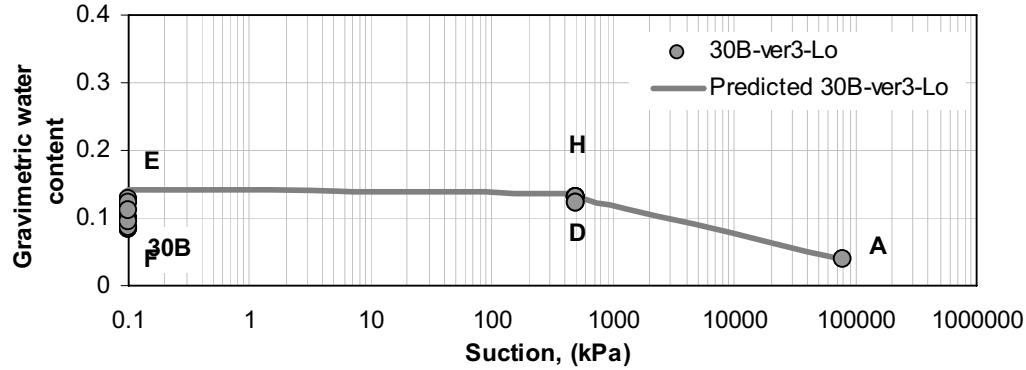

c

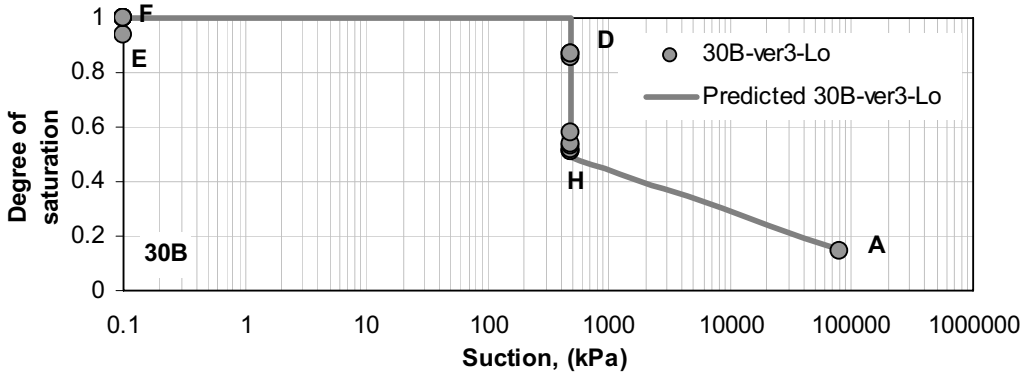

d

Figure 6.42 Experimental and model predictions of 30B-ver3-com test for 30B soil.

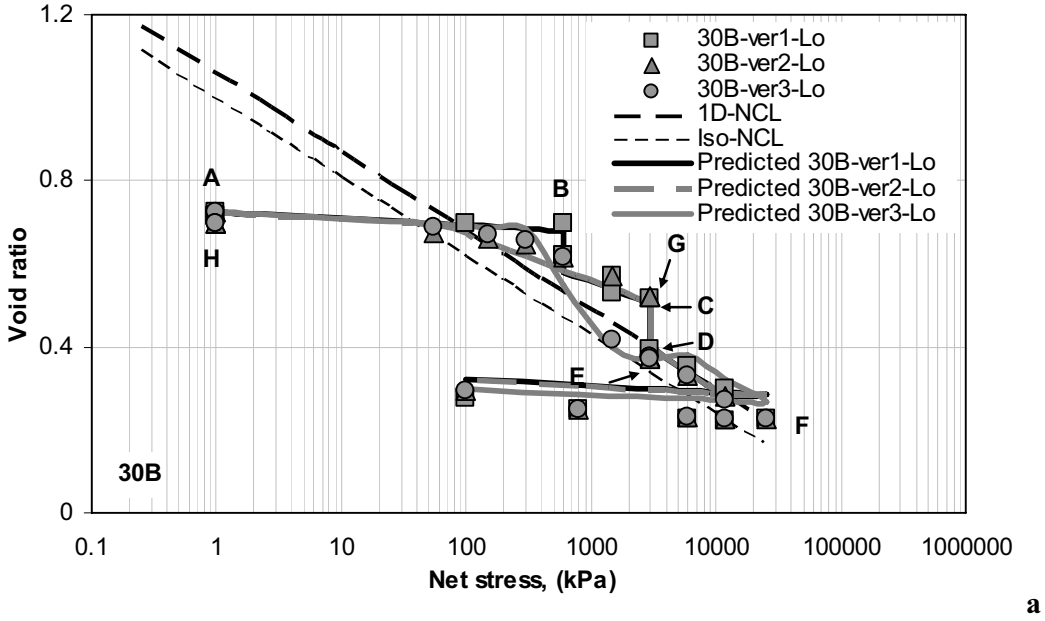

a

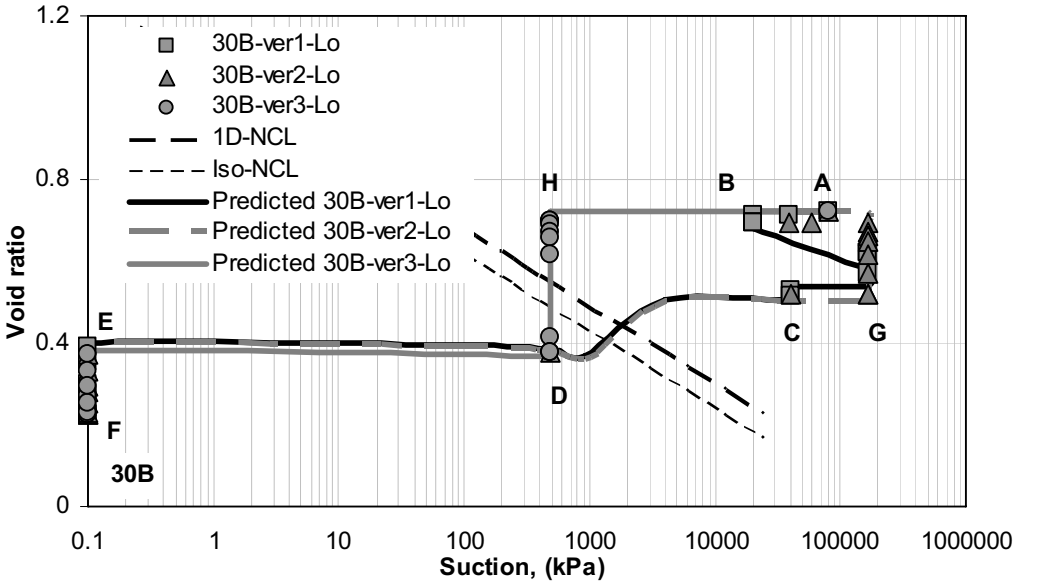

b

Figure 6.43-1 Experimental and model predictions of all uniqueness of the state surface tests for 30B soil.

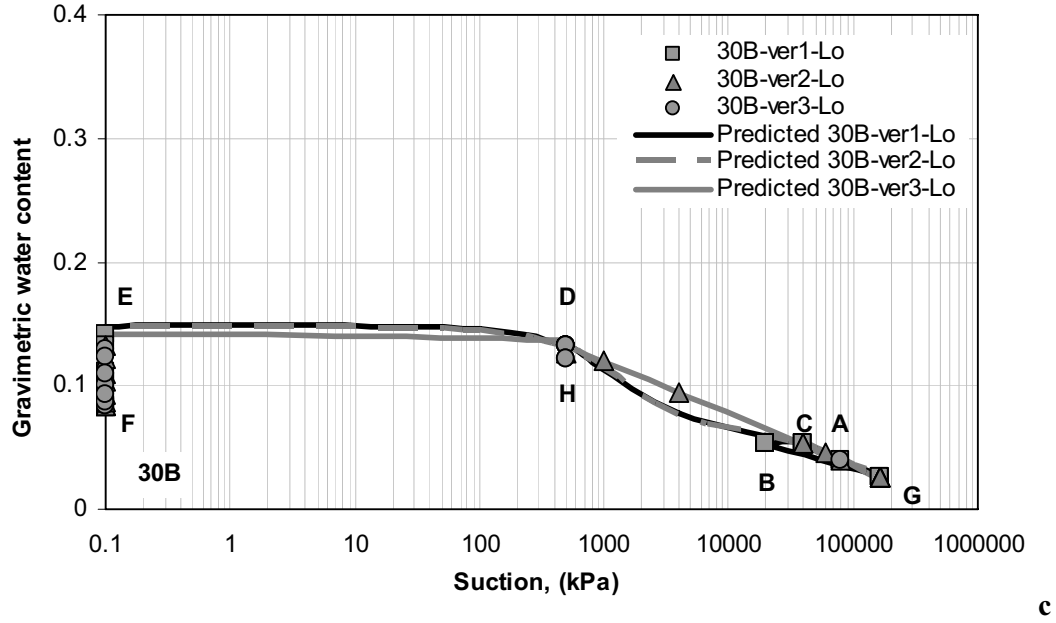

c

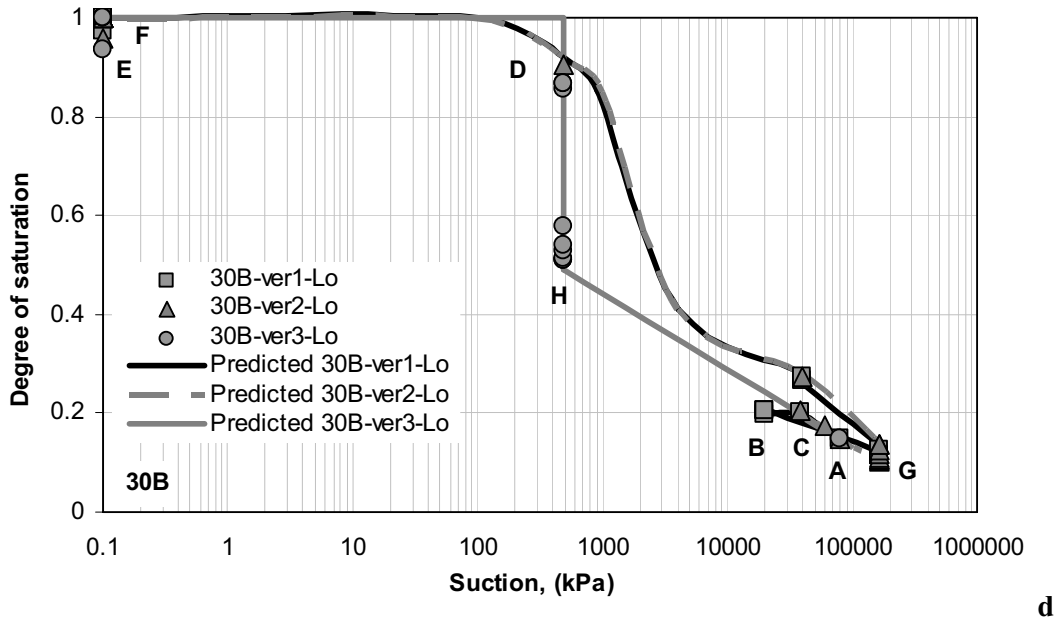

d

Figure 6.43-2 Experimental and model predictions of all uniqueness of the state surface tests for 30B soil.

6.7 Applications

Pereira and Fredlund (2000): wetting under constant net stress "collapse" test

The first soil for application of the proposed model is a residual silty sand soil that was investigated by Pereira and Fredlund (2000). The soil is representative of a typical soil used in the construction of "Alka-Seltzer" dams in northeast Brazil. The soil was classified as SM-ML according to Unified Soil Classification System (USCS) and soil properties are: the specific gravity (G_s) = 2.64, liquid limit (LL) = 29 %, plasticity index (PI) = 12 %. The initial conditions of the statically compacted specimens were: dry density (γ_d) = 1.475 gm/cm^3, water content (w) = 0.105, degree of saturation (S_r) = 0.367, and suction = 370 kPa. Four volume changes (collapse) tests were investigated using a triaxial permeameter system where the stress variables (net mean stress and matric suction) were independently controlled. Wetting stress paths were utilized to reflect field conditions associated with collapsing earth structures. The specimens were compressed isotropically under initial suction (370 kPa) and then were followed by wetting paths under different confined stresses (20 kPa, 50 kPa, 100 kPa, and 200 kPa as TPT1, TPT2, TPT3, and TPT4 respectively). Measurements of total volume change and water content change were made at specified matric suction values followed a wetting paths stress under the given loading. Each predicted curve is divided into two ranges: the over consolidated, OC, and normal consolidated, NC, ranges. The predicted OC part is determined by using the rebound index (C_r). The predicted NC part or unsaturated NCL is determined by using Equation (6.4). The predicted NC part requires the isotropic saturated void ratio at each net stress (from isotropic saturated NCL), the critical degree of saturation S_{rc} = 0.86 (from optimum water content, OWC, of compaction test), the parameter R = 0.4 (from one unsaturated compression test), and the water content w (from wetting curve of suction-gravimetric water content relationship). The isotropic saturated NCL was calculated from the experimental data (compression index, C_c, and rebound index, C_r, are back-estimated from saturated experimental data). The state of specimen, drying or wetting and over consolidated or normal consolidated, has been considered. Figure (6.44) shows the experimental and model predictions of the four collapse tests for the residual silty sand soil. The model predictions show that the state of all four specimens before wetting was over consolidated (OC). The model predictions for the collapse tests with 20 kPa and 50 kPa confined stress (TPT1 and TPT2 tests) fit well with experimental data. The state of specimens in these two tests was over consolidated (OC) during the wetting due to the fact that the void ratios of the specimens before wetting were lower than the saturated NCL. The model predictions for the collapse tests with 100 kPa and 20 kPa confined stress (TPT3 and TPT4 tests) show the same three stages of collapse as the experimental data. The predicted voids ratio of the second stage of

collapse (the collapse phase as mentioned in the reference) are higher than the experimental data. The difference between the predicted and experimental results may be attributed to that the transitions between the intervals of the predicted state surface are considered as points, Figure (6.24c). Possibly these transitions behave as smooth curves in the experimental results. The predicted result of the third stage of 100 kPa confined stress (TPT3 test) matches very good with experimental data. While the predicted voids ratio of the third stage of 200 kPa confined stress (TPT4 test) are slightly lower than the experimental data. This difference can be attributed to the wetting path stress in the experimental test. The suction in the experimental wetting path for TPT4 test was reduced directly from 30 kPa to 10 kPa which means, according to model predictions from the new model, that the specimen transit from the second to third stage of collapse (from third to fourth interval of state surface) without passing the suction of the lowest of void ratio at critical degree of saturation. The suction at critical degree of saturation, under 200 kPa confined stress, equals to 12 kPa according the new model. The wetting path that followed in the TPT4 test may produce higher void ratio in comparison with a wetting path passes by the suction at critical degree of saturation as in case of the model predictions.

Sun et al. (2007): constant suction test

The compacted Pearl clay that has been studied by Sun et al. (2007) is used as a second soil for application of the model. The specimens were prepared by different vertical stress of static compaction (300,400, and 600 kPa) at constant water content (0.26). The initial void ratio is ranging from 1.0 to 1.5 and degree of saturation is ranging from 0.40 to 0.65, and an initial suction from 90 kPa to 130 kPa. The compacted soil was tested in a controlled-suction triaxial cell. In the triaxial cell, the soil specimen was first dried to a suction of 147 kPa and then isotropically compressed to different net stresses. Two tests with different initial void ratio were chosen (e_o = 1.28 and e_o = 1.36). The isotropic saturated NCL was calculated from the experimental data (C_c and C_r are back-estimated from saturated experimental data). The predicted curve is divided into two ranges: the over consolidated, OC, and normal consolidated, NC, ranges. The predicted OC part is determined by using the initial void ratio and C_r. Each point in the predicted NC part or unsaturated NCL is determined by using Equation (6.4), which requires the isotropic saturated void ratio at each net stress (from isotropic saturated NCL), the critical degree of saturation S_{rc} = 0.84 (from *OWC* of compaction test), the parameter $R = 0.5$ (from one unsaturated compression test), and the water content w (from wetting curve of gravimetric water content-suction relationship). The condition of specimen, drying or wetting and over consolidated or normal consolidated, has

been considered during predicting the gravimetric water content and void ratio respectively. Figure (6.45) shows that the predicted curves match very well with the experimental data.

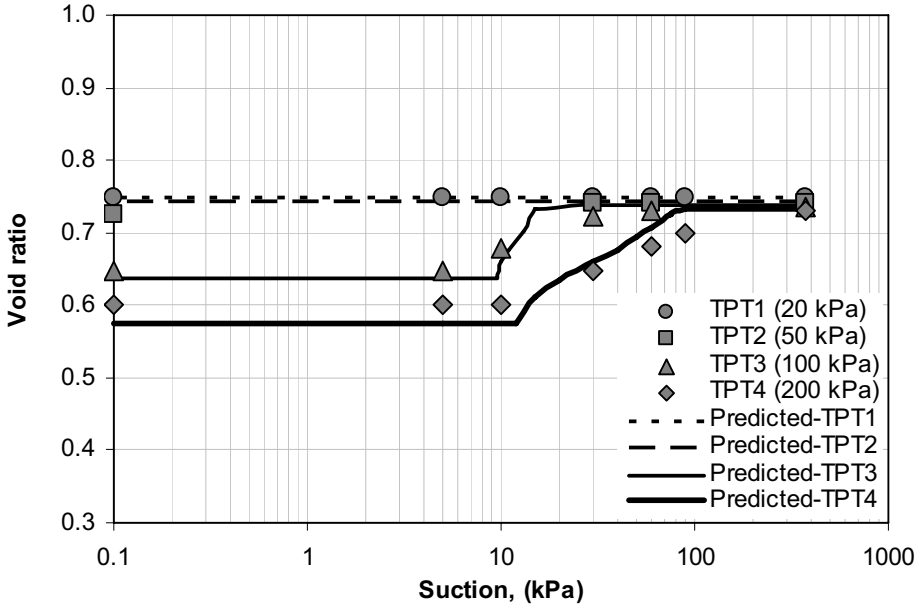

Figure 6.44 Experimental and model predictions of collapse tests under isotropic stress for compacted residual silty sandy soil (experimental data from Pereira and Fredlund, 2000).

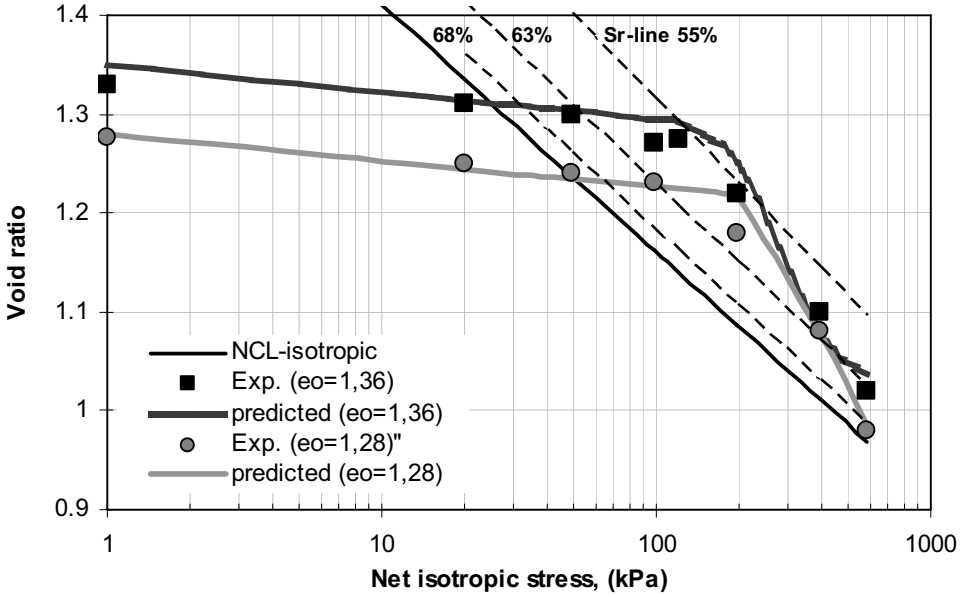

Figure 6.45 Experimental and model predictions of controlled-suction isotropic compression tests for compacted Pearl clay (experimental data from Sun et al., 2007).

6.8 Summary

A new model of the state surface for unsaturated fine-grained soils is presented. The position of the state surface is defined by the NCL of constant degree of saturation, S_r-lines (Al-Badran, 2001), which is modified according to the microstructural consideration of (Nagaraj et al, 2006a and b). The modifications are that the S_r-lines are not parallel, but they have slightly different slopes, and empirical equations can be proposed to determine the volumetric yielding at each degree of saturation. According to the proposed model, for constant net applied vertical stress, the entire range of the degree of saturation (from fully dry to fully saturated condition) shows five different trends (intervals). The basic parameters of the new model are net stress, degree of saturation, critical degree of saturation, SWCC, the parameter that controls the influence of the degree of saturation to the increase of the void ratio under constant net stress in the third interval (R), and the parameter that controls the position of e_{max} in the second interval (M). Moreover the model was developed depending on three hypotheses. The proposed model is validated against the experimental results (present study) and experimental data reported in literature. The model predictions match very well with the experimental data. The proposed model provides additional understanding to the volume change behavior of unsaturated soils such as: compression, compaction, collapse.

Chapter 7
Modelling the Compaction Curve Using the New Volumetric Yielding Model

7.1 Introduction

This chapter amid to model the compaction curves at various compaction efforts for the entire range of water content for fine-grained soils. It is assumed that the compaction curves reproduce the state surface at yield state of unsaturated state (case *i* of loading stated in chapter 6). Specifically each point in the compaction curve represents a normal consolidated or yield state results in increase the applied net stress or compaction effort till specific value under constant water content condition for initially loose state soil. Thus, for each applied compaction effort, the compaction curve relates to one yielding point at saturated NCL. In this model, the parameters involved are functions of: void ratio of the saturated NCL (e_{NCL}) of effective stress equivalents to the compaction effort, degree of saturation S_r, critical degree of saturation S_{rc} (degree of saturation at *OWC*), parameter that controls the influence of the degree of saturation to increase the void ratio under constant compaction effort (R), and parameter that controls the position of maximum value of void ratio under each net stress or compaction effort (M). However, for a given soil, the model requires NCL, S_{rc}, and one point from any compaction curve to predict the compaction curves for different compaction efforts. The prediction of any further compaction curve for a specific compaction effort requires only the e_{NCL} of equivalent effective stress. Moreover, the lines of equal suctions on the compaction curves can be determined, if SWCC (wetting path) is known.

7.2 Prediction of compaction test: Description of the model

In this section the description of the model will present. Main assumption is that the compaction curves represent the state surface of unsaturated state, as proposed in chapter 6. The model assumes that the maximum dry density γ_{dmax} for all compaction efforts is reached at one and the same degree of saturation, and this saturation is the critical degree of saturation. The critical degree of saturation, S_{rc}, is the degree of saturation at the air-entry value when the air phase state starts to be continuous. This condition (change of phase's state) occurs also at

optimum water content, *OWC* (Pandian et al,. 1997), therefore the critical degree of saturation is assumed to be equal to the degree of saturation at *OWC*.

Modelling the compaction curve using the volumetric yielding model (chapter 6) is discussed below. The saturated NCL for initially slurry state specimen is adopted in this model to determine the parameter e_{NCL}. The validity of the main assumptions (or hypotheses) in the new model will be not discussed (see chapter 6 for details). It is worthwhile to mention that the 2nd hypothesis is valid only for dry of optimum DOP. Therefore, for water content less than the *OWC*, the water content-dry density relationship for constant suction represents a vertical line (different dry densities at constant water content that corresponds to the wetting path). For the wet of optimum WOP, the contour line of constant suction can be calculated by adopting a linear relationship between the degree of saturation and suction to consider the effect of density on the wetting path. Moreover, the behavior of soil in the second interval produces maximum void ratio that the soil can reach under a specific net stress or compaction effort. Furthermore, this increase in void ratio may create another peak to the compaction curve on the dry side.

The main assumption in the modelling of compaction curve is that the compaction curves reproduce the state surface at yield state (chapter 6). In compaction process the volume change behavior response according to the two independent stress variables; net stress and suction. Generally, to prepare soil before compaction test, firstly the soil is mixed with water, then the mixture disintegrates to make loose soil structure in unsaturated state. To unify all states, the value of 1 kPa will be considered as preconsolidation stress for this initial loose unsaturated soil. This initially unsaturated loose soil will produce volumetric yielding when the following two points are ensured (i) considerable stress (>1 kPa) and (ii) sufficient time under load to reach the equilibrium. Any applied compaction effort value more than 1 kPa on the DOP will produce volumetric yielding and soil structure reaches to the equilibrium within very short time. During this process the air expels out only making the time for equilibrium very short. The initial value of suction keeps constant because the water content is constant throughout the process (2nd hypothesis in section 6.3). While at WOP, the process is the combination of compaction and consolidation, therefore the complete process to reach volumetric yielding needs sufficient time to take place. In other words, the experimental results of compaction curve at WOP do not reach to the yield state due to the short duration of compaction test. As a result, on WOP, there is some difference between the predicted (normal consolidated or yield state) and the experimental results. Moreover, with passage of time the suction will increase in case of compacted expansive soils due to incomplete hydration (Schanz et al., 2010). This may leads to change in the state of soil from the yield state to the

over consolidated state (hardening due to drying). The unsaturated soil exhibit very small amount of volume changes during this process. Therefore the volume change for long time will be neglected. Additionally, in DOP, both dynamic and static compaction techniques give the same horizontal alignment of soil particle groups (Mitchell, 1993). However, the alignment of soil particles in WOP will effect by the compaction type, which is not taken into account in this model. Therefore, the model does not consider the dynamic and static compaction explicitly. From above, the compaction curve in the DOP can consider representing the yield state. While that compaction curve in the WOP it is expected some difference between the predicted (normal consolidated or yield state) and the experimental results.

Figure (7.1) summarises the different steps to predict the compaction curve. The curve of compaction effort equivalent to the effective stress P1 can be estimated based on the point (A) that represents the e_{NCL} corresponding to P1 effective stress. From point (A), by using the additional model parameter (i. e., S_{rc}, R, and M), the void ratio for any degree of saturation or water content can be calculated (according to the equations 6.1 to 6.5 for S_r-lines in chapter 6). The next step will be the conversion of the void ratio to the dry density to obtain the compaction curve. The parameters S_{rc}, R, and M are constant for each soil and each parameter requires only one experimental point to be determined. To predict the curve for other compaction effort, such as equivalent to the effective stress P2, it requires no more than updating the parameter e_{NCL} which corresponding to P2 effective stress, point (B). Figure (7.2) represents the predicted compaction curves of different compaction efforts using the new model for 30B soil.

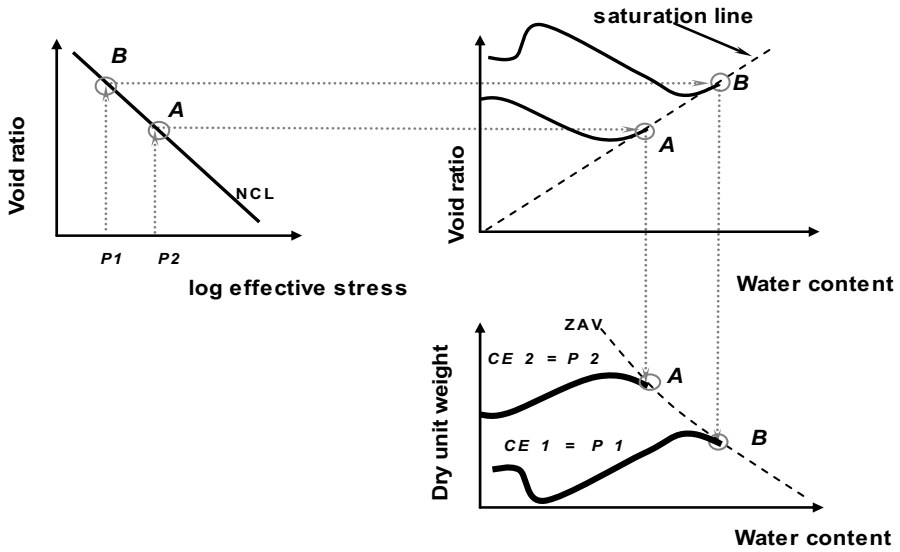

Figure 7.1 Sketch showing the steps using the proposed model to predict the compaction curve.

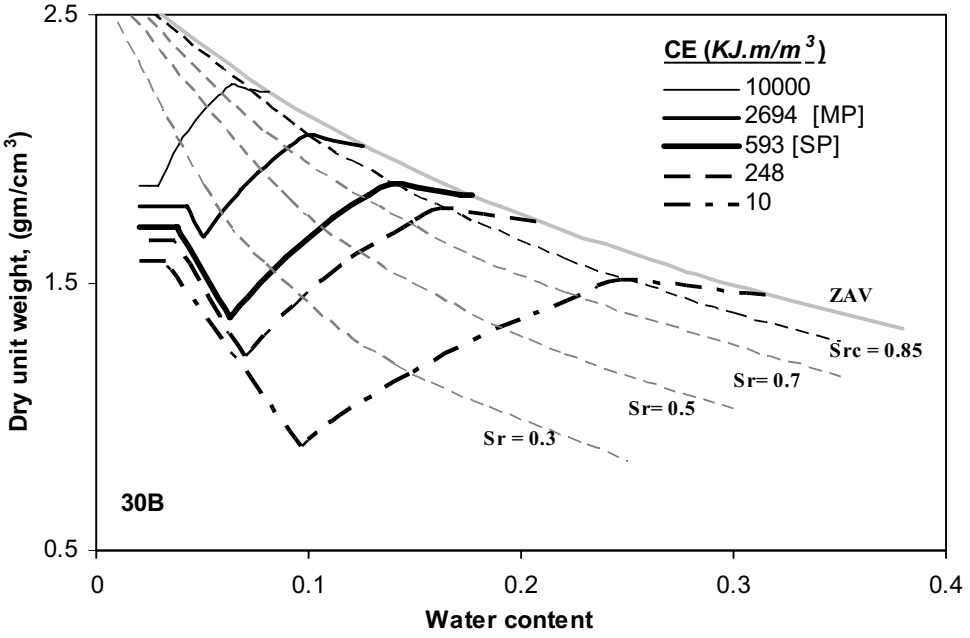

Figure 7.2 The model predictions of compaction curves of different compaction energies (CE's) using the proposed model for 30B soil.

7.3 Shape and properties of compaction curve according to the new model

In the proposed model, the compaction curve can have two peaks (for dry unit weight). One peak has low water content, and is labelled as dry peak compaction point, *DPCP*, (point B in Figure 2.32); the second peak has high water content and is labelled as wet peak compaction point, WPCP (point D in Figure 2.32). When the compaction effort increases, the amplitudes of the two peaks (i.e., dry and wet) increase. Moreover, by increasing the compaction effort, the dry peak tends to decrease with respect to the wet peak. This trend continues until the dry peak vanishes: the curve attains a horizontal line in the low water content range (Figure 7.2). The water content of the wet peak (wet optimum water content *WOWC*) decreases, while the water content of the dry peak (dry optimum water content *DOWC*) increases and then decreases as the compaction effort increases (Figure 7.2). However, the water content of the concave point (*CP*) decreases with the increase of compaction effort. The dry peak compaction point (*DPCP*) in the compaction curve does not appear in most cases because the compaction curve starts with a water content higher than the dry optimum water content (*DOWC*) regarding for the applied compaction effort. If more than one curve exists for the same soil with different compaction efforts (e.g., standard and modified) starting from the same water content, then the following scenarios are possible: (i) the dry peak compaction points do not appear for both low and high compaction efforts; (ii) the dry peak compaction

points for both low and high compaction effort appear; and (iii) the dry peak compaction point for either low or high compaction effort appears, and the concave point of the other one appears. Case (i) happens when the compaction curve initially starts with water content more water than the dry optimum water content for both of the compaction efforts. Case (ii) occurs when the initial moulding water content is less than the dry optimum water content for both of the compaction efforts (Figure 2.32 for SP and RP). Case (iii) occurs when the initial moulding water content falls between the two dry optimum water contents (Figure 2.32 for MP and SP). At the wet peak compaction point (*WPCP*) (at $W\gamma_{dmax}$ and *WOWC*), the degree of saturation is constant for all compaction efforts, and it equals the critical degree of saturation Src, while the degree of saturation of *DPCP* (at $D\gamma_{dmax}$ and *DOWC*) increases as the applied compaction effort increases. The other significant feature of the compaction curve, with regard to the state surface model for fine-grained soils, is that the value of the degree of saturation of the *DPCP* remains constant when the dry unit weight decreases with increasing water content (the second interval in the model) for the same applied compaction effort (Figure 2.32, B-C). This trend continues until the dry unit weight begins to increase (the third interval in the model). In other words, the degree of saturation in the compaction curve remains constant between the *DPCP* and the *CP* (from point B to C in Figure 2.32). Then, the degree of saturation increases as the water content increases until it reaches the *WPCP*, after which the saturation increases slightly until it reaches the fully saturated condition.

7.4 Verification of model

The new compaction curve model has been verified in two ways: first quantitatively, by experimental results and second qualitatively, by examining the relationships from other models in the literature.

Experimental tests and materials used

The compaction curve model assumptions were verified by analysing the residuals between the predicted and the experimental compaction curves (static and dynamic). The predicted curve is determined by using the equations (6.1-6.5) for all five intervals of volumetric yielding behavior. These equations require the value of the void ratio of e_{NCL} of net stress equivalent to each compaction effort, the critical degree of saturation, and the degree of saturation or water content (input data). The net stresses equivalent to each compaction efforts are 248 kPa for RP, 593 kPa for SP, and 2694 kPa for MP. As stated in chapter 6, the critical degrees of saturation, S_{rc}, are 0.90 and 0.85 for 100B and 30B, respectively. The R values

(Equation 6.4) are 0.43 and 0.5, and the M values (Equation 6.3) are 0.4 and 0.24 for 100B and 30B, respectively.

In water content-dry density relationship, contour lines of equal suctions are vertical in DOP (2nd hypothesis). For WOP, the contour lines of constant suction are calculated by adopting a linear relationship between the degree of saturation and suction to consider the effect of density on the wetting path.

Figure (7.3 and 7.4) show the experimental, predicted compaction curves, and the contours line locations of constant suction for 100B and 30B soils. The results show that the model fits well with the experimental results of the compaction tests. The predicted constant suction lines almost perfectly match the experimental data with a slight shift towards less water content due to the model predictions represent the wetting path (3rd hypothesis). The measured suction values seem to follow a scanning path due to drying or reduced water content while taking a specimen from the compaction mould till measuring suction in chilled mirror.

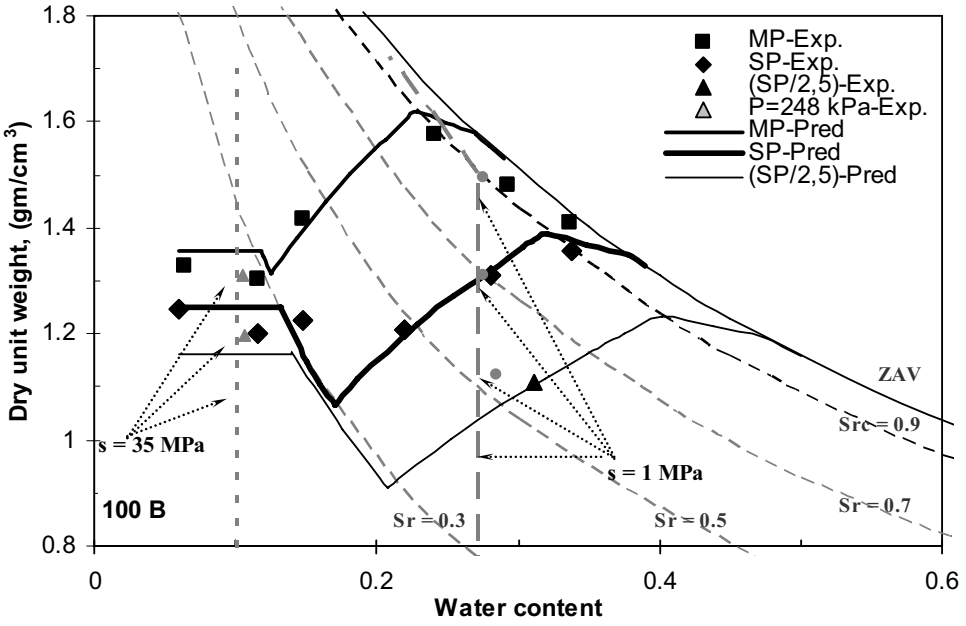

Figure 7.3 Dynamic and static compaction curves for different compaction efforts for 100B soil, the points are the experimental results and lines are the model predictions.

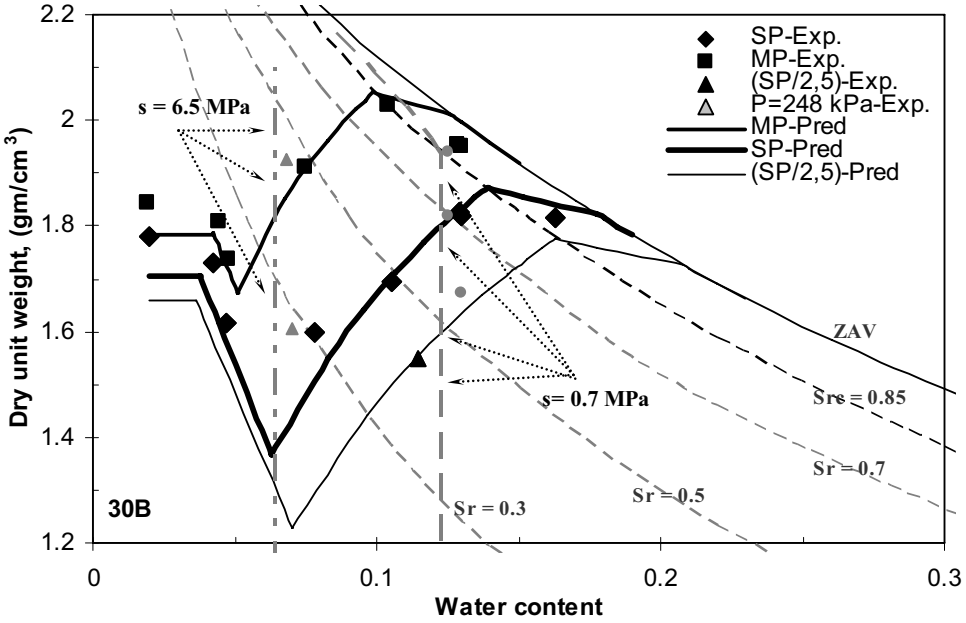

Figure 7.4 Dynamic and static compaction curves for different compaction efforts for 30B soil, the points are the experimental results and lines are the model predictions.

Verifying the relationships of previous compaction curve models

The usefulness of the proposed model is its ability to explain most of the relationships that other compaction models introduced, such as the linear relationships between Atterberg limits (liquid limits *LL* and *PL*), G_s, water content w, degree of saturation S_r, and the void ratio of constant water content $e_{(cons\ w)}$, and between the compaction effort on a logarithmic scale (Al-Kafaji, 1993, Pandian et al., 1997, Blotz et al., 1998, Sridharan and Nagaraj, 2005 and Gurtug and Sridharan, 2002, Nagaraj et al., 2006, Jesmani et al., 2008). All the above relationships can be explained by the semi-linear relationship between void ratio and net stress in the saturated NCL under constant or different values of liquid limit (*LL*) for the same soil or different types of soils, respectively. It is important to mention that all the presented relationships came from regression analysis (fitting) of experimental results.

Honda et al., (2007) presented equations based on the assumptions that the unsaturated normal compression lines in the constant water content condition (although the degree of saturation is increasing) are straight in the void ratio-ln (σ) plot, as long as the degree of saturation is not close to 1.0. This assumption, according to the proposed model, is correct because the compression lines in the yield state follow the S_r-lines according to its degree of saturation. The positions of the S_r-lines are fixed for each soil. Therefore, all the normal compression lines for different initial dry densities (under the same water content) follow one straight line according to:

$$G_s.w = S_r.e \longrightarrow e_{uns} = G_s.w / S_r \tag{7.1}$$

The work of Horpibulsuk et al., (2008a), specifically (Equation 2.22), can be explained by the relationship between NCL and liquid limit (*LL*) by using different values of liquid limits to cover the range of fine-grained soils. The optimum water content (*OWC*), according to equation (6.5) is as the following:

$$OMC = e_{NCL} \frac{1}{G_s} (S_{rc})^{2-R} \tag{7.2}$$

$$OMC = e_{NCL} K \tag{7.3}$$

$$K = \frac{(S_{rc})^{2-R}}{G_s} \tag{7.4}$$

where K is constant for each soil (G_s, S_{rc} and R are constant for the same soil). Thus, the ratio between OMC/OMC_{SP} can be calculated as:

$$\frac{OMC}{OMC_{SP}} = \frac{e_{NCL}}{e_{NCL\ (593\ kPa)}} \tag{7.5}$$

Now, if the saturated NCL general equation presented by Nagaraj and Murthy (1986), (Equation 7.6), is used, Equation (7.5) is rewritten as in Equation (7.7).

$$e_{NCL} = G_s \cdot LL\ (1.122 - 0.2343 \log \sigma) \tag{7.6}$$

$$\frac{OMC}{OMC_{SP}} = 2.375 - 0.496 \log(CE) \tag{7.7}$$

As shown in Figure (7.5), Equation (7.7) is close to Equation (2.22). It is believed that the difference between Equations (2.22) and (7.7) is a result of the fact that Equation (7.6) is a fitting equation for only 11 different soils with a limited range of LL (36%< LL < 160%) and a limited range of stresses (about 800 kPa). However, Equation (2.22) was generated by fitting 24 different soils with LL (17%< LL<256%) and a larger range of compaction effort (356 to 2694 kJ·m/m^3).

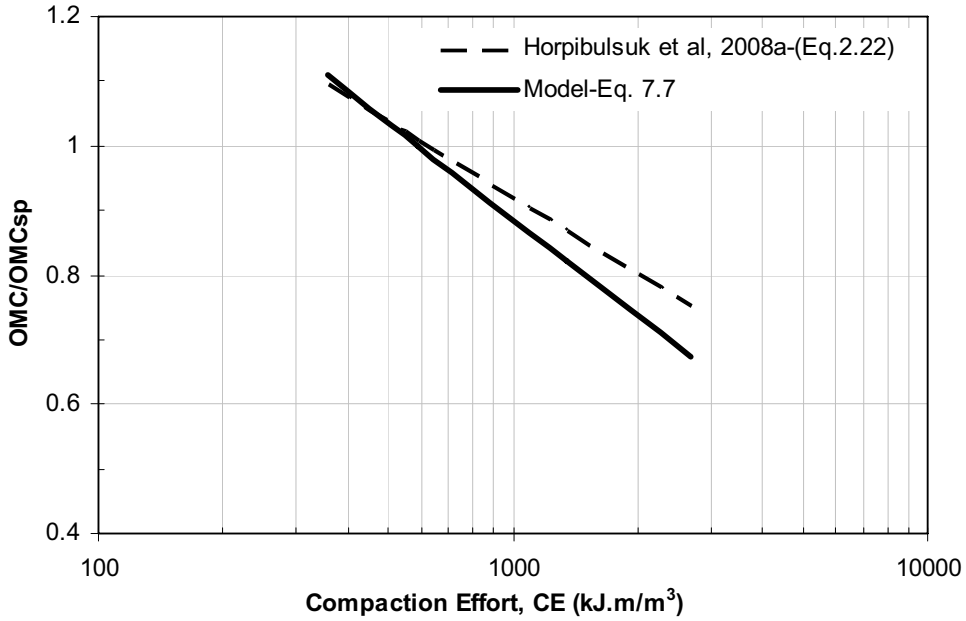

Figure 7.5 Normalization of OMC-compaction effort relationship.

7.5 Applications

The model was applied to several datasets from the literature with a large range of liquid limit values (37 % to 180 %). Four different soils were chosen (Table 7.1): natural Boom clay [Boom] (Romero, 1999); pure calcigel (calcium-type) bentonite [100B2]; bentonite-sand mixture [50B2]; and [30B2] from (Agus, 2005 and Arifin 2008). Fifteen experimental datasets of compaction curves for the four soils were collected: nine static compaction curves for the natural Boom clay, and two dynamic compaction curves for each bentonite-sand mixture.

The critical degrees of saturation were determined directly from the experimental results. The one dimensional saturated NCL and SWCC of natural Boom Clay were taken from Romero (1999). The one dimensional saturated NCL of 100B2 was taken from Baille et al., (2010), and that for 50B2 was provided in Figure (5.52) in chapter 5. For 30B2 mixture, the one dimensional saturated NCL test results were taken from Al-Badran and Schanz (2009b). The SWCC of all bentonite-sand mixtures were obtained from Arifin (2008).

Figures (7.6-7.9) present the predicted and measured compaction curves for the above selected soils. The model predictions show good agreement with the experimental results for both compaction and suction data.

Table 7.1 Properties of the soils used in application for the compaction model.

Soil Symbol	G_s	*LL*	S_{rc}	*R*	*M*
		%			
Boom	2.7	58	0.90	0.35	0.35
100B2	2.8	180	0.90	0.04	-
50B2	2.725	74	0.865	0.15	-
30B2	2.695	37	0.85	0.45	-

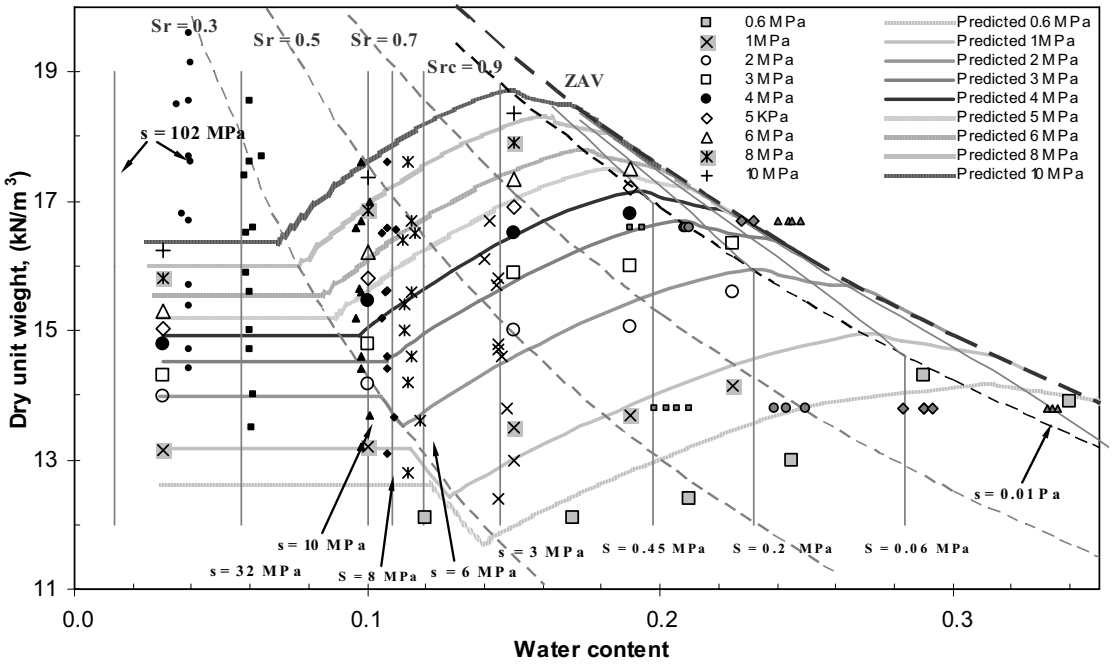

Figure 7.6 Static compaction curves and contour lines of equal suction for natural Boom clay (exp. Data from Romero, 1999), the points are the experimental results and the lines are the model predictions.

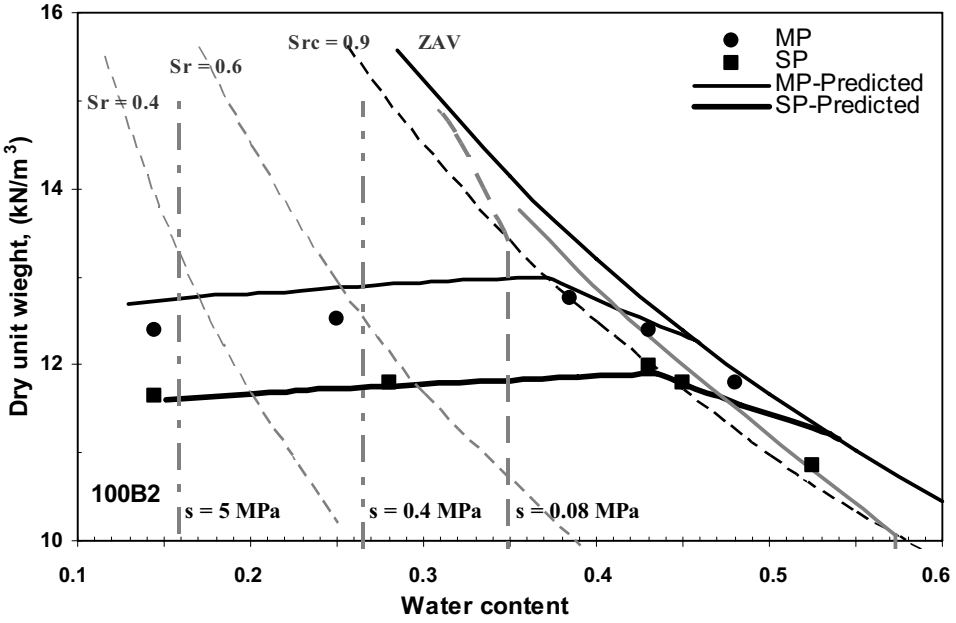

Figure 7.7 Experimental and the model predictions of dynamic compaction curves and contour lines of equal suction for 100B2 soil (exp. Data from Agus, 2005 and Arifin, 2008).

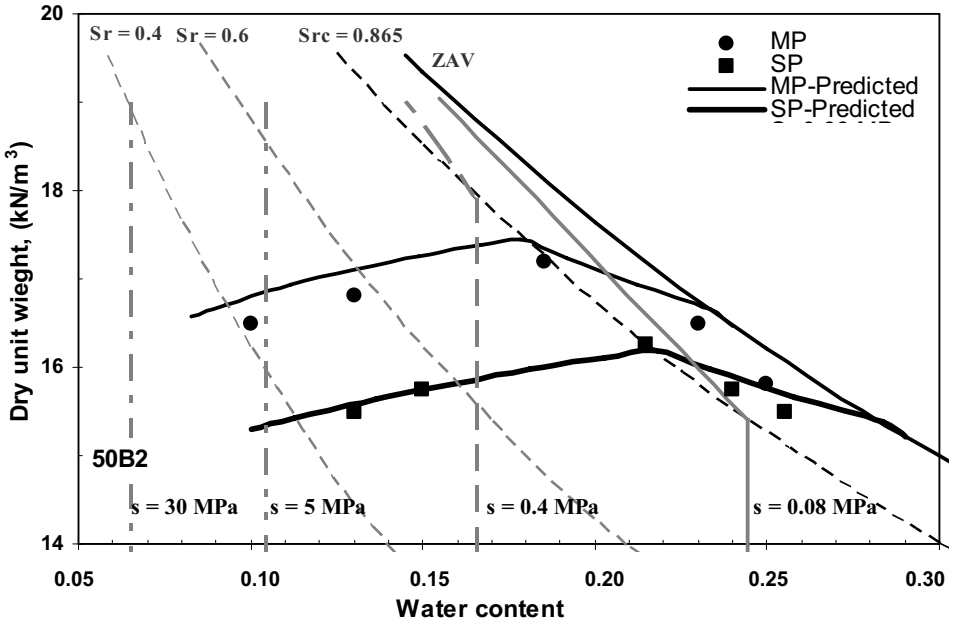

Figure 7.8 Experimental and the model predictions of dynamic compaction curves and contour lines of equal suction for 50B2 soil (exp. Data from Agus, 2005 and Arifin, 2008).

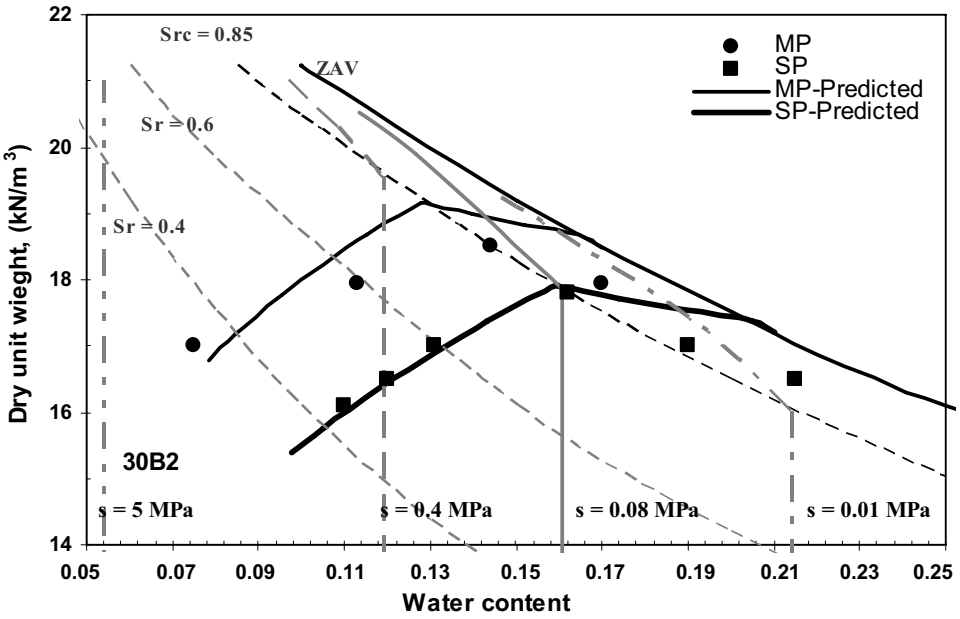

Figure 7.9 Experimental and the model predictions of dynamic compaction curves and contour lines of equal suction for 30B2 soil
(exp. Data from Agus, 2005 and Arifin, 2008).

7.6 A stepwise procedure for fast estimation of optimum water content (*OWC*) and maximum dry unit weight (γ_{dmax})

A simple chart based on liquid limit values for straight forward estimation of the maximum dry density (γ_{dmax}) and the optimum water content (*OWC*) without performing laboratories proctor tests is presented in this section. This chart depends on Equation (7.2) to determine the maximum dry density and the optimum water content. Equation (7.6) from Nagaraj and Murthy (1986) is used to predict the NCL from the LL to identify the value of e_{NCL} with different compaction efforts. To simplify the model, it is assumed that the specific gravity, G_s, taken equal to 2.7, and based on the experimental results, the following values are adopted: S_{rc} = 0.87 and R = 0.5 for the range of liquid limit from 20 % to 120 %. Figure (7.10) shows the relationship between the maximum dry density (γ_{dmax}) and the optimum water content (*OWC*) for a large range of liquid limit values (20%-120%) for Reduced Proctor RP (*CE* = 356 $kJ{\cdot}m/m^3$), Standard Proctor SP (*CE* = 593 $kJ{\cdot}m/m^3$) and Modified Proctor MP (*CE* = 2694 $kJ{\cdot}m/m^3$). The maximum dry density for each compaction effort decreases with increasing liquid limit. The behavior of the optimum water content is the reverse of that of the maximum dry density. The rate of increase in the maximum dry density increases slightly as the compaction effort increases. Figure (7.11) presents the comparison between the charts using the new model and the other charts using regression analysis from Al-Khafaji (1993) and Blotz et al. (1998) for different compaction energies. Al-Khafaji (1993) established two charts for Standard

proctor test for range of liquid limit from 20 % to 80 %: one for USA soils and the second for Iraqi soils. In these charts the liquid limit and plastic limit were used in the regression analysis (Figure 7.11 shows the chart of Al-Khafaji, 1993, for plastic limit = 20 % only). Blotz et al. (1998) established chart for Reduced Proctor RP (CE = 356 $kJ{\cdot}m/m^3$), Standard Proctor SP (CE = 593 $kJ{\cdot}m/m^3$) and Modified Proctor MP (CE = 2694 $kJ{\cdot}m/m^3$) using liquid limit for range from 20 % to 70 %.

As it can be seen in Figure (7.11) there are some discrepancies between the curves in the initial part till 40 % liquid limit. Generally, the curves of the proposed model have the highest values of the maximum dry density (γ_{dmax}), and the curves of the Al-Khafaji (1993) give the lowest values. The discrepancies of the new chart may be attributed to the fitting equation of the saturated NCL by Nagaraj and Murthy (1996), Equation (7.6). After 50 % liquid limit all the curves indicate very close behavior except the curves related to the USA soils by Al-Khafaji (1993). The curves related to the USA soils decreases when compared with the other curves as the liquid limit increases. The curves related to the optimum water content have an opposite behavior related to the maximum dry density curves.

Data for 147 different fine-grained soils (LL: 17%-110%) from 24 reported literatures and the present study (Table 7.2) were used to validate the proposed chart. The total data comprise of 211 peak compaction points PCPs: 42 for MP, 147 for SP, and 22 for RP, respectively. Figure (7.12) presents the comparison between the new chart for the peak compaction points and the experimental data. The figure shows that the new chart results generally show good agreement with the experimental data. Thus, the proposed chart can be used for fast estimation of maximum Dry density (γ_{dmax}) and Optimum water content (OWC).

Table 7.2. Peak compaction points data for 147 different fine-grained soils used in the verification of the proposed chart.

Nr.	Soil	LL	Reduced Proctor		Standard Proctor		Modified Proctor		References
			Max. γ_{dry}	*OWC*	*Max.* γ_{dry}	*OWC*	*Max.* γ_{dry}	*OWC*	
		%	kN/m^3	%	kN/m^3	%	kN/m^3	%	
1	A	33	17.1	18.5	17.7	17.5	19.3	12.2	Blotz et al., 1998
2	B	31	17.2	18.5	17.8	16.5	19.4	12.5	Blotz et al., 1998
3	C	35	17	18.5	17.5	16.6	19.4	11.5	Blotz et al., 1998
4	D	27	18.6	14.4	19.1	13	20.5	9	Blotz et al., 1998
5	E	41	16.2	20	16.7	18	18.7	13.3	Blotz et al., 1998
6	F	17	19.8	10.1	20.4	9.4	21.7	7.9	Blotz et al., 1998
7	G	18	19.9	9.3	20.5	8.9	22	7.3	Blotz et al., 1998
8	H	55	15.2	26	15.7	23	17.7	16	Blotz et al., 1998
9	I	55	14.1	30.6	14.4	29.4	15.8	23.5	Daniel and Benson, 1990
10	J	34	16.8	19.4	17.3	17.5	18.8	13.1	Daniel and Benson, 1990
11	K	70	13.8	27.5	15.4	24	17.1	19	Benson and Trast, 1995
12	L	49	17	21	17.6	18	19.4	12.5	Benson and Trast, 1995
13	M	27	18.5	14	19.1	12.5	20.5	8	Benson and Trast, 1995
14	N	53	16.6	19	17.9	16	19	12	Benson and Trast, 1995
15	O	67	15.6	23	16.3	21.5	18.4	16	Benson and Trast, 1995
16	P	29	18.5	13	19	12	20.4	10	Benson and Trast, 1995
17	Q	37	16.7	15	17.5	14	19.5	12	Benson and Trast, 1995
18	R	24	18.7	13.5	20.4	10	21.2	9	Benson and Trast, 1995
19	S	43	16	21	16.5	20	18.6	14	Daniel and Wu, 1993
20	T	32	18.3	14	19.5	13	20.6	10	Blotz et al., 1998
21	U	30	17.6	16	18.4	14	19	12	Blotz et al., 1998
22	V	32	17.5	15.8	18	15.2	19.5	10.9	Blotz et al., 1998
23	AGC(K-treated)	54.5	-	-	14.1	23.5	-	-	Al-Zoubi, 2008
24	AGC(Ca-treated)	72	-	-	14.3	23	-	-	Al-Zoubi, 2008
25	AGC(Untreated)	107.8	-	-	12.8	31.5	-	-	Al-Zoubi, 2008
26	Low plasticity clay	41	-	-	16.8	17	18.8	13	Benson et al., 1997
27	Residual soil	31	-	-	18.8	12.8	-	-	Leong et al., 2007
28	Silty clay	51	-	-	15.8	22.5	17.4	17	Horpibulsuk et al., 2006
29	Lateritic soil	53	-	-	19	11.5	19.8	8.7	Horpibulsuk et al., 2006
30	Silty clay1	39.7	-	-	17.6	15.6	20	10.8	Horpibulsuk et al., 2008a
31	Silty clay2	42.3	-	-	17.5	16.5	19.3	11.9	Horpibulsuk et al., 2008a
32	Silty clay3	47.5	-	-	15.1	22	16.4	18.1	Horpibulsuk et al., 2008a
33	Silty clay4	49.3	-	-	16.9	17.7	18.9	12.4	Horpibulsuk et al., 2008a
34	Kaolinite	52	-	-	14	29.3	15.4	23.3	Horpibulsuk et al., 2008a
35	Weathered clay	63.5	-	-	14.4	27.2	16.2	20.3	Horpibulsuk et al., 2008a
36	silty clay	70	-	-	14.55	30	17	22	Ellis, 1980
37	Kaolinite	28.2	-	-	15.9	18	-	-	Gurtug and Sridharan, 2002
38	Degrirmenlik	37	-	-	17	18.5	-	-	Gurtug and Sridharan, 2002
39	Tuzla	52.9	-	-	15.35	23	-	-	Gurtug and Sridharan, 2002
40	Akdeniz	49.6	-	-	15.5	23	-	-	Gurtug and Sridharan, 2002
41	Montmorillonitic clay	98	-	-	12.5	32	-	-	Gurtug and Sridharan, 2002
42	CL-Lean clay	42	-	-	16.2	22	-	-	Sawangsuriya et al., 2008
43	MI-Silt	28	-	-	17.75	15	-	-	Sawangsuriya et al., 2008
44	SC-Clayly sand	28	-	-	18.6	13.8	19.3	12	Sawangsuriya et al., 2008
45	A	100	-	-	12.7	35	14.9	26	Tripathy et al., 2002
46	B	74	-	-	14.1	30	17.1	21	Tripathy et al., 2002
47	Silty sand	29	-	-	18.4	14	-	-	Pereira & Fredlund , 2000
48	1	84	-	-	13.8	28	-	-	Pandian et al., 1997
49	2	62	-	-	15.2	24	-	-	Pandian et al., 1997

		LL	Reduced Proctor		Standard Proctor		Modified Proctor		
			Max. γ_{dry}	*OWC*	*Max.* γ_{dry}	*OWC*	*Max.* γ_{dry}	*OWC*	
50	**3**	48	-	-	16.2	21	-	-	Pandian et al., 1997
51	**Jossigny silt**	37	-	-	16.7	18	-	-	Delage et al., 1996
52	**Kaolin Speswhite**	64	-	-	13.3	31	-	-	Trantino and DeCol, 2008
53	**Embankment soil**	18.7	-	-	23.2	6.6	-	-	Hoffmann and Tarantino, 2008
54	**Granite residual soil**	68	-	-	14.47	26.2	16.36	20.7	Kabir and Taha. 2004
55	**100B1**	90	-	-	14	32	16	26	Experimental results
56	**30B1**	30	-	-	18.5	13	20.3	10	Experimental results
57	**Pearly clay**	63	-	-	14.2	28			Sun et al.,2007
58	**70M+20K+10C**	29	-	-	18	15.5	20.2	12	Jotisankasa et al., 2007
59	**1-Balad-Ruz**	32	-	-	18.2	16	-	-	Al-Khafaji, 1993
60	**2-Balad-Ruz**	49	-	-	17.9	16	-	-	Al-Khafaji, 1993
61	**3-Balad-Ruz**	41	-	-	17.8	17	-	-	Al-Khafaji, 1993
62	**4-Balad-Ruz**	46	-	-	17.5	18	-	-	Al-Khafaji, 1993
63	**5-Balad-Ruz**	35	-	-	17.68	17	-	-	Al-Khafaji, 1993
64	**6-Balad-Ruz**	36	-	-	17.4	18.2	-	-	Al-Khafaji, 1993
65	**7-Balad-Ruz**	52	-	-	16.7	19.8	-	-	Al-Khafaji, 1993
66	**8-Balad-Ruz**	40	-	-	16.8	20	-	-	Al-Khafaji, 1993
67	**9-Balad-Ruz**	43	-	-	17.3	18.2	-	-	Al-Khafaji, 1993
68	**10-Balad-Ruz**	40	-	-	17.3	17.2	-	-	Al-Khafaji, 1993
69	**11-Balad-Ruz**	38	-	-	17.2	19	-	-	Al-Khafaji, 1993
70	**12-Balad-Ruz**	43	-	-	17.39	18.2	-	-	Al-Khafaji, 1993
71	**13-Balad-Ruz**	40	-	-	17.61	17.4	-	-	Al-Khafaji, 1993
72	**14-Balad-Ruz**	48	-	-	17.6	19.6	-	-	Al-Khafaji, 1993
73	**15-Balad-Ruz**	44	-	-	16.9	19.3	-	-	Al-Khafaji, 1993
74	**16-Balad-Ruz**	38	-	-	18.25	16	-	-	Al-Khafaji, 1993
75	**17-Balad-Ruz**	33	-	-	17.5	18.2	-	-	Al-Khafaji, 1993
76	**18-Balad-Ruz**	37	-	-	17.9	16.6	-	-	Al-Khafaji, 1993
77	**19-Balad-Ruz**	34	-	-	18.2	16	-	-	Al-Khafaji, 1993
78	**20-Balad-Ruz**	33	-	-	18.3	15	-	-	Al-Khafaji, 1993
79	**21-Balad-Ruz**	33	-	-	18	17	-	-	Al-Khafaji, 1993
80	**22-Balad-Ruz**	39	-	-	17.5	18.6	-	-	Al-Khafaji, 1993
81	**23-Balad-Ruz**	49	-	-	16.7	20	-	-	Al-Khafaji, 1993
82	**24-Balad-Ruz**	49	-	-	16.7	20	-	-	Al-Khafaji, 1993
83	**25-Balad-Ruz**	45	-	-	16.8	19.5	-	-	Al-Khafaji, 1993
84	**26-Balad-Ruz**	34	-	-	17.7	17	-	-	Al-Khafaji, 1993
85	**27-Balad-Ruz**	43	-	-	17.2	18.5	-	-	Al-Khafaji, 1993
86	**28-Balad-Ruz**	43	-	-	16.82	20	-	-	Al-Khafaji, 1993
87	**29-Balad-Ruz**	35	-	-	17.53	18.4	-	-	Al-Khafaji, 1993
88	**30-Balad-Ruz**	38	-	-	17.13	19.5	-	-	Al-Khafaji, 1993
89	**1-Abu-Ghraib**	54	-	-	15.8	22.3	-	-	Al-Khafaji, 1993
90	**2-Abu-Ghraib**	64	-	-	15.1	24.8	-	-	Al-Khafaji, 1993
91	**3-Abu-Ghraib**	56	-	-	15.62	23.3	-	-	Al-Khafaji, 1993
92	**4-Abu-Ghraib**	66	-	-	15.2	24.5	-	-	Al-Khafaji, 1993
93	**5-Abu-Ghraib**	63	-	-	15.22	24.3	-	-	Al-Khafaji, 1993
94	**6-Abu-Ghraib**	50	-	-	15.86	23	-	-	Al-Khafaji, 1993
95	**7-Abu-Ghraib**	62	-	-	15.2	25.5	-	-	Al-Khafaji, 1993
96	**8-Abu-Ghraib**	64	-	-	14.85	26	-	-	Al-Khafaji, 1993
97	**9-Abu-Ghraib**	59	-	-	15.1	26	-	-	Al-Khafaji, 1993
98	**10-Abu-Ghraib**	41	-	-	16	22.7	-	-	Al-Khafaji, 1993
99	**11-Abu-Ghraib**	46	-	-	16.2	23.5	-	-	Al-Khafaji, 1993
100	**12-Abu-Ghraib**	59	-	-	15.66	24.5	-	-	Al-Khafaji, 1993
101	**13-Abu-Ghraib**	60	-	-	15.48	25.5	-	-	Al-Khafaji, 1993
102	**14-Abu-Ghraib**	51	-	-	16.08	22.5	-	-	Al-Khafaji, 1993

		LL	Reduced Proctor		Standard Proctor		Modified Proctor		
			Max. γ_{dry}	*OWC*	*Max.* γ_{dry}	*OWC*	*Max.* γ_{dry}	*OWC*	
103	**15-Abu-Ghraib**	54	-	-	15.86	23	-	-	Al-Khafaji, 1993
104	**16-Abu-Ghraib**	54	-	-	16.48	22	-	-	Al-Khafaji, 1993
105	**1-Suwaira**	27	-	-	17.84	17	-	-	Al-Khafaji, 1993
106	**2-Suwaira**	34	-	-	17.73	17	-	-	Al-Khafaji, 1993
107	**3-Suwaira**	33	-	-	17.81	17.5	-	-	Al-Khafaji, 1993
108	**4-Suwaira**	35	-	-	17.4	17.5	-	-	Al-Khafaji, 1993
109	**5-Suwaira**	35	-	-	17.84	16.5	-	-	Al-Khafaji, 1993
110	**7-Suwaira**	27	-	-	18.39	16	-	-	Al-Khafaji, 1993
111	**8-Suwaira**	27	-	-	17.82	17.3	-	-	Al-Khafaji, 1993
112	**9-Suwaira**	30	-	-	17.51	17.8	-	-	Al-Khafaji, 1993
113	**10-Suwaira**	36	-	-	17.29	18.7	-	-	Al-Khafaji, 1993
114	**11-Suwaira**	31	-	-	17.51	18	-	-	Al-Khafaji, 1993
115	**12-Suwaira**	33	-	-	17.4	18	-	-	Al-Khafaji, 1993
116	**13-Suwaira**	32	-	-	17.47	17	-	-	Al-Khafaji, 1993
117	**14-Suwaira**	36	-	-	16.9	20	-	-	Al-Khafaji, 1993
118	**15-Suwaira**	39	-	-	16.56	21.5	-	-	Al-Khafaji, 1993
119	**1-Kamaliya**	31	-	-	17.24	18.7	-	-	Al-Khafaji, 1993
120	**2-Kamaliya**	23	-	-	17.52	17.5	-	-	Al-Khafaji, 1993
121	**3-Kamaliya**	20	-	-	19.18	13.5	-	-	Al-Khafaji, 1993
122	**4-Kamaliya**	36	-	-	16.78	20.5	-	-	Al-Khafaji, 1993
123	**5-Kamaliya**	34	-	-	16.6	21.5	-	-	Al-Khafaji, 1993
124	**6-Kamaliya**	26	-	-	17.4	18.5	-	-	Al-Khafaji, 1993
125	**7-Kamaliya**	32	-	-	17.2	19	-	-	Al-Khafaji, 1993
126	**8-Kamaliya**	54	-	-	15.34	26	-	-	Al-Khafaji, 1993
127	**9-Kamaliya**	42	-	-	16.4	22	-	-	Al-Khafaji, 1993
128	**11-Kamaliya**	31	-	-	17.45	17.6	-	-	Al-Khafaji, 1993
129	**12-Kamaliya**	41	-	-	16.42	20.5	-	-	Al-Khafaji, 1993
130	**13-Kamaliya**	57	-	-	15.54	24.5	-	-	Al-Khafaji, 1993
131	**14-Kamaliya**	36	-	-	17.74	18.9	-	-	Al-Khafaji, 1993
132	**15-Kamaliya**	36	-	-	17.5	18	-	-	Al-Khafaji, 1993
133	**16-Kamaliya**	35	-	-	18.14	16.2	-	-	Al-Khafaji, 1993
134	**17-Kamaliya**	36	-	-	17.7	16.2	-	-	Al-Khafaji, 1993
135	**18-Kamaliya**	39	-	-	17.66	16.7	-	-	Al-Khafaji, 1993
136	**19-Kamaliya**	29	-	-	17.64	17.2	-	-	Al-Khafaji, 1993
137	**20-Kamaliya**	39	-	-	16.5	20.7	-	-	Al-Khafaji, 1993
138	**21-Kamaliya**	43	-	-	16.6	20.8	-	-	Al-Khafaji, 1993
139	**22-Kamaliya**	31	-	-	18.14	16.2	-	-	Al-Khafaji, 1993
140	**23-Kamaliya**	29	-	-	18.14	16.5	-	-	Al-Khafaji, 1993
141	**24-Kamaliya**	28	-	-	18.44	15.3	-	-	Al-Khafaji, 1993
142	**25-Kamaliya**	33	-	-	17.34	18.5	-	-	Al-Khafaji, 1993
143	**26-Kamaliya**	35	-	-	17.2	17	-	-	Al-Khafaji, 1993
144	**Natural Boom**	60	-	-	14.3	29	16.5	22	Romero, 1999
145	**100B3-Calcigle**	110	-	-	12	37	-	-	Experimental results
146	**30B2**	37	-	-	17.8	16	18.5	14	Arifin,. 2008+Agus, 2005
147	**50B2**	63	-	-	16.3	20.5	17.2	18.5	Arifin, 2008+Agus, 2005

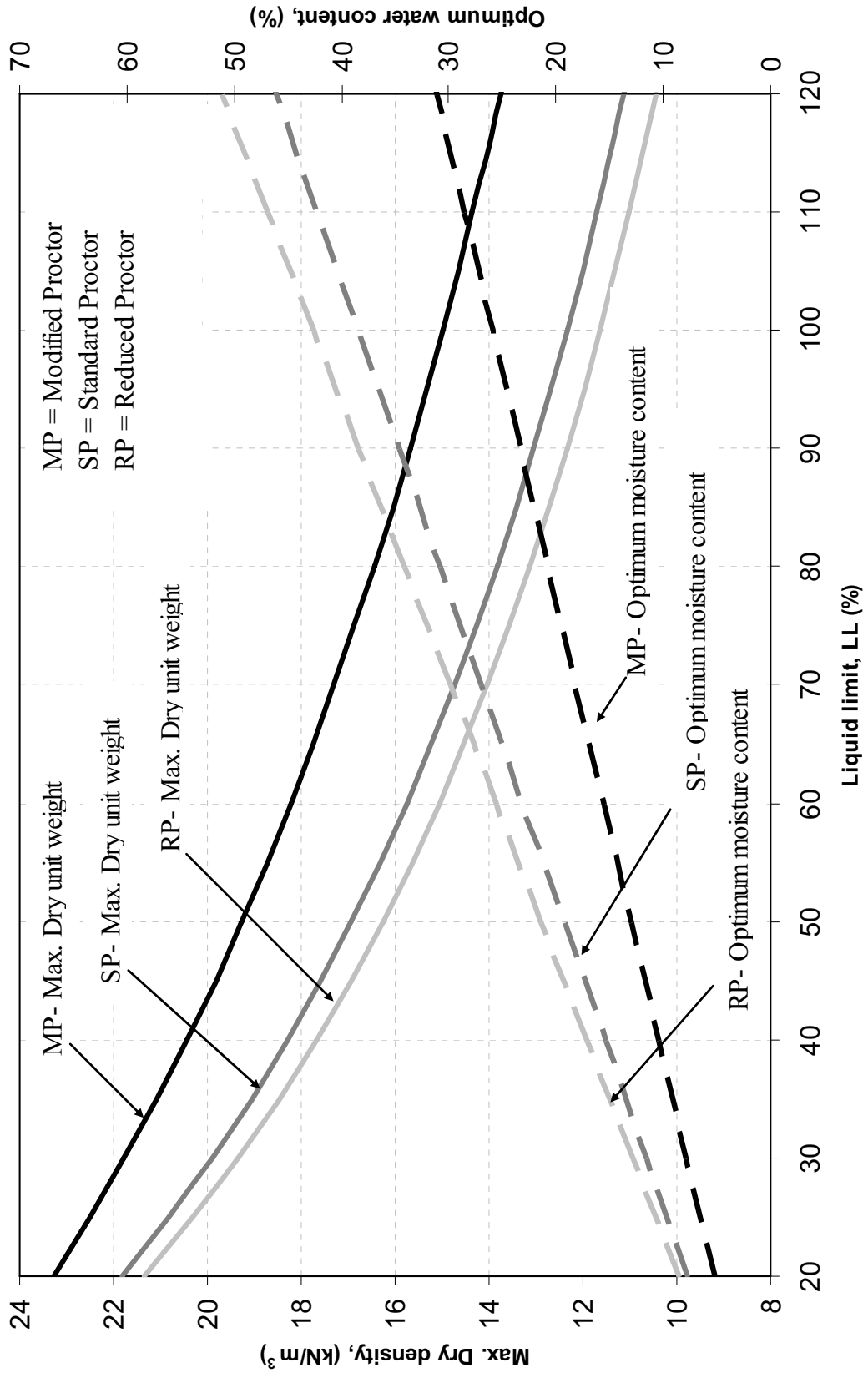

Figure 7.10 Optimum water content (*OWC*)-max. Dry unit weight (γ_{dmax}) chart using the proposed model depending upon LL.

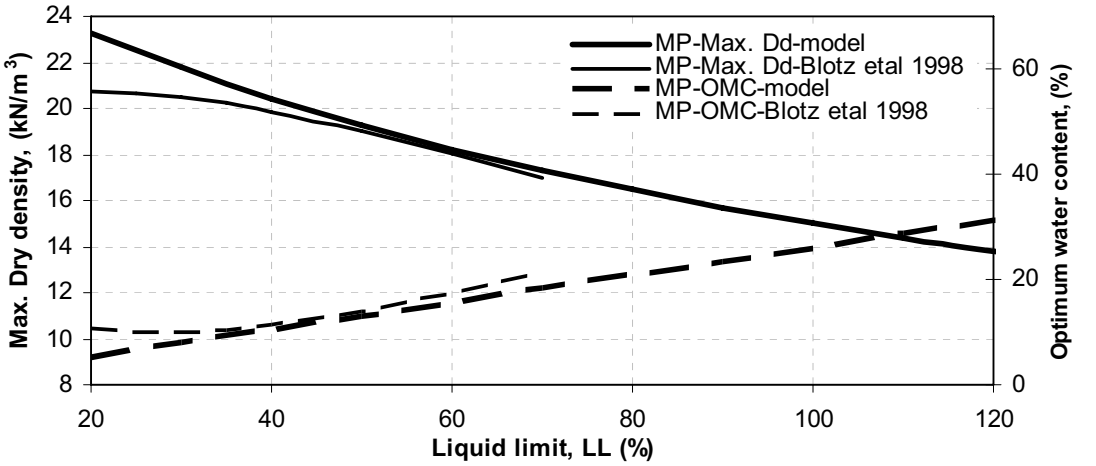

a

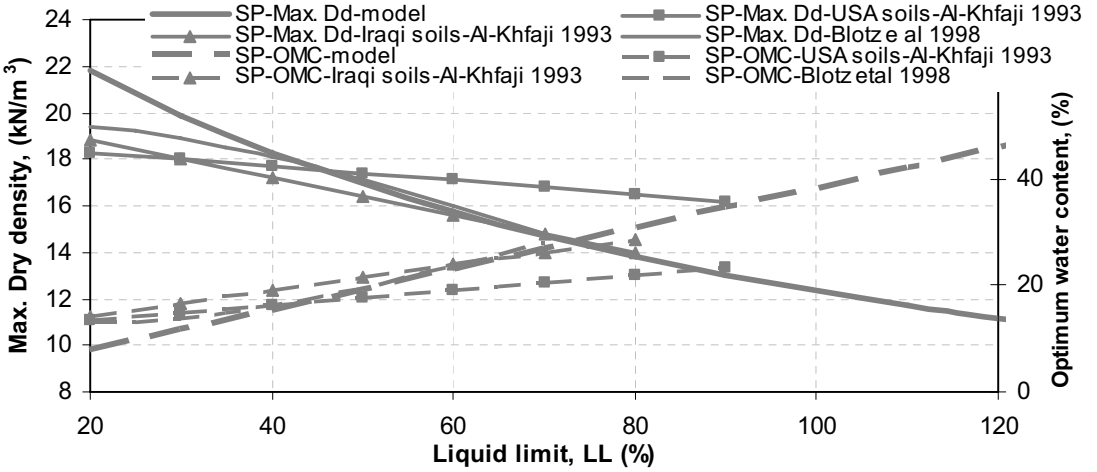

b

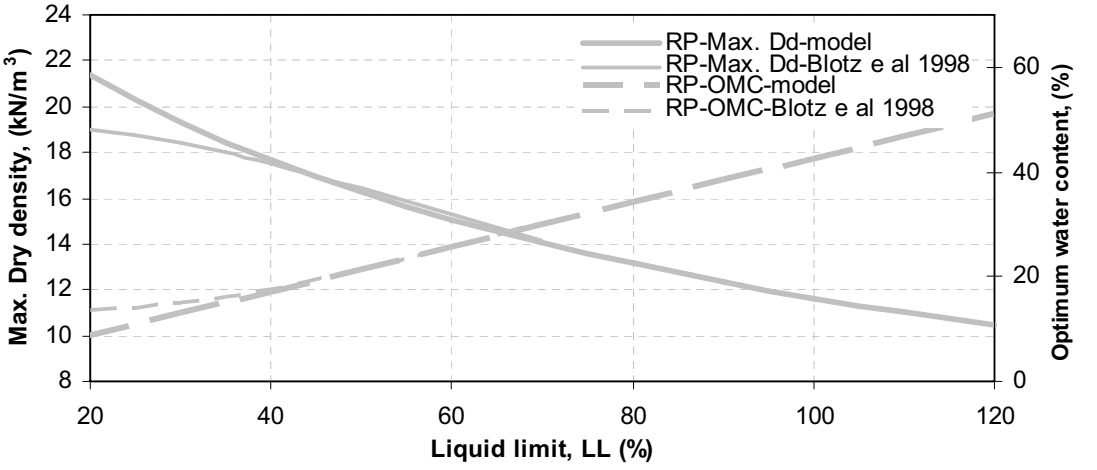

c

Figure 7.11 Optimum water content (*OWC*)-max. Dry unit weight (γ_{dmax}) charts for: Al-Khafaji, 1993; Blotz et al, 1998; and the present study using the proposed model: a-Modified Proctor (MP), b-Standard Proctor (SP), and c-Reduced Proctor (RP).

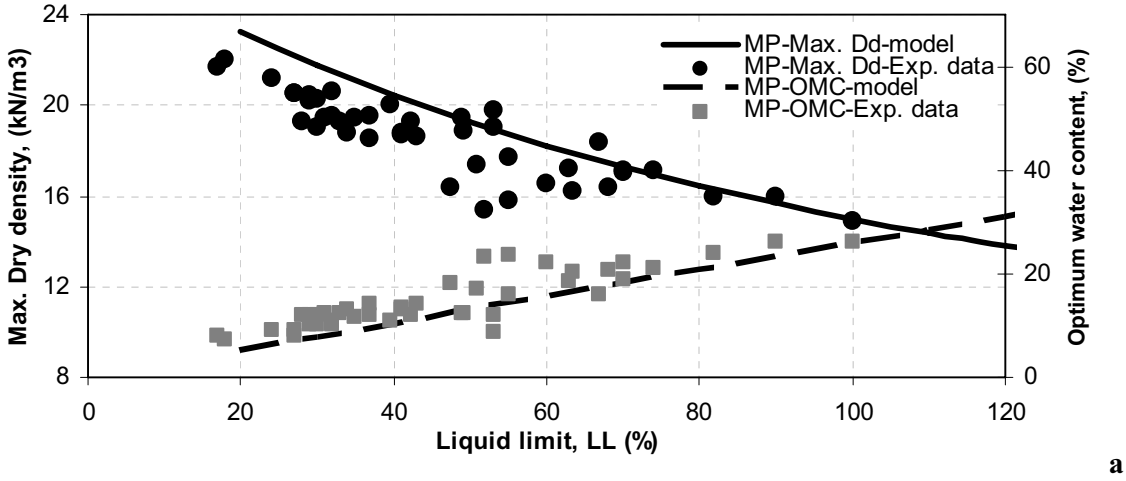

a

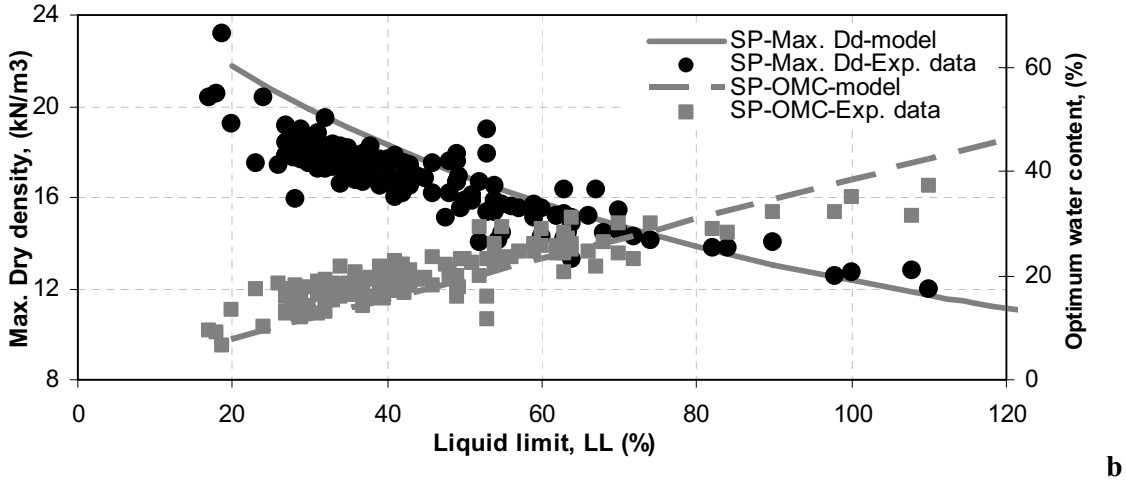

b

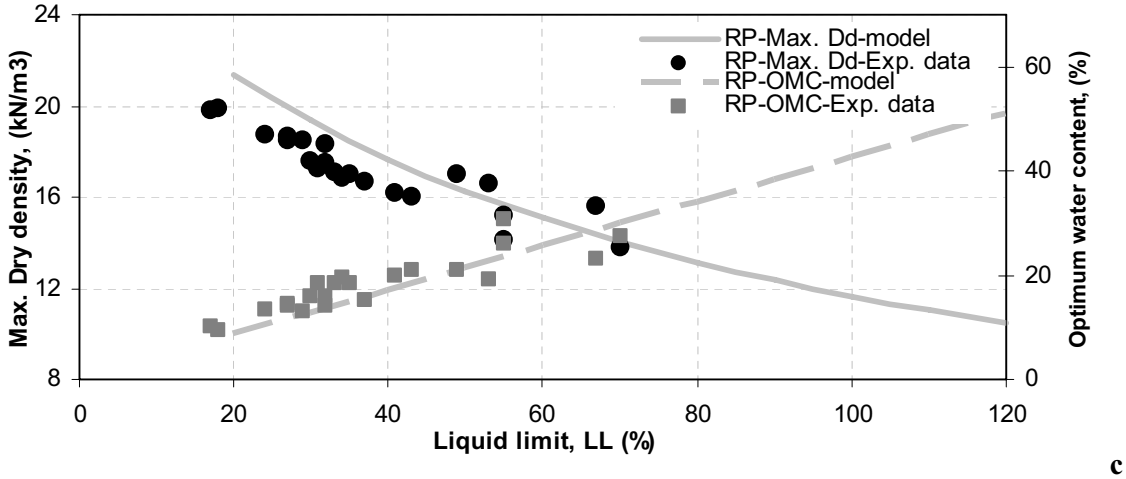

c

Figure 7.12 Optimum water content (*OWC*)-max. Dry unit weight (γ_{dmax}) chart using the proposed model depending upon LL and the experimental results from literature (Table 7.2): a-Modified Proctor (MP), b-Standard Proctor (SP), and c-Reduced Proctor (RP).

7.7 Summary

A model of the compaction curve for fine-grained soils is presented. Main assumption is that the compaction curves represent the state surface of unsaturated state (as proposed in chapter 6), and the maximum dry density γ_{dmax} for all compaction efforts occurs at constant degree of saturation, and this saturation is the critical degree of saturation. In the proposed model, the compaction curve can have two peaks. One peak has low water content, and the second peak has high water content. The compaction model can describe the lines of equal suction on the compaction curves. The new compaction curve model has been verified in two ways: first quantitatively, by the experimental results of present study and the experimental data reported in literature and second qualitatively, by examining the relationships from other models in the literature. The model predictions match very well with the experimental data. A simple chart based on this model and using liquid limit is presented to estimate γ_{dmax} and *OWC*. This chart covers a large range of LL values (20 %-120 %). The proposed chart has been validated using reported data for 147 different clay soils. The chart generally shows good agreement with the experimental data.

Chapter 8
Summary and Outlook

8.1 Introduction

In this chapter a summary of the main outcomes of the study and the outlook for further work is outlined. In this thesis, a new volumetric yielding model for unsaturated fine-grained soils has been presented. The summary is categorized into three sections as follows: summary of the experimental results, summary of new volumetric yielding mode for unsaturated fine-grained soils, and finally the summary connected to the modelling of the compaction curve.

8.2 Summary

8.2.1 Experimental results

The results of experimental tests for 30B and 100B soils are presented and discussed. The set of tests to asses the volumetric yielding or the volume change at yield state consists of five different types of 1D-compression controlled-suction tests: constant degree of saturation test, constant net stress test, constant suction test, changing both net stress and suction test, and the compaction tests. Slurry and unsaturated loose conditions are chosen as initial states in the experimental program.

1. The results of constant degree of saturation tests show that the NCL's are almost straight in semi-log scale, and have slopes slightly more than the slope of the saturated NCL. This behavior depicts almost the same behavior as it was assumed in Al-Badran (2001) and Kanazawa et al. (2009).
2. The results of drying under constant net stress condition show that for all initial densities the volume decreased with increasing suction until reaching air-entry value, then the reduction in volume reduced. The gravimetric water content continued decreasing as suction increased, and all gravimetric water content curves for different constant net stress joined as suction increases.
3. The results of wetting under constant net stress for initial loose condition (collapse test) show three different phases during reducing the suction (wetting) process.

4. The results of constant suction tests that show the position and the slope of NCL's depend on both net stress and suction. The NCL's either, for low suction value, has void ratio lower than the saturated NCL (associated with lower slope than the saturated NCL), or the NCL has void ratio higher than the saturated NCL (associated with higher slope than the saturated NCL) for higher suction value.
5. The verification tests (changing both net stress and suction test) showed that the state surface at yield state for unsaturated soil is unique.
6. Double peaks are observed in compaction curves. The contour lines of equal suction were established in the dry of optimum (DOP) state only. All contour lines of equal suction show vertical lines in dry density-water content relationship.
7. The results of SWCC tests under unconfined condition show, (i) significant hysteresis behavior associated with absence of residual suction; (ii) for low expansive soil (e.g., 30B soil) the value of air-entry suction of initial slurry condition remains constant initially then increases as the density increases; (iii) while for high expansive soil (e.g., 100B soil) the density has no effect on the value of air-entry value of initial slurry condition for the tested range of density.

8.2.2 New volumetric yielding model for unsaturated fine-grained soils

A new model of the state surface at yield state for unsaturated fine-grained soils is presented. It contents the following:

1. The position of the state surface is defined by the NCL's of constant degree of saturation, S_r-lines (Al-Badran, 2001), which is modified according to the microstructural consideration of (Nagaraj et al, 2006a and b).
2. According to the new model, for constant net applied vertical stress, the entire range of degree of saturation (from fully dry to fully saturated condition) one can distinguish five different trends (intervals).
3. The basic parameters of the new model are net stress, degree of saturation, critical degree of saturation, SWCC, the parameter that controls the influence of the degree of saturation to the increase of the void ratio under constant net stress in the third interval of degree of saturation (R), and the parameter that controls the position of e_{max} in the second interval of degree of saturation (M).
4. The model shows that the unsaturated NCL's for constant degree of saturation (S_r-lines) are not parallel, but they have slightly different slopes, and empirical equations can be proposed to determine the volumetric yielding at each degree of saturation.
5. The model predictions of the model show that the slope of the S_r-lines firstly decreases as the degree of saturation decreases until reaching the critical degree of saturation

(S_{rc}), then the slope increases until finally the slope reduce rapidly to the slope of the fully dry NCL.

6. The model predictions show that the behavior of NCL's under constant suction condition in void ratio-log net stress plane is very complicated and depends on the value of suction and net stress.
7. The slope of NCL under low constant suction condition decreases as the suction increases until reaching the air-entry value. Then the slope of the NCL increases with increasing the constant suction condition. Consequently, with increasing the suction the slope starts to decrease again until reaching the slope of the fully dry condition.
8. In case of curve for constant void ratio cross-section of state surface (CSSS), the yield net stress of CSSS curve initially decreases as the suction increases, then increases after air-entry value. The yield net stress continues increasing as suction increases until reaching the maximum value, in which the yield net stress decreases again with increasing the suction. Finally the yield net stress reaches the yield net stress at the fully dry condition. Beyond this value the yield net stress remains constant with increasing the suction.
9. In case of very low density, the CSSS curve consists only of parts from the third and second intervals of degree of saturation (when the yield net stress increases then decreases with increasing the suction). While in case of high density, the second interval of degree of saturation in the CSSS curve (when the yield net stress decreases as suction increases) will disappear.
10. The study proposed three stages of collapse behavior during wetting according to the proposed volumetric yielding model.
11. The validity of the proposed model was tested against experimental results from the present study and experimental data reported in literature. The model predictions match very well with the experimental data.
12. The proposed model provides additional understanding to the volume change behavior of unsaturated soils such as: compression, compaction, collapse.

8.2.3 Modelling the compaction curve

A model of the compaction curve for fine-grained soils is presented.

1. Main assumption is that the compaction curves reproduce the state surface at yield state of unsaturated state (as proposed in chapter 6), and the maximum dry density

γ_{dmax} for all compaction efforts occurs at one and the same degree of saturation, and this saturation is the critical degree of saturation.

2. In the proposed model, the compaction curve can have two peaks. One peak has low water content, and the second peak has high water content.
3. The compaction model can describe the lines of equal suction on the compaction curves.
4. The new compaction curve model has been verified in two ways: firstly quantitatively, against the experimental results of the present study and the experimental data reported in literature and secondly qualitatively, via examining the relationships from other models in the literature. The model predictions match very well with the experimental data.
5. A simple chart based on this model and using liquid limit is presented to estimate γ_{dmax} and *OWC*. This chart covers a large range of LL values (20 %-120 %). The proposed chart has been validated using reported data for 147 different clay soils. The chart generally shows good agreement with the experimental data.

8.3 Outlook

Based on the finding of the experimental work and the proposed models in this thesis the following further works are suggested:

1. Investigate the behavior of swelling pressure during constant volume test regarding to the proposed model in this thesis.
2. The proposed model has the ability to taken into the account the volumetric yielding behavior of unsaturated fine-grained soils. Comparison of proposed model with the other existing models for fine-grained unsaturated soil is suggested to check its applicability and compatibility.
3. As there has been little previous work done on normal consolidated lines at high suction value, a comprehensive study for the first and second intervals of degree of saturated is recommended.
4. More investigation on the wet side of optimum to enhance the results of the compaction model.

References

Abeyesekera, R. A. (1977) Stress-deformation and strength characteristics of compacted shale. Report No.**JHRP-77-24** Purdue University, West Lafayette, Ind.

Agus S.S., Schanz T. (2007) Error in total suction measurement. Proc. **2nd** International Conference: Mechanics of Unsaturated Soils (Ed. Tom Schanz), Weimar, Germany. Springer proceedings in physics. Vol. 1, pp. 59-70.

Agus, S.S. and Schanz, T. (2008) A method for predicting swelling pressure of compacted bentonites. *Acta Geotechnica*, **3**:125–137

Agus S.S. and Schanz T. (2005) Swelling pressure and total suction of compacted Bentonitesand mixtures. Proceeding of International Conference on Problematic Soils (Eds. Bilsel, H and Nalbantoglu, Z). North Cyprus. V**1**: 61-70.

Agus, S.S. (2005) An experimental study on hydro-mechanical characteristics of compacted bentonite-sand mixtures. PhD Dissertation. Faculty of Civil Eng., Bauhaus-Universität Weimar, Germany.

Aitchison, G. D. (1960) Relationships of moisture stress and effective stress functions in unsaturated soils. Proc. Conf. pore pressure. Butterworths. London: 47-52.

Aitchison, G. D. and Donald, I. B. (1956) Effective stresses in unsaturated soils." Proc. 2nd Aust. N.Z. Conf. Soil Mech.: 192-199.

Aitchison, G.D. (1965) Moisture equilibrium and moisture changes in soils beneath covered areas. A symposium in Print, (Australia), Butterworth (Ed. G.D. Aitchison).

Al-Badran, Y. (2001) Collapse behavior of Al-Tharthar gypseous soil. M.Sc. Thesis, Civil Eng., Baghdad University, Iraq.

Albrecht, B.A., Benson, C.H. and Beuermann, S. (2003) Polymer capacitance sensors for measuring gas humidity in drier soils. *Geotechnical Testing Journal*, **26**(1): 3-11.

Al-Kafaji, A. N. (1993). Estimation of soil compaction parameters by means of Atterberg limits. *Quarterly Journal of Engineering Geology*, **26**: 359-368.

Al-Mukhtar M., Qi Y., Alcover J.F., and Bergaya F. (1999) Oedometric and water-retention behavior of highly compacted unsaturated smectites. *Canadian Geotechnical Journal,* **36**: 675-684.

Alonso E. E., Gens A. and Hight D. W. 1987. Special problems soils. General report. Proc. 9th European. Conf. Soil Mech., Dublin: 1087-1146.

Alonso, E.E., Vaunat, J., and Gens, A. (1999) Modelling the mechanical behaviour of expansive clays. *Engineering Geology*, **54**: 173-183.

Alonso, E.E., Romero, E. Hoffmann, C., and Escudero, E. (2005) Expansive bentonite–sand mixtures in cyclic controlled-suction drying and wetting. *Engineering Geology*, **81**: 213–226.

Alonso, E. E., Gens, A. and Josa, A. (1990) A constitutive model for partially saturated soils. *Géotechnique,* **40** (3): 405-430.

Al-Zoubi, M. S. (2008) Swell characteristics of natural and treated compacted clays. *EJGE*, V. **13**, Band D.

Arifin, Y. and Schanz, T. (2009) Osmotic suction of highly plastic clays. *Acta Geotechnica*, **4**:177–191.

Arifin, Y.F. (2008) Thermo-Hydro-Mechanical behavior of compacted bentonite-sand mixtures: An experimental study. PhD thesis. Faculty of Civil Eng., Bauhaus-Universität Weimar, Germany.

ASTM (1997) Annual Book of Standards. Volumes **04.08** and **04.09**, Soil and rock, *ASTM International*. West Conshohocken. PA.

Aziz, A., Ali, F., Heng, C., Mohammed, T.,and Huat, B. (2006) Collapsibility and volume change behavior of unsaturated residual soil. *American Journal of Environmental Sciences*, **2** (4): 161-166, 2006

Backer, R. and Frydman, S. (2009) Unsaturated soil mechanics: critical review of physical foundations. *Engineering Geology Journal*, **106**: 26-39.

Baille, W., Tripathy, S. and Schanz, T. (2010). Swelling pressure and one-dimensional compressibility behavior of bentonite at high pressure, *Applied Clay Sci.* doi:10.1016/j.clay.2010.**01.00**2: 1-10.

Barden, L., McGown, A., and Collins, K. (1973) The collapse mechanism in partly saturated soil. *Engrg. Geol.*, **7**(1), 49-60.

Basheer, I. A. (2001). Empirical modeling of the compaction curve of cohesive soils, *Can. Geotech. Journal*. **38**: 29-45.

Basheer, I.A. (1998) Neuromechanistic-based modeling and simulation of constitutive behavior of fine-grained soils. Ph.D. dissertation, Kansas State University, Manhattan, Kans.

Basheer, I.A., and Najjar, Y.M. (1995). A neural network for soil compaction. In Numerical models in geomechanics, numerical methods in geomechanics, *NUMOG*. A.A. Balkema, Rotterdam, The Netherlands, V **5**: 435–440.

Benatti, J.C.B., Miguel, M.G., Rodrigues, R.A., and Vilar, O.M. (2010) Collapsibility study for tropical soil profile using oedometric tests with controlled suction. **5th** Int. Conf. of Unsaturated Soils-Alonso & Gens (eds), 6-8 Sep 2010, Barcelona, Spain: 193-198.

Benson, C. and Trast J. (1995). Hydraulic conductivity of thirteen compacted clays. *Clays and Clay Minerals*, **43** (6): 669-681.

Benson, C. H., Gunter, A. G., Boutwell, G. P., Trautwein, S. J. and Berzanskis, P. H. (1997). Comparison of four methods to assess hydraulic conductivity. *Journal Geotechnical and Geoenvironmental Engrg., ASCE*, V **123** (10): 929-937.

Biot, M.A. (1941) General theory of three-dimensional consolidation. *Journal App. Phys.*, V **42**: 155-164.

Bishop, A. W. and Blight, G. E. (1963) Some aspects of effective stress in saturated and partially saturated soils. *Géotechnique*, GE130301:177-197

Bishop, A. W. and Donald, I. B. (1961) The experimental study of partly saturated soil in the triaxial apparatus. Proc. **5th** International Conf. of Soil Mech. 1 : 13-21.

Bishop, A. W. (1959). The principle of effective stress. *Tecknish Ukeblad*, **106**: 859-863.

Blatz, J.A. and Graham, J. (2003) Elastic-plastic modelling of unsaturated soil using results from a new traixial test with controlled suction. *Géotechnique*, **53**(1): 113-122.

Blotz, L.R., Benson, C., and Boutwell, G. (1998). Estimating optimum water content and maximum dry unit weight for compacted clays. *J. of Geotech. Eng., ASCE*, **124**: 907–912.

Bolt, G.H. and Miller, R.D. (1958) Calculation of total and component potentials of water in soils. *American Geophysicist Union Transportaion*, **39**: 917-928.

Bolzon G, Schrefler A, and Zienkiewicz O.C. (1996) Elasto–plastic constitutive laws generalised to partially saturated states. *Géotechnique*, **46**(2):279–289.

Brackley, I.J.A. (1975) Swell under load. Proc. **6th** Reg. Conf. for Africa on Soil Mech and Found. Eng., Durban, V. 1:65-70.

Brackley, I.J.A. (1971) Partial collapse in unsaturated expansive clay. Proc. **5th** Reg. Conf. Soil Mech. Found. Eng., South Africa: 23-30.

Brookins D. (1984) *Geochemical aspects of radioactive waste disposal*. Springer-Verlag: 267- 278.

Buckingham, E. (1907) Studies of the movement of soil moisture. *USDA Bureau of Soils Bulletin*, **38**.

Burland, J. B. (1965) Some aspects of the mechanical behaviour of partly saturated soils. Moisture Equilibria and Moisture Changes in the Soils Beneath Covered Areas, G. D. Aitchison, ed., Butterworth, Sydney, Australia: 270–278.

Casini, F., Vassallo, R. , Mancuso, C. and Desideri, A. (2007) Interpretation of the behavior of compacted soils using Cam-clay extended to unsaturated conditions. **2nd** Int. Conference Mech. of Unsaturated Soil.7-9 March, Weimar, Germany.

Cerato A.B. and Lutenegger A.J. (2002) Determination of surface area of fine-grained soils by the ethylene glycol monoethyl ether (EGME) method. *Geotechnical Testing Journal, ASTM*, **25**(3): 315-321.

Clemence, S. P. and Finbarr, A. O. (1981) Design Considerations for Collapsible Soils. *Journal of the Geotechnical Engineering. Division.*, Vol. **107**, No. GT3.

Croney, D. and Coleman, J.D. (1961) Pore pressure and suction in soil. In Proceedings of Conference on Pore Pressure and Suction in Soils, London, Butterworths: 31-37.

Croney, D., Coleman, J. D. and Black, W. P. M. (1958) Movement and distribution of water in soil in relation to highway design and performance. Highw. Res. Bd, Spec. Report No. 40.

Cui, Y.J., Yahia-Aissa, M., and Delage, P. (2002) A model for the volume change behavior of heavily compacted swelling clays. *Engineering Geology*, **64**: 233-25

Cui, Y.J. and Delage, P. (1996) Yielding and plastic behavior of unsaturated compacted silt. *Géotechnique*, **46** (2): 291-311.

Cunningham, M. R. 2000. The mechanical behaviour of a reconstituted, unsaturated soil. Ph.D. thesis, Imperial College of Science, Technology and Medicine, University of London.

Daniel, D. and Benson, C. (1990). Water content-density criteria for compacted soil liners. *J. Geotech. Engrg., ASCE*, **116** (12): 1181-1130.

Daniel, D. and Wu, Y. (1993). Compacted clay liners and covers for arid sites. *J. Geotech. Engrg., ASCE*, **119** (2): 223-237.

Datcheva, M. and Schanz, T. (2003) Hardening for unsaturated frictional materials. *Journal de Physique IV*, **105**:305-311.

Davidson, D. T., and Gardiner, W. F., (1949). Calculation of Standard Proctor Density and Optimum Moisture Content from Mechanical, Analysis, Shrinkage and Factors and Plasticity Index. *Highw. Res. Board, Proceeding Annual Meeting*, V **29**: 447–481.

Delage, P. and Graham, J. (1995). Understanding the behaviour of unsaturated soils requires reliable conceptual models: state of the art report. In Proceedings of the first international conference on unsaturated soils (eds E. E. Alonso and P. Delage), pp. 1223–1256. Rotterdam: Balkema.

Delage, P. and Graham, J. (1996) Mechanical behaviour of unsaturated soils: Understanding the behaviour of unsaturated soils requires reliable conceptual models. In Proceedings of the **1st** International Conference on Unsaturated Soils (UNSAT 95), Paris, France (Eds. E.E. Alonso and P. Delage), Balkema, Rotterdam: 1223-1256.

Delage, P., Hawat, M., and Cui, Y.J. (1998) The relationship between suction and swelling properties in a heavily compacted unsaturated clay. *Engineering Geology*, **50**(1-2): 31-48.

Delage, P., Cui, Y.J., and Antoine, P. (2005) Geotechnical problems related with loess deposits in Northern France. International Conference on Problematic Soils, Famagusta, North Cyprus : Cyprus. 25-27 May 2005: 1-24.

Delage, P., Audiguier, M., Cui, Y., and Howat. M. (1996) Microstructure of a compacted silt. *Can. Geotech. Journal,* V. **33**: 150-158.

DIN (1987) Baugrund und Grundwasser. Benenen und Beschreiben von Boden und Fels, , *Deustche Institut für Normung e.V., Beuth Verlag GmbH, Berlin*.

Dixon, D. A., Gray, M. N., and Thomas, A. W. (1985). A study of the compaction properties of potential clay-sand buffer mixtures for use in nuclear fuel waste disposal, *Engineering Geology*, **21**: 247-255.

Drumright, E. E. (1989). The contribution of matric suction to the shear strength of unsaturated soils. PhD thesis, Colorado State University, Fort Collins.

Dudley, J. H. (1970) Review of Collapsing Soils. *Journal of Soil Mech. Found. Div., ASCE*, **96**(3), 925-947.

Edlefsen, N.E. and Anderson, A.B.C. (1943) Thermodynamics of soil moisture. *Hilgardia*, **15**: 31-298.

Ellis, C. I. (1980) Soil compaction at low moisture content-field trials in Sudan. 7th Regional conference for Africa on soil mechanics and foundation eng., *Accra, Ghana*, 1-7 June.

Escario, V. & Saez, J. (1986). The shear strength of partly saturated soils. *Géotechnique,* **36**(3): 453-456.

European Standard EN-ISO 11885 (1985) Water Quality-Ditermination of 33 Elements by Inductively Coupled Plasma (ICP) emission spectroscopy.

Feng, M. and Fredlund, D.G. (1999) Hysteretic influence associated with thermal conductivity sensor measurements. In Proc. from Theory to the Practice of Unsat. Soil Mech- in Association with the **52nd** Canadian Geotechnical Conf- and the Unsat- Soil Group, Regina, Sask., 23–24 October 1999: 14:2:14–14:2:20.

Ferber, V., Auriol, J., Cui, Y., and Magnan, J. (2008) Wetting-induced volume changes in compacted silty clay and high-plasticity clays. *Canadian Geotechnical Journal*, **45**: 252-265.

Ferrari, A. (2007) Caratterizzazione meccanica di un'argilla a scaglie compattata non satura: effetti della suzione sulla resistenza al taglio. Ph.D. thesis, Universita` degli Studi di Palermo, Palermo, Italy. [In Italian].

Fisher, R. A. (1926) On the capillary forces in an ideal soil; correction of formulas by W.B. Haines. *J. Agric. Sci.* **16**, 492–505.

Fleureau, J.M., Verbrugge, J.C., Huergo, P.J., Correia, A.G., and Kheirbek-Saoud, S. (2002) Aspects of the behaviour of compacted clayey soils on drying and wetting paths. *Canadian Geotechnical Journal*, **39**: 1341-1357.

Fleureau, J. M., Kheirbek-Saoud, S., Soemitro, R., and Taibi, S. (1993) Behavior of clayey soils on drying-wetting paths. *Can. Geotech. Journal*, **30**: 287–296.

Fleureau, J.M., Verbrugge, J.C., Huergo, P.J., Correia, A.G. (2002) Aspects of the behaviour of compacted clayey paths. *Canadian Geotechnical Journal*, **39**: 1341-1357.

Fredlund, D.G. and Pham, H.Q. (2006) A volume-mass constitutive model for unsaturated soils in term of two independent stress state variables. Keynote Address, **4th** International Conference on Unsaturated Soils, ASCE, April, 2-6, Carefree, Arizona: 105-134,

Fredlund, D.G. and Pham, H.Q. (2007) Independent Roles of the Stress State Variables on Volume–Mass Constitutive Relations. **2nd** International Conference Mech. of unsaturated soils, 7th-9th March 2007, Bauhaus-Universität Weimar, Germany: 37-44.

Fredlund, D. G. and Morgenstern, N. R. (1977) Stress state variables for unsaturated soils. *J. Geotech. Eng. Div., ASCE*, **103**, No. GT5: 447-466.

Fredlund, D.G. and Rahardjo, H. (1993) *Soil mechanics for unsaturated soils*. John Wiley & Sons.

Fredlund, D.G. (2000) The 1999 R.M. Hardy Lecture: The implementation of unsaturated soil mechanics into geotechnical engineering. *Canadia. Geotech. Journal*, **37**: 963–986.

Fredlund, D.G. (1989) Negative pore-water pressures in slope stability. In Simposio Suramericano de Deslizamiento, Paipa, Columbia: 1-31.

Gallipoli, D. (2000) Constitutive and numerical modeling of unsaturated soils. Ph.D. thesis, The University of Glasgow, UK.

Gallipoli, D., Wheeler, S. J. and Karstunen, M. (2002) Importance of modeling degree of saturation: the pressuremeter test. *Numerical models in Geomechanics- NUMOG VIII* (eds Pande & Pietruszczak): 627-633.

Gallipoli, D., Wheeler, S. J. and Karstunen, M. (2003**a**). Modelling the variation of degree of saturation in a deformable unsaturated soil. *Géotechnique,* **53**, No. 2. 105-112

Gallipoli, D., Gens, A., Sharma, R. and Vaunat, J. (2003**b**). An elasto-plastic model for unsaturated soil incorporating the effects of suction and degree of saturation on mechanical behaviour, *Géotechnique,* **53**, No. 1, 123–135

Gens A, Śanchez M., and Sheng D. (2006) On constitutive modelling of unsaturated soils. *Acta Geotechnica*, **1**:137–147.

Gens A. (1996) Constitutive modelling, application to compacted soil. First International Conference on Unsaturated Soils, Paris, France, Alonso E, Delage P (eds), vol. **3**. Balkema: Rotterdam; 1179–1200.

Gens A., Alonso E.E., Suriol J., and Lloret A. (1995) Effect of the structure and volumetric behaviour of a compacted soil. Proceedings of the 1st International Conference on Unsaturated Soils (Eds. Alonso and Delage), Paris, France, Vol. 1: 83-88.

Gens, A. and Alonso E.E. (1992) A framework for the behavior of unsaturated expansive clays. *Can. Geot. Journal*, **29**: 1013-1032.

Georgiadis, K. (2003). Development, implementation and application of partially saturated soil models in finite element analysis. Ph.D. thesis, Imperial College of Science, Technology and Medicine, University of London.

Gurtug, Y., and Sridharan, A. (2002). Prediction of compaction characteristics of fine-grained soils. *Géotechnique*, V. **52**, No. 10: 761–763.

Haines, W.B. (1930) Studies in the physical properties of soil – V: The hysteresis effect in capillary properties and the modes of water distribution associated therewith. *Journal of Agricultural Science*, **20**: 97–116.

Hilf, J.W. (1956) An investigation of pore water pressure in compacted cohesive soils. US Bureau of Reclamation. Technical Memo No. 654, Denver, Colorado.

Hilf, J.W. (1991) *Compacted fill. In Foundation engineering handbook*. Edited by H.-Y. Fang. Chapman and Hall Ltd., London, U.K.: 249–316.

Hillel, D. (1998) *Environmental soil physics*. Academic Press, San Diego., CA.

Hindi, A. R. O. (1967). Identification, physical properties and compaction of swelling soils in western Egypt. *Bulletin of College of Eng., Basrah University*, V. **1**, No. 1: 15-38.

Ho, D. Y. F. (1988) The relationship between the volumetric deformation moduli of unsaturated soils. PhD thesis, Dep. Of Civil Eng., Univ. of Saskatoon, Sask., Canada..

Ho, D.Y.F., Fredlund, D. G. and Raharadjo H. (1992) Volume change indices during loading and unloading of an unsaturated soil. *Can. Geotec. Journal*, **29**: 195-207.

Hoffmann, C. and Tarantino, A. (2008) Effect of grain size distribution on water retention behavior of well graded coarse material, Unsaturated Soils: Advances in Geo-Engineering, Proc. **1st** European Conf. on Unsaturated Soils, Durham, UK (ed. Toll, D.G., Augarde, C.E., Gallipoli, D. and Wheeler, S.J.), Leiden: CRC Press/Balkema: 291-298.

Honda, M., Ohno, S., Iizuka, A., Kawai, K. and Ohta H. (2007) A study on yield stress in unsaturated clay. **3rd** Asia Conference on Unsaturated Soils. China: 219-222.

Horpibulsuk, S., Katkan, W., and Apichatvullop, A. (2008a). An Approach for Assessment of Compaction Curves of Fine- Grained Soils at Various Energies Using a One Point Test. Soils Found., *Japan Geotechnical Society (JGS)*, V. **48**, No. 2: 115–126.

Horpibulsuk, S., Katkan, W., and Naramitkornburee A. (2008b). Modified Ohio's Curves: A rapid estimation of compaction curves for coarse- and fine-grained soils. *Geotechnical Testing Journal*, V. **32**, No. 1: 1-12.

Horpibulsuk, S., Rachan, R, and Katkan, W. (2006) Prediction of compaction curves at various energies using a one point tests. International Symposium of Lowland Technology, September 14-16 2006 in Saga, Japan.

Houlsby G. T. (1997). The work input to an unsaturated granular material. *Géotechnique*, **47**, No1: 193-196.

Howell, J.L., Shackelford, C.D., Amer, N.H., and Stern, R.T. (1997). Compaction of sand-processed clay soil mixtures. *Geotechnical Testing Journal*, **20**(4): 443–458.

Hutter K, Laloui L., and Vulliet L. (19999 Thermodynamically based mixture models for saturated and unsaturated soils. *Mechanics of Cohesive-frictional Materials*; 4:295–338.

JNC (2000) H12: Project to establish the scientific and technical basis for HWL disposal in Japan. Supporting Report 2. Repository design and engineering technology, JNC TN1410 2000-003. Japan Nuclear Cycle Development Institute, Tokai, Japan.

Jeng, Y. S., and Strohm, W. E. (1976) Prediction of the Shear Strength and Compaction Characteristics of Compacted Fine- Grained Cohesive Soils. United States Waterways Experiment Station, Soil and Pavement Laboratory, Vicksburg, Miss.

Jennings, J. E. B. and Burland, J. B. (1962) Limitations to the use of effective stresses in partly saturated soils. *Géotechnique*, Vol. **12**, No. 2.

Jennings, J. E., and Knight, K. (1957) The Addition Settlement of Foundations Sandy Subsoil on Wetting. Proc. of **4th** Int. Conf. on Soil Mech. and Foud. Eng., **1**: 316-319.

Jesmani, M, Manesh A. N., and Hoseini S. M. R. (2008). Optimum water content and maximum unit weight of clayey gravels at different compactive efforts. *EJGE*, V. **13**, L.

Johnson, J. M., and Lovell, C. W. (1979) The Effect of Laboratory Compaction on the Shear Behavior of a Highly Plastic Clay after Saturation and Construction. Report No. JHRP-79-7, Purdue University, West Lafayette, Ind.

Jommi, C. (2000) Remarks on the constitutive modelling of unsaturated soils. Proceedings of the international workshop on unsaturated soils, Trento: 139–153.

Jommi, C. and Di Prisco, C. (1994) Un semplice approccio teorico per la modellazione del comportamento meccanico dei terreni granulari parzialmente saturi (in Italian). *In Atti Convegno sul Tema: Il Ruolo deiFluidi nei Problemi di Ingegneria Geotecnica*, Mondovı´: 167–188.

Josa, A. (1988) Un medelo elastoplastico para siels no saturados. PhD thesis, Universidad Politecnica de Catluna, Barcelona, Spain.

Josa, A., Balmaceda, A., Gens, A., and Alonso, E.E. (1992) An elasto-plastic model for partially saturated soils exhibiting a maximum of collapse. Proc. 3rd Int. Conference Computational Plasticity, Barcelona, 1: 815-826.

Joslin, J.C. (1959). Ohio's typical moisture–density curves. American Society for Testing and Materials, *Special Technical Publication STP,* **239**: 111–118.

Jotisankasa, A. (2005) Collapse behaviour of compacted silty clay. Ph.D. thesis, Imperial College of Science, Technology and Medicine, University of London.

Jotisankasa, A., Ridley, A. and Coop, M. (2007). Collapse behavior of compacted silty clay in suction-monitored oedometer apparatus. *Journal of Geotech. and Geoenvironmental Eng. ASCE,* V. **133**, No. 7: 867-877.

Kabir, M. H. and Taha, M. R. (2004). Assessment of physical properties of a granite residual soil as an isolation barrier. *EJGE*, V. **9**, Bundle B.

Kanazawa, S., Kawai. K., Iizuka, A., Ohno, S., Tachibana. S., Thirapong. P., and Takeyama, T. (2009) A finite element simulator for mechanical behavior of unsaturated earth structures exposed to evaporation and moisturization. 4th Asia-Pacific Conference on Unsaturated Soils, 23-25 November 7 2009, Newcastle, Australia: 711-717.

Karube, D. and Kawai, K. (2001). The role of pore water in the mechanical behavior of unsaturated soils. *Geotech. Geol. Eng*. **19**, 211–241.

Kayadelen, C.(2008). Estimation of effective stress parameter of unsaturated soils by using artificial neural networks. Int. *J. Numer. Anal. Meth. Geomech*, **32**:1087–1106

Kezdi, A. (1960) *Soil Mechanics*. Budapest: Tankonyv Kiado.

Khalili N, Geiser F, and Blight G.E. (2004) Effective stress in unsaturated soils: review with new evidence. *International Journal of Geomechanics*, **4**(2):115–126.

Khalili N, Habte M.A, and Zrgarbashi S. (2008) A fully coupled flow-deformation model for cyclic analysis of unsaturated soils including hydraulic and mechanical hystereses. *Computers and Geotechnics,* **35**(6):872–889.

Khalili N. and Khabbaz M.H. (1998) A unique relationship for _ for the determination of the shear strength of unsaturated soils. *Géotechnique,* **48**(5):681–688.

Khalili, N., and Loret, B., (2001) An Elasto-Plastic Model for Non-Isothermal Analysis of Flow and Deformation in Unsaturated Porous Media: Formulation, *Int. Journal Solids and Structures*, **38**:8305-8330.

Klausner, Y. (1991) *Fundamentals of continuum mechanics of soils*. Springer-Verlag, New York.

Knight, K. (1963) The Origin & Occurrence of Collapsing Soils. Proc. of **3rd** Regional Conference of Africa on Soil Mechanics and Foundation Engineering, **1**: 127-130.

Kohgo, Y., Nakano, M., and Miyazaki, T. (1993a) Theoretical aspects of constitutive modeling for unsaturated soils. Soil Mech. Found. Eng. (Engl. Transl.), **33**(4): 49–63.

Kohgo, Y., Nakano, M., and Miyazaki, T. (1993b) Verification of the generalized elastoplastic model for unsaturated soils. Soil Mech. Found. Eng. (Engl. Transl.), **33**(4): 64–73.

Komine H. and Ogata N. (2003) New equations for swelling characteristics of bentonite based buffer materials. Canadian Geotechnical Journal, **40**: 460-475.

Korfiatis, G.P., and Manikopoulos, C.N. (1982). Correlation of maximum dry density and grain size. Journal of Geotechnical Engineering, ASCE, **108**: 1171–1176.

Krahn J. and Fredlund D.G. (1972) On total, matric and osmotic suction. Soil Science, **115**(5): 339-348.

Kurucuk, N., Kodikara, J. and Fredlund, D. G. (2008) Theoretical modelling of the compaction curve. 1st Unsaturated Soils Conf., Advances in Geo-Eng., Durham, UK: 375-379.

Lambe, T. W., and Whitman, R. V. (1979) Soil Mechanics. Wiley, New York.

Lang A.R.G. (1967) Osmotic coefficients and water potentials of sodium chloride solution from 0 to 40°C, *Australian Journal of Chemistry*, **20**: 2017-2023.

Blatz, J.A. and Graham, J. (2003) Elastic-plastic modelling of unsaturated soil using results from a new triaxial test with controlled suction. *Géotechnique*, **53**(1): 113-122.

Lawton, E. C., Fragaszy, R. J., and Hardcastle, J. H. (1989) Collapse of Compacted Clayey Sand. *Journal of Geotech. Engrg. , ASCE*, **115**(9): 1252-1267.

Lawton, E.C., Fragaszy, R. J., and Hardcastle, J. H. (1991) Stress ratio effects on collapse of compacted clayey sand. *J. Geotech. Eng. ASCE*, **117** (5): 714-730.

Lawton, E.C., Fragaszy, R. J., and Hetherington, M. D. (1992) Review of wetting-induced collapse in compacted soil. *J. Geotech. Eng., ASCE*, **117** (9): 1376-1394.

Lee, P. Y. and Suedkamp, R. J. (1972) Characteristics of irregularly shaped compaction curves of soils. National academy of sciences, Washington, DC, Highway Research Record No. **3811-9**.

Leong E.C., Tripathy S., and Rahardjo R. (2003) Total suction measurement of unsaturated soils with a device using the chilled-mirror dew-point technique. *Géotechnique*, **53**(2): 173-182.

Leong, E. C., Wee, H. S. and Rahardjo, H. (2007) One-dimensional compressibility of unsaturated soils. **3rd** Aian Conference on Unsaturated Soil, China: 237-242.

Li, Z.M. (1995) Compressibility and collapsibility of compacted and saturated lossial soils. Proc. **1st** Int. Conf. On Unsaturated Soils, Paris. EE. Alonso and P. Delage (eds.), Balkema, 1:139-144.

Li, H., and Sego, D.C. (2000). Equation for complete compaction curve of fine-grained soils and its applications. In Construction and controlling compaction of earth fills. Edited by D.W. Shanklin, K.R. Rademacher, and J.R. Talbot. *American Society for Testing and Materials*, Special Technical Publication STP **1384**: 113–125.

Lins, Y. (2009) Hydro-mechanical properties of partially saturated sand. PhD. Thesis, Ruhr-Universität Bochum, Germany.

Livneh, M., and Ishai, I. (1978) Using indicative properties to predict the density–moisture relationship of soils. Transportation Research Record **690**: 22–28.

Lloret, A. and Alonso, E. E. (1980). Consolidation of unsaturated soil including swelling and collapse behaviour. *Géotechnique,* **30**(4): 449-477.

Lloret, A., Villar, M.V., Sánchez, M., Gens, A., Pintado, X., and Alonso, E.E. (2003) Mechanical behaviour of heavily compacted bentonite under high suction changes. *Géotechnique*, **53**(1): 27-40.

Loret B. and Khalili N. (2000) A three-phase model for unsaturated soils. *International Journal for Numerical and Analytical Methods in Geomechanics,* **24**: 893–927.

Loret B. and Khalili N. (2002) An effective stress elastic-plastic model for unsaturated porous media. Mechanics of Materials; **34**:97–116.

Lu, Ning and Likos, William (2006) Suction stress characterstic curve for unsaturated soil. *J. of Geotechnical and Geoenvironmental Eng.* **132** (2): 131-142.

Marinho F.A.M. (2005) Nature of soil-water characteristic curve for plastic soils. *Journal of Geotechnical and Geoenvironmental Engineering, ASCE,* **131** (5): 654-661.

Mašín D. and Khalili N. (2008a) A hypoplastic model for mechanical response of unsaturated soils. *International Journal for Numerical and Analytical Methods in Geomechanics,* **32**(15):1903–1926.

Mašín D. and Khalili N. (2008b) Modelling of the collapsible behavior of unsaturated soils in hypoplasticity. First European Conference on Unsaturated Soils, Durham, U.K., Toll DG, Augarde CE, Gallipoli D, Wheeler SJ (eds). CRC Press, Balkema: Boca Raton, The Netherlands; 659–665.

Mašín, D. (2009) 3D modelling of a NATM tunnel in high K0 clay using two different constitutive models. *Journal of Geotechnical and Geoenvironmental Engineering, ASCE,*.

Mašín, D. (2010) Predicting the dependency of a degree of saturation on void ratio and suction using effective stress principle for unsaturated soils. *International Journal for Numerical and Analytical Methods in Geomechanics,* **34**, No. 1, 73-90.

Maswoswe, J. (1985). Stress path for a compacted soil during collapse due to wetting. PhD thesis, Imperial College, London. Matyas, E. L.

Matsuoka, H., Sun, D., Kogane, A., Fukuzawa, N., and Ichihara, W. (2002) Stress-strain behaviour of unsaturated soil in true triaxial tests. *Canadian Geotech. Journal*, **39**: 603-619.

Matyas, E.L. and Radhakrishna H.S. (1968) Volume change characteristic of partially saturated soils. *Géotechnique*, **18**, 432-448.

Mitchell, J. K. (1993) *Fundamentals of soil behavior*, 2nd edition. Wiley, New York.

Modaressi, A., and Abou-Bekr, N. (1994) A unified approach to model the behavior of saturated and unsaturated soils.'' Siriwardane, ed., Proc., **8th** Int. Conf. on Computer Methods and Advances in Geomechanics, Morgantown, Balkema, Rotterdam: 1507–1513.

Müller-Vonmoos, M. and Kahr, G. (1982) Bereitstellung der Bentonite für die Laboruntersuchung. Technischer Bericht 82-04, The Swiss National Cooperative for the Storage of Radioactive Waste (NAGRA), Wettingen, Switzerland.

Nagaraj, T.S. Srinivasa Murthy,B.R and Vatsala,A. (1990) Discussion on change in pore size distribution due to consolidation of clays by D.J. Griffiths and Joshi, R.C. *Géotechnique*, **40**(2),303-305.

Nagaraj, T.S., Srinivasa Murthy, B.R. and Vatsala, A., (1994) *Prediction of soil behaviour*. Wiley Eastern Publishers.

Nagaraj, T. S., Lutenegger, A., Pandian, N. S., and Manoj, M. (2006b). Rapid Estimation of Compaction Parameters for Field Control. *Geotech. Test. Journal*, V **29**, No 6: 1–10.

Nagaraj, T. S., Pandian, N. S. and Narasimha Raju, P. S. R. (1998) Compressibility behaviour of soft cemented soils. *Géotechnique*, **48**(2): 281-287.

Nagaraj, T.S. (1994). Analysis and prediction of compaction characteristics of soils. *Indian Institute of Science, Bangalore, India.*

Nagaraj, T.S., and Bindumadhava, J. (1992) Analysis of compaction characteristics of fine grained soils. *Indian Geotechnical Conference, Calcutta,* V. **1**: 441–444.

Nagaraj, T.S., and Srinivasa Murthy, B.R. (1986). A critical reappraisal of compression index Eq.s. *Géotechnique*, **36**(1): 27–32.

Nagaraj, T.S., Lutenegger, A.J., Pandian, N.S. and Monaj, M., (2007) Phenomenological model for rapid field compaction control. *Geotechnical Testing J. ASTM*, **29**(6), 1-10.

Nagaraj, T.S., Schanz, T. and Prasad, K. N. (2006a) Generalized state parameter for constitutive relations. *Indian Geotechnical Society ING, Chennai, INDIA*, 14-16 December.

Nagaraj, T. S., Lutenegger, A., Pandian, N. S., and Manoj, M. (2006b). Rapid estimation of compaction parameters for field control. *Geotech. Test. Journal*, V **29**, No 6: 1–10.

Nagaraj. T.S. & Miura, N. (2001) *Soft Clay Behaviour -Analysis and assessment*. AA Balkema Pub, Rotterdam, Netherlands.

Najjar, Y.M., and Basheer, I.A. (1996). Utilizing computational neural networks for evaluating the permeability of compacted clay liners. *Journal of Geotechnical and Geological Engineering*, **14**: 193–212.

Nelson, J.D. and Miller, D.J. (1992) *Expansive soils: problems and practice in foundation and pavement engineering*. John Wiley & Sons, NY.

Olson, R.E. and Langfelder, L.J. (1965) Pore-water pressures in unsaturated soils. *Journal of Soil Mechanics and Foundation Division*, Proceedings of American Society of Civil Engineers, **91**(SM4): 127-160.

Pandian, N. S., Nagaraj, T. S., and Manoj, M. (1997). Reexamination of compaction characteristics of fine-grained soils. *Geotech. Test. Journal*, V. **47**, No. 2: 363–366.

Pereira, J.H.F., and Fredlund, D.G. (2000) Volume change behaviour of a residual soil of gneiss compacted at metastable-structured conditions. *Journal of Geotechnical and Geoenvironmental Engineering, ASCE*, **126**(10): 907–916.

Pham Q.H. and Fredlund, D. (2005) A volume-mass constitutive model for unsaturated soils. Proc. Of the **58th** Canadian Geotechnical Conf., Saskatchewan, Canada. V. 2.

Pham, Q.H., Fredlund, D.G., and Barbour, S.L. (2005) A study of hysteresis models for soil-water characteristic curves. *Can. Geotech. Journal*, **42**: 1548-1568.

Proctor, R. R., (1933) Fundamental Principles of Compaction. *Eng. News-Rec*., V. **111**, No. 9-10: 12–13.

Pusch R., and Yong R. (2003) Water saturation and retention of hydrophilic clay buffermicrostuctural aspects, *Applied Clay Science, Elsevier*. **23**: 61-68.

Ramiah, B.K., Viswanath, V., and Krishnamurthy, H.V. (1970) Interrelationships of compaction and index properties. Proceedings of the **2nd** Southeast Asian Conference on Soil Engineering, Singapore: 577–587.

Rao S.M. and Shivananda P. (2005) Role of osmotic suction in swelling of salt amended clays, *Canadian Geotechnical Journal*, **42**: 307-315.

Razouki, S. S., Haik, M., Spyridon, G., Mosa, S., Wazir, H., Majead, G. and Ibrahim, E. (1980). On the compaction and CBR behavior of Basrah soil. *Bulletin of the college of engineering, University of Basrah*, **4**, No. 1: 107-133.

Razouki, S., Kuttah, D., Al-Damluji, O. and Nashat, I. (2008). Using gypsiferous soil for embankments in hot desert areas. *ICE, Construction Materials*, **6**, CM2: 63-71.

Rethati, L. (1988) *Probabilistic solutions in geotechnics*. Elsevier, New York.

Reznik, Y.M. (1995) Comparison of results of oedometer and plate load tests performed on collapsible soils. *Engineering Geology*, **39**: 17-30.

Richards, B.G. (1965) Measurement of the free energy of soil moisture by the psicrometric technique using thermistors. In Moisture Equilibria and Moisture Changes in Soil Beneath Covered Area. A. symposium in Print. Australia: Butterworths: 39-46.

Ridley, A.M. and Wray, W.K. (1996) Suction measurement: a review of current theory and practices. In Proceedings of the **1st** International Conference on Unsaturated Soils (UNSAT 95), Paris, 1995 (Eds. E.E. Alonso and P. Delage), Balkema, Rotterdam: 1293-1322.

Ring, G.W., Sallgerb, J.R., and Collins, W.H. (1962). Correlation of compaction and classification test data. *Highway Research Board*, Bulletin **325**: 577–587.

Romero, E. (1999) Characterisation and T-H-M behavior of unsaturated Boom clay: an experimental study. PhD thesis, Uni. Polytecnica de Catalunya.

Roscoe, K.H. and J.B. Burland. (1968) On the generalized stress-strain behaviour of wet clay. *In Engineering Plasticity, eds. Journal of Heyman and F.A. Leckie*, Cambridge, England: Cambridge University Press: 535-609.

Russell A. R. and Khalili N. (2006) A unified bounding surface plasticity model for unsaturated soils. I*nternational Journal for Numerical and Analytical Methods in Geomechanics,* **30**(3):181–212.

Sacchi E., Michelot J.L., Pitsch H., Lalieux P., Aranyossy J.F. (2001) Extraction of water and solutes from argillaceous rocks for geochemical characterisation: Methods, processes, and current understanding. *Hydrology Journal, Spinger*. **9**: 17-33.

Sawangsuriya, A., Edil, T. and Bosscher, P. (2008). Modulus-suction-moisture relationship for compacted soils. *Can. Geotech. Journal*, **45**: 973-983.

Schanz, T., Arifin, Y., Agus, S., and Khan, M. (2010) Time effect on the total suction of bentonites. *Soil and Found. Journal, Japanese Geotech. Society*, V. **50**, No. 2:195-202.

Sharma, R. S. (1998). Mechanical behaviour of unsaturated highly expansive clays. PhD thesis, University of Oxford, UK.

Sheng, D. Fredlund, D and Gens, A. (2008a) A new modelling approach for unsaturated soils using independent stress variables. *Canadian Geotech. Journal,* **45**: 511-534.

Sheng, D. Gens, A. Fredlund, D. and Sloan, S. (2008b) Unsaturated soils: From constitutive modelling to numerical algorithms. *Computers and Geotechnics*, **35**: 810–824.

Sivakumar, V. (1993). A critical state framework for unsaturated soil. PhD thesis, University of Sheffield, UK.

Sposito G. (1981) *The thermodynamic of soil solution*. Oxford Clarendon Press. London.

Sridharan, A., Sreepada Rao, A. and Sivapullaiah, P.V. (1986) Swelling pressure of clays. *Geotechnical Testing Journal, GTJODJ*, **9**(1): 24-33.

Sridharan, A. and Nagaraj, H. B. (2005). Plastic limit and compaction characteristics of fine-grained soils. *Ground Improvement*, **9** (1): 17-22.

Sridharan, A. and Nagaraj, H.B. (1999) Absorption water content and liquid limit of soils. *Geotechnical Testing Journal, GTJODJ*, **22**(2): 121-127.

Sun, D.A., Sheng, D., and Xu, Y.F. (2007). Collapse behavior of unsaturated compacted soil with different initial densities. *Canadian Geotech. Journal*, **44**(6): 673-686.

Swedish Nuclear Fuel and Waste Management Company (1983) Final storage of spent nuclear fuel-KBS-3, III barriers. Swedish Nuclear Fuel Supply Company, Division KBS Technical Report: 9:1–16:12.

Tamagnini, R. (2004) An extended Cam-clay model for unsaturated soils with hydraulic hysteresis. *Géotechnique*, **54**(3): 223-228.

Tarantino, A. and Tombolato, S. (2005) Coupling of hydraulic and mechanical behaviour in unsaturated compacted clay. *Géotechnique*, **55**(4): 307–317.

Thomson W.T. (1871) *Philosophical Magazine*. **42**: 448.

Trantino, A. and DeCol, E. (2008) Compaction behaviour of clay. *Géotechnique*, **58**(3): 199-213.

Tripathy , S., Subba, F.S., and Fredlund, D.G. (2002) Water content-void ratio swell-shrink paths of compacted expansive soils. *Canadian Geotech. Journal*, **39**: 938-959.

Turnbull, W.J. (1948) Computation of the optimum moisture content in the moisture–density relationship of soils. Proceedings of the **2nd** International Conference on Soil Mechanics and Foundation Engineering, Rotterdam, V **4**: 256–262.

USDA (1950) *USDA Agricultural Handbook 60*. Diagnosis and improvement of saline and alkali soils.

Vanapalli S.K., Fredlund, D.G., and Pufahl, D.E. (1999) Influence of soil structure and stress history on the soil-water characteristics of a compacted till. *Géotechnique*, **49**(2):143-159.

Vesga, L.F. (2008) Equivalent Effective Stress and Compressibility of Unsaturated Kaolinite Clay Subjected to Drying. *Journal of Geotechnical and Geoenvironmental Engineering, ASCE*, Vol. **134**, No. 3:1090-0241.

Villar M.V. and Lloret A. (2004) Influence of temperature on the hydro-mechanical behaviour of a compacted bentonite, *Applied Clay Science, Elsevier*. **26**: 337-350.

Villar MV, Rivas P, Campos R, Lloret A, Romero E, and Mariano A (2001) First report on thermo-hydro-mechanical laboratory tests. Report 70-IMA-L-0-86

Wang, M.C., and Huang, C.C. (1984). Soil compaction and permeability prediction models. *Journal of Environmental Engineering, ASCE*, **110**: 1063–1083.

Wheeler, S. J., and Karube, D. (1996) Constitutive Modelling. Proc. **1st** Int. Conf. Unsaturated Soils, Paris, France: 1323-1356.

Wheeler, S. J., Gallipoli, D., and Karstunen, M (2002) Comments on use of the Barcelona Basic Model for unsaturated soils. *International Journal Numer. Anal. Meth. Geomech.,* **26**:1561–1571.

Wheeler, S. J., Sharma, R. J. and Buisson, M. S. R. (2003). Coupling of hydraulic hysteresis and stress–strain behaviour in unsaturated soils. *Géotechnique*, **53**, No 1, 41- 54.

Wheeler, S.J. and Sivakumar, V., (1995) An elasto-plastic critical state framework for unsaturated soils. *Géotechnique*, **45** (1): 35–53.

Schriftenreihe des Lehrstuhls für Grundbau, Boden- und Felsmechanik der Ruhr-Universität Bochum

Herausgeber: H.L. Jessberger

Heft Nr.

1	(1979)	**Hans Ludwig Jessberger** Grundbau und Bodenmechanik an der Ruhr-Universität Bochum
2	(1978)	**Joachim Klein** Nichtlineares Kriechen von künstlich gefrorenem Emschermergel
3	(1979)	**Heinz-Joachim Gödecke** Die Dynamische Intensivverdichtung wenig wasserdurchlässiger Böden
4	(1979)	**Poul V. Lade** Three Dimensional Stress-Strain Behaviour and Modeling of Soils
5	(1979)	**Roland Pusch** Creep of soils
6	(1979)	**Norbert Diekmann** Zeitabhängiges, nichtlineares Spannungs-Verformungsverhalten von gefrorenem Schluff unter triaxialer Belastung
7	(1979)	**Rudolf Dörr** Zeitabhängiges Setzungsverhalten von Gründungen in Schnee, Firn und Eis der Antarktis am Beispiel der deutschen Georg-von-Neumayer- und Filchner-Station
8	(1984)	**Ulrich Güttler** Beurteilung des Steifigkeits- und Nachverdichtungsverhaltens von ungebundenen Mineralstoffen
9	(1986)	**Peter Jordan** Einfluss der Belastungsfrequenz und der partiellen Entwässerungsm öglichkeiten auf die Verflüssigung von Feinsand
10	(1986)	**Eugen Makowski** Modellierung der künstlichen Bodenvereisung im grundwasserdurchströmten Untergrund mit der Methode der finiten Elemente
11	(1986)	**Reinhard A. Beine** Verdichtungswirkung der Fallmasse auf Lastausbreitung in nichtbindigem Boden bei der Dynamischen Intensivverdichtung
12	(1986)	**Wolfgang Ebel** Einfluss des Spannungspfades auf das Spannungs-Verformungsverhalten von gefrorenem Schluff im Hinblick auf die Berechnung von Gefriersch¨achten
13	(1987)	**Uwe Stoffers** Berechnungen und Zentrifugen-Modellversuche zur Verformungsabhängigkeit der

Ausbaubeanspruchung von Tunnelausbauten in Lockergestein

14 (1988) **Gerhard Thiel**
Steifigkeit und Dämpfung von wassergesättigtem Feinsand unter Erdbebenbelastung

15 (1991) **Mahmud Thaher**
Tragverhalten von Pfahl-Platten-Gründungen im bindigen Baugrund, Berechnungsmodelle und Zentrifugen-Modellversuche

16 (1992) **Rainer Scherbeck**
Geotechnisches Verhalten mineralischer Deponieabdichtungsschichten bei ungleichf¨ormiger Verformungswirkung

17 (1992) **Martin M. Bizialiele**
Torsional Cyclic Loading Response of a Single Pile in Sand

18 (1993) **Michael Kotthaus**
Zum Tragverhalten von horizontal belasteten Pfahlreihen aus langen Pf¨ahlen in Sand

19 (1993) **Ulrich Mann**
Stofftransport durch mineralische Deponieabdichtungen: Versuchsmethodik und Berechnungsverfahren

20 (1992) **Festschrift anlässlich des 60. Geburtstages von Prof. Dr.-Ing. H. L. Jessberger**
20 Jahre Grundbau und Bodenmechanik an der Ruhr-Universität Bochum

21 (1993) **Stephan Demmert**
Analyse des Emissionsverhaltens einer Kombinationsabdichtung im Rahmen der Risikobetrachtung von Abfalldeponien

22 (1994) **Diethard König**
Beanspruchung von Tunnel- und Schachtausbauten in kohäsionslosem Lockergestein unter Berücksichtigung der Verformung im Boden

23 (1995) **Thomas Neteler**
Bewertungsmodell f¨ur die nutzungsbezogene Auswahl von Verfahren zur Altlastensanierung

24 (1995) **Ralph Kockel**
Scherfestigkeit von Mischabfall im Hinblick auf die Standsicherheit von Deponien

25 (1996) **Jan Laue**
Zur Setzung von Flachfundamenten auf Sand unter wiederholten Lastereignissen

26 (1996) **Gunnar Heibrock**
Zur Rissbildung durch Austrocknung in mineralischen Abdichtungsschichten an der Basis von Deponien und Baugrund infolge stoßartiger Belastung

27 (1996) **Thomas Siemer**
Zentrifugen-Modellversuche zur dynamischen Wechselwirkung zwischen Bauwerken

28 (1996) **Viswanadham V. S. Bhamidipati**
Geosynthetic Reinforced Mineral Sealing Layers of Landfills

29 (1997) **Frank Trappmann**
Abschätzung von technischem Risiko und Energiebedarf bei Sanierungsmaßnahmen f¨ur Altlasten

30 (1997) **Andr´e Schürmann**
Zum Erddruck auf unverankerte flexible Verbauwände

31 (1997) **Jessberger, H. L. (Herausgeber)**
Environment Geotechnics, Report of ISSMGE Technical Committee TC 5 on Environmental Geotechnics

Herausgeber: Th. Triantafyllidis

32 (2000) **Triantafyllidis, Th. (Herausgeber)**
Boden unter fast zyklischer Belastung: Erfahrung und Forschungsergebnisse (Workshop)

33 (2002) **Christof Gehle**
Bruch- und Scherverhalten von Gesteinstrennflächen mit dazwischenliegenden Materialbrücken

34 (2003) **Andrzej Niemunis**
Extended hypoplastic models for soils

35 (2004) **Christiane Hof**
Über das Verpressankertragverhalten unter kalklösendem Kohlensäureangriff

36 (2004) **Rene´ Schäfer**
Einfluss der Herstellungsmethode auf das Verformungsverhalten von Schlitzwänden in weichen bindigen Böden

37 (2005) **Henning Wolf**
Zur Scherfugenbänderung granularer Materialien unter Extensionsbeanspruchung

38 (2005) **Torsten Wichtmann**
Explicit accumulation model for non-cohesive soils under cyclic loading

39 (2008) **Christoph M. Loreck**
Die Entwicklung des Frischbetondruckes bei der Herstellung von Schlitzwänden

40 (2008) **Igor Arsic**
Über die Bettung von Rohrleitungen in Flüssigböden

41 (2009) **Anna Arwanitaki**
Über das Kontaktverhalten zwischen einer Zweiphasenschlitzwand und nichtbindigen Böden

Herausgeber: T. Schanz

42 (2009) **Yvonne Lins**
Hydro-Mechanical Properties of Partially Saturated Sand

43 (2010) **Tom Schanz (Herausgeber)**
Geotechnische Herausforderungen beim Umbau des Emscher-Systems
Beiträge zum RuhrGeo Tag 2010

44 (2010) **Jamal Alabdullah**
Testing Unsaturated Soil for Plane Strain Conditions: A New Double-Wall Biaxial Device

45 (2011) **Lars Röchter**
Systeme paralleler Scherbänder unter Extension im ebenen Verformungszustand

46 (2011) **Yasir Al-Badran**
Volumetric Yielding Behavior of Unsaturated Fine-Grained Soils

ISSN 2190-3255